TRANSLATION

FUNDAMENTALS OF HEAT TRANSFER IN AVIATION AND
ROCKET ENGINEERING

By

V. S. Avduyevskiy, Yu. I. Danilov, et. al.

FOREIGN TECHNOLOGY
DIVISION

AIR FORCE SYSTEMS COMMAND

WRIGHT-PATTERSON AIR FORCE BASE

OHIO

UNEDITED ROUGH DRAFT TRANSLATION

FUNDAMENTALS OF HEAT TRANSFER IN AVIATION AND
ROCKET ENGINEERING

BY: V. S. Avduyevskiy, Yu. I. Danilov, et. al.

English Pages: 591

Ministerstvo Vysshego i Srednego Spatsial'nogo
Obrazovaniya RSFSR

OSNOVY TEPLOPEREDACHI V AVIATSIONNOY I RAKETNOY TEKHNIKE

Gosudarstvennoye Nauchno-Tekhnicheskoye Izdatel'stvo
Oborongiz, Moskva, 1960

Pages: 1-389

TABLE OF CONTENTS

CHAPTER I

TYPES OF HEAT EXCHANGE, FUNDAMENTAL CONCEPTS AND DEFINITIONS

CHAPTER II

THERMAL CONDUCTIVITY UNDER STEADY-SSTATE CONDITIONS

CHAPTER III

CONVECTIVE HEAT EXCHANGE AND FUNDAMENTALS OF THEORY OF SIMILARITY

CHAPTER IX

HEAT EXCHANGE DURING CHEMICAL REACTIONS IN THE BOUNDARY LAYER

CHAPTER X

HYDRODYNAMIC METHODS OF FIRMLY PROTECTING SURFACES. SWEAT COOLING

CHAPTER XI

BARRIER AND COMBINED COOLING OF COMBUSTION CHAMBER WALLS AND NOZZLES IN JET ENGINES.

CHAPTER XII

FILM COOLING OF WALLS OF COMBUSTION CHAMBER AND NOZZLES IN LIQUID PROPELLANT ROCKET ENGINES.

CHAPTER XIII

CONCEPT OF HEAT EXCHANGE IN RAREFIED GASES

CHAPTER XIV

SOME ASPECTS OF THE CALCULATION OF THE HEAT-UP OF WINGED FLYING CRAFT; METHODS OF THERMAL PROTECTION

CHAPTER XV

SOME FEATURES OF HEAT TRANSFER CALCULATIONS IN LIQUID PROPELLENT ROCKET ENGINES

CHAPTER XVI

HEAT CONDITONS IN CRAFT FLYING IN UPPER LAYERS OF ATMOSPHERE (ARTIFICIAL EARTH SATELLITES)

CHAPTER XII

SOME FEATURES OF HEAT TRANSFER IN NUCLEAR POWER REACTORS

vii

Chapter 1.

TYPES OF HEAT EXCHANGE, FUNDAMENTAL CONCEPTS AND DEFINITIONS

Section 1. Types of Heat Exchange

The concept of heat exchange (heat transfer) covers a whole series of phenomena involving the transfer of heat from one set of bodies to another or from parts of one body to other parts of the same body *as a result* of difference in temperature.

The process of heat transfer can be carried out in three ways. On the basis of this we distinguish three fundamental types of heat exchange:

1. Thermal conductivity.

2. Convective heat exchange .

3. Radiant heat exchange.

Thermal conductivity is the transfer of heat between directly touching parts of a body. Thermal conductivity is not related to the macromovement of the bodies or parts of a body. This process of heat exchange is due to the transfer of energy from one lot of elementary particles of the body to others *as a result* of the micromotion of these elementary particles. In the case of gases, these particles are molecules.

Molecules of a gas in the part of it which is at a higher temperature possess greater mean kinetic energy. When the gas molecules collide, they exchange kinetic

energy, as a result of which the heat is transferred from the hotter parts of the gas to the cooler parts.

In its pure form, thermal conductivity is observed in solid bodies and stationary fluids, *provided that* convective currents are possible in them.

In fluids thermal conductivity is usually connected with a whole number of other physical phenomena, for example, macromotion of the gas mass and the related transfer of heat. Study of thermal conductivity in metals shows that the propagation of heat in them is similar to that of electricity.

According to the present-day theory, it is electrons which play the main part in electric conductivity, *hence)* in metals thermal conductivity is also associated with the motion of electrons, which play the part of the heat transmitters.

In the simplest theory of thermal conductivity of metals it is assumed that there are free electrons in the metals which behave as gas molecules; these electrons move between the atoms of the solid body and thereby transfer the heat.

Convective heat exchange. This type of heat exchange is effected by particles of liquid shifting through space. It is always accompanied by *an* exchange between particles in direct contact.

- 2 -

According to the reason for the motion of the fluid, convective heat

exchange is subdivided into two types:

a) convective heat exchange with free motion of the medium (free convection)

b) convective heat exchange with enforced motion of the medium (forced

convection).

Free convection occurs whenever the motion of the fluid is due . solely to

different densities in different parts of the medium under consideration, which

in its turn is due to uneven heating of these parts.

Example. If we heat a vessel containing a liquid (Fig. 1), particles of

the liquid at a higher temperature ($t_2 > t_1$), are forced upwards x by the colder layers

as a result of the reduction in their specific gravity ($\gamma_2 > \gamma_1$)

of liquid and carry the heat away with them. Convective currents are produced in

the vessel. The x intensity with which the heat is transferred obviously depends

on the temperature difference ($t_2 - t_1$), the coefficient of volumetric expansion,

the specific gravity and the viscosity of the liquid.

. forced convection occurs whenever the motion of the fluid is due to

outside factors (a current caused by a pump, compressor, the motion of an aircraft

with respect to the air, a ventilation blast, engine cooling systems, etc.).

Heat exchange during forced convection usually exceeds heat exchange

- 3 -
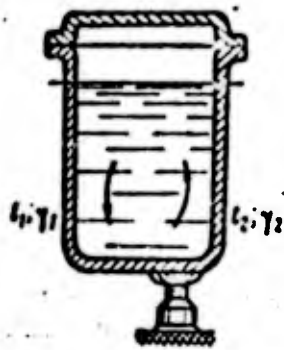
Fig. 1. Conception of natural convection

during free convection by a large factor, and forced convection is ~~utilised~~ for that

reason in engineering ~~in~~ problems involving the transfer of large amounts

of heat.

Radiant heat exchange. Heat transfer effected by radiation, or radiant

heat transfer, occurs when a heated body is able to transform some of the energy

belonging to ~~it~~ into radiant energy, which is transferred from ~~that~~ body to

another. If they encounter a body in their path, the heat rays are partially

absorbed and are reconverted into heat, partly reflected and partly passed through

the body.

Heat rays obey the same laws as light rays: *i.e., the laws of* reflection, refraction and

absorption. According to present-day views, the nature of radiant heat exchange

is the transfer of heat and energy by electromagnetic waves possessing a quantum

nature and conforming to the laws of thermodynamics.

Analysis of specific phenomena connected with the transfer of heat shows

that we usually deal with *all* three ~~a~~ types of heat exchange at the same time, i.e.,

in practice we encounter complex heat exchange.

The combined study of the regularities controlling complex heat exchange

is mathematically difficult, however. Hence we usually study the three types of

heat exchange separately, after which we can go on to calculate the complex heat

- 4 -

exchange fairly easily.

When solving specific tasks in practice, the amount of heat transferred in one way or another may be quite different, hence in the calculations we often disregard the type of heat exchange which is of little importance in the case in point, and conduct the whole calculation for the basic type determining the effect as a whole.

For example, convective heat exchange is always accompanied by thermal conductivity, but in engineering calculations, particularly during forced convection, the effect of thermal conductivity is disregarded.

Section 2: Fundamental Concepts and Definitions.

The following concepts are introduced for the study of complex heat exchange due to the simultaneous effect of thermal conductivity and convection.

Heat exchange between a wall and a fluid touching it is termed heat transfer. The body at the higher temperature t_1 is called the source and the second body at the lower temperature t_2 is called the receiver.

On account of the temperature difference between these bodies $(t_1 > t_2)$ there occurs the phenomenon of heat exchange, characterised by the presence of a heat flux.

The amount of heat passing through the given surface per unit time is called the heat flux and is designated $\frac{\#}{i}$kcal/hour. The heat flux passing through a unit of surface is called the heat flux density and is designated q kcal/m/hour.

Heat exchange between fluids (gases or gas and liquid) separated by a solid wall is called heat transfer through a wall (Fig. 2). If $t_1 > t_2$, then the medium on the left in Fig. 2 is called the source and the medium on the right is termed the receiver. There is a flow of heat between these heat exchanging media.

Any physical phenomenon occurs both in space and time. Hence the study of the physical phenomenon can be reduced to study of the spatial-temporal variations in its characteristic values.

From now on all matter will be regarded as homogeneous and isotropic and possessed of identical physical properties in all directions. Mathematical physics introduces the concept of the field of a physical value, by which we mean the totality of instantaneous values at all points on the space under study. For example, the totality of temperatures at all points in a given region is called a temperature field. The mathematical expression of the concept of a field is an equation.
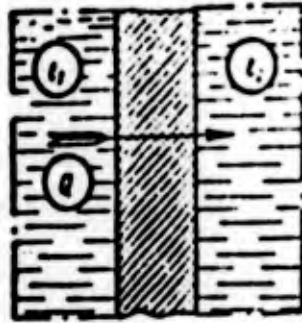
Fig. 2. Conception of
heat transfer
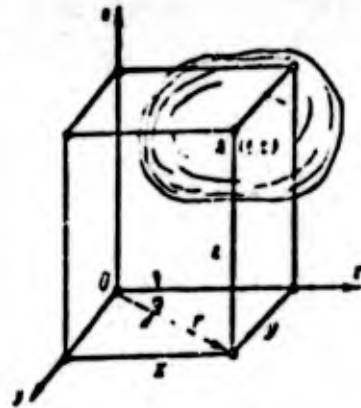
Fig. 3. Conception of
temperature field

The temperature field equation (Fig. 3) in Cartesian coordinates is written in the form

$$t = f(x, y, z, \tau). \qquad (1.1)$$

Here t is the field temperature as a function of the coordinates and time, x, y and z are the coordinates of the given point, and τ is the time.

The temperature t is scalar, hence the temperature field is a scalar field.

This definition of a field is valid as well for vector physical quantities characterised both by direction and value (velocity, acceleration, force). A field of this kind is called a vector field. In certain calculations the temperature field equation can be conveniently expressed in a cylindrical system of coordinates (Fig. 3).

For the system Eq. (1.1) is written in the form

$$t = f(r, \varphi, z, \tau). \qquad (1.2)$$

Here t is the temperature, r is the radius vector, φ is the angle of deflection of the radius vector from the selected initial direction, z is the coordinate axis perpendicular to the plane of variation of the radius vector, and τ is the time.

A shift from any point in the temperature field in an arbitrary direction over an infinitely small distance is characterized by a change in temperature. If the infinitely small shifts of any point in the field correspond to infinitely small

changes in temperature, the temperature field is termed continuous. In this case

the derivative of the temperature in any direction is a finite value. If the

infinitely small shifts, be it only from ~~one~~ point in the field, correspond to

a finitely or infinitely large variation in temperature, the field is termed

discontinuous.

The following arguments will only refer to continuous temperature fields.

The temperature fields described by Eq. (1.1) are termed three-dimensional,

since the temperature t varies along each of the three axes of the coordinates x, y

and z. In practice, we encounter cases of two-dimensional and uni-dimensional fields.

For these . the derivatives of the temperature along the directions in which

the temperature does not vary disappear.

For example, an equation of the type

$$t = f(x, y, z) \tag{1.3}$$

is an equation for a non-stationary $\left(\frac{\partial t}{\partial \tau} \neq 0\right)$ two-dimensional $\left(\frac{\partial t}{\partial z} = 0\right)$ temperature field.

An equation of the type

$$t = \varphi(x) \tag{1.4}$$

is an equation for a steady state $\left(\frac{\partial t}{\partial \tau} = 0\right)$ uni-dimensional $\left(\frac{\partial t}{\partial y} = 0 \text{ and } \frac{\partial t}{\partial z} = 0\right)$ temperature field.

The heat conditions described by the variation in temperature in time

- 8 -

are termed either non-stationary or non-steady-state. For such heat conditions there is a non-steady state heat flux varying with time. Non-stationary heat conditions have non-stationary temperature fields. Equations (1.1) or (1.2) for a non-steady-state temperature field are the most general expression for the temperature field when the temperatures are different points on the body and vary with time. Consequently non-steady-state heat conditions, on the one hand, are due to variation in temperature woth time, and, on the other, to the difference in the amount of heat supplied and removed.

Heat conditions described by non-variation of temperature with time are termed stationary or steady state. These heat conditions have a stationary or steady-state heat flux which does not vary with time. Stationary heat conditions have stationary temperature fields. Under steady-state conditions the heat flux in any body is equal to the heat flux emerging from the body through the corresponding surface.

The equation for a steady-state temperature field is an equation of the type

$$t = \varphi(x, y, z),\tag{1.5}$$

which is derived on the basis of the invariability of a temperature with time

$$\frac{\partial t}{\partial \tau} = 0.\tag{1.6}$$

- 9 -

Consequently, steady-state heat conditions are conditioned by the invariability of the temperature with time, which in its turn is determined by the equality of the amount of heat removed and supplied.

In accordance with the classification of heat conditions and the temperature fields corresponding to them, we distinguish two cases of heat transfer: non-steady-state and steady-state.

Isothermal surface. Surfaces representing a geometric site of points with equal temperature are called isothermal surfaces or level surfaces. Let us assume we have the body shown in Fig. 4. If there is no heat source, all the points on this body will be at the same temperature:

$$t_A = t_B = t_C = \text{const};$$

If a certain amount of heat is imparted to it, there will be a Heat flux distorting the original pattern of equal distribution of temperature over the body, so that

$$t_A > t_B > t_C.$$

By joining all the points on the body which have the same temperature, we get an isothermal surface. We can make as many isothermal surfaces as we want. The totality of isothermal surfaces uniquely defines the temperature field in time at a given moment.

The very definition of an isothermal surface implies two of its properties, to wit:

- 10 -

Fig. 4. Definition of an isothermal surface

1. Isothermal surfaces cannot intersect with each other, since the line

of intersection would not be characterized by one, but by several temperatures.

Such lines cannot exist in the temperature field.

2. Isothermal surfaces cannot break off inside the field - they are

either closed or else they break off at the outside boundaries of the body.

When isothermal surfaces intersect with a plane, we find traces on the

latter in the form of families of isotherms. Fig. 5 shows isotherms resulting from

intersection of isothermal surfaces and the plane xOy. The isotherms differ one

from the other by the value $\triangle$ t.

Temperature gradient. Let us consider two extremely close isothermal

surfaces with temperatures $\underline{t}$ and $\underline{t}+ \Delta \underline{t}$ (Fig. 6).

It follows from this second law of thermodynamics and the property of the

isometric surface as a geometrical site of points with the same temperature that the

heat flux cannot be propagated along an isothermal surface. By shifting from point $\underline{A}$

in any direction $\underline{S}$ intersecting the isotherms we find a change in temperature. Here

the greatest change in $\underline{t}$ per unit of length is observed . when shifting along the

direction of the normal $\underline{n}$ to the isothermal surface.

The temperature gradient is the limit of the ratio $\left(\frac{\Delta t}{\Delta n}\right)$ when isothermal

- 11 -
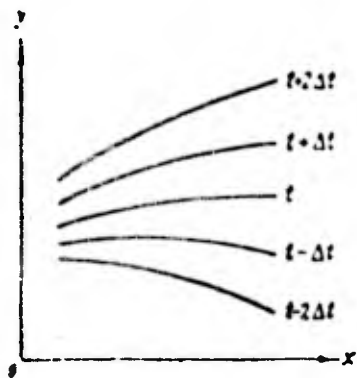
Fig. 5. Conception of a
level surface
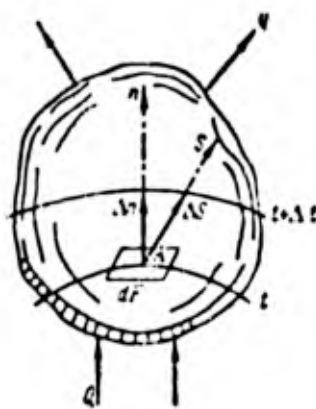
Fig. 6. The Fourier
hypothesis

surfaces come together to an infinite extent and $\Delta_n \rightarrow 0$.

Thus, according to the definition,

$$\operatorname{grad} t = \lim_{\Delta n \to 0} \left[\frac{\Delta t}{\Delta n} \right] = \frac{\partial t}{\partial n} \quad \mathit{град. \, \varkappa.} \tag{1.7}$$

The temperature gradient is a vector directed along the normal to

the isothermal surface at $\underline{A}$. As the positive direction on the gradient we take

the direction of temperature increase. The gradient is different for different

points on the same level surface; it is greater where ever the distance Δn between

the surfaces of the level is less.

The temperature gradient determines the temperature increment per unit of

length of the normal to the isothermal surface, and is a measure of the intensity

of the variation in temperature.

Temperature waves. In a number of practical cases a non-steady-state

temperature regime is very often brought about by periodic temperature effects on a

body (walls of cylinders in internal combustion engines and boilers, walls of

combustion chambers in jet engines are subjected to periodic heat effects through

the cyclic nature of the processes involved). Periodic heat effects on a building

are due to diurnal t variation in the outside temperature and the effect of solar

radiation. In industrual plants the periodic nature of the heat processes is often

- 12 -

associated with corresponding daily interruptions in operations and with the very

nature of the manufacturing process. Thus, a whole number of cases of heat exchange

involve the presence of periodic heat phenomena.

The effect of these phenomena on a body cause periodic temperature changes

in it. These periodic changes are called temperature waves.

References

1. Kutateladze S. S., Fundamentals of theory of heat exchange, ch. 1, 2 and 7. Mashgiz, 1957.

2. " and others. Liquid-metal heat-transfer agents, Atomizdat, 1958.

3. ? " . Reference book on heat exchange, ch. 1 and 2, Gosenergoizdat, 1959.

4. Mikheyev M. A. Fundamentals of heat transfer, ch. 1. Gosenergoizdat, 1956.

5. Predvoditelev A. S., Some invariant quantities in theory of thermal conductivity and viscosity of liquid, "J. Phys. Chem.", vol. XXII, issue 3, 1948.

6. Romanovskiy P. I. Fourier series. Field theory, analytical and special functions. Laplace transforms, ch. 5, Gostekhizdat, 1957.

7. Shirokov M. F. Physical fundamentals of gas-dynamics, ch. 4 and 8. Fizmat-izdat, 1958.

8. Shirokov M. F. Viscosity of liquids and transfer of momentum by waves, Acad. Sci. Press, 1944.

9. Shorin S. N. Heat transfer, Ch. 1, 2, 3 and 4. Stroyizdat, 1952.

10. Greber G and others. Fundamentals of heat exchange, For. Lit. Press, 1958.

THERMAL CONDUCTIVITY UNDER STEADY-STATE CONDITIONS

Section 3. *The* A fundamental law of thermal conductivity in the general form.

The A quantitative evaluation of the heat passing through the given body

as a result of thermal conductivity is based on a hypothesis put forward in 1822 by

the French scientist Fourier. This hypothesis states that the _elementary_

quantity of heat dQ passing through an element of the isothermal surface dF in the

time interval $d\tau$ is proportional to the temperature gradient

$$dQ = -\lambda \frac{\partial t}{\partial n} dF\, d\tau. \tag{2.1}$$

The proportionality factor λ in Eq. (2.1) is called the thermal conductivity.

The minus sign on the right hand side of the equation is there because

the temperature decreases in the direction of propagation of the heat, as a result of

which the temperature gradient $\frac{\partial t}{\partial n}$ is a negative value, though the amount of heat dQ

is considered positive. Equation (2.1) is called the _fundamental law of

thermal conductivity, or Fourier's law. If we refer the amount of heat transferred

by thermal conductivity to a unit of isothermal surface and a unit of time, we

get the heat flux density

$$\bar{q} = \frac{dQ}{dF\, d\tau} \quad \text{kcal/m}^2 \text{ hr.} \tag{2.2}$$

The vector

$$\bar{q} = -\lambda \frac{\partial t}{\partial n} = -\lambda \operatorname{grad} t.$$ (2.3)

known as the heat flux, is normal to the level surface and directed towards the decrease in temperature.

Consequently, the vectors $\bar{q}$ and grad $\underline{t}$ lie along a straight line, but are directed in different directions (Fig. 7).

The projections of the vector $\bar{q}$ on the axis of the coordinates $\underline{x}$, $\underline{y}$, $\underline{z}$ are equal, respectively, to

$$\left. \begin{array}{l} q_x = -\lambda \dfrac{\partial t}{\partial x} \\[2mm] q_y = -\lambda \dfrac{\partial t}{\partial y} \\[2mm] q_z = -\lambda \dfrac{\partial t}{\partial z} . \end{array} \right\}$$ (2.4)

If we plot the elements of the normals $\triangle \underline{n}$ to the isometric surfaces at each point on the isotropic body (that is to say, a body possessing identical properties in all directions), the totality of these normals gives us a family of curves called the heat flux lines. They indicate the direction of the heat flux.

The tangents to the stream lines show the lines of action of the vectors $\bar{q}$ and grad $\underline{t}$ directed in diametrically opposite directions (Fig. 7).

Section 4. Thermal conductivity.

Let us determine the thermal conductivity on the basis of the basic Eq. (2.1).

$$\lambda = \frac{dQ}{\dfrac{\partial t}{\partial n} dF \, d\tau},$$ (2.5)

- 16 -
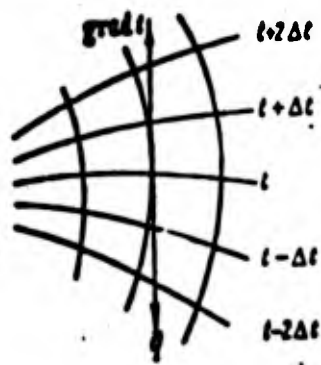
Fig. 7. Thermal streamlines

after which we will find its dimensionality.

$$\lambda = \left[\frac{dQ}{\frac{\partial t}{\partial n} dF \, \partial \tau} \right] \text{kcal} \bigg/ \frac{\text{deg.}}{u} \cdot u^2 \cdot \text{hr} = \text{kcal} / u \cdot \text{hr} \cdot \text{deg.}$$

Numerically the thermal conductivity λ is equal to the amount of heat passing through a unit of isometric surface per unit of time, on condition that the temperature gradient at the point under consideration is equal to unity.

The thermal conductivity ~~is one of~~ of a substance is one of the physical characteristics it indicates the ~~xxx~~ ability of the given substance to conduct heat through thermal conductivity. The quantity λ differs for different substances. The best conductor of heat is metal and the worst is gas.

Different bodies possess very different thermal conductivities in accordance with the structure of the material and the mechanism of the propagation of heat. The Thermal conductivity of a material is determined by means of special experiments on the appropriate laboratory apparatus, which are contingent upon the type of material and its aggregate state. Figs. 8 - 10 show the dependence on temperature of the thermal conductivity of certain metals and alloys /4, 9/.

As shown by experience, in the majority of materials the dependence of thermal conductivity on temperature t can be expressed approximately in the form of a linear function

$$\lambda = \lambda_0 (1 + bt),$$

- 17 -

Fig. 10. Thermal conductivity of aluminum alloys: 1) alusil with 20% Si; 2) silumin with 12.5% Si; 3) duralumin: 4% Cu, 0.5% Mg; 4) alpax with 13% Si; 5) alloy with 15% Cu; 6) alloy with 10% Vn and 2% Cu; 7) cast with 8% Cu; 8) thermally worked alloy with 8% Mg; 9) cast with 8% Mg; 10) cast with 2% Mg; 11) thermally worked alloy with 14% Mg.

Fig. 9. Thermal conductivity of different alloys: 1) brass with 18% zinc; 2) brass with 30% zinc; 3) brass with 12% zinc; 4) alloy of chromium, nickel and iron; 5) bronze; 85% Cu, 7% Vn, 6% Sn; 0.6% Ni; 6) managanese bronze: 57% Cu, 37% Vn, 2.3% Mn; 7) instrument bronze; 85% Cu, 9% Sn, 4% Zn; 8) alloy of lead and zinc; 92% SN, 8% Vn; 9) phosphorus bronze; 88% Cu, 11% Sn, 4% P; 10) white metal; 88% Sn, 8% Sb, 4% Cu; 11) constantan; 60% Cu, 40% Ni; 12) metal; 67% Ni, 29% Cu; 13) manganin; 84% Cu, 1.2% Mn and 4% Ni; 14) nickel steel with 30% Ni; 15) liquid alloy of lead and zinc; 92% Sn, 8% Zn.

Fig. 8. Thermal conductivity of metal: 1) pure copper; 2) copper - 99.9%; 3) aluminum 99.7%; 4) aluminum 99.0%; 5) pure manganese; 6) manganese 99.6%; 7) zinc 99.8%; 8) pure platinum; 9) 99% nickel; 10) 99.2% nickel; 11) iron - 99.2%; 12) pure industrial lead.

in which λ_0 is the thermal conductivity at 0°C, and b is a constant determined experimentally.

The dependence of λ on t may be an increasing or decreasing function in different materials. Most heat-insulating and building materials are of a porous nature. The complex process of the propagation of heat through these bodies is evaluated by a mean thermal conductivity, the increase in which with temperature is explained both by the increase in λ for gases filling the pores, as well as a strong increase in radiant heat-exchange between the surfaces of the material through the gas-filled pores separating them. The relationship $\lambda = f(t)$ is very often disregarded in engineering calculations and the problem is worked out on the basis of certain mean values of the thermal conductivity λ_m.

Table 1 shows λ_m for certain materials

Thermal conductivity of gases. According to the kinetic theory of gases, the transfer of heat through gases by means of thermal conductivity is brought about by a molecular transfer of energy during the collison between molecules. The coefficient of molecular transfer in a gas is determined by the following relationship for the thermal diffusivity /9/.

$$a = \frac{\lambda}{c_p \gamma} = \frac{1}{3} w_m l_m.$$

- 18 -

Thermal conductivity λ and thermal diffusivity $\underline{a}$ of different materials

№	Material	λ kcal/м·hr·deg
1	Heat insulation	0,02—0,5
2	Building materials	0,8—3
3	Metals and their alloys	10—110

Material (at 20° C)	a м²/hr	Material (at 20 C)	a м²/hr
Copper	0,37	Glass	0,00222
Aluminum	0,311	Brick	0,00118
Iron	0,0555	Wood	0,0005

This formula can be used to determine the thermal conductivity of gases

$$\lambda = \frac{1}{3} v_m l_m c_v \gamma.$$

Here v_m is the mean velocity of motion of the gas molecules in m/sec or m/hour;

l_m is the mean free path length of the gas molecules in between collisions

in m;

c_v is the thermal capacity of the gas at $V = $ const in kcal/kg·deg;

γ is the specific gravity of the gas in kg/m³.

For ideal gases $l_m \gamma = $ const, since γ increases and l_m decreases to an

equal extent when the pressure is increased. Hence the thermal conductivity of gases

hardly *changes* with variation in the pressure. But for very small pressures, when

the free path length of the molecules begins to exceed the dimensions of the vessel

containing the gas, the thermal conductivity of a highly rarefied gas ($p < 10^{-4}$ atm)

becomes a strong function of pressure and declines as the pressure falls.

At very high gas pressures, the forces of intermolecular interaction

begin to have a marked effect, and the thermal conductivity increases with the

pressure.

The temperature of a gas affects the mean velocity of motion of the

molecules v_m and the thermal capacity c_v , as a result of which the thermal

conductivity of gases increases as the temperature rises.

Fig. 11 shows data for the thermal conductivity of different gases obtained by N. B. Vargastik at the All-Union Heat Engineering Institute. Helium and hydrogen are marked by a high thermal conductivity (Fig. 12), which is greater than in other gases by a factor of 5 - 10 /3/.

Fig. 13 shows data for λ for superheated steam as a function of its pressure and temperature.

Thermal conductivity of liquids. The variation in the thermal conductivity of different liquids with temperature is shown in Figs. 14 and 15. For organic liquids, with the exception of glycerine, the thermal conductivity decreases somewhat as the temperature rises. The thermal conductivity of water increases with temperature and on the saturation line reaches a maximum value $\lambda = 0.59$ kcal/m · hour · deg at $t \approx 120°$. If the temperature is raised further, λ declines.

Fig. 16 shows the dependence of thermal conductivity of liquid metals and their alloys on temperature, determined by the method of consecutive steady-states /2/. Variation in thermal conductivity of liquids with their temperature may be explained by representing the mechanism of the propagation of heat in drop liquids as the transfer of energy through disorderly elastic oscillations. This representation

- 20 -
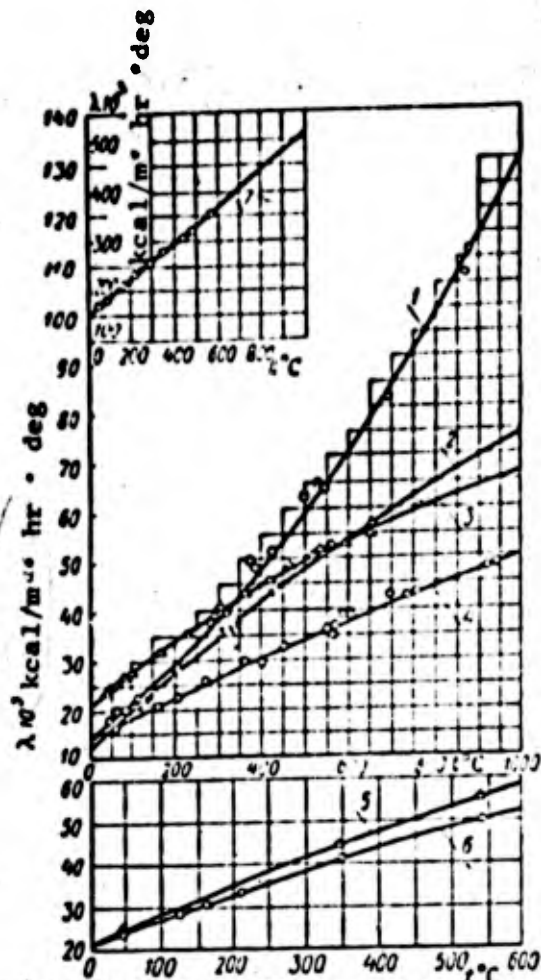
Fig. 11. Thermal conductivity of different gases (according to Vagraftik): 1) water vapor; 2) carbon dioxide; 3) air; 4) argon; 5) oxygen; 6) nitrogen; 7) hydrogen.
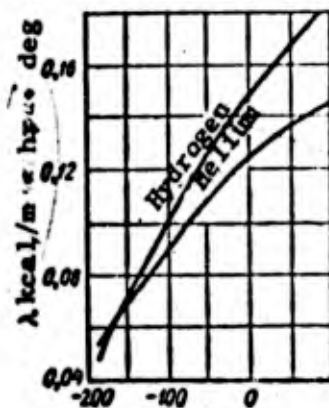
Fig. 12. Coefficient of thermal conductivity of helium and hydrogen (9).

- 20a -
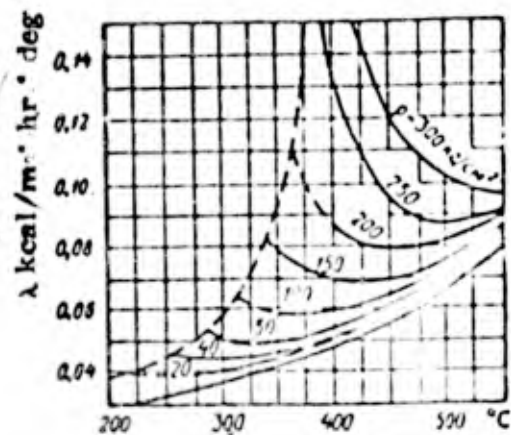
Fig. 13. Thermal conductivity of superheated
steam according to Timrot (broken line shows
curves for extrapolated experimental values).
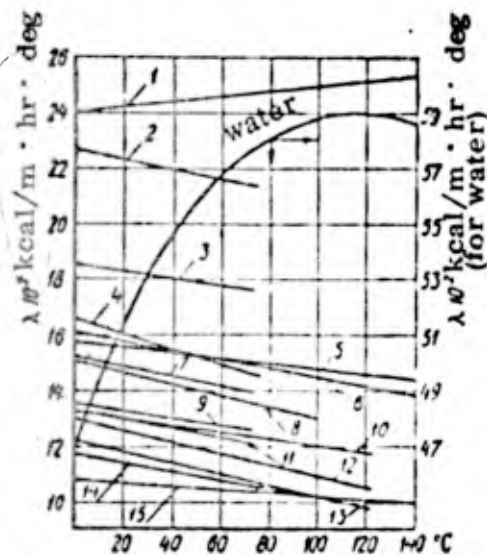
Fig. 14. Thermal conductivity of different fluids (according
to Vagraftik): 1) anhydrous glycerine; 2) formic acid;
3) methyl alcohol; 4) ethyl alcohol; 5) castor oil; 6) anyline;
7) acetic acid; 8) acetone; 9) butyl alcohol; 10) nitro-benzene;
11) isopropyl alcohol; 12) benzene; 13) toluene; 14) xylene;
15) vaseline oil.
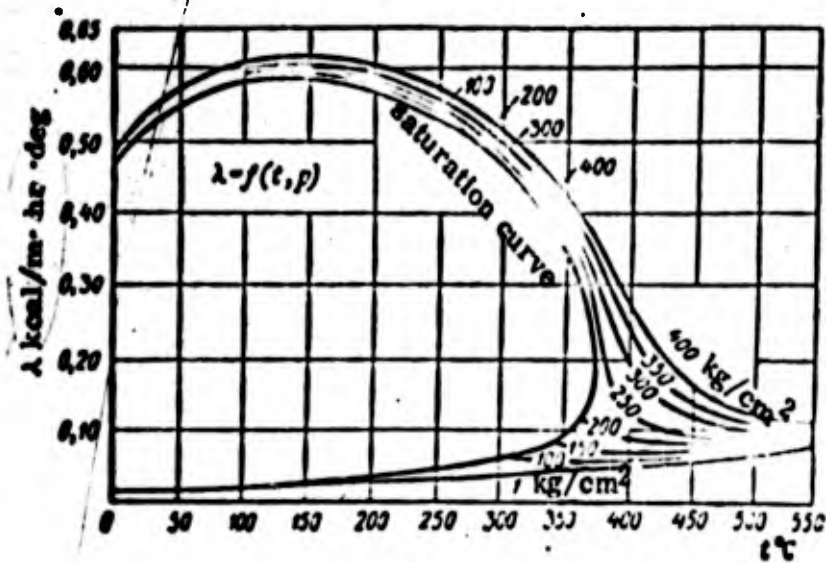
Fig. 15. Thermal conductivity of water and steam (according to Timrot and Vagraftik).

Fig. 16. Variation in thermal conductivity of liquid metals and alloys with temperature, determined by consecutive steady states:

1 – Na (mp= 97.3°C, b.p. = 878°C); 2 - Li (m.p. = 186°C, b.p. = 1317°C); 3 - K (m.p. = 63.7°C, b.p. = 760°C); 4 - Sn (m.p. 231.9°C, b.p. = 2270°C); 5 - Na-K alloy (25%Na + 75% K) (m.p. = -11°C, b.p. = 784°C); 6 - Bi (m.p. = 271°C, b.p. = 1490°C); 7 - Pb-   (m.p. = 327.4°C, b.p. = 1740°C); 8 - Pb-Bi alloy (44.5% Pb + 55.5% Bi) (m.p. = 123.5°C, b.p. = 1670°C); 9 - Hg (m.p. = -38°C, b.p. = 357°C).

- 20c -

suggested by M. F. Shirokov, /7, 8/, and the theoretical premises of A.S. Predvoditelev

/5/ were used by Vargaftik а to describe the experimental data on thermal

conductivity ~for~ different liquids, and in most cases they were well confirmed. These

premises have suggested the following formula for the thermal conductivity of

liquids

$$\lambda = A \frac{c_p \gamma^{\frac{4}{3}}}{\mu^{\frac{1}{3}}},$$

in which c_p is the thermal conductivity of a liquid at $\rho = \text{const}$;

γ is the specific gravity of the liquid; and

μ is the molecular weight.

The coefficient A is proportional to the rate of propagation of elastic

waves ~through~ the liquid and is not a function of the nature of the liquid. As the

temperature varies, the coefficient A changes according to the relationship

$Ac_p = \text{const.}$ For $t = 0^\circ$, $A = 3.58 \cdot 10^{-3}$.

In view of the fact that the molecules of a number of liquids are inclined

to association, their molecular weight may vary. The data for λ for liquids

can therefore be supplemented with data for the association coefficient of molecules

in a liquid.

More detailed data on thermal conductivity of different materials are

given in the textbooks "Fundamentals of Heat Transfer" by M. A. Mikheyev /4/ and

"Heat Transfer" by F.N. Shorin /2/.

Section 5. Derivation of Basic Differential Thermal Conductivity Equation

When solving absolutely all thermal conductivity problems both under steady-state and non-steady-state conditions, it is essential to know the temperature field.

But to determine the type of function describing the spatial-temporal temperature distribution throughout the field is not possible by the general laws of physics.

Hence in order to find the temperature distribution in a body due to the effect of thermal conductivity, we have to use the following method. The phenomenon is first studied in an arbitrary singled-out element of the body (elementary parallelepiped with sides dx, dy and dz, over an infinitely small interval of time $d\tau$, rather than for the whole of the body under consideration and over a finite interval of time. When deriving the differential thermal-conductivity equation, let us consider that the physical parameters λ (thermal conductivity), c (thermal capacity) and γ (specific gravity) are not functions of the coordinates or time within the entire field.

Let us single out from a space occupied by a homogeneous and isotropic body (Fig. 17) an elementary parallelepiped with the edges dx, dy and dz, parallel to the corresponding coordinate axes. Let us compile the heat balance for this elementary

- 22 -
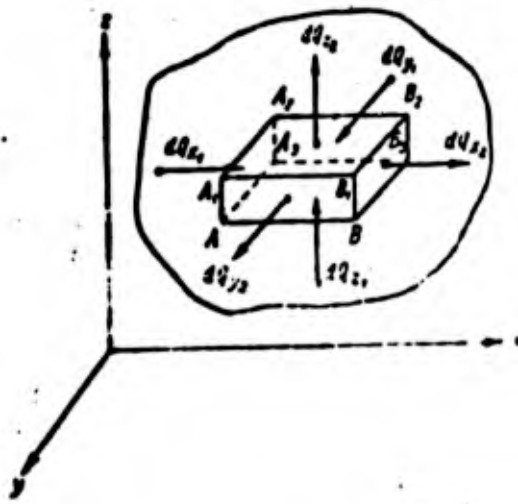
Fig. 17. Derivation of differential thermal conductivity equations

parallelepiped.

To do this, let us calculate the amount of heat supplied to and removed through its faces.

According to the fundamental law of thermal conductivity, the amount of heat dQ_{x_1} entering the parallelepiped through the face A, A_1, A_2, A_3 in the direction of the x-axis is equal to

$$dQ_{x_1} = -\lambda \left(\frac{\partial t}{\partial x}\right)_{x_1} dF\, d\tau;$$

In the given case $dF = dydz$ and

$$dQ_{x_1} = -\lambda \left(\frac{\partial t}{\partial x}\right)_{x_1} dy\, dz\, d\tau.$$

Here $\left(\frac{\partial t}{\partial x}\right)_{x_1}$ is the temperature gradient on the face $AA_1 A_2 A_3$. Correspondingly, the temperature gradient for the outlet section $BB_1 B_2 B_3$ in the direction of the x-axis will be $(\partial t, \partial x)_{x_1}$.

The amount of heat leaving the parallelepiped through the face $BB_1 B_2 B_3$ is then determined by the relationship

$$dQ_{x_2} = -\lambda \left(\frac{\partial t}{\partial x}\right)_{x_2} dy dz d\tau.$$

Subtracting the heat dQ_{x_2} which has left the through the face $BB_1 B_2 B_3$ from the heat dQ which has entered through the face $A A_1 A_2 A_3$ we find the amount of heat left in the elementary parallelepiped over the time $d\tau$

$$dQ_1 = dQ_{x_1} - dQ_{x_2} = -\lambda \left[\left(\frac{\partial t}{\partial x}\right)_{x_1} - \left(\frac{\partial t}{\partial x}\right)_{x_2}\right] dy dz d\tau.$$

- 23 -

The temperature gradient $\dfrac{\partial t}{\partial x}$ represents a continuous function of $\underline{x}$, hence the difference in the partial values of the gradient $\left[\left(\dfrac{\partial t}{\partial x}\right)_{x_2} - \left(\dfrac{\partial t}{\partial x}\right)_{x_1}\right]$ can be decomposed into a Taylor series

$$\left(\frac{\partial t}{\partial x}\right)_{x_2} - \left(\frac{\partial t}{\partial x}\right)_{x_1} = (x_2 - x_1)\frac{\partial^2 t}{\partial x^2} + \frac{(x_2 - x_1)^2}{2}\frac{\partial^3 t}{\partial x^3} + \cdots$$

Since $x_2 - x_1 = dx$, then by discarding infinitely small values of the higher order we get

$$\left(\frac{\partial t}{\partial x}\right)_{x_2} - \left(\frac{\partial t}{\partial x}\right)_{x_1} = \frac{\partial^2 t}{\partial x^2}dx,$$

from which

$$dQ_x = \lambda \frac{\partial^2 t}{\partial x^2}dx\,dy\,dz\,d\tau. \tag{2.6}$$

The result obtained relates to the projection of the heat flux onto the x-axis. In similar fashion we get for the y- and z-axes

$$dQ_y = \lambda \frac{\partial^2 t}{\partial y^2}dx\,dy\,dz\,d\tau \tag{2.7}$$

and

$$dQ_z = \lambda \frac{\partial^2 t}{\partial z^2}dx\,dy\,dz\,d\tau. \tag{2.8}$$

The total amount of heat accumulated in the elementary volume of the body under consideration is made up of the sum of the values determined by Eqs. (2.6), (2.7) and (2.8).

$$dQ = dQ_x + dQ_y + dQ_z$$

or

$$dQ = \lambda \left(\frac{\partial^2 t}{\partial x^2} + \frac{\partial^2 t}{\partial y^2} + \frac{\partial^2 t}{\partial z^2} \right) dx dy dz d\tau. \qquad (2.9)$$

The product $dxdydz$ is the volume of the elementary parallelepiped dV.

$$dV = dxdydz.$$

The sum of the second partial derivatives of any function in a mathematical

analysis is termed **a** Laplace operator and is designated in the following way

$$\frac{\partial^2 t}{\partial x^2} + \frac{\partial^2 t}{\partial y^2} + \frac{\partial^2 t}{\partial z^2} = \nabla^2 t. \qquad (2.10)$$

Consequently, Eq. (2.9) can be finally written in the form

$$dQ = \lambda \nabla^2 t \, dV \, d\tau. \qquad (2.11)$$

In accordance with the law of conservation of energy, the amount of

heat dQ accumulated in the elementary volume dV causes in it a corresponding rise

in temperature (heating up of the body).

The temperature of a solid body is in the general case a function of four

variables x, y, z, and τ. In a solid body, however, the spatial coordinates of

the field points x, y and z are not linked with the time coordinates. Hence, when

considering thermal conductivity in a solid body, variation in temperature over an

infinitely small interval of time $d\tau$ is expressed in the form of a partial

differential $\frac{\partial t}{\partial \tau} d\tau$.

Thus, we arrive at the following conventional heat equation.

- 25 -

$$dQ = c\gamma dV \frac{\partial t}{\partial \tau} d\tau. \qquad (2.12)$$

Here γ is the specific gravity in kg/m^3; c is the thermal capacity in kcal/kg·deg. Since the left-hand sides of Eqs. (2.11) and (2.12) are equal, their right-hand sides are also equal

$$c\gamma dV \frac{\partial t}{\partial \tau} d\tau = \lambda \nabla^2 t\, dV\, d\tau;$$

and this, designating $\lambda / c\gamma = a$, gives us

$$\frac{\partial t}{\partial \tau} = a\nabla^2 t. \qquad (2.13)$$

Equation (2.13) is called the basic differential thermal conductivity equation. It establishes the relationship between the temporal and spatial variation in temperature at any point in the field.

The value

$$a = \frac{\lambda}{c\gamma} \qquad (2.14)$$

is called the thermal diffusivity of the body.

Its dimensionality is found by simple substitution of the dimensionalities of the physical parameters making up the right hand side of Eq. (2.14).

$$a = \frac{\lambda}{c\gamma} = kcal \cdot kg \cdot m^3 \cdot deg/m \cdot hour \cdot kcal \cdot kg \cdot deg = m^2/hour.$$

Thermal diffusivity is a physical constant. Its value for different materials is shown in Table 1.

The physical meaning of thermal diffusivity as a proportionality factor

between the spatial and temporal change in temperature is that it is a measure of

the rate of *the balancing* of temperatures at different points in a given temperature field.

The greater the value a, the quicker all the points in the field will attain the

same temperature.

Consequently, whereas the thermal conductivity λ describes the heat-

conducting ability of bodies, thermal diffusivity a describes the heat-inertial

properties of these bodies. Equation (2.13) relates to a case of non-steady-state

conditions.

For a steady-state heat condition

$$\frac{\partial t}{\partial z} = 0,$$

and Eq. (2.13) can be rewritten in the form $\nabla^2 t = 0$ or

$$\frac{\partial^2 t}{\partial x^2} + \frac{\partial^2 t}{\partial y^2} + \frac{\partial^2 t}{\partial z^2} = 0. \tag{2.15}$$

In engineering it is often necessary to study heat exchange and temperature

distribution in cylindrical bodies (flat discs, round rods, and so on). In these

cases it is most convenient to study the basic thermal-conductivity equation in

a cylindrical system of coordinates rather than in cartesian coordinates. The method

of translating the Laplace operator from one coordinate system to another is set forth

in Romanovskiy's book /5/.

Let us write down again the expression for the Laplace operator in rectangular (cartesian) systems

$$\frac{\partial^2 t}{\partial x^2} + \frac{\partial^2 t}{\partial y^2} + \frac{\partial^2 t}{\partial z^2} = \nabla^2 t.$$

This expression relates to a certain moment in time.

In this case thet temperature $\underline{t}$ is a function of three arguments - the coordinates x, y and z,   i.e.,

$$t = f(x, y, z).$$

In the cylindrical system the coordinates are:

$\underline{r}$ is the radius vector of the point, φ is the polar angle, and $\underline{c}$ is the coordinate of the point (distance from the main plane) - Fig. 18.

The cartesian coordinates x, y and z can be expressed in terms of cylindrical coordinates (Fig. 19) using the following expressions

$$x = r\cos\varphi, \quad y = r\sin\varphi, \quad z = z. \tag{2.16}$$

Substituting x and y as functions of $\underline{r}$ and φ into the expression for temperature, we get

$$t = t[x(r, \varphi), y(r, \varphi), z] = t_1(r, \varphi, z).$$

Thus, the temperature may be represented as a function of cylindrical coordinates.
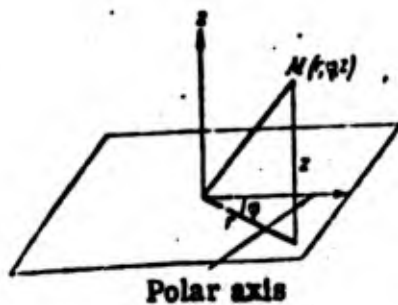
Fig. 18. Diagram of cylindrical coordinates of points
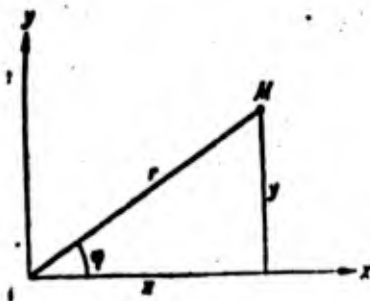
Fig. 19. Relationship between rectangular and cylindrical coordinate systems

- Let us introduce an expression for the Laplace operator in cylindrical coordinates.

Since the coordinate z both in cartesian and cylindrical coordinates is the same, to obtain the Laplace operator we need only find expressions for the partial derivatives $\frac{\partial^2 t}{\partial x^2}$ and $\frac{\partial^2 t}{\partial y^2}$ in cylindrical coordinates.

Compiling expressions for the first and second derivatives for the function $\underline{t} = \underline{t}_1(r, \varphi, \mathcal{L})$ and taking it into account that

$$\frac{\partial z}{\partial x} = 0; \ \frac{\partial z}{\partial y} = 0; \ \frac{\partial r}{\partial z} = 0 \ \text{и} \ \frac{\partial \varphi}{\partial z} = 0,$$

we get

$$\frac{\partial^2 t}{\partial x^2} + \frac{\partial^2 t}{\partial y^2} = \frac{\partial^2 t}{\partial r^2} + \frac{1}{r^2}\frac{\partial^2 t}{\partial \varphi^2} + \frac{1}{r}\frac{\partial t}{\partial r}.$$

Hence the Laplace operator in cylindrical coordinates is expressed as

$$\nabla^2 t = \frac{\partial^2 t}{\partial r^2} + \frac{1}{r^2}\frac{\partial^2 t}{\partial \varphi^2} + \frac{1}{r}\frac{\partial t}{\partial r} + \frac{\partial^2 t}{\partial z^2}, \tag{2.17}$$

and

$$t = t_1(r, \varphi, z).$$

Section 6. Marginal conditions. Theoretical heat-transfer equation.

The basic differential thermal conductivity equation describes the spatial-temporal variation in temperature at any point in the field by uniting absolutely all thermal-conductivity phenomena, irrespective of the geometrical shape of the body, its physical properties or conditions under which it interacts with the

surrounding medium.

This differential equation describes a class of phenomena of thermal conductivity. In order to single out one phenomenon from the whole class, we have to supplement the differential equations with additional conditions, for the specific case in point.

These additional partial data which describe the single phenomenon under consideration are termed the marginal conditions or uniqueness conditions.

The following may be uniqueness conditions: geometrical conditions describing the shape and size of the body in which the heat exchange takes place; physical conditions describing the physical properties of the body; temporal conditions describing the occurrence of the process in time; or boundary conditions describing the features of the process on the boundaries of the body.

The uniqueness conditions enable us to single out a specific process and define it uniquely, i.e., give a full mathematical description of it. The marginal temporal conditions is defined by setting the temperature distribution in the body under consideration at any moment in time preceding the moment under consideration. The marginal temporal condition is usually defined by setting the temperature distribution throughout the body for an initial moment of time $\tau = 0$. The temperature field equation for this case is written in the form

$$t = \varphi(x, y, z).$$

The marginal boundary conditions are related to the interaction of the body under consideration and the surrounding medium (for example, the temperature distribution of the body on the surface at any moment in time). The boundary marginal conditions in their turn may be set in three ways:

1. The first-order boundary condition is set by the temperature distribution along the surface of the body at any moment in time.

2. The second-order boundary condition is set by the heat flux at each point on the surface of the body at each moment of time.

3. The third-order boundary condition consists in setting the temperature of the medium surrounding the body, and the law of heat transfer between the surfaces and surrounding medium.

This third method of setting the boundary conditions directly touches on the problem of heat exchange between a solid body and a medium *flowing past* it, the process which is termed heat transfer.

The intensity of the heat exchange in the given case is determined both by the temperature difference between the heat exchanging bodies as well as the heat resistance which is created in the path of the heat flux *by*

the physical-mechanical nature of the phenomena occurring on the boundary between

- 31 -

the solid body and the medium _surrounding_ it. Difficulties of a mathematical nature arising in formulation of the analytical theory of heat transfer force us to select a simpler mathematical formula and _shift_ the _bulk_ of the study to the region of experimental investigation.

This simplified mathematical law of heat transfer was first put forward by Newton. According to Newton's law, the amount of heat dQ supplied (or received) by a [element surface] of a solid body dF in the time $d\tau$ is proportional to the temperature difference of the surface t_w and the surrounding medium t, the value dF and the time interval $d\tau$.

The corresponding equation can be written in the form

$$dQ = \alpha (t_w - t) dF \, d\tau. \tag{2.18}$$

In Eq. (2.18) the proportionality factor is termed the heat-transfer coefficient it is equal to

$$\alpha = \frac{dQ}{(t_w - t) dF \, d\tau}.$$

Equation (2.18) easily gives us the dimensionality of the heat-transfer coefficient.

$$\alpha = \text{kcal/m}^2 \cdot \text{hour} \cdot \text{deg}$$

The heat-transfer coefficient is numerically equal to the amount of heat supplied or received by the surface element per unit of time at a temperature

difference between the wall and the heat receiving medium equal to 1°.

The heat-transfer coefficient α was regarded by Newton as a constant value. This coefficient takes into account all the features of heat exchange occurring near the boundary between two heat-exchanging bodies, and is a function of a large number of variables, for example: the rate of motion of the medium, the temperatures t_w and t, the position of the body in the stream, the size of the body, the physical parameters (thermal conductivity, viscosity, thermal capacity, etc.).

When using the basic t_i heat-transfer equation in tax practice, we have to make a number of experiments and find the heat-transfer coefficient from the data obtained.

Hence all the difficulties involved in calculating heat transfer, which are due to the abundance of influencing factors, are concentrated in the heat-transfer coefficient a, and the theoretical equations for heat transfer put forward by Newton despite the apparent simplicity, do not in fact offer any particular simplification.

Section 7. Plane wall

Using the basic differential thermal-conductivity equation under steady-state conditions, wex get

$$\nabla^2 t = 0$$

from Eq. (2.15) in a cartesian system of coordinates

$$\frac{\partial^2 t}{\partial x^2} + \frac{\partial^2 t}{\partial y^2} + \frac{\partial^2 t}{\partial z^2} = 0.$$

The plane one-layer wall, in which we are considering thermal conductivity, is assumed to have infinitely greater length and width than its thickness δ (Fig. 20).

On account of the infinite extent of the wall in the directions y and z it may be assumed that the removal of heat from its ends is non-existent and that the heat flux is directed perpendicular to the wall surface. Hence the temperature of the wall only changes along the x-axis, i.e., we have a uni-dimensional, steady-state temperature field, for which

$$\frac{\partial t}{\partial y} = \frac{\partial t}{\partial z} = 0$$

$$\frac{\partial^2 t}{\partial y^2} = \frac{\partial^2 t}{\partial z^2} = 0.$$

The basic thermal conductivity equation (2.15) in this case takes the form

$$\frac{\partial^2 t}{\partial x^2} = 0. \tag{2.19}$$

The temperature distribution through the wall is found by double integration of Eq. (2.19). After the first integration we get $\frac{\partial t}{\partial x} = C_1$. After the second integration we get

$$\bar{t} = C_1 x + C_2. \tag{2.20}$$

Here C_1 and C_2 are the integration constants.

It is clear from Eqs. (2.20) that the temperature distribution in the wall
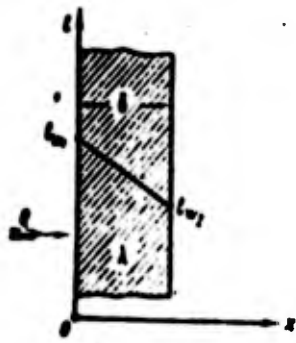
Fig. 20. Plane wall

obeys the law of a straight line. The isothermal surfaces represent planes parallel

to the surfaces of the wall and normal to the x-axis.

In order to determine the integration constants C_1 and C_2 in Eq. (2.20)

let us use the first order boundary conditions, i.e., let us set outselves the

following temperature distribution on the surface of the body for any moment of time:

at $x = 0$, $t = t_{W_1}$

at $x = \delta$, $t = t_{W_2}$

Here t_{W_1} is the temperature of the hotter surface of the wall in °C

and t_{W_2} is the temperature of the other, colder surface of the wall, hence

$$t_{w_1} > t_{w_2}.$$

Equation (2.20), which expresses the temperature distribution, takes the

following form at $x = 0$

$$t_{w_1} = C_2.$$

at $x = \delta$, corresponding, $t_{W_2} = C_1 \delta + t_{W_1}$; hence

$$C_1 = \frac{t_{w_2} - t_{w_1}}{\delta}. \tag{2.21}$$

Substituting C_1 and C_2 into Eq. (2.20), we get

$$t = \frac{t_{w_2} - t_{w_1}}{\delta} x + t_{w_1}. \tag{2.22}$$

Equation (2.22) is the final solution of the problem, since the temperature

distribution described by us satisfies both the differential equation (2.19) as well

- 35 -

as the boundary conditions applied.

In order to determine the amount of heat passing through the element of the wall per unit of time $(d\tau = 1)$, let us use the Fourier law (2.1), according to which

$$dQ = -\lambda \frac{\partial t}{\partial x} \, dF \text{ kcal/hr,}$$

Equations (2.19) and (2.21) give us

consequently,

$$\frac{dt}{dx} = C_1 = \frac{t_{w_1} - t_{w_2}}{\delta},$$

$$dQ = \lambda \frac{t_{w_1} - t_{w_2}}{\delta} \, dF.$$

For the area of surface F in size, we get

$$Q = \frac{\lambda}{\delta}(t_{w_1} - t_{w_2}) \int_F dF$$

or finally

$$Q = \frac{\lambda}{\delta}(t_{w_1} - t_{w_2}) F \text{ kcal/hr.} \tag{2.23}$$

Let us designate

$$t_{w_1} - t_{w_2} = \Delta t_w. \tag{2.24}$$

Eq. (2.23) then can be rewritten in the form

$$Q = \frac{\lambda}{\delta} \Delta t_w F \text{ kcal/hr.} \tag{2.25}$$

The amount of heat passing through a unit of surface of wall per unit of time is determined by the relationship

$$q = \frac{Q}{F} = \frac{\lambda}{\delta}(t_{x_1} - t_{x_2}) \quad \text{kcal/m}^2\text{hr} \tag{2.26}$$

or, taking into account (2.24), ¹

$$q = \frac{\lambda}{\delta} \Delta t_w \quad \text{kcal/m}^2 \text{ hr} \tag{2.27}$$

It is clear from Eqs. (2.23) and (2.26) that the amount of heat passing through the wall is a function of the temperature difference on the surfaces Δt_w. The ratio λ/δ is usually termed the thermal conductivity of the wall, while its reciprocal δ/λ is the thermal resistance.

Section 8. Plane multilayer wall; heat-transfer coefficient, thermal resistance

Let us now consider the thermal conductivity of a plane, multilayered wall (Fig. 21), consisting of $\underline{n}$ closely packed layers. Let us assume that the thermal conductivities for each layer are equal $\lambda_1, \lambda_2, \ldots, \lambda_n,$ and that the thicknesses of the layers are, respectively, $\delta_1, \delta_2, \ldots, \delta_n,$

Since we are investigating a steady-state heat flux, described by the equality of the amount of heat supplied and removed from the body, the flux density entering | per unit of surface | the first layer of an infinitely plane wall | does not change when it passes through the other layers.

We will therefore have

$$q = \frac{\lambda_1}{\delta_1}(t_{w_1} - t_{w_2})$$
$$q = \frac{\lambda_2}{\delta_2}(t_{x_2} - t_{w_3})$$
$$q = \frac{\lambda_3}{\delta_3}(t_{w_3} - t_{x_4})$$
$$\cdots \cdots \cdots \cdots$$
$$q = \frac{\lambda_n}{\delta_n}(t_{w_n} - t_{w_{n+1}}).$$

$$\tag{2.28}$$

- 37 -
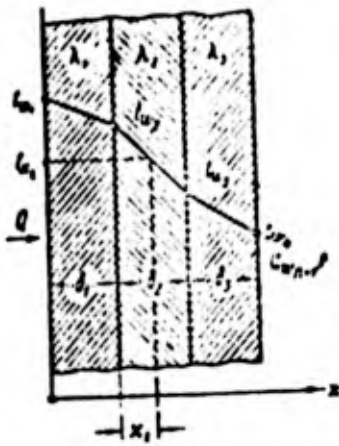
Fig. 21. Multilayer plane wall

Let us write Eq. (2.28) in the following form

$$q\frac{\delta_1}{\lambda_1} = t_{w_1} - t_{w_2}$$
$$q\frac{\delta_2}{\lambda_2} = t_{w_2} - t_{w_3}$$
$$q\frac{\delta_3}{\lambda_3} = t_{w_3} - t_{w_4}$$
$$\cdots\cdots\cdots\cdots$$
$$q\frac{\delta_n}{\lambda_n} = t_{w_n} - t_{w_{n+1}}$$

(2.29)

Adding term by term, we get

$$q\left(\frac{\delta_1}{\lambda_1} + \frac{\delta_2}{\lambda_2} + \frac{\delta_3}{\lambda_3} + \cdots + \frac{\delta_n}{\lambda_n}\right) = t_{w_1} - t_{w_{n+1}}.$$

from which

$$q = \frac{t_{w_1} - t_{w_{n+1}}}{\frac{\delta_1}{\lambda_1} + \frac{\delta_2}{\lambda_2} + \frac{\delta_3}{\lambda_3} + \cdots + \frac{\delta_n}{\lambda_n}}$$

or, what is the same thing,

$$q = \frac{t_{w_1} - t_{w_{n+1}}}{\sum\limits_{i=1}^{n}\frac{\delta_i}{\lambda_i}}.$$

(2.30)

in which $\underline{i}$ is the number of the layer.

Sometimes we introduce for consideration the equivalent heat

$$\sum\limits_{i=1}^{n}\delta_i$$

this dependence, according to /31/, is shown in Fig. 12.   Thus, consideration for

the hydraulic resistances does not vary the nature of the dependence of the main

characteristics

$$q = \frac{\lambda_{eq}}{\sum\limits_{i=1}^{n}\delta_i}(t_{w_1} - t_{w_{n+1}});$$

(2.31)

$$\lambda_{m.e} = \frac{\sum\limits_{i=1}^{n} \delta_i}{\sum\limits_{i=1}^{n} \frac{\delta_i}{\lambda_i}}. \qquad (2.32)$$

The equivalent thermal conductivity enables us to compare the heat-conducting properties of a multilayer wall composed of unlikes materials with a single layer wall made of a homogeneous material. The temperature distribution through a section of a multilayer wall (Fig. 21) is represented by a broken line, the distribution being described inside each layer by the equation

$$t_{x_i} = t_{w_i} - q \frac{x_i}{\lambda_i}. \qquad (2.33)$$

Here $\underline{x}_i$ is the distance inside the $\underline{i}$-th layer from the surface $(\underline{i}-1)$-th layer with the temperature $t_{\underline{w}_i}$.

Let us derive theoretical equations for a plane, multilayer wall, using the third-order boundary conditions which are set by the temperature of the surrounding medium and the heat exchange on the surface of the wall.

Let $\underline{t}_1$ be the temperature of the heat-supplying medium and $\underline{t}_2$ the temperature of the receiving medium. There is a heat flux through the plane multilayer wall between these media.

The heat flux density from the source to the wall according to Newton's law is

$$q = a_1(t_1 - t_{w_1}). \qquad (2.34)$$

Under steady-state conditions this quantity of heat is transferred by

thermal conductivity through all the layers to the opposite wall surface at a

temperature $l_{w_{n+1}}$. According to Eq. (2.30) we can write

$$q = \frac{l_{w_1} - l_{w_{n+1}}}{\sum\limits_{i=1}^{s} \frac{\delta_i}{\lambda_i}}.$$

The same amount of heat is entirely transferred to the receiving medium at

temperature t_{-2}, i.e.,

$$q = a_2 (l_{w_{n+1}} - l_2). \tag{2.35}$$

Let us rewrite Eqs. (2.30), (2.34) and (2.35) in the following way

$$q \; \frac{1}{a_1} = l_1 - l_{w_1},$$

Adding term by term , we get
$$q \sum\limits_{i=1}^{s} \frac{\delta_i}{\lambda_i} = l_w - l_{w_{n+1}},$$

$$q \frac{1}{a_2} = l_{w_{n+1}} - l_2.$$

from which we get
$$q \left(\frac{1}{a_1} + \sum\limits_{i=1}^{s} \frac{\delta_i}{\lambda_i} + \frac{1}{a_2} \right) = l_1 - l_2;$$

$$q = k (l_1 - l_2) \;\; \text{kcal/m}^2 \cdot \text{hr} \tag{2.36}$$

in which

$$k = \frac{1}{\frac{1}{a_1} + \sum\limits_{i=1}^{s} \frac{\delta_i}{\lambda_i} + \frac{1}{a_2}} \;\; \text{kcal/m}^2 \cdot \text{hr} \cdot \text{deg} \tag{2.37}$$

The value $\underline{k}$ is termed the heat-transfer coefficient.

The reciprocal of the heat-transfer coefficient

$$\frac{1}{k} = \frac{1}{a_1} + \sum\limits_{i=1}^{s} \frac{\delta_i}{\lambda_i} + \frac{1}{a_2} \;\; \text{m}^2 \; \text{hr} \cdot \text{deg/kcal} \tag{2.38}$$

is termed the total thermal or thermal resistance of the multilayer wall.

Correspondingly, the values $\frac{1}{\alpha_1}$ and $\frac{1}{\alpha_2}$ are termed the thermal or heat

resistances of heat transfer, while the ~~quantity~~ $\left(\sum_{i=1}^{n} \frac{\delta_i}{\lambda_i} \right)$ is called the thermal resistance

of the multilayer wall, in which $\frac{\delta_i}{\lambda_i}$ is the thermal resistance of a separate layer.

Thus, the total thermal resistance is equal to the sum of all the partial thermal

resistances and, like the heat-transfer coefficient, therefore depends on the

conditions of heat transfer between the surfaces and the surrounding media, on the

thicknesses and thermal conductivities of the individual wall layers.

Section 9. Graphic methods of determining temperatures t_{w_1} and t_{w_2}

of surfaces of a plane wall.

1. Single-layer wall.

Let us assume that the temperatures t_1 and t_2 of the media *flowing over* the

surface of a plane single-layer wall are known. Furthermore, we know the thickness

of the wall δ, the thermal conductivity of the material of which the wall is made

and we are given the heat-transfer coefficients α_1 and α_2 for both wall surfaces.

Under steady-state conditions, given the temperatures of both wall surfaces t_{w_1} and t_{w_2}

the temperature distribution inside the wall can be determined by means of the

following graph.

Along the horizontal in the drawing, on any particular scale, we plot the

- 41 -

thickness of the wall, $\delta = E_1 \ E_2$; the segments $\overbrace{\frac{\lambda}{\alpha_1} = E_1 O_1}$ and $\overbrace{\frac{\lambda}{\alpha_2} = E_2 O_2}$ are plotted on the

same scale on the opposite sides _from points E_1 and E_2)_ we erect the perpendiculars $O_1 A_1$ and $O_2 A_2$ from the

ends of the segments obtained to the horizontal axis (Fig. 22).

The corresponding temperatures t_1 and t_2 of both media are plotted to

scale along these perpendiculars. By joining the points A_1 and A_2, obtained thereby,

by a straight line, we get a line the intersection of which with the surfaces of

the wall gives us the corresponding temperatures of the wall surfaces t_{W_1} and t_{W_2}

in the form of the vertical segments FB_1 and FB_2. Here the temperature distribution

inside the wall is given by the line $B_1 B_2$.

First graphic method. Let us assume that there is heat transfer through

a plane wall possessing the thermal conductivity λ. The temperatures of the

surfaces of this wall are, respectively, t_{W_1} and t_{W_2}, while the temperatures of the

source and receiving media are, respectively, t_1 and t_2 (Fig. 22).

Let us imagine another plane wall with the same thermal conductivity λ,

as in the actual wall we are considering. Let the temperatures of the surfaces of

this imaginary wall be equal, respectively, to the temperatures of both media t_1 and

t_2, and let the amount of heat passing through it be equal to the amount of heat

passing through an actual wall of thickness δ.

Fig. 22. First graphic method

Then, applying Eqs. (2.28) and (2.36) we can determine the thickness Δ of

this imaginary wall

$$q = k(t_1 - t_2) = \frac{\lambda}{\Delta}(t_1 - t_2);$$

from which

$$\Delta = \frac{\lambda}{k} = \lambda\left(\frac{1}{a_1} + \frac{\delta}{\lambda} + \frac{1}{a_2}\right) = \frac{\lambda}{a_1} + \delta + \frac{\lambda}{a_2}.$$

Let us determine the dimensionality of the value λ/α

$$\frac{\lambda}{a} = \frac{\text{kcal}}{\text{m} \cdot \text{hr} \cdot \text{deg}} \Big/ \frac{\text{kcal}}{\text{m}^2 \cdot \text{hr} \cdot \text{deg}} = M.$$

i.e., the values $\frac{\lambda}{\alpha_1}$ and $\frac{\lambda}{\alpha_2}$ possess length. Let us plot them in the form of

segments on the left and right of the thickness of our actual wall δ (Fig. 22);

then, drawing a horizontal line through the points O_1 and O_2 we can plot the

temperatures t_1 and t_2 along the vertical on a certain scale.

The points thus obtained A_1 and A_2 will be joined by a straight line.

Then, according to the similarity of the triangles $A_1 CB_1$ and $A_1 DA_2$ we get

$$\frac{A_1 C}{A_1 D} = \frac{CB_1}{DA_2}$$

or

$$\frac{A_1 C}{t_1 - t_2} = \frac{\dfrac{\lambda}{a_1}}{\left(\dfrac{1}{a_1} + \dfrac{\delta}{\lambda} + \dfrac{1}{a_2}\right)\lambda},$$

from which

$$A_1 C = \frac{t_1 - t_2}{a_1} \cdot \frac{1}{\dfrac{1}{a_1} + \dfrac{\delta}{\lambda} + \dfrac{1}{a_2}} = k\frac{t_1 - t_2}{a_1}.$$

But

$$k(t_1 - t_2) = q.$$

consequently,

$$A_1 C = \frac{q}{e_1}.$$

and, according to Eq. (2.29),

$$A_1 C = t_1 - t_{w_1}.$$

On the other hand,

$$A_1 C = A_1 O_1 - B_1 E_1;$$

By substituting the segments $A_1 C$ and $A_1 O_1$ we get

$$B_1 E_1 = t_{w_1}.$$

Similarly we find

$$\frac{B_2 F}{A_2 F} = \frac{A_1 D}{A_2 D}$$

or

$$B_2 F = \frac{\frac{\lambda}{a_q}(t_1 - t_2)}{\frac{\lambda}{e_1} + \delta + \frac{\lambda}{a_2}}.$$

from which

$$B_2 F = \frac{t_1 - t_2}{e_2} \frac{1}{\frac{1}{e_1} + \frac{\delta}{\lambda} + \frac{1}{e_2}} = \frac{t_1 - t_2}{e_2} k = \frac{q}{e_2}.$$

Consequently, the segment $B_2 F$ on the scale chosen is equal to

$$B_2 F = t_{w_2} - t_2;$$

- 44 -

On the other hand,

$$B_2F = B_2E_2 - A_2O_2.$$

Substituting the segments B_2F and A_2O_2, we get

$$B_2E_1 = t_{x_\mu}$$

i.e., the points of intersection of the straight line A_1 and A_2 plotted by the above method with the surfaces of our wall give the temperatures T'_{W_1} and T'_{W_2} of these surfaces, while the segment of the straight line $B_1 \frown B_2$ gives the distribution of temperature through the wall.

The temperature distribution in the first and second mobile media (line segments A_1B_1 and B_1A_2) do not correspond to reality. The true temperature distribution when there is convective heat exchange is shown in Fig. 23.

Second graphic method. Let us plot the following segments on an arbitrarily chosen horizontal line

$$O_1E_1 = \frac{1}{\alpha_1}; \quad E_1E_2 = \frac{\delta}{\lambda}; \quad E_2O_2 = \frac{1}{\alpha_2}$$

(Fig. 24). Let us plot the segments $O_1A_1 = t_1$ and $O_2A_2 = t_2$ as verticals from points O_1 and O_2. Let us join the points A_1 and A_2 by a straight line. The points of intersection B_1 and B_2 of this straight line with the surfaces of the walls then determine the unknown temperatures $t_{w_1} = E_1B_1$ and $t_{w_2} = E_2B_2$.

- 45 -
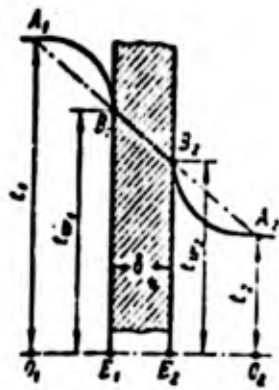
Fig. 23. Temperature
distribution during
convective heat exchange
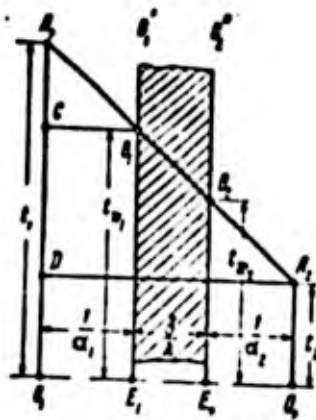
Fig. 24. Second graphic
method

Indeed,

$$\frac{A_1C}{CB_1} = \frac{A_1D}{DA_2},$$

and, according to Fig. 24, we get

$$A_1C = \frac{1}{e_1}\frac{t_1 - t_2}{\frac{1}{e_1} + \frac{\delta}{\lambda} + \frac{1}{e_2}} = \frac{k(t_1 - t_2)}{e_1} = \frac{q}{e_1},$$

since

$$k(t_1 - t_2) = q.$$

Hence, $A_1C = t_1 - t_{z_1}.$

and from this $B_1E_1 = t_{z_1}.$

It can be shown in exactly the same way that

$$B_2E_2 = t_{z_1}.$$

The second graphic method is also applicable to the case of heat transfer

through a plane multilayer wall.

Example 1. Let us determine the thermal conductivity λ of the walls of

an aircraft) cowling

engine if the thickness of the walls δ = 5 mm, the surface F = 0.5 m^2,

the temperature of the inside surface of the cowling t_{w_1} = 70°, the outside temperature

t_{w_2} = 65°, and the amount of heat passing through the cowling walls is q = 87,500

kcal/hour. indicate what material the cowling is made of.

- 46 -

Solution. The thermal conductivity is determined from Eq. (2.23)

$$\lambda = \frac{Q \cdot \delta}{F(t_{w_1} - t_{w_1})} = \frac{87\,500 \cdot 0.005}{0.5(70 - 65)} = 175 \text{ kcal/m} \cdot \text{hr} \cdot \text{deg}$$

According to reference data (see Mikheyev's book) we can presume the

is made of

aluminum.

Example 2. A brick tunnel-type dryer has the following dimensions: length

A = 20 m; width b = 9 m, height h = 3 m. The walls are made of ordinary building

brick with a thermal conductivity λ = 0.8 kcal/m hour deg, and the thickness

δ = 400 mm. By measurement it is found that the temperature of the outside surfaces

of the walls t_{w_2} = 50°, and of the inside walls t_w = 60°.

How much heat passes through the side walls of the dryer per hour?

Solution. Let us find the area of the side walls of the dryer.

$$F = 2ah + 2bh = 2 \cdot 20 \cdot 3 + 2 \cdot 9 \cdot 3 = 168 \; m^2.$$

2. From Eq. (2.23) we can determine the amount of heat passing through

the side walls of the dryer.

$$Q = \frac{\lambda}{\delta}(t_{x_1} - t_{x_1})F = \frac{0.8}{0.4} \cdot 80 \cdot 168 = 26\,880 \text{ kcal/hr}$$

Example 3. What is the heat-transfer coefficient k and the heat resistance

for the brick wall (λ = 0.76 kcal/m hour deg) of thickness δ = 380 mm, if

the heat-transfer coefficient for the inside surface of the wall is α_1 = 5 kcal/m^2 · hour ·

deg, and for the inside wall α_2 = 20 kcal/m^2 · hour · deg.

- 47 -

Solution

1) the heat transfer coefficient is determined from $Eq.$ (2.37);

$$k = \frac{1}{\frac{1}{a_1} + \frac{\delta}{\lambda} + \frac{1}{a_2}} = \frac{1}{\frac{1}{5} + \frac{0.380}{0.76} + \frac{1}{20}} = 1.33 \text{ kcal/m}^2 \cdot \text{hr} \cdot \text{deg}$$

2) the total heat resistance is determined by $Eq.$ (2.38)

$$\frac{1}{k} = 0.75 \text{ m}^2 \cdot \text{hr} \cdot \text{deg/kcal}$$

Example 4. The heating surface consists of an iron plate $\lambda = 50$ kcal/m hour deg) of thickness $\delta = 10$ mm. Water flows past ± one side of the plate, and the heat-transfer coefficient from the water to the wall is $\alpha_v = 2000$ kcal/m² hour · deg.

We are required to determine the heat transfer coefficient, when there are on the other side of the plate:

a) running water $\alpha_2 = 2000$ kcal/m² hour · deg;

b) moving air $\alpha_2 = 50$ kcal/m² hour · deg;

c) stationary air $\alpha_2 = 5$ kcal/m² hour · deg.

Solution

Let us first determine the total heat resistance of the water → wall and the wall proper

$$\frac{1}{k_1} = \frac{1}{a_1} + \frac{\delta}{\lambda} = \frac{1}{2000} + \frac{0.010}{50} = 0.0007 \text{ m}^2 \cdot \text{hr} \cdot \text{deg/cal}$$

But the total heat resistance is obviously calculated from the formula

Substituting numerical values, we get $\frac{1}{k} = \frac{1}{k_1} + \frac{1}{\alpha_2}$.

a) running water

$$\frac{1}{k} = 0.0007 + \frac{1}{2000} = 0.0012; \quad k = 1250 \text{ kcal/m}^2 \cdot \text{hr} \cdot \text{deg}$$

b) moving air

$$\frac{1}{k} = 0.0007 + \frac{1}{50} = 0.0207; \quad k = 48.3 \text{ kcal/m}^2 \cdot \text{hr} \cdot \text{deg}$$

c) stationary air

$$\frac{1}{k} = 0.0007 + \frac{1}{5} = 0.2007; \quad k = 4.98 \text{ kcal/m}^2 \cdot \text{hr} \cdot \text{deg}$$

Example 5. We are required to find the temperatures t_{W_1} and t_{W_2} of both surfaces of a sheet of boiler iron ($\lambda = 50$ kcal/m hour deg, thickness $\delta = 20$ mm, and the boiler wall is considered plane) and the amount of heat q passing through 1 m^2 of heating surface from the gases to the water in 1 hour, given the following

gas temperature $t_1 = 1000°$;

water temperature $t_2 = 200°$;

heat-transfer coefficients

gas $\rightarrow$ wall $\alpha_1 = 100$ kcal/m$^2 \cdot$ hour $\cdot$ deg;

wall $\rightarrow$ water $\alpha_2 = 2000$ kcal/m$^2 \cdot$ hour $\cdot$ deg.

Solution

1. Let us determine the heat resistance from Eq. (2.38)

$$\frac{1}{k} = \frac{1}{a_1} + \frac{\delta}{\lambda} + \frac{1}{a_2} = \frac{1}{100} + \frac{0.02}{50} + \frac{1}{2000} = 0.0109 \ m^2 \cdot hr \cdot deg/kcal$$

2. The heat-transfer coefficient k is

$$k = \frac{1}{0.0109} = 91.7 \ kcal/m^2 \cdot hr \cdot deg$$

3. The amount of heat passing through $1 \ m^2$ in one hour is determined from Eq. (2.36).

$$q = k(t_1 - t_2) = 91.7(1000 - 200) = 73390 \ kcal/m^2 \cdot hr$$

4. To determine the temperatures t_{w_1} and t_{w_2} let us use Eqs. (2.34) and (2.35)

$$t_{w_1} = t_1 - \frac{q}{a_1} = 1000 - \frac{73390}{100} = 266.1^\circ C$$

$$t_{w_2} = t_2 + \frac{q}{a_2} = 200 + \frac{73390}{2000} = 236.5^\circ C.$$

Example 6. A plane iron wall ($\lambda_1 = 50 \ kcal/m \cdot hour \cdot deg$) of thickness $\delta_1 = 0.025 \ m$ is insulated from heat loss by a layer of asbestos ($\lambda_2 = 0.2 \ kcal/m \cdot hr \cdot deg$ of thickness $\delta_2 = 0.1 \ m$, and a layer of cork ($\lambda_3 = 0.05 \ kcal/m \cdot hour \cdot deg$) of thickness $\delta_3 = 0.1 \ m$.

We have to determine the thickness of al .ol insulation that would be required for this sheet instead of the asbestos and cork in order for the heat insulation properties of the system to remain unchanged.

Solution

1. Let us determine the equivalent thermal conductivity of a three-layer wall (iron, asbestos, cork) from Eq. (2.26)

$$\lambda_{eq} = \frac{\delta_1 + \delta_2 + \delta_3}{\frac{\delta_1}{\lambda_1} + \frac{\delta_2}{\lambda_2} + \frac{\delta_3}{\lambda_3}} = \frac{0.025 + 0.1 + 0.1}{\frac{0.025}{50} + \frac{0.1}{0.2} + \frac{0.1}{0.05}} = 0.09 \text{ kcal/m} \cdot \text{hr} \cdot \text{deg}$$

Clearly, the thickness of the alfol insulation x should be such that the equivalent thermal conductivity of the new two-layer wall (iron-alfol) is equal to the thermal conductivity of the three-layer wall, i.e., 0.09 kcal/m hour deg;

thus

$$0.09 = \frac{\delta_1 + x}{\frac{\delta_1}{\lambda_1} + \frac{x}{\lambda_4}} = \frac{0.025 + x}{\frac{0.025}{50} + \frac{x}{0.03}}.$$

Solving this equation with respect to x, we get $x = 0.2$ m.

Example 7. The following data is possessed for an iron flue pipe ($\lambda_1 = 500$ kcal/m · hour · deg) of thickness $\delta = 20$ mm (the wall is considered plane on account of its slight curvature):

(Gas $\rightarrow$ wall $\alpha_1 = 50$ kcal/m² · hour · deg) $t_1 = 900°$; (wall - water $\alpha_2 = 1000$ kcal/m² · hour · deg) $t = 180°$.

We are to determine the temperature of the wall surfaces.

a) when the surface of the iron wall is clean;

b) when there is a layer of boiler scur ($\lambda_2 = 1$ kcal/m · hour · deg)

1 mm thick on the water side;

c) the same when the thickness of the fur is 10 mm.

<u>Solution.</u> Case a)

$$\frac{1}{k} = \frac{1}{a_1} + \frac{\delta_1}{\lambda} + \frac{1}{a_2} = \frac{1}{50} + \frac{0.02}{50} + \frac{1}{1000} = 0.0214 \quad m^2 \cdot hr \cdot deg/kcal$$

The heat-transfer coefficient k is equal to

$$k = \frac{1}{0.0214} = 46.73 \quad kcal/m^2 \cdot hr \cdot deg$$
$$q = 46.73 (900 - 180) = 33\,615 \quad kcal/m^2 \cdot hr$$
$$t_{w_1} = t_1 - \frac{q}{a_1} = 900 - \frac{33\,645}{50} = 227.1^\circ C.$$
$$t_{w_2} = t_2 + \frac{q}{a_2} = 180 + \frac{33\,645}{1000} = 213.7^\circ C.$$

Case b)   See page 52a

The temperature on the surface of the iron is

$$t_{w_1} = 900 \frac{32.40}{50} = 257.1^\circ C.$$

The temperature on the boundary between the iron and the *fur* is

$$t_{w_2} = t_{w_1} - q \frac{\delta_2}{\lambda_2} = 257.1 - 32\,140 \frac{0.02}{50} = 244.24^\circ C.$$

The temperature on the surface of the *fur* is

$$t_{w_3} = t_{w_2} - q \frac{\delta_2}{\lambda_2} = 244.24 - 32\,140 \frac{0.01}{1} = 212.1^\circ C.$$

Case c)   See page 52a

As can be seen from the calculation, the presence of a layer of scale
reduces the heat-transfer coefficient, and   the insulating properities
of the *fur* scale the temperature of the iron greatly increased, and this may cause

an accident to the boiler.

Case b)

$$\frac{1}{b} = 0,0214 + \frac{b_2}{\lambda_2} = 0,0214 + \frac{0,001}{1} = 0,0224 \ . \ m^2 \cdot hr \cdot deg/kcal$$

$$b = \frac{1}{0,0224} = 44,64 \ kcal/m^2 \cdot hr \cdot deg$$

$$q = 44,64 (900 - 150) = 32\,140 \ kcal/m^2 \cdot hr$$

Case c)

$$\frac{1}{b} = 0,0214 + \frac{b_2}{\lambda_2} = 0,0214 + \frac{0,010}{1} = 0,0314 \ \ m^2 \cdot hr \cdot deg/cal$$

$$b = \frac{1}{0,0314} = 31,84 \ kcal/m^2 \cdot hr \cdot deg$$

$$q = 31,84 (900 - 150) = 22\,9.5 \ kcal/m^2 \cdot hr$$

$$t_{w_1} = t_1 - q \ \frac{1}{a_1} = 900 - \frac{22\,925}{50} = 441,5^\circ \ C.$$

$$t_{w_2} = t_{w_1} - q \ \frac{b_1}{\lambda_1} = 441,5 - 22\,925 \ \frac{0,02}{50} = 432,3^\circ \ C$$

$$t_{w_3} = t_{w_2} - q \ \frac{b_2}{\lambda_2} = 432,3 - 22\,925 \ \frac{0,01}{1} = 203^\circ \ C.$$

Section 10. Cylindrical wall

Let us consider the process of heat transfer through a cylindrical wall. Let us assume that the cylinder is of infinite length so that the heat transfer through its ends can be ignored.

At each point on the wall of the tube (Fig. 25) the heat flux is directed along the radius, while the isothermal surfaces represent the surfaces of cylinders, whose axes coincide with the axis of the cylinder under consideration. The temperature field in the given problem is steady and unidimensional and is expressed by the following equation

$$t = f(r).$$

Here r is the operating coordinate of the cylindrxical system.

The equation for the temperature distribution through the cylindrical wall and the equation for the amount of heat passing through the wall could be derived by double integration of Eq (2.15), by expressing the Laplace operator in cylindrical coordinates. But to simplify the mathematical transformations we will argue along different lines.

According to the Fourier law, the amount of heat passing through any cylindrical surface of radius r per unit of time is equal to the amount of heat passing through the entire thickness of the tube, i.e.,

- 53 -
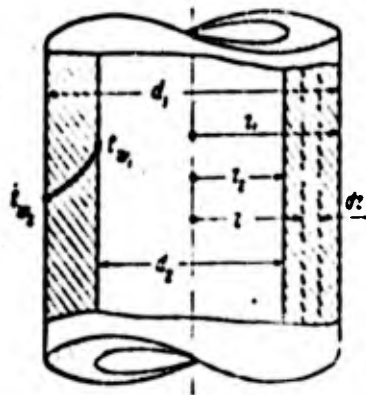
Fig. 25. Cylindrical wall.

$$Q = -\lambda \frac{dt}{dr} 2\pi r l \quad \text{Kcal/hr} \tag{2.39}$$

Here $\underline{l}$ is the length of the area of the pipe under consideration.

Let us designate the constants in Eq. (2.39)

$$\frac{Q}{2\pi\lambda l} = A. \tag{2.40}$$

Equation (2.39) will be then be rewritten in the form

$$dt = -A \frac{dr}{r}. \tag{2.41}$$

Integration of Eq. (2.41) gives us

$$t = -A \ln r + C, \tag{2.42}$$

in which $\underline{C}$ is the integration constant.

It is clear from Eq. (2.42) that the temperature distribution in the wall

of the tube obeys a logarithmic law.

First-order boundary conditions. In order to determine the integration

constants $\underline{C}$ and $\underline{A}$ in Eq. (2.40) let us apply the first-order boundary conditions,

i.e., let us set ourselves the temperature distribution on the surface of the

cylinder under consideration for any interval of time.

Let us assume that at

$$r = r_1 \quad t = t_{w_1},$$
$$r = r_2 \quad t = t_{w_2}.$$

Substituting these boundary conditions into Eq. (2.42) we get

$$\left. \begin{array}{l} t_{w_1} = -A \ln r_1 + C \\ t_{w_2} = -A \ln r_2 + C. \end{array} \right\} \tag{2.43}$$

Eq. (2.43) actually constitute a system of linear equations with two

unknowns C and A (since A is expressed in terms of the unknown value Q).

By . . . . solving them with respect to C and A we get

$$A = \frac{t_{x_1} - t_{x_2}}{\ln \frac{r_2}{r_1}} = \frac{t_{x_1} - t_{x_2}}{\ln \frac{d_2}{d_1}}.$$

Substitution of A into Eqs. (2.43) and their solution with respect to C

gives us the following two equations

$$C = \frac{t_{x_1} - t_{x_2}}{\ln \frac{r_2}{r_1}} \ln r_1 + t_{x_1.}$$
(2.44)

$$C = \frac{t_{x_1} - t_{x_2}}{\ln \frac{r_2}{r_1}} \ln r_2 + t_{x_2}.$$
(2.45)

After elementary transformations we find the integration constant

$$C = \frac{t_{x_1} \ln r_2 - t_{x_2} \ln r_1}{\ln \frac{r_2}{r_1}}.$$
(2.46)

Substituting A and C into Eq. (2.42) we get the following expression

for the temperature distribution in the cylindrical wall

$$t = \frac{t_{x_1} \ln \frac{r_2}{r} + t_{x_2} \ln \frac{r}{r_1}}{\ln \frac{r_2}{r_1}}.$$
(2.47)

It follows from Eq. (2.47) that at

$$r = r_1 \qquad t = t_{x_1}$$
$$r = r_2 \qquad t = t_{x_2}.$$

The amount of heat Q passing through the cylindrical wall per unit of

time is determined from Eq (2.40).

$$Q = 2\pi \lambda A.$$

Substituting the expression for A into this, we get

$$Q = \frac{1}{\ln\frac{d_2}{d_1}}(t_{w_1} - t_{w_2}) 2\pi l \quad \text{kcal/hr} \tag{2.48}$$

It is clear from Eq. (2.48) that Q depends both on the thickness of

the wall as well as on the ratio of the external and internal diameters.

In engineering calculations it is usual to ~~refer~~ the amount of heat

passing through the wall of the cylinder to a unit of length of the tube

$$q_1 = \frac{Q}{l} = \frac{2\pi\lambda}{\ln\frac{d_2}{d_1}}(t_{w_2} - t_{w_1}) \quad \text{kcal/hr} \tag{2.49}$$

For the case of a multilayer cylindrical wall (Fig. 26) the following

equation can be derived by methods which are exactly the same as those used for

the case of a multilayer plane wall (see Section 8)

$$q_1 = \frac{(t_{w_1} - t_{w_{n+1}})\pi}{\frac{1}{2\lambda_1}\ln\frac{d_2}{d_1} + \frac{1}{2\lambda_2}\ln\frac{d_3}{d_1} + \cdots + \frac{1}{2\lambda_n}\ln\frac{d_{n+1}}{d_n}} \cdot \tag{2.50}$$

In exactly the same way for a cylindrical multilayer wall the

concept of the equivalent thermal conductivity, which was introduced for a multi-

layer plane wall, remains valid

$$q_1 = \frac{\lambda_{equi}}{\ln\frac{d_{n+1}}{d_1}}(t_{w_1} - t_{w_{n+1}}) 2\pi. \tag{2.51}$$

Balancing the right-hand sides of Eqs. (2.50) and (2.51), we get

$$\lambda_{equi} \cdot \frac{\ln\frac{d_{n+1}}{d_1}}{\frac{1}{\lambda_1}\ln\frac{d_2}{d_1} + \frac{1}{\lambda_2}\ln\frac{d_3}{d_2} + \cdots + \frac{1}{\lambda_n}\ln\frac{d_{n+1}}{d_n}}. \tag{2.52}$$

Using Eq. (2.50) we can write the equation for determining the temperature

t   on the boundary between the i-th and the $(i+1)$-th layers.
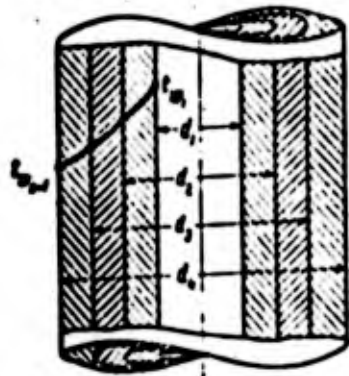
Fig. 26. Multilayer
cylindrical wall

Fig. 27. Boundary
conditions of third
kind

$$l_{w_{i+1}} - l_{x_i} - \frac{q_i}{2\pi}\left(\frac{1}{\lambda_1}\ln\frac{d_2}{d_1} + \frac{1}{\lambda_2}\ln\frac{d_3}{d_2} + \cdots + \frac{1}{\lambda_i}\ln\frac{d_{i+1}}{d_i}\right). \tag{2.53}$$

<u>Third-Order Boundary Conditions.</u> Let us now consider the problem of a cylindrical wall, using boundary conditions of the third kind, the essence of (_principle_) which is to set the temperatures t_1 and t_2 of the liquids (_flowing past_) the wall, and the law of heat transfer between the surfaces of the wall.

Consequently, the task of heat exchange is determined by the corresponding heat-transfer coefficients α_1 and α_2 (Fig. 27).

The amount of heat q_i passing through the wall of _a_ tube of length 1 m from the hot liquid (t_1) to the cold liquid (t_2) can be expressed by three

equations

$$\left.\begin{aligned} q_1 &= \alpha_1(l_1 - l_{w_1})\pi d_1 \\ q_1 &= \frac{\lambda}{\ln\frac{d_2}{d_1}}(l_{w_1} - l_{w_2})2\pi \\ q_1 &= \alpha_2(l_{w_2} - l_2)\pi d_2. \end{aligned}\right\} \tag{2.54}$$

Let us write Eqs. (2.54) in the following transformation

$$q_1 \cdot \frac{1}{\pi d_1 \alpha_1} = l_1 - l_{x_1}$$

$$q_1 \cdot \frac{1}{2\pi\lambda}\ln\frac{d_2}{d_1} = l_{x_1} - l_{x_2}$$

$$q_1 \cdot \frac{1}{\pi d_2 \alpha_2} = l_{x_2} - l_2.$$

Summing the left-hand and right-hand sides of the equalities, we get

$$\frac{q_1}{\pi}\left(\frac{1}{d_1 \alpha_1} + \frac{1}{2\lambda}\ln\frac{d_2}{d_1} + \frac{1}{d_2 \alpha_2}\right) = l_1 - l_2. \tag{2.55}$$

From here

$$q_1 = \pi k_a(l_1 - l_2)\ \text{kcal/m}\cdot\text{hr}$$

in which

$$\pi k_a = \frac{\pi}{\frac{1}{\alpha_1 d_1} + \frac{1}{2\lambda}\ln\frac{d_2}{d_1} + \frac{1}{\alpha_2 d_2}}\ \text{kcal/m}\cdot\text{hr}\cdot\text{deg} \tag{2.56}$$

- 57 -

The coefficient k_c is called the heat-transfer coefficient of a cylindrical wall. Its dimensionality, as can be seen from equations (2.56), differs from that of the heat transfer coefficient k for a plane wall. The coefficient k_c is numerically equal to the amount of heat passing through the wall of the tube 1 m in length per unit of time from 1 liquid to another, providing the temperature gradient between them is 1°C.

The reciprocal of the heat-transfer coefficient k_c is

$$\frac{1}{k_s} = \frac{1}{a_1 d_1} + \frac{1}{2\lambda} \ln \frac{d_2}{d_1} + \frac{1}{a_2 d_2} -$$ (2.57)

and is termed the total heat or thermal resistance of the tube, and the summands $1/a_1 d_1$ and $1/a_2 d_2$ are termed the heat or thermal resistances to heat transfer, while the summand $1/2\lambda \ln d_2/d_1$ is called the heat or thermal resistance of the wall of the tube.

Thus, in the case of a cylindrical wall the thermal resistance of heat transfer is not only a function of α_1 and α_2, but also of the diameters d_1 and d_2.

For the case of a multilayer cylindrical wall with n tightly packed layers with the corresponding thermal conductivities $1/2\lambda \ln d_2/d_1$ $\lambda_1, \lambda_2, \lambda_3 \ldots \lambda_n$, on an analogy with the plane, multilayer wall, we can write the expressions for the thermal conductivity

$$k_s = \frac{1}{\frac{1}{a_1 d_1} + \frac{1}{2\lambda_1} \ln \frac{d_2}{d_1} + \frac{1}{2\lambda_2} \ln \frac{d_3}{d_2} + \cdots + \frac{1}{2\lambda_n} \ln \frac{d_{n+1}}{d_n} + \frac{1}{a_2 d_{n+1}}}$$ (2.58)

- 58 -

and thermal resistance

$$\frac{1}{k_s} = \frac{1}{a_1 d_1} + \frac{1}{2\lambda_1}\ln\frac{d_2}{d_1} + \frac{1}{2\lambda_2}\ln\frac{d_3}{d_2} + \cdots + \frac{1}{2\lambda_s}\ln\frac{d_{s+1}}{d_s} + \frac{1}{a_s d_{s+1}}. \qquad (2.59)$$

The temperature $t_{w_{i+1}}$ on the boundary between the i-th and $(i + 1)$-th layers

is determined from the equation

$$t_{w_{i+1}} = t_i - \frac{q}{s}\left(\frac{1}{a_1 d_1} + \frac{1}{2\lambda_1}\ln\frac{d_2}{d_1} + \frac{1}{2\lambda_2}\ln\frac{d_3}{d_2} + \cdots + \frac{1}{2\lambda_i}\ln\frac{d_{i+1}}{d_i}\right). \qquad (2.60)$$

Example 8. The power developed in a internal combustion engine cylinder

is $N_i = 50$ hp. The specific consumption of fuel is $c_i = 0.220$ kg/hp hour. The

calorific value of the fuel is $H_u = 10,100$ cal/kg. We are to determine the

thermal conductivity of the cylinder wall, assuming that 14% of the total heat

of the fuel is removed through the cylinder wall into water. The temperature drop

in the wall of the cylinder $t_{w_1} - t_{w_2} = 10°$.

The dimensions of the engine cylinder are as follows: $D = 160$ mm, $l = 175$ mm,

and the thickness of the wall $\delta = 3$ mm.

Solution.

1) Let us determine the hourly fuel consumption

$$G_{v_i} = N_i c_i = 50 \cdot 0.220 = 11 \text{ kg/hr}$$

2) Let us determine the Q_i -hourly amount of fuel given off in the engine

cylinder.

$$Q_i = G_{v_i} H_u = 11 \cdot 10\,100 = 111\,100 \text{ kcal/hr}$$

3) let us determine the amount of heat removed through the cylinder wall

$$Q = 0.14 \cdot Q_1 = 0.14 \cdot 111\,100 = 15\,554 \text{ kcal/hr}$$

4) the thermal conductivity of the cylinder is determined from Eq. (2.48)

$$\lambda = \frac{Q \ln \frac{d_2}{d_1}}{2\pi l (t_{w_1} - t_{w_2})} = \frac{15\,554 \cdot 2.3 \cdot 1g \frac{166}{160}}{2 \cdot 0.175 \cdot 10} = 50 \text{ kcal/m} \cdot \text{hr} \cdot \text{deg}$$

, **Example 9.** An iron tube ($\lambda = 50$ kcal/m · hour · deg) with an internal diameter 16 cm and external diameter 17 cm is covered with a layer of refractory insulation ($\lambda = 0.11$) 2 cm thick. On top of this insulation is a layer of cork ($\lambda = 0.035$) 5 cm thick. The temperature of the internal surface of the iron tube is 300 °C. The temperature on the outside surface of the cork insulation is 40 °C. Determine the heat losses in the tube over 1 m of its length, the equivalent thermal conductivity, and the temperatures on the surface separating the individual layers.

<u>Solution.</u>

$$d_1 = 0.16 \text{ м}, \quad \lambda_1 = 50 \text{ kcal/m} \cdot \text{hr} \cdot \text{deg}$$
$$d_2 = 0.17 \text{ м}, \quad \lambda_2 = 0.1 \text{ kcal/m} \cdot \text{hr} \cdot \text{deg}$$
$$d_3 = 0.21 \text{ м}, \quad \lambda_3 = 0.035 \text{ kcal/m} \cdot \text{hr} \cdot \text{deg}$$
$$d_4 = 0.31 \text{ м},$$
$$t_{w_1} = 300° \text{ C}, \quad t_{w_4} = 40° \text{ C}.$$

Further,

$$\ln \frac{d_2}{d_1} = 0.05; \quad \ln \frac{d_3}{d_2} = 0.21; \quad \ln \frac{d_4}{d_3} = 0.38.$$

According to Eq. (2.50) we get

$$q_1 = \frac{(300 - 40)\, 2\pi}{\frac{1}{50} 0.05 + \frac{1}{0.1} 0.21 + \frac{1}{0.035} 0.38} = 126 \text{ kcal/m} \cdot \text{hr}$$

- 60 -

To determine λ_{eq} let us use Eq. (2.52)

$$\lambda_{eq} = \frac{\ln\dfrac{0.31}{0.16}}{\dfrac{1}{50}0.05 + \dfrac{1}{0.1}0.21 + \dfrac{1}{0.035}\cdot 0.38} = 0.51\,\text{kcal/m}\cdot\text{hr}\cdot\text{deg}$$

The temperature t_{w_2} on the outside surface of the iron tube is found from

Eq. (2.53)

$$t_{w_2} = t_{w_1} - \frac{q_1}{2\pi}\frac{1}{\lambda_1}\ln\frac{d_2}{d_1} = 300 - \frac{126}{2\pi}\frac{1}{50}\ln 0.5 = 299.98° \approx 300°\,\text{C}.$$

In exactly the same way we find t_{w_2}

$$t_{w_3} = t_{w_4} + \frac{q}{2\pi}\frac{1}{\lambda_3}\ln\frac{d_4}{d_3} = 40 + \frac{126}{2\pi}\frac{1}{0.035}0.38 = 258°\,\text{C}.$$

The temperature of the internal surface of the cork insulation is

extremely high, on account of the small thickness of the refractory insulation.

Example 10. A pipe feeding a refrigerating solution has cork insulation

($\lambda \approx 0.045$) 75 mm thick. The outer diameter of the insulation is 250 mm.

Measurement has shown that the temperature of the outside surface of insulation is

$t_{w_1} = 20°$ and that of the internal surface t_{w_2} is $-10°$. The length of the pipe is

1 - 20 m. How much heat will pass from the surrounding medium to the internal

surface of the insulation in 24 hours?

Solution. Let us apply Eq. (2.48)

$$Q = \frac{\lambda}{\ln\dfrac{d_2}{d_1}}(t_{w_1} - t_{w_2})2\pi l\ \text{cal/hr}$$

Substituting numerical values, we get

$$Q = \frac{0.045}{\ln\dfrac{0.250}{0.100}}[20 - (-10)]2\pi\cdot 20 = 185.33\,\text{cal/hr}$$

or

$$Q = 24 \cdot 185.33 = 4448 \text{ cal}$$

Example 11. The outside diameter of the iron steam pipe is 17 cm, and the inside diameter 16 cm. The pipe is covered with a layer of asbestor ($\lambda = 0.15$) 5 cm thick. On top of the asbestos is a layer of cork ($\lambda = 0.04$ kcal/m · hour · deg) 5 cm thick. The temperature of the steam flowing through the pipe is $t_1 = 250°$, while that of the air surrounding thepipe is $t_2 - 20°$. The heat transfer coefficient from the steam to the pipe is $\alpha_1 = 100$ cal/m^2 · hour · deg. The heat transfer coefficient from the pipe to the air is $\alpha_2 = 10$ cal/m^2 · hour · deg.

Let us determine the heat-transfer coefficient and thermal resistance per unit of length of pipe.

Solution. The thermal resistanceof the pipe is determined from Eq. (2.59)

$$\frac{1}{k_s} = \frac{1}{a_1 d_1} + \frac{1}{2\lambda_1} \ln \frac{d_2}{d_1} + \frac{1}{2\lambda_2} \ln \frac{d_2}{d_3} + \frac{1}{2\lambda_3} \ln \frac{d_4}{d_3} + \frac{1}{a_2 d_4}.$$

Let us total up the individual heat resistances

$$\frac{1}{a_1 d_1} = \frac{1}{100 \cdot 0.16} = 0.0625 \text{ m} \cdot \text{hr} \cdot \text{deg/cal}$$

$$\frac{1}{2\lambda_1} \ln \frac{d_2}{d_1} = \frac{1}{2 \cdot 50} \ln \frac{0.17}{0.16} = 0.00061 \text{ m} \cdot \text{hr} \cdot \text{deg/cal}$$

$$\frac{1}{2\lambda_2} \ln \frac{d_3}{d_2} = \frac{1}{2 \cdot 0.15} \ln \frac{0.27}{0.17} = 1.54 \text{ m} \cdot \text{hr} \cdot \text{deg/cal}$$

$$\frac{1}{2\lambda_3} \ln \frac{d_4}{d_3} = \frac{1}{2 \cdot 0.04} \ln \frac{0.37}{0.27} = 3.94 \text{ m} \cdot \text{hr} \cdot \text{deg/cal}$$

$$\frac{1}{a_2 d_4} = \frac{1}{10 \cdot 0.37} = 0.27 \text{ m} \cdot \text{hr} \cdot \text{deg/cal}$$

The total heat resistance is

$$\frac{1}{k_\mathrm{q}} = 0.0625 + 0.00061 + 1.51 + 3.94 + 0.27 = 5.81 \; \text{м·час·град/кал}$$

and the heat-transfer coefficient is

$$k_\mathrm{q} = \frac{1}{5.81} = 0.172 \, \text{kcal/m} \cdot \text{hr} \cdot \text{deg}$$

Section 11. Critical thickness of heat insulation of pipe

Let us consider a case in which a cylindrical wall (pipe) is covered with a single layer of heat insulating material. The values $a_1, a_2, d_1, d_2, \lambda_1, \lambda_2, l_1, l_2$ are assumed to be given and to be constant. Let us ascertain the variation in the total heat resistance during variation in the thickness of the insulatingmaterial through variation in its diameter (Fig. 28).

Using Eq.(2.59) we can write

$$\frac{1}{k_\mathrm{q}} = \frac{1}{a_1 d_1} + \frac{1}{2\lambda_1}\ln\frac{d_2}{d_1} + \frac{1}{2\lambda_2}\ln\frac{d_3}{d_2} + \frac{1}{a_2 d_3}.$$

When the external diameter of the insulating material d_3 increases, the term $\frac{1}{2\lambda_2}\ln d_3/d_2$ increases, while the term $1/a_2 d_3$ decreases, i.e., when the thickness of the insulating material is increased, the heat resistance of the material itselfis increased and the beat resistance to heat transfer on the outside surface of the

material decreases.

Thus we have to study the function

$$\frac{1}{k_\mathrm{q}} = f(d_3).$$

- 63 -

Taking the first derivative of the right-hand side of Eq. (2.59) with respect to d_3 and equating it with zero, we get

$$\left(\frac{1}{k_u}\right)' = \frac{2}{2\lambda_2 d_3} - \frac{1}{e_2 d_3^2} = 0.$$

This gives us

$$d_{\kappa p} = \frac{2\lambda_2}{e_2}. \qquad (2.61)$$

Substituting into the second derivative

$$\left(\frac{1}{k_u}\right)'' = -\frac{1}{2\lambda_2 d_3^2} + \frac{2}{e_2 d_3^3} = \frac{1}{d_3^2}\left(\frac{2}{e_2 d_3} - \frac{1}{2\lambda_2}\right)$$

the critical value of the diameter, we get

$$\left(\frac{1}{k_u}\right)'' = \frac{e_2^2}{4\lambda_2^3}\left(1 - \frac{1}{2}\right) = \frac{e_2^2}{8\lambda_2^3} > 0.$$

Consequently, at the critical value

$$d_3 = d_{\kappa p} = \frac{2\lambda_2}{e_2}.$$

the thermal resistance $1/k_c$ is minimal, while the heat transfer coefficient k_c is maximum (Fig. 29), i.e., the heat losses at $d_3 = d_{cr}$ are greatest. If $d_3 < d_{cr}$ the heat losses decrease on account of a decrease in the heat removing surface.

If $d_3 > d_{cr}$, the heat losses are also decreased on account of an increase in the thickness of the insulating material. Experiments show that in practice d_{cr} is mainly a function of the properties of the insulating material, i.e., a function of λ_2.
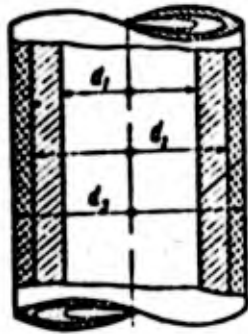
Fig. 28. Determination critical
thickness of thermal insulation
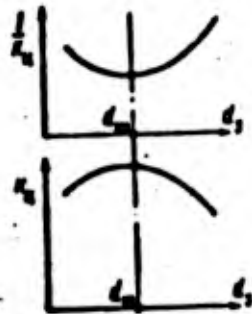
Fig. 29. Variation in thermal-resistance and
heat-transfer coefficients as function of
external insulation diameter

Section 12. Spherical Wall

Let us consider the process of thermal conductivity in a spherical wall with internal and external surface radii r_1 and r_2 (Fig. 30) and a thermal conductivity λ. Steady-state conditions ensure that the temperatures on the internal (t_{w_1}) and external (t_{w_2}) surfaces are constant. Obviously, in this case the temperature$t$ is only a function of the radius r and the Fourier law expressing the amount of heat passing per unit of time through the spherical surface r can be written in the form

$$Q = -\lambda \frac{dt}{dr} 4\pi r^2 \ \text{ккал/час}. \tag{2.62}$$

Designating the constant $\frac{Q}{4\pi\lambda} = A$ and separating the variables, we get

$$dt = -A \frac{dr}{r^2}. \tag{2.63}$$

Integrating Eq. (2.63) we get

$$t = \frac{A}{r} + C. \tag{2.64}$$

in which C is an integration constant.

It is clear from Eq. (2.64) that the curve expressing the variation in temperature in a spherical layer is a hyperbola.

In order to find the unknown A and C let us use the first-kind boundary conditions.

Fig. 30. Spherical wall

At

$$r = r_1 \qquad t = t_{x_1}$$
$$r = r_2 \qquad t = t_{x_2}$$

Substituting these conditions into Eq. (2.64) we get

$$t_{w_1} = \frac{A}{r_1} + C_1$$

$$t_{w_2} = \frac{A}{r_2} + C_2$$

(2.65)

Solving the obtained system of linear equations, we get

$$A = \frac{t_{x_2} - t_{x_1}}{\frac{1}{r_1} - \frac{1}{r_2}},$$

and therefore

$$Q = \frac{4\pi\lambda}{\frac{1}{r_1} - \frac{1}{r_2}} (t_{w_1} - t_{w_1}) \text{ cal/hr}$$

(2.66)

The integration constant is determined from the following *relationship in*

Eqs. (2.65)

$$C = \frac{r_2 t_{w_1} - r_1 t_{w_1}}{r_2 - r_1}.$$

Substituting A and C into Eq (2.64) we get

$$t = \frac{t_{w_1}\left(\frac{1}{r} - \frac{1}{r_2}\right) + t_{w_1}\left(\frac{1}{r_1} - \frac{1}{r}\right)}{\frac{1}{r_1} - \frac{1}{r_2}}.$$

(2.67)

For a multilayer spherical wall consisting of n layers with thermal conductivities $\lambda_1, \lambda_2, \lambda_3, \ldots, \lambda_n$, and radii $r_1, r_2, \ldots, r_{n+1}$, we get on an analogy with the multi-layer plane and cylindrical walls

$$Q = \frac{4\pi(t_{w_1} - t_{w_n+1})}{\frac{1}{\lambda_1}\left(\frac{1}{r_1} - \frac{1}{r_2}\right) + \frac{1}{\lambda_2}\left(\frac{1}{r_2} - \frac{1}{r_3}\right) + \cdots + \frac{1}{\lambda_n}\left(\frac{1}{r_n} - \frac{1}{r_{n+1}}\right)}.$$

(2.68)

The temperature distribution inside any i-th layer of the spherical wall obeys the equation

$$\ell_i = \frac{\ell_{w_i}\left(\frac{1}{r} - \frac{1}{r_{i+1}}\right) + \ell_{w_{i+1}}\left(\frac{1}{r_i} - \frac{1}{r}\right)}{\frac{1}{r_i} - \frac{1}{r_{i+1}}}. \tag{2.69}$$

Section 13. Infinitely long rod

Let us consider steady-state heat transfer through a rod of infinite length (Fig. 31). One end of the rod is kept at a constant temperture $\underline{t}_1$. The rod is ~~Surrounded~~ by a medium with a constant temperature $\underline{t}_0$. The heat-transfer coefficient from the surface of the rod to the medium is considered constant throughout the length of the rod. The thermal conductivity of the material of the rod λ is assumed to be fairly high, while the transverse dimensions of the rod are so small compared with the length that we can ignore the variation in tempeeature from the axis of the rod to its surface in the sections perpendicular to its axis. The temperature of the rod $\underline{t}$ is considered a function of one coordinate alone

$$t = f(x).$$

For the temperature of the rod to exceed that of the surrounding medium we will ~~assume that~~

$$t - t_0 = \theta.$$

For the beginning of the rod at $\underline{x} - 0$

$$t_1 - t_0 = \theta_1.$$

Let us consider the thermal equilibrium of a rod element bounded by two perpendicular sections at a distance $\underline{x}$ from the origin of the coordinates.

The length of the element dx, the area of the section of the rod is F and the perimeter of the section is U.

The amount of heat Q_x entering the element under consideration through the section I - I per unit of time is determined by the equation

$$Q_x = -\lambda\left(\frac{d\theta}{dx}\right)_x \cdot F. \tag{2.70}$$

The amount of heat Q_{x+dx} leaving the element through the section II - II situated at a distance $x + dx$ from the origin of the coordinates is

$$Q_{x+dx} = -\lambda\left(\frac{d\theta}{dx}\right)_{x+dx} \cdot F. \tag{2.71}$$

During this time the lateral surface of the rod $U\,dx$ will give up the following amount of heat

$$dQ = \alpha U\theta\,dx. \tag{2.72}$$

Compiling the heat balance for the rod element we get

$$Q_x - Q_{x+dx} = dQ, \tag{2.73}$$

$$-\lambda\left(\frac{d\theta}{dx}\right)_x F + \lambda\left(\frac{d\theta}{dx}\right)_{x+dx} \cdot F = \alpha U\theta\,dx. \tag{2.74}$$

Taking it into account that

$$\frac{\left(\frac{d\theta}{dx}\right)_{x+dx} - \left(\frac{d\theta}{dx}\right)_x}{dx} = \frac{d^2\theta}{dx^2}, \tag{2.75}$$

we get

$$\lambda F\frac{d^2\theta}{dx^2} = \alpha U\theta. \tag{2.76}$$
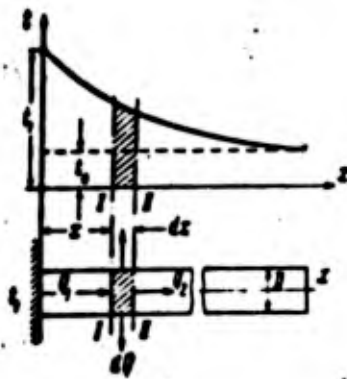
Fig. 31. Rod of infinite length

Introducing the quantity

$$\beta^2 = \frac{\alpha U}{\lambda F},$$ (2.77)

we get

$$\frac{d^2\theta}{dx^2} = \beta^2\theta.$$ (2.78)

The solution of the derived linear differential equation of the second

order can be represented in the general form

$$\theta = C_1 e^{\beta x} + C_2 e^{-\beta x}.$$ (2.79)

The constants C_1 and C_2 can be found by means of the boundary

conditions

At

$$x = 0 \qquad \theta = \theta_1 = C_1 + C_2,$$
$$x = \infty \qquad \theta = 0 = C_1 e^{\infty}.$$

At

The last equality is only varied on condition $C_1 = 0$.

Consequently,

$$\theta_1 = C_2 \quad \text{и} \quad \theta = \theta_1 e^{-\beta x}.$$

The hourly amount of heat given up by the whole lateral surface of the

rod can be found as the heat flux entering the rod through its base

$$Q_1 = -\lambda F \left(\frac{d\theta}{dx}\right)_{x=0}.$$ (2.80)

Since

$$\left(\frac{d\theta}{dx}\right)_{x=0} = -\beta\theta_1,$$ (2.81)

- 69 -

Therefore,

$$Q = \lambda F \beta \theta_1 \qquad (2.82)$$

or

$$Q = \theta_1 \sqrt{\alpha U \lambda F}. \qquad (2.83)$$

If the heat transfer from the rod to the medium does not take place along the whole surface of the rod, the value $\underline{U}$ should be taken to mean the part of the section perimeter along which the heat transfer occurs. For a rod of circular section with diameter $\underline{D}$ with heat transfer over the whole surface, we get

$$\beta = 2 \sqrt{\frac{\alpha}{\lambda D}}, \qquad (2.84)$$

$$Q_1 = \frac{\pi}{2} \theta_1 \sqrt{\lambda \alpha D^3}. \qquad (2.85)$$

Section 14. Rod of finite length

If the cold end of the rod is at a temperature higher than that of the surrounding medium, we have to use different formulae when calculating the heat transfer through it.

Let us designate the length of the rod $\underline{L}$ and the amount by which the temperature of the cold end exceeds that of the surrounding medium $\theta_{\underline{\Delta}}$. We will ignore heat transfer from the end of the rod or we will take it into account by increasing the length of the rod so that the lateral surface when elongated is equal to the total (lateral and end) surface of the actual rod.

- 70 -

The general solution of the differential equation (2.79)

$$\theta = C_1 e^{\beta x} + C_2 e^{-\beta x}$$

is applicable to a rod of finite length. The derivation of this equation coincides

with that given for a rod of infinite length, except that the boundary conditions vary

at $\qquad x = 0 \quad \theta = \theta_1 = C_1 + C_2 \quad$ or $\quad C_2 = \theta_1 - C_1;$ $\qquad$ (2.86)

at $\underline{x} = \underline{L}$, ignoring the heat transfer from the end of the rod, we get

$$\left(\frac{d\theta}{dx}\right)_{x=L} = 0, \qquad (2.87)$$

$$\left(\frac{d\theta}{dx}\right)_{x=L} = \beta C_1 e^{\beta L} - \beta C_2 e^{-\beta L} = 0. \qquad (2.88)$$

Equations (2.86) and (2.88) give us

$$C_1 (e^{\beta L} + e^{-\beta L}) - \theta_1 e^{-\beta L} = 0, \qquad (2.89)$$

from which

$$C_1 = \frac{\theta_1 e^{-\beta L}}{e^{\beta L} + e^{-\beta L}} = \theta_1 \frac{e^{-\beta L}}{2 \operatorname{ch}(\beta L)} \qquad (2.90)$$

and

$$C_2 = \theta_1 - C_1 = \theta_1 \left(1 - \frac{e^{-\beta L}}{e^{\beta L} + e^{-\beta L}}\right) = \theta_1 \frac{e^{\beta L}}{2 \operatorname{ch}(\beta L)}. \qquad (2.91)$$

Equation (2.79) for the temperature distribution in the rod can be

expressed more conveniently in hyperbolic functions. Substituting the derived

values $\underline{C}_1$ and $\underline{C}_2$ into Eq. (2.79) and changing to hyperbolic functions, we get

$$\theta = \frac{\theta_1}{2 \operatorname{ch}(\beta L)} (e^{\beta x} e^{-\beta L} + e^{-\beta x} e^{\beta L}) \qquad (2.92)$$

or

$$\theta = \frac{\theta_1 (e^{-\beta(L-x)} + e^{\beta(L-x)})}{2 \operatorname{ch}(\beta L)} = \theta_1 \frac{\operatorname{ch}[\beta(L-x)]}{\operatorname{ch}(\beta L)}. \qquad (2.93)$$

At $\underline{x - L}$ we get

$$\theta_L = \frac{\theta_1}{\operatorname{ch}(\beta L)}. \qquad (2.94)$$

The heat flux entering the rod and transferred byx the lateral surface

of the rod to the surrounding medium can be found from Eqs. (2.79) and (2.80)

$$Q = -\lambda F \left(\frac{d\theta}{dx}\right)_{x=0} = -\lambda F \beta (C_1 - C_2) = \lambda F \beta \frac{\theta_1 (e^{-\beta L} - e^{\beta L})}{2 \operatorname{ch}(\beta L)} \qquad (2.95)$$

or

$$Q = \theta_1 \sqrt{\lambda F a U} \frac{\operatorname{sh}(\beta L)}{\operatorname{ch}(\beta L)} = \theta_1 \operatorname{th}(\beta L) \sqrt{a U \lambda F}. \qquad (2.96)$$

$$\beta^2 = \frac{4a}{\lambda D} \qquad (2.97)$$

and

$$\sqrt{a U \lambda F} = \sqrt{\frac{a \lambda \pi D^2 \pi D}{4}} = \frac{\pi D}{2} \sqrt{a \lambda D} \quad \text{kcal/hr} \qquad (2.98)$$

Example 13. It is known that the temperature at the end of the inlet

valve stem in an internal combustion engine is $\underline{t_2} = 180^\circ$ (Fig. 32). Determine the

temperature of the valve at the beginning of the stem $\underline{t_1}$, if it is known that

the diameter of the valve stem is $\underline{D} = 10$ mm and its length is $\underline{L} = 120$ mm. The

valve is made of a special steel with thermal conductivity $\lambda = 25$ kcal/m · hour · deg.

The heat-transfer coefficient from the surface of the valve stem to the

bushing is $\alpha = 15$ kcal/m² /hour · deg. The temperature of the bushing is

is taken to be constant throughout the length and is equal to $t_{-\overline{v}} = 65'$.

Note. The valve stem is considered a rod of finite length.

Solution. Equation (2.94) gives us

$$\theta_L = \frac{\theta_1}{ch\,(\beta L)}\,.$$

from which

$$\theta_1 = \theta_L\,ch\,(\beta L).$$

From the given data we find

$$\theta_L = t_2 - t_0 = 180° - 65° = 115°.$$

Fig. 32. Calculation of temperature field of inlet valve in engine

From Eq. (2.97) we calculate

$$\beta = 2\sqrt{\frac{a}{\lambda D}} = 2\sqrt{\frac{15}{25 \cdot 0.01}} = 15.5,$$
$$\theta_1 = 115\,ch\,(15.5 \cdot 0.12) = 115\,ch\,(1.86) = 378°$$
$$\theta_1 = t_1 - t_0,\ t_1 = \theta_1 + t_0 = 378° + 65° = 443°.$$

Section 15. Round Plane Fins

The problem of correctly designing fins for air-cooled engine cylinders, economizers, heaters and other heat-exchanging apparatus consists in obtaining maximum removal of heat at the given consumption of the cooling agent, while keeping the weight and the size of the apparatus itself down to a minimum.

We have to determine the shape, height and distance between fins.

The most advantageous fin-shape for the given weight or height can be decided mathematically. If the weight and area of the transverse fin are constant,

- 73 -

the maximum heat removal is ensured if the lateral surfaces of the fin are concave-

parabolic in shape (Fig. 33a). In a fin of this kind the temperature

gradient is constant all the way up. By   virtue of the difficulties of a

technological nature, in practice use is made of fins with a cross-section in the

form of a trapezium (Fig. 33b) or a rectangle (Fig. 33c).

An analytical solution of the problem of the propagation of heat through

a fin and, chiefly, the heat transfer from its outer surface *involves*   a number

of difficulties of a mathematical and physical nature. The chief difficulty is

the necessity to know the distribution of the heat-transfer coefficient α over

the surface of the fin. Hence the analytical solution of the propagation of heat

in fins, possible at the present stage of development of the study of heat transfer,

gives a very approximate result on account of the assumptions made to   simplify

the physical picture of the given phenomenon.

Let us therefore consider the heat flux for a rectangular fin under the

following conditions:

1) The temperature conditions are steady-state. The temperature of the

base of the fin is constant and equal to t_1 ;

2) the amount of heat *dissipated* over a unit of time from any part of the
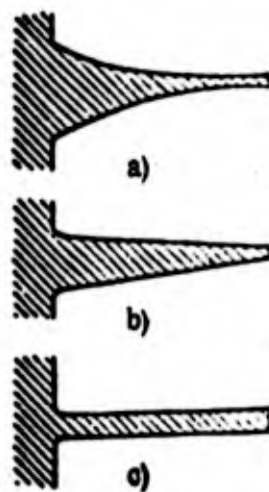
Fig. 33. Shape of fins

surface of the fin is proportional to the temperature difference between the fin and

the surrounding medium;

3) the heat transfer coefficient α is the same at all points on the surface

of the fin;

4) if h is the height of the fin and δ is its thickness, the heat loss

from the end of width   may be taken into consideration by replacing the actual

height h by

$$h_1 = h + \frac{\delta}{2};$$

5) in view of the fact that the thickness δ is small compared with the

other dimensions of the fin, we will take it that the temprature is a function of

one coordinate x (operating value of the height of the fin), i.e., we are dealing

with a uni-dimensional steady-state temperature field.

$$t = f(x).$$

Let us use θ to designate the temperatured difference at any point on

the fin t and the surrounding medium t_0, $\theta = t - t_0$ then $\theta = f(x)$.

Let us develope the round, plane fin along the mean diameter as shown in

Fig. 34. From now on the task is reducible to heat transfer through a rod of finite

length. Let us consider the heat balance of the element of the fin πD_m in length,

δ in   height and dx in width.

- 75 -

The amount of heat entering the element under consideration through the

section I - I per unit of time, according to the Fourier law, is

$$Q_1 = -\lambda \frac{d\theta}{dx} \pi D_{cp} \delta \quad \text{Kcal/hr}$$

The amount of heat leaving the element through the section II.- II per

unit of time is

$$Q_2 = -\lambda \frac{d}{dx}\left(\theta + \frac{d\theta}{dx}\,dx\right)\pi D_{cp}\delta \;\; \kappa\kappa a\lambda/\nu a c.$$

The difference between the amount of heat $\underline{dQ}$ entering the element Q_1 and

the amount leaving it Q_2 is the heat transferred to the surrounding medium. Thus

$$dQ = Q_1 - Q_2 = \lambda \frac{d^2\theta}{dx^2}\pi D_{cp}\delta\,dx. \tag{2.99}$$

But, on the other hand, this amount of heat, $\underline{dQ}$ can be determined by

Newton's law of heat transfer

$$dQ = \alpha\theta 2\pi D_{cp}\,dx. \tag{2.100}$$

Equating the right-hand sides of Eqs. (2.99) and (2.100), we get

$$\lambda \frac{d^2\theta}{dx^2}\pi D_{cp}\delta = \alpha\theta 2\pi D_{cp}\delta,$$

from which

$$\frac{d^2\theta}{dx^2} = \frac{2\alpha}{\lambda\delta}\theta. \tag{2.101}$$

Equation (2.101) is a linear differential equation with constant

coefficients without a right-hand side, exactly the same in form as Eq. (2.78).
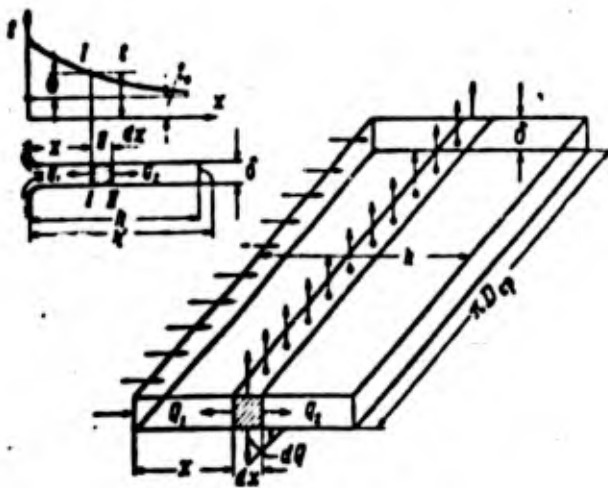
Fig. 34. Calculation of cooling fins

Let us designate

$$\frac{2\alpha}{\lambda\delta} = \mu^2,$$

(2.102)

and write the solution of this differential equation in the form

$$\theta = Ae^{\mu x} + Be^{-\mu x},$$

(2.103)

in which _A_ and _B_ are integration constants.

If we substitute the hyperbolic functions into Eq. (2.103), after

transformation, we get

$$\theta = M\,\mathrm{ch}\,\mu\,(x - \beta_1).$$

(2.104)

The link between the constants in Eqs. (2.103) and (2.104) is expressed

in the following way

$$\left.\begin{aligned} M &= 2\sqrt{AB} \\ \mathrm{th}\,\beta_1 &= \frac{B-A}{B+A} \end{aligned}\right\}$$

(2.105)

The constants _M_ and β_1 in Eq. (2.104) are determined by using first-kind

boundary conditions.

At $x = 0$ $\theta = \theta_0 = t_1 - t_0$.

At $\underline{x} = \underline{h}'$ there can be no further variation in Θ (extreme point in fin).

Hence, $\left(\dfrac{d\theta}{dx}\right)_{x=h'} = 0.$ Thus, $\theta_0 = M\,\mathrm{ch}\,\mu\beta_1$, i. e., $M = \dfrac{\theta_0}{\mathrm{ch}\,\mu\beta_1}$ and

$$\frac{d\theta}{dx} = M\frac{d}{dx}\left[\mathrm{ch}\,\mu\,(x - \beta_1)\right]_{x=h'} = \left[M\,\mathrm{sh}\,\mu\,(x - \beta_1)\right]_{x=h'} = 0.$$

Consequently,

$$\mathrm{sh}\,\mu\,(h' - \beta_1) = 0$$

- 77 -

or according to the definition of a hyperbolic sine,

$$e^{\mu(\kappa-\beta_1)}-e^{-\mu(\kappa-\beta_1)}=0,$$

from which

$$\beta_1=h'.$$

Thus, we finally get the following dependence for the temperature variation along the length of the fin

$$\theta=\theta_0\frac{ch\,\mu\,(x-h')}{ch\,\mu\,h'}.\qquad(2.106)$$

The amount of heat transferred by the fin to the surrounding medium per unit of time can be determined b integrating Eq. (2.110).

$$Q=2\pi D_{cp}\int_0^{h'}\theta\,dx.$$

Substituting for θ the value of it obtained from Eq. (2.106), and removing the integral sign from the constants, we get

$$Q=\frac{2\pi D_{cp}\theta_0}{ch\,\mu\,h'}\int_0^{h'}ch\,\mu\,(x-h')\,dx$$

or

$$Q=\frac{2\pi D_{cp}\theta_0}{\mu}\frac{sh\,(\mu h')}{ch\,(\mu h')}=\frac{2\pi D_{cp}\theta_0}{\mu}th\,(\mu h').\qquad(2.107)$$

If the fin had a constant temperature difference, i.e., a constant temperature θ_0 throughout the height of the fin and a constant temperature of the surrounding medium t_0, the amount of heat transferred by it to the surrounding

medium would be expressed by the following equation

$$Q_o = 2 a \theta_o \pi D_{cp} h'.$$ (2.108)

The ratio of the heat actually *dissipated* by the fin to the amount of heat which the fin could *dissipated* if the temperature difference along the height were constant and equal to θ_o, is called the efficiency of the fin (η_f).

$$\eta_p = \frac{Q}{Q_o}.$$ (2.109)

Substituting the values Q and Q₀ from Eqs. (2.107) and (2.108) into Eq. (2.109), we get

$$\eta_p = \frac{2 a \pi D_{cp} \theta_o}{\mu h' 2 a \pi D_{cp} \theta_o} \, \text{th} \, \mu h'.$$

By makingg reductions we finally get

$$\eta_p = \frac{\text{th} (\mu h')}{\mu h'}.$$ (2.110)

Fig. 35 gives, for purposes of illustration, a graphic expression of the functional dependence of the efficiency of the fin on the value $\mu h'$

$$\eta_p = f (\mu h')$$

Furthermore, Table 2 shows the efficiency of the fin η_f for different fins, the heat-transfer coefficient being taken as identical for all fins and equal to 108 kcal/m^2 hour · deg, which corresponds to the rate of free flow around the surface of 145 km hour.
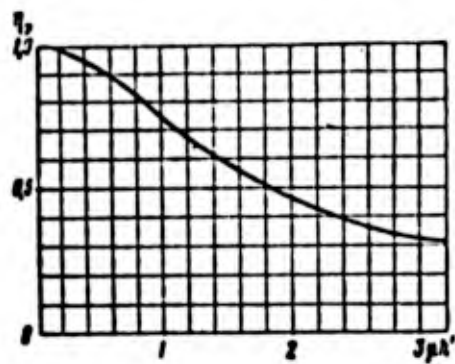
Fig. 35. Efficiency of fin $\eta_p = f(\mu h')$.

Table 2

Tin material	Height of tin, h, $мм$	Thickness of tin, δ $мм$	$\mu = \sqrt{\dfrac{2s}{\lambda\delta}}$	$\dfrac{h'}{\mu}$	$\mu h'$	τ_φ
Aluminum	25	2,3	22,8	0,0261	0,595	0,9
Steel	16	0,8	83	0,0164	1,36	0,65
Copper	25,4	0,5	36,4	0,0256	0,93	0,75

Thus (from the point of view of heat transfer per unit weight) it is

an advantage to have a large number of light, thin fins. This holds till such time

as the air stream flowing round the fin begins to be distorted by the proximity of

the neighboring fins.

The chief problem in designing fins is how near they can be placed to

each other without ~~a~~ seriou~~ly~~ *impairing* their efficiency through a reduction in

the amount of air passing between them.

Example 14. What is the efficiency of a fin in an air-cooled aircraft

engine cylinder if the fin height is $\underline{h} = 12$ mm, the thickness $\delta = 0.8$ mm? The

heat-transfer coefficient between the surface of the fin and the surrounding medium

$\alpha = 190$ kcal/m² hour, deg. The cylinder is made of steel with thermal conductivity

$\lambda = 45$ kcal/m · hour · deg.

Solution.

1) Let us determine the value μ from Eq. (2.102)

$$\mu = \sqrt{\frac{2\alpha}{\lambda\delta}} = \sqrt{\frac{2 \cdot 190}{45 \cdot 0.0008}} = 102;$$

2) Let us determine $\underline{h'}$

$$h' = h + \frac{\delta}{2} = 0.012 + 0.0004 = 0.0124 \ m;$$

3) Let us determine $\mu\underline{h'}$

$$\mu h' = 102 \cdot 0.0124 = 1.26.$$

- 80 -

The table of hyperbolic functions for $\mu \, \underline{b'} = 1.26$ gives us

$$th\,(\mu A') = 0.85106;$$

4) From Eq. (2.110) we can determine the fin efficiency

$$\eta_\varphi = \frac{th\,(\mu A')}{\mu A'} = \frac{0.85106}{1.26} = 0.675.$$

In conclusion we give Tables 3 - 11 showing the thermal conductivity of

different materials /1, 3, 4, 9/.

TABLE 3

Thermal Conductivity of Metals

Material	Temperature in °C	λ kcal/m hour deg
1. Pure metals		
Bismuth	18	7.0
Bismuth	100	5.8
Tungsten	20	138
Pure iron	18	58
Pure Iron	100	54.5
Forged iron	18	52
Forged iron	100	51.6
Gold	18	252
Gold	100	253
Cadmium	18	80
Cadmium	100	77.8
Magnesium	0—100	137
Platinum	18	60
Platinum	100	62.4
Mercury	0	5.4
Mercury	50	6.9
Steel (1% C)	18	39
Steel (1% C)	100	38.6
Antimony	0	15.8
Antimony	100	14.5
Pig iron	54	41
Pig iron	102	40

TABLE 3 (contd)

2. Alloys

Constantin (60Cu, 40Ni)	18	19.5
Constantan (60Cu, 40Ni)	100	23.1
Manganin (84Cu, 4Ni, 12Mn)	18	19.1
Manganin (84Cu, 4Ni, 12Mn)	100	22.6
Nickel alloys (70Ni, 28Cu, 2Fe)	20	30
Nickel alloys (62Ni, 12Cu, 26Fe)	20	11.6
Ballbearing metal (white)	20	20.4

Table 4

Effect of temperature on heat conductivity of metals and alloys, according to International Critical Tables; λ in (kcal/m · hr · deg)

	Temperature,°C							Melting point,°C
	0	100	200	300	400	500	600	
Aluminum	174	177	197	234	274	319	364	617
Brass (90—10)	89	101	115	128	143	155	168	1050
" (70—30)	91	91	95	98	100	103	104	910
" (67—33)	86	92	97	104	110	116	130	910
" (60—40)	91	103	118	131	145	160	172	891
Copper (pure)	337	331	327	322	315	311	307	1083
Nickel	50.6	50.3	49.2	48.9	47.8	47.5	46.2	1452
Tin	54	51	46	—	—	—	—	231
Lead	29.9	29.5	28.3	27.4	—	—	—	315
Silver	361	358	353	318	311	339	334	960
Steel (soft)	54	49	45	40	36	31	27	1530
Tantalum (at 18°)	47	—	—	—	—	—	—	2900
Zinc	97	92	88	84.5	80	—	—	419
Pig iron	43	42	30	34	48	67	82	1200
Pig iron with a high silicon content	45	—	—	—	—	—	—	1200

Table 5

Thermal conductivity of steels λ (in kcal/m · hr · deg) as function of temperature

Type of steel	Temperature, °C						
	100	200	300	400	500	600	700
Carbon							
15	46,8	43,2	39,6	36,0	32,4	28,8	—
30	43,2	39,6	36,0	32,4	28,8	25,2	—
Molybdenum: 15M, 20M 0,5% Mo	36	—	—	—	—	—	—
Chrome-molybdenum:							
12MX; 1% Cr, 0,5% Mo, EI107	32,4	31,6	25,8	—	—	—	—
10% Cr, 0,8% Mo	15,8	—	18,7	—	—	21,2	18,9
Chrome-nickel-tungsten heat resistant EI69, 13-15% Cr, 13-15% Ni, 2-2,8% W	13,3	—	15,6	—	—	18,2	18,9
Chrome stainless EZh-1 15% Co, 12-14% Cr, 0,5% Mn	19,3	18,2	—	20,2	—	18,9	—
Chrome-nickel, acid resistance stainless EYa-T; 18% Cr, 9% Ni	13,4	—	16,7	—	—	20,3	21,3

Table 6

Thermal conductivity of different liquids from data supplied
by N. B. Vargaftik $\lambda \cdot 10^2$ (in kcal/m · hr · deg)

Name of liquid	Temperature, in °C						
	0	25	50	75	100	125	150
Butyl alcohol	13,4	13,1	12,75	12,4	—	—	—
Isopropane "	13,2	12,9	12,55	12,2	—	—	—
Methyl alcohol	18,4	18,12	17,8	17,6	—	—	—
Ethyl alcohol	16,2	15,75	15,25	14,75	—	—	—
Acetic acid	15,2	14,75	14,30	13,9	—	—	—
Formic acid	22,40	22,0	21,65	21,25	—	—	—
Acetone	15,0	14,5	14,0	13,55	13,0	—	—
Nitrobenzene	13,25	12,9	12,6	12,3	12,0	11,7	—
Xylene	11,75	11,3	10,9	10,45	10,1	9,57	—
Benzene	12,15	11,7	11,1	10,6	10,2	9,65	—
Toloune	13,0	12,45	11,9	11,35	10,8	10,35	—
Aniline	16,0	15,6	15,2	14,8	14,45	14,05	13,7
Glycerine	23,8	24,05	24,35	24,6	24,85	25,1	25,4
Vaseline	10,75	10,65	10,5	10,4	10,2	10,1	9,95
Castor oil	15,8	15,55	15,25	15,0	14,7	14,45	14,2

Table 7

Thermal conductivity of certain gases at different
pressures and temperatures
A. Thermal conductivity of air at different pressures
and temperatures $\lambda \cdot 10^4$ (in kcal/m · hr · deg)

p in kg/cm^2	t in °C		
	20	100	180
1	221	263	311
100	239	265	314
200	328	323	351
300	390	371	660
400	431,5	404	418

B. Thermal conductivity of hydrogen at different pressures and temperatures $\lambda \cdot 10^4$ (in kcal/m $\cdot$ hr $\cdot$ deg)

p in kg/cm^2	t in °C			
	15	100	200	300
1	1508	1818	2169	2520
100	1551	1840	2183	2530
200	1607	1877	2211	2554
300	1642	1896	2226	2568
400	1653	1909	2236	2572
500	1660	1917	2239	2576

C. Thermal conductivity of helium $\lambda \cdot 10^4$ (in kcal/m $\cdot$ hr $\cdot$ deg) and t = 43°C at different pressures

p in kg/cm^2	λ	p in kg/cm^2	λ
1	1340	120	1412
10	1345	130	1418
20	1352	140	1424
30	1357	150	1430
40	1363	160	1436
50	1370	170	1442
60	1375	180	1448
70	1382	190	1454
80	1387	200	1460
90	1393	210	1467
100	1400	220	1474
110	1406		

D. Thermal conductivity argon $\lambda \cdot 10^4$ (in kcal/m $\cdot$ hr $\cdot$ deg) and t = 41°C at different pressures

p in kg/cm^2	λ	p in kg/cm^2	λ
1	161	70	183
10	166	80	188
20	169	90	194
30	172	100	199
40	174	110	204
50	176	120	208
60	180	130	213

p in kg/cm²	λ	p in kg/cm²	λ
140	217	180	236
150	222	190	241
160	226	200	246
170	230		

Table 8

Thermal conductivity of nitrogen at different temperatures and pressures $\lambda \cdot 10^4$ (in kcal/m · hr · deg)

p in kg/cm²	t в °C						
	15	25	50	75	100	200	300
1	216	227	233	253	265	317	371
100	243	281	283	292	274	323	373
200	313,5	352	350	350	326,5	354	395
300	374	428	414	407	378	392	425,5
400	406	495	474	463	405	414	444
500	459	556	535	518	455	457	481
600	—	616	592	570	—	—	—
700	—	666	640	618	—	—	—
800	—	712	687	663	—	—	—
900	—	760	734	705	—	—	—
1000	--	804	772	743	--	—	--
1100	—	844	810	780	--	—	--
1200	—	833	846	817	—	—	—
1300	—	922	883	854	—	—	—
1400	—	961	920	889	—	—	—
1500	—	1000	956	925	—	—	—
1600	—	1034	992	959	—	—	—
1700	—	1068	1026	994	—	—	—
1800	—	1103	1060	1027	—	—	—
1900	—	1139	1094	1060	--	—	—
2000	—	1174	1126	1092	—	—	—
2100	—	—	1158	1122	—	—	—
2200	—	—	1189	1153	—	—	—
2300	—	—	—	1182	—	—	—
2400	—	—	—	1212	—	—	—
2500	—	—	—	1240	—	—	—

Note: Thermal conductivity of hydrogen, helium, argon and nitrogen given in Tables 7 and 8 are taken from [3]

Table 9

Thermal conductivity of insulating materials at high temperatures
λ (in kcal/m · hr · deg)

Materials	Up to what temp.	Mean temperature in °C									
		38	93	149	204	260	316	371	427	482	53,
Layer of asbestos felt (about 40 layers per 25 mm)	370	0,049	0,055	0,05	0,065	0,071	—	—	—	—	—
Same (about 20 layers per 25 mm)	260	0,067	0,075	0,082	0,090	0,097	—	—	—	—	—
Wavy asbestos (four folds per 25 mm)	150	0,075	0,086	0,103	—	—	—	—	—	—	—
85% magnesia	315	0,058	0,061	0,061	0,069	—	—	—	—	—	—
Diatomite with asbestos and bond	870	0,067	0,070	0,073	0,075	0,079	0,052	0,090	0,097	—	—
Diatomit brick	870	0,080	0,083	0,086	0,090	0,094	0,097	0,103	0,100	—	—
	1100	0,189	0,191	0,108	0,201	0,208	0,213	0,223	0,235	0,262	—
	1370	0,191	0,195	0,201	0,207	0,213	0,201	0,231	0,243	0,273	0,30
Diatomite powdery (bulk density 290 kg/m³)	—	0,059	0,062	0,066	0,071	0,076	0,080	0,091	0,101	—	—

Table 10

Thermal conductivity of insulating materials at mean temperatures
λ (in kcal/m · hr · deg)

Materials	Bulk density kg/m³	Temperature in °C						
		0	38	93	149	204	316	427
Asbestos	577	0,130	0,145	0,164	0,175	0,180	0,186	0,194
Fired infusor earth for lagging pipes	200	0,064	0,068	0,077	0,085	0,092	0,103	0,127
Insulation (loose)	400	0,060	0,068	0,075	0,079	0,082	—	—
Cotton	80	0,018	0,052	0,055	—	—	—	—
Silk thread	146	0,039	0,045	0,050	—	—	—	—
Silk	100	0,037	0,042	0,050	—	—	—	—
Wool	136	0,033	0,040	0,049	—	—	—	—
Cork powder	160	0,031	0,039	0,048	—	—	—	—
Infusor earth (loose)	350	0,052	0,058	0,067	0,070	0,075	0,079	—

Table 11

Thermal conductivity of insulating materials at low
temperatures λ (in kcal/m · hr · deg)

Materials	Bulk density kg/m³	Temperature in °C				
		0	—45,5	—73,3	—129	—184
Asbestos	700	0,20	0,196	0,194	0,186	0,149
Asbestos	465	0,1330	0,1280	0,1220	0,1072	0,0812
Cotton	80	0,0484	0,0450	0,0411	0,0380	0,0295
Silk	100	0,0432	0,0381	0,0350	0,0292	0,0231

References

1. Kutateladze, S. S. Fundamentals of theory of heat exchange, Chapters 1, 2 and 7. Mashgiz, 1957.

2. Kutateladze, S. S. and others. Liquid-metal heat-transfer agents. Atomizdat, 1958.

3. Kutateladze, S. S. and others. Reference book on heat transfer, Chapters 1 and 3, Gosenergozidat, 1959.

4. Mikheyev, M. A. Fundamentals of heat transfer, Chapter 1, Gosenergozidat, 1956.

5. Predvoditelev, A. S. Certain invariant quantities in theory of heat transfer and viscosity of fluids. "Journal of Physical Chemistry", V. XXII, Issue 3, 1948.

6. Romanovskiy, P. I., Fourier series. Field theory. Analytical and special functions. Laplace transformations, Chapter 5, Gostekhizdat, 1957.

7. Shirokov, M. F. Physical fundamentals of gas dynamics, Chapters 4 and 8. Fizmatizdat, 1958.

8. Shirokov, M. F. Viscosity of fluids and transfer of momentum by waves. Acad. Sci. Press, 1944.

9. Shorin, S. N. Heat transfer, Chapters, 1, 2, 3 and 4. Stroyizdat, 1952.

10. Graber, G., and others. Fundamentals of teaching on heat exchange, For. Lit. Press, 1958.

CHAPTER 3

CONVECTIVE HEAT EXCHANGE AND FUNDAMENTALS OF THEORY OF SIMILARITY

Convective heat exchange or heat transfer is the process of heat exchange which is effected between any solid surface and a fluid *surrounding* it. The process of heat transfer is a complex form of heat exchange and depends both on thermal as well as hydrodynamic phenomena.

In the first section in this book it was pointed out that the heat flux density q kcal/$m^2 \cdot$ hour may be determined by Newton's formula (2.34)

$$q = a \Delta t,$$

in which Δt is the temperature gradient, i.e., the difference between the temperature of the wall and the *fluid surrounding* it; α kcal/$m^2 \cdot$ hour $\cdot$ deg is the heat-transfer coefficient, numerically equal to the amount of heat transferred or received by an element of surface per unit time at a temperature difference between the wall and the receiver of 1°. The heat-transfer coefficient α depends on a whole number of factors: *e.g.,* on the thermodynamic state and physical properties of the medium *surrounding* (the surface (its temperature, pressure, density, viscosity, thermal conductivity, and other parameters); the velocity and conditions of motion of the medium (laminar or turbulent), and on the shape and size of the heat-exchange surface.

- 84 -

It is not possible to study experimentally the effect of any of these factors

on the heat transfer coefficient α , since the variation in one of them inevitably

results in variation of the others. For example, if we change the temperature of the

~~then~~)
medium, (its density, viscosity and thermal conductivity are inevitably changed as

surrounding
well, and the rate and conditions of motion of the medium   the surface may also

change. By virtue of this, the heat-transfer coefficient arrived at experimentally

would only be varied in the conditions under which the test was carried out.

Theoretical analysis of the dependence   of the heat-transfer coefficient

on the factors mentioned above is also difficult, and sometimes impossible. For a

mathematical description of the complex physical phenomena use is made, as is known,

of differential equations of mathematical physics. The differential equations can

be compiled also for processes involving heat transfer.

But to study this complex phenomenon of heat exchange we would have to

use a whole system of differential equations: differential thermal-conductivity

equations, convective heat-exchange equations; motion and solidity equations. On

the   involved
account of mathematical difficulties this system of differential equations cannot

be integrated.

When studying   complex phenomena which cannot be investigated by

strictly mathematical analysis and which it is difficult to investigate experimentally

on account of the large number of variables, we use the methods of the theory of

similarity.

Section 16. Fundamentals of theory of similarity

The study of different cases of heat exchange by mathematical analysis

makes it possible to   obtain a final result in *only very* rare cases. In

most cases it is only possible to give a mathematical formulation of the problem, i.e.,

1) to compile a differential equation describing the phenomenon under

consideration;

2) to determine uniqueness conditions which pick out one specific

phenomenon from a whole class of others described by the differential equation.

But the final solutions of most differential equations are impossible

in most cases on account of   mathematical difficulties. In such cases we have

to turn to the experimental study of a *given, particular* case of heat exchange and find

an   empiric equation providing a link between the characteristic physical parameters

for the phenomenon, derived experimentally.

But the experimental dependences obtained   only relate to the

specific case for which they were *derived*   The extension of them to cover other

phenomena leads to gross errors, which shows how unfounded it is to generalize the

results of investigation of individual cases of heat exchange.

For example, let us assume we have determined the heat-transfer coefficient

from a liquid moving in a pipe to the surrounding medium. The variations in the

rate of motion of the liquid, the conditions of the surrounding medium, and so on

cause a varition in the heat transfer, which is such that the experiment only

specific application

Thus, it transpires that the application of mathematical analysis to

heat exchange leads in most cases to insoluble differential equations, and some

experiments prevent the results being generalized for the whole group of phenomena

under investigation.

The way out of this apparently hopeless situation has been found in the

theory of similarity. This theory makes it possible to extend the results of a single

experiment to a whole group of phenomena. The similarity method enables us to draw

a number of generalizing conclusions from differential equations and uniqueness conditions

without resorting to integration, but merely *by applying* experimental data. We can thereby

determine the limits of generalization of the results of the one experiment.

The term "similarity" is derived from geometry. Geometrically similar

figures possess the property that the ratio of *corresponding* dimensions is the same

number. Figures expressing this characteristic of similarity are known by that name.

It has been found that in heat exchange, too, we can point out a whole

number of similarities between the *relevant* temperature, kinematic and geometric

relationships. If we take, for example, the temperature relationships during heat

exchange, then, as is known, the totality of the temperature relationships provides the

temperature field. It turns out that all the temperature fields can be divided into

a number of groups, reach of which may possess an identical characteristic of

similarity for all cases united by the group. This group of temperature fields possess-

ing identical similarity characteristics is said to be similar.

Analogously, all of the kinematic fields can be divided into a number

of groups, each of which possesses a similarity characteristic, and all the relation-

ships united by this group are therefore known as similar; in other words, all the

kinematic fields making up the said group with the identical characteristics are

similar   among themselves. All this clearly relates to mechanical, geometrical,

physical and other phenomena.

Thus, for similar groups of phenomena and for similar fields we can

give a finite mathematical interpretation without integrating the initial differential

equation. Furthermore, for a   group of fields *of this kind* it is possible to extend

a single experiment to cover a whole group of phenomena.

The methods of the similarity theory are used in aerodynamics, hydraulics,

the theory of ships and other branches of science. The theory   was

- 88 -

first applied to the investigation of heat exchange in 1910 by Nusselt, and has

acquired particular importance in connection with the development of the so-called

thermal simulation, i.e., the method of investigating heat exchange apparatus using

models, put forward by Kirpichev in 1923.

In subsequent years Kirpichev, Mikheyev and other Soviet scientists

carried out a great deal of work on further substantiating and developing this method.

At the present time the theory of similarity is being widely employed in the study

of convective heat exchange, and when applied to it, can produce reliable mathematical

dependences describing the process under investigation.

Concept of Similarity

Geometrical similarity.   AS is well known, the term geometrically

similar figures means figures in which the *corresponding* sides are proportional, *and*

the *corresponding* angles are equal so that if the three triangles shown in Fig. 36 are

geometrically similar, the following relationships can be compiled for them

$$\frac{l_1}{l_1} = \frac{l_2}{l_2} = \frac{l_3}{l_3} = C.$$

This dependence shows that the ratio of the *corresponding* sides of two

similar triangles is the same; the number is designated $\underline{C}$ and is known as the

geometric similarity constant. Thus, the similarity constants of two geometrically

similar figures are the numerical values of the ratio of any *corresponding*.

- 89 -
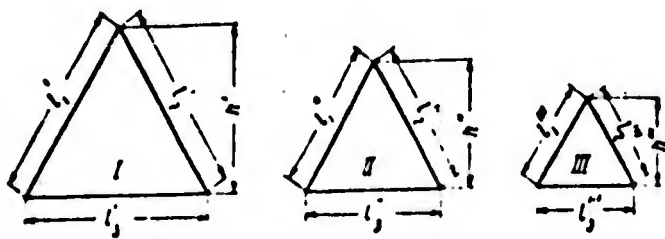
Fig. 36. Geometrically similar triangles

linear dimensions of these figures.

If we consider triangles I and III, a similarity constant can also be obtained for them.

$$\frac{l_1}{l_1} = \frac{l_2}{l_2} = \frac{l_3}{l_3} = C'.$$

Similarly, for triangles II and III

$$\frac{l_1'}{l_1} = \frac{l_2'}{l_2} = \frac{l_3'}{l_3} = C''.$$

In the general case, the values of these constants may be different from each other

$$C \neq C' \neq C''.$$

Other relationships may be compiled on the basis of the geometric similarity of these triangles.

For example, the ratios of like sides of triangles and heights would also be the same

or

$$\frac{l_1}{h'} = \frac{l_1'}{h'} = \frac{l_1''}{h''} = i$$

$$\frac{l_2}{h'} = \frac{l_2'}{h'} = \frac{l_2''}{h''} = i'.$$

These values, as distinct from the similarity constants, are termed similarity invariants and are designated i.

Thus, the similarity invariants of geometrically similar figures are the numerical ratios of two linear dimensions in the same figure. It is not difficult to see that when the figures change, the similarity invariant remains unchanged, while the similarity constant varies while both during a change in segments in the same figure the similarity constant is retained while the similarity invariant changes.

Similarity of physical phenomena. When two physical phenomena are similar, there must be a similarity of the fields of all homogeneous values characterizing the phemonenon in question. This means that at *corresponding* points in the space under study at *corresponding* moments of time, *homogeneous values* of the first phenomenon are proportional to *homogeneous* values of the second phenomenon. Like values hould be taken to mean values which have the same physical significance and the same dimensionality.

Geometric similarity is an essential precondition for the similarity of physical phenomena. For example, if two streams of liquid are to be hydrodynamically similar, they have to be bounded by walls of geometrically similar configuration, and, moreover, there have to be similar velocity fields, accelerations, densities and other parameters in these streams. Similarity constants and invariants can also be compiled for physically similar phemomena.

- 91 -

The similarity constant of physical phenomena is the ratio of like values

at two *corresponding* points in a system under consideration. Here each physical value

has its own similarity constant, which is given a special subscript. For example,

c_u is the velocity similarity constant, c_ρ is the density similarity constant, and

so forth.

If the three streams of liquid shown in Fig. 37 are similar, they must

be bounded by walls of the same shape (for example, cylindrical shape) and here it

is essential to keep the condition

$$\frac{h'}{d'} = \frac{h''}{d''} = \frac{h'''}{d'''} .$$

The condition of physical similarity of the streams may be expressed in

terms of the similarity constant in the following way. Let us take on the axes of

the streams at distances from the initial section $x = d$ the like points in the

streams $0'$, $0''$ and $0'''$ and the points a', a'' and a''' in the same sections at distances

from the tube axis $y = d/4$.

At the given points the velocities and densities of the streams are

designated, respectively,

$$u_0'; \ u_0''; \ u_0'''; \ u_a'; \ u_a''; \ u_a''';$$
$$\rho_0'; \ \rho_0''; \ \rho_0'''; \ \rho_a'; \ \rho_a''; \ \rho_a'''.$$

The velocity similarity constants then take the form

- 92 -
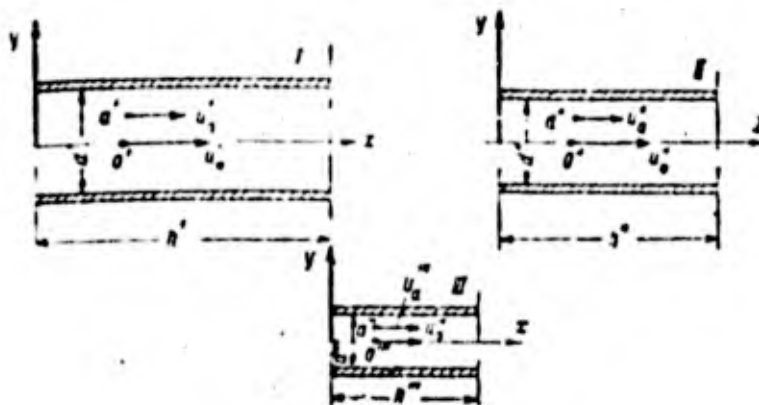
Fig. 37. Hydrodynamically similar fluid flows

$$C_s = \frac{u_0'}{u_0''} = \frac{a_0'}{u_0''}$$

$$C_s = \frac{s_0'}{u_0} = \frac{u_0'}{u_0}$$

$$C_s' = \frac{u_0'}{u_0''} = \frac{u_0'}{u_0}.$$

(3.1)

The [density] similarity constants [are]

for

$$C_t = \frac{t'_a}{t'_o} = \frac{t''_a}{t_a}$$

$$C_t = \frac{t'_a}{t_o} = \frac{t''_a}{t_a}$$

$$C_t = \frac{t''_o}{t_o} = \frac{t'_a}{t_a}.$$

(3.2)

In the general case

$$C_a \neq C_a \neq C_a^{\cdot}.$$
$$C_t \neq C_t \neq C_t.$$

The similarity invariants of these streams may be   represented in the

following way

$$i_a = \frac{u'_a}{u_o} = \frac{u'_a}{u_o} = \frac{u''_1}{u_o}$$

$$i_t = \frac{t'_a}{t_o} = \frac{t'_a}{t_o} = \frac{t''_a}{t_o}.$$

(3.3)

Clearly, when the streams change, the similarity invariant remains

unchanged, but the similarity constant varies. The similarity invariants which

represent the ratio of two like physical values, are called invariant simplexes.

Given the physical similarity of complex phenomena, x the similarity

invariants can be derived in the form of dimensionless complexes made up of unlike

physical   quantities   describing the phenomenon under consideration. These dimensionless

complexes are termed dimensionless numbers.

The dimensionless numbers can be obtained for any physical phenomenon ,

provided there is an analytical dependence between the variable physical values of

the particular phenomenon. This was first shown by Newton for the case of mechanical

similarity.

- 93 -

Let us illustrate this with an example. According to Newton's second law,

equals

force is/mass times acceleration

$$P = m\frac{du}{d\tau}.$$ (3.4)

Here $\underline{m}$ is the mass of a body in kg $\cdot$ sec^2/m; $\underline{u}$ is the velocity in m/sec, and τ is time

in seconds.

If we have two similar systems, then by applying this equation to two

corresponding

$\to$ points in these systems we can write

$$P' = m'\frac{du'}{d\tau'},$$ (3.5)

for the first system, and

$$P'' = m''\frac{du''}{d\tau''}.$$ (3.6)

for the second. The similarity constants in this case take the form

$$C_p = \frac{P''}{P'}; \quad C_m = \frac{m''}{m'}; \quad C_u = \frac{u''}{u'}; \quad C_\tau = \frac{\tau''}{\tau'}.$$

Let us express the variables making up Eq. (3.6) in terms of the similarity

constants and the variables in the first system

$$C_p P' = C_m \frac{C_u}{C_\tau} m'\frac{du'}{d\tau'}$$

or

$$\frac{C_p C_\tau}{C_m C_u} P' = m'\frac{du'}{d\tau'}.$$ (3.7)

It is clear from comparison of the expressions derived with Eq. (3.6)

that the complex composed of the similarity constants $\frac{C_p C_\tau}{C_m C_u}$ should be equal to unity.

- 94 -

These complexes composed of similarity constants are termed similarity

indicators

$$\frac{C_p C_\tau}{C_m C_u} = 1. \tag{3.8}$$

If in the latter expression we replace the similarity constants by

variables, the expression takes the form

$$\frac{\frac{p''}{p'} \cdot \frac{\tau''}{\tau'}}{\frac{m''}{m'} \cdot \frac{u''}{u'}} = 1,$$

from which

$$\frac{p' \tau'}{m' u'} = \frac{p'' \tau''}{m'' u''} . \tag{3.9}$$

It appears that if we had a third similar system, it would have been

possible to write for it

$$\frac{p' \tau'}{m' u'} = \frac{p'' \tau''}{m'' u''} = \frac{p''' \tau'''}{m''' u'''} .$$

When going from one system to another, the complex invariant derived

remains unchanged. It is not difficult to see that the invariant complex is

dimensionless. It is termed the Newton dimensionless number and is designated Ne

$$Ne = \frac{p \tau}{mu} . \tag{3.10}$$

Three Theorems of Similarity

First theorem of similarity. The theory of similarity is based on three

theorems of similarity.

The first theorem is as follows: in phenomena similar to themselves

- 95 -

like dimensionless numbers are identical, and the similarity indicators are equal to

unity. As was shown above for a case of mechanical similarity, the dimensionless

numbers are ascertained on the basis of *the* analytical dependence between *the* *quantities* physical

describing the phenomenon under consideration.

The arithmetical dependences between the physical *quantities* are established

on the basis of the general laws of physics and in the case of complex phenomena

can be represented in the form of differential equations. The importance of the

first theorem of similarity is that it indicates the possibility of obtaining a d

dimensionless number from the differential equations of mathematical physics without

having to integrate them. In order to obtain the dimensionless numbers,

these differential equations should undergo so-caled similarity transformations.

The similarity transformations consist in the following: on the basis of

an analytical description of the phenomena for two similar systems we ascertain the

similarity constants; then the variables in the equation for the second system are

expressed in terms of like variables of the first system, multiplied by the

corresponding similarity constants. After this the values in the equations derived

are grouped in such a way that the similarity constants make up similarity indicators,

which should be equal to unity. The similarity constants making up the similarity

indicators derived are then replaced by the ratio of the corresponding variables and

- 96 -

we get the dimensionless numbers. A very simple

example of a similarity transformation was considered above when deriving the Newton

dimensionless number Ne.

As was pointed out, when studying complex phenomena we have to use a

system of differential equations.

For example, *textbooks* courses on hydrodynamics, use differential

equations for motion and the equation for solidity (when *discussing* the hydrodynamic

similarity of two geometrically similar streams of liquid) in order to ascertain the

dimensionless numbers. When deriving these equations, we select a system of coordinates

: xyz and in the medium under consideration we single out an elementary

parallelepiped, the sides of which are designated dx, dy and dz, respectively,

in the same way as was done to derive the thermal-conductivity differential equation

in the first section in this book. After that we consider the forces acting on this

element.

When deriving differential equations *of* motion we use Newton's second

law, and as a result obtain the following system of equations, which *are* termed

the Navier-Stokes equations

(See page 97a) (3.11)

in which ρ is the density of the medium in kg sec^2/m^4;

- 97 -

$$\rho \frac{\partial u_x}{\partial t} + \rho \left(u_x \frac{\partial u_x}{\partial x} + u_y \frac{\partial u_x}{\partial y} + u_z \frac{\partial u_x}{\partial z} \right) = \rho g_x - \frac{\partial p}{\partial x} + \mu \nabla^2 u_x$$

$$\rho \frac{\partial u_y}{\partial t} + \rho \left(u_x \frac{\partial u_y}{\partial x} + u_y \frac{\partial u_y}{\partial y} + u_z \frac{\partial u_y}{\partial z} \right) = \rho g_y - \frac{\partial p}{\partial y} + \mu \nabla^2 u_y \qquad (3.11)$$

$$\rho \frac{\partial u_z}{\partial t} + \rho \left(u_x \frac{\partial u_z}{\partial x} + u_y \frac{\partial u_z}{\partial y} + u_z \frac{\partial u_z}{\partial z} \right) = \rho g_z - \frac{\partial p}{\partial z} + \mu \nabla^2 u_z.$$

u_x, u_y, u_z — are projections of the velocity $\underline{u}$ of motion of the element on the corresponding

coordinate axes in m/sec;

g_x, g_y, g_z — are the same for acceleration due to gravity in m/sec

μ — is the viscosity coefficient in kg · sec/m

τ — is the time in sec;

$\underline{p}$ is the pressure in kg/m^2

The differential solidity equation is derived by means of the law of

conservation of mass, and takes the form

$$\frac{\partial \rho}{\partial \tau} + \frac{\partial (\rho u_x)}{\partial x} + \frac{\partial (\rho u_y)}{\partial y} + \frac{\partial (\rho u_z)}{\partial z} = 0. \tag{3.12}$$

If these equations undergo similarity transformations, the following

dimensionless numbers are obtained.

Geometrical similarity dimensionless number $\quad \frac{h}{d} = i;$ (3.13)

The homochronic similarity number $Ho = \frac{u\tau}{l}$;

(3.14)

The Froude number $\quad Fr = \frac{gl}{u^2};$

(3.15)

The Euler number $\quad Eu = \frac{p}{\rho u^2};$ (3.16)

The Reynolds number $\quad Re = \frac{ul}{\nu};$ (3.17)

in which $\underline{h}$ and $\underline{d}$ are the length and diameter of the stream in m;

ν — is the coefficient of kinematic viscosity in m^2/sec;

$\underline{l}$ is the characteristic dimension;

If the stream is of circular section, then $\underline{l} = \underline{d}$, and in the case of a

stream with rectangular section

$$l = d_{м.з.} = \sqrt{\frac{4F}{\pi}}$$

and $\underline{F}$ is the area of the cross-section of the stream in $\underline{m}^2$.

Consequently, if two streams of liquid are hydrodynamically similar,

(h/d, Ho, Fr, Eu, Re)

the dimensionless groups obtained (/) must have the same numerical value at

any corresponding points in the streams.

The equality of the dimensionless groups, $\frac{l_1}{d} = \underline{L}$, as pointed out, is an

Similarity of

essential precondition for physical phenomena. The quality of the homochronous

numbers Ho is essential in studying non-steady-state, but periodically repeated

detachment of vortices [around a body

phenomena (for example,   during   flow]).

Second theorem of similarity. The second theorem of similarity

establishes the possibility of representing the mathematical description of the

phenomenon under consideration in the form of a functional dependence between the

dimensionless groups. This functional dependence is termed the dimensionless

characteristic

equation. Here the dimensionless groups are divided into the   and the

unknown groups)

The *unknown* dimensionless group is one which contains an unknown value.

The *characteristic* groups are ones composed of values set by uniqueness conditions.

The dimensionless equation should establish the functional dependence of
the *unknown* number *on* the other *characteristic* dimensionless numbers. For example,

when studying the hydraulic resistance of horizontal tubes in a case of steady-state
isothermal flow, the *characteristic* dimensionless numbers are the Reynolds number

$Re = ul/v$ and the geometric dimensionless number $h/d = 1$, while the Euler number,

which in this case is represented in the form $Eu = \Delta p / \rho u^2$, in which Δp is the pressure

drop at two points in the system under consideration is the *characteristic*

dimensionless number. This is due to the fact that when studying hydraulic

resistances of pipes the unknown value is the pressure difference Δp which *appears* in

the Euler number numerator.

The other hydrodynamic dimensionless numbers - the homochronous number
$Ho = u\tau/l$ and the Froude number $Fr = gl/u^2$ - are not *characteristic* in steady-state

isothermal flow, and need not be introduced to the differential equation. In the

case in point, the dimensionless equation takes the form

$$Eu = f\left(Re, \frac{h}{d}\right).$$

The form of this function is established on the basis of careful analysis of

experimental data derived for the given phenomenon.

Thus, it follows from the second theorem of similarity that the mathematical description of the phenomenon in question can be represented in the form of a functional dependence between the dimensionless groups. In certain cases the form of the function can be established theoretically, although it is more often established on the basis of experimental data.

The importance of the second similarity theorem is that it shows which of the results should be processed. They have to be represented in the form of a dimensionless equation.

If the investigation is based on experiment, the results of the experiments should be processed in such a way that the dependence between the dimensionless complexes composed of these variable physical values rather than in such a way that the dependence between the individual variable dimensionless numbers was represented. Consequently, the experimental data should be processed in such a way that we can establish the dependence between the dimensionless groups and obtain a dimensionless equation.

Third theorem of similarity. The dimensionless equations based on the precepts of the second theorem of similarity are valid both for a phenomenon for which they were obtained and also for all phenomena similar to the one studied.

The third theorem of similarity answers the question, which phenomena

should be considered similar. According to this theorem, similar phenomena are x those

characteristics

for which the mathematical description coincides and the like   dimensionless

groups are numerically equal.

The significance of this theorem may be explained with the example given

above. The following dependences can be compiled for two steady-state, isothermal

streams:

For the first stream $Eu' = f'\left[Re', \left(\frac{\hbar}{d}\right)' \right].$

For the second stream $Eu'' = f\left[Re'', \left(\frac{\hbar}{d}\right)'' \right].$

These streams are similar to one another xon condition that the dimensionless

groups in the equation have the same value at corresponding points in the streams

$$Re' = Re''; \quad \left(\frac{\hbar}{d}\right)' = \left(\frac{\hbar}{d}\right)''; \quad Eu' = Eu''$$

and if the forms of the functions f' and f'' are similar.

Thus, the third theorem of similarity points out the requirements necessary

and sufficient to satisfy in order for the phenomena to be similar. The practical

importance of the third theorem of similarity is that it enables us to single out a

group of phenomena, to which we can extend data for single experiments, represented

in the form of dimensionless equations. Furthermore, the third theorem has been

used to establish a new method of investigation - the method of models.

- 102 -

The application of the method of models to the study of heat exchange at

the present time is very common and is termed thermal simulation. The research model

is constructed in such a way that it reproduces the design elements of the specimen,

important for the process under study, which is carried out in the ∮ model in the same

way as it would *be done* in the specimen.

The third theorem of similarity shows which conditions have to be satisfied

here, *i.e.,* the like *characteristic* groups *at* corresponding points in the specimen and

model should have the same numbrical value; furthermore, the mathematical descriptions

of the processes occurring in the specimen and model should be identical.

The main difficulty in using the theory of similarity is correct selection

of the *characteristic* dimensionless groups. Groups which in one case are *characteristic*

may be *unknown* in another case, or of no importance at all for the phenomenon in

question. When selecting the *characteristic* dimensionless groups, a large part is played

by self-similarity and stability.

Stability, self-similarity and the approximate simulation method.

When studying complex phenomena it is difficult to provide all the

conditions ensuring complete similarity between the model and the specimen, and in

certain cases it is not necessary. In practice, when studying such complex phenomena

as convective heat exchange, *a* part of the set of interacting processes is studied,

- 103 -

rather than the whole. In this case we use the method of so-called approximate

simulation. This is based on *special* properties of a viscous liquid, which

are termed stability and self-similarity.

Stability is the ability of a viscous liquid to follow a fully determined

velocity distribution law when moving in channels of different shape.

Experience shows that during the motion of a liquid in a horizontal channel at

some distance from the channel inlet the velocity distribution in the cross-section

of the stream is always the same, irrespective of the nature of the velocity

distribution in the channel inlet section.

Self-similarity *can be defined,* as follows: investigation shows that the variation

within certain limits of a *characteristic* dimensionless group does not always result

in variation in the *unknown* group, i.e., it does not have an effect on the

process under consideration. For example, when liquid moves through a channel,

the variation within certain set limits in the Re number has no effect on the

velocity distribution in the channel cross-section. This phenomenon is termed

self-similarity.

Self-similarity and stability make it possible to simplify the

differential equations and marginal conditions by disregarding the unimportant

factors. Furthermore, self-similarity and stability make it possible to use the

- 104 -

so-called local heat similarity method ~for~ studying heat exchange.

This method is as follows: when studying the operation of any aggregate the similarity (is ~principle applied~ in certain parts of it rather than in the whole aggregate. Then, on the basis of a careful study of the processes taking place in these areas, a general conclusion is drawn with regard to the work as a whole. This method is widely used to study processes occurring in the combustion chambers of jet engines, in study of various heat-exchange apparatus, and in other cases.

The model method enables us tom study a process to the fullest and simplest extent, and to apply the results to the specimen on the ~basis of the~ (theory of similarity.

The simulation method is used in various branches of engineering and is a reliable and powerful instrument for studying the work of both existing apparatus as well as ~devices~ under construction.

Determining Dimensionless Groups from Averaged Values

When using the methods of the theory of similarity the dimensionless groups making up the dimensionless equations are not usually established for individual corresponding points in the systems s under consideration, but for averaged parameters. The possibility of averaging parameters describing processes in similar systems is the result of the similarity of these systems. For example, during laminar flow by a liquid in a closed channel ~it moves at~ different velocities at

different points in the cross-section. The mean velocity of motion of the liquid in

the cross-section of the channel may be represented in the following way

$$u_{cp} = \frac{\int u_w dF}{F},$$

in which u_w is the local velocity and F is the cross-section of the channel.

If there are two similar streams of liquid, then obviously the velocity

similarity constants C_u have the same value for all corresponding points in the

corresponding sections of the streams. It follows from this that the ratio of

the velocities averaged for the section in corresponding sections of the streams are

numerically equal to the same similarity constant C_u.

Consequently, the Reynolds number may be calculated from the averaged

velocity when studying these streams.

What has been outlined above shows that the theory of similarity is of

extremely great importance in studying complex phenomena. Every complex physical

phenomenon is described by a large number of unlike, interconnected parameters.

If an attempt is made to establish the dependence between these values on the basis

of experimental data, the dependence is only valid under the experimental conditions

and cannot be used if they in any way deviate. The study of these complex physical

phenomena should be based on the theory of similarity.

We can obtain a dimensionless group on the basis of the first theorem of

similarity from differential equations describing various aspects of the complex

phenomenon in question. Here the equations may undergo similarity transformations

without resorting to integrations. Then, on the basis of the second theorem, we have

to ascertain the functional dependence between the dimensionless groups established.

In this way, the results of the investigations should be represented in the form of

dimensionless equations. The equations obtained are valid for all phenomena similar

to *the one* investigated. The similarity of the phenomena is established on the basis of

the third theorem of similarity.

It should be kept firmly in mind, however, that the theory of similarity

does not provide a general solution. Equations *derived on the basis* of this

theory generalize experimental data for the phenomena similar to each other.

The theory is called the theory of experiment, since it is of very great importance

in a study of processes which is based chiefly on experiment. The convective heat

exchange is just one such process.

Section 17. Application of Theory of Similarity to Study of Convective

Heat Exchange

Differential Equation for Convective Heat Exchange and
Dimensionless Groups

As shown above, convective heat exchange is a complex form of heat

exchange and depends on a whole number of factors, including the nature of motion of

medium *slowly past* the solid surface.

There are two types of motion - free and forced motion - according to the

origin of it. Free motion is the motion of a liquid which occurs through a difference

in densities between the hot and cold parts of the liquid (i.e., on account of a

temperature difference). Forced motion is the motion of a liquid which is caused by

extraneous agents (pumps, fans, bodies moving *through a* liquid, and so on). In the

general case free motion may exist side-by-side with forced motion.

The motion of a liquid is also distinguished by the nature of the motion.

It is known from hydraulics that there are two different types of motion - laminar

and turbulent. In laminar flow the streams of liquid (gas) move in parallel without

mixing. In laminar flow heat exchange is chiefly conditioned by thermal conductivity

in the liquid (gas),

During turbulent flow there is no parallel motion in the streams of liquid.

Some volumes of *liquid* move in disorderly fashion, and mix with each other in a

chaotic way. When flowing round different solid surfaces, the velocity of the stream

drops near the circumvented surface and on the surface of the circumfented

body becomes equal to zero on account of viscosity. If the liquid flowing round the

body is not very viscous (for example, air ar other gases) the effect of viscosity
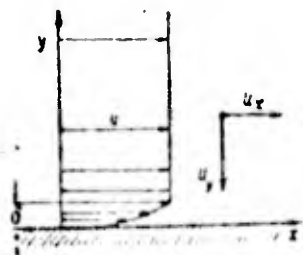
Fig. 38. Concept of boundary layer

only shove$ up in a thin layerof liquid near the circumvented surface.

If the stream of fluid moves along a surface at a constant rate, as shown in Fig. 38, the equal distribution of velocities is *disturbed* in a thin layer of thickness δ located near the solid surface.

In this layer the velocity of the stream u drops to zero on the surface of the solid body on account of viscosity. The thin layer in which the properties of the fluids are manifested is called the boundary layer.

Study has shown that in many cases the boundary layer may be regarded as a layer in which laminar flow is retained. But this idea is *conditional* tentative, and in actual fact the boundary layer is not laminar. In the main turbulent flow, some *the moves in* of liquid complex spirals, on account of which there occur in the stream pulsati*ng*, transverse velocity components u, u_y which are damped by the wall in the boundary layer. On account of the smallness of the pulsation transverse components in the layer adjoining the circumvented surface, it is regarded conditionally as laminar. The thickness of this layer δ is a function of the viscous properties of the liquid, its velocity of motion and the temperature.

In the boundary layer the transfer of heat depends mainly on the thermal conductivity of the liquid and in the bulk of the turbulent flow the transfer of heat is brought about by turbulent mixing. This *notion* of the transfer of heat during motion

- 109 -

of a liquid along a solid surface may be used to find an equation describing the heat transfer on the boundaries of the body.

If the heat is transferred through the laminar boundary layer of liquid on account of thermal conductivity, we can write the following on the basis of the Fourier law

$$dq = -\lambda \frac{\partial t}{\partial y}.$$

On the other hand on the basis of Newton's law this elementary heat flux can be determined by the dependence

$$dq = \alpha(t_j - t_u),$$

in which t_j is the mean of the liquid and t_w is the mean temperature of the surface.

Equating the right-hand sides of these equations, we get

$$-\lambda \frac{\partial t}{\partial y} = \alpha(t_j - t_u),$$

from which

$$\alpha = -\frac{\lambda}{\Delta t} \cdot \frac{\partial t}{\partial y} \qquad (3.18)$$

or

$$\alpha \Delta t = -\lambda \frac{\partial t}{\partial y}.$$

Here

$$\Delta t = t_j - t_u.$$

Equation (3.18) is termed the differential equation of convective heat exchange.

An essential condition in the thermal similarity of streams is the presence

of geometric and hydrodynamic similarity. Hence, at like points of systems similar

in a thermal respect the hydrodynamic dimensionless group and the thermal group should

have the same value.

The hydrodynamic dimensionless groups Ho, Fr, Eu and Re were established

earlier. In order to ascertain the thermal dimensionless groups we have to have

differential equations describing the process in question.   When studying convective

heat exchange, the following can be used as these equations:

1) the differential convective heat-exchange equation (3.18) $\alpha \Delta t = -\lambda \frac{\partial t}{\partial y}$.

2) the differential thermal-conductivity equation for a medium in motion
$$\frac{dt}{d\tau} = a \nabla^2 t,$$

$$(3.19)$$

$$\frac{dt}{d\tau} = \frac{\partial t}{\partial \tau} + u_x \frac{\partial t}{\partial x} + u_y \frac{\partial t}{\partial y} + u_z \frac{\partial t}{\partial z},$$

in which $\frac{dt}{d\tau}$ is the substantial derivative and $a = \frac{\lambda}{c_p \gamma}$ is the thermal conductivity.

If there are two systems similar in a heat respect, then Eqs. (3.18)

and (3.19) can be compiled for each of them.

For the first system

$$a' \Delta t' = -\lambda' \frac{\partial t'}{\partial y'},$$ $$(3.20)$$

$$\frac{\partial t'}{\partial \tau'} + u'_x \frac{\partial t'}{\partial x'} + u'_y \frac{\partial t'}{\partial y'} + u'_z \frac{\partial t'}{\partial z'} = a' \nabla^2 t',$$ $$(3.21)$$

for the second system

- 111 -

$$a'' \Delta t'' = -\lambda'' \frac{\partial t''}{\partial y''}. \tag{3.22}$$

$$\frac{\partial t''}{\partial \tau''} + u_x' \frac{\partial t''}{\partial x''} + u_y' \frac{\partial t''}{\partial y''} + u_z' \frac{\partial t''}{\partial z''} = a'' \varsigma^2 t''. \tag{3.23}$$

These equations have to undergo similarity transformations in order to ascertain the determining dimensionless groups.

As in the example of mechanical similarity quoted above, in order to carryout similarity transformations we have to ascertain the similarity constants and express the variables in Eqs. (3.22) and (3.23) in terms of the similarity constants and variables of the first system.

The similarity constants in the case in point are as follows

(See page 112a)   (Eq.)

Expressing the variables of the second system in Eqs. (3.22) and (3.23) in terms of the variables of the first system and the similarity constants, we get the following equations

$$C_a C_t x' \Delta t' = -C_\lambda \frac{C_t}{C_l} \lambda' \frac{\partial t'}{\partial y'}. \tag{3.24}$$

$$\frac{C_t}{C_\tau} \cdot \frac{\partial t'}{\partial \tau'} + \frac{C_u C_t}{C_l} \left(u_x' \frac{\partial t'}{\partial x'} + u_y' \frac{\partial t'}{\partial y'} + u_z' \frac{\partial t'}{\partial z'} \right) =$$

$$= \frac{C_a C_t}{C_l^2} a' \left(\frac{\partial^2 t'}{\partial x'^2} + \frac{\partial^2 t'}{\partial y'^2} + \frac{\partial^2 t'}{\partial z'^2} \right). \tag{3.25}$$

Joint solution of Eqs. (3.24) and (3.20), and then (3.25) and (3.21) gives us

$$\frac{C_t}{C_\tau} = \frac{C_u C_t}{C_l^2} ; \quad \frac{C_u C_t}{C_l} = \frac{C_a C_t}{C_l^2}, \quad C_a C_l = \frac{C_\lambda C_t}{C_l}.$$

$$\frac{x}{x'} = \frac{y}{y'} = \frac{z}{z'} = C_1; \quad \frac{z}{z'} = C_2; \quad \frac{a'_x}{a'_z} = \frac{a'_y}{a'_y} = \frac{a'_z}{a'_z} = C_3;$$

$$\frac{t}{t'} = \frac{\Delta t''}{\Delta t'} = C_4; \quad \frac{d}{d'} = C_5;$$

$$\frac{v}{v'} = C_6; \quad \frac{a'}{a'} = C_7.$$

The similarity indicators can be obtained from here

$$\frac{C_c C_\gamma}{C_i^2} = 1, \quad \frac{C_a C_l}{C_a} = 1, \quad \frac{C_a C_l}{C_\lambda} = 1.$$

Expressing the similarity constants in terms of variables, we get the

invariant complexes.
$$\frac{c\tau}{l^2} = \text{inv}.$$

$$\frac{ul}{a} = \text{inv}, \quad \frac{ul}{\lambda} = \text{inv}.$$

The dimensionless invariant-complexes derived are thermal dimensionless

groups and possess the following names: $c\tau/l^2 = \text{Fo}$ — is the Fourier number, describing

the similarity of physical fields in time; $ul/a = \text{Pe}$ is the Péclet number. It can

. be represented in other ways, if we multiply and divide the complex by the

kinematic viscosity coefficient

$$\text{Pe} = \frac{ul}{a} \cdot \frac{\nu}{\nu} = \frac{ul}{\nu} \cdot \frac{\nu}{a}. \tag{3.26}$$

As is ~~~~~~ known, the complex $ul/\nu = \text{Re}$ is the hydrodynamic Reynolds number.

The ratio between the kinematic viscosity coefficient ν and the thermal

diffusivity a is known as the Prandtl number $\text{Pr} = \nu/a$. The Prandtl number describes

the physical properties of a medium flowing round a solid body (surface). The

coefficient of kinematic viscosity a describes the viscous properties of a liquid,

which condition the molecular transfer of the amount of motion. The thermal

diffusivity a which is equal to the ratio between the thermal conductivity and the

volumetric thermal capacity $a = \lambda/c_p\gamma$, expresses the intensity of the molecular

heat transfer. The Prandtl number can be regarded as a measure of the similarity

of the velocity and temperture fields, since experiment shows that for liquids in which

Pr ≈1, the velocity and temperture fields in the boundary layer are similar. In the

case of gases the Pr number is close to unity and depends chiefly on the atomicity

of the gas. The Pr number for gases with different atomicity is shown in Table 12.

The complex $a//\lambda = Nu$ is the Nusselt number. This number is *an unknown* when

studying heat exchange, since it contains the *an* unknown value - the heat transfer

coefficient α.

An essential precondition for thermal similarity, as has already been

pointed out, is hydrodynamic similarity. Consequently, given the thermal

similarity of two geometrically similar systems, at corresponding points the

following dimensionless groups must have the same values

$$Nu, \ Pr, \ Re, \ Fo, \ Ho, \ Fr, \ Eu.$$

The type of dimensionless groups may be altered by a corresponding

regrouping of the physical values describing the phenomenon in question. A third,

derivative group can be made from two *characteristic* groups. This is usually done

on the basis of the *possibilities for* the experiment.

For example, when studying convective heat exchange the Froude number

$Fr = gl/u^2$ describing the ratio between gravity and inertia is represented in a

- 114 -

Table 12

Atomicity gas	2	3	4
Pr	0.72	0.8	1.0

different way.

In free motion of a liquid caused by a density difference, the rate of motion of the liquid cannot be measured and the Grashof number is introduced instead of the Fr number

$$Gr = Fr \, Re^2 \beta \Delta t, \tag{3.27}$$

in which β is the coefficient of volumetric expansion (for gases $\beta = \frac{1}{T}$), and Δt is the temperature difference at ~~the two plates~~ in the system.

Substituting the Fr and Re numbers into the expression for the Gr number we get

$$Gr = \frac{g l^3}{\nu^2} \Delta t,$$

For gases

$$Gr = \frac{g l^3}{\nu^2} \frac{\Delta t}{T}.$$

The ~~unknown~~ dimensionless group which includes the heat-transfer coefficient α may also be altered. In certain cases, the Nusselt number is replaced by the Stanton number, St, which is equal to the ratio of the Nusselt number $Nu = \alpha l / \lambda$ and the Péclet number $Pe = u l / a$:

$$St = \frac{\alpha l}{\lambda} \cdot \frac{a}{u l}.$$

Taking it into account that the thermal diffusivity is equal to $a = \lambda / c_p \gamma$, we can derive the following ~~Stanton~~ number $St = \frac{\alpha}{c_p \gamma u}.$

- 115 -

When determining the Stanton and Péclet numbers we have to keep it in mind that the thermal diffusivity a is usually measured in hour/m^2; hence the velocity u must be expressed in m/hour.

Hence

in the most general form the dimensionless equation should be represented as a functional dependence of the Nusselt or Stanton number on the other numbers considered above

$$Nu = f(Ho, Gr, Eu, Re, Fo, Pr)$$

or

$$St = f(Ho, Gr, Eu, Re, Fo, Pr).$$

When investigating steady-state processes the Ho and Fo numbers are not *characteristic*. Furthermore, as shown by experiment, when the gas flow is subsonic, the Eu number can be excluded from the dimensionless equation on account of self-similarity, since the hydrodynamic similarity in this case is retained even if there is no similarity between the absolute pressure fields.

Study shows that in certain cases the intensity of heat exchange is influenced by the temperature gradient and direction of the heat flux.

Mikheyevich has suggested that in order to take these phenomena into account we should add the ratio of $Pr_{\hat{f}}/Pr_{\hat{w}}$ to the dimensionless equation, where Pr is the Prandtl number for the mean temperature of the liquid, and $Pr_{\hat{f}}$ is the Prandtl number for the temperature of the surface. The dimensionless equation for a steady-state process can then be represented as

$$Nu = f\left(Re,\ Gr,\ Pr,\ \frac{Pr_f}{Pr_w}\right)$$

or

$$St = f\left(Re,\ Gr,\ Pr,\ \frac{Pr_f}{Pr_w}\right).$$

The form of the function f is established on the basis of experimental data with a careful analysis of the process in question. When studying more complex phenomena, for example the motion of gas at a high velocity, or variation in the aggregate state, we have to introduce *additional characteristic* numbers for the phenomena under investigation.

Averaging of Temperature

Newton's formula $q = \alpha(t_{\hat{f}} - t_{\hat{w}})$ contains the temperature of the medium (fluid) *flowing over* the surface. The temperature differs at different points in the stream during heat exchange. In this case, the temperature of the *fluid* $t_{\hat{f}}$ is taken to *be* a mean temperature. There are several methods of averaging the temperature of the *fluid*

- 117 -

If we can disregard variation in the rate of motion of the liquid in
the channel section, t_f can be calculated as the mean temperature of the liquid
through the section

$$t_f = \frac{\int t\, df}{F}$$

(3.28)

or approximately,

$$t_f = \frac{\Sigma t f}{F}.$$

In this case the transverse section of the stream F is broken down into
a number of elements of area Δf. The value t is determined by measuring the
temperature at different points in the stream section and is mean for an element
with area Δf.

If the rate of motion of the fluid is not constant throughout the stream
section, t_f is defined as the mean volumetric temperature

$$t_f = \frac{\int t\, dv}{v},$$

(3.29)

in which dv is the volume of liquid passing through the element per second, and
v is the volume of liquid passing through the cross-section of the stream per second.

If the temperature of the moving medium varies along the stream, then
we average the temperature gradient Δt by the following equation

$$\Delta t = \frac{t_f - t_f'}{\ln \dfrac{t_f - t_w}{t_f' - t_w}}.$$

(3.30)

- 118 -

in which t_f' and t_f'' are the mean temperature of the liquid at the initial and
terminal sections of the stream, respectively.

Characteristic
temperature. The various physical parameters $(c, \lambda, \rho$ etc.)
making up the determining dimensionless numbers vary with temperature, hence when
choosing these parameters they should be related to a certain temperature, which
is indeed called the *characteristic* temperature.

This temperature may be selected in different ways, in accordance with
the premises of the problem. In certain cases the mean temperature of the *fluid* t_f
is taken as the *characteristic* temperature while in other cases they take the arithmetic
mean temperature of the boundary layer (t_m)

$$t_m = \frac{t_1 + t_2}{2}.$$

Sometimes the *characteristic* temperature is taken to be the mean temperature
of the washed surface t_w. In dimensionless equations it is usually pointed out
which temperature has been taken as the *characteristic* one, and subscripts are used
for this. For example, Nu_m means that when determining the values making
up the Nusselt number, the mean temperature of the boundary layer (t_m) was taken
as the *characteristic* temperature. The *characteristic* temperaures t_f and t_w correspond
to the Nu_f and Nu_w numbers.

- 119 -

Study of Different Types of Heat Exchange

Convective heat exchange depends on the physical properties of the liquid and the nature of its motion. Study has shown that heat exchange between a solid surface and liquids, for which the Prandtl number is considerably less than unity, exhibits specific features.

In liquids for which $\Pr = v.a \ll 1$, the molecular transfer of heat is considerably more intensive than the transfer of momentum, since in this case the numerical value of the thermal conductivity α is many times greater than that of the coefficient of kinematic viscosity ν . Such liquids include liquid metals, for which the Prandtl number is of the order of $1 \cdot 10^{-2}$. Hence the study of convective heat exchange in liquid metals will be considered separately.

In this section we deal with convective heat exchange with different types of motion of fluids, in which the Prandtl number is of the order of unity or more.

Convective heat exchange with free motion of medium. As has been pointed out above, the motion of a medium _flowing over_ a solid surface is _said to be_ free. If it is due to the differences in density between the hot and cold particles.

Thus, a temperature difference is essential for the occurrence of free motion. A distinction is made between the heat exchange occurring in a "infinite" space, compared with the dimensions of the body, and heat exchange taking place in a "finite" space.

Convective heat exchange with free motion in an infinite space.
Heat transfer during free motion of a medium due to local heating or cooling in an infinite space is of great importance in constructional engineering.

For example, during the heating of air in buildings with heating devices and when cooling certain parts of buildings and in other cases. This type of heat exchange has been studied thoroughly. A great deal of research has been carried out along these lines by Kirpichev and Mikheyev.

Study of the equations describing heat transfer on the basis of the theory of similarity shows that the *characteristic* dimensionless numbers are the following

$$Gr = \beta \frac{gl^3}{\nu^2} \Delta t \text{ и } Pr = \frac{\nu}{a}.$$

As in all heat transfer, the *unknown* number is the Nusselt number $Nu = \alpha l / \lambda$. Hence on the basis of the experimental data we can ascertain the *form the* of function

$$Nu = f(Gr, Pr).$$

Mikheyev has shown that numerous experimental data on heat exchange

for differently-shaped bodies (cylinders, spheres, plates, and so on) *immersed* in

different fluids which are large compared with the size of the bodies can give

us a dimensionless equation of the type

$$Nu = C(Gr \cdot Pr)_m^n. \qquad (3.31)$$

The coefficient $\underline{C}$ and the exponent $\underline{n}$ are functions in their turn of

the numerical complex $Gr \cdot Pr$, but do not depend on the shape of the body.

In order to select $\underline{C}$ and $\underline{n}$, Table 13 *textbooks give* the values obtained by Mikheyev.

The subscript $\underline{m}$ in the latter equation means that the determining

temperature is t_m

In problems involving aviation engineering, heat exchange through natural

convection in an infinite space is of no great practical importance.

Investigation of convective heat exchange with natural, free convection

closed
in a finite (ℓ) space is of great interest since the data obtained from this

study can be used to calculate the air layers employed as thermal insulation.

Convective heat exchange with free motion in a finite, closed space.

The nature of free motion in a finite space depends to a considerable extent on the

Table 13

Gr · Pr	C	a
$1 \cdot 10^{-3} \div 5 \cdot 10^2$	1,18	$^1/_8$
$5 \cdot 10^2 \div 2 \cdot 10^7$	0,54	$^1/_4$
$2 \cdot 10^7 \div 10^{13}$	0,135	$^1/_3$
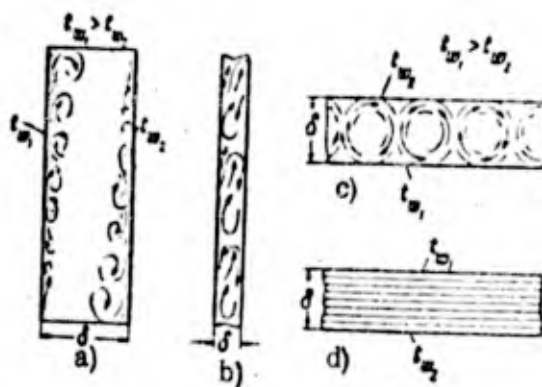
Fig. 39. Convective currents infinite space

shape of the enclosed space and on the mutual arrangement of the source and receiving surfaces. For example, if the closed space is shaped like a vertical slot, the free motion is determined by the width of the slot, δ as shown in Figs. 39a and b.

If the space is shaped like a horizontal slot, the nature of the free motion depends on where the source surface with temperature t_w is located.

If the source surface is located below (Fig. 39c), then both ascending and descending currents occur in the closed space. If the source surface is at the top, there are no convective currents (Fig. 39d).

A great deal of research has shown that when calculating these fluid layers, the processes occurring in them can be tentatively regarded as thermal conductivity phenomena, i.e., we can determine the thermal resistance of a layer of this kind as the thermal resistance of a solid, homogeneous wall of the same shape. The thermal conductivity of this layer is termed the equivalent thermal conductivity and is designated λ_{eq}.

Obviously, λ_{eq} is greater than the thermal conductivity λ of a stationary fluid filling the layer, since in actual fact in the layer there is free convection. It is conventional to determine λ_{eq} in calculations from the

- 123 -

formula

$$t_{cp} - t_{cp} = \frac{\varepsilon_q}{\varepsilon} \cdot c$$

in which ε_c is the coefficient making allowance for convection.

Numerous experimental data obtained from study of different layers shapes enables us to   establish the dependence of the convection coefficient on the complex Gr · Pr , determining the convective heat exchange in the free stream,

$$\varepsilon - f(GrPr).$$

In textbooks on heat transfer the form of this function is given as a graph. Furthermore, ε_c may be calculated from the following formulae

$$\varepsilon_c = 0{,}105\,(GrPr)_f^{0{,}3} \ (\text{at} \ \ GrPr = 10^3 \div 10^5). \tag{3.32}$$

$$\varepsilon_c = 0{,}4\,(GrPr)_f^{0{,}2} \ (\text{at} \ \ GrPr = 10^6 \div 10^{10}). \tag{3.33}$$

The subscript f means that the temperature t_f is the characteristic one,

Convective heat exchange with forced motion of the medium. In

studying heat exchange with forced motion of the medium, we distinguish the

problems of internal and external flow around the body. The problem of internal   flow around the body (includes heat exchange between the wall of the channel and the stream of fluid

in the channel. The problem of external   flow includes heat exchange arising

when the fluid flows around differently shaped bodies.

- 124 -

For example, heat exchange between the surface of an aircraft and the medium through which it is passing, heat exchange between a gas ^stream and the surface of the protective thermocouple casing, in this stream, and so on.

Heat exchange with forced motion and internal ~~around a body~~ flow. As is well known, on the basis of the type of motion we distinguish turbulent and laminar flow. In hydraulics the dimensionless group evaluating the motion of the stream in tubes is the ^{R}eynolds number. If the Reynolds number is $Re < 2300$, the stream can be regarded as laminar, but if it is $Re > 10^4$ the flow is turbulent.

This division of ^flow into laminar and turbulent in accordance with the Reynolds number, however, is only valid for isothermal streams. If the stream is non-isothermal, as a result of the temperature difference, there is always natural, free convection which agitates the stream. Hence when investigating heat exchange we cannot speak of purely laminar flow. The streams in which $Re < 2300$ are called streams with poorly developed turbulence. Streams for which the Reynolds number exceeds 10^4 ($Re > 10^4$) are termed streams with a highly developed turbulence.

Heat exchange in a stream with poorly developed turbulence. $Re < 2300$. In a stream with poorly developed turbulence, apart from the forced motion of the

- 125 -

fluid, there is also free, natural convection, and the effect of this convection increases with the rate of motion of the stream.

When a liquid moves in closed pipes the intensity of the heat transfer along the pipe is non-uniform. The heat-transfer coefficient α shows a maximum directly at the inlet, then decreases and at a certain distance from the inlet acquires a set value which remains unchanged throughout the pipe.

This phenomenon can be explained in the following way. In the initial area of the pipe the drop in temperature occurs in a rather thin layer alongside the wall on account of the comparatively low thermal conductivity of liquids and gases. Hence in the initial sections the temperature gradient dt/dy and the temperature difference $\Delta t = t_f / t_w$ are greater than in the subsequent section.

The decrease in the heat-transfer coefficient along the pipe is due to the fact that as the liquid moves along, the temperature gradient decreases more rapidly than the temperature difference. This produces a reduction in α according to Eq. (3.18).

$$a \,\Delta t = -\lambda \frac{\partial t}{\partial y}.$$

The length of the section of the tube over which there is a drop in the

heat transfer coefficient α depends on the conditions of motion and physical

parameters of the fluid, and also on the size and shape of the pipe and other

factors.

Usually, if the length of the pipe h exceeds its diameter by a factor

of 50 (h/d > 50), the process of heat transfer is fully stabilized.

characteristic

Investigation shows that in this case the   dimensionless groups are

$$ \text{Re, Gr, Pr } \text{and} \frac{Pr_f}{Pr_w} . $$

and the *unknown*   is the Nusselt number. Hence the dimensionless equation

should take the form

$$ Nu = f\left(Re, \ Gr, \ Pr, \ \frac{Pr_f}{Pr_w} \right). $$

Extensive investigation enables us to obtain the following dimensionless

equation for calculating horizontal pipes

$$ Nu_f = 0,17 Re_f^{0,33} Pr_f^{0,43} Gr_f^{0,1} \left(\frac{Pr_f}{Pr_w} \right)^{0,25} . \qquad (3.34) $$

Heat exchange in a stream with highly developed turbulence. When

the Reynolds number is Re > 10^4, the development of free motion in the fluid is

characteristic

impossible and the Gr number drops out of the (groups   .   .

The dimensionless equation in this case takes the form

$$ Nu = f\left(Re, \ Pr, \ \frac{Pr_f}{Pr_w} \right). $$

- 127 -

In order to calculate heat exchange in pipes and channels with differently shaped cross-sections, Mikheyev suggests the following dimensionless equation

$$Nu_f = 0.021 Re_f^{0.8} Pr_f^{0.43} \left(\frac{Pr_f}{Pr_\bullet}\right)^{0.25}.$$
(3.35)

For air and diatomic gases, the Pr number is constant ($Pr \approx 0.27$) and Eq. (3.35) takes the form

$$Nu_f = 0.018 Re_f^{0.8}.$$

The _characteristic dimension_ for cylindrical pipes and channels is the diameter $\frac{d}{D}$, and d_{eq} for pipes and channels of a different shape.

For air at high temperatures when $Re > 30,000$, we can use the Ditrus Bolter equation /4/.

$$Nu_m = 0.021 Re_m^{0.8} Pr_m^{0.4} \left(\frac{T_f}{T_m}\right)^{0.4}.$$
(3.36)

The dimensionless equations (3.34), (3.35) and (3.36) are valid for pipes _will_ $h/d > 50$: for short pipes the calculation is made by the same equations and the correction ε_l is added to the number derived.

$$\theta_{\text{кор}} = \varepsilon_l \lambda.$$

The value ε_l is determined experimentally as a function of the Re number and the ratio h/d from Table 14, suggested by Alad'yev.

- 128 -

Table 14

Value ε_l

Re \ l/d	1	2	5	10	15	20	30	40	50
$<2.3\cdot10^3$	1,90	1,70	1,41	1,28	1,18	1,13	1,05	1,02	1,0
$1\cdot10^4$	1,65	1,50	1,34	1,23	1,17	1,13	1,07	1,03	1,0
$2\cdot10^4$	1,51	1,40	1,27	1,18	1,13	1,10	1,05	1,02	1,0
$5\cdot10^4$	1,34	1,27	1,18	1,13	1,10	1,08	1,04	1,02	1,0
$1\cdot10^5$	1,28	1,22	1,15	1,10	1,08	1,06	1,03	1,02	1,0
$1\cdot10^6$	1,14	1,11	1,08	1,05	1,04	1,03	1,01	1,01	1,0
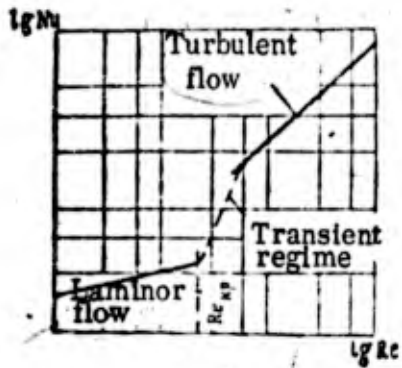
Fig. 40. Busselt number as function of Reynolds number
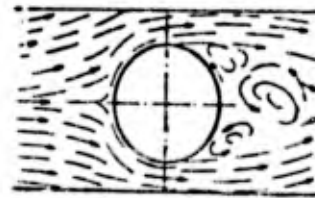
Fig. 41. Cross-flow around cylinder

in it

If the pipe has bends/(for example, right-angle bend, coils), the

nature of motion is disturbed on account of the centrifugal effect and the

additional turbulence due to it. In this case the calculation is made in

the same way as for a straight pipe, and the corresponding correction ε_R is

added . to the heat-transfer coefficient obtained, and

$$\varepsilon_{\text{bend}} = \varepsilon_R^2.$$

The correction coefficient ε_R is established from the relationship

$$\varepsilon_R = 1 + 1.77 \frac{l}{R},$$

in which $\underline{l}$ is the *characteristic dimension* of the pipe, *and* $\underline{R}$ is the radius of the bend.

It should be pointed out that the dimensionless equations (3.34), (3.35) and

(3.36) cannot be used to calculate heat exchange if the Reynolds number is

$$2300 < \text{Re} < 10^4.$$

For these conditions of motion, which are termed transient, there are

no generalizing formulae and only occasional experimental data are found in

literature.

Fig. 40 shows the variation in the Nu number as a function of the Re

number in a logarithmic system of coordinates. In order to evaluate the heat-

transfer coefficients for *in* transient conditions, in the first approximation we

can use the *broken* line shown in Fig. 40. Here it should be taken into account

- 129 -

that the shape and size of the channels in transient conditions have a marked

effect on the heat-transfer coefficient.

Convective heat exchange with forced motion and external circumflow.

Heat exchange *with transverse passage of fluid across*
~~the pipe~~ . . . . If a stream of fluid flows

round a body, for example a cylinder set perpendicularly to the direction of

motion of the flow, as shown in Fig. 41, the stream moves smoothly around the

leading, frontal part of the cylinder, after which there is ~~dieruption~~ of

the stream and the rear section of the cylinder is washed by a stream with

complex vort*ical* flow.

On account of the variation in the motion of the stream *flowing round* the

cylinder, the heat-transfer coefficient *for* the surface of the cylinder is

non-uniform. Investigation shows that the coefficient is greatest in the

leading and rear points on the surface of the cylinder.

This may be explained in the following way: a boundary layer is

formed on the frontal surface of the cylinder, *after which* its thickness increases,

reaching a maximum, *and* there is *detachment* of the

boundary layer. This layer, as it were, *'isolates'?* the surface of the cylinder

from the bulk of the liquid. The heat exchange in the boundary layer is mainly

- 130 -

determined by the thermal conductivity; the thermal conductivity λ of the fluid

is comparatively small, hence the heat-transfer coefficient decreases as the

thickness of the boundary layer increases. The minimum value of α corresponds to

the   point of the boundary layer from the cylinder surface. In the

back region the surface of the cylinder is washed by a stream with complex vortical

motion, and the heat transfer coefficient is increased.

Thus, heat transfer   is here

determined by the nature of the motion of the liquid while flowing round the

body and the parameters of the liquid (viscosity, thermal conductivity,

etc.). The determining groups are the Re and Pr numbers. The dimensionless

equation therefore takes the form

$$Nu = f\left(Re, Pr, \frac{Pr_f}{Pr_w}\right).$$

On the basis of experimental data the following formula has been

established

$$Nu_f = C\,Re_f^n Pr_f^{0.38}\left(\frac{Pr_f}{Pr_w}\right)^{0.25}. \tag{3.37}$$

The values $\underline{C}$ and $\underline{n}$ depend on the Re number and the shape of the

body around which the stream flows. For example, for round pipes, they are

usually selected from Table 15.

Table 15

Re	C	n
$1\cdot10^4 \div 1\cdot10^3$	0,59	0,47
$1\cdot10^3 \div 2\cdot10^5$	0,21	0,62

For air and diatomic gases at $Pr \approx 0.7 =$ const, Eq.(3.37) can be simplified: $Nu_f = 0.52 Re_f^{0.47}$ at $Re = 1 \cdot 10 \div 1 \cdot 10^3$; $Nu_f = 0.1 S Re_f^{0.62}$ at $Re = 1 \cdot 10^3 \div 2 \cdot 10^5$.

Stuart MacLain /4/ suggests the following dimensionless equation for large Reynolds numbers

$$Nu_m = 0.26 Re_m^{0.6} Pr_m^{0.3}. \qquad (3.38)$$

The heat-transfer coefficient α calculated with Eq. (3.37) and (3.38) is the mean for the entire cylinder surface. It should be pointed out that Eqs. (3.37) and (3.38) are only valid at an angle of attack of 90°. If the angle of attack φ is lower, α is lower, which is taken into account in the calculation by the relevant correction ε_φ, which is established experimentally for differently-shaped bodies at different angles of attack.

Consequently,

$$\varepsilon_\varphi = \varepsilon_\varphi \alpha.$$

If the cross-stream of liquid flows past a bank of tubes, heat transfer is made still more complicated, since the motion of the liquid over the surfaces of the tubes is to a considerable extent a function of the arrangement of the tubes. It has been established on the basis of available data that the heat-transfer coefficient of the second and third rows of tubes is greater than for the first; beginning at the third row the heat-transfer coefficient

- 132 -

remains constant.

On the basis of a great deal of research, Mikheyev suggests the
following dimensionless equation

$$Nu_f = C\,Re_f^n Pr_f^{0.11}\left(\frac{Pr_f}{Pr_\omega}\right)^{0.25}. \qquad (3.39)$$

The values $\underline{C}$ and $\underline{n}$ are functions of the arrangement of the pipes:
for the corridor arrangement (Fig. 42) $\underline{C} = 0.23$ and $\underline{n} = 0.65$; for staggered
arrangement (Fig. 43) $\underline{C} = 0.41$ and $\underline{n} = 0.6$.

For air and diatomic gases at $Pr \approx 0.7 = \text{const}$, Eq. (3.39) takes
the form: $Nu_f = 0.21 Re_f^{0.65}$ (for a corridor bank) and $Nu_f = 0.37 Re_f^{0.6}$ (for a staggered bank).

When calculating the heating surfaces of heat-exchanging apparatus
we usually calculate the mean heat-transfer coefficient α_m of the entire bank.
The value α_m can be established from the following relationship

$$\alpha_{cp} = \frac{a_1 F_1 + a_2 F_2 + \ldots + a_m F_m}{F_1 + F_2 + \ldots + F_m}, \qquad (3.40)$$

in which $a_1, a_2, \ldots, a_m$ are the heat-transfer coefficients of separate rows of pipes,
given a total number of pipes $\underline{m}$, while $F_1, F_2, \ldots, F_m$ are the heating surfaces of all
the pipes in each row.

Heat exchange with longitudinal flow around a flat plate. If the
liquid flows round a flat plate, a laminar boundary layer forms on the plate
surface and its thickness increases in the direction of motion of the liquid,

- 133 -

as shown in Fig. 44.

It has been established that when the Reynolds number is Re = 4.85 · 10^5
the laminar boundary layer *is disturbed* and changes to a turbulent layer with a
thin laminar sublayer (Fig. 44).

When determining the Reynolds number $\underline{1}$ should be taken to mean distance from the
edge of the plate, and $\underline{U}$ should be taken to mean the velocity of the stream
beyond the boundary layer.

When calculating heat exchange occurring when different *fluids* flow
round flat plates, Mikheyev suggests the following equation

$$Nu_f = C \, Re_f^n Pr_f^{0.43} \left(\frac{Pr_f}{Pr_w}\right)^{0.25}. \tag{3.41}$$

For air and diatomic gases at Pr ≈ 0.7 = const, E_q. (3.41) takes the
form: $\underline{Nu_f = 0.032 Re_f^{0.5}}$, and at Re < 4.85 · 10^5 $\underline{C}$ = 0.76, $\underline{n}$ = 0.5; at Re > 4.85 · 10^5, $\underline{C}$ = 0.037,
$\underline{n}$ = 0.8.

Sec. 18. Connection Between Friction Coefficient and Heat-Transfer Coefficient.

The theory establishing the connection between the heat-transfer coefficient
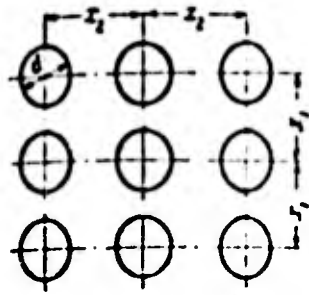
Fig. 42. Corridor arrangement
of tubes in bundle
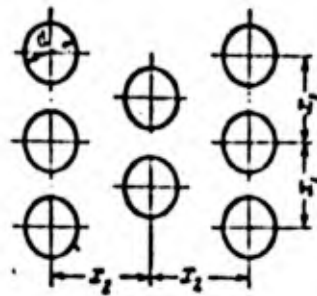
Fig. 43. Staggered arrangement
of tubes in bundle

laminar sublayer
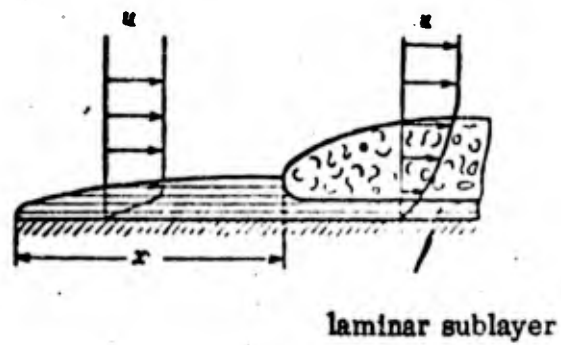
Fig. 44. Boundary layer during longitudinal flow
around flat plate

and the friction coefficient is conventionally termed the hydrodynamic theory of heat exchange. The main concept in this theory is the assumption that when a liquid experiences forced motion, the mechanisms of the transfer of momentum and the propagation of heat are identical. It was shown above that when studying flow around diffeent surfaces, turbulent flow is regarded, as it vere, as consisting of two parts: the bulk of the flow and a laminar sublayer occurring near the wall.

It should be remembered, however, that this representation is tentative and there is actually no clearly marked boundary between the bulk of the flow and the laminar bublayer. In actual fact, particles of liquid penetrate freely from the bulk of the stream into the boundary layer and/come back again, thereby transferring the momentum.

The identity, assumed in the hydrodynamic theory of heat exchange, of the transfer of momentum and heat is based on the assumption that both these phenomena are effected by the same elementary volumes of liquid.

In the case of certain fluids, over a large ange of variation in temperature the $P_r$andtl number is approximately equal to unity. Gases closely fulfil this condition. If a liquid (gas) flows round a surface,

-135 -

as shown by experiments, the distributions of velocity and temperature in the

boundary layer of this liquid are similar. This means that the temperature and

velocity of motion of the liquid in the boundary layer vary in accordance with

the same law. Hence the ratio of the temperature gradients $\partial t/\partial n$ and velocity

$\partial u/\partial n$ can be replaced by the ratio of the temperature increment Δt and Δu of the

velocity increment

$$\frac{\frac{\partial t}{\partial n}}{\frac{\partial u}{\partial n}} = \frac{\frac{\Delta t}{\Delta y}}{\frac{\Delta u}{\Delta y}} = \frac{\Delta t}{\Delta u}.$$

This ratio is valid for any area inside the boundary layer. On the

boundary of the boundary layer and the bulk of the flow $(y = \delta)$, the values

Δt and Δu can be expressed as

$$\Delta t = t_f - t_w.$$
$$\Delta u = U - u_w.$$

in which t_f , U and t_w, u_w are the temperatures and velocities of the flow

beyond the boundary layer and on the surface of the immersed body.

Taking it into account that $u_w = 0$, we can write

$$\frac{\frac{\partial t}{\partial n}}{\frac{\partial u}{\partial n}} = \frac{t_f - t_w}{U}.$$

It was pointed out above that the principal type of heat exchange in the

boundary layer is thermal conductivity. Hence the expression for the heat flux

density based on the Fourier equations can be represented in the following way

$$q = -\lambda \frac{\partial t}{\partial n}.$$

If we take it that the boundary layer consists of separate elementary

layers of liquid moving at different velocities, then viscosity obviously

causes friction between these two layers. As is known from hydrodynamics, the

friction R can be expressed in terms of the viscosity coefficient μ and the

velocity gradient

$$R = \mu \frac{\partial u}{\partial n}.$$

According to the equations given above, the ratios can be represented

as follows

$$\frac{q}{R} = \frac{\lambda}{\mu} \frac{t_w - t_f}{U},$$

and by transferring R to the right-hand side of the equation we get

$$q = \frac{\lambda}{\mu} \frac{t_w - t_f}{U} R. \qquad (3.42)$$

This expression is the fundamental equation in the hydrodynamic theory

of heat exchange. By using this equation for the investigation of flow in pipes and

tubes we can establish the connection between the heat-transfer coefficient

and the coefficient of hydraulic resistance of pipes ζ. For example, for pipes

of circular section the relationship can be established in the following way.

It is known from hydrodynamics that in this case R can be found from the

relationship

$$R = \frac{\zeta}{8} \rho U^2. \qquad (3.43)$$

in which ζ is the coefficient of hydraulic resistance of the pipe, and depends

on the ^{R}eynolds number

$$\zeta = f(Re).$$

If the amount of heat given up to the wall by the liquid is expressed

in Eq. (3.42) in terms of the heat-transfer coefficient and the temperature

gradient,

$$-q = \alpha(t_f - t_w).$$

while $\underline{R}$ is replaced by ^{E}q. (3.43) we get

$$-\alpha(t_f - t_w) = \frac{\lambda}{\mu} \frac{(t_w - t_f)}{U} \frac{\zeta}{8} \rho U^2.$$

Taking it into account that $\mu = \nu\rho$, in which μ is the

viscosity coefficient, ν is the coefficient of kinematic viscosity and ρ is

the density, we finally get the following dependence between the heat-transfer

coefficient and the coefficient of hydraulic resistance for circular-section

tubes

$$\alpha = \frac{1}{8} \zeta \frac{\lambda}{\nu} U. \qquad (3.44)$$

This relationship may be represented in form of a dimensionless equation.

In order to do this, we can use as a rough approximation the dependence $\zeta = f(Re)$

for isothermal turbulent flow in pipes $\qquad \zeta = \frac{0.3164}{Re^{0.25}}.$

Then Eq. (3.44) takes the form

$$a = \frac{0.3164}{8} Re^{-0.25} \frac{U}{\nu} \lambda;$$

By transferring λ to the left-hand side and multiplying both sides of the equation by the characteristic dimension l, we get

$$\frac{\dot{a}l}{\lambda} = \frac{0.3164}{8} Re^{0.75}$$

or

$$Nu = 0.0395 Re^{0.75}. \qquad (3.45)$$

If it is taken into account that this expression has been obtained for liquids in which $Pr \approx 1$, it can be considered that Eq. (3.45) approaches the earlier quoted equation of Mikheyev, obtained from investigating flow in pipes and tubes with forced motion of the liquid. It can be considered that the coincidence would be greater if the dependence on the temperature distribution in the flow had been taken into account.

When solving the problem of external flow round a body, i.e., when the heat exchange takes place during flow around differently-shaped bodies, by means of the basic equation of the hydrodynamic theory of heat exchange (3.42) we can establish the connection between the heat-transfer coefficient α and the friction coefficient c_f.

- 139 -

As is well known from hydrodynamics, the friction is proportional to the velocity gradient

$$R = c_f \frac{U^2}{2}. \qquad (3.46)$$

in which c_f is the proportionality coefficient, which is termed the friction coefficient. If we substitute R from Eq. (3.46) into Eq. (3.42) and express q in terms of the heat-transfer coefficient, then we can obtain the dependence between α and c_f in the following form

$$\alpha = \frac{1}{2} \frac{\lambda}{\nu} U c_f.$$

In its dimensionless form this dependence can be expressed as follows:

$$Nu_f = \frac{1}{2} c_f Re_f. \qquad (3.47)$$

The dimensionless equation obtained is fully confirmed by experimental data for liquids with $Pr \approx 1$. Investigation of boundary layers of different liquids /5/ with $Pr \neq 1$ introduce a correction for the Prandtl number to this equation

$$Nu_f = \frac{1}{2} c_f Re_f Pr_f^{\frac{1}{3}}. \qquad (3.48)$$

Thus, by means of the hydrodynamic theory of heat exchange we can establish the connection between heat-transfer and hydrodynamic phenomena.

The established connection between the heat-transfer and friction coefficient[s]

enables us to use extensive experimental data from the aerodynamic study of

the resistance of differently shaped bodies in order to find the numerical

value α. But the chief importance of the hydrodynamic theory is that is

discloses the physical *meaning* of heat exchange during forced flow of a

liquid, since the heat transfer coefficients calculated from equations derived

on the basis of the theory coincide with experimental data, and thereby confirm

the assumption made in the theory with respect to the identity of the transfer

of heat and the transfer of momentum.

Sec. 19. Study of Convective Heat Exchange using Liquid Metals

as Transfer Agents.

The development of heating installations which use nuclear energy has

given rise to the question of the use of heat-transfer agents ensuring large

heat fluxes at high working tempeatures. The heat-transfer agents used can be

liquid metals, the advantages of which over other transfer agents are due to the

following of their properties.

Liquid metals exhibit high thermal conductivity, high *thermal* capacity,

and a high boiling point. Furtermore, liquid metals do not cause a great deal

of corrosion to construction materials, which means that steel as well as other

- 141 -

alloys can be used ~~for this purpose~~ .

The high boiling point, high thermal conductivity and high thermal capacity enable great quantities of heat to be removed at high temperatures. This makes it possible to use liquid-metal heat-transfer agents for cooling nuclear reactors in which the removal of heat can be *effected* at temperatures of the order of 500 - 650°. The use in this case of water as a heat-transfer agent becomes difficult, since it requires a considerable increase in pressure. For example, in order to have a mean water temperature of the order of $\underline{t} = 550°$, we have to create a pressure of more than 300 atm abs.

The low melting points of certain metals enables them to be converted to the liquid state very easily and kept in the plant in that form. The high critical temperatures of liquid metals give them considerable advantages as heat-transfer agents in steam plants utilizing nuclear energy. For example, the critical temperature of water is |lower than that of mercury |about 4 times| $(\underline{t}_{c.Hg} = 1400°)$. On account of this, the use of steam *limits* the possibility of raising the temperature of the steam in a turbine. This prevents us improving the thermal efficiency of the steam cycle to any great degree.

The regularities governing the flow of ⱡ liquid metals are similar
~~true for~~
to other incompressible liquids. On account of this the pressure loss in

communicating units with a heat-conducting contour does not hamper the use of

liquid-metal heat-transfer agents.

As such agents liquid metals possess certain negative properties which

have to be taken into account when using them. One ~~drawback of~~ these metals when

used for cooling nuclear reactors is their tendency to become radioactive, thus

creating difficulties in designing and servicing the heat-removal system.

The use of liquid metals in atomic power plants is further complicated

by the need to create low pressures in the condenser in order to obtain the

corresponding low temperatures. But these shortcomings are not insuperable.

By dint of the properties mentioned above, liquid metals are being widely used

in contemporary heat-exchanging apparatus.

Heat transfer with liquid-metal heat-transfer agents

On account of the high thermal conductivity of liquid metals, the

molecular transfer of heat in them is considerably more intensive than that of

the momentum. The physical properties of heat-transfer agents, as is known,

are described by the P_r-andtl number. This number is considerably less than

unity in the case of liquid metals, as already pointed out. In this case the

thickness of the temperature boundary layer is considerably greater than that of

- 143 -

the dynamic boundary layer, and the effect of molecular thermal conductivity shows

up both within the boundary layer add in the region of the main stream.

The physical parameters of some liquid metals as a function of temperature

are shown in Tables 16, 17 and 18.

In practice the most interesting process in studying heat transfer with

liquid-metal transfer agents is heat transfer with forced motion of a in liquid metal

in a closed pipe. Numerous investigations show that the resistance during flow through

pipes and the local hydraulic resistances coincide when both liquid metals and other

non-metallic liquids flow through them.

The investigation of numerous experimental data shows that the temperature

gradient and direction of the heat flux have virtually no effect on heat exchange in

liquid metals, this being due to the high thermal conductivity and comparatively poor

dependence of the physical parameters of liquid metals on temperature. Hence the

ratio Pr_f / Pr_w is excluded from the characteristic groups.

The processing of experimental data in the dimensionless form shows that

at $Pr \ll 1$ the Nu number for liquid metals is a function mainly of the Pe number. Hence,

if the dimensionless equation for non-metallic liquids flowing through pipes can be

- 144 -

Table 16

Mercury ($t_m = -39°C$; $t_b = 357°C$)

t °C	γ kg/m³	λ kcal/m·hr·deg	c_p kcal/kg·deg	$a·10^2$ m²/deg	$v·10^4$ m²/sec	$Pr·10^2$
0	13 590	6,70	0,0334	1,48	12,4	3,02
10	13 570	6,81	0,0333	1,51	11,8	2,81
20	13 550	6,92	0,0332	1,54	11,4	2,65
50	13 470	7,25	0,0329	1,64	10,4	2,30
100	13 350	7,80	0,0328	1,78	9,4	1,90
150	13 230	8,35	0,0328	1,92	8,6	1,61
200	13 110	8,90	0,0328	2,07	8,0	1,39
250	13 000	9,45	0,0328	2,22	7,5	1,22
300	12 880	10,00	0,0328	2,37	7,1	1,08
350	12 800	10,50	0,0329	2,50	6,8	0,98
400	12 700	10,85	0,0329	2,60	6,6	0,91
450	12 600	11,15	0,0329	2,69	6,4	0,86
500	12 480	11,45	0,0330	2,78	6,2	0,80

Table 17

Potassium ($t_m = 63,7°C$; $t_b = 760°C$)

t °C	γ kg/m³	λ kcal/m·hr·deg	c_p kcal/kg·deg	$a·10^2$ m²/deg	$v·10^4$ m²/sec	$Pr·10^2$
100	818	40,0	0,195	25,1	56,1	0,60
150	807	39,9	0,192	25,8	48,0	0,67
200	795	39,5	0,189	26,3	42,8	0,59
250	784	38,6	0,187	26,3	38,6	0,53
300	773	37,3	0,185	26,1	35,2	0,49
350	761	35,8	0,184	25,6	32,4	0,46
400	750	34,0	0,183	24,8	29,8	0,43
450	738	32,0	0,183	23,7	27,6	0,42
500	727	30,0	0,183	22,6	25,7	0,41
550	716	28,2	0,184	21,4	24,1	0,41
600	704	26,6	0,184	20,5	22,1	0,39
650	692	25,3	0,185	19,8	21,6	0,37
700	681	24,3	0,185	19,3	20,5	0,35

Table 18

Tin ($t_m = 231.9°C$; $t_b = 2270°C$)

t °C	γ kg/m³	λ kcal/m·hr·deg	c_p kcal/kg·deg	$a \cdot 10^2$ m²/deg	$v \cdot 10^8$ m²/sec	$Pr \cdot 10^2$
240	6985	26.2	0.061	6.15	27.3	1.60
250	6950	26.4	0.061	6.20	26.7	1.55
300	6940	27.20	0.061	6.42	24.1	1.35
350	6905	28.0	0.061	6.65	21.9	1.19
400	6865	28.9	0.061	6.89	20.1	1.05
450	6830	29.7	0.061	7.13	18.6	0.91
500	6790	30.5	0.061	7.36	17.4	0.85
550	6755	31.4	0.061	7.62	16.5	0.73
600	6720	32.2	0.061	7.85	15.6	0.72
650	6680	33.0	0.061	8.10	15.0	0.67
700	6640	33.9	0.061	8.37	14.3	0.61

represented in the general form by the dependence

$$Nu = f\left(Re, Pr, \frac{Pr_f}{Pr_\bullet}\right),$$

then for liquid metals the dimensionless equation should take the form

$$Nu = f(Pe),$$

or taking into account $Pe = Re \cdot Pr$, we get

$$Nu = f(Re \cdot Pr).$$

The form of the function f depends on the conditions of motion.

There is a great deal of experimental data available at the present time on heat transfer with different liquid-metal transfer agents /2/. Generalization of the studies made shows that the chief feature of fused metals affecting heat transfer is the non-wettability of the ground which line is low surface.

For example, mercury does not wet carbon steel at $t < 600°$. Non-wettability reduces the heat-transfer coefficients. But it is not possible as yet to make a quantitative evaluation of this phenomenon.

On the basis of the study of flow in pipes in which contamination and non-wettability of the surface are possible, we can recommend the following dimensionless equation

$$Nu_f = 3.3 + 0.014 Pe_f^{0.9}. \qquad (3.49)$$

- 145 -

Equation (3.49) is recommended for use over the range $200 < Pe < 20,000$.
In the region of small Péclet numbers $20 < Pe < 200$ a rough calculation may be made from the formula

$$Nu_f = 0.7 Pe_f^{\frac{1}{3}}.$$ (3.50)

If we consider the surface non-contaminated and completely wettable, the following formula can be used

$$Nu_f = 4.8 + 0.014 Pe_f^{0.8}.$$ (3.51)

These equations can determine the mean heat transfer coefficient for long pipes ($h/d \geqslant 30$). Calculation of heat transfer for short pipes is made with the same equations, but the correction ε_{ℓ} is added to the heat-transfer coefficient α obtained

$$\alpha_{\text{кор}} = \varepsilon_{\ell} \alpha.$$ (3.52)

The value ε_{ℓ} depends on the ratio h/d and can be established from the equation

$$\varepsilon_{\ell} = 1.72 \left(\frac{d}{h}\right)^{0.16}.$$ (3.53)

It should be pointed out that when liquid metal flows through pipes and flows continuously around different shapes, no corrosion is found on the solid surfaces. But when the boundary layer becomes detached or when the flux branches, the solid surfaces undergo destructive corrosion.

At the present time extensive experimental data is available on different solid specimens in liquid metal media /2/.

In conclusion to this chapter we give a list of the basic similarity groups:

$$Ho = \frac{u\tau}{l}$$ Homochronous number

$$Fr = \frac{gl}{u^2}$$ Froud number

$$Eu = \frac{\Delta p}{\rho u^2}; \quad Eu = \frac{p}{\rho u^2}$$ Euler number

$$Re = \frac{ul}{\nu}$$ Reynolds number

$$Fo = \frac{a\tau}{l^2}$$ Fourier number

$$Pe = \frac{ul}{a}$$ Peclet number

$$Pr = \frac{\nu}{a}$$ Prandtl number

$$Nu = \frac{\alpha l}{\lambda}$$ Nusselt number

$$Gr = g \frac{\beta l^3 \Delta t}{\nu^2}$$ Grashof number

$$St = \frac{\alpha}{c_p \rho u}$$ Stanton number

REFERENCES

1. Kutateladze, S. S. Fundamentals of theory of heat exchange, Chapters VI and IX. Mashgiz, 1957.

2. Kutatelandze, S. S. and others. Liquid metals as heat-transfer agents. Atomizdat, 1958.

3. Mikheyev, M. A. Fundamentals of heat transfer, Chapters II, III and IV, Gosenergozidat, 1956.

4. Stuart MacLane, Lecture, No. 9 on Reactor construction. Sudpromgiz, 1957.

5. Schlichting, G. Theory of boundary layer, Chapters XIV, For. Lit. Press, 1956.

CHAPTER IV

HEAT EXCHANGE WITH VARIATION IN AGGREGATE STATE OF MATTER

This section deals with the process of heat exchange between a solid

surface and a liquid when the latter is boiling, and between a solid surface and steam

when the latter is condensing*. These processes are accompanied by a variation

in the aggregate state of the working solid, which distinguishes them

from heat exchange with a single phase liquid or gas to a considerable extent.

The processes of heat exchange when the liquid boils is of great

importance in present-day engineering. They are *encountered*, first, in steam

boilers, and, second, in heat exchange apparatus for cooling surfaces with high

heat flux densities, *such as* atomic reactors, systems for cooling nozzles

and combustion chambers in liquid propellant engines, for tempering steels in liquid

media, and so on. The processes of heat exchange when steam condenses are

found in condensers, which are essential parts of stationary power plants

utilizing steam.

The *aim* of the study of heat exchange between a solid surface and a

liquid or steam is to establish the connection between the heat-transfer

coefficient α kcal/m^2 · hour · deg and the parameters determining these processes.

Using

the ~~·known~~ heat-transfer coefficient α , the amount

of heat which has to be transferred from the wall to the liquid $\underline{Q}$ kcal/hour, and

the given *difference,* ~~y~~ between the temperature of the wall $\underline{t}_w$ and the saturation

point of the liquid t'' $\underline{}$ $\overline{(M = t_w - t'')}$, and using the known Eq.(2.19), we can determine the

total area of surface of the heat exchanger $\underline{(S, m^2)}$

$$Q = a\,M\,S.\qquad\qquad (4.1)$$

Sec. 20. Heat ^{T}ransfer when Liquids Boil. Temperature Field
of Boiling Liquid

By boiling we mean the process of the formation of a vapor inside a

liquid when the latter is heated. The temperature of the vapor formed is called

the saturation point $\underline{t}''$. The saturation point $\underline{t}''$ is determined by the pressure $\underline{p}$

of the boiling liquid. Experience shows that the boiling point of a liquid $\underline{t}_f$

is always higher than the saturation point $\underline{t}''$, i.e., when boiling the liquid is

Super
·heated with respect to the saturation point. The characteristic variation

in the temperature of boiling water at different distances from the heated bottom

surface is shown in Fig. 45 /6/.

$\ast$ ────────

An analysis of heat exchange during melting and solidification of the working

solid can be found in /5/.

At the interface between the liquid and vapor there is a small temperature difference $t_f - t''$, which is determined by the physical properties of the liquid and the intensity of vaporization. A sharp increase in the temperature of the liquid is only observed in the layer 2 - 5 mm thick directly adjoining the bottom of the vessel. The temperature of the liquid particles adjoining the heated surface is equal to the temperature of the surface. The super heating of the liquid is maximum here . Observations have shown that as the heat flux density increases over the heating surface (q kcal/m^2 · hour), the value Δt increases.

The possibility of super heating a liquid is due to the presence of surface tension which restricts the bubbles of vapor. On account of surface tension the vapor pressure inside the bubble (p_1) is always greater than that of the surrounding liquid (p). Hence the vaporization temperature on the heated surface ($t'' = t_w$) is always higher than the saturation point t'' above the flat liquid surface.

The vapor pressure inside the bubble p_1, and therefore the super heat temperature t'', increases as the surface tension coefficient σ, and the radius of curvature σ of the surface of the bubble decrease .

This relationship can be expressed by the Laplace equation

$$p_1 = p + \frac{2\sigma}{\rho} . \qquad (4.2)$$
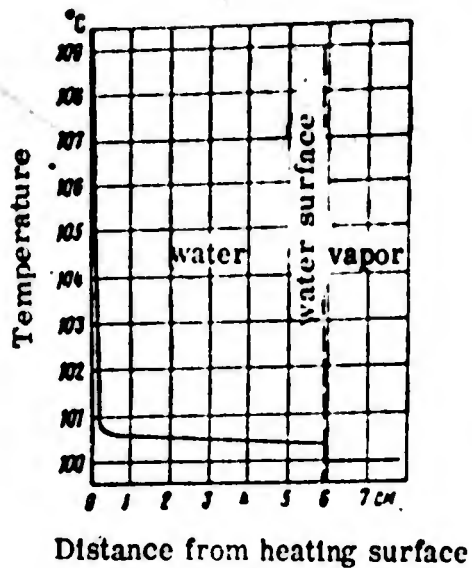
Fig. 45. Variation in boiling point of water
when heated from below $(q=19.0 \text{ kcal/m}^2 \cdot \text{hr},$
$t_s = 109.1° C)$.

Apart from maintaining pressure in the bubble, according to the Laplace

equation, super heating the liquid is essential to create a temperature gradient

which ensures the movement of heat from the liquid to the vapor. Furthermore, the

occurrence of the /new phase is accompanied by a wastage of work in forming the

interface ($\delta \underline{F}$) and the work of expansion. The super heating $\Delta \underline{t}$ /can vary over a

wide range.

For example, when pure water boils in a special vessel, it is possible to

produce steam bubbles of small size and . . . . . . superheat   the water

by several tens of degrees, after which there is violent vaporization throughout

the water.

Speaking

Theoretically, we can imagine the occurrence of the embryonic cavities

- 151 -

in the bulk of the liquid through fluctuation of the density during thermal motion of the molecules, with the center of vaporization being a cavity in which the thermodynamic potential of the vapor phase is equal to that of the liquid phase (or greater than it). In practice the vaporization centers occur on the interface of phases present in the given system. They may be either liquid or solid phases (heating surface, dust particles) or the liquid and gaseous phases, for example bubbles of air or some other gas. Here the initial bubble radius generated in the boundary layer is of the order of

$$\rho_0 = 4{,}65 \cdot 10^{-3} \frac{T'_0}{r \Delta t},$$
(4.3)

in which r is the latent heat of vaporization.

For example, for water boiling at atmospheric pressure ($\sigma = 6 \cdot 10^{-3}$ kg/m)

at $\quad \Delta t = t_w - t'' = 5^\circ C \quad \rho_0 = 6{,}7 \cdot 10^{-6}$ м.

at $\quad \Delta t = t_w - t'' = 25^\circ C \quad \rho_0 = 1{,}3 \cdot 10^{-6}$ м.

After this the steam bubble grows rapidly through the heat supplied from the surrounding liquid until it attains a maximum size termed the detachment size, after which it leaves the heating surface. For a certain period of time the vaporization center remains covered with liquid, after which a new bubble is generated and the cycle repeats itself.

The number of bubbles of steam formed per unit of time on the given

center is termed the detachment frequency. The diameter of the bubble at the

moment of detachment under conditions of natural convection is determined by the

equation

$$D_{otp} = 0.0185 \sqrt{\frac{\theta}{\gamma'\gamma}},$$ (4.4)

in which θ is the edge angle between the bubble and the heating surface or the

marginal?

wetting angle.

A case may be encountered in which the heating surface is higher in

temperature than the saturation point, while the bulk of the cold liquid has not

yet reached this temperature (cooling of liquid propellent rocket engines, quenching

of metals). This process is known as surface boiling. In this case we have an iso-

thermal surface on one side of which the liquid is superheated while on the other

it is not yet up to the saturation point. The superheated region in this is

called the boiling boundary layer, while the underheated region is termed the

subheated?

cold nucleus. The steam bubbles condensing in this region are formed in the

boiling boundary layer. The superheat of the liquid is determined by the

heat flux density q, the state of the heating surface, the radius of the steam

and

bubbles formed and the nature of the liquid (σ). Furthermore, the superheat

depends on the motion of the liquid with respect to the heating surface.

Section 21. Two fundamental types of boiling.

There are two fundamental types of boiling - _nucleate_ and film boiling.
They may also be combined.

The transition from one type to another and the regions in which they exist are determined by the heat flux density q passing through the heated surface, the physical properties of the liquid and the hydrodynamic state of the flow.

The differences in the different types of boiling can be illustrated more clearly by means of the experimental graph in Fig. 46, which shows the variation in heat-transfer coefficient from the wall to the water α and the heat flux density q as a function of the _superheat_ of the wall compared with the saturation point of the water $\Delta t = t_v - t_s^{"}$. The wall is the bottom of _a large-capacity_ vessel containing boiling water. For any other liquid wetting the wall, the difference is merely quantitative. At small degrees of _superheat_ of the wall and therefore small heat flux densities, in the region AB the heat-transfer coefficient is small and is determined by the conditions of free convection of homogeneous liquid. At atmospheric pressure this region is restricted by the temperature gradient $t = 5°$ and, correspondingly, the thermal load $q = 5000$ kcal/m^2. hour. As Δt increases, _nucleate_ boiling begins (the lines BC and BD in Fig. 46), during which there _runs_ /the above described increase in the steam bubbles

- 154 -

and their detachment.
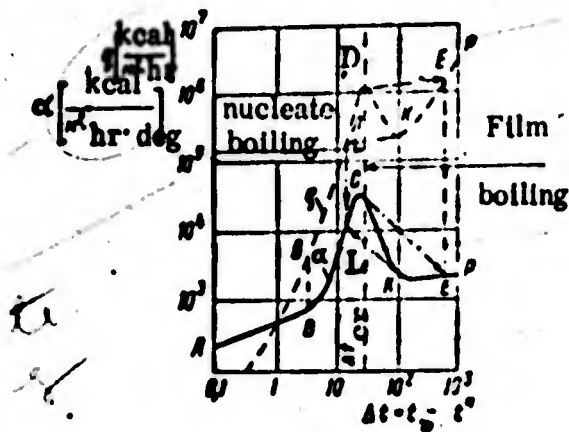

Fig. 46. Nature of variations in heat flux and heat-transfer
coefficient for boiling water as function of temperature
head $(p = 1\ ara)$

The occurrence and motion of bubbles causes circulation and migration

of the liquid at the heated surface. Hence α during boiling does not

remain constant, but increases with intensification, i.e., with an increase in the

number of vaporization centers and detachment frequency of the bubbles. But the

number of centers and detachment frequency increases with the heat flux density q,

i.e., when the of the wall Δt is increased. Hence, during

boiling the heat-transfer coefficient to the liquid α when q and Δt are increased

rises sharply (line BC and BD in Fig. 46). For example, at $\Delta t = 5°C$ $q \approx 10$ kcal/$m^2 \cdot$ hour $\cdot$ deg

and $q = 5 \cdot 10^3$ kcal/$m^2 \cdot$ hour, while at $\Delta t = 25°C$ $q \approx 1 \cdot 10^1$ kcal/$m^2 \cdot$ hour $\cdot$ deg, and $q = 1 \cdot 10$ kcal/m

hour.

Thus, when the boiling conditions are most intensive (point C and D

- 155 -

in Fig. 46) 500 times more heat may be transferred than at the initial stage of

the boiling ($\Delta V = 5°C$) and, what is particularly important in practice, at a very

slight superheat of the wall - only 25° in all. These nucleate boiling conditions

are termed the first critical regime (q_{cr_i}; Δt_{cr_i}; α_{cr_i}) because from then on, even if the

increase in the heat flux density is very slight, nucleate boiling turns into film

boiling, and there is a sharp drop in the heat-transfer coefficient.

Film Boiling.

When the heat flux density approaches the first critical value $(q \rightarrow q_{cr_i})$,

the number of vaporization centers is increased so much that there is rearrangement

of the boundary layer. The layer of liquid, typical of nucleate boiling, which is

permeated by bubbles and streams of vapor, is replaced by a layer of vapor,

permeated with streams and films of liquid, which still provides a flow of liquid

to the heating surface and a high heat-exchange intensity. When q becomes greater

than q_{cr}, the amount of vapor formed becomes so considerable that it carries away

the liquid in the thin streams, the stability of the streams is destroyed and a solid

steam blanket is formed, forcing the liquid away from the heated wall.

In film boiling, the heat is transferred from wall to

liquid through the film of vapor by conduction, convection and radiation.

The formation of the vapor from the liquid occurs on the surface of the vapor film.

On account of the low conductivity of the vapor, the heat-transfer

coefficient from the wall to the liquid in film boiling is reduced (by a factor

of 20 or 30), compared with its value during critical nucleate boiling. The

reduction in α leads to the transfer of the same amount of heat from the wall

to the liquid q_{cr} becoming possible only when there is a corresponding increase

in the superheat~~ed~~ temperature of the wall, compared with Δt_{cr}.

In our example, the superheat of the wall becomes dangerous for the wall

at $\Delta t \approx 750°$ or $t_w \approx 850°$. Hence, the film regime often leads to the wall burning

through, which *(a risk cannot be tolerated)* in heat exchanges. The transition to film boiling
occurs in the form of discontinuities,

(see the broken lines CE and DE in Fig. 46).

Under steady-state film *conditions* (line ___ in Fig. 46) α retains a

permanently low value and q increases solely through an increase in the superheat

of the wall Δt. The reverse transition from the film regime to the nucleate

regime (when q and $\Delta t'$ decrease) occurs, as shown by experiment, when the heat

flux is comparatively small (lines KL in Fig. 46).

Thus, we have two critical heat flux densities: q_{cr_1} at which there is

transition from nucleate to film boiling, and q_{cr_2} which corresponds to a transition

from film to nucleate boiling.

It follows from this description of the heat-exchange regimes during

boiling that the most effective one is nucleate boiling with heat flux densities

close to the first critical value (q_{cr}). In order for the ~~heat-exchanger~~ *heat-exchanger* to be of minimum

size, and the coolant consumption to be as *low* as possible at the *tolerated degree*

ing/
superheat /of the wall, the process is carried out in such a way that the heat-

transfer coefficient α is as near to (α_{cr}) as possible, but slightly less than it,

so as not to cause an accident and destruction of the tubes.

Determining heat-transfer coefficient (α) from heating surface

to boiling liquid in free convection

The most complete experimental observations and theoretical investigations

of boiling have been made for the case of free convection of a liquid boiling on

a surface immersed on a large volume, for example on the flat bottom of a capacious

vessel.

Fig. 47 shows the results of experiments on heat transfer during nucleate

boiling in a large volume of water at atmospheric pressure, plotted in logarithmic

coordinates /4/.

Experiment shows that the heat-transfer coefficient is not a function

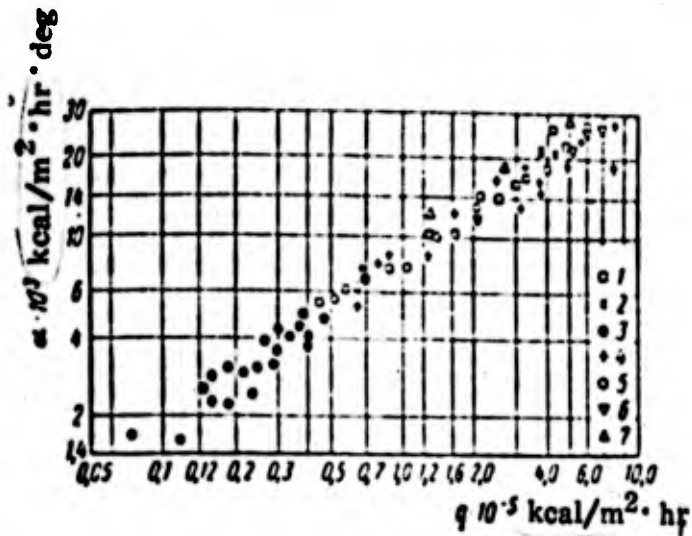of the size of the heating surface. Furthermore, the dependence of α on q is

- 158 -

Fig. 47. Effect of dimensions of heating surface on heat transfer
to boiling water:
1 - Minchenko, brass 9 mm in diameter; 2 - Borishanskiy, brass 11 mm
in diameter; 3 - Kutateladze, pipes 31 and 45 mm in diameter; 4 - Kutateladze,
graphite 2 mm in diameter; 5 - MacAdams, copper 13 mm in diameter;
6 - Nikaima, platinum 0.14 mm in diameter; 7 - Kichelli, chrome plate.

rectilinear in logarithmic coordinates. This means that $a \sim q^n$ and $a \sim (\Delta t)^m$ with α

depending on Δt to a larger extent than on q. Experimental data are usually

expressed by the empiric formulae (see, for example, Tables 12 - 1 in the

reference book on heat transfer /9/). Two formulae of this kind for water /4/

take the form

$$a = Aq^{0.77} \qquad\qquad (4.5)$$

and

$$a = B(\Delta t)^{2.33}, \qquad\qquad (4.6)$$

in which $B = A^{3.33}$.

Experiments show that m and n drop as the pressure approaches critical

$(p \to p_{cr})$, as well as when q approaches q_{cr} and Δt approaches Δt_{cr}. Both values

- 159 -

A and B are functions of the type of liquid, state of the heating surface and pressure.

Examples showing the effect on the type of liquid on α. 1. If the liquid does not wet the surface, the vapor accumulates in bubbles with wide bases (Fig. 48) and a great deal of buoyancy is required to detach them, i.e., a greater bubble size. The detachment frequency of the bubbles reduces, the liquid phase is forced away from the surface by the vapor and the heat-transfer coefficient is also reduced.
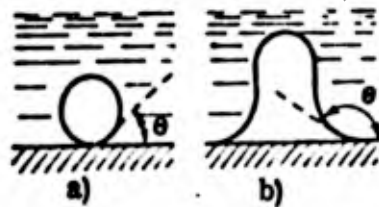
Fig. 48. Shape of vapor bubbles on wetted (a) and unwetted (b) surfaces

The boiling of mercury on steel surfaces, which it hardly wets at all at temperatures below 600°, is of great interest /10/. In view of this, low heat-transfer coefficients are characteristic of the boiling of pure mercury, and in certain conditions they decreases as the heat flux increases. The addition of a small amount of titanium, magnesium or other impurity to the mercury leads

- 160 -

to the   formation of amalgams /10/.   Here the boiling varies sharply and

becomes the same as for other liquids wetting the surface. x Certain data on

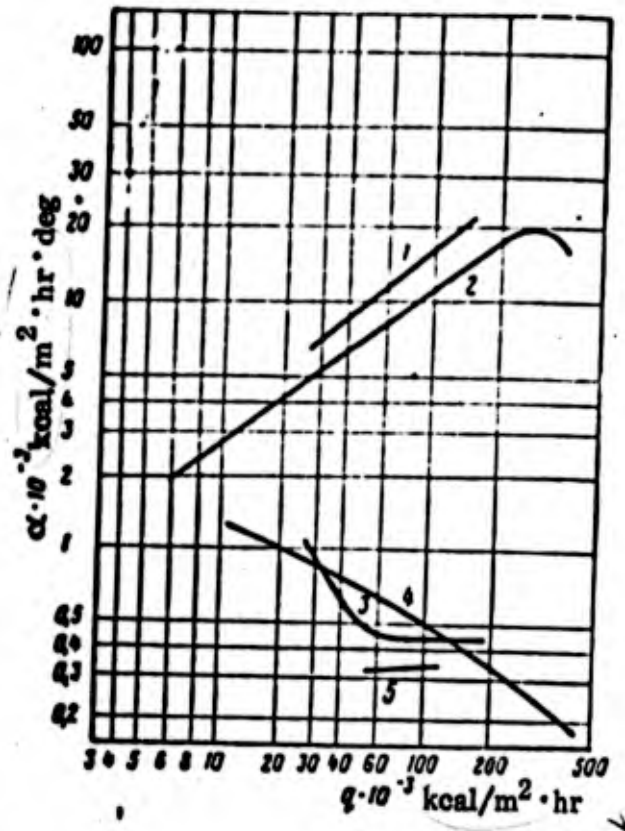heat-transfer coefficients during the boiling of metals are shown in Fig. 49.

Fig. 49. Data on intensity of heat transfer to metals boiling
at atmospheric pressure on steel heating surfaces /10/:

1 - magnesium amalgam with mercury inside vertical pipe;
2 - magnesium amalgam of mercury on heating surface of pipe;
3 - film boiling of magnesium amalgam with mercury;
4 - boiling of pure mercury;   5 - cadmium

2. An increase in the surface tension coefficient and viscosity coefficient

of a liquid also leads to a reduction in the intensity of the motion of a liquid

during boiling on the surface, and therefore to a reduction in α .

According to experimental data /4/

$$a \sim \sigma^{-0.33}, \tag{4.7}$$
$$a \sim \mu^{-0.45}, \tag{4.8}$$

in which μ is the viscosity coefficient of the liquid, kg sec/m^2.

Effect of state of heating surface on α . A metal heating surface is

often coated with a layer of oxide. On the one hand, the oxide layer reduces

the heat transfer, since it adds to the thermal resistance of the oxide film

(R_{ox}) between the metal and the liquid

$$R_{ox} = \frac{\delta_{ox}}{\lambda_{ox}},$$

in which δ_{ox} is the thickness of the oxide layer in m, and

λ_{ox} is the thermal conductivity of the layer in kcal/m $\cdot$ hour $\cdot$ deg.

On the other hand, a rough oxide film surface creates more

favorable conditions for the formation of vapor bubbles and this intensifies the

heat transfer. Hence the heat-transfer coefficient from the surface of the oxide

film to the boiling liquid may be greater than α for a clean surface.

Dependence of α on pressure. When the pressure is increased, the saturation point in t" increases, and the surface-tension coefficient of the liquid is decreased. The diameter of the vapor bubbles is therefore decreased at which they are detached from the surface, i.e., the number of active vaporization xxxx centers and the detachment frequency are increased. Hence, the coefficient α increases with pressure at a constant Δt until critical temperature difference $\Delta t_{cr} = t_{cr} - t''$, is reached, and at this temperature the boiling becomes film boiling, and α is reduced.

Fig. 50 shows experimental data for the heat-transfer coefficient when boiling water as a function of the temperature difference and pressure.

In the case of water we can recommend the following theoretical empirical formula (at $p < 30$ atm abs) /4/

$$\alpha = 2.5 p^{0.3} q^{0.7} \quad (p \text{ in kg/cm}^2 \text{ and q in kcal/m}^2 \cdot \text{hr}) \tag{4.9}$$

Dimensionless Equations for Determining Heat-Transfer

Coefficient During Nucleate Boiling

The quantitative results of individual experiments, formulated by empirical equations, cannot be transferred directly to other liquids or other conditions for the process. The transfer is possible only if the relationships derived are expressed in the form of dimensionless equations arrived at by means
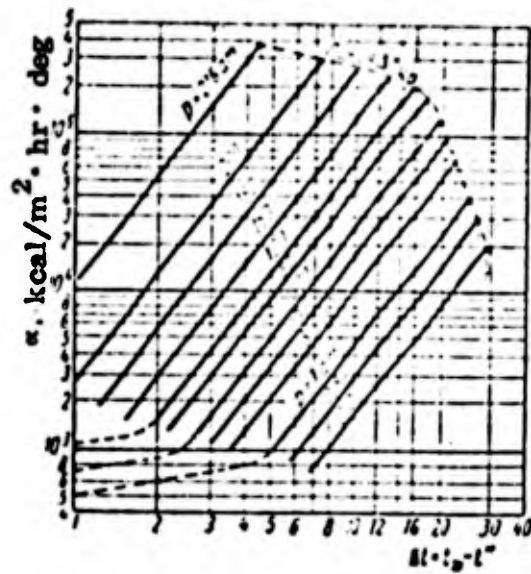
- 163 -

Fig. 50. Heat-transfer coefficient for boiling water as function of temperature and pressure difference

the theory of similarity. These equations are of great interest, since they show

the actual possibility of generalizing experimental data even for such complicated

processes as boiling. The derivation of the existing dimensionless equations is

based on the fundamental assumption that during developed boiling with free

convection the ~~$ motion~~ motion of the liquid near the heating surface is completely

determined by the vaporization, and, as pointed out above, the dimensions of

the surface have little effect on the heat transfer coefficient α.

Kruzhilin /3/ has used the similarity theory method to investigate

a system of differential equations describing the growth conditions of a vapor

bubble and the transfer of heat from the wall to the liquid during the action

of one vaporization _center_ . In this case, to calculate the heat-transfer

coefficient α during boiling use was made of the dimensionless relationship

$$\frac{a}{\lambda}\sqrt{\frac{a}{\gamma'-\gamma''}}=0{,}0325\left(\frac{a}{v}\right)^{0.5}\cdot\left[\frac{qr''\gamma''}{\Delta T''\lambda\left(\gamma'-\gamma''\right)^2}\right]^{0.7}\times$$
$$\times\left[\frac{\Delta T''c_p a^{0.5}(\gamma'-\gamma'')^{1.333}}{(r''\gamma'')^2}\right]^{0.333},$$

(4.10)

which was subsequently reduced to the following form after transformation and

improvement in accuracy

$$a=6{,}9\cdot10^{-3}\frac{\lambda^{0.75}q^{0.7}}{\mu^{0.45}c_p^{0.117}T^{0.37}}\left(\frac{r''}{\gamma'-\gamma''}\right)^{0.033}\cdot\left(\frac{\gamma'}{a}\right)^{0.333};$$

(4.11)

here all the physical parameters were compressed in technical units.

Kutateladze has _studied_ the processes occurring in the liquid and

vapor phase, irrespective of one another, and compiled two independent systems of

equations describing the hydrodynamic and thermal phenomena occurring in each of them. Both systems are united by the general boundary conditions on the interface, which express the specific nature of heat exchange during boiling. Processing of the differential equations derived by the similarity theory has given a dimensionless relationship, similar in the final analysis to the results of calculations made by Kruzhilin. The final form of the equation for the coefficient α was obtained by Kutateladze in collaboration with Borishanskiy, and is

$$\alpha = 0.44\lambda \left(\frac{\gamma - \gamma''}{\sigma} \right)^{0.5} \cdot \left(\frac{\nu}{a} \right)^{0.35} \cdot \left[\frac{q\rho}{3600 r \gamma'' g^{\frac{3}{2}}} \cdot \frac{\gamma'}{(\gamma' - \gamma'')} \right]^{0.7} . \qquad (4.12)$$

In the equations given the following quantities are conventional:

α is the heat-transfer coefficient during nucleate boiling in kcal/m^2·hour· deg

λ is the thermal conductivity of the boiling liquid at the given pressure in kcal/m hour deg

σ is the surface tension coefficient in kg/m;

γ', γ'' is the specific gravity of the liquid and saturated liquid in kg/m^3;

a is the thermal diffusivity of the liquid in m^2/hour;

ν is the coefficient of kinematic viscosity in m^2/hour;

q is the heat flux density in kcal/m^2· hour;

r is the latent heat of vaporization in kcal/kg;

- 164 -

$A = \frac{1}{427}$ is the heat equivalent of mechanical work in kcal/kg·m;

c_p is the specific heat capacity of the liquid in kcal/kg·deg;

T' is the vapor saturation point in ° abs;

μ is the coefficient of viscosity of the boiling liquid at the given

pressure in kg sec/m².

In Eqs. (4.10), (4.11) and (4.12) the values α are represented as

functions of the physical parameters alone. Hence if we have reliable

values for these parameters and if we ~~only~~ the formulae, we can calculate Δt and

as a function of q for any liquid and any pressure.

To do this we have to select the cooling liquid and saturation pressure.

The remaining parameters are found from tables.

Nucleate Boiling with Forced Motion of Liquid in Pipe

The organized motion of a liquid may lead to an increase in the heat-

transfer intensity during boiling (an increase in α). The degree of this

intensification is determined by the ratio of turbulent pertubations of the

boundary layer caused by the organized motion of the liquid and by the vaporization

process proper.

Intensive boiling often exerts the greatest effect on heat transfer, since

- 165 -

it developes right in the wall layer of the liquid. In this case the heat exchange in the circulating liquid is no different from heat exchange during boiling of a freely convective liquid in a large volume.

The joint effects of the rate of forced circulation of the liquid and the heat flux on heat transfer in a boiling liquid is shown schematically in Fig. 51 /8/.

Curve 1 corresponds to the relationship $\alpha = f(q)$ for a case of free convection. At small values of q, the addition of forced circulation agitates the boundary layer and α is considerably increased when the rate of forced circulation is stepped up (see curves U_1, U_2 and U_3). When the heat flux q is increased, agitation in the boundary layer due to vaporization becomes the determining factor, and the effect of the rate of circulation on the heat transfer is reduced to zero, and the curves U_1, U_2, and U_3 merge.

When analyzing the processes of boiling accompanying forced convection of a liquid we must keep it in mind that there are three zones:

1st zone: from the site of the commencement of heating to the section L_1, in which the pipe wall attains the saturation point. Over this area the liquid is only heated up by convection, and α remains low (see convective heat exchange).

- 166 -

For a pipe the length of this zone is determined by the formula (see ref. book /9/)

$$\frac{L_1}{D} = \frac{3600 c_p \gamma U_0 (t_1' - t_1)}{4q} - 10.4 \left(\frac{\nu}{a}\right)^{0.6} \left(\frac{U_0 D}{\nu}\right)^{0.2}. \qquad (4.13)$$
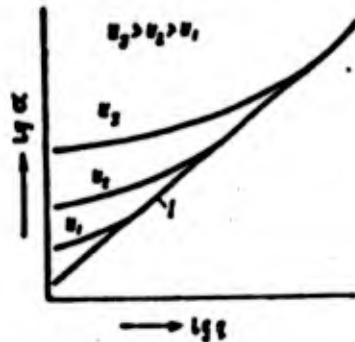

Fig. 51.   as function of q and U during boiling:

1) curve for developed boiling with free convection

2nd zone: *between* the section L_1 *and* the (*Commencement of heating*) . in which the liquid

attains saturation point throughout ~~the section~~. In this zone there is gradual

development of vaporization on the wall with partial condensation in the flow

nucleus. Both in the section L_2 and beyond it the whole of the liquid boils

$$\frac{L_2}{D} = \frac{3600 c_p \gamma U_0 (t_2' - t_1)}{4q}. \qquad (4.14)$$

Here t_1' is the saturation point in the section L_1 ;

t_2' is the saturation point in the section L_2 ;

t_1 is the temperature of the liquid and the pipe inlet;

D is the diameter of the pipe

U_0 is the velocity of the liquid at the pipe inlet.

- 167 -

3rd zone: the zone of developed boiling, for which the regularities

nucleate boiling are valid.

The boiling points t_1' and t_2' are determined as a function of the

pressure drop along the pipe

$$t_i = t_0' + 21.8 \frac{\zeta_{ip} T_0'(\gamma' - \gamma'') U_0^2 L_i}{\gamma'' D}. \qquad (4.15)$$

in which t_0' is the boiling point at the pressure p_0 in the inlet section of

$T_0' = t_0' + 273.2; \; t_i''$

the pipe, $\wedge$ is the boiling point at pressure p_i at a distance L_i from the

inlet section; $\zeta_\wedge$ is the coefficient of hydraulic resistance over the length L_i.

In zone (1) heat transfer is calculated by the convective heat exchange

formulae. In zone (3) the heat-transfer coefficient can be determined from Eqs.

(4.11) or (4.12) for a large volume. In the transition zone (2) the presence of

organized motion of the liquid in the pipe effects the intensity of the heat exchange

until the pertubations contributed by vaporization begin to have a decisive effect.

In practice the coefficient $\propto$ is calculated twice - from the convection equations and

the boiling equations - and the greater of the two values is selected.

During developed boiling, in the third zone the effect of the vapor

content in the flow is manifested and it can be taken into account by the equations

in /9/

$$\alpha = 14 q^{0.7} \left(1 + \frac{\gamma'}{\gamma''} \frac{\Delta t}{r}\right)^{0.4}. \qquad (4.16)$$

in which Δi is the difference in heat content in the liquid at the pipe inlet and

outlet in kcal/kg.

Critical Heat Flux Densities

In order to calculate heat exchanging apparatus, it is particularly

important to know the critical heat flux densities q_{cr_1} and q_{cr_2}. In most cases

we need only know (q_{cr_1}), since this determines the limits within which the

apparatus works reliably.

The values q_{cr_1}, z_{cr_1}, Δt_{cr_1}, q_{cr_2}, z_{cr_2}, Δt_{cr_2} and are determined by the physical properties of

the liquid, pressure in the system, state of the surface, underheating of the bulk

of the liquid up to the temperature t'' or vapor content in the flow, and the

intensity of forced circulation of the liquid.

Determining q_{cr_1} in conditions of forced convection in a large volume

of liquid. At the present time the phenomenon of the peak heat flux has been studied more

fully for free convection in a large volume of liquid. It is now taken for granted

that the boiling peak occurs through destruction of the hydrodynamic stability

of the developed structure of the boundary layer during nucleate boiling. In the

case of a liquid which thoroughly wets the heating surface during developed boiling

in a large volume, when the whole of the liquid is at a temperature t'',

Kruzhilin has derived the dimensionless equation for determining q_{cr_1}

$$\frac{q_{cr}\gamma'\gamma''}{\Delta T^2\lambda(\gamma'-\gamma'')^2} = 855\left(\frac{\nu}{a}\right)^{0.5}\left[\frac{(r\gamma'')^2}{\Delta T^2 c_p\gamma''^{0.5}(\gamma'-\gamma'')^{1.5}}\right]^{0.666} \times$$

$$\times\left[\frac{\gamma'\sigma^{1.5}}{g^{0.5}(\gamma'-\gamma'')^{0.5}}\right]^{0.25}. \qquad (4.17)$$

Using their own system of dimensionless groups, Kutateladze and

Borishanskiy /9/ have obtained an equation for q_{cr}, in which, like Kruzhilin's,

contains the dimensionless group

$$\left[\frac{\gamma'\sigma^{1.5}}{g^{0.5}(\gamma'-\gamma'')^{0.5}}\right]:$$

$$\frac{q}{r(\gamma'')^{0.5}[\sigma(\gamma'-\gamma'')]^{0.25}} = 1470\left\{1 + 30\left[\frac{g^{0.5}(\gamma'-\gamma'')^{0.5}}{\gamma'\sigma^{1.5}}\right]^{0.4}\right\}. \qquad (4.18)$$

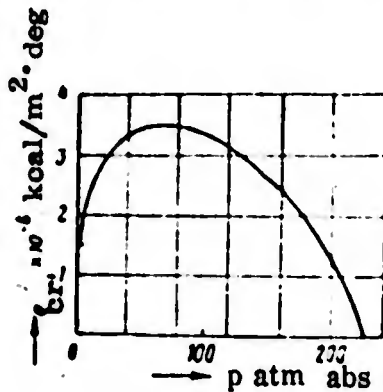Here g is the acceleration due to gravity ($g = 9.81$ m/sec).

Fig. 52. First critical density of heat flux as
function of pressure (boiling of water
in large volume) [9].

Fig. 52 shows q_{cr}, as a function of pressure for

boiling water derived by Eq. (4.18). Equation (4.17) gives similar results. In

both cases the maximum q_{cr} is found in the pressure area between 70 and 100 atm abs,

which corresponds to $(0.3 - 0.4) p_{cr}$. In the region of the vacuum and the region

of the near critical pressure (in the thermodynamic sense) q_{cr} tends to zero.

Similar relationships are satisfied roughly for other liquids as well. For liquified

gases, for example CO_2, O_2 or N_2, the heat-up of q_{cr} on ~~engineering~~ surfaces is

roughly half that calculated by Eqs. (4.17) or (4.18).

For surface boiling, when apart from the boundary layer the whole of the

remaining liquid has not yet been heated to t'', the critical heat flux q_{cr_1} is

increases, ~~xx~~ since condensation of vapor bubbles in the cold liquid makes the

boiling boundary layer more stable. On the basis of experimental observations,

Kutateladze /4/ has put forward a relationship which takes into account the

effect of the ~~sub~~ heating on the peak heat flux, which is as follows

$$q_{cr_1}' = q_{cr}' \left[1 + 0.065 \left(\frac{\gamma'}{\gamma''} \right)^{0.8} \frac{c_p \Delta t_n}{r} \right].$$ (4.19)

$\Delta t_n = t'' - t_f$.

in which Δ is the difference between the bulk of the liquid at temperature t_f

and the saturation point t''.

<u>Effect of state of heating surface on q_{cr_1}.</u> When the heating surface

is made rougher, q_{cr_1} is increased. This is due to the increased stability of the

liquid films as they adhere to the rough surface.

If a heated plate is ~~immersed~~ horizontally, q_{cr_1} is less than for the same

plate set on ~~its side~~. This is due to the fact that large vapor bubbles accumulate on

the bottom of the horizontal plate and make the generation of a vapor film easier.

Data from numerous experiments and theoretical calculations show that

there is a constant ratio between q_{-cr_1} and q_{-cr_2} for each liquid

$$\frac{q_{cr_1}}{q_{w'}} = k. \qquad (4.20)$$

According to the limited number of experimental data available, q_{-cr_1} can

be determined for different liquids, including/liquified gases O_2 and N_2; for the

case of boiling in a large volume /9/

$$q_{w'} = 300r(\gamma'')^{\frac{1}{2}}[s(\gamma'-\gamma'')]^{\frac{1}{4}}. \qquad (4.21)$$

It should be kept in mind however, that q_{-cr_2} is of no practical importance

and is rarely used.

Determining q_{-cr} during flow of liquid through pipes. When a liquid is

forced through pipes, the two-phase boundary layer proves more stable than during

free convection; this is partly because the inflow of cold liquid is greater, and

partly because of destruction of the nascent vapor film. Hence q_{-cr_1} increases with

an increase in the rate of flow as shown in Fig. 53. It can be seen from this

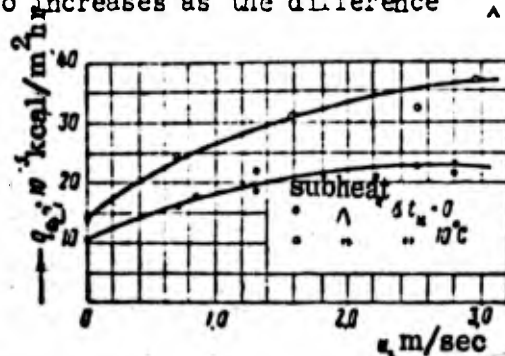graph that q_{-cr_1} also increases as the difference $\Delta t_s = t'' - t_{\tilde{\kappa}}$ increases.

Fig. 53. Effect of fluid velocity on first critical thermal
load (water $p \approx 1$ atm abs)

- 172 -

Numerous investigations of q_{cr_1} during motion of vapor-liquid mixtures

through pipes show that the walls overheat as a result of the normal peak heat flux

with the formation of an insulating vapor film in the boundary layer, and also as

a result of the drying up of the liquid film, some of the liquid in this case

continuing to move in the form of drops in the vapor stream. It has been pointed

out that in the high-pressure region close to critical the peak heat flux

degenerates in the   thermodynamic sense and the   pipe heats up bit by bit

rather than in the usual leaps and bounds, as the thermal load q increases. This

is more clearly marked at higher rates $U_0 > 10$ m/sec, when the vapor content

increases, and is greater for organic liquids than for water.

The importance of different conditions influencing the peak heat flux

has not been studied to an equal extent. Better known is the effect of pressure,

velocity and   sub heating on q_{cr}, the effect of vapor content has been studied to

a lesser extent, and it is only recently that the investigation of such factors as

the shape and size of channels has been begun.

Kutateladze /9/ recommends calculation of the first critical heat flux

density q_{cr} during the flow of low-viscosity liquids (water, alcohols, etc.) through

a cylindrical pipe and slotted channels by the following equation

$$q_w = A\eta^{-0.5} \cdot [\mathfrak{z}(\gamma' - \gamma'')]^{0.3} \cdot \left[U_c \left(\frac{\gamma - \gamma''}{\mathfrak{z}''}\right)^{0.25}\right]^m \times$$

$$\times \left[1 + B\left(\frac{\gamma}{\gamma''}\right)^n \frac{c_p \Delta t_s}{r}\right]. \qquad (4.22)$$

in which the coefficients A and B and the exponents m and n are determined empirically from experimental data. This equation is suitable for moderate values $U_0 < 20$ m/sec.

For higher velocities the Power Engineering Institute of the Academy of Sciences of the USSR has derived the following equation

$$q_{cr} = q_{cr_0} (1 + \delta \Delta t_s) \times$$

$$\times \left(1 + \frac{U}{W_0}\right)^{0.3}. \qquad (4.23)$$

in which q_{cr_0}, B and W_0 are coefficients calculated from experimental data for each liquid. Fig. 54 gives these coefficients for water as a function of pressure. Here the coefficient q_{cr_0} has the dimensionality of the heat flux [kcal/m² hour] for zero subheat and represents the hypothetically maximum value q_{cr} and zero velocity. It should be pointed out that q_{cr_0} is not equal to q_{cr_1}, since in a large volume the rate of motion of a liquid with natural convection is different from zero. The coefficient W_0 has the dimensionality of velocity [m/sec] and expresses the proportion of the mixing of the boundary layer which can be attributed to the nascent vapor bubbles. At low flow velocities, this proportion is high and q_{cr} varies only slightly with the velocity U. When the flow velocity increases, the relative effect of W_0 is decreased and the line $q_{cr} = f(U)$ becomes parallel to the line $q_{H.K} = f(U)$. The coefficient B has the dimensionality

$[1/\tau]$ and takes account of ᴛʜᴇ ᴇꜰꜰᴇᴄᴛ ᴏꜰ ꜱᴜʙ heating on the peak heat flux during flow through

a pipe, and is not the same as the effect of Δt_{H} on the peak in a large volume,
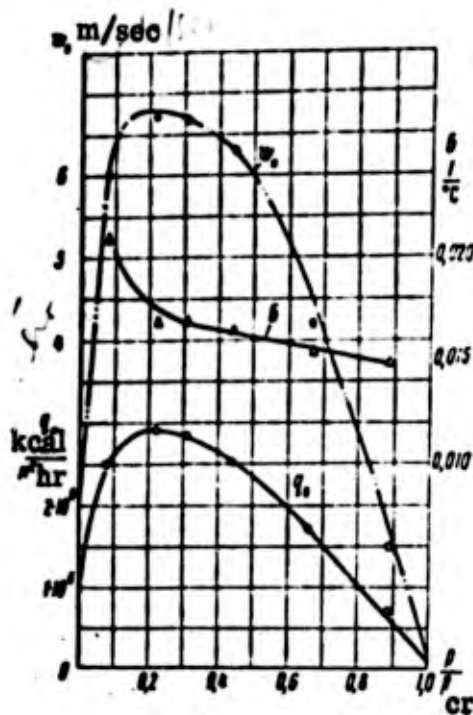
determined by Eq. (4.19)

Fig. 54. Coefficients q_0, W_0 and $\underline{B}$ as function of
pressure for water

The vapor content has a very complex affect on $\underline{q}_{\text{cr}}$ during flows through

a pipe. But there is no single opinion so far on this problem. It can only be

said that the effect of the vapor content is different at different weight

consumptions in the pipe.

It is known /4/ that when the perimeter of a pipe is heated up non-uniformly,

the peak . . . occurs at higher values of the heat flux q_{cr} than is the case

during uniform heating of the perimeter. The effect of the ratio of the length of

the heated area of the pipe and its diameter (L/D) has also been established, and

an increase in L/D leads to a decrease in q_{cr}. This effect is mainly appreciable

during the motion of a vapor-liquid mixture and at very low degrees of subheating

of the order of 5°. When the subheating is greater than 10°, the effect becomes

negligible, except for very short pipes L/D < 4, in which a further decrease in L/D

sharply increases q_{cr}.

An important part is played by the occurrence of the peak heat flux during

the flow of organic liquids when the phenomenon of thermal decomposition of the

liquids is imposed upon heat exchange during nucleate and film boiling, and there

is precipitation of a layer of fur and a sharp reduction in the heat-transfer

coefficient α. For the moment very little study has been made of this phenomenon.

Heat Transfer with free flow of liquid over heating surface

During cooling, quenching and other operations used in working cutting tools,

there is free flow of a liquid over the heating surface. Fig. 55 shows the

dependence of the total evaporation time of a drop of water on the temperature of

a horizontal metal plate /4/. As long as the temperature of the surface is
lower than the saturation point, the drops of liquid reaching the surface flow
along it and slowly evaporate. When the temperature of the surface exceeds the
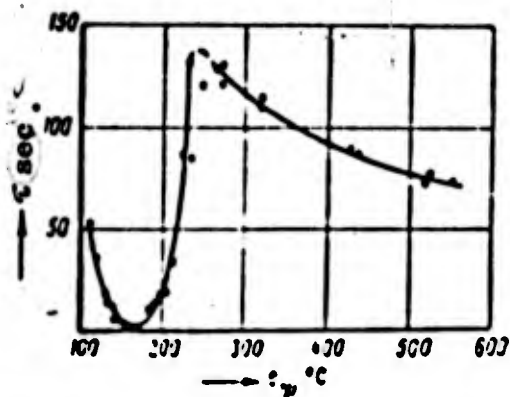

Fig. 55.   Evaporation time for drops (V = 0.0465 cm^3) as
function of wall temperature

saturation point, nucleate boiling is observed in the flowing liquid, the heat
transfer coefficient is sharply increased, and the evaporation time drops as the
nucleate boiling is intensified.

As soon as the temperature of the wall reaches a certain limit, a drop
reaching the surface . . .   no longer flows around it, but gathers into
a globule which intermittently comes into contact with the heating surface throughout
the evaporation time. A further increase in the temperature of the surface brings
about a reduction in the frequency of contact between the drop and the surface, and
the evaporation time begins to increase through a reduction in the heat-transfer

- 177 -

intensity to the liquid.

The maximum evaporation time corresponds to a cessation of contact between the drop and the surface and to the formation of a stable vapor layer separating the heating surface and the liquid. From then on the evaporation time for the drop is reduced through an increase in the surface temperature. Thus, the foregoing suggests the following:

1. There are two different types of boiling - nucleate and film.

2. The transition from nucleate boiling to film, and from film to nucleate boiling occurs at different specific thermal loads of the wall $q > q_{cr_1} , q_{cr_2}$ and corresponding heating of the wall

$$\Delta t_{cr_2} > \Delta t_{cr_1}$$

3. During nucleate boiling the heat-transfer coefficient increases with the heat flux density q and the of the wall Δt and reaches a maximum on the boundary between nucleate and film regimes.

4. During film boiling the heat-transfer coefficient retains a constant value which is less than the maximum α during nucleate boiling by a factor of 20 or 30.

5. Nucleate boiling of a liquid which does not wet a surface is close in nature to the film boiling of a liquid which does wet the surface.

- 178 -

6. Heat exchanges should operate on [the principle of] nucleate boiling.

Sec. 22. Heat Transfer with Vapor Condensation

If a vapor [comes into contact with] a wall with a temperature t_w lower than the saturation

point t'', the vapor condenses and the condensate settles on the wall.

There are two types of condensation: dropwise, when the condensate

settles in the form of separate drops, and film condensation, when the condensate

settles in the form of a film. Furthermore, there may be cases of mixed

condensation.

Dropwise condensation is marked by a particularly intensive heat

transfer, since direct contact with the cold wall is maintained throughout.

Dropwise condensation is only possible if the condensate does not wet the surface*

In practice there is always film condensation of the vapor in present-day

condensers. The only exception is the mercury vapor condenser in which there is

dropwise condensation. Hence below we only consider film condensation. Dropwise

---

* In the case of water vapor dropwise condensation can be artificially produced

on a polished surface covered with a thin layer of fat. The heat-transfer coefficients

during the condensation of water vapor at atmospheric pressure are as follows:

for film condensation $\alpha = 6000 \div 10\,000$ kcal/m². hour,

x with dropwise condensation $\alpha = 40\,000 \div 100\,000$ kcal/m². hour.

- 179 -

condensation is considered in /4/ and /3/.

In film-type condensation all the heat released during condensation of the vapor passes to the wall through the film of condensate. The motion of a liquid film is usually laminar, the transfer of heat through it is effected by molecular conductivity and the thermal resistance of the film is decisive for the heat transfer of the vapor to the surface of the body (the thicker the film, the less the heat transfer).

Let us assume the temperature of the condensate particles coming in contact with the wall is equal to that of the wall t_w , while the temperature of the particles in contact with the vapor is equal to the condensation point of the vapor t''; the specific heat flux from the vapor to the wall can then be determined by the following qualities

$$q_x = \frac{\lambda}{\delta_x}(t'' - t_w)$$ (4.24)

$$q_x = \alpha_x(t'' - t_w).$$ (4.25)

in which α_x is the heat-transfer coefficient during condensation of the vapor on the surface of the cooled body in the section x;

λ is the thermal conductivity of the condensate;

δ_x is the thickness of the film of condensate in the section x.

Equating the right-hand sides of equalities (4.24) and (4.25) we get

$$s_x = \frac{\lambda}{\delta_x} \quad kcal/m^2 \cdot hr \cdot deg \qquad (4.26)$$

The value λ of a liquid can always be taken from tables, hence the calculation of the heat-transfer coefficient in the given case reduces to determination of the thickness of the condensate layer δ_x, which should be found from the condition of equilibrium of friction, gravity, surface tension and inertia of the condensate element.

When vapor condenses on a vertical wall, the thickness of the dripping film of condensate gradually increases toward the bottom (see Fig. 56 /6/).

Below we give the formula derived by Nusselt* /6/ for the thickness of the condensate film

$$\delta_x = \sqrt[4]{\frac{4\lambda \mu x (t'' - t_w)}{\gamma^2 r}} \; M, \qquad (4.27)$$

in which x is the distance of the section under consideration from the upper edge of the wall.

---

* When deriving Eq. (4.27) the following simplifications were made: the film was taken as laminar; the surface tension of the film, inertia occurring in the film, convection transfer of heat in the film, friction between the condensate and the vapor, variation in specific gravity, thermal conductivity and viscosity of the condensate with temperature were all ignored.

The variation in the thickness of the film as a function of x calculated
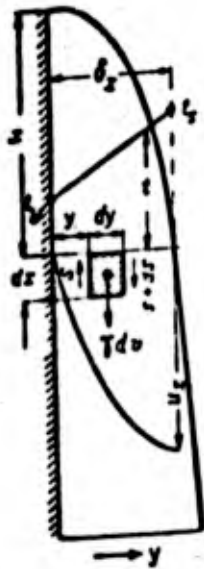
from Eq. (4.27) is shown in Fig. 57.
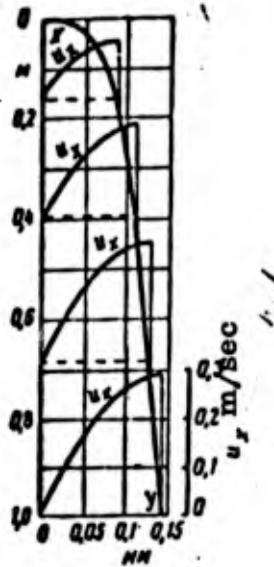

Fig. 56. Film condensation on
vertical wall

Fig. 57. Variation in film thickness and
velocity distribution in film of condensate

The variation in the velocity component $\underline{u}_{\underline{x}}$ in each section is shown in the sections marked with a broken line.

The mean heat-transfer coefficient during laminar flow of the film along a vertical wall and vertical pipe of height $\underline{H}$ can be determined by means of (4.26) and (4.27)

$$\alpha = \frac{1}{H}\int_0^H \alpha_x\,dx = 0.94\,\sqrt[4]{\frac{r\eta^3}{\mu H(t^{\prime}-t_{c})}}\cdot \text{kcal/m}^2\cdot\text{hr}\cdot\text{deg} \qquad (4.28)$$

For a wall sloping towards the horizon at an angle ψ , the heat-transfer coefficient α_ψ can be determined from the formula

$$\alpha_\psi = \alpha_{\text{vert}}\,\sqrt[4]{\sin\psi}. \qquad (4.29)$$

It was taken into account when deriving Eq. (4.29) that we should substitute the component parallel to the plane rather than the gravity of the film element into the equation of motion for a film element along an inclined plane /6/.

The surface of a horizontal pipe can be considered to consist of small plane elements at different angles ψ to the horizon. If we integrate with respect to ψ from 0 to 180°, the theoretical formula for the heat-transfer coefficient for a horizontal pipe takes the form

$$\alpha = 0.72\,\sqrt[4]{\frac{r\eta^3}{\mu d(t^{\prime}-t_{c})}}. \qquad (4.30)$$

in which d is the diameter of the pipes in meters.

Equations (4.28) and (4.30) are applicable to the vapor of any liquid
wetting surface. The values λ, γ and μ are selected from the mean temperature
of the film $\left(t_m = \frac{t'' + t_w}{2}\right)$, while r is taken from the condensation temperature t''. Nusselt's
derivations are approximate. When compared with experimental results, it transpires that
the theory reflects the general regularity of the theory correctly, but the actual
heat-transfer coefficients are approximately 20 - 22% greater than those derived
by Eq. (4.28). Academician Kapitsa has suggested the reason for this
discrepancy between theory and practice.

When a thin liquid film flows in an open channel, we have to take into
account the surface tension, which was omitted by Nusselt. In this case the
calculations show that for a motion of a film, it is not laminar motion, but
undular motion (which is observed in practice) that is the more stable. The
thermal conductivity of the film during motion of this kind proves to be 21%
greater than during laminar flow. Hence for vertical pipes we must introduce
the correction

$$\frac{\alpha}{\alpha_v} = 1.21_a.$$
(4.31)

in which α is the heat-transfer coefficient calculated from (4.28) and (4.29)
and α_v is the true heat-transfer coefficient for vertical pipes.

- 184 -

This correction cannot be extended to cover horizontal pipes, since on
account of the short length of the film there is no undular flow.

At the bottom of _long, vertical_ tubes, the flow becomes turbulent as a
result of the accumulation of a large amount of condensate, and the thermal
resistance of the film is sharply reduced. In this case, as well as during
dropwise condensation, the heat-transfer coefficient is greater than during film-
type condensation and undular flow of the nascent condensate film /4/.

The problem of heat exchange during condensation of a vapor can also be
solved on the basis of the similarity theory. By using the differential equations
describing the motion of an element of liquid film, and the processes of the
propagation of heat through it, plus the equation for the heat balance during the
condensation of the vapor, Kutateladze /4/ has found the following similarity
group for this case

$$Nu = \frac{al}{\lambda}; \quad Pr = \frac{\nu}{a}; \quad Ga = \frac{gl^3}{\nu^2} \text{ and } K = \frac{r}{c(t'' - t_x)}.$$

in which c is the thermal capacity of the liquid and,

l is the characteristic dimension on the condensation surface.

for pipes this is the length h and for horizontal pipes it is the diameter D.

According to the second theorem of similarity, the ~~~~~~ following general functional relationship between these dimensionless groups *must exist*

$$Nu = f(Ga, Pr, K).$$

(4.32)

This dependence is also confirmed by Eqs. (4.28) and (4.30), which can be represented in the following generalized form

$$Nu = C(Ga \cdot Pr \cdot K)^{0.25}.$$

(4.33)

Fig. 58 shows the results of experiments on heat transfer of *condensing* vapor from different liquids (on horizontal and vertical pipes. The experimental points for horizontal pipes lie along a straight line, for which $\underline{C} = 0.72$ and $\underline{n} = 0.25$, and thus satisfactorily confirm Eq. (4.33). For vertical pipes E·s. (4.28) and (4.31) are confirmed for a case $(Ga \cdot Pr \cdot K) < 10^{15}$, and in this region $\underline{C} = 1.15$ and $\underline{n} = 0.25$. For the region $(Ga \cdot Pr \cdot K) > 10^{15}$ $C = 0.06$ and $\underline{n} = 0.33$.
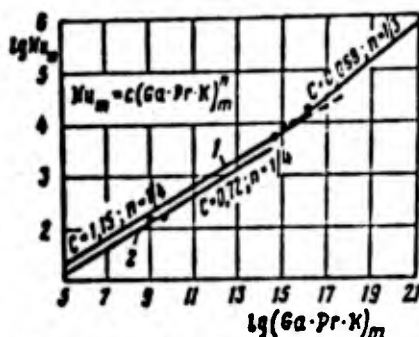
Fig. 58. Heat transfer of condensing steam:
1) on vertical tube; 2) on horizontal tubes

- 186 -

Thus, the equations for the heat-transfer coefficient during the condensation of vapor of vertical pipes acquire the following final form

$$Nu = 1.15 (Ga \cdot Pr \cdot K)^{0.25} \quad (Ga \cdot Pr \cdot K < 10^{15}).$$ (4.34)

$$Nu = 0.068 (Ga \cdot Pr \cdot K)^{0.13} \quad (Ga \cdot Pr \cdot K > 10^{15}).$$ (4.35)

Effect of Different Factors on Heat Transfer During Condensation

of Vapor

Effect of rate and direction of vapor flow. Equations (4.29), (4.30) and (4.31) are valid for rate of motion of the vapor of up to 10 m/sec. At high degrees of velocity there is marked friction between the vapor and the film. If the motion of the vapor . coincides with the flow of the film, the rate of flow of the latter is increased, its thickness is decreased and the heat-transfer coefficient rises.

When the vapor moves in the reverse direction, the film flow is decelerated, the thickness increases and α decreases. At high vapor velocities on account of which the friction may exceed gravity, the film begins to be carried upwards by the detached) vapor and is from the surface. Here α increases as the vapor velocity is increased. At low vapor pressures (0.1 atm abs), the effect of the vapor velocity on α is small (right up to $U = 75$ m/sec), but as the pressure is increased, even at 1 atm abs, the effect is greatly stepped up (see Fig. 59).

- 187 -

There is no explanation in literature for this experimental fact.

Effect of state of surface. An increase in the roughness of the surface

leads to increased friction of the film. Hence the thickness increases, and the

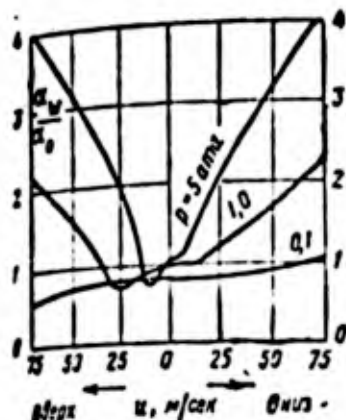reduction in the heat-transfer coefficient may be as much as 30% or more.

Fig. 59.   Variation in heat transfer coefficient during condensation
as function of velocity and direction of motion of water
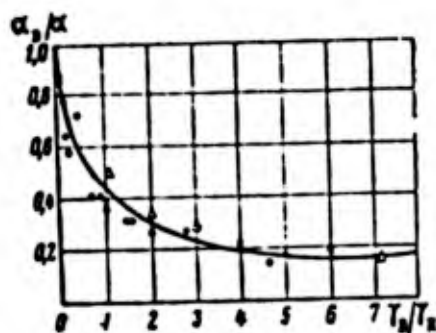vapor at different pressures

Fig. 60.   Relative variation in heat-transfer coefficient during
condensation as function of air content in vapor

The thermal resistance of the oxide film also reduces α to a great

extent.

- 188 -

Effect of _Super_ heating the vapor. In the case of condensation of a superheated vapor, it is essential to take the superheat. $q_s = c_s(t_s - t)$ kcal/kg into acount, and for the heat of vaporization r we have to substitute $r' = r + q_s$ into the theoretical formulae. Instead of the temperature difference we substitute $(t'' - t_w)$ into the formulae as before. In the case of superheated vapor the heat-transfer coefficient is only increased to a very slight degree (by 2 - 3%).

Effect of content of uncondensed gases (for example, air) in vapor.

If there are uncondensed gases in the vapor, the heat transfer is greatly reduced during condensation. This is due to the fact that the noncondensing gas flowing towards the surface is cooled together with the vapor and stays near the surface in the form of a concentrated layer of gas molecules, which hampers access to the film surface by the vapor.

The diffusion of vapor through this layer of gas molecules contributes a great degree of extra thermal resistance. Even a small content of air in water vapor appreciably reduces the heat-transfer coefficient. For example, 1% air contained in vapor reduces the coefficient by 60% (see Fig. 60 /6/).

In order to remove the air from the vapor, industrial condensers contain special air separators or air pumps.

Effect of design of heat exchanger. A single tube is most advantageously

placed in a horizontal position. It follows from Eqs. (4.30) and (4.28) that

$$\frac{\alpha_{hor}}{\alpha_{vert}} = \frac{0.72}{1.15}\sqrt[4]{\frac{H}{d}}. \tag{4.36}$$

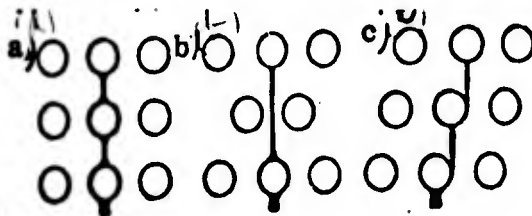For a pipe $\underline{d} = 0.02$ m and $\underline{l} = 1$ m, $\alpha_{hor}/\alpha_{vert} = 1.7$.

Fig. 61. Condensation of vapor in banks with different tube
arrangements. a) corridor arrangement; b) staggered
arrangement; c) arrangement for most favorable dripping
of condensate

This means that given equal condensation conditions, the heat-transfer

coefficient for a horizontal pipe is 1.7 times greater than for a vertical one.

But this is only valid for one pipe or for the upper row of pipes in a bank. In

banks with *a large number of rows* /8/ the condensate drips from the top rows to the bottom

ones (Fig. 61). Hence in the bottom rows the film is considerably thicker while

the heat-transfer coefficient is lower. The mean heat-transfer coefficient $\tilde{\alpha}$ for

the whole bank of horizontal tubes is determined by the correction coefficient ε,

which is selected from the experimental graph shown in ^{F}ig. 62, taking the layout

- 190 -

of the pipes into account /8/

in which α is the heat-transfer coefficient for one horizontal pipe, determined
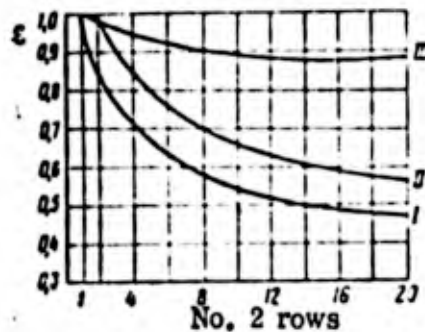
by Eq. (4.30).

Fig. 62. Correction coefficient for reduction in heat transfer of
condensing vapor in different banks of horizontal pipes:
1) corridor arrangement; 2) staggered arrangement;
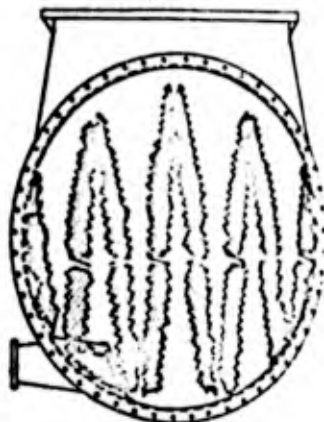3) same arrangement as in c in Fig. 61

Fig. 63. Arrangement of pipes in
industrial condensor

Fig. 64. Arrangement of caps
on vertical pipes for removing
condensate

- 191 -

In large condensers special sloping baffles (see Fig. 63) are usually inserted to remove the condensate at an intermediate stage /6/.

For vertical pipes the heat-transfer coefficient in a downward direction is reduced through thickening of the film. In this case the mean coefficient can be xx increased by installing caps to remove the condensate at different levels up the pipe (Fig. 64).

If placed every ~ 10 cm along a pipe of height $H = 3$ m, these caps double or treble the mean α .

Thus, the material which has been considered suggests that when vapor condenses the heat transfer is rather high. But we should pay particular attention to precautionary measures to prevent it being reduced by the presence of air, a method of wrong (removal of the condensate, deposits of oil on the surface, or other contaminations. It is precisely these extraneous factors which may explain the unsatisfactory operation of a condenser.

REFERENCES

1. Bolgarskiy, A. V. and other. Working processes in liquid-jet engines. Oborongiz, 1956.

2. Ziblend, I. Problems of heat transfer in rocket engines. "Problems of Rocketry", For. Lit. Press., 1956, No. 4.

3. Kruzhilin, G. N. Heat transfer from heating surface to boiling liquid with free convection. Reports of AS USSR, Vol 58, Issue 8, 1947; Heat transfer from horizontal plate to boiling liquid with free convection. Herald of AS USSR, OTN, Issue 7, 1948; Generalization of experimental data on heat exchange with boiling liquid under natural convection. Herald of AS USSR, OTN, Issue 5, 1949; Improvement of Nusselt's theory of heat exchange during condensation, Zhtf, Vol. 7, Issue 20/2, 1937.

4. Kutateladze, S. S. Fundamentals of theory of heat exchange, Chapters XIV, XV, XVI and XVII, Mashgiz, 1957.

5. Kutateladze, S. S. "Problems of heat exchange with variation in aggregate state of matter", Collection of articles, Gosenergozidat, 1953.

6. Mikheyev, M. A. Fundamentals of heat transfer, Chapter V, Gosenergozidat, 1956.

7. Sinyarev, G. B. and others. Liquid-fuel rocket engines, Chapter VII, Sec. 42 - 44 Oborongiz, 1956.

8. Shorin, S. N. Heat transfer, Chapters 11 and 12, Stroizdat, 1952.

9. Kutateladze, S. S. and others. Reference book on heat transfer, Chapters 11 and 12. Gosenergozidat, 1959.

10. Kutateladze, S. S. and others. Liquid-metal heat-transfer agents. Atom izdat, 1958.

CHAPTER V.

RADIANT HEAT EXCHANGE

Sec. 23. General Concepts and Definitions.

x   When a body is heated, some of the thermal energy is turned into

radiant energy and propagates into the surrounding space in the form of electro-

magnetic waves. Among these are the well-known X-ray, ultra-violet, light (visible)

rays and electromagnetic waves. The radiated waves spread through a vacuum at

the speed of light c = 300,000 km/sec and are distinguished, first and foremost,

by their frequency or wavelength, λ .

At moderate temperatures (up to 1500°) the bulk of the radiation energy

consists of rays with wavelength λ = 0.7 to 50 microns. This region of the

spectrum includes infra-red and, partially, light rays. At 6000°, about half

the radiant energy consists of visible and ultra-violet rays (λ = 0.3 - 0.6

microns).

Different bodies possess   powers of radiating energy *differing* both in

quantity and in the type of spectrum at the same temperature. Radiation is

inherent in all bodies with a temperature higher than absolute zero, and each

body radiates energy continuously. When it strikes other bodies, the energy

is partially absorbed and partially reflected, and partially passes through the body. The absorbed energy is turned into heat, while the reflected and transmitted parts strike other bodies, and are also partially absorbed. As a result of multiple absorption and reflection, the energy radiated by the body is fully distributed between the surrounding bodies.

Thus all bodies have the power to absorb radiant energy. If the temperature of bodies participating in mutual irradiation is different, radiant heat exchange occurs between them. The amount of heat received or given off by each body is equal to the difference in the amounts of absorbed and radiated energy. But if the bodies are at the same temperature, despite the fact that they are all continuously radiating and absorbing energy, they are in a state of thermal equilibrium, since the amount of energy received by them is equal to that given off. Radiant energy is measured in kilocalories. The amount of energy radiated from 1 m^2 of surface per 1 hour is termed the emissivity of a body or the surface hemispherical density of radiation, and is designated E

$$E = \frac{Q}{F} \text{ kcal/m}^2 \cdot \text{hr} \qquad (5.1)$$

Of the entire amount of irradiant energy incident on a body Q_0, part of it Q_A is absorbed, part Q_R is reflected, and part Q_D passes through (Fig. 65).

- 194 -

Hence

$$Q_A + Q_R + Q_D = Q_0$$

or

$$\frac{Q_A}{Q_0} + \frac{Q_R}{Q_0} + \frac{Q_D}{Q_0} = 1.$$

Introducing the new quantities, we get

$$A + R + D = 1. \tag{5.2}$$

Here $\underline{A}$ is the absorptivity of the body,

$\underline{R}$ is the reflectivity of the body,

$\underline{D}$ is the transmissivity.

The values, $\underline{A}$, $\underline{R}$ and $\underline{D}$ are dimensionless and may vary from 0 to 1.
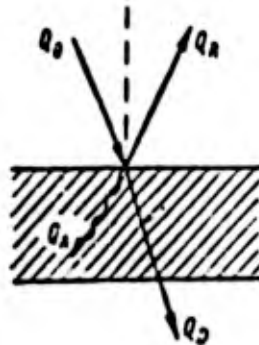
Fig. 65. Distribution of radiant energy

If $\underline{A} = 1$, then $\underline{R} = \underline{D} = 0$. This means that all the radiant energy

incident on the body is absorbed by it. Such bodies are said to be absolutely black.

If $\underline{R} = 1$, then $\underline{A} = \underline{D} = 0$, i.e., all the energy incident on the body

is reflected by it. If the reflection is directed and obeys the laws of geometric

optics, the bodies are said to be specular; but if the reflection is diffuse they

are said to be absolutely white.

If $\underline{D} = 1$ and $\underline{A} = \underline{R} = 0$, i.e., if all the energy incident passes through the

body, the bodies are said to be absolutely transparent.

In nature we do not find any absolutely black, absolutely white ones

or absolutely transparent ones. $\underline{A}$, $\underline{R}$ and $\underline{D}$ for actual bodies depend on their

nature, temperature and the wavelength of the radiation. Most solid bodies and

liquids are opaque for practical purposes; for them $\underline{D} \approx 0$. Certain bodies are

only transparent to rays of definite wavelengths, and are opaque to others.

For example, quartz is opaque to heat rays $(\lambda > 4\mu)$, but is transparent to

light and ultra-violet rays. Rock salt, on the contrary, is transparent to heat

rays and opaque to ultra-violet rays. Window glass is only transparent to light

rays, and practically opaque to heat and ultra-violet rays.

If the body is opaque, $\underline{A} + \underline{R} = 1$. Hence the better the body reflects,

the less energy it absorbs. That is why objects are painted with light colors

to reduce the effect of heating by the sun's rays. Light colors only help to

reflect visible rays, while the state of the surface has a greater effect on the

reflection and absorption of heat rays.

Smooth, polished surfaces, irrespective of color, reflect many times

better than rough ones. Bodies with an uneven coating of black paint may absorb

up to 90 - 96% of the energy.

The theory of thermal radiation, as well as in the experimental study

of emissivity and absorptivity, the concept of a black body, a model of which can

be constructed artificially, if is of very great importance. The properties of

an absolutely black body are possessed, for example, by a small opening in the

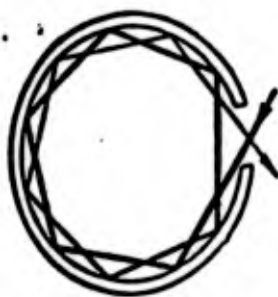wall of a hollow body (Fig. 66).

Fig. 66. Hollow body and behavior of ray inside it

Planck's Law

In order to evaluate the distribution of radiant energy over different

wavelengths, we utilize the concept of spectral radiation intensity J_λ (or

abbreviated to radiation intensity)

$$\lambda = \frac{dE}{d\lambda}. \qquad (5.3)$$

Hence, the emissivity E, which represents the total radiant energy through 1 m^2 of surface, is equal to

$$E = \int_{\lambda=0}^{\lambda=\infty} J_\lambda d\lambda. \qquad (5.4)$$

Planck established theoretically the following dependence between the spectral intensity of radiation of an absolutely black body J_{λ_s} and the wavelength and temperature (Planck's law)

$$J_{\lambda, s} = \frac{c_1 \lambda^{-5}}{e^{\frac{c_2}{\lambda T}} - 1} \quad \text{kcal/m}^3 \cdot \text{hr} \qquad (5.5)$$

in which λ is the radiation wavelength in m;

T is the absolute temperature in °K;

$c_1 = 3.21 \cdot 10^{-k}$ kcal $\cdot$ m^2/hour;

$c_2 = 1.44 \cdot 10^{-2}$ m $\cdot$ deg;

e is the natural logarithm base.

Planck's equation is easily confirmed by experiment. His law is shown graphically in Fig. 67.
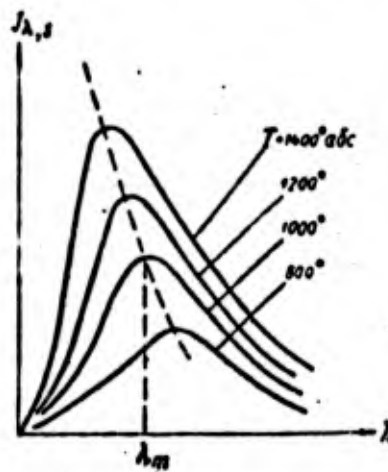

Fig. 67. Energy distribution of black radiation over spectrum

An analysis of this equation shows that at all temperatures the

radiation intensity $J_{\lambda,s}$ is equal to zero at very low and very high wavelengths λ,

while it exhibits a maximum at an intermediate value λ_m.

Thus, an absolutely black body reflects waves of all lengths from zero

to infinity at all temperatures, except $T = 0°$ abs. For all wavelengths the

radiation intensity increases with temperature.

Wien's Displacement Law

The "displacement" law follows from Planck's equation and establishes

the following relationship between the wavelength λ_m corresponding to maximum

radiation intensity and the temperature

$$\lambda_m T = \text{const} = 2.9 \text{ mm} \cdot \text{deg} \tag{5.6}$$

In order to obtain this relationship we need only equate the derivative

$dJ_{\lambda,s}/d\lambda$ with zero. But it was derived by Wien from thermodynamic principles

nine years before Planck developed his equation.

Wien's law shows that as the temperature rises, the maximum intensity

is displaced towards the shorter waves. A qualitative illustration of this law

incandescent
is the fact that metal first becomes red as the temperature rises, then

acquires other colors (orange, yellow) corresponding to shorter wavelengths in

the region of the visible spectrum.

Stefan-Boltzmann Law

The emissivity of an absolutely black body E_s is equal to the total

energy radiated from 1 m^2 of surface per hour and is determined by an equation

similar to (5.4)

$$E_s = \int_0^\infty J_{\lambda,s}\, d\lambda \;\; \text{kcal/m}^2 \cdot \text{hr}$$

Substituting $J_{\lambda,s}$ from Planck's equation into this one, we get

$$E_s = \int_0^\infty \frac{c_1 \lambda^{-5}}{e^{\frac{c_2}{\lambda T}} - 1}\, d\lambda$$

After transformation we finally get

$$E_s = c_s \left(\frac{T}{100}\right)^4 \text{kcal/m}^2 \cdot \text{hr} \tag{5.7}$$

in which $c_s = 4.6$ kcal/m$^2 \cdot$ hour $\cdot$ deg - is the radiation factor of an

absolutely black body. Thus the emissivity of an absolute black body E

is proportional to the fourth power of the absolute temperature. This law

was established experimentally by Stefan and theoretically substantiated by

Boltzmann twenty years before Planck established his law.

Radiation and Absorption of Non-Black Bodies

The radiation spectra of actual bodies differ from the spectrum of

an absolutely black. The radiation intensity at different areas of the wavelengths

are different, but at no point do they exceed the radiation intensity of an

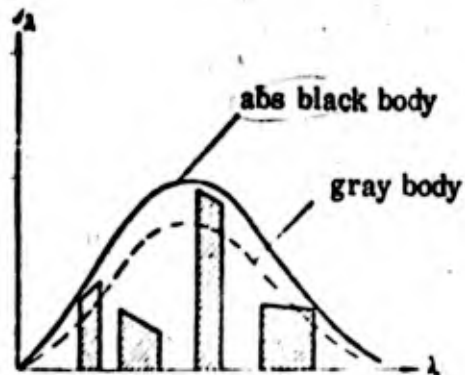absolutely black body at the same wavelength (Fig. 68).

Fig. 68. Radiation spectra

Many bodies have an intermittent (selective) variation spectrum. In this case the radiation intensity is equal to zero over certain areas of the wavelength.

A particular case of non-black radiation is the so-called "gray" radiation, which means that the intensity of radiation J_λ at all wavelengths comprises the same proportion ε of radiation intensity of an absolutely black body

$$\varepsilon = \frac{J_\lambda}{J_{o,\lambda}}. \qquad (5.8)$$

The value ε is called the degree of blackness or the black body coefficient. Most ~~used in engineering~~ solid bodies, with the exception of metals, can be

- 201 -

considered gray bodies with fair approximation. The blackness factor ε is

determined on the basis of experimental data.

The Stefan-Boltzmann law can be applied to gray bodies. The emissivity

of a gray body E is

$$E = \int_0^\infty \, \iota J_{\lambda,s}\, d\lambda = \varepsilon E_s = \varepsilon c_s \left(\frac{T}{100}\right)^4 = c \left(\frac{T}{100}\right)^4 \; \text{kcal/m}^2 \cdot \text{hr} \qquad (5.9)$$

in which c is the radiation factor $\text{kcal/m}^2 \cdot$ hour $\cdot \deg^4$.

The radiation factor c depends on the type of material, the temperature

and to a very great extent on the state of the surface. For example, for polished

copper $c = 0.20$, whereas for rolled copper it is $c = 3.18$.

Kirchhoff's Law

Kirchhoff's law relates emissivity and absorptivity of a body in a

state of equilibrium. Let us consider two parallel surfaces placed so near to

one another, compared with their dimensions, that the rays emitted by each of

them inevitably fall on the opposite surface (Fig. 69). Let us consider that

surface I is gray, that II is absolutely black, and that both surfaces are at

the same temperature $T_1 = T_2$.

The system is in a state of thermal equilibrium, and the amount of

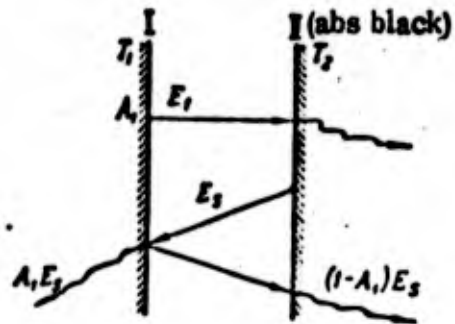energy emitted by each surface is inevitably equal to the amount absorbed.

- 202 -

Fig. 69. Derivation of Kirchhoff's law

The gray wall emits E_1, but only absorbs part of the energy incident on it from the black wall in accordance with its absorptivity $A_1 E_s$. Hence, $E_1 = A_1 E_s$ or $E_1 / A_1 = E_s$. But since surface I has been taken arbitrarily, the relationship derived is valid for any bodies

$$\frac{E_1}{A_1} = \frac{E_2}{A_2} = \ldots$$
$$\ldots = \frac{E}{A} = E_s = f(T).$$

(5.10)

Thus, the ratio of the emissivity and the absorptivity at thermal equilibrium is the same for all bodies, is equal to the emissivity of an absolutely black body at the same temperature, and is only a function of temperature. This is, in fact, Kirchhoff's law.

The law is valid as well for rays of any wavelength, i.e., for monochromatic radiation. In this case

$$\frac{J_\lambda}{A_\lambda} = J_{\lambda,s} = f(\lambda, T);$$

(5.11)

Hence the ratio of the monochromatic intensity of radiation J_λ at the given

wavelength to the absorptivity at the same wavelength for all bodies is the

same, and solely a function of the wavelength and temperature. In particular,

for gray bodies $A_\lambda = \varepsilon$ and is the same at all wavelengths, since

$$\frac{J_\lambda}{J_{\lambda,s}} = \varepsilon.$$

It follows from Kirchhoff's law that the more intensively the body

emits rays of a given wavelength, the more strongly it absorbs them. If the

body does not absorb energy at a particular wavelength ($A_\lambda = 0$), it does not

emit it either ($I_\lambda = 0$).

Absorption of Energy by transparent media

Let us assume we have a certain medium which is impinged upon by a

beam of rays with monochromatic intensity J_λ' (Fig. 70). As they pass through

the medium, the intensity is reduced. In the elementary layer dS the drop in intensity

dJ_λ is equal to

$$dJ_\lambda = -\beta_\lambda J_\lambda \, dS, \qquad\qquad (5.12)$$

in which β_λ is the coefficient of absorption of radiant energy by the material
at the given wavelength λ, and is a function of the physical
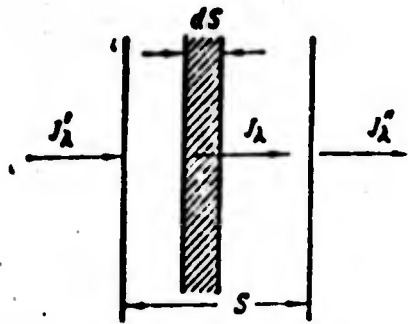properties of the medium and the temperature.

Fig. 70.   Variation in intensity of radiant energy
when passing through body

Separating the variables and integrating *over* the whole
layer S, we get

$$\frac{dJ_\lambda}{J_\lambda} = -\beta_\lambda dS;$$

$$\ln\frac{J_\lambda}{J_\lambda'} = -\beta_\lambda \cdot S; \quad \frac{J_\lambda}{J_\lambda'} = e^{-\beta_\lambda S}.$$

Subtracting the right-hand and left-hand sides of the equality from
unity, we get

$$\frac{J_\lambda' - J_\lambda}{J_\lambda'} = 1 - e^{-\beta_\lambda S} \qquad (5.13)$$

or

$$A_\lambda = 1 - e^{-\beta_\lambda S}. \qquad (5.14)$$

in which A_λ is the absorptivity of the medium for rays of wavelength λ.

It is clear from this equation that even at a low coefficient of
absorption β_λ, though with a (layer *very thick*, the absorption may be

considerable. If β_λ is very *high* , as in most solid bodies, absorption occurs in

a very thin surface layer. In this case we can tentatively consider that the

absorption   occurs on the surface.

Lambert's Law

The Stefan-Boltzmann law determines the total amount of energy emitted

by a body in all directions. The variation in emission for different directions

is determined by Lambert's law.

Let us consider radiation into space with an elementary area dF on the

surface of a body (Fig. 71). The total amount of energy emitted in all directions

within the hemisphere from 1 m^2 of surface per unit time is equal to the

emissivity E *k* cal/m^2· hour. The amount of energy emitted per unit time

from the elementary area dF on the surface of a body in a beam *bounded* by the

elementary solid angle dΩ and directed at an angle φ to the normal to the surface
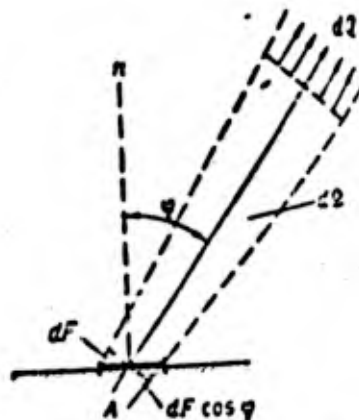
is equal to dQ kcal/hour.

Fig. 71. From Lambert's Law

Let us introduce the two concepts:

E_φ is the amount of energy emitted in the direction φ per unit of solid

angle through 1 m² of area on the surface of a body per unit time,

$$E_\varphi = \frac{dQ}{d\Omega \cdot dF} \text{ kcal/m}^2 \cdot \text{hr} \cdot \text{steradian} \qquad (5.15)$$

J_φ is the amount of energy emitted in the direction φ per unit solid

angle per unit time through 1 m² area normal to the given direction.

$$J_\varphi = \frac{dQ}{d\Omega \cdot dF \cdot \cos\varphi} \text{ kcal/m}^2 \cdot \text{hr} \cdot \text{steradian} \qquad (5.16)$$

The value J_φ is termed the intensity of radiation in the given direction

(as distinct from the monochromatic intensity of radiation J_λ). It is similar

to the concept of brightness in optics. The value J_φ may be different for

different directions. But if J_φ is constant in all directions, this radiation

is termed diffuse.

The relationship between E_φ and J_φ is clear from the definitions

$$E_\varphi = J_\varphi \cos\varphi.$$

This relationship is indeed Lambert's law. In particular, for diffuse

radiation (J_φ = const) the amount of energy emitted from 1 m² of surface per unit

solid angle per unit time E_φ is proportional to the cosine of the angle between

the direction of radiation and the normal to the surface.

J_φ can be expressed in terms of the emissivity E by taking the integral within the hemisphere

$$E = \iint_{\theta = 2\pi} J_\varphi \cos \varphi\, d\Omega.$$

(5.17)

Since $d\Omega = \dfrac{df}{r^2}$ (see Fig. 72),

$$d\Omega = \frac{r\, d\varphi\, r \sin \varphi\, d\psi}{r^2} = d\varphi \sin \varphi\, d\psi$$

and

$$E = J_\varphi \iint_{\theta = 2\pi} \cos \varphi\, d\Omega = J_\varphi \int_{\psi=0}^{\psi=2\pi} d\psi \int_{\varphi=0}^{\varphi=\frac{\pi}{2}} \sin \varphi \cdot \cos \varphi\, d\varphi = J_\varphi \cdot \pi.$$

(5.18)

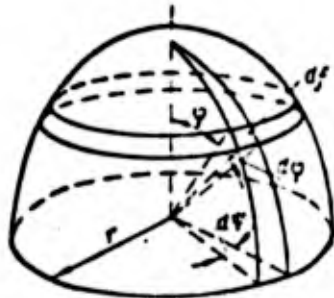Fig. 72. Determining spatial angle in spherical coordinates

Thus, for diffuse radiation $E = \pi J_\varphi$, i.e., the emissivity E is greater numerically than the intensity of radiation in any direction J_φ by a factor of π.

- 208 -

Let us recall that E and J_φ have different dimensionality. After

substitutions, we finally get

$$E_\varphi = \frac{c \cdot \epsilon_0}{s}\left(\frac{T}{100}\right)^4 \cos\varphi \;\; \textit{ккал}/\textit{м}^2 \cdot \textit{час} \cdot \textit{стерад}. \qquad (5.19)$$

Experience shows that for most actual bodies the intensity of radiation J_φ

only varies very slightly over a range ⁓‿‿ angles φ from 0 to $60°$.

Examples of the variation $J_\varphi / J_{\varphi,s}$, for different materials are shown in

Fig. 73. Here $J_{\varphi,s}$ is the intensity of radiation of an absolutely black body in
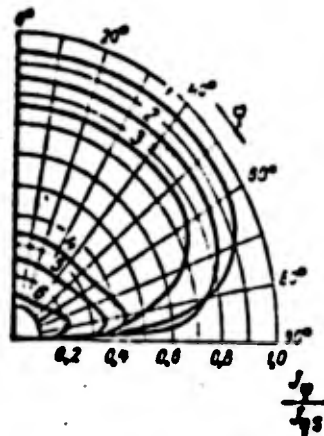
the given direction.

Fig. 73. $J_\varphi / J_{\varphi,s} = f(\varphi)$ for rough and smooth
bodies. 1 - wood; 2 - corundum; 3 - oxidized
copper; 4 - bismuth; 5 - aluminum-bronze;
6 - brass

1, 2, 3 - rough
4, 5, 6 - polished

So far we have been evaluating the radiation source from the amount of energy emitted from 1 m² of area of its surface. Another characteristk of the source is the amount of energy per 1 m² of surface irradiated by it. This is

irradiance?

the so-called irradiation power of the source e similar to the concept of illuminance in optical engineering.

In the case of radiation from a point source uniform in all directions Q_1 kcal/hour for a sphere of radius r

$$e = \frac{Q_1}{4\pi r^2}.$$

If the irradiated area dF is set at an angle φ to the surface of the sphere, the amount of energy falling on it from the point source A (Fig. 72) is equalt to

$$dQ = e \cos\varphi\, dF = \frac{Q_1}{4\pi r^2} \cos\varphi\, dF. \tag{5.20}$$

The law of inverse proportion $dQ \sim 1/r^2$ becomes less applicable as the dimension of the source increases, compared with r. At the limit the irradiation power does not depend on distance for an infinitely large source.

(For example, in radiation pyrometers the readings are not a function of distance as long as the surface covers the entire field of vision of the pyrometer).

For ~medium~ -size sources

$$dQ \sim \frac{1}{r^m}, \text{ where } m = 0 \div 2.$$

Radiant heat exchange between two parallel surfaces

Let us consider ~the~ very simple problem of radiant heat exchange between two bodies with plane parallel surfaces (Fig. 74). For each of the bodies we are given the temperature T, the emissivity E and the absorptivity A. Furthermore, $T_1 > T_2$.

The first surface radiates E_1 per hour ~per~ 1 m^2. Of this amount the second absorbs $E_1 A_2$ and reflects $E_1 (1 - A_2)$. Of this the first surface absorbs $E_1(1-A_2)A_1$ and the second $E_1(1-A_2)(1-A_1)$. The second surface reabsorbs $E_1(1-A_2) \times$ ~and~ $\times (1-A_1)A_2$ reflects $E_1(1-A_2)^2(1-A_1)$.

Of this amount the first surface reabsorbs $E_1(1-A_2)^2(1-A_1)A_1$, and so on ad infinitum.
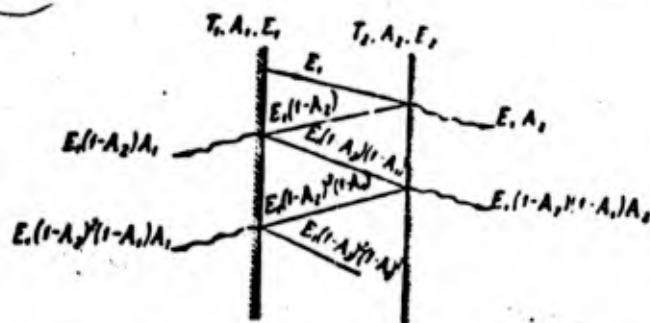

Fig. 74. Radiant heat exchange between plane-parallel surfaces

Similar arguments can be put forward for the transients of the energy E_2 emitted by the second surface. To find the energy q ∧ which is received by the second surface through mutual irradiation with the first, we calculate the total amount of energy absorbed by each of the surfaces.

The second surface receives through radiation by the first

$$q_{1-2} = E_1 A_2 + E_1 (1 - A_2)(1 - A_1) A_2 + \cdots$$
$$\cdots + E_1 (1 - A_2)^{s-1}(1 - A_1)^{s-1} A_2.$$

$$\underline{p = (1 - A_2)(1 - A_1)}$$

This series represents a geometric progression with the denominator ∧

and can easily be worked out

$$q_{1-2} = \frac{a_1}{1 - p} = \frac{E_1 A_2}{1 - (1 - A_2)(1 - A_1)}. \qquad (5.21)$$

Similarly the amount of energy received by the first wall through radiation from the second is equal to

$$q_{2-1} = E_2 A_1 + E_2 (1 - A_1)(1 - A_2) A_1 + \cdots$$
or
$$\cdots + E_2 (1 - A_1)^{s-1}(1 - A_2)^{s-1} A_1$$

$$q_{2-1} = \frac{E_2 A_1}{1 - (1 - A_1)(1 - A_2)}. \qquad (5.22)$$

As a result of mutual irradiation, the second surface receives

$$q_2 = q_{1-2} - q_{2-1} = \frac{E_1 A_2}{1 - (1 - A_1)(1 - A_2)} - \frac{E_2 A_1}{1 - (1 - A_1)(1 - A_2)} =$$
$$= \frac{E_1 A_2 - E_2 A_1}{A_1 + A_2 - A_1 A_2} \text{ kcal/m}^2 \cdot \text{hr} \qquad (5.23)$$

Substituting in accordance with the Kirchhoff and Stefan-Boltzmann laws

- 212 -

and

$$E_1 = A_1 E_s = A_1 c_s \left(\frac{T_1}{100}\right)^4$$

$$E_2 = A_2 E_s = A_2 c_s \left(\frac{T_2}{100}\right)^4,$$

and after the substitutions we get

$$q_a = \frac{A_1 c_s \left(\frac{T_1}{100}\right)^4 A_2 - A_2 c_s \left(\frac{T_2}{100}\right)^4 A_1}{A_1 + A_2 - A_1 A_2} = A_a c_s \left[\left(\frac{T_1}{100}\right)^4 - \left(\frac{T_2}{100}\right)^4\right]. \tag{5.24}$$

in which

$$A_a = \frac{1}{\frac{1}{A_1} + \frac{1}{A_2} - 1} = \varepsilon_a$$

is the reduced absorptivity of the system of bodies or the reduced degree of

blackness of the system $\left(\varepsilon_a = \overline{A_a}\right)$.

Having replaced A by the equivalent values for gray bodies $(A = \varepsilon)$,

we get

$$A_1 = \frac{c_1}{c_s} \quad \text{и} \quad A_2 = \frac{c_2}{c_s},$$

$$A_a c_s = \frac{1}{\frac{1}{c_1} + \frac{1}{c_2} - \frac{1}{c_s}} = c_a. \tag{5.25}$$

Here c_a is the reduced radiation factor of the system of bodies

between which there is radiant heat exchange.

The final theoretical equation for heat exchange takes the form

$$q_a = c_a \left[\left(\frac{T_1}{100}\right)^4 - \left(\frac{T_2}{100}\right)^4\right] \text{ kcal/m}^2 \cdot \text{hr} \tag{5.26}$$

The problem of heat exchange between two surfaces in an enclosed space

is more complex than plane parallel surfaces, but can be solved in a similar fashion.

In this case only part of the emission by one of the surfaces strikes the other,

while the bulk of it misses by and again strikes the first surface.

The final theoretical equation takes the form

$$Q_a = c_a F_1 \left[\left(\frac{T_1}{100} \right)^4 - \left(\frac{T_2}{100} \right)^4 \right] \text{ kcal/hr} \qquad (5.27)$$

in which c_a is the reduced radiation factor of the system

$$c_a = \frac{1}{\frac{1}{c_1} + \frac{F_1}{F_2} \left(\frac{1}{c_2} - \frac{1}{c_s} \right)} \qquad (5.28)$$

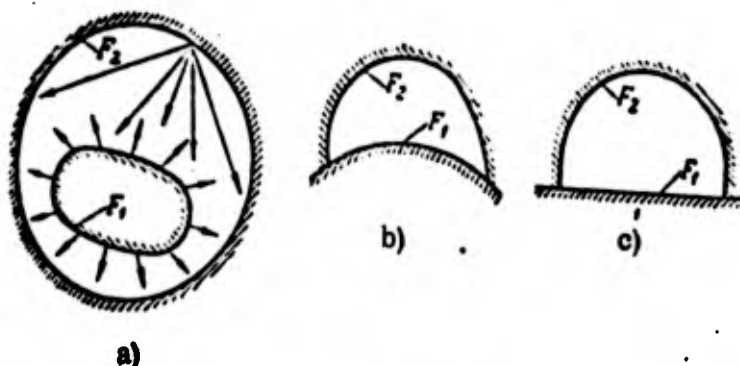and F_1 is the area of the smaller surface.

a)

Fig. 75. Simple calculation systems for radiant heat exchange in enclosed spaces

The equation is applicable to bodies of any shape, provided the smaller

one is convex. In particular, it is applicable to calulation of heat exchange

between long cylinders, and also when the convex body, 1, and the concave body, 2,

form an enclosed space (Fig. 75).

Radiant heat exchange between two surfaces placed arbitrarily

in space

The solutions given above for the problem of radiant heat exchange for very simple cases cannot be extended to cover the more complex cases which are usually encountered in practice.

It is only possible to produce approximate solutions in most of the engineering problems. Let us consider one such solution in greater detail. Let there be two elements of a surface dF_1 and dF_2, arranged arbitrarily in space (Fig. 76). The temperature, emissivity and absorptivity of the surfaces are known and equal, respectively, to $T_1, E_1, A_1; T_2, E_2, A_2$.

Let us *use the following quantities*

r is the distance between the elements dF_1 and dF_2,

and *φ_1 and φ_2* are the angles between normals and a line joining their centers

(φ_1 and φ_2 may be situated in different planes),

$d\Omega_1$ is an elementary spatial angle.

According to Lambert's law, the element dF_1 radiates in the direction of element dF_2

$$dQ_1 = \frac{E_1}{\pi} dF_1 d\Omega_1 \cos \varphi_1 \quad \text{kcal/hr}. \qquad (5.29)$$

in which

$$d\Omega_1 = \frac{dF_2 \cos \varphi_2}{r^2}.$$

Then,

$$dQ_1 = \frac{1}{\pi} E_1 dF_1 \frac{dF_2 \cos \varphi_2}{r^2} \cos \varphi_1. \qquad (5.30)$$
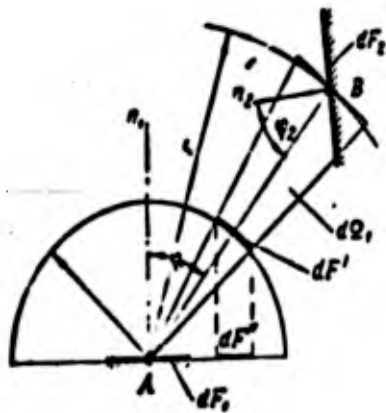

Fig. 76. Derivation of equations for radiant heat exchange between surfaces Df_1 and Df_2
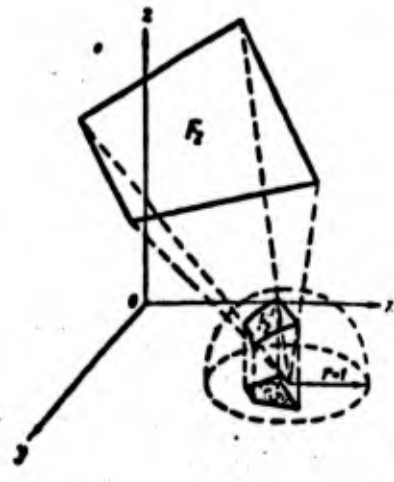

Fig. 77. Graphic determination of angular coefficient

Of this amount of energy the element dF_2 absorbs

$$dQ_{1\to2} = A_2 dQ_1. \qquad (5.31)$$

Since A is large (0.8 - 0.9) for most ~~encountered in engineering~~ bodies, we need only

take the first absorption into account.

The amount of energy absorbed by the element dF_1 through radiation

from dF_2 is calculated in similar fashion

$$dQ_{2\to1} = A_1 \frac{1}{\varkappa} E_2 dF_2 \frac{dF_1 \cos \bar\varphi_1}{r^2} \cos \bar\varphi_2. \qquad (5.32)$$

The amount of energy transmitted through mutual irradiation by the first

element to the second one is found as the difference

$$dQ_{12} = dQ_{1\to2} - dQ_{2\to1} =$$
$$= \frac{1}{\varkappa} (A_2 E_1 - A_1 E_2) \frac{\cos \bar\varphi_1 \cos \bar\varphi_2}{r^2} dF_1 dF_2 \quad \text{kcal/hr} \qquad (5.33)$$

Replacing $E_1 = A_1 c_s \left(\frac{T_1}{100}\right)^4$ and $E_2 = A_2 c_s \left(\frac{T_2}{100}\right)^4$,

we get $\quad dQ_{12} = A_1 A_2 c_s \left[\left(\frac{T_1}{100}\right)^4 - \left(\frac{T_2}{100}\right)^4\right] \frac{\cos \bar\varphi_1 \cos \bar\varphi_2}{\varkappa r^2} dF_1 dF_2. \qquad (5.34)$

For surfaces of finite dimensions, the amount of heat transferred

by radiation is determined by the integration of dQ_{12} with respect to F_1 and F_2.

We get

$$Q_{12} = A_1 A_2 c_s \left[\left(\frac{T_1}{100}\right)^4 - \left(\frac{T_2}{100}\right)^4\right] \int_{F_1} dF_1 \int_{F_2} \frac{\cos \bar\varphi_1 \cos \bar\varphi_2}{\varkappa r^2} dF_2. \qquad (5.35)$$

Abreviated quantities are usually found in literature

and the last equation is written as follows

$$Q_{12} = \varepsilon_n c_s F_p \left[\left(\frac{T_1}{100}\right)^4 - \left(\frac{T_2}{100}\right)^4\right] \varphi_{12} \quad \text{kcal/hr} \qquad (5.36)$$

- 217 -

$$c_s = 4.9 \ \text{ккал}\ м^2\cdot час\cdot град^4;$$

$\left(\frac{1}{\varepsilon} = \varepsilon_1 \varepsilon_2 = A_1 A_2\right)$ is the reduced degree of blackness of the system;

F_h is the conditional theoretical surface of heat exchange;

φ_{12} is the mean angular coefficient or irradiation factor.

The mean angular coefficient is a purely geometric parameter

$$\varphi_{12} = \frac{1}{F_9} \int_{F_9} dF_1 \int_{F_9} \frac{\cos \varphi_1 \cos \varphi_2}{\pi r^2} \, dF_2 = \frac{2}{F_9} \int_{F_9} \varphi' \, dF_2. \qquad (5.37)$$

The numerical value of φ' shows the portion of energy emitted by the element dF_1 for the whole semi-space which strikes the surface F_2. The value φ_{12} is an averaged value of φ' for the whole of the surface of F_2. In certain cases φ' can be determined graphically (see Figs. 76 and 77).

Let us draw a tangent plane through the element dF_1 and let us plot a hemisphere with a radius of unity from the center A. The elementary area of the cross section of the solid angle $d\Omega$ of the hemisphere $r = 1$ is equal to

$$dF_2' = \frac{dF_2}{r^2} \cos \varphi_2.$$

The projection dF_2' onto the principal tangent plane is

$$dF_2' = dF_2' \cos \varphi_1 = \frac{\cos \varphi_1 \cos \varphi_2}{\pi r^2} \, dF_2.$$

The area of the circle at the base ($r = 1$) is equal to π,

$$\frac{dF_2^\circ}{\pi} = d\varphi' = \frac{\cos \varphi_1 \cos \varphi_2}{\pi r^2} \, dF_2.$$

That was how the elementary angular coefficient $d\varphi'$ was determined.

In order to find the angular coefficient φ' for the entire surface we have to take the integral

$$\varphi' = \int_{F_2} \frac{\cos \varphi_1 \cos \varphi_2}{\pi r^2} dF_2.$$
(5.38)

Graphically this can be reduced to determining by the above method the projection F''_2, after which we take its ratio to the area of the circle $r = 1$ (see Fig. 77)

$$\varphi' = \frac{F'_2}{\pi}.$$
(5.39)

Similar plottings can be made for each element into which the surface F_1 divides up. Integration with respect to F_1 is replaced by summation. Graphically this can be reduced to finding the volume of a body, the base of which has the area F_1, and the height of which is φ'. Finally, by dividing this volume by the theoretical surface F_{th}, we get the mean angular coefficient φ_{12}

$$\varphi_{12} = \frac{V}{F_\varphi}.$$

It is very difficult to determine the angular coefficient by this method in the case of complex systems. Since the angular coefficients are equal for geometrically similar systems, their values may be determined on the basis of experiments with models.

The angular coefficients have been calculated for certain cases of radiant heat exchange encountered in practice and are given in the form of graphs, /2/. The arrangement of the surfaces for these cases is shown in Fig. 78.
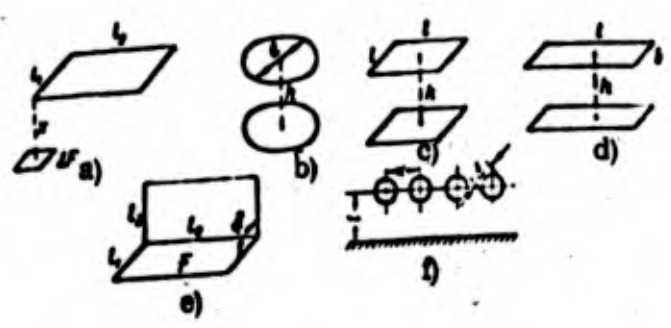
Fig. 78. Systems of radiant heat exchange

Solar radiation

In a number of problems of engineering involving heat exchange, solar radiation plays a substantial part. The amount of energy emitted by the sun per 1 m^2 of area perpendicular to its rays per hour at an average distance between the sun and earth (beyond the limits of the atmosphere) is constant and equal to S

S_0 = 1140 kcal/m^2. hour. S_0 is known as the solar constant.

The density of the stream of direct solar radiation at the earth's surface S is less than S_0 and is a function of the degree of transparency of the atmosphere.

For example, at mid-day in Moscow *according to the* seasons S ranges

from 480 to 740 kcal/m^2 · hour.

The density of the stream of solar radiation S' incident on *the* horizontal

surface of the earth is a function of the angular elevation of the sun above the

horizon h_0 and is equal to

$$S' = S \sin h_c.$$

The theoretical equation for the radiant heat exchange *between* a body *and*

the surrounding medium, taking into account *solar* radiation, takes the form

$$Q_{12} = \epsilon_1 c_s F_1 \left[\left(\frac{T_1}{100} \right)^4 - \left(\frac{T_2}{100} \right)^4 \right] - A_{1(s)} F_0 S. \qquad (5.40)$$

in which

Q_{12} is the amount of heat supplied or received by the body in kcal/hour;

T_1 is the temperature of the body in °K

T_2 is the temperature of the surrounding space in °K,

S is the density of the stream of solar radiation in kcal/m^2 · hour;

F_1 is the surface of a body radiating energy in m^2;

F_0 is the surface of the body illuminated by the sun in m^2;

$A_{1(s)}$ is the absorptivity of the body with respect to the sun's rays

(given in Table /2/);

ϵ_1 is the degree of blackness of the surface of the body.

<u>Note</u>. The formula has been derived from a general formula for radiant heat exchange between two surfaces in an enclosed space (see 5.27)

$$Q_a = \frac{1}{\frac{1}{\varepsilon_1} + \frac{F_1}{F_2}\left(\frac{1}{\varepsilon_2} - 1\right)}\, \varepsilon_s F_1\left[\left(\frac{T_1}{100}\right)^4 - \left(\frac{T_2}{100}\right)^4\right] \tag{5.41}$$

taking into account the surface ratio $\left(\frac{F_1}{F_2} \approx 0\right)$.

Protection from radiation

In order to reduce radiation heat exchange use is made of shields. Let us consider two parallel surfaces between which there is a shield in the form of a thin plate made of the same material $(c_1 = c_2 = c_3)$.

The temperature of the surfaces and the shield are equal, respectively, to T_1, T_2 and T_3 (Fig. 79).

If the shield were not there, the heat flux per 1 m^2 of surface would be equal to

$$q_{1,2} = c_s\left[\left(\frac{T_1}{100}\right)^4 - \left(\frac{T_2}{100}\right)^4\right] \text{ kcal/m}^2 \cdot \text{hr} \tag{5.42}$$

Fig. 79. Positioning of screen

When the screen is there, the following amount is transmitted from

the surface I to the shield

$$q_{1,0} = c_s \left[\left(\frac{T_1}{100} \right)^4 - \left(\frac{T_0}{100} \right)^4 \right].$$

and from the shield to the surface II

$$q_{0,2} = c_s \left[\left(\frac{T_0}{100} \right)^4 - \left(\frac{T_2}{100} \right)^4 \right].$$

Under steady-state heat conditions, $q_{1,0} = q_{0,2}$ and

$$\left(\frac{T_1}{100} \right)^4 - \left(\frac{T_0}{100} \right)^4 = \left(\frac{T_0}{100} \right)^4 - \left(\frac{T_2}{100} \right)^4.$$

from which

$$\left(\frac{T_0}{100} \right)^4 = \frac{1}{2} \left[\left(\frac{T_1}{100} \right)^4 + \left(\frac{T_2}{100} \right)^4 \right];$$

but since

$$q_{1,0} = q_{0,2} = c_s \left[\left(\frac{T_1}{100} \right)^4 - \left(\frac{T_0}{100} \right)^4 \right] = c_s \left[\left(\frac{T_1}{100} \right)^4 - \frac{1}{2} \left(\frac{T_1}{100} \right)^4 - \frac{1}{2} \left(\frac{T_2}{100} \right)^4 \right];$$

therefore

$$q_{1,0} = q_{0,2} = \frac{1}{2} c_s \left[\left(\frac{T_1}{100} \right)^4 - \left(\frac{T_2}{100} \right)^4 \right]. \tag{5.43}$$

i.e., when there is one shield, the amount of heat transferred by radiation is

halved.

It can be seen that if there are two shields, the amount of heat

is reduced by a factor of three, and if there are n shields, it is reduced by

a factor of $(n + 1)$.

The efficiency of the screen increases to a great extent when made of a good heat-reflecting material, i.e., one with a low ε .

Irradiation and absorption of gases.

Gases also possess the power of irradiation and absorbing radiant energy. The power differs with different gases. In monotopic and diatopic gases it is insignificant. For example, N_2, C_2 and H_2 are for practical purposes transparent to heat rays. But, Considerable emissivity, of great importance in practice, is possessed by polyatomic gases, in particular, carbon dioxide (CO_2) water vapor (H_2O), sulphur anhydride (SO_2), ammonia (NH_2), and other substances.

Compared with solid bodies, the radiation and absorption of gases exhibit two different and important features:

1. As distinct from solid bodies which mainly have continuous, uninterrupted radiation spectra, the radiation of gases is selective in nature. This means that gases only radiate energy over a certain range of wavelengths, or so-called bands.

According to Kirchhoff's law which we considered earlier, gases can only emit rays with the wavelengths which they can absorb ($J_\lambda = A_\lambda J_{\lambda_s}$). Hence the absorption of gases is also selective.

2. As distinct from solid, opaque bodies, in which absorption and radiation occur in the thin surface layer, gases radiate and absorb throughout their volume.

The energy of heat rays passing through a layer of gas is reduced. Here the degree of absorption depends on the number of molecules encountered on the way. The latter is proportional to the wavelengths of the x ray 1 and to the partial gas pressure p. Hence the absorptivity of a gas for any wavelength A_λ is a function of the product pl. Furthermore, A_λ depends on the temperature of the gas T_g. Hence,

$$A_\lambda = f(T_g, pl). \tag{5.44}$$

Engineering calculations of gas radiation are based on the Stefan-Boltzmann law. Although in actual fact the radiation of gases does not always obey the law of proportionality T^4 exactly (for example for CO_2 the radiation is proportional to $T^{3.5}$, and for water vapor T^3), the conditional nature of the figure (is obtained, fully acceptable on account of its convenience.

The radiation energy of the gas per 1 m^2 of surface per hour is

$$q_g = \varepsilon_g c_s \left(\frac{T_g}{100}\right)^4 \text{ kcal/m}^2 \cdot \text{hr} \tag{5.45}$$

in which ε_g is the degree of blackness of the gas, determined experimentally (taken from tabular data).

This formula gives us the ~~radiated~~ energy of a gas into a cavity which can be regarded as an absolutely black space at $T = 0°K$. In actual fact, the gas x is usually protected by a solid surface, shell, with a temperature T_w above absolute zero and a degree of blackness $\epsilon_w < 1$.

The equation for calculating radiant heat exchange between the gas and the shell takes the form

$$q_{rz} = \epsilon'_w C_s \left[\epsilon_r \left(\frac{T_r}{100}\right)^4 - A_r \left(\frac{T_z}{100}\right)^4 \right] \text{ kcal/m}^2 \cdot \text{hr} \qquad (5.43)$$

in which ϵ'_w is the effective degree of blackness of the shell;

$\epsilon_{\hat{z}}$ is the degree of blackness of the gas at a gas temperature T °K;

$A_{\hat{z}}$ is the absorptivity of the gas at the shell temperature T_w.

The values ϵ'_w, $\epsilon_{\hat{z}}$ and $A_{\hat{z}}$ are taken from experimental data /3/.

This equation is valid for non-luminous gases and gaseous combustion products. It is usually enough in the calculation to consider the radiation of CO_2 and H_2O, while the remaining components in the combustion products can be disregarded, since the part played by them in the radiation is very small.

Radiation from flames

When there is complete combustion of x a gas or benzene fuel, the flames are almost colorless with a slight bluish tinge. The radiation from these flames is of a

- 226 -

selective kind and can be calculated by the equations derived for non-luminous gases.

Radiation from luminous flames is mainly determined by the radiation from the decomposition products of hydrocarbons, red-hot soot particles, coal, ash contained in them, and depends on the type of particle, quantity and size. In actual character, radiation from luminous flames is closer to radiation from solid bodies than from gases.

An approximate calculation of radiant heat exchange between a luminous flame and the wall can be made by the equation

$$Q_{\text{w}} = \varepsilon_{\text{w}} \varepsilon_{\text{w}} c_{\text{s}} F_{\text{w}} \left[\left(\frac{T_{n1}}{100} \right)^4 - \left(\frac{T_{\text{w}}}{100} \right)^4 \right] \text{ kcal/hr} \qquad (5.47)$$

Here $T_f = \sqrt{T_1 T_2}$ is the effective flame temperature;

T_1 is the theoretical combustion temperature;

T_2 is the temperature of the combustion products at the firebox outlet;

F_w is the radiation surface in m ;

T_w is the temperature of the wall;

and ε_w and ε_f are the degree of blackness of the walls and flame (taken from experimental data).

REFERENCES

1.   Kondrat'yev, K. Ya. Radiant heat exchange in atmosphere, Gidrometeoizdat, 1956.

2.   Mikheyev, M. A. Fundamentals of heat transfer, Chapter VI, Gosenergozidat, 1956.

3.   Stalder, J. and other. Transfer of heat to bodies traveling at high velocities in upper layers of atmosphere. "Problems of Rocketry" For. Lit. Press, 1952, No. 5.

4.   Shorin, S. N. Heat transfer, Chapters 13, 14, 15. Stroyizdat.

CHAPTER VI

THEORY AND CALCULATION OF HEAT EXCHANGERS

Sec. 24. Fundamentals of Calculation of Heat Exchangers

A heat exchanger is a device intended to transfer heat from one heat-transfer agent to another. According to the working   principle, heat exchangers divide up into surface and contact   types. Surface heat exchangers are either continuous or periodic in action.

In continuous (heat exchanges the heat is transferred from one agent to another through a dividing wall and the process of heat transfer is stationary. Among such equipment are condensers, steam boilers, heating system radiators, gas turbine regenerators.

In periodic heat exchangers, the heating surface is comes in contact alternately with a flow of cold and hot liquid. The walls of these exchangers receive (accumulate) heat while they are in contact with the hot liquid and give it out when in contact with the cold liquid. An example of this type of exchanger are the regenerators in open-hearth and   glass- forming furnaces, air heaters for blast furnaces and so on.

In contact exchangers, the heat is exchanged by means of direct contact

and   mixing ^between the Hot and cold liquids.   These include different types of heaters,

steam jets, water jets and so on.

The effectiveness of heat exchangers and the temperature distribution

in them are functions of the flow arrangement of the working liquids. There are

three ^principal   simple systems - parallel flow ^(coflow), counter flow and cross flow (Fig. 80).

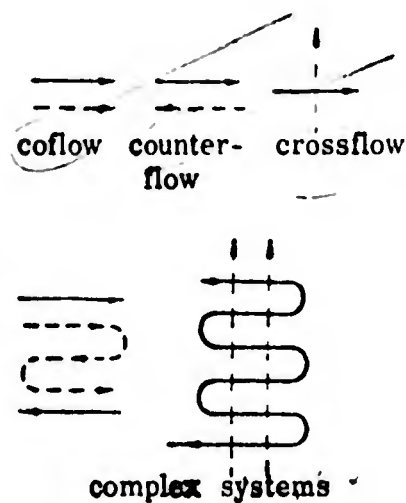coflow   counter-   crossflow
          flow

complex systems

Fig. 80. Types of motion of fluid in heat exchangers

In ^co flow the hot and cold liquids move in parallel in the

same direction. In counter flow they move in parallel, but in the opposite

direction. In cross flow the liquids cross each other. Apart from these

simple systems of motion, there may be more complex ones, combining the simple

systems.

When designing new exchangers, the aim of the calculation is to determine the heating surface. But if the surface is known, the aim of the calculation is to establish operating conditions for the equipment and to determine the final temperature of the working ~~fluid~~.

In both cases the basic theoretical formulae are the heat-transfer equation (2.18)

$$Q = kF(t_1 - t_2) \text{ kcal/hr}$$

and the heat balance equation

$$Q = u_1 f_1 \gamma_1 c_{p_1}(t_1' - t_1'') = u_2 f_2 \gamma_2 c_{p_2}(t_2'' - t_2') \text{ B kcal/hr} \tag{6.1}$$

in which Q is the amount of heat given off in kcal/hour;

   F is the heating surface in m^2;

   k is the heat transfer coefficient in $kcal/m^2 \cdot hour\text{-}deg$;

   u is the velocity of the liquid in m/hour;

   f is the cross-sectional area of the stream in m^2;

   γ is the specific gravity of the liquid in kg/m^3;

   c_p is the thermal capacity at constant pressure in $kcal/kg \cdot deg$;

   t is the temperature of the liquid.

Here and from now on the subscripts 1 and 2 relate

to the hot and cold liquids, while the superscripts prime and double prime ($''$) ~~respectively,~~ $(')$

refer to the parameters of the liquid at the exchanger inlet and outlet.

χ   Mean temperature gradient

In the general case the temperatures of the liquid inside the exchanger

do not remain constant. Hence the heat-transfer equation is only applicable

in differential form to the element of the surface dF

$$dQ = k \Delta t_i \, dF.$$

while the total amount of heat passing through the whole surface F is found as

the integral

$$Q = \int_F k \Delta t_i \, dF \ \text{kcal/hr}$$

In order to simplify the calculation, we will introduce the concept of

the mean temperature gradient Δt, and the last equation can be represented

in the form

$$Q = k \Delta t F \ \text{kcal/hr}$$

For certain simple systems of heat exchangers, the mean temperature

gradient can be calculated analytically.

Let us derive the equation for the mean temperature gradient for a

very simple heat exchanger using   co-flow (Fig. 81). The amount of heat

- 231 -

transferred through the element dF of the surface per hour is

$$dQ = k(t_1 - t_2)\, dF \text{ kcal/hr}$$

Here the temperature of the hot liquid is reduced by dt_1, and that

of the cold liquid rises by dt_2. Consequently,

$$dQ = -G_1 c_{p_1}\, dt_1 = G_2 c_{p_2}\, dt_2$$

in which G_1 and G_2 are the consumptions of hot and cold liquid in kg/hour;

while c_{p_1} and c_{p_2} are the thermal capacities.

Hence

$$dt_1 = -\frac{dQ}{G_1 c_{p_1}}$$

and $$dt_2 = \frac{dQ}{G_2 c_{p_2}}.$$

Subtracting the left and right hand sides of the last equalities, we get

$$d(t_1 - t_2) = -dQ\left(\frac{1}{G_1 c_{p_1}} + \frac{1}{G_2 c_{p_2}}\right).$$

After substitution of $dQ = k(t_1 - t_2)\,dF$ and separation of the variables, we get

$$\frac{d(t_1 - t_2)}{t_1 - t_2} = -\left(\frac{1}{G_1 c_{p_1}} + \frac{1}{G_2 c_{p_2}}\right)k\,dF.$$

The values $G_1 c_{p_1}$ and $G_2 c_{p_2}$ can be found from the thermal balance

equations for the whole exchanger

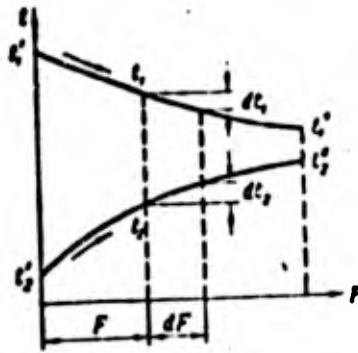$$Q = G_1 c_{p_1}(t_1' - t_1'').$$
$$Q = G_2 c_{p_2}(t_2'' - t_2').$$

Fig. 81. Distribution of temperature in coflowing
heat exchanger

Then

$$\frac{d\,(t_1-t_2)}{t_1-t_2}=-\left[\frac{t_1'-t_1''}{Q}+\frac{t_2''-t_2'}{Q}\right]k\,dF.$$

Integration then gives us

$$[\ln\,(t_1-t_2)]\,{}_{t_1'-t_2'}^{t_1''-t_2''}=-[(t_1'-t_1'')+(t_2''-t_2')]\frac{k}{Q}\,F.$$

Finally,

$$Q=\frac{(t_1'-t_2')-(t_1''-t_2'')}{\ln\dfrac{t_1'-t_2'}{t_1''-t_2''}}\,kF \quad \text{kcal/hr} \tag{6.2}$$

Thus, for parallel flows the mean temperature gradient Δt is equal to

$$\Delta t=\frac{(t_1'-t_2')-(t_1''-t_2'')}{\ln\dfrac{t_1'-t_2'}{t_1''-t_2''}}. \tag{6.3}$$

We can derive the equation for Δt for counterflow in a similar way (Fig. 82).

$$\Delta t=\frac{(t_1'-t_2'')-(t_1''-t_2')}{\ln\dfrac{t_1'-t_2''}{t_1''-t_2'}}. \tag{6.4}$$

If we designate the greatest temperature difference between the hot

and cold liquids as Δt_δ, and the least difference as Δt_m, then we get one general

formula for *coflow* and counterflow

- 233 -

$$\Delta t = \frac{\Delta t_\delta - \Delta t_M}{\ln \frac{\Delta t_\delta}{\Delta t_M}} \qquad (6.5)$$

and

$$Q = kF \frac{\Delta t_\delta - \Delta t_M}{\ln \frac{\Delta t_\delta}{\Delta t_M}}. \qquad (6.6)$$

The equations are derived on the assumption that the consumption of

liquids and the heat-transfer coefficient throughout the length of the heat

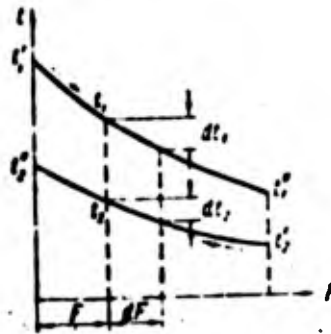exchanger remain unchanged. Since, in actual fact, this is only roughly the case,

Fig. 82.   Distribution of temperature in counterflowing
heat exchanger

$\Delta \underline{t}$ is also approximate.

For small variations in temperature of the hot and cold liquids,
when $\widehat{0.5 < \frac{\overline{\Delta t_M}}{\Delta t_\delta} < 1}$, the mean temperature gradient $\Delta \underline{t}$ can be calculated without too

much error (less than 4%) from the mean arithmetic

$$\Delta t = \left(\frac{t_1' + t_1''}{2} - \frac{t_2' + t_2''}{2} \right). \qquad (6.7)$$

For crossflow and   combined   flow the calculation of Δt is very   cumbersome.

Solutions are given for the most frequently encountered cases in the form of

graphs /2/.

By knowing Δt, the heat flux Q and the mean heat-transfer coefficient k,

the heating surface can be calculated from the formula $F = \frac{Q}{kM} \, \kappa^2.$

Selection of heat-transfer coefficient

When calculating heat exchangers the selection of the heat-transfer

coefficient k involves great difficulty. This is due to the variation in

temperature of the working liquids and the complexity of the shape of the

surface. In practice in most cases in which the heat-transfer coefficient

at the beginning (k') and the end (k'') of the heating surface are fairly

close together, we can take the arithmetic mean as the theoretical value

$$k = \frac{k' + k''}{2}. \tag{6.8}$$

But if k' and k'' are very far apart, the heating surface has to

be broken up into areas within which the difference between k' and k'' is

small, and the heat transfer is calculated separately for each area.

. We   operate in the same way in cases in which the conditions of

flow pas^{t} the heating surface by the working liquid vary sharply. By

dividing the surface into areas, in each of which the flow conditions can be

considered identical, we average k using the following equation

$$k = \frac{k_1 F_1 + k_2 F_2 + \ldots + k_n F_n}{F_1 + F_2 + \ldots + F_n}.$$ (6.9)

Calculating final temperature of working liquid

If the heat exchanger is given, the aim of the calculation is to

determine the final temperature of the liquid. The following are known in

the problem: heating surface F, heat-transfer coefficient k, consumptions G_1 and G_2,

thermal capacity c_{p_1} and c_{p_2}, and the initial temperatures t'_1 and t'_2. The

unknowns are the final temperatures t''_1 and t''_2, and the amount of heat transferred Q.

In approximate calculations we can adopt the following methods.

$$Q = c_{p_1} G_1 (t'_1 - t''_1) = c_{p_2} G_2 (t''_2 - t'_2)$$

From the heat balance equation we get the relationship between the final

temperatures of the hot and cold liquids and the amount of heat Q (unknown for

the moment):

$$t''_1 = t'_1 - \frac{Q}{c_{p_1} G_1}; \quad t''_2 = t'_2 + \frac{Q}{c_{p_2} G_2}.$$ (6.10)

If we take it that the temperatures of the working liquids vary

within small limits, then

$$Q = kF\left(\frac{t'_1 + t''_1}{2} - \frac{t'_2 + t''_2}{2}\right).$$

- 236 -

Substituting for t''_1 and t'_2 the expressions *derived,* ~~for them~~ from (6.10),

we find after simple transformations

$$Q = \frac{i'_1 - i'_2}{\dfrac{1}{hF} + \dfrac{1}{2G_1 c_{p_1}} + \dfrac{1}{2G_2 c_{p_1}}} \quad \text{kcal/hr} \tag{6.11}$$

The unknown final temperatures t''_1 and t''_2 can now be found from Eq. (6.10).

This system of calculation is very simple, but is only applicable to rough calculations when the variation in temperature of the liquids is small. In the general case, the final temperature is a function of the motion of the working liquid.

Literature gives more exact solutions for simple systems - co *flow* and counter flow. In view of the restricted nature of their use we will not consider the *actual* (solutions . We will only deal with the derivations implied by these solutions on the basis of comparison of the two given heat-exchange systems.

Comparison of effectiveness of heat exchange in co *flow* and counter flow.

Fig. 83 shows the theoretical dependence of the heat transfer efficiency for co *flow* with respect to counter flow at identical local values of the heat-transfer coefficient h for the whole surface. Here Q_{max} is the

amount of heat transferred during co͞   flow, and Q_2 is the amount of heat

transferred during counter͞   flow,

$\frac{kF}{G_1 c_{p_1}}$ is the dimensionless parameter characterizing the relationship

between the mean temperature gradient Δt and the variation in temperature of

the hot liquid (since $\frac{kF}{G_1 c_{p_1}} = \frac{t_1' - t_1'}{\Delta t}$)

$G_1 c_{p_1} : G_2 c_{p_2}$ is the ratio of the hourly thermal capacities of the working

liquids (or the so-called water equivalents).

It describes   the relationship between the variation in the temperatures

of the working liquids (since $\frac{G_1 c_{p_1}}{G_2 c_{p_2}} = \frac{t_2' - t_2'}{t_1' - t_1'}$).
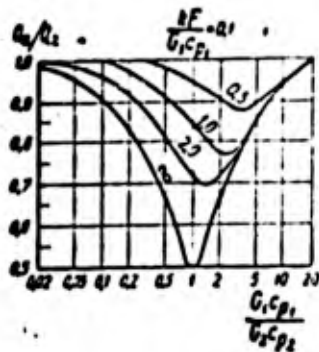

Fig. 83.   Comparison of coflow and
counterflow

The graph shows that co flow   and counter͞   flow can be

considered of equal value, provided the hourly thermal capacities (or water equivalents)

- 238 -

of the working liquids are considerably different, to wit, at

$$\frac{G_1 c_{p_1}}{G_2 c_{p_2}} < 0.05 \quad \wedge \quad \frac{G_1 c_{p_1}}{G_2 c_{p_2}} > 10$$

or if the parameter $kF/G_1 c_{p_1}$ is small.

The first conditions is tantamount to a variation in the temperature one of the liquids slight compared with that of the other. The second condition is for a case in which the mean temperature gradient is considerably greater than the variation in the working liquid temperatures.

In all other cases in co-flow a smaller quantity of heat is transferred than in counter-flow. Hence from the point of view of heat engineering, we should always give preference to counter-flow, provided we are not forced by other considerations (for example, the design) to use co-flow.

It should be kept in mind here that in counter-flow more difficult temperature conditions are created for the material of the heat exchanger walls, since some of the areas on the hot liquid inlet side come into contact with maximum temperature liquids on both sides.

Optimum make-up and deficiency of heat exchangers

The effectiveness of the exchange of heat in heat-exchange apparatus is a function of a large number of factors, including the rate of motion of the

- 239 -

working _fluids_, the shape and composition of the heating surfaces. The shape
of the surfaces is often determined by the purpose for which the apparatus is
designed, and the selection of the composition and rate of motion are left to
the designer to a considerable extent.

Improvement in the heat-exchange intensity by increasing the rate
is accompanied by an increase in hydraulic resistance and output required to
overcome _it_. Hence the composition of the heating surface as well as
artificial intensification of heat transfer must be solved by making
allowance for the relationship between the heat exchange intensity and the
theoretical power required to pump through the working liquid and creating the
required velocity.

Thus, the calculation of heat exchanges is not restricted to
determining the heating surfaces and final temperatures of the working liquids,
but also includes calculating the hydraulic resistances, selecting the optimum
size and composition of the heating surfaces and determining the most
advantageous rate of motion of the liquids. The solution to this complex
task must also take into account the initial expenditure on erecting the
apparatus and operatinal costs, which is particularly important when designing

- 240 -

industrial and other types of stationary heat exchangers.

The basic requirement in heat exchangers *for use in aircraft* is a

high degree of effectiveness with small dimensions and hydraulic resistances.

The degree of perfection of a heat exchanger from the point of view of power

engineering can be evaluated by the following equation

$$\psi = \frac{Q}{AR},$$

in which Q is the amount of heat transferred in kcal/hour;

AR is the amount of heat equivalent to the energy spent on pumping

the liquid through in kcal/hour.

The greater ψ, the better the heat exchanger is.

The basic characteristics showing the economic nature of the heat

exchange in any *device* is the efficiency η which describes the

proportion of heat from the hot liquid used to heat up the cold liquid

$$\eta = \frac{Q_1}{Q_{avail}} = \frac{G_2(i_2'' - i_2')}{G_1(i_1' - i_1'')}. \tag{6.12}$$

Here Q_1 is the amount of heat received by the cold liquid in kcal/hour;

Q_{avail} is the *available* amount of heat from the hot liquid;

G_1 and G_2 are the consumptions *flow rate?* of hot and cold liquid in kg/hour;

i_2'' and i_2' are the heat contents of the cold liquid at the outlet and inlet

in kcal/kg;

i'_1 is the heat content of the hot liquid at the inlet;

i^0_1 is the heat content of the hot liquid at the temperature of the

surrounding medium.

In cases in which the system includes several heat exchangers in series,

there is no point in determining the efficiency for each of them in the same

way, since ~~any~~ non-utilized heat from the hot liquid is partly utilised in the

subsequent heat exchangers and cannot be regarded as lost.

The second characteristic showing the economic nature of an exchanger

is the so-called heat retention ~~coefficient~~ ratio ε , which takes into account the

heat loss into the surrounding medium and is the ratio of the amount of heat

received by the cold liquid Q_1 and the amount supplied by the hot liquid

Q_2

$$\varepsilon = \frac{Q_1}{Q_2}.$$

Since $Q_2 = Q_1 + Q_\pi.$, in which Q_π is the heat loss to the surrounding medium,

$$\varepsilon = \frac{Q_1}{Q_1 + Q_\pi} = \frac{1}{1 + \dfrac{Q_\pi}{Q_1}}.$$

The value ε is a function of the design of the apparatus and the quality of

the heat insulation.

REFERENCES

1. Kutateladze, S. S. Fundamentals of heat exchange, Chapter 19, Mashgiz, 1957.

2. Mikheyev, M. A. Fundamentals of heat transfer, Chapter 8, Gosenergoizdat, 1956.

3. Shorin, S. N. Heat transfer, Chapter 16, Stroyizdat, 1952.

THERMAL CONDUCTIVITY IN NON-STATIONARY CONDITIONS

As has been shown earlier, the temperature field in a steady-state regime does not vary with time, i.e., $\frac{\partial t}{\partial \tau} = 0$. In a non-steady-state heat regime in which the body is heated or cooled, the temperature field varies with time $\left(\frac{\partial t}{\partial \tau} \neq 0\right)$. There is variation in the enthalpy of the body at the same time as the variation in the temperature field.

The process of heating or cooling can be divided into three regimes. The first is characterized by a gradual penetration of the temperature variation into the body from layer to layer, the rate of variation in the temperature being different at different points. During the process the temperature field is affected to a considerable extent by the initial state, which may be completely arbitrary. The first regime is termed a non-ordered process.

Next comes an orderly regime, which means that at a certain moment the initial temperature distribution in the body loses its value, and from the on the process is governed solely by the conditions on the boundary. Here the temperature at all points is a function of the shape of the body, its physical parameters and the heat-exchange conditions on the boundary. Kondrat'yev /3,'4/ has termed this orderly process of heating or cooling a

regular regime, and has formulated a corresponding theory for it.

Furthermore, he has put forward a number of methods for solving practical

problems. As time passes - theoretically after an infinitely long period has

elapsed - the variation in temperature at different points on the body comes

to an end, i.e., we arrive at a third regime with a constant temperature

distribution, where $\frac{\partial t}{\partial \tau} = 0$, which is the basic characteristic of the steady-state

regime. A case in which the temperature of the body is identical throughout and

equal to that of the surrounding medium is conventionally called the thermal

equilibrium.

To illustrate heat exchange in non-steady-state conditions, let us

consider two different examples.

Example 1. A body is placed in a medium at a higher temperature t_f.

The heating process begins at this point and passes through the three mentioned

regimes:

1. The temperatures on the outer layers of the body increase. The

variation in temperature is gradually carried into the body.

2. The non-steady-state regime covers the whole body. The temperatures

vary at all points on the body.

3. The temperature of the body is equalized and equal to t_f. The non-steady-state regime is complete. The body arrives at a state of thermal equilibrium.

Graphs showing the variation in temperature on the boundary of the body t_w and at its center t_0 as a function of the duration of the process are given in Fig. 84.
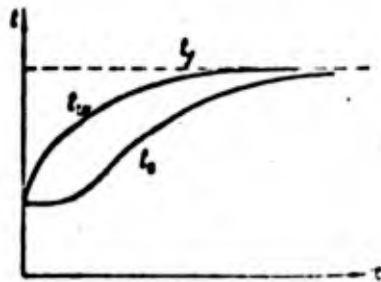

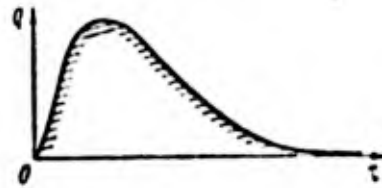**Fig. 84.** Nature of variation in temperature of body with time

Fig. 85. Amount of heat imparted to body with time

In non-steady-state heating conditions, the amount of heat accumulated by the body per unit time Q kcal/hour, is not constant. The area under the curve $\int Q$ (Fig. 85) shows the total amount of heat which has been used to heat the body, i.e., to raise its heat content over the time τ. When the body cools, its heat content decreases, and the amount of heat released is transferred to the surrounding medium.

- 245 -

Example 2. Let us consider heat transfer through dividing wall in a non-steady-state regime.

The non-steady-state process is preceded by a stationary regime which is described by the earlier-established dependence of the temperature field for a flat dividing wall (Fig. 86).

If the temperature of the hot medium now jumps from t'_{f_1} to t''_{f_2} (Fig. 87), while the temperature of the cold medium is left the same as before t_{f_2}, the process becomes nonsteady-state for a certain time, and (in the process) the temperature curve continues to vary, beginning at the initial stationary regime described by the curve $t_{f_1} - t'_{w_1} - t'_{w_2} - t_{f_2}$, right up to the advent of the new stationary regime with the temperature line

$$t_{f_1} - t''_{w_1} - t''_{w_2} - t_{f_2}.$$

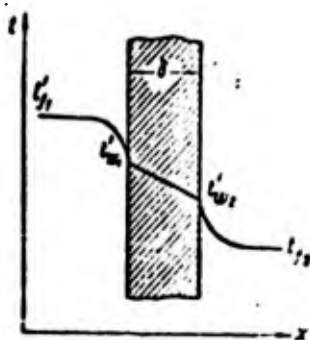The variation in temperature t_{w_1} and t_{w_2} with time is shown in Fig. 88.

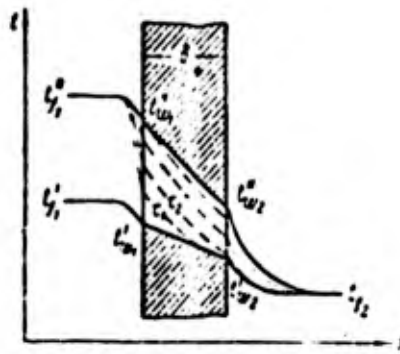Fig. 86. Nature of variation in temperature in plane wall under steady-state conditions

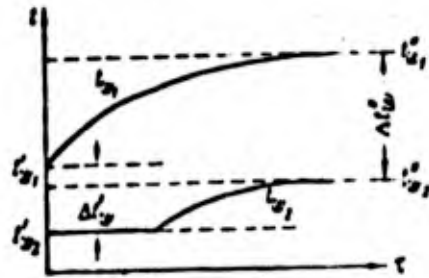Fig. 87. Nature of variation in temperature in plane wall under non-steady-state conditions

- 246 -

Fig. 88. Variation in temperature
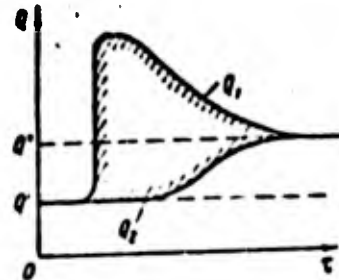t_{w1} and t_{w2} of plane wall with
time

Fig. 89. Amount of heat Q_1 and
Q_2 transferred through heat-
receiving and heat-supplying
surfaces of wall under non-steady-
state conditions

Correction: Curve Q_1 should start at $\tau = 0$

It is clear from this that the rise in temperature of the second

surface of the wall takes place after the corresponding increase in the first

surface, and its that temperature increases by fewer degrees.

The variation in the amount of heat transferred per unit time is shown

in Fig. 89, in which Q' and Q" are the amounts of heat corresponding to a

stationary regime, while Q_1 and Q_2 are the amounts of heat transferred through

the   receiving and   transferring wall surfaces during a non-stationary

regime. The area contained between the curves Q_1 and Q_2 shows the amount of

heat which is used to increase the enthalpy of the wall.

The rate of the thermal process in non-steady-state conditions is

determined by the thermal diffusivity $a = \dfrac{\lambda}{c\gamma}$ m^2/hour. The established

- 247 -

relationships between the variation in temperature and amount of heat transferred

are strictly valid for solid bodies alone. When fluids are heated, we can

only consider the variation in the mean temperatures, which are the result of

inevitable equalization when convection occurs. Consequently, the rate of

the non-stationary heat process is a function of the nature of the body, its

physical parameters, size and shape, and the conditions under which there is

heat exchange with the outside medium.

Solving a problem of non-stationary thermal conductivity means finding

the dependence between the variation in temperature and the amount of heat

transferred in time for any point on the body. But these decisions may be derived

on the basis of a whole number of simplifications, only when the solid bodies are of simple shape, i.e.,

plates, cylinders or spheres. These solutions are usually given

for practical use in the form of graphs or tables.

A number of experimental methods for solving the problem have been worked out of late, for

example, the hydrothermal analogue method developed by Luk'yanov /5/. This method is

based on the analogy between the propagation of heat and laminar motion of a

liquid. Gutenmakher /2/ has developed a method of electro-thermal analogy,

based on the similarity between thermal and electric phenomena.

- 248 -

Above we derived a differential thermal-conductivity equation determining

the relationship between the temperature, time and coordinates of the body for

an infinitely small volume, i.e., an equation which mathematically describes

the heat transfer inside the body. In the general case of a solid body it takes

the form of (2.13)

$$\frac{\partial t}{\partial \tau} = a \left(\frac{\partial^2 t}{\partial x^2} + \frac{\partial^2 t}{\partial y^2} + \frac{\partial^2 t}{\partial z^2} \right).$$

In order to solve this equation, i.e., in order to find the temperature

field inside the body at any moment of time, we have to preset the marginal conditions:

1. The initial temperature distribution in the body which is given

by the temperature distribution inside the body at the initial moment of time

$$t(x, y, z, 0) = t(x, y, z).$$

If the temperature distribution at the initial moment of time in the

body is uniform, then

$$t(x, y, z, 0) = t_0 = \text{const}.$$

2. The boundary condition describing the geometrical shape of the

body and the interaction between the surrounding medium and the body surface. The

boundary condition may be given in three ways:

a) for a boundary condition of the first kind we set the temperature distribution on the surface of the body for any moment of time, i.e,

$$l_\bullet(\tau) = f(\tau).$$

If the temperature of the surface is the same throughout and the heat exchange is constant throughout the process, then

$$l_\bullet(\tau) = l_\bullet = \text{const.}$$

This latter condition is graphically expressed by setting point A (Fig. 90). The amount of heat flowing from inside the body to its boundary can be determined by the equation

$$dQ = -\lambda \frac{\partial l}{\partial n} dF. \qquad (7.)$$

In order to determine the amount of heat passing through the surface, we have to find the slope of the tangent to the temperature curve at the surface of the body, i.e., the angle

$$\varphi = \arctan \left(-\frac{\partial l}{\partial n}\right);$$

b) the boundary condition of the second kind is set by the density of the heat flux at each point on the surface as a function of time, to wit

$$q(\tau) = \dot{f}(\tau).$$

A particular case of the second-kind boundary condition is when the heat flux density is constant $q(\tau) = q = \text{const.}$
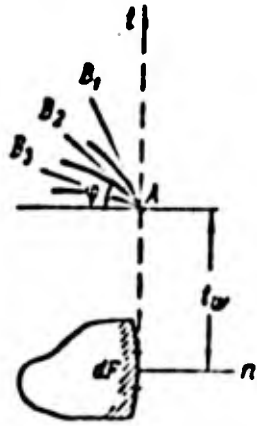
- 250 -

Fig. 90. Graphic representation
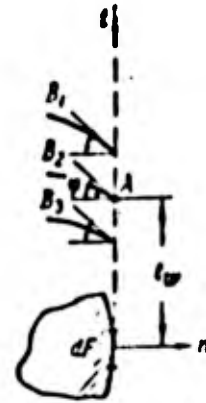of boundary condition of first
kind

Fig. 91. Graphic representation of
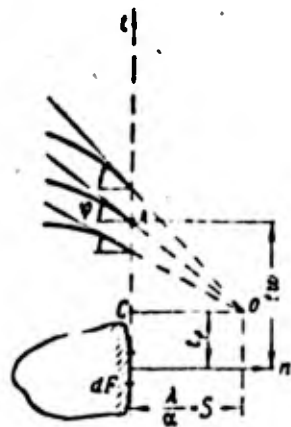boundary condition of second kind

Fig. 92. Graphic representation of
boundary condition of third kind

Thus, the boundary condition of the second kind is of a reciprocal nature, i.e., we know the amount of heat passing through the surface and therefore the tangent of the [angle] [slope] of the tangent to the temperature curve on the surface of the body is given. The aim of the problem is to determine the surface temperature, i.e., to determine the position of point $\underline{A}$ (Fig. 91);

c) the boundary condition of the third kind is determined by presetting the temperature of the surrounding medium and the heat exchange between the body surface and the surrounding medium

$$q(\tau) = \alpha\,[t_w(\tau) - t_f] = -\lambda\left(\frac{\partial t}{\partial n}\right). \qquad (7.2)$$

In problems with boundary conditions of the third kind, the surface temperature of the body and the tangent of the slope angle of the tangent to the temperature curve are variable, but we are given on the outside normal the point $\underline{0}$ through which all the tangents to the temperature must pass (Fig. 92). It follows from condition (7.2) that

$$-\frac{\partial t}{\partial n} = \frac{t_w(\tau) - t_f}{\frac{\lambda}{\alpha}} \qquad (7.3)$$

or

$$\operatorname{tg}\varphi = -\frac{\partial t}{\partial n} = \frac{t_w(\tau) - t_f}{\frac{\lambda}{\alpha}}. \qquad (7.4)$$

- 252 -

The value $\tan \varphi$ is equal to the ratio of the side $\frac{\hat{t_w(\tau)} - t_i}{\lambda}$ to the side λ/α

of a corresponding right-angled triangle. The adjoining side λ/α is constant,

while $\frac{t_w(\tau) - t_i}{\lambda}$ varies continuously in proportion to $\tan \varphi$ during the heat exchange.

Hence, the boundary condition of the third kind determines the point $\underline{0}$, the

position of which remains unchanged, and through which all the tangents to

the temperature curve at the point lying on the body surface must pass.

The point $\underline{0}$ is termed the direct$^{\text{ri}x}$ and lies at a distance $\lambda/\alpha = \underline{S}$

from the surface. The segment $\underline{S}$ is a subtangent to the temperature curve; its

value does not depend on the shape of the surface

$$\frac{1}{S} = h = \frac{\alpha}{\lambda}, \tag{7.5}$$

in which $\underline{h}$ is the relative heat-transfer coefficient.

Thus, the differential equation, given the geometric shape, initial

and boundary conditions, can be solved, i.e., we can find the distribution

temperature function at any moment of time

$$t(x, y, z, \tau) = f(x, y, z, \tau).$$

For engineering purposes we need usually only concern ourselves with the

process occurring in one particular direction $\underline{x}$. In this case the general

solution takes the following form for a flat wall

$$t = bx + c + \sum_{n=1}^{\infty} A_n (\cos m_n x + p_n \sin m_n x) e^{-\alpha m_n^2 \tau} \tag{7.6}$$

- 253 -

and for a cylindrical wall

$$t = b \ln r + c + \sum_{a=0}^{\infty} A_a [J_0(m_a r) + p_a Y_0(m_a r)] e^{-a m_a^2 \tau},$$ (7.7)

in which J_0 and Y_0 are Bessel functions of the first and second kind. The

constants b and c are determined from the conditions of steady-state (at $\tau = \infty$);

p_n and m_n are determined from the boundary conditions and A_n is determined

from the initial conditions (at $\tau = 0$).

A detailed descriptions of these solutions can be found in the books

by Graber, Erk. and Grigull' /1/ and Lykov /6/.

It follows from the last two equations that the unknown function depends

on a large number of variables, but it turns out that these variables can be

grouped into three dimensionless complexes which are derived from Eqs. (7.1) and

(7.2):

$$\frac{\alpha l}{\lambda} = Bi - \text{Biot number}$$

$$\frac{\alpha \tau}{l^2} = Fo - \text{Fourier number}$$

$$\frac{x}{l} = L - \text{Geometric similarity number}$$

On the basis of the second theorem of similarity the unknown function

is the same in the form of a dimensionless temperature ϑ / ϑ_0' for all corresponding

processes and can be represented in the form of the relationship

$$\frac{\vartheta}{\vartheta_0} = \Phi (Bi, Fo, L).$$ (7.8)

- 254 -

The Biot and Fourier numbers are thermal similarity groups. The

$$Bi = \frac{\alpha l}{\lambda} = \frac{\alpha}{\lambda/l}$$

physical meaning of the Biot number α can be interpreted as follows:

at a certain temperature difference the heat-transfer coefficient α determines

the removal of heat from the cooling surface, while the supply of heat to this

surface from inside the body is determined by the thermal conductivity λ/l.

Consequently, the ratio between these characteristic values $\frac{\alpha}{\lambda/l}$ constitutes the

relative intensity of heat transfer from the body surface compared with that of

the flow of heat from inside it to the surface. The smaller the Biot number,

the less heat is removed from the surface of the cooling body compared with

the efflux of heat from inside. As an example let us look at the problem of

the thermal conductivity of an infinitely long rod of constant section. The

assumption has been made in this problem that the temperature is constant in

the selected cross-section. This assumption is possible either when the

thermal conductivity is high or when the heat transfer on its surface is small,

i.e., whenever the rod is ~~is made~~ thin and/from a thermally conducting material.

The number Bi $\leqslant$ 1 corresponds to these conditions.

Considering the physical meaning of the Fourier number, we can

represent it in the form
$$Fo = \frac{\alpha \tau}{l^2} = \frac{\frac{\lambda}{l} \beta \tau}{c \gamma l^3}.$$

- 255 -

As can be seen, the ^{F}ourier number represents the ratio of the scale of heat *supplied* through thermal conductivity to the scale of variation in the heat content of the body $c\gamma\ell^3$, i.e., it is a measure of the rate of change of the body temperature in a non-steady state.

Let us go on to apply the equations derived to *individual* problems in which we are required to find the temperature distribution and heat consumption for any moment of time in the given body.

Flat wall./ We have to consider here the cooling (or heating) of an infinite flat wall of thickness 2δ (Fig. 93). The wall is cooled on both sides and the coefficient α is constant throughout with time and identical for both surfaces.

We are also given the coefficients λ, c and γ. These values are constant throughout the field. Hence we also know the thermal diffusivity $a = \dfrac{\lambda}{c\gamma}$.

The differential thermal conductivity equation (2.13) for the case in point of a unidimensional temperature field takes the form

$$\frac{\partial t}{\partial \tau} = a \frac{\partial^2 t}{\partial x^2}.$$ (7.9)

Boundary conditions of the third kind (7.3) are used *for* the boundary

- 256 -

$$-\left(\frac{\partial t}{\partial x}\right)_w = \frac{t_w(\tau) - t_f}{\frac{\lambda}{\alpha}}$$

or

$$-\left(\frac{\partial t}{\partial x}\right)_w = h[t_w(\tau) - t_f].$$

since $\alpha / \lambda = h$

As can be seen, the thermal conductivity equation and the boundary condition only include the temperature difference and the derivatives from the temperature.
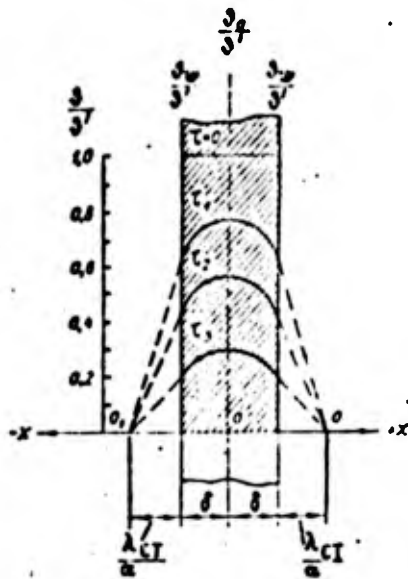

Fig. 93. Variation in temperature field
during cooling of plane infinite wall

Hence if we take the temperature of the surrounding medium t_f as the initial one, i.e., as the first reading, then the temperature head of the wall can be designated as $\theta = t_f - t_\infty$.

Thus, Eqs. (7.9) and (7.3) can be represented in the form

$$\frac{\partial \theta}{\partial \tau} = a \frac{\partial^2 \theta}{\partial x^2} \quad \text{и} \quad -\left(\frac{\partial \theta}{\partial x}\right)_\infty = h\theta.$$

The initial condition is set in the form of a uniform distribution of temperature with respect to the entire volume of the body at the initial moment of time, i.e., at $\tau = 0 \; \theta = \theta'$, and therefore $\theta/\theta' = 1$.

The boundary conditions can be written in the form

$$\frac{\partial \theta}{\partial x} = -h\theta, \quad \text{при} \; x = +\delta;$$

$$\frac{\partial \theta}{\partial x} = +h\theta, \quad \text{при} \; x = -\delta.$$

In the last two equalities the value $\frac{\partial \theta}{\partial x}$ is a projection of the vector grad t onto the direction of the external normal to the surface of the wall. Since the direction of this normal coincides with the positive direction of the x-axis at $x = +\delta$, and the external normal is directed towards the negative x-axis at $x = -\delta$, the opposite sign has been taken on the right-hand side of the equalities. This system of equations is a mathematical formulation of the problem under consideration. Its solution can be reduced to finding the temperature as a function of the coordinates x, the time τ and the

the parameters a, h, δ and ϑ'.

Thus, we are required to find the function

$$\vartheta = \Phi(x, \tau, a, h, \delta, \vartheta'). \tag{7.10}$$

As has already been pointed out above, these variables can be grouped into three dimensionless complexes, which are the Biot, Fourier and geometrical similarity numbers, i.e.,

$$\frac{\vartheta}{\vartheta'} = \Phi(Bi, Fo, L).$$

When solving engineering problems it is usually enough to know the temperature on the surface ϑ_w and in the mid-plane of the wall ϑ_0. In this case Eq. (7.8) is simplified, since the argument L becomes a constant number (at $x = 0$, $L = \dfrac{x}{\ell} = 0$ and at $x = \delta$, $L = 1$).

Consequently

$$\frac{\vartheta_w}{\vartheta'} = \Phi_w(Bi, Fo) \tag{7.11}$$

and

$$\frac{\vartheta_0}{\vartheta'} = \Phi_0(Bi, Fo). \tag{7.12}$$

The amount of heat Q_τ transferred in the time τ is determined from the variation in heat content of the body and is equal to the initial heat content $Q' = 2\delta\gamma c\vartheta'$. multiplied by the relative variation in the mean temperature of the body ϑ_m/ϑ' over the time τ.

- 259 -

Hence, the relative variation in the heat content is also a function of the two numbers Bi and Fo

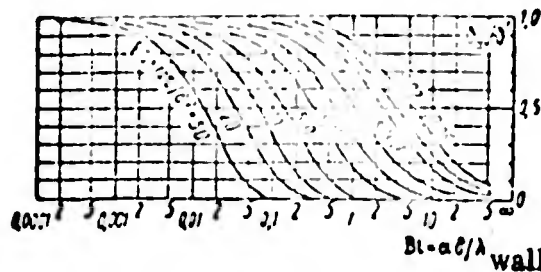$$\frac{Q_1}{Q'} = \Phi_Q(Bi, Fo). \qquad (7.13)$$

Fig. 94. $\dfrac{\vartheta_x}{\vartheta'} = f(Bi, Fo)$ as function of plane infinite wall

Figs. 94, 95 and 96 show graphs for the functions Φ_w, Φ_0 and Φ_u. When determining the unknowns, we have first to calculate the numbers $Bi = \alpha\delta/\lambda_{wall}$ and $Fo = a\tau/\delta^2$, from which we determine the graphs ϑ_w/ϑ'_1, ϑ_0/ϑ' and Q_1/Q'. By knowing these ratios and the values ϑ' and Q', we can calculate the unknown ϑ_w, ϑ_0, Q_1.

The temperature ϑ_w and ϑ_0 are used to plot a rough curve showing the temperature distribution in the body (See Fig. 93). At $\underline{x} = \pm\delta$ the rays drawn from points $\underline{0}$ and $\underline{0}_1$ should be tangents to the temperature curve, and at $\underline{x} = 0$ the tangent is horizontal by dint of the symmetry of the temperature curve.
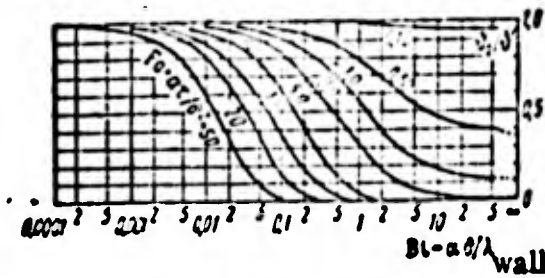
- 260 -

Fig. 95. $\frac{\vartheta_0}{\vartheta'} = f(\text{Bi, Fo})$ as function of plane infinite wall
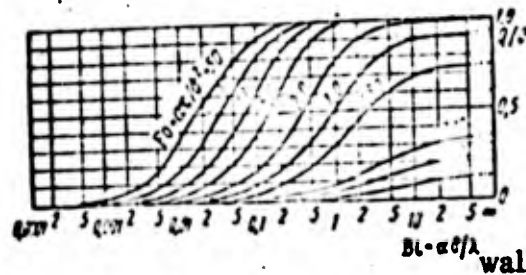

Fig. 96. $\frac{Q}{Q'} = f(\text{Bi, Fo})$ as function of plane infinite wall

Thus, temperature curves can be plotted for any moment of time.

The temperatures t on the surface of the wall and at its center t_0 may be determined for any moment of time τ from the following relationship

$$\frac{\vartheta_w}{\vartheta'} = \frac{t_w - t_f}{t' - t_f},$$

$$\frac{\vartheta_0}{\vartheta'} = \frac{t_0 - t_f}{t' - t_f}. \tag{7.14}$$

in which t_f is the temperature of the surrounding medium;

t' is the initial temperature of the body;

- 261 -

t_w is the temperature of the surface of the body;

t_0 is the temperature in the middle plane of the body.

The solution of the problem in question is applicable both to cases of cooling as well as heating of the plate. It should be pointed out that if the process is unilateral rather than bilateral, then δ has to be taken to mean the total thickness of the wall.

Cylinder. A cylinder with a length considerably exceeding in diameter can be regarded as an infinite cylinder, in which the length is infinite compared with the diameter.

If the heat exchange over the entire surface with the surrounding medium proceeds uniformly, the temperature inside the cylinder only varies as a function of time and radius.

The values λ, c, γ (and therefore a) are considered to be known and are regarded as constant throughout the field. At the initial moment of time, the temperature of the cylinder at all points is the same.

Assuming that the temperature field is a function solely of the radius vector (r) and does not depend on the polar angle of turn (φ) and the applicate (z), Eqs. (2.13) and (2.17) give us the following differential thermal-conductivity equation in cylindrical coordinates for the formulated unidimensional problem

- 262 -

$$\frac{\partial \theta}{\partial \tau} = a\left(\frac{\partial^2 \theta}{\partial r^2} + \frac{1}{r}\cdot\frac{\partial \theta}{\partial r}\right). \qquad (7.15)$$

The boundary condition is such that at $\underline{r} = \underline{R}$ the following

relationship is satisfied

$$-\frac{\partial \theta}{\partial r} = \frac{\alpha}{\lambda}\theta_{\text{wall}} \qquad (7.16)$$

The initial condition is such xthat at $\tau = 0$
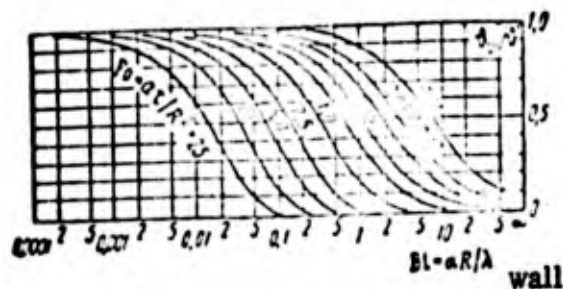
$$\theta = \theta' \qquad (7.17)$$

Fig. 97. $\frac{\theta_{\nabla}}{\theta'} = f(\text{Bi, Fo})$ as function of
infinitely long cylinder

The solution with respect to

$$\frac{\theta_{\nabla}}{\theta'}, \quad \frac{\theta_0}{\theta'} \quad \text{and} \quad \frac{Q}{Q'}$$

is also a function of the two numbers alone

$$Bi = \frac{\alpha R}{\lambda_{\text{wall}}} \text{ and } Fo = \frac{a\tau}{R^2}.$$

These relationships are shown in Figs. 97 - 99 in the form of graphs.

The initial thermal content of an area of cylinder of length 1 is equal to

$$Q' = \pi R^2 c_\gamma l\theta' \text{ kcal} \qquad (7.18)$$

Sphere/ When converted to spherical coordinates the differential

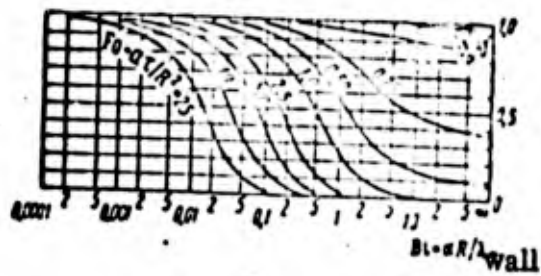thermal conductivity equation for the unidimensional problem under consideration

- 263 -

Fig. 98. $\frac{\vartheta_0}{\vartheta'} = f$(Bi. Fo) as function
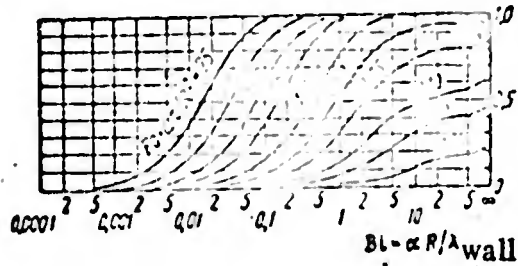of infinitely long cylinder

Fig. 99. $\frac{Q}{Q'} = f$(Bi. Fo) as function
of infinitely long cylinder
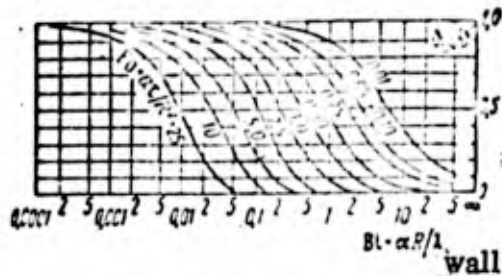
Fig. 100. $\frac{\vartheta_T}{\vartheta'} = f$ (Bi. Fo) as
function of sphere

takes the following form

$$\frac{\partial \vartheta}{\partial \tau} = a \left(\frac{\partial^2 \vartheta}{\partial r^2} + \frac{2}{r} \frac{\partial \vartheta}{\partial r} \right). \qquad (7.19)$$

The boundary condition is: at $r = R$

$$-\frac{\partial \vartheta}{\partial r} = \frac{\alpha}{\lambda} \vartheta. \qquad (7.20)$$
$$\text{wall}$$

- 264 -

The initial condition is: at $\tau = 0$

$$\theta = \theta'.$$

(7.21)

In this case the solution with respect to $\widehat{\theta_o/\theta'}, \widehat{\theta_s/\theta'}$ and $\widehat{Q/Q'}$ is also a

function of the two numbers alone

$$Bi = \frac{aR}{\lambda_{\text{wall}}} \text{ and } Fo = \frac{a\tau}{R^2}.$$

These relationships are shown in Figs. 100 - 102 in the form of graphs.

The initial thermal content of the sphere is equal to

$$Q' = \frac{4}{3} \pi R^3 \gamma c \theta' \text{ kcal}$$

(7.22)

After consideration of non-steady-state heat exchange in an infinite

wall, cylinder or sphere, we should give due regard to the fact that the process

of the propagation of heat depends to a tremendous extent both on the geometrical

shape of the body, which determines the ratio of the surface to its volume,
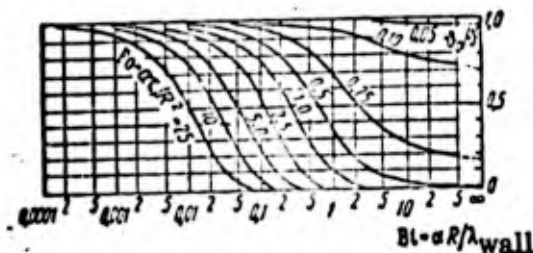
as well as on its size.

$$Bi = aR/\lambda_{\text{wall}}$$

Fig. 101. $\dfrac{\theta_0}{\theta'} = f(Bi, Fo)$ as function
of sphere

Fig. 102. $\frac{Q}{Q'} = f(\text{Fo, Bi})$ as
function of sphere
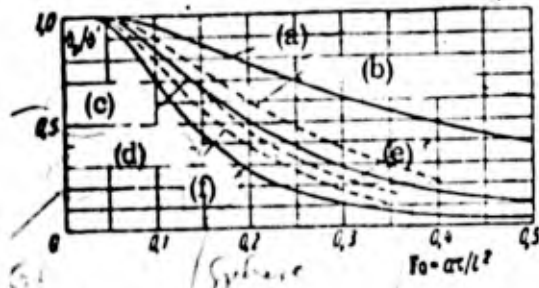
Fig. 103. Curves showing $\frac{\theta}{\theta'} = f(\text{Fo})$ for bodies of
different shapes at Bi = const.

(a) plate
(b) square beam, length
(c) cylinder length
(d) cylinder length = diameter
(e) cube
(f) sphere

The rate of the process is greater in bodies of finite length, for example short cylinders, prisms, and increases as the ratio of the body surface to its volume is increased. Fig. 103 shows a comparison of the dimensionless temperature $\frac{\theta}{\theta'} = f(\text{Fo})$ at Bi = const for differently shaped bodies. It is clear from this figure that for spherical bodies the rate of the process is higher than for those with other shapes.

The textbook /7/ gives examples of the calculation for a cylinder of finite length.

Conductivity Problems

All methods used to solve thermal conductivity problems are based on certain simplifications and assumptions valid for specific problems. Let us consider one of the commone methods.

Method of finite differences

As an illustration we can use the problem of finding the temperature field in an infinite plate, given boundary conditions of the third kind.

The method of finite differences permits us to replace a continuous process by one which is discontinuous both in time and space. Here the differential thermal-conductivity equation for a flat wall is

$$\frac{\partial t}{\partial \tau} = a \frac{\partial^2 t}{\partial x^2}$$

and can be replaced by an equation in finite differences, which for a unidimensional temperature field takes the form

$$\frac{\Delta t}{\Delta \tau} = a \frac{\Delta^2 t}{\Delta x^2}. \tag{7.23}$$

Fig. 104 shows a flat wall divided into separate layers of identical thickness Δ x with the numbers $(\Delta x_1, \Delta x_2, \ldots \Delta x_n, \Delta x_{n+1})$. Time over which process is being considered should also be divided into separate periods $\Delta\tau$, after which each period is marked with the corresponding number $(\tau_1, \tau_2, \ldots \tau_n, \tau_{n+1})$.

For the given segment of time $\Delta \tau$ the temperatures remain constant at the same points.
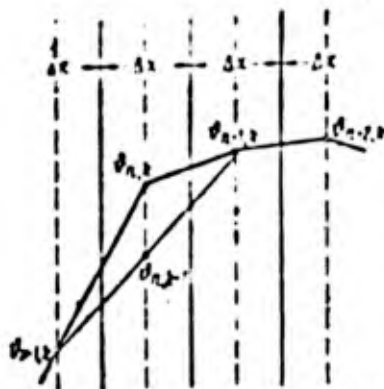

Fig. 104. Graphic explanation of finite difference methods
and conventional signs

For the system described, in which we only take one temperature value for any moment in time τ_k in any layer, for example, $t_{n,k}$ in the middle, the continuous temperature distribution curve $t(x)$ is replaced by a broken one. Here the slope angle of the temperature curve for the n-th layer with respect to its middle line is different, and the derivative of the temperature with respect to the coordinate should have two values

$$\left(\frac{\Delta t}{\Delta x}\right)_+ = \frac{t_{n+1,k} - t_{n,k}}{\Delta x} \tag{7.24}$$

$$\left(\frac{\Delta t}{\Delta x}\right)_- = \frac{t_{n,k} - t_{n-1,k}}{\Delta x}. \tag{7.25}$$

in which the plus or minus signs show the direction of the approach through the layer n, the plus sign standing for the right and the minus sign for the left.

- 268 -

The second derivative in the finite differences is expressed as follows

$$\frac{\Delta^2 t}{\Delta x^2} = \frac{1}{\Delta x}\left[\left(\frac{\Delta t}{\Delta x}\right)_+ - \left(\frac{\Delta t}{\Delta x}\right)_-\right] = \frac{1}{\Delta x^2}(t_{n+1,\,k} + t_{n-1,\,k} - 2t_{n,\,k}). \qquad (7.26)$$

The temperature derivative with respect to time in the finite

differences for the given layer takes the following form

$$\frac{\Delta t}{\Delta \tau} = \frac{t_{n,\,k+1} - t_{n,\,k}}{\Delta \tau}. \qquad (7.27)$$

The differential equation in the finite differences (7.25) after

substitution of (7.26) and (7.27) into it is then transformed in the following way

$$\frac{t_{n,\,k+1} - t_{n,\,k}}{\Delta \tau} = a\frac{1}{\Delta x^2}(t_{n+1,\,k} + t_{n-1,\,k} - 2t_{n,\,k})$$

or

$$t_{n,\,k+1} - t_{n,\,k} = \frac{2a\Delta\tau}{\Delta x^2}\left(\frac{t_{n+1,\,k} + t_{n-1,\,k}}{2} - t_{n,\,k}\right).$$

This last equation can be used to determine the temperature in the

middle of any layer for the subsequent moment of time $(k + 1)$, if we know the

temperature distribution for the k-th period of time

$$t_{n,\,k+1} = \frac{2a\Delta\tau}{\Delta x^2}\cdot\frac{t_{n+1,\,k} + t_{n-1,\,k}}{2} - \left(\frac{2a\Delta\tau}{\Delta x^2} - 1\right)t_{n,\,k}. \qquad (7.28)$$

In a case in which we select the period of time $\Delta\tau$ and the size of

the layer Δx in such a way that $\dfrac{2a\Delta\tau}{\Delta x^2} = 1$, Eq. (7.28) takes the form

$$t_{n,\,k+1} = \frac{t_{n+1,\,k} + t_{n-1,\,k}}{2}. \qquad (7.29)$$

As can be seen from Eq. (7.29) the temperature in the middle of the n-th

layer for the subsequent moment of time $\hat{t}_{n,k+1}$ is the arithmetic mean of $t_{n+k,1}$ and

$t_{n-1,k}$. Equation (7.29) can also be solved simply by means of a graph. To do

this, when solving a specific problem, we first select Δx and the time intervals

are determined from (7.30)

$$\Delta \tau = \frac{\Delta x^2}{2a}. \tag{7.30}$$

The known temperature distribution is then plotted as a broken curve 0, 1, 2

for the initial moment (Fig. 105).
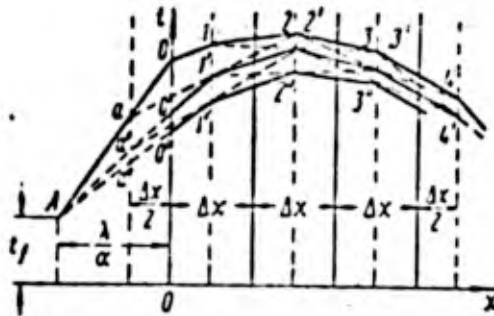

Fig. 105. Graphic solution of problem of non-steady-state
thermal conductivity

At the following moment of time the temperature distribution is

found in the following way: point 1 is joined to 3 by a straight line. At

the point of intersection between this straight line and the central line

on the second layer we obtain point 2', which determines the mean arithmetic

- 270 -

temperature in this layer for the following period of time. By joining point 2 with point 4 by a straight line, we get point 3' and so on. In order to obtain points 1' and 0' we have to determine the guide point A, which is

λ/α away from the outer surface of the wall and in accordance with the boundary conditions of the third kind a temperature of the surrounding medium t_f as the ordinate.

Furthermore, on the left of the plate surface we draw a straight line parallel to it at a distance of $\frac{\Delta x}{2}$. The straight line corresponding to the plate surface is then, as it were, the central line of an auxiliary layer $\left(-\frac{\Delta x}{2}, +\frac{\Delta x}{2} \right)$.

After these extra plottings, the guide point A is joined to the point 0, the line $0A$ intersects the auxiliary line at the point a. By joining point a to point 2, we get the point $1'$, which determines the temperature in the first layer for the subsequent moment of time. The temperature on the surface of the plate $0'$ at this moment is found from the guide to point A, i.e., as an approximation we joined point $1'$ to point A with a straight line. As a result we obtain a new broken line $0'$, 1', 2', 3'..., corresponding to the temperature distribution for the moment of time τ_{k+1}.

For the subsequent period of time τ_{k+2} we have to carry out a similar

plotting operation, as a result of which we get the temperature distribution $\underline{0}$", 1", 2", 3"... etc.

As time passes, the distribution curves for the same periods $\Delta\tau$ come closer together, since the cooling process is gradually slowed down. In the graph method this makes it difficult to plot the result and reduces its accuracy. In order to avoid this, we have to increase $\Delta\tau$ by increasing $\Delta\underline{x}$, but in such a way that the multiplier remains equal to unity. Here the increase of $\Delta\underline{x}$ was a factor of 2 leads to a four-fold increase in $\Delta\tau$.

It can be seen from consideration of this method that it does not impose any restrictions on the temperature of the medium t_f or on the thermal coefficients λ, a and α . If t_f or λ/α vary, the directional point $\underline{A}$ is displaced. Hence for each moment of time we should take the directional point from the new set t_f and $\frac{\lambda}{\alpha}$.

If there is variation in the thermal diffusivity $\underline{a}$ contained in the expression $_\wedge$, the period of time $\Delta\tau$ should also change, i.e., the temperature distribution graphs correspond to different time intervals.

The finite difference method may be applied to solution of problems of determining the temperature field of a sphere or cylinder under non-steady-state conditions. A disadvantage of this method, as pointed out above, is its comparatively low accuracy, the latter being governed by the thoroughness by which the

- 272 -

distribution graphs are plotted.

Sec. 27.   Regular Regime Method

It follows from what has been said that the process of cooling of a

body when there are no internal heat sources in it and the temperature of the

surrounding medium t_f and the heat-transfer coefficient α in time are constant,

can be divided into the disorder ed stage and regular-regime stage. The latter

occurs at the end of a certain time after the cooling has begun, when the

initial temperature state of the body ceases to have an effect, and means that

at the moment it occurs, the temperature field of the system varies according

to an exponential law.

The moment the regular regime occurs, the natural logarithm of the

temperature head ϑ , equal to the distance between the temperature t at any

point on the body and the permanent temperature of the medium t_f , decreases

with time according to a linear law

$$\ln\vartheta = -m\tau + C, \qquad (7.31)$$

its rate of change

$$\frac{\partial(\ln\vartheta)}{\partial\tau} = -m \qquad (7.32)$$

being the same for all points. The coefficient m is a positive number describing

the   cooling rate irrespective, as a whole, of the selection of the

point on the body M_1, M_2 M_1. The value m is determined entirely by the size and

shape of the body, its thermal parameters, heat-exchange conditions and does

not depend on the initial temperature field , which is a characteristic sign

of the advance of the regular regime. This is still the case during heating,

i.e., when $t_f > t$.

Fig. 106 shows a graph for the variation in the natural logarithm of

the temperature head for two points M_1 and M_2 as a function of the heat
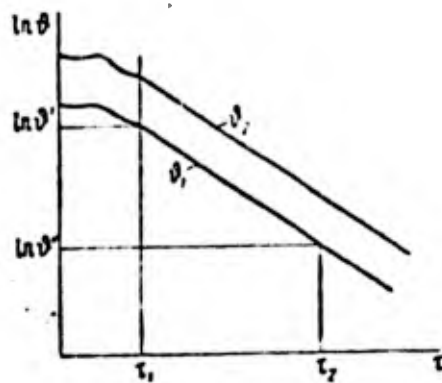
exchange time.

Fig. 106. Logarithm of temperature difference as function
of time during cooling

When the time τ_1 has elapsed since the beginning of the cooling, the

is reached

second stage (- the regular regime in which the variation $\ln \vartheta_1$ and $\ln \vartheta_2$ for

points M_1 and M_2 with time is rectilinear with the identical and constant

- 274 -

angle of coefficient ω ..... As can be seen from the graph in Fig. 106,

up to the advent of the regular regime (i.e., for $\tau < \tau_l$), there is an orderly

process (first stage), during which the $\boxed{\text{graph} \cdot \text{cooling}}$ does not show any

rectilinear law and the temperature at the point is still influenced by the

initial conditions, location of the point and other factors mentioned above.

If at the initial moment of time $\tau = 0$ the temperature at all points

on the body is the same, the curve should start from the same point on the

ordinate, otherwise, as shown in Fig. 106, the curve should start from different

points. Using Eq. (7.19) for the two arbitrary moments of time, and subtracting

one from the other, we find the coefficient m describing the rate of the

regular regime. We find

$$m = \frac{\ln \vartheta' - \ln \vartheta''}{\tau_2 - \tau_1} \, 4ac^{-1}. \tag{7.33}$$

Thus, the coefficient m is the tangent of the slope angle of the

rectilinear segment of the curve to the x-axis on the coordinates $\tau, \ln \vartheta$. The

angular coefficient of the straight line is always negative, since ϑ tends to

zero at τ_l tending to infinity. This formula enables us to determine

the cooling rate experimentally by measuring the temperature at any point on

the body for two consecutive moments of time during the regular regime.

The mathematical solution of the problem based on the regular regime

theory, worked out by Kondrat'yev, establishes the connection between the cooling

rate m, on the one hand, and the physical and geometrical values of the body

and the external cooling conditions, on the other. The theory of the regular

regime may be applied to the solution of practical problems, for example,

evaluation of the heating and cooling time.

Equation (7.34) makes it possible to determine the time of change

in temperature from ϑ' to ϑ'' at any point on the body

$$\tau = \frac{1}{m} \ln\left(\frac{\vartheta'}{\vartheta''}\right). \tag{7.34}$$

m can be calculated theoretically if the geometrical shape of the

body, its size and the thermal parameters of the material are known.

Methods of determining the thermal parameters of a material a, λ, c the

heat transfer coefficient α, the emissive coefficient c and the thermal

resistances have been worked out on the basis of the regular regime theory.

The   theory has been further developed) to cover

bodies and systems of bodies with internal heat sources.

REFERENCES

1. Graber, G. and others. Fundamentals of teaching on heat exchange, Chapter III. For. Lit. Press, 1958.

2. Gutenmakher, L. I. Electric models, Chapter 109 Academy of Sciences Press, 1949.

3. Kondrat'yev, G. M. Regular heat regime, Gostekhizdat, 1954.

4. Kondrat'yev, G. M. Thermal measurements, Chapter 3, 4, 5, 8. Mashgiz, 1957.

5. Luk'yanov, V. S. Hydraulic devices for engineering calculations, Herald of AS USSR, OTN, No. 2, 1939.

6. Lykov, A. V. Thermal conductivity theory. Gostakhizdat, 1952.

7. Mikheyev, N. A. Fundamentals of heat transfer, Chapter 10, Gosenergozidat, 1956.

HEAT EXCHANGE AT HIGH VELOCITIES AND HIGH TEMPERATURE OF

GAS FLOW

The development of jet engines and the appearance of *unmanned* flying craft
and ballistic missiles moving at supersonic velocities has led to the *creation* of a
whole number of new branches of science. First and foremost, this applies to gas
dynamics and the theory of gas transfer. In a number of cases the heat-transfer
problems involved in calculating the heating of bodies around which there is a
gas flow cannot be separated from problems of gas dynamics, which has resulted in a
new branch of science called gas dynamic theory of heat exchange.

At the present time the designer 2 of a supersonic flying craft is
forced to *make* both an aerodynamic calculation as well as a total heat
calculation. When | velocities | flight | of 1 - 5 km/sec are attained, the
calculation of the heating up and methods of protecting the parts of the craft
is a decisive one.

A very difficult problem has been the cooling of combustion chambers,
nozzles, *and* / gas-turbine blades in a jet engine. The high temperatures and heat fluxes
have forced designers to switch to new materials, on the one hand, and have

- 277 -

necessitated intensive cooling of parts *with the inevitably* accompanying increase in weight

and reduction in economy, on the other. All this has been an incentive to

develop completely new and more economical *cooling* methods - sweat cooling, film

cooling and *barrier* cooling.

Let us consider in greater detail what *governs* the heating up of

surfaces at high flight velocities. When a body moves through a fluid,

particles of the fluid adjoining the wall are carried away by the latter on

account of friction, or, *which* is the same thing, are decelerated *at* the wall

when flowing round the body *in a stream*, thus forming a boundary layer.

The deceleration of the particles on account of friction is

accompanied by the release of heat, *i...* ("dissipation"of the kinetic energy of the

flow, and this leads to the gas heating up. If there is no *system of* heat removal from

the wall (if the wall in insulated), the gas temperature at the wall, and therefore

the temperature of the surface, is increased to *a* value close to the drag

temperature of the stream $(T_{00})\infty$. The drag temperature of the flow is determined

in the following way

$$(T_{00})_\infty = T_\infty \left(1 + \frac{k-1}{2} M^2\right).$$

Here T_∞ is the gas temperature;

- 278 -

$k = \dfrac{c_p}{c_v}$ is the ratio of thermal capacities, for air $k = 1.4$;

$M = \dfrac{U}{a}$ is the M number of the flight;

U is the velocity of the flight and a is the speed of sound; for

air $(T_\omega)_- = T_-(1 + 0.2M^2)$.

The variation in T_∞ as a function of the M number for two altitudes

is shown in Fig. 107. As can be seen; during a flight with $M = 2.5$, the

temperature of the heat-insulated elements is greater than $300°$, and so instead

of duralumin, usually used in aircraft parts, a more spalling-resistant material

has to be employed. x On an analogy with the "sound barrier", the term "heat

barrier" is now being used in literature. The concept of the "sound barrier" is

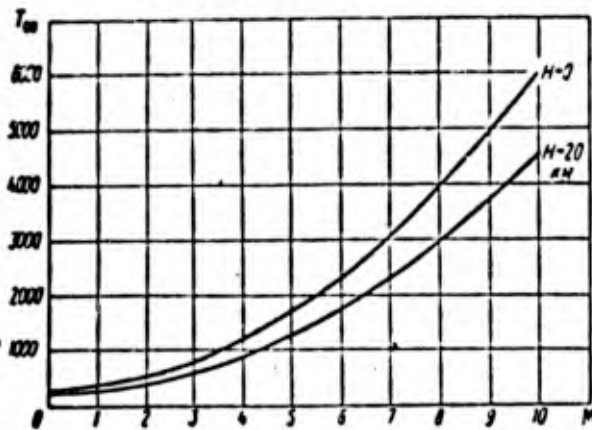associated with the increase in resistance with a flight velocity at an M number close

Fig. 107. Variation in drag temperature as function
of M number

- 279 -

to unity. The concept of a "heat barrier" is associated with the increase in the temperature of the wall. The temperature of the non-cooled surface increases continually with the M number of the flight. At M = 5, steel parts have to be protected by ceramic coverings. At greater M numbers it is no longer possible to produce a non-cooled part /16/. Here it should be kept in mind that as the M number increases, the wall temperature of the flying craft begins to lag behind the increase int the drag temperature on account of heat-transfer through radiation from the surface.

In the general case the surface temperature is determined from the balance of the heat fluxes supplied and removed from the wall. The amount of heat supplied depends to a great extent on the velocity and altitude of the flight and the geometric dimensions of the body. The heat fluxes to the surface of the body may attain 10^4 to 10^9 $kcal/m^2 \cdot$ hour. Thus, for example, a surface of this kind is water cooled, using the latent heat of vaporization in its entirety, from 20 to 2000 tons of water an hour would be needed to cool $1 \, m^2$. It is clear from this how important it is to be able to calculate the heat fluxes correctly so that the most advantageous trajectories and flight velocities can be chosen from the point of view of weight.

In the combustion chambers and nozzles of jet engines heat fluxes may also

be tremendous. The tendency to "gun" the engine lead to an increase in thermal

load. The specific thrust of a liquid propellent engine $R_{sp} = \dfrac{K}{G_{sec}}$ is equal to

the thrust referred to the consumption per second of combustible components, and

is directly proportional to the exhaust velocity. An increase in the exhaust

velocity may be achieved by increasing the thermal content of the gases in the

combustion chamber. In order to reduce the size of the engine, the working pressure

in the combustion chamber must be increased. The joint action of these two factors

leads to a sharp increase in the heat flux densities, particularly in the region

of the critical nozzle section.

Just as important is the calculation of the heat transfer and thermal

protection of the combustion chambers in an air jet engine. In this type of engine

some of the air entering the combustion x chamber is removed for cooling

purposes. The efficiency of the cooling is stepped up when internal jet and

barrier cooling is employed. When the M number of the flight is increased, the

drag temperature of the oncoming *stream* is increased. The amount of air required for

cooling is also increased, and this means an appreciable drop in the thrust and
efficiency?
economic advantage of the engine. Xx

Very serious problems involving heat transfer have arisen in rocketry.

Modern ballistic rockets may attain flight velocities of 6 - 7 km/sec. When

they enter the atmosphere, the surfaces of the rockets heat up intensively, and

melting or combustion of the surface material occurs. For example, if the shell

is made of steel, the time the rocket reaches the earth, to a depth of several centimeters,

the shell may have melted. Here we face the question of selecting a covering,

determining the optimum trajectory, accurately calculating the loss of material or

determining the rated weight of the coolant. The difficulties involved in

calculating these factors are aggravated by the fact that oxygen and nitrogen

molecules in the air begin to dissociate at such high temperatutes and there is

a chemical reaction between the covering and the air. Similar difficulties are

encountered by designers of winged rockets moving through the atmosphere at

velocities of - 2 - 5 km/sec when calculating the descendent trajectories of

artificial earth satellites or instrument cassettes, when calculating take-off

devices, craft with liquid propellant engines, and so on.

In all these cases we have to solve both problems of determining

the heat flux to the surface as well as the propagation in time of heat inside

a complex assembly.

New problems of heat transfer also arise when switching to jet engines

using atomic energy. Here the chief problems are the removal of heat from the

reacting matter and the protection of the craft from the joint action of aerodynamic

heating and nuclear radiation. In order to increase the removal of heat from the reactor it has proved advisable to use intermediate liquid-metal heat-transfer agents.

When ~~dealing with~~ high velocities it has been advisable to increase the flight altitude more than 20 kilometers. The rarefaction of the atmosphere acquires great importance during motion at an altitude. The air ceases to obey the laws of a solid medium, and the normal hydrodynamic equations become invalid. Over the last few years a new branch of hydrodynamics - superaerodynamics, or the aerodynamics of rarefied gases and high M numbers - has been widely developed. The need has |risen accordingly| for the stabilization of the heat regimes of these craft, and therefore the need to find methods of calculating the heat under these conditions.

The ~~point~~ described above, which far from exhaust the (range of ~~problems~~ facing the designers of modern jet engines and flying craft, show the need for extensive development of theoretical and experimental research on heat exchange and the need for aviation engineers to master all the achievements of the theory of heat transfer.

The present section in our book is intended for students specializing in aviation. About half the section deals with convective heat exchange at high

temperatures and flow velocities, and with hydrodynamic methods of thermal

protection. The second half gives methods of calculating the heating of specific

aircraft and rocket assemblies encountered in engineering practice.

Sec. 28. General Concepts of Hydrodynamic Theory of Heat Exchange

Let us use q to designate the heat flux passing through a unit of area

per unit time $(kcal/m^2 \cdot hour)$, then

$$q = -\lambda \left(\frac{\partial T}{\partial y} \right).$$

Here λ is the thermal conductivity in $kcal/m \cdot hour \cdot deg$;

q is the heat flux through the area normal to the direction y (Fig. 108).

If we are considering heat exchange between two areas, at different

temperatures T_1 and T_2, it is usually more convenient to employ the concept of

thermal resistance $R \; m^2 \cdot hour \cdot deg/kcal$

$$q = \frac{T_1 - T_2}{R}.$$

For example, during steady-state flow of heat through a flat plate made

of material with a thermal conductivity λ

$$q = \frac{\lambda}{\delta} (T_1 - T_2); \quad \left(R = \frac{\delta}{\lambda} \right).$$

The thermal resistance in more complicated cases may be determined

in a similar way.

In the hydrodynamic study of convective heat transfer it is more convenient to use the heat-exchange coefficient α kcal/m·hour·deg, i.e., $q = \alpha (T_1 - T_2)$. Hence $a = \dfrac{1}{R}$.
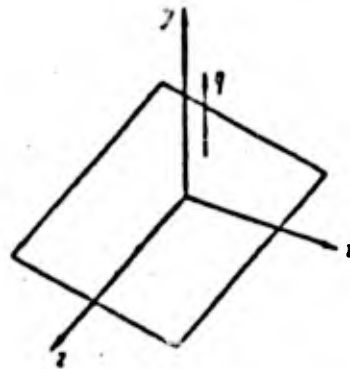

Fig. 108. Coordinate system

Given a definition of this kind, α or R are weak functions of the temperature difference ⟨ frat ⟩ which is very convenient for calculating heat fluxes. By singling out a strong function q of the temperature difference in the form of a multiplier, we reduce the problem to calculation of α or R. When studying turbulent convective heat exchange, it is convenient to single out the flux density ρU as the multiplier

$$q = g c_{p} U (T_1 - T_2) c_{11}. \qquad (8.1)$$

- 285 -

Here c_H is a dimensionless value; since we have separated the basic terms affecting the heat flux, c_H is a function of the flow conditions to a lesser extent than

$$a = g c_p \cdot L' c_H. \tag{8.2}$$

In literature the Stanton number, St, is sometimes used instead of c_H. The dimensionless heat-exchange coefficient is also introduced in the form of the Nusselt number $Nu = \propto L/\lambda$, in whibh L is the characteristic dimension.

In the general case of convective heat exchange, c_H and Nu are functions of dimensionless groups determining the flow conditions; $M = U/a$; Reynolds number $Re = U_\rho L/\mu$, in which μ is the viscosity ($kg \cdot sec/m^2$); Prandtl number $Pr = \quad$; ratio of wall and stream temperatures $T_w = T_w /T_\infty$; adiabatic index $k = c_p /c_v$. $\frac{c_p}{\mu}$

Furthermore, there are dependences on certain other parameters, but we will not deal with them in detail at this point. The aim of the theory of convective heat exchange is to determine these relationships.

convective heat exchange is always accompanied by an exchange of momentum. Here the layers of fluid moving at a greater rate are slowed down, while those moving more slowly are speeded up, i.e., there is friction between them. In the event of two-dimensional flows, the friction stress along the area perpendicular to the direction y is determined by the Newton equation

$$\tau = \mu \frac{\partial u}{\partial y} \; kg/m^2 \qquad (8.3)$$

This force acts along the x-axis. Fig. 109 shows the friction factor produced by the effect of the speeded-up top layers of liquid on the lower ones.
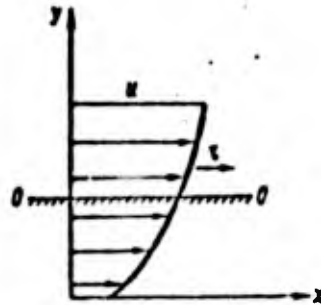

. Fig. 109. Plane flow with viscosity

The friction is proportional to the velocity head, hence it is advisable to introduce the dimensionless quantity c_f

$$\tau_w = c_f \frac{\rho u_\infty^2}{2}. \qquad (8.4)$$

Here τ_w is the local friction stress on the wall;

$\left(\frac{\rho u_\infty^2}{2} \right)$ — is the velocity head of the oncoming stream.

The value c_f is a function of the same parameters as c_H and Nu. A very important achievement in the hydrodynamic theory of heat exchange has been the establishment of the relationship between c_H and c_f , or Nu and c_f. In the first approximation for gases at moderate temperatures

$$c_H \approx \frac{1}{2} c_f.$$

In cases in which there are different concentrations of material in

different layers of flow, the heat exchange is accompanied by a transfer of matter — diffusion and mass exchange.

Let us designate

$$Q = g_? D_{12} \frac{\partial C_1}{\partial y} \text{ kg/m}^2 \cdot \text{hr}, \qquad (8.5)$$

in which D_{12} is the diffusion factor in m^2/hour;

C_1 is the concentration by weight in kg/kg;

Q_1 is the transfer of matter 1 with respect to matter 2 through an

area one square meter in size in the course of one hour.

This equation holds for a binary mixture. On ananalogy with the

heat-exchange coefficient we introduce the mass-exchange coefficient — β kg/m^2· hour —

which is the amount of matter transferred through an area equal to 1 square meter

per hour at a concentration difference equal to unity. We get

$$(8.6)$$

$$Q = \beta [(C_1)_i - (C_1)_{ii}].$$

In dimensionless form $\qquad Nu_1 = \frac{\beta L}{\rho D}.$

In the general case, the heat exchange, mass exchange and friction

coefficients are interrelated. This is due to the unity of the physical processes

of the transfer of heat, matter and momentum. It follows from the molecular

theory of gases that $\qquad \frac{\mu}{\rho} \sim \frac{\lambda}{\rho c_\rho} \sim D \quad$ or $\quad \nu \sim a \sim D.$

- 288 -

During turbulent flow the transfer of heat energy, matter and momentum is effected through the intermingling of whole volumes and moles of gas. In this case the link between the transfer processes shows up all the more strongly.

It should be pointed out that during flow at high velocities, when chemical reactions occur, the transfer of energy is due to all three processes: the direct transfer of heat, the transfer of chemical energy and the release of heat during dissipation of the energy *through* friction. All these phenomena should be regarded together.

We will leave out in all these operations the multipliers coordinating the dimensionality of different values in the engineering system, and will only introduce them in the final equations.

Sec. 29. Some Preliminary Information on the Boundary Layer

Calculation of convective heat exchange can be reduced to calculating the boundary layer. In actual fluid flows, the effect of viscosity, thermal conductivity and diffusion are usually manifested in a relatively *narrow* region near the surface, termed the boundary layer.

We will only consider two-dimensional flows. In this case all the values are functions of two coordinates x and y. From now on the velocity vector components along the coordinate axes x and y will be termed u and v, *respectively*,

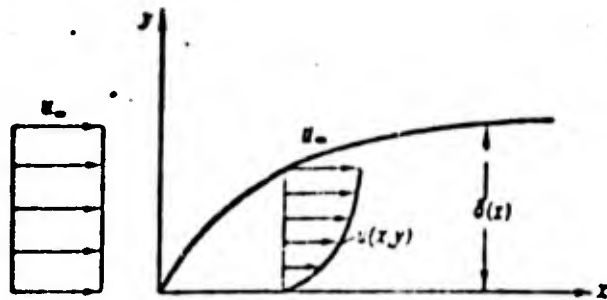$\underline{u}_x = \underline{u}$ and $\underline{u}_y = \underline{v}$

Fig. 110. Dynamic boundary layer

When a *fluid* flows round a body, the velocity of the *fluid* on the

body surface is equal to the velocity of the surface (there is "adhesion" of the

fluid). Inside the boundary layer the velocity varies sharply between its

value at the wall and the velocity in the outside flow. On account of the fact

that the boundary layer is *thin*, the pressure across it is constant, or $\partial p / \partial y = 0$.

This is the fundamental characteristic of the boundary layer.

The thickness of the boundary layer δ is conventionally *regarded as*

the distance from the wall at which the velocity $\underline{u}$ is 99% of the velocity of

the oncoming stream, i.e., $\underline{u} = u/u_\infty = 0.99$. In the general case of two-dimensional

flow, $\underline{u}$ is a function of the coordinates $\underline{x}$, $\underline{y}$: $\underline{u} = \underline{u}\,(\underline{x},\,\underline{y})$.

To describe the shape of the profile in the given section $\underline{x}$ use is

made of the dimensionless coordinate $\eta = y/\delta$. This condition is written down

- 290 -

$$u = u(y/\delta) = u(\eta)$$

as $\rightarrow$. In order to show that we are considering a boundary layer in which

there is a change in velocity, it is termed the "dynamic" boundary layer (Fig. 110).

The thickness of the dynamic layer δ/increases with distance. In the

case of a laminar layer on a plate plate $\dfrac{\delta}{x} \sim \dfrac{1}{\sqrt{Re}}$; in the case of a turbulent layer

$\dfrac{\delta}{x} \sim \dfrac{1}{Re^{0.2}}$. It is clear from this that the layer is $\lfloor$ thin only $\rfloor$ at large Re numbers.

Hence all the derivations in the theory of the boundary layer only hold for large

Re numbers, or for streams with high velocity and low viscosity.

For a case of flow with heat exchange, we introduce the concept of the

thermal or temperature boundary layer. The thermal boundary layer is the

layer adjoining the surface of the region of flow in which there is variation

in the temperature of the liquid between its value at the wall and the temperature

of the external flow. Here the wall temperature and the liquid temperature at

the wall are taken as being equal.

The thickness of the dynamic and thermal boundary layers may not

coincide. On a flat plate with a constant surface temperature the thickness of

the laminar thermal layer δ_t is approximately equal to

$$\frac{\delta_t}{x} \sim \frac{1}{\sqrt{\dfrac{U_l c_p x}{\lambda}}} = \frac{1}{\sqrt{Re\, Pr}}.$$

For the product RePr use is sometimes made of the quantity RePr = Pe -
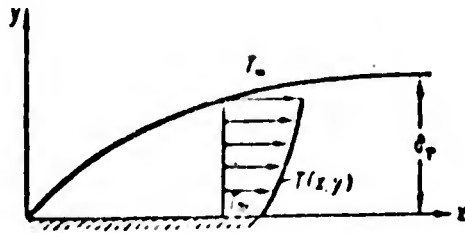
the Péclet number.

Fig. 111. Temperature boundary layer

At $P_T = 1$ $R_e = f_e$ and the thicknesses of the dynamic and layers coincide. In the general case the Pr number may differs considerably from unity, attaining several tens or even hundreds in certain liquids. At Pr ≥ 1, the thermal layer is many times thinner than the dynamic one. The variation in the temperature across the thermal layer (Fig. 111) in dimensionless form can be written down as

$$\theta = \frac{T - T_w}{T_\infty - T_w} = \theta\left(\frac{y}{\delta_T}\right).$$

When there is diffusion, we introduce the concept of the diffusion boundary layer. This is the region of flow near the wall, in which there is variation in the concentration of the admixture between its value at the wall and the value in the external stream. The thickness of the laminar diffusion boundary layer on a flat plate is

$$\frac{\delta_d}{x} \sim \frac{1}{\sqrt{u_\infty L/D}}.$$

In the general case the thickness of the diffusion layer may differ from that of the dynamic and thermal layers.

The concentration profile in dimensionless form is written as

- 292 -

$$\bar{c} = \frac{c}{c_\infty} = \bar{c}\left(\frac{y}{\delta_s}\right).$$

The determination of the thicknesses of the boundary layer is made difficult by the fact that the velocity, temperature and concentration in the boundary layer approach their values in the outside flow very smoothly. Hence it is more convenient to use the integral values. The thickness of the displacement is

$$\delta^* = \int_0^\infty \left(1 - \frac{\rho u}{\rho_\infty u_\infty}\right) dy. \tag{8.7}$$

The amount of liquid flowing through an area   in height at the velocity of the external stream is equal to the amount of liquid by which the consumption through the boundary layer has been reduced.

The thickness of the loss in impulse is

$$\delta^{**} = \int_0^\infty \frac{\rho u}{\rho_\infty u_\infty} \left(1 - \frac{u}{u_\infty}\right) dy. \tag{8.8}$$

Multiplying (8.8) by $\rho_\infty u_\infty^2$, we get

$$\delta^{**} \rho_\infty u_\infty^2 = \int_0^\infty \rho u \left(u_\infty - u\right) dy.$$

The flow of momentum at the velocity of the outside stream through an area δ^{**} in height is equal to the momentum lost in the boundary layer through friction at a true consumption flowing through the boundary layer. The thickness δ^{**} takes into account the friction losses on the surface, but does not make allowance for the reduction in momentum of the outside stream through a reduction

in consumption.

The thickness of the energy loss

$$\delta_T^{**} = \int_0^{\bar{\delta}} \frac{\rho u}{\rho_\infty u_\infty} \left(\frac{T_\infty - T}{T_\infty - T_w} \right) dy \tag{8.9}$$

and the thickness of the loss of matter (through diffusion)

$$\delta_i^{**} = \int_0^{\bar{\delta}} \frac{\rho u}{\rho_\infty u_\infty} \frac{C_\infty - C}{C_\infty - C_w} dy. \tag{8.10}$$

have similar physical meaning.

Sec. 30. Calculation of Heat Exchange during Laminar Flow in Boundary Layer (In Incompressible Liquid)

During laminar flow the processes of transfer are due to molecular

viscosity, thermal conductivity and diffusion. Laminar motion exists at small

Reynolds numbers. For example, during flow along a plate, the laminar regime

is established at $Re = \frac{u_\infty x}{\mu} < 5 \cdot 10^5$. The exact value of this number is a function of

the state of the surface, the sharpness of the leading edge, the surface

temperature, and so on.

Laminar flow may be found near the leading edges *during flow around a* /body

low/ (x) or at flights at a high altitude. Attempts are being made to produce

artificial laminarization of the stream at $Re > 5 \cdot 10^5$ as well, since here the

heat fluxes are considerably reduced.

In practice we encounter a tremendous variety of cases of flow round

- 294 -

surfaces, but for the calculation we have to take the fundamental ones.

When there is flow around the outside of a wing, gas-turbine blade or aircraft fusilage (Fig. 112), we can single out the neighborhood of the leading critical point A at which there is a strong increase in velocity, and the lateral surface described by slight variation in velocity and pressure. In the neighborhood of the critical point, the heat fluxes are maxim$^{\mathcal{l}}$, while the fluxes on the lateral surface are much smaller, but act over a larger area.
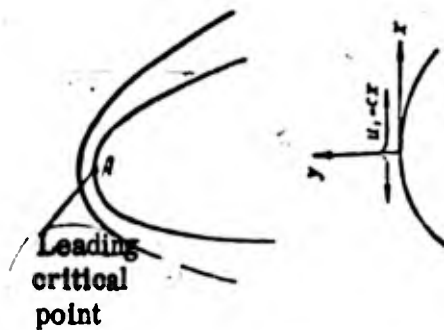

Fig. 112. Flow in neighborhood
of leading critical point
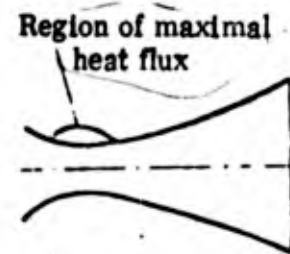

Region of maximal
heat flux

Fig. 113. Supersonic nozzles

When gas flows through the nozzle of an engine (Fig. 113), the maximum heat fluxes occur in the critical section of the nozzle, where the stream is densest and greatly speeded up. In the diverging part the flow density is smaller, the velocity variation is slighter, and the heat fluxes are considerably lower.

The simplest case of flow is flow around a flat plate, in which the velocity of the outside stream u_∞ = const. The solution of this problem can be used approximately to calculate the heating of lateral wing surfaces, gas-turbine blades, fusilage, combustion chambers, diverging sections of a nozzle, and in all cases of flow at slight acceleration or deceleration of the stream.

Let us first consider the boundary layer in an incompressible liquid with a constant density ρ , viscosity μ and thermal conductivity λ so that we may then further refine the calculations for the case of a compressible liquid at high temperatures and M numbers.

Equations for two-dimensional laminar boundary layer at

low velocities

The motion of a viscous liquid is described by the Navier-Stokes differential equations, the continuity equation, thermal-conductivity equations and diffusion equations. During flow with high Re numbers,

$$Re = \frac{u_\infty \rho x}{\mu}, \quad Pe = \frac{u_\infty \rho x c_p}{\lambda} \text{ and } Re_A = \frac{u_\infty x}{D}$$

(diffusion analogue of the Re number), the equations for the viscous liquid are simplified and transformed into boundary layer equations, first derived by Prandtl.

1. Equation of motion

$$\rho u \frac{\partial u}{\partial x} + \rho v \frac{\partial u}{\partial y} = -\frac{dp}{dx} + \frac{\partial}{\partial y}\left(\mu \frac{\partial u}{\partial y}\right). \qquad (8.11)$$

This equation represents the projection of the momentum equation onto the x-axis directed along the surface (Fig. 114). The additional equation obtained when projecting the equation of motion onto the y-axis is $dp/dy = 0$ or $t = $ const. Hence the pressure across the boundary layer is constant. This important property considerably facilitates the calculations.

2. The continuity equation

$$\frac{\partial \rho u}{\partial x} + \frac{\partial \rho v}{\partial y} = 0. \tag{8.12}$$

The continuity equation expresses the law of conservation of mass for an elementary volume of liquid.

3. The energy equation

$$\rho u \frac{c_p \partial T}{\partial x} + \rho v \frac{c_p \partial T}{\partial y} = \frac{\partial}{\partial y} \left(\lambda \frac{\partial T}{\partial y} \right). \tag{8.13}$$

The energy equation expresses the thermal balance conditions in the elementary volume of liquid.

4. The diffusion equation for any admixture in a gas express the law of conservation of matter for this admixture. For a mixture consisting of two gases, the diffusion equations are written in the following form

$$\left. \begin{array}{l} \rho u \dfrac{\partial C_1}{\partial x} + \rho v \dfrac{\partial C_1}{\partial y} = \dfrac{\partial}{\partial y} \left(\rho D_{12} \dfrac{\partial C_1}{\partial y} \right). \\[2mm] \rho u \dfrac{\partial C_2}{\partial x} + \rho v \dfrac{\partial C_2}{\partial y} = \dfrac{\partial}{\partial y} \left(\rho D_{21} \dfrac{\partial C_2}{\partial y} \right). \end{array} \right\} \tag{8.14}$$
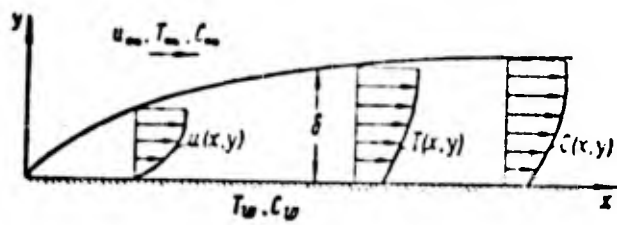
Fig. 114. Flow at $Pr = Pr_d = 1$

The subscripts (1) and (2) designate the first and second components in the mixture. Since $C_1 = C_2$, $\dfrac{\partial C_1}{\partial y} = -\dfrac{\partial C_2}{\partial y}$. Furthermore, the diffusion coefficient $D_{12} = D_{21}$.

To solve the equations of motion we have to indicate the conditions which are *satisfied* on the boundaries of the area in question by the functions describing the distribution of velocity, temperature and concentration.

Boundary conditions

In the coordinate system bound to the wall, at $y = 0$, $u = 0$, $T = T_w$, $v = 0$ and $C = C_w$. Using these conditions, the boundary layer equations at $y = 0$ give us the additional equations

$$\frac{\partial}{\partial y}\left(\mu \frac{\partial u}{\partial y}\right) = -\frac{\partial p}{\partial x}; \quad \frac{\partial}{\partial y}\left(\lambda \frac{\partial T}{\partial y}\right) = 0; \quad \frac{\partial}{\partial y}\left(D \frac{\partial C}{\partial y}\right) = 0.$$

If $\dfrac{\partial p}{\partial x} = 0$ (case of flat plate) and μ, λ, ρ remain constant, the final conditions acquire the form: at $y = 0$ $\quad \dfrac{\partial^2 u}{\partial y^2} = 0; \quad \dfrac{\partial^2 T}{\partial y^2} = 0; \quad \dfrac{\partial^2 C}{\partial y^2} = 0.$

On the external boundary, the velocity, diffusion and temperature should change to these values in the external stream

$$u = u_\infty, \quad T = T_\infty, \quad C = C_\infty \quad \text{and} \quad y \to \infty \, (y = \ell).$$

The boundary conditions may also vary in accordance with the physical conditions of the problem. For example, the wall temperature is sometimes an unknown, and the set value $(\partial T/\partial y)_{y=0}$ for vertical gas feed through a porous surface $(v)_{y=0} = v_0$ is used as the boundary condition. An exact solution of the two-dimensional

- 298 -

boundary layer equations in the general case is extremely complex, since all the

values in the equations are functions of two variables, since the boundary layer

equations are differential ones в in partial derivatives. In certain special

cases, the motion equations can be transformed into ordinary, differential ones

with one independent variable. This is possible whenever the temperature, velocity

and concentration profiles are not functions of the coordinate x. In this case

the relationships

$$\frac{u}{u_\bullet}=\bar{u}(y,z); \quad \frac{T-T_w}{T_\bullet-T_w}=\theta(y,z); \quad \frac{C-C_z}{C_\bullet-C_z}=\bar{C}(y,z)$$

remain the same at different sections. When going on to the ordinate proportional

to the ratio y/δ, the dependence of x in the boundary-layer equations should

disappear. Such flows with low longitudinal pressure gradients are ones in which

the velocity distribution in the outside stream is

$$u_\bullet=cx^m \quad \text{и} \quad u_\bullet=ce^x.$$

at constant T_w and C_w.

The solution of these problems have been numerically calculated and

tabulated. It should be pointed out that these laws cover certain important cases

encountered in practice. For example at $m = 0$, $u_\infty=$ const, we find flow along

a flat plate, at $m = 1$, $u_\infty= \frac{c}{x}$ we find flow in the neighborhood of the critical

point on the flat body (for example, a turbine blade or wing). The solution for

- 299 -

$\underset{\sim}{m} = 1/3$ may be used to calculate flow in the neighborhood of the critical point

of an obtuse, axial-symmetric body. The values $\underset{\sim}{m} \geqslant 1$, correspond to flow near the

critical section of a supersonic nozzle. In cases in which it is not possible to

use the exact solutions, we resort to approximate methods. These methods enable

us to transform the boundary-layer equations into ordinary differential equations

by using the . integral boundary-layer relationships.

The relationship between friction, heat transfer and diffusion.

If a case of flow in which $\underset{\sim}{dp/dx = 0}$, under certain conditions we can

establish a link between the friction and heat transfer directly from the equations

without having to solve them.

Let us assume that $\dfrac{dp}{dx} = 0$ (flow along a plate),

$$Pr = \frac{\mu c_p}{\lambda} = 1 \text{ and } Pr_{_A} = \frac{\mu}{\rho D} = 1.$$

In this case the equations of motion, thermal conductivity and diffusion

become similar

$$\rho u \frac{\partial u}{\partial x} + \rho v \frac{\partial u}{\partial y} = \frac{\partial}{\partial y}\left(\mu \frac{\partial u}{\partial y}\right),$$

$$\rho u \frac{c_p \partial T}{\partial x} + \rho v \frac{c_r \partial T}{\partial y} = \frac{\partial}{\partial y}\left(\mu \frac{c_r \partial T}{\partial y}\right),$$

$$\rho u \frac{\partial C}{\partial y} + \rho v \frac{\partial C}{\partial y} = \frac{\partial}{\partial y}\left(\mu \frac{\partial C}{\partial y}\right).$$

- 300 -

If we now consider the variables

$$\bar{u}=\frac{u}{u_\infty}, \quad \theta=\frac{T-T_w}{T_\infty-T_w}, \quad \bar{C}=\frac{C-C_w}{C_\infty-C_w},$$

the equations become identical, since $\bar{u}, \theta, \bar{C}$ vary between zero at the wall and unity on the outer boundary. The equations hold if

$$\bar{u}=\theta=\bar{C}.$$

Thus, we find an important condition of similarity for the velocity, temperature and concentration profiles

$$\frac{u}{u_\infty}=\frac{T-T_w}{T_\infty-T_w}=\frac{C-C_w}{C_\infty-C_w}. \tag{8.15}$$

This condition is a result of the fact that the transfer of momentum, energy and concentration is effected by identical, physical molecular processes.

If the profile velocity is known, the friction stress τ is determined by the formula $\tau=\mu\frac{\partial u}{\partial y}$. Applying the similarity conditions, we get

$$\tau=\mu\frac{\partial u}{\partial y}=\mu u_\infty\frac{\partial\bar{u}}{\partial y}=\frac{\mu u_\infty}{T_\infty-T_w}\frac{\partial T}{\partial y}.$$

Multiplying the numerator and denominator by λ and taking it into account that

$$\lambda\cong\mu c_p, \quad \text{and} \quad q=-\lambda\frac{\partial T}{\partial y}, \quad \text{we will obtain}$$

$$\tau=\frac{\mu u_\infty}{(T_w-T_\infty)\lambda}\lambda\frac{\partial T}{\partial y}=\frac{u_\infty}{c_p}\frac{q}{(T_w-T_\infty)}.$$

we get

$$\frac{\tau}{u_\infty}=\frac{q}{c_p(T_w-T_\infty)}.$$

- 301 -

Similarly, for the transfer of matter

$$\frac{\tau}{u_\infty} = \frac{q}{c_p(T_v - T_\infty)} = \frac{Q}{C_v - C_\infty}.$$

These expressions are transformed into the dimensionless form. For

$$\tau = \tau_w, \quad -q = q_w, \quad -Q = Q_w,$$

conditions on the wall $_w$. Multiplying all the sides of the equality by the

$$\lambda = \mu c_p = \rho D c_p$$

length $\underline{L}$ and dividing by $_\lambda$, we get

$$\frac{q_w L}{(T_\infty - T_w)\lambda} = \frac{\tau_w}{\mu u_\infty} L = \frac{Q_w L}{(C_\infty - C_w)\rho D}.$$

After multiplication and division of the first term by ρu_∞ we get

$$\frac{q_w L}{(T_\infty - T_w)\lambda} = \frac{\tau_w}{\rho u_\infty^2} \frac{u_\infty L \rho}{\mu} = \frac{Q_w L}{(C_\infty - C_w)\rho D}.$$

According to definition $\dfrac{q_w}{T_\infty - T_w} = \alpha, \quad \dfrac{\tau_w}{\rho u_\infty^2} = \dfrac{1}{2} c_f$ and $\dfrac{Q_w}{C_\infty - C_w} = \beta.$

The values $\dfrac{\alpha L}{\lambda} = \mathrm{Nu}, \quad \dfrac{u_\infty L \rho}{\mu} = \mathrm{Re}$ and $\dfrac{\beta L}{\rho D} = \mathrm{Nu_d}$. The relation between friction, heat

transfer and diffusion finally takes the dimensionless form of

$$\mathrm{Nu} = \mathrm{Nu}_d = \frac{1}{2} c_f \mathrm{Re}. \qquad (8.16)$$

The equation derived expresses the thermodynamic analogy between the

friction, diffusion and heat transfer at the numbers Pr = 1 and $\mathrm{Pr_d}$ = 1.

In the general case Pr $\neq$ 1 the formulae are derived in the form

$$\mathrm{Nu} = \frac{1}{2} c_f \mathrm{Re} \, f(\mathrm{Pr}).$$

During laminar flow $\underline{f}(\mathrm{Pr}) \approx \mathrm{Pr}^{\frac{1}{3}}$, approximately, and in turbulent flow $f(\mathrm{Pr}) \approx \mathrm{Pr}^{0.4}$.

These relationships can also be written in the form

$$\frac{c_v}{\mu_\infty c_p (T_\infty - T_s)} = \frac{\tau_T}{\mu u_\infty^2}, \quad \tau. \; e. \; c_H = \frac{1}{2} c_f \quad \text{for} \quad Pr = 1$$

and

$$c_H = \frac{1}{2} c_f Pr^{-\frac{2}{3}}, \tag{8.17}$$

$$c_H = \frac{1}{2} c_f Pr^{-0.6} \tag{8.18}$$

at $Pr \neq 1$ for laminar and turbulent flow. The equations derived for the relationship) between friction and heat transfer are widely used in calculations and can be extended to cover a case of high velocity.

Methods of calculating boundary layer

One of the methods of simplifying the boundary-layer equations is to satisfy the differential equations as an average for the boundary-layer thickness, rather than the equations for each individual particle.
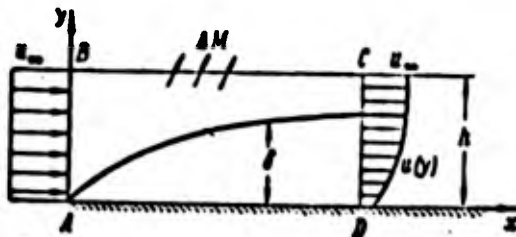

Fig. 115. Derivation of integral relationship
of momentum on plate

Let us consider a very simple example of flow along a flat plate. Let us look for a solution satisfying the momentum and energy equations for two sections of the boundary layer.

Let us construct a control surface near the plate (Fig. 115). Let

R be the force acting on the liquid on the plate side, and Δ M the mass of

liquid emerging from the contour by virtue of the fact that the consumption

through the face CD is less than through AB.

The projection of the momentum equation onto the x-axis gives us

$$\int_0^\delta \rho u^2 dy + \Delta M u_\infty - \int_0^\delta \rho_\infty u_\infty^2 dy = -R.$$

$$\Delta M = \int_0^\delta \rho_\infty u_\infty dy - \int_\delta^\delta \rho u dy.$$

$$R = \int_0^\delta \rho u \left(u_\infty - u \right) dy = \rho_\infty u_\infty^2 \int_0^\delta \frac{\rho u}{\rho_\infty u_\infty}\left(1 - \frac{u}{u_\infty} \right) dy = \rho_\infty u_\infty^2 \delta^{**}.$$

The friction stress $\tau_w = dR/dx$. Hence

$$\tau_w / \rho_\infty u_\infty^2 = d\delta^{**}/dx. \tag{8.19}$$

The friction acting on the liquid side of the plate is directed towards the

motion of the liquid.

This equation is called the integral momentum relationship. Here
$\tau_w = \tau_w(x)$ and $\delta^{**} = \delta^{**}(x)$. In this equation (there is) one independent invariable x and two unknown

functions τ_w and δ^{**}. To solve the equation we have to find a further

connection between τ_w and δ^{**}.

For this purpose the velocity profile in the boundary layer is

approximated with a function selected in such a way that it satisfies the physical

conditions of the problem. Let us assume that in the case of an incompressible

- 304 -

Kind

(ρ = const) the velocity profile is given as the function $\bar{u}/u_\infty = f(\eta)$, in which

$\eta = y/\delta$. The friction stress is then

$$\tau_0 = \mu\left(\frac{\partial u}{\partial y}\right)_w = \mu\left(\frac{u_\infty}{\delta}\right)\left(\frac{\partial f}{\partial \eta}\right)_w.$$

The thickness of the layer δ at the known $f(\eta)$ may be expressed in

terms of δ^{**}.

$$\delta^{**} = \int_0^\delta \frac{\rho u}{\rho_\infty u_\infty}\left(1 - \frac{u}{u_\infty}\right)dy = \delta\int_0^1 f(1-f)\,d\eta.$$

Substituting τ_w and δ^{**} into the integral relationship we get an

equation for δ , and also for τ_w and δ^{**}. The velocity profile is often given

in the form of a step polynomial

$$\frac{u}{u_\infty} = a_0 + a_1\eta + a_2\eta^2 + a_3\eta^3.$$

The profile has to satisfy the boundary conditions established by

us earlier on: at $\widehat{\eta = 0 \; u = 0}$ and $\frac{\partial^2 u}{\partial\eta^2} = 0$; at $\widehat{\eta = 1 \; u = u_\infty}$. In addition, we adopt the condition

of smooth conjugation between the velocity profile and the outer stream profile:

at $\widehat{\eta = 1 \; \partial u/\partial\eta = 0}$.

Applying these conditions we get $a_0 = 0;\; a_2 = 0;\; a_1 = \frac{3}{2};\; a_3 = \frac{1}{2}.$ Hence

$$\frac{u}{u_\infty} = \frac{3}{2}\eta - \frac{1}{2}\eta^3.$$

$$\tau_0 = \frac{3}{2}\mu\frac{u_\infty}{\delta};\quad \delta^{**} = \frac{39}{280}\delta.$$

The integral relationship takes the form

$$\frac{3}{2}\mu\frac{u_\infty}{\rho u_\infty^2}\frac{280}{39}dx = \delta\,d\delta.$$

After integration

$$\delta = 4.5 \sqrt{\frac{\mu x}{\rho u_\infty}}; \quad \frac{\delta}{x} = \frac{4.5}{\sqrt{\frac{u_\infty \rho_\infty x}{\mu}}} = \frac{4.5}{\sqrt{Re}}.$$

$$\frac{\tau_w}{\rho u_\infty^2} \sqrt{Re} = 0.323$$

from which ▲ . The exact solution of the differential equation for this case

give us

$$\frac{\tau_w}{\rho u_\infty^2} \sqrt{Re} = 0.332.$$

It is now easy to derive formulae for the heat flux by using the

hydrodynamic analogy between friction and heat transfer. We get

$$Nu = \frac{1}{2} c_f Re \, Pr^{\frac{1}{3}};$$

$$\text{но} \quad \frac{1}{2} c_f \sqrt{Re} = 0.332.$$

Hence

$$Nu = 0.332 \sqrt{Re} \, Pr^{\frac{1}{3}}.$$

$$\frac{\alpha x}{\lambda} = 0.332 \sqrt{\frac{u_\infty \rho x}{\mu}} \, Pr^{\frac{1}{3}};$$

$$\alpha = 0.332 \lambda \sqrt{\frac{u_\infty \rho}{\mu x}} \, Pr^{\frac{1}{3}};$$

$$q_w = 0.332 \lambda (T_\infty - T_w) \sqrt{\frac{u_\infty}{\nu x}} \, Pr^{\frac{1}{3}}.$$

Thus, the heat flux density drops as x increases. The mean heat flux

is determined from the expression

$$q_{cp} = \frac{\int_0^x q \, dx}{x} = 0.664 \, \lambda (T_\infty - T_w) \sqrt{\frac{u_\infty}{\nu x}} \, Pr^{\frac{1}{3}}.$$

In cases in which the velocity distribution in the outer stream

obeys the power law $u_\infty = c x^m$, we can derive exact solutions. Here the heat-

transfer coefficient can be written in the general form

$$\alpha = \theta' \lambda \sqrt{\frac{u_\infty}{\nu x}} \, Pr^{\frac{1}{3}}, \qquad (8.20)$$

m	θ'
0	0.332
1/3	0.44
1	0.57

and u_∞ is a function of x and $\theta' = [\partial \theta / \partial \eta]_{\tau=0}$.

- 306 -

The values θ' for certain cases are shown in the table.

The values θ' at $\underline{m} = 1$ can be used to calculate the heat exchange in the neighborhood of the leading critical point. In this region $\underline{u}_\infty = \underline{cx}$ in which $\underline{x}$ is the distance reckoned from the critical point and

$$a = 0.57 \lambda \sqrt{\frac{c}{\nu}} \, Pr^{\frac{1}{3}}.$$

For air $Pr \approx 0.7$. In the neighborhood of the leading critical point on the axial symmetric body $u_\infty = \underline{cx}$ as well and

$$a = \sqrt{3} \lambda \theta' \sqrt{\frac{c}{\nu}} \, Pr^{\frac{1}{3}} = 0.763 \sqrt{\frac{c}{\nu}} \, Pr^{\frac{1}{3}}.$$

Sec. 31. Laminar Boundary Layer in A Compressible Gas

When calculating the boundary layer during flow at high velocities and high temperature differences we have to take into account the variation in the density of the gas as a function of the variation in the pressure and temperature (compressibility of a gas) and also the dependence of the temperature of the physical parameters of the gas: μ, λ, c_p, Pr. Furthermore, at high velocities the release of heat through the work of friction (displacement of energy) and through the work of pressure becomes substantial. At superhigh velocities and temperatures about 2000 - 3000°, we have to take into account as well the chemical changes in the gas, dissociation, the transfer of heat by radiation, ionization and other factors.

Compressibility is the power of a liquid to alter its volume when

acted on by outside pressure. If the ratio $\frac{\Delta\rho}{\rho_0}\ll 1$, throughout the flow area under

consideration, the liquid is regarded as incompressible. Here $\Delta\rho=\rho-\rho_0$ and ρ_0 is

the density at a fixed point in the area under consideration.

When a gas flows round an obtuse body, a pressure is established at

the forward critical point in sub-sonic flow which is equal to the pressure of

the total adiabatic drag. Here the density of the gas assumes the value

$$\frac{(\rho)_{00}}{\rho_0}=\left(1+\frac{k-1}{2}M^2\right)^{\frac{1}{k-1}}\approx 1+\frac{1}{2}M^2 \quad (\rho_0=\rho_\infty).$$

$$\rho_{00}/\rho_0\approx 1.1; \; \Delta\rho/\rho_0=0.1$$

At M = 0.45, the value (Λ). If we take an accuracy of 10% to

be satisfactory, the gas moving at $M \leqslant 0.45$ can be regarded as an incompressible

fluid. At $M > 0.45$ we have to take the compressibility of the gas into account.

When considering heat exchange, we must make allowance as well for

the variation in the gas density in the boundary layer through a large difference

in temperature $\rho_0=\rho/RT_0$. If the temperature is T_1 at any point on the boundary

layer and the pressure remains the same, then

$$\rho_1=\frac{\rho}{RT_1} \text{ and } \frac{\Delta\rho}{\rho_0}=\frac{T_1-T_0}{T_1}=1-\frac{T_0}{T_1}.$$

The compressibility has to be taken into account with an accuracy of

10%, whenever the temperature ratio at the two points $T/T \geqslant 0.9$ or $T_0/T_1 \leqslant 1.1$.

Variation in the temperature in the boundary layer also occurs when there is no

heat exchange, but when the gas is slowed down through friction.

If the wall is firmly insulated, i.e., if there is no heat removal,

the gas temperature at the surface is close to the drag temperature

$$T_{00} = T_\infty \left(1 + \frac{k-1}{2} M^2\right); \qquad \text{for air} \qquad k = 1.4 \text{ и } T_{00} = (1 + 0.2 M^2) T_\infty.$$

$T_{00}/T_\infty = 1.1$ occurs at M = 0.7. Hence in a case of flow along an

insulated flat surface when there is no adiabatic drag, the compressibility has

to be taken into account at $M \geqslant 0.7$.

When there is strong variation in temperature, apart from the change

in density, there is also a variation in the physical properties of the liquid

or gas

$$\mu = \mu(T); \quad \lambda = \lambda(T); \quad D = D(T).$$

If, furthermore, there is diffusion of gases with different physical properties

in the boundary layer, then

$$\mu = \mu(T, C); \quad \lambda = \lambda(T, C); \quad D = D(T, C); \quad \rho = \rho(T, C).$$

Here C is the concentration of the impurity.

Thus, when investigation the flow of a compressible gas, we must make

allowance for the dependence of the physical properties of the medium on temperature,

concentration and pressure. In certain specific cases some of these factors can

be disregarded.

Boundary layer equations for high velocities

On account of friction in the boundary layer there is an emission of heat. The kinetic energy of the outer stream is transformed into heat energy and there is dissipation.

The amount of heat released through friction is

$$\Phi = \frac{\mu}{gE}\left(\frac{\partial u}{\partial y}\right)^2 \cdot 3600 \text{ kcal/m}^3 \cdot \text{hr} \tag{8.21}$$

If there is a longitudinal pressure drop, heat is released through the work of pressure. The amount of heat released in this case is equal to

$$\frac{u}{gE}\frac{dp}{dx} \cdot 3600 \text{ kcal/m}^3 \cdot \text{hr} \tag{8.22}$$

Taking these terms into account, the equations now become (the multipliers showing dimensionality has been left out)

$$\rho u \frac{\partial u}{\partial x} + \rho v \frac{\partial u}{\partial y} = \frac{\partial}{\partial y}\left(\mu \frac{\partial u}{\partial y}\right) - \frac{\partial p}{\partial x}, \tag{8.23}$$

$$\rho u c_p \frac{\partial T}{\partial x} + \rho v c_p \frac{\partial T}{\partial y} = \frac{\partial}{\partial y}\left(\lambda \frac{\partial T}{\partial y}\right) + \mu\left(\frac{\partial u}{\partial y}\right)^2 + u\left(\frac{\partial p}{\partial x}\right). \tag{8.24}$$

The equations can be transformed into another form. Let us multiply the first equation by u and add it to the second. Here we must make allowance for the fact that

$$u \frac{\partial u}{\partial y} = \frac{\partial (u^2/2)}{\partial y}; \qquad u \frac{\partial u}{\partial x} = \frac{\partial (u^2/2)}{\partial x} \quad \text{and}$$

$$u \frac{\partial}{\partial y}\left(\mu \frac{\partial u}{\partial y}\right) = \frac{\partial}{\partial y}\left[\mu \frac{\partial (u^2/2)}{\partial y}\right] - \mu\left(\frac{\partial u}{\partial y}\right)^2.$$

We get the following equation

$$\rho u \left[c_p \frac{\partial T}{\partial x} + \frac{\partial (u^2/2)}{\partial x}\right] + \rho v \left[c_p \frac{\partial T}{\partial y} + \frac{\partial (u^2/2)}{\partial y}\right] =$$

$$= \frac{\partial}{\partial y}\left(\lambda \frac{\partial T}{\partial y}\right) + \frac{\partial}{\partial y}\left[\mu \frac{\partial (u^2/2)}{\partial y}\right].$$

- 310 -

From the definition of the drag temperature

$$c_p dT + d(u^2/2) = c_p dT_\infty.$$

The equation then takes the following form:

$$\rho u \frac{c_p \partial T_{00}}{\partial x} + \rho v c_p \frac{\partial T_{00}}{\partial y} = \frac{\partial}{\partial y}\left(\lambda \frac{\partial T}{\partial y}\right) + \frac{\partial}{\partial y}\left[\mu \frac{\partial(u^2/2)}{\partial y}\right].$$

If in the right-hand side we now add and subtract the expression $\frac{\partial}{\partial y}\left[\frac{\lambda}{c_p}\frac{\partial(u^2/2)}{\partial y}\right]$ and take

it into account that $\mu c_p / \lambda = \mathrm{Pr},$ we finally get

$$\rho u \frac{c_p \partial T_{00}}{\partial x} + \rho v \frac{c_p \partial T_{00}}{\partial y} = \frac{\partial}{\partial y}\left(\lambda \frac{\partial T_{00}}{\partial y}\right) + \frac{\partial}{\partial y}\left[\mu \left(1 - \frac{1}{\mathrm{Pr}}\right)\frac{\partial(u^2/2)}{\partial y}\right]. \qquad (8.25)$$

This equation can be used instead of the energy equation for the

temperature T. Its chief feature is that at $\mathrm{Pr} = 1$ it acquires a similar form to

that of the equation for low flow velocities

$$\rho u \frac{c_p \partial T_{00}}{\partial x} + \rho v \frac{c_p \partial T_{00}}{\partial y} = \frac{\partial}{\partial y}\left(\lambda \frac{\partial T_{00}}{\partial y}\right). \qquad (8.26)$$

The distinction is that instead of the temperature T the equation

contains T_{00}. Thus, all the conclusions drawn by us with regard to heat

exchange at low velocities are still valid if we use T_{00} instead of T.

Consequently, the heat flux at high velocities is determined by the

variation in drag temperature in the boundary layer. The transfer of heat

occurs when there is a difference between the drag temperature of the flux and

the temperature of the wall. In a more general case, when variable thermal

capacity is taken into account, we introduce the concept of the total drag

enthalpy $J_\infty = \int c_p dT + \frac{u^2}{2}$, which is equal to the product of thermal capacity and drag

temperature, provided c_p = const. The energy equation for Pr = 1 can

be written in the form

$$\rho u \frac{\partial J_{00}}{\partial x} + \rho v \frac{\partial J_{00}}{\partial y} = \frac{\partial}{\partial y}\left(\frac{1}{c_p}\frac{\partial J_{00}}{\partial y}\right). \qquad (8.27)$$

Thus, in the general case heat exchange depends on the difference

between the total drag energy of the flow and the energy of the gas at wall

temperature. For the sake of simplicity let us consider a case c_p = const.

Let us look at flow along a flat plate at a constant velocity of the outer

stream u_∞ = const and dp/dx = zero. It is easy to see that by means of the

equality $T_{00} = \frac{u}{u_\infty}(T_{00_\infty} - T_w)$ the energy equation at Pr = 1 becomes identical with the

motion equation. The solution of the energy equation is determined from this

$$\frac{T_{00} - T_w}{(T_{00})_\infty - T_w} = \frac{u}{u_\infty}.$$

Thus, at higher velocities of the flow in the boundary layer, there

is similarity between the velocity and drag temperature profiles at Pr = 1.

Temperature distribution in boundary layer on insulated

surface at Pr = 1

Let us see how the temperature varies inside the boundary layer at

large velocities and at Pr = 1. If the wall is thermally insulated, the heat

flux is equal to zero $\quad q_w = \lambda\left(\frac{\partial T}{\partial y}\right)_w = 0 \quad$ и $\quad \left(\frac{\partial T}{\partial y}\right)_w = 0;$

but

$$T = T_{00} - \frac{u^2}{2c_p}.$$

Consequently,

$$\frac{\partial T}{\partial y} = \left(\frac{\partial T_{00}}{\partial y}\right) - \frac{u}{c_p}\frac{\partial u}{\partial y}.$$

At the wall $\underline{u} = 0$ and

$$\left(\frac{\partial T}{\partial y}\right)_w = \left(\frac{\partial T_{00}}{\partial y}\right)_w = 0.$$

Since

$$\frac{\partial T_{00}}{\partial y} = \frac{\partial T_{00}}{\partial u}\frac{\partial u}{\partial y}, \quad a$$

$$\left(\frac{\partial u}{\partial y}\right)_w \neq 0,$$

therefore

$$\left(\frac{\partial T_{00}}{\partial u}\right)_w = 0.$$

Differentiating the expression for $\underline{T}_{00}$ with respect to $\underline{u}$, we find

that $\frac{(T_{00})_w - T_w}{U_w} = 0$ or $T_w = (T_{00})_w$. A temperature equal to the drag temperature of the outside

stream is established on the insulated wall at Pr = 1. But if $(T_{00})_w - T_w = 0$, then at any
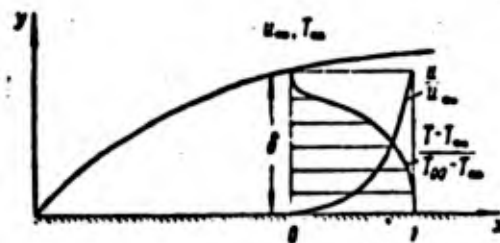
Fig. 116. Velocity and temperature distribution in boundary
layer at high velocities in Pr = 1 on insulated wall

point on the boundary layer $T_{00} = (T_{00})_-$. At all points on the boundary on the insulated

surface when Pr = 1 the drag ⌒ temperature is constant.

Let us find now the temperature distribution across the boundary layer

$T = T_{00} - \frac{a^2}{2c_p}$. From this

$$T = T_- + \frac{a_-^2}{2c_p}\left(1 - \frac{a^2}{a_-^2}\right).$$ (8.28)

Thus, the gas temperature varies smoothly between the temperature of the outside

stream and the drag temperature at the wall (Fig. 116).

Temperature distribution in boundary layer on insulated

surface at Pr $\neq$ 1.

If the Prandtl number Pr $\neq$ 1, a temperature is established on the

thermally insulated wall which is different from the drag temperature on the

outer stream. For gases Pr < 1, for example, in air Pr ⪰ 0.71. In this case

the temperature of the insulated wall is lower than the drag temperature of the

outside stream. Let us designate the temperature acquired by the insulated wall

as $\underline{T}_e$. Then $T_e < (T_{00})$. At a high velocity two processes occur simultaneously in

the boundary layer - the emission of heat through friction and the removal of

heat through conduction and convection. At Pr < 1 these processes are balanced,

at $\underline{T}_e < (\underline{T}_{00})_\infty$.

Let us introduce the concept of the temperature recovery coefficient

$$r = \frac{T_e - T_\infty}{(T_{00})_\infty - T_\infty}. \quad (8.29)$$

or in other words

$$r = \frac{T_e - T_\infty}{\dfrac{w_\infty^2}{2c_p}}$$

and

$$T_e = T_\infty + r \frac{w_\infty^2}{2c_p}.$$

The temperature recovery coefficient $\underline{r}$ indicates the proportion of

kinetic energy from the outside stream which has gone into the heat content on

the wall. In laminar flow along a flat plate $\underline{r} \approx \sqrt{Pr}$. For air $\underline{r} \approx 0.84$ and

$$T_e = T_\infty \left(1 + \frac{k-1}{2} \sqrt{Pr} M_\infty^2\right) \qquad (8.30)$$

or

$$T_e = T_\infty \left(1 + 0.168 M_\infty^2\right).$$

The distribution of velocity, temperature and the drag temperature

on an insulated surface at $Pr \neq 1$ is shown in Fig. 117. As can be seen from this

figure, the drag temperature at the wall is below that of the outside stream.

Some of the energy has been transferred from this region to the outside of the

boundary layer on account of which the drag temperature in this area has become

greater than that of the outside stream.

In a case in which the velocity of the outside stream is variable
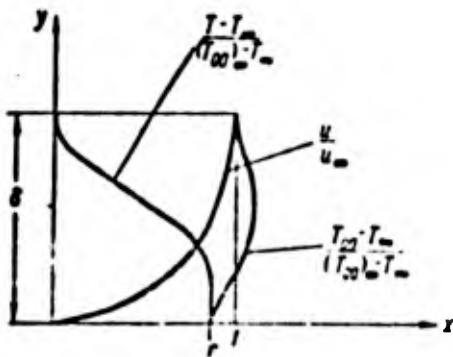
Fig. 117. Velocity and temperature distribution across boundary layer at high velocities and Pr < 1 on heat insulated wall

$u_\infty \neq$ const and $dp/dx \neq 0$, the recovery coefficient varies along the length.

During laminar flow an approximate value can be found theoretically

$$T_e = T_\infty + \frac{u_\infty^2}{2c_p}\left[1 + \frac{u_{1\infty}^2}{u_\infty^2}\left(\sqrt{\mathrm{Pr}} - 1\right)\right].\qquad(8.31)$$

Here u_∞ is the velocity of the stream approaching the body;

$u_{1\infty}$ is the local velocity at the surface of the immersed .

body beyond the boundary layer, and

T_∞ is the temperature of the oncoming stream.

If we designate the recovery coefficient as before, as $r = \dfrac{(T_e - T_\infty)}{(u_\infty^2/2c_p)}$,

we get

$$r = 1 + \frac{u_{1\infty}^2}{u_\infty^2}\left(\sqrt{\mathrm{Pr}} - 1\right).\qquad(8.32)$$

It can be seen from this that at the leading critical point $u_{1\infty} = 0$; $r = 1$;
$T_e = (T_\infty)_\infty$; on the plate $u_{1\infty} = u_\infty$, $r = \sqrt{\mathrm{Pr}}$.

When there is flow round the surface, the local velocity $u_{1\infty}$ in an

extreme case may attain the so-called maximum velocity, which is related to the

parameters of the oncoming flow in the following way

$$\frac{u_{1\infty}^2}{2c_p} = T_\infty.$$

Here

$$T_e = \sqrt{\mathrm{Pr}}\, T_\infty.$$

The recovery coefficient can be obtained by direct measurement of the temperature of the insulated surface. For a case of flow along a plate, Fig. 118 shows the dependence of r on the Reynolds number for the flow of air. As can be seen from this graph, in laminar flow the recovery coefficient does not depend for practical purposes on the Re number. At Re $\approx 10^6$ there is a sharp increase in the recovery coefficient to $r \approx 0.89$ through transition to turbulent flow.
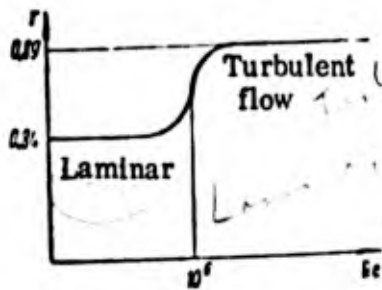

Fig. 118. Experimental values of temperature recovery coefficients
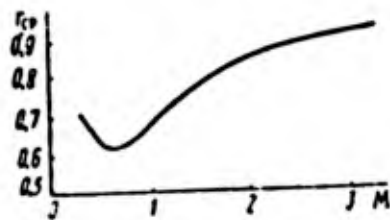
Fig. 119. Variation in mean temperature recovery coefficient of cylinder as function of M

For M > 1 the dependence of the recovery coefficient on M in the case of a flat plate proves to be only slight. An investigation was made of the experimental dependence of the mean temperature recovery coefficient on the M number for thin wires

$$t_{cp} = \frac{T_{cp} - T_\infty}{\frac{a_\infty^2}{2c_p}},$$
(8.33)

in which $T_{\hat{m}}$ is the mean wire temperature as determined from measurement of its

electric resistance. The results of the measurements are shown in ^{F}ig. 119.

Temperature distribution in boundary layer of compressible

gas when there is heat exchange

$$\frac{T_{00} - T_v}{(T_{00})_\infty - T_v} = \frac{u}{u_\infty}$$

Let us consider first the case $Pr = 1$. Here $\sim$; taking it into

$T_{00} = T + \frac{u^2}{2c_p}$

account that $\sim$, after transformation we get

$$T = T_v + (T_\infty - T_v)\frac{u}{u_\infty} + \frac{u_\infty^2}{2c_p}\frac{u}{u_\infty}\left(1 - \frac{u}{u_\infty}\right).$$
(8.34)

Since $\frac{u_\infty^2}{2c_p} = \frac{k-1}{2}M_\infty^2 T_\infty,$ then

$$\frac{T}{T_\infty} = \frac{T_v}{T_\infty} + \left(\frac{T_\infty - T_v}{T_\infty}\right)\frac{u}{u_\infty} + \frac{k-1}{2}M_\infty^2\frac{u}{u_\infty}\left(1 - \frac{u}{u_\infty}\right).$$

If the M number is small ($M \approx 0$), we get the well-known relationship

for small velocities

$$\frac{T - T_v}{T_\infty - T_v} = \frac{u}{u_\infty}.$$

The temperature distribution and velocity distribution the across the

boundary layer are shown in ^{F}ig. 120.

For the case $Pr = 1$, when $T_w < T_{00}$, the wall heats up. At $T_w > T_{00}$ the

wall cools down, at $T_w = T_{00}\left(\partial T \partial y\right) = 0$ and heat flux $q_w = \lambda\,(\partial T\,\partial y)_w = 0$.

If $T_v < (T_{00})_\infty$, the curve showing the temperature distribution has a maximum/

- 318 -

In the outside of the boundary layer the gas heats up through friction, while there is a drop in temperature at the wall through removal of heat through it. Thus, the temperature inside the boundary layer may be considerably higher than that of the stream and the wall. It is interesting to evaluate the maximum temperature. Assuming $Pr = 1$, let us differentiate the expression for T with respect to y and let us equate the derivative ($\partial T/\partial y$) to zero. T_{max} is determined by the equation

$$\frac{T_{max} - T_w}{(T_{00})_\infty - T_w} = \frac{1}{4}\left(\frac{1 - \dfrac{T_w}{T_\infty}}{\dfrac{k-1}{2}M^2} + 1\right). \qquad (8.35)$$

If $M \gg 1$ or if $T_w \approx T_\infty$, then $\dfrac{T_{max} - T_w}{(T_{00})_\infty - T_w} = \dfrac{1}{4}$.

For example, at a flight number $M \approx 20$, $T_\infty = 250°$ abs; $T_w \approx 1000°$ abs; $T_{max} \approx 5700°$. Thus, although the temperature of the stream by the wall does not
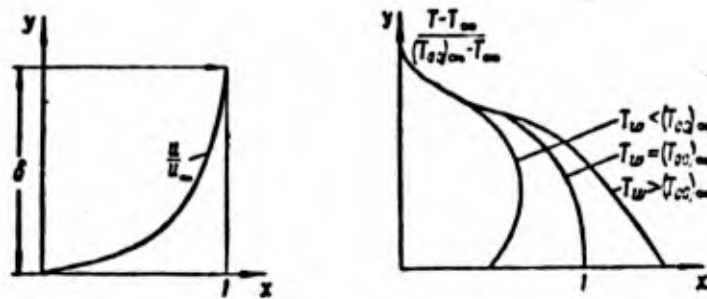
Fig. 120. Velocity and temperature distribution in boundary layer at Pr = 1 and with heat exchange

exceed 1000°, an extremely high temperature is attained inside the boundary layer.

If $Pr \neq 1$, the temperature distribution on the wall with heat exchange is similar in form. But since the temperature established on the wall when there is no heat exchange is different from the drag temperature $T_e \neq T_{00}$, the wall is cooled by the outside stream, if it is kept at $T_w > T_e$, and is heated by the outside stream if it is kept at $T_w < T_e$.

Calculation of heat exchange in laminar flow in boundary layer

of compressible gas

At high velocities the heat-transfer coefficient is determined by the equation $q_w = a(T_e - T_w)$. Defined in this way, it might be thought that the main effect of the high stream velocity had been taken into account by the fact that the temperature T_e has been taken instead of T_∞. Furthermore, if $T_w^\wedge = T_e^\wedge$ here, then $q_w = 0$, which is in full accordance with the experiment.

The problem is to determine the heat-transfer coefficient $\propto$, which is in the general form a function of the Re number, the M number, the temperature ratio $\dfrac{T_w}{T_e}$, the Pr number, and so on.

In order to determine $\propto$ we have to find a solution to the system of equations(8.23) and (8.24), and then find the temperature field inside the boundary layer. The heat flux density to the wall is equal to $q_w = \lambda_w (\partial T / \partial y)_w$.

In certain special types of velocity distribution in the outside stream, and if there are further limitations, Eqs. (8.23) and (8.24) can be transformed into ordinary differential equations. Exact numerical solutions have been derived for these cases. In flow with an arbitrary velocity distribution in the outside stream, and with variable temperature of the wall, the integral relationships of momentum and energy (see also Secs. 30 and 37) can be successfully used to plot the approximate methods.

The integral momentum and energy relationships for a flat case take the form

$$\frac{d}{dx}\left(\rho_1 u_1^2 \delta^{**}\right) + \rho_1 u_1 \frac{du_1}{dx} \delta^* = \tau_w.$$

$$\frac{d}{dx}\left[g\rho_1 u_1 c_p (T_e - T_w) \delta_t^{**}\right] = q_w.$$

Here δ^{**} is the thickness of the loss in impulse), δ^* is the displacement thickness, δ_t^{**} is the thickness of the loss in energy, ρ_1 and μ_1 are the density and velocity on the boundary of the boundary layer, τ_w is the friction on the wall, and q_w is the heat flux density to the wall.

Thus, the two differential equations in the partial derivatives have been replaced by two ordinary differential equations. But these contain five unknowns: $\delta^{**}, \delta^*, \tau_w, \delta_t^{**}$ and q_w. Hence to solve them we have to derive another three relationships relating these values. These may be obtained by setting the

velocity and temperature profile in dimensionless coordinates, for example

i.e.,

$$\frac{u}{u_1} = f(\eta) \quad \text{и} \quad \frac{T_{(0)} - T_{\scriptscriptstyle w}}{(T_{(0)})_{\scriptscriptstyle \infty} - T_{\scriptscriptstyle w}} = f_1(\eta).$$

here

$$\tau_{\scriptscriptstyle w} = \frac{\mu u_1}{\xi_{\scriptscriptstyle \bullet \bullet}}\left(\frac{\partial f_1}{\partial \eta}\right)_{\scriptscriptstyle w}.$$

$$q_{\scriptscriptstyle w} = \frac{\lambda\left[(T_{01})_{\scriptscriptstyle \infty} - T_{\scriptscriptstyle w}\right]}{\xi_{\scriptscriptstyle \bullet \bullet}}\left(\frac{\partial f_1}{\partial \eta}\right)_{\scriptscriptstyle w}.$$

The ratio

$$H = \frac{\xi^{\scriptscriptstyle \bullet}}{\xi^{\scriptscriptstyle \bullet \bullet}} = \frac{\displaystyle\int_0^{\scriptscriptstyle \infty}\left(1 - \frac{\rho u}{\rho_1 u_1}\right)dy}{\displaystyle\int_0^{\scriptscriptstyle \infty}\frac{\rho u}{\rho_1 u_1}\left(1 - \frac{u}{u_1}\right)dy}$$

may also be expressed in terms of the function $\underline{f}$ and $\underline{f}_1$.

The result depends on the selection of the type of function $\underline{f}$ and $\underline{f}_1$. But, as shown by the calculations, the effect of the type of function on the solution is insignificant. Particularly good results are obtained by the use in the integral relationships of velocity and temperature distributions taken from calculations obtained for partial velocity distribution laws in the outside stream, when exact solutions can be obtained.

For the flow of a compressible liquid, exact solutions are possible if we use special transformations of the coordinates, worked out by Dorodnitsin /5/ and Stuartson /13/. For flow along a flat plate   an exact solution is obtained by taking into account the dependence μ, ρ and $c \hat{p}$ on temperature.

Calculations show that the dependence of $\propto$ on the Re and Pr numbers

remains the same in the case of a compressible gas as for an incompressible liquid.

For a flat plate

$$\frac{ax}{\lambda} = Nu = 0.332 \cdot Re^{1/2} Pr^{1/3} f\left(M, \frac{T_w}{T_e}\right). \tag{8.36}$$

The effect of compressibility shows up in the form of the multiplier $f(M, T_w, T_e)$.. The nature of the dependence of the Nu on the M number for a plate is shown in Fig. 121. When the M number increases, the heat-transfer coefficient, all other conditions being equal, (Re = const, x = const) is decrease . Fig. 122 shows the deformation of the velocity profile due to the compressibility of the gas: as the M number increases, the velocity distribution tends to be linear.

The temperature ratio T_w/T_e affects the heat transfer during the flow of air in such a way that the heat transfer increases when the wall cools.

For calculating the flow along a plate we can use the equation

$$q_w = a(T_e - T_w) = 0.332 \left(\frac{\mu_w \rho_w}{\mu_e \rho_e}\right)^{\frac{1}{15}\frac{T_w}{T_e}} \left(\frac{\mu^* \rho^*}{\mu_e \rho_e}\right)^{1/3} \sqrt{\frac{u_e}{\nu_e x}} \times$$
$$\times (T_e - T_w)\sqrt[3]{Pr.} \tag{8.37}$$

The values μ^* and ρ^* are taken at $T^* = T_{max}$ /Eq. (8.35)/ or, at $T^* = T_w$, if $T_x > T_e$, of at $T^* = T_w$.if $\frac{k-1}{2} M^2 < 1 - \frac{T_w}{T_e}$.

Exact values can be determined from the graphs in the publications described, which give the values of α, also making allowance for dissociation of

- 323 -

air molecules at high temperatures.

When there is supersonic flow around _an_ obtuse leading edge, a shock wave is created in front of the body and presonic ~~x~~ flow is created behind it.

The heat flux at the leading critical point can be calculated from the equations

$$q_\bullet = 0.763\,\lambda_w\,[(T_{0_j})_\infty - T_w]\,\sqrt{\frac{\beta}{\nu_w}}\cdot Pr^{0.4}\left(\frac{\mu_\infty \rho_\infty}{\mu_w \rho_x}\right)^{0.4} \qquad (8.38)$$

for an axial‑symmetric body and

$$q_\bullet = 0.57\,\lambda_w\,[(T_\omega)_\infty - T_w]\,\sqrt{\frac{\beta}{\nu_w}}\,Pr^{0.4}\left(\frac{\mu_\infty \rho_\infty}{\mu_w \rho_w}\right)^{0.44} \qquad (8.39)$$

for a flat body.

Here it is taken that $Pr \approx 0.7$; λ_w and ν_w are taken at wall temperature and pressure equal to the total adiabatic drag pressure beyond the direct discontinuity, and $\left(T_{0_j}\right)_\infty$ is the drag temperature in the outside stream.

$$\beta = (\partial u_\infty /\partial x)_{\ldots}$$

The value is determined from the experimental pressure distribution in the neighborhood of the critical point. For a rounded end, $\beta \approx 2a_\pi/b$, in which α_{cr} is the critical speed of sound, $b/2$ is half the thickness of the edge. If the end is spherically or cylindrically rounded, $b/2$ is the distance between the critical point and the point $\varphi \approx 45°$ (Fig. 123).

The heat exchange on the lateral surface of a cone around which there is supersonic flow can be calculated with the same equations as for the plate. But here the heat flux has to be multiplied by $\sqrt{3}$, and u_∞ and T_e have to be

- 324 -
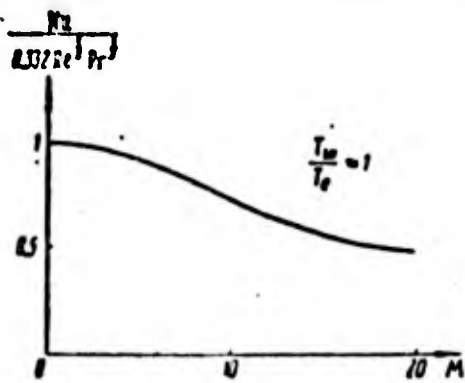
Fig. 121. Heat transfer coefficient as function of M number during laminar flow along a flat plate
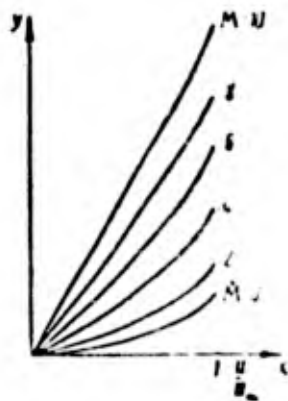
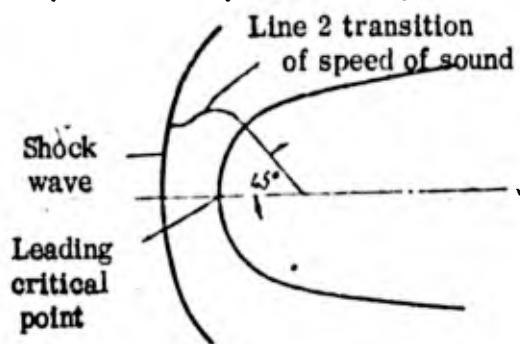Fig. 122. Deformation of velocity profiles at large M numbers and laminar flow

Fig. 123. Flow in neighborhood of leading critical point

determined for flow beyond the boundary layer on the surface of the cone.

Sec. 32.   Heat exchange in Turbulent Flow in Boundary Layer

So far we have considered laminar flow in the boundary layer, in which

the transfer of momentum, heat and matter is due to the molecular processes of

friction, conduction and diffusion. Here the stresses due to friction, the heat

and diffusion fluxes were known functions of the distribution of velocity,

temperature and concentration.

In laminar flow we can write down boundary layer equations and their

solution as determined to a larges extent by mathematical techniques. The

calculations required experimental improvement on account of the inevitably

sketchy nature of the phenomena, although the corrections introduced are small.

The role of the laminar layer theory becomes particularly important at the present

time in view of the development of flying craft⌉ designed to fly at very great heights at

low Re numbers, in which the laminar flow is retained.

Main features of turbulent flow

At high Re numbers the orderliness of the flow is disturbed, and there

is general interm mixing of the liquid to a great extent. If one of the streams

of liquid is colored in laminar flow, we see that it diffuses only to a slight

extent. During turbulent flow, the entire liquid in the tube becomes colored within

- 326 -

a small distance. Transverse motion which becomes interwoven with the principal

motion and there arises an "interwoven turbulent motion". Here the resistance

of the tube is increased, which is due to the intensified exchange of momentum

between individual streams. This exchange leads to equilization of the velocity
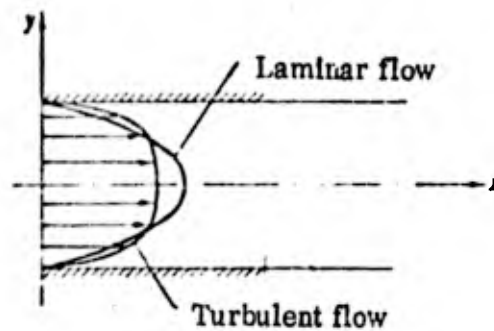
profile in the tube cross-section (Fig. 124).

Fig. 124. Velocity profiles in channel or pipe

The velocity gradient at the wall $(\partial u/\partial y)_w$ increases accordingly

compared with laminar flow, and therefore the friction is increased.

Conditions of transitions from laminar to turbulent flow.

The first systematic investigation was carried out by Reynolds, who

found the law of similarity, according to which the transition from laminar to

turbulent flow occurs approximately at the same Reynolds $Re = u_m d/\nu$, in which u_m

is the mean flow velocity.

It was established that at Re $<$ 2000, the flow is always laminar.

The exact value of the critical Re number, at which the transition occurs, depends

on the conditions of inlet to the tube, the degree of roughness, and so on, and

can vary between 2000 and 10,000.

Flow in the boundary layer when the body is immersed may also be

laminar or turbulent. The transition occurs when the Re number reaches $Re = Ux/\nu$

equal to Re_{cr}, which for a plate is $3 \cdot 10^5 < Re_{sp} < 5 \cdot 10^5$. These values correspond roughly to

$$(Re_\delta)_{sp} = (u_\infty \delta/\nu)_{sp} \approx (2700 - 3000).$$

At the transition from a laminar to a turbulent boundary layer, the

thickness of the latter is increased, the velocity profile becomes fuller, the

friction is increased, and so are the heat-transfer and mass-transfer coefficient.

A diagram of the experimental pattern of transition from a laminar to a turbulent

boundary layer is shown in Fig. 125.

Laminar flow   Turbulent flow
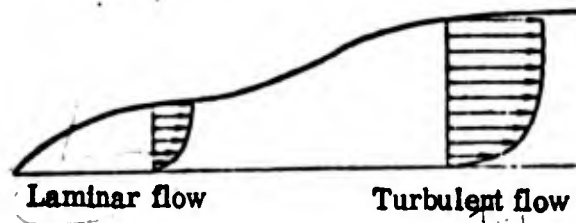
Fig. 125. Flow in boundary layer of plate

Averaged motion and pulsating motion

The study of turbulent flow shows that the velocity and pressure at a given point are not constant in time, but vary frequently and non-uniformly (Fig. 126). These variations which are known as pulsations are the most characteristic property of turbulent flow. During turbulent motion along and across a stream
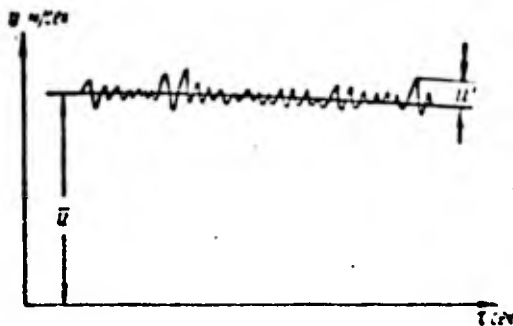
Fig. 126. Pulsation and averaged velocities

Here is pulsation conglomerations

of complete (of fluid, or moles; As a rule the pulsations only comprise

several percent of the mean velocity, but they exert a very great influence on the development of the flow.

In order to make a mathematical analysis, the flow is divided into the mean and pulsating flow. Let us designate the time-averaged velocity $\overline{u}'$ and the pulsations velocity u', the pressure $\overline{p}$ and p' and so on.

The velocity can then be determined in the following way

- 329 -

The average velocity is equal to

$$u = \bar{u} + u'.$$

$$\bar{u} = \frac{1}{\Delta t} \int_{t_0}^{t_0 + \Delta t} u \, dt.$$

(8.40)

To average the values we have to take a fairly large interval of time Δt so that the average value is not a function of time.

The velocity pulsates in all directions. The mean pulsation components are equal to zero

$$\bar{u}' = 0, \quad \bar{v}' = 0, \quad \bar{w}' = 0, \quad \bar{p}' = 0.$$

Averaging the products of the values with respect to time, we get

$$\overline{\bar{u}u'} = 0, \quad \overline{\bar{u}u} \neq 0.$$

The mean products of the pulsation components in the general case may also differ from zero $\overline{u'v'} \neq 0$.

Pulsation motion at velocities $\underline{u}'$, $\underline{v}'$ and $\underline{w}'$ affects the average motion $\overline{\underline{u}}$, $\overline{\underline{v}}$ and $\overline{\underline{w}}$ in such a way that the resistance to friction increases in the average motion and an additional, apparent viscosity is created.

Let us draw the line $x\text{-}x$ parallel to the wall in the boundary layer (Fig. 127). In view of the flow of liquid through the area there is a flow of momentum $J = \rho u v$. If there are pulsations $J = \rho (\bar{u} + u')(v + v') = \rho u v + \rho u' v + \rho v' u + \rho v' u'$.

- 330 -

The mean momentum flow is equal to

$$J = \rho \bar{u} \bar{v} + \rho \overline{v' u'}.$$

As we see, the presence of pulsations changes the momentum flow by $\rho \overline{v' u'}$.

But the flow of momentum through the area is equivalent to an oppositely directed

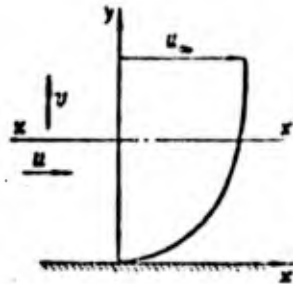force with which the surrounding medium acts on the area. Hence, if there are

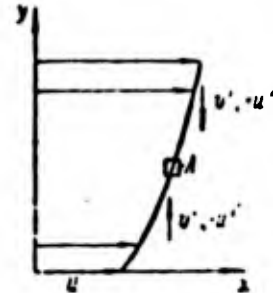Fig. 127. Determining values
of apparent friction

Fig. 128. Correlation between
pulsation velocity

pulsations, there is an additional force exerted by the top of the flow on the

bottom, producing the friction

$$\tau = -\rho \overline{v' u'}. \tag{8.41}$$

This friction differs from zero and is directed in a positive direction

of the x-axis, which is clear from the following arguments. Let us consider which

sign the products u'v' possess at any point A on the boundary layer Fig. 128).

- 331 -

Particles of fluid reach this point from the top and from the bottom on account of pulsations. The particles coming from the bottom have a pulsation component directed upwards, i.e., positively. Having reached point A, these particles have a velocity less than the mean velocity at this point, i.e., they create a negative pulsation $(-u')$.

By exactly the same argument we can prove that in the case of particles coming from the top, the product $\overline{v'u'}<0$. Hence

$$\tau = -\rho\overline{v'u'} > 0,$$

and the friction acting from the top on the bottom is directed, when the velocity distribution corresponds to the drawing, in the positive direction of the x-axis, i.e., the top accelerates the bottom, while the bottom resists the top.

Theory of the mixing length

In accordance with this friction

$$\tau = -\rho\overline{u'v'} = \rho\varepsilon\frac{\partial\bar{u}}{\partial y}.$$

Here we introduce the quantity ε - the conditional turbulent viscosity coefficient. On an analogy with molecular friction, ε corresponds to μ/ρ. To calculate ε, Prandtl has put forward a simplified flow system.

Let us consider two layers of liquid at a distance Δy from each other (Fig. 129). The velocities in these layers are different, and on account

of pulsation there is an exchange of momentum between individual streams. Prandtl

has assumed that the *conglomeration,* (of liquid shifting on account of pulsation from one

layer to another retains the momentum component in the direction of the x-axis

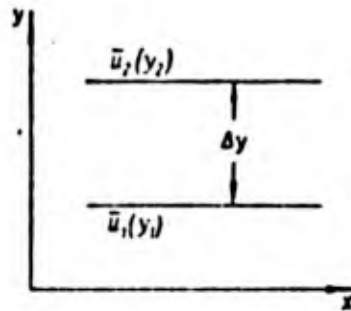over a certain distance. The distance over which the particles retain the

Fig. 129. Determining mixing length

properties which they possessed in the first layer has been called the . *mixing*

length . Let us designate this value as $\underline{l}$. If the distance between the

layers in Fig. 129 are selected in such a way that $\Delta \underline{y} = \underline{l}$, then the particles

traveling from ———— the bottom layer to the top one retain their horizontal

velocity components which is $\overline{\underline{u}}_1$.

The difference between the mean flow velocity at the points $\underline{y}_2$ and the

velocity of the particles reaching this point from the bottom layer gives us the

pulsation in the velocity at this point

$$u' = \Delta u_1 = \overline{u}_2(y_2) - \overline{u}_1(y_1).$$

But if $\underline{l}$ is small, then $\wedge$ $\Delta u_1 = \widehat{l(\partial \overline{u}/\partial y)}$. Thus, the pulsation is $u' = l\frac{\partial \overline{u}}{\partial y}$.

- 333 -

The pulsation of the velocity in a transverse direction $\overset{\prime}{v} \sim \overset{\prime}{u}$. Thus, the friction is

$$\tau = \mu l^2 \left(\frac{\partial \bar{u}}{\partial y}\right)^2 \text{and} \quad \epsilon = l^2 \left(\frac{\partial \bar{u}}{\partial y}\right). \tag{8.42}$$

In the formula derived, l remains undetermined. But in a number of cases by using experimental data we can find the connection between the mixing length l and the linear dimensions of the flow.

Turbulent flow nucleus and laminar sublayer

During turbulent flow the total friction in the boundary layer is made up of friction through molecular viscosity and turbulent viscosity

$$\tau = (\mu + \rho l^2)\, \frac{\partial u}{\partial y}.$$

Over a wide distance from the wall the turbulent viscosity greatly exceeds the molecular viscosity. The part of the boundary layer in which we can disregard molecular viscosity is called the turbulent nucleus (Fig. 130).
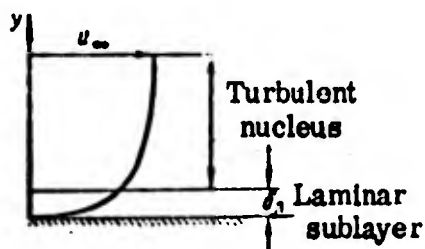
Fig. 130. Turbulent flow nucleus and laminar sublayer

Near the wall the turbulent pulsations are damped and the molecular

viscosity plays the major role. This section of the boundary layer is termed the

laminar sublayer. On the boundary between the turbulent nucleus and the laminar

sublayer there is a transient region in which the molecular and turbulent

viscosities are of the same order. When calculating the turbulent boundary layer

we must consider each region separately and introduce further assumptions with

regard to the conditions at the point where the region is joined.

Universal laws of velocity distribution

The experimental study of turbulent flow in pipes and boundary layers

has shown that velocity profiles can be represented as $u/u_\infty = (y/\delta)^{\frac{1}{n}}$. The value $\underline{n}$ ranges

from 7 to 9 when the Reynolds number $Re = u_\infty x/v$ ranges from 10^5 to 10^8. The

representation of the velocity profile by means of power laws has become common

and is convenient for supersonic flow as well.

A second expression for the velocity distribution can be derived by using

the hypothesis of the turbulent friction $\tau = \rho l^2 (\partial u/\partial y)^2$. It is roughly assumed that

across the boundary layer τ = const = τ_ω.

The mixing length $\underline{l}$ - the scale of turbulence by the wall - must be equal

to zero and can be taken as a first approximation as proportional to the distance

from the wall $\underline{l} = \underline{ky}$ at which $\underline{k}$ is the proportionality factor.

- 335 -

After substitution we get

$$\tau_{\omega} = \rho k^2 y^2 \left(\frac{\partial u}{\partial y}\right)^2$$

and

$$\frac{\partial u}{\partial y} = \sqrt{\frac{\tau_{\omega}}{\rho}} \, \frac{1}{ky}.$$

Integrating, we get

$$u = \frac{1}{k} \sqrt{\frac{\tau_{\omega}}{\rho}} \ln y + \text{const.}$$

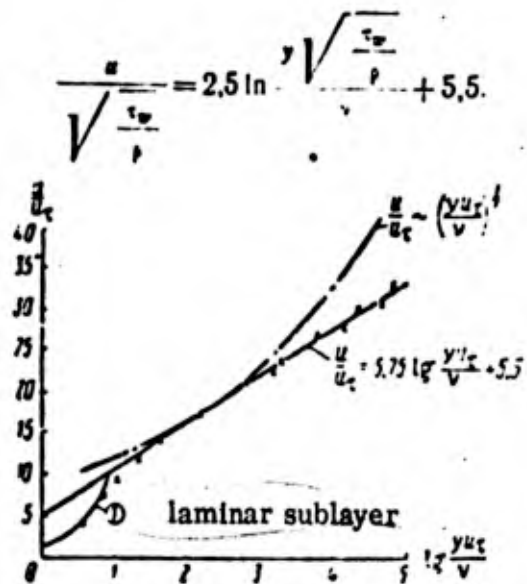k and the integration constant are determined experimentally

$$\frac{u}{\sqrt{\frac{\tau_{\omega}}{\rho}}} = 2.5 \ln \frac{y \sqrt{\frac{\tau_{\omega}}{\rho}}}{\nu} + 5.5.$$

Fig. 131. Velocity distirbution in dimensionless coordinates

The value $\sqrt{\dfrac{\tau_w}{\rho}}$ has the dimensionality of velocity and is designated

$$u_\tau = \sqrt{\frac{\tau_w}{\rho}}. \tag{8.43}$$

The logarithmic law of velocity distribution can be written in the form

$$\frac{u}{u_\tau} = 2{,}5 \ln \frac{yu_\tau}{\nu} + 5{,}5 \quad \text{or} \quad \frac{u}{u_\tau} = 5{,}75 \lg \frac{yu_\tau}{\nu} + 5{,}5. \tag{8.44}$$

Fig. 131 ~~compares~~ experimental data for the velocity distribution with the ~~suggested~~ laws.

As can be seen, the logarithmic law accords satisfactorily with experimental data at $\log (yu_\tau/\nu) > 1{.}5$. Below this point near the wall there is a laminar sublayer with a linear distribution of velocity (curve 1 in the logarithmic scale).

Sec. 33. Turbulent Heat Exchange

In turbulent flow, the pulsations produce further friction stresses and an additional transfer of heat. The mechanism of transfer in both cases is the same and the analogy between friction and heat transfer in turbulent flow is closer than in laminar flow.

Without repeating the arguments which we put forward in the preceding sections, let us write down the expression for the heat flux density in the form

$$q = g \rho c_p (\overline{v'T'}). \tag{8.45}$$

Here v' is the vertical pulsation of velocity and $\dfrac{T'}{t_b}$ is the temperature pulsation $\odot$

On the basis of the motion of the mixing length, we get

$$v' \sim l\left(\frac{\partial \bar{u}}{\partial y}\right), \quad T' \sim l_1\left(\frac{\partial \bar{T}}{\partial y}\right), \quad l \sim l_1.$$

Here $\bar{T}$ is the mean temperature, $\quad T = \bar{T} + T'.$

Hence

$$q = -g \kappa c_p l^2\left(\frac{\partial \bar{u}}{\partial y}\right)\left(\frac{\partial \bar{T}}{\partial y}\right); \quad q = -g \kappa c_p \varepsilon_1\left(\frac{\partial \bar{T}}{\partial y}\right).$$

$$\varepsilon_1 = l^2 (\partial \bar{u}/\partial y)$$

The value $\wedge$ is the analogue of the molecular thermal

diffusivity $\lambda/g \rho \leq \hat{k}$ $\odot$

Assuming that the

mixing paths $\ell_T \approx \ell$, we took it that $\varepsilon_1 \approx \varepsilon$.

By analogy with molecular weight $Pr = \mu c_p / \lambda$, let us introduce the

turbulent number $Pr_T = \varepsilon / \xi_1$, which represents the ratio between the turbulent

viscosity and the thermal conductivity. The molecular number P_T for air

is

is approximately equal to 0.71, and the turbulent number $Pr_T \approx 0.86$. Thus,

in the case of turbulent flow we can take it roughly that $Pr_T \approx 1$.

The temperature distribution across the boundary layer can be represented

by the same laws as the velocity distribution.

The power law

$$\frac{T - T_w}{T_\infty - T_w} = \left(\frac{y}{\delta_1}\right)^{\frac{1}{n}}.$$ (8.46)

in which $\underline{n} = 7$ to 9 and δ_T is the thickness of the thermal boundary layer.

The velocity and temperature profiles are similar to each other.

$$\frac{T - T_w}{T_\infty - T_w} = \frac{u}{u_\infty}.$$

<u>Link between friction and heat transfer.</u> The similarity between the

process of transfer of momentum and heat leads, as in the case of laminar flow,

to a link between friction and heat exchange.

Assuming the velocity and temperature profiles to be similar

$$\frac{u}{u_\infty} = \frac{T - T_w}{T_\infty - T_w}.$$

we get $\qquad q_w = \tau_w \frac{c_p (T_\infty - T_w)}{u_\infty}, \quad a = \frac{\tau_w}{u_\infty} c_p.$

Near the wall there is a laminar sublayer in which we have to take the difference between Pr and unity, and moreover, in the turbulent nucleus $Pr_t \approx 0.85$. Hence between the friction and heat transfer the following relationships have been experimentally established

$$c_H = \frac{1}{2} c_f f(Pr).\tag{8.47}$$

This condition is only valid when the thermal and dynamic layers begin at the same point and when the longitudinal pressure gradient is slight.

Approximately $f(Pr) \approx Pr^{0.4}$.

Sec. 34. Semi-empirical Methods of Calculating Turbulent

Boundary Layer

At the present time it is not possible to write down any exact differential equations for momentum and energy in turbulent flow in the boundary layer, since there are no reliable expressions for determining the friction.

Hence the calculation of the turbulent layer is chiefly based on experimental data. The commonest methods are those in which we use the equations in their integral form. But the direct use of the integral method, similar to Polhausen's method for laminar flow, in which the velocity profile is replaced by a polynomial or some other function, satisfying the boundary conditions, is

- 340 -

unsuitable for a case of turbulent boundary layer.

This is due to the fact that the above-mentioned power and logarithmic
laws of velocity distribution in the turbulent boundary layer are only true *for the*
turbulent nucleus of the layer and are inapplicable to the laminar sublayer.

Let us consider the integral relationship for momentum in the case of
a flat plate

$$\frac{\tau_w}{\rho u_\infty^2} = \frac{d\delta^{**}}{dx}.$$

This formula contains two unknowns τ_w and δ^{**}. In a laminar boundary
layer we introduce a further assumption regarding the velocity profile

$$\frac{u}{u_\infty} = f\left(\frac{y}{\delta}\right).$$

This condition can express the friction τ_w and the thickness of the
energy loss in terms $\left(\text{of } \delta \quad \delta^{**}\right)$, and give us an equation with one unknown function

$$\tau_w = \mu \left(\frac{\partial u}{\partial y}\right)_w = \mu \frac{u_\infty}{\delta} f'\left(\frac{y}{\delta}\right).$$

$$\delta^{**} = \delta \int_0^1 f(1-f)\, d\left(\frac{y}{\delta}\right).$$

In the case of *a* turbulent layer, this approach is impossible. Having
set the velocity profile $u/u_\infty = f(y/\delta)$ η , we can express δ^{**} in terms of δ fairly accurately.

But we cannot express the friction on the wall with this profile since the velocity
profile in *the* turbulent nucleus is inapplicable directly at the wall in the laminar

- 341 -

sublayer.

Thus, we must derive an additional equation linking the thickness of the boundary layer δ or δ^{**} with the friction on the wall. This equation is termed the resistance law. It can be obtained from a semi-empirical logarithmic velocity distribution, or else experimentally.

The most complete experimental data at the present time describe flow through a tube at presonic velocities and flow along a flat plate at high supersonic velocities.

Example of calculation of boundary layer on flat plate on

basis of experimental law of resistance for flow through pipe

During flow through a cylindrical pipe (Fig. 132), the friction can be determined by measuring the pressure distribution along the wall. The condition
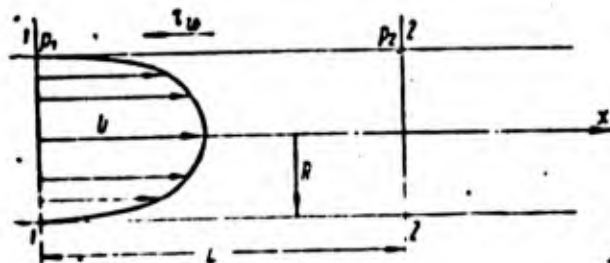
Fig. 132. Momentum equation for fluid flow in pipe or channel

of balance of the liquid column contained between sections 1 and 2 gives us

$$\tau_w 2\pi R L = (p_1 - p_2)\pi R^2.$$

$$\tau_w = \frac{p_1 - p_2}{L}\frac{R}{2}.$$

The friction when determined experimentally for $R = \dfrac{U\rho R}{\mu} < 100,000$ is

equal to

$$\frac{\tau_w}{\rho U^2} = 0.0225 \frac{1}{\left(\dfrac{U\rho R}{\mu}\right)^{0.25}}.$$

During flow through the pipe the boundary layer fills the entire section and

the radius of the pipe is the thickness of the layer. The velocity at the axis

of the pipe $\underline{U}$ corresponds in the case of the boundary layer to the velocity

beyond this layer.

Thus, we have an unknown resistance law in the form

$$\frac{\tau_w}{\rho u_\infty^2} = \frac{0.0225}{\left(\dfrac{u_\infty \rho \delta}{\mu}\right)^{0.25}}.$$

Using the power law of velocity distribution with the exponent $1/7$

we get the connection between δ^{**} and δ.

$$\frac{u}{u_\infty} = \left(\frac{y}{\delta}\right)^{\frac{1}{7}}, \quad \delta^{**} = \delta\int_0^1 \left(\frac{y}{\delta}\right)^{\frac{1}{7}}\left[1 - \left(\frac{y}{\delta}\right)^{\frac{1}{7}}\right]d\left(\frac{y}{\delta}\right) = \frac{7}{72}\delta.$$

Thus, substituting this result into the momentum equation, we get

$$0.0225\left(\frac{\nu}{u_\infty \delta}\right)^{\frac{1}{4}} = \frac{7}{72}\frac{d\delta}{dx}.$$

Solving this equation, we get

- 343 -

$$\frac{\delta}{x} = \frac{0.37}{\left(\frac{u_\infty x}{\nu}\right)^{0.2}}$$

and then
$$c_f = \frac{\tau_w}{\frac{1}{2}\rho u_\infty^2} = 0.057\,\mathrm{Re}_x^{-0.2}\left(\mathrm{Re}_x = \frac{u_\infty x}{\nu}\right).$$

The mean friction stress
$$c_{f_{cp}} = \frac{R}{\frac{\rho u_\infty^2}{2}\,lx}.$$

in which R is the total resistance of the plate with width 1 over the length, and

x is equal to
$$c_{f_{cp}} = \frac{l\int_0^x \tau_w\,dx}{\frac{\rho u_\infty^2}{2}\,lx} = \frac{1}{x}\int_0^x c_f\,dx = \frac{c_f}{0.8} = 0.072\,\mathrm{Re}_x^{-0.2}.$$

These equations hold throughout the range of Reynolds numbers from $5\cdot10^5$ to 10^7.

Using the condition of hydrodynamic analogy between friction and heat exchange, we can easily find the corresponding expression for the thermal fluxes.

Taking $c_H = \frac{1}{2}c_f\,\mathrm{Pr}^{-0.6}$, we obtain
$$c_H = \frac{\alpha}{g\rho u_\infty c_p} = 0.029\,\mathrm{Re}_x^{-0.2}\,\mathrm{Pr}^{-0.6}$$

or
$$q = \alpha(T_\infty - T_w) = 0.029\cdot3600 g\rho u_\infty c_p(T_\infty - T_w)\,\mathrm{Re}_x^{-0.2}\,\mathrm{Pr}^{-0.6}.$$

. The mean heat flux per unit length in kcal/m^2. hour for the case

$$5\cdot10^5 < \mathrm{Re}_x < 10^7 \qquad \text{is equal to}$$
$$q_{cp} = \frac{q}{0.8} = 0.037\cdot3600 g\rho u_\infty c_p(T_\infty - T_w)\,\mathrm{Re}_x^{-0.2}\,\mathrm{Pr}^{-0.6}.$$

In the dimensionless form

$$\mathrm{Nu} = \frac{\alpha x}{\lambda} = 0.029\,\mathrm{Re}_x^{0.8}\,\mathrm{Pr}^{-0.6}. \tag{8.48}$$

As we can see, the variation in the thickness of the boundary layer δ, resistance to friction and heat flux density as a function of the Reynolds number in the turbulent flow differ from the corresponding laws for laminar flow.

Flat plate

Laminar flow	Turbulent flow

$$\frac{\delta}{x} \sim \frac{1}{\sqrt{Re}}\,; \quad \delta \sim x^{0,5} \qquad\qquad \frac{\delta}{x} \sim \frac{1}{Re^{0,2}}\,, \quad \delta \sim x^{0,8}$$

$$\frac{\tau_w}{\rho u_\infty^2} \sim \frac{1}{\sqrt{Re}}\,; \quad \tau_{\tau_{cp}} = 2\tau_w \qquad \frac{\tau_w}{\rho u_\infty^2} \sim \frac{1}{Re^{0,2}}\,; \quad \tau_{\tau_{cp}} = \frac{\tau_w}{0,8}$$

$$\frac{q_w}{\rho u_\infty c_\rho (T_\infty - T_w)} \sim \frac{1}{\sqrt{Re}}\,, \quad Nu \sim Re_x^{0,5} \bigg| \frac{q_w}{\rho u_\infty c_\rho (T_\infty - T_w)} \sim \frac{1}{Re^{0,2}}\,,$$

$$Nu \sim Re_x^{0,8}\,.$$

Thus, during turbulent flow the basic characteristics of the boundary layer are a function of the Reynolds number to a lesser extent than during laminar flow. The effect of the Reynolds number is due to the action of the molecular viscosity. When the Reynolds number is increased, the effect of it is still weaker. This is because the thickness of the laminar sublayer in which the molecular forces play the main part, is reduced as the Reynolds number is increased.

Example of use of semi-empirical logarithmic law of velocity

distribution to calculate boundary layer on the flat plate

In the equation for the velocity distribution

$$\frac{u}{\sqrt{\frac{\tau_w}{\rho}}} = 2,5 \ln \frac{\sqrt{\frac{\tau_w}{\rho}}\, y}{\nu} + 5,5$$

the constants are determined experimentally on the basis of measurement of the velocity distribution and friction on the wall of the pipe (see Fig. 131.)

This equation interlinks the velocity in the boundary layer and the friction on the wall. By using the integral relationship for momentum we can obtain expressions for the friction. Leaving out the cumbersome operations /10, 14/, we arrive at the final forms

$$c_{f_{cp}} = \frac{0.455}{(\lg Re)^{2.58}}, \quad Nu_{cp} = \frac{a_{cp}x}{\lambda} = \frac{0.237 Re}{(\lg Re)^{2.58}}.$$

These equations are rather superior to those derived on the basis of the power law for the velocity profile with the exponent $1/7$ since they are applicable up to $Re \approx 10^9$.

Sec. 35. Turbulent boundary layer on flat plate in compressible gas

At high flight velocities, the kinetic energy of the outside stream is transformed into the heat content by the wall on account of friction. The heat flux at high flight velocities is determined by the difference between the drag temperature of the stream and the temperature of the wall, rather than by the temperature drop.

Temperature of thermally insulated wall

The degree of transformation of kinetic energy into heat is described by the coefficient temperature recovery

$$r_1 = \frac{T_s - T_\infty}{(T_\infty)_s - T_\infty} = \frac{T_s - T_\infty}{\frac{k-1}{2} M_\infty^2 T_\infty}, \quad T_s = T_\infty \left(1 + r \frac{k-1}{2} M^2 \right).$$

Here T_A is the temperature of the heat-insulated wall. Experimentally the value has been determined as $r \approx 0.89$.

Thus, in turbulent flow the temperature recovery coefficient is greater than in laminar flow. This is because the Prandtl number for the principal turbulent area of the boundary layer is closer to unity ($Pr_\tau \approx 0.86$ for air, and $Pr = \mu c_p/\lambda = 0.71$).

Determining heat exchange coefficient

In order to take the energy dissipation $\widehat{f}$ through friction into account, the heat exchange coefficient is determined by the equation $q_w = a(T_c - T_w)$.

When determining in this way, it might be thought that the effect of the compressibility would show up in α solely through variation in the physical properties of the medium.

Distribution of velocity, temperature and drag temperature

When there is flow along a flat plate at high velocities of the outside stream, there is approximate similarity between the velocity and drag temperature profiles

$$\frac{T_{00} - T_w}{(T_{00})_e - T_w} = \frac{u}{U_e} .$$

The distribution of the drag temperature and velocity across the boundary layer can be described fairly well by either a power or a logarithmic law, given

earlier for the case of an incompressible gas. The distribution of temperature across the boundary layer coincides qualitatively with the temperature distribution in the laminar boundary layer at high flight velocities.

Sec. 36. Experimental Graphs and Theoretical Formulae

At the present time there are reliable experimental data for the variation in the friction coefficient as a function of the M number.

Fig. 133 shows a composite graph for the experimental ratios of the friction coefficient c_f and the corresponding value of it for an incompressible liquid c_{f_H}. The friction values were determined by direct measurement. The following extrapolating curve is also plotted on this graph

$$\frac{c_f}{c_{f_H}} = \left(1 + \frac{k-1}{2} r M^2\right)^{-0.55}.$$

These points were obtained basically for the case of a thermally-insulated wall or at the ratio T_w / T_e, hardly differing from unity. Taking the effect of the temperature ratio into account, we can recommend the following formula for the local friction coefficient

$$c_f = 0.058 \mathrm{Re}_x^{-0.2} \left(\frac{T_w}{T_e}\right)^{-0.27} \left(1 + \frac{k-1}{2} r M^2\right)^{-0.55}. \tag{8.49}$$

and
$$r \approx 0.89, \quad c_f = \frac{\tau_w}{\frac{\rho_e u_e^2}{2}}.$$

- 348 -
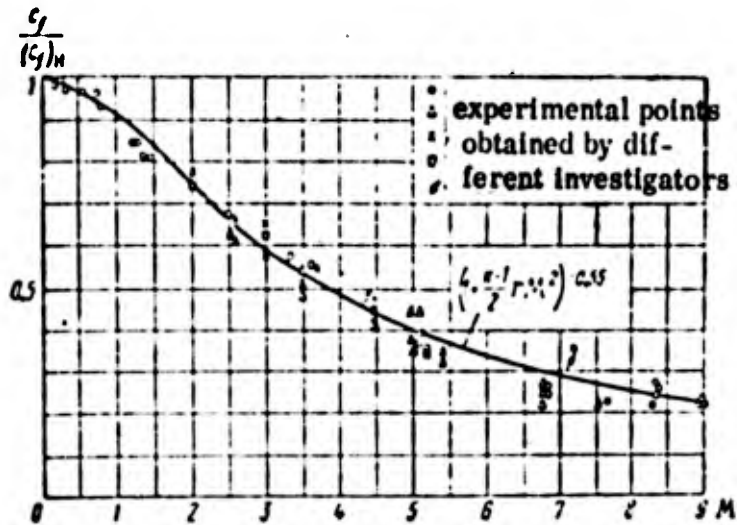
Fig. 133. Experimental data on friction coefficient as function
of M number in turbulent flow in boundary layer of plane plate

The heat-exchange coefficient can be determined from the equation

$$Nu = \frac{ax}{\lambda_{\bullet}} = 0.029 Re_{x}^{0.9} Pr^{0.4} \left(\frac{T_{c}}{T_{\ell}}\right)^{+0.39} \left(1 + \frac{k-1}{2} r M^2\right)^{0.1:}. \qquad (8.50)$$

$$\rho_{\bullet}/\mu = (T_{\bullet}/T)^{2.7}, \quad \lambda_{\bullet}/\lambda = (T_{\bullet}/T)^{0.85}$$

Here, if we take the relationship λ , the following relationship

exists between friction and heat transfer

$$Nu_{\bullet} = \frac{1}{2} c_{f_{\flat}} Re_{x} Pr^{0.4}.$$

The thermal flux on the cone at the same value $Re_{x\bullet}$ is approximately

1.17 times greater than on a plate.

Here

$$Nu_{\bullet} = \frac{ax}{\lambda_{\bullet}}, \quad c_{f_{\bullet}} = \frac{\tau_{\bullet}}{\frac{\rho_{\bullet} u_{\infty}^2}{2}}, \quad Re_{\bullet} = \frac{u_{\infty}\rho_{\bullet} x}{\mu_{\bullet}}.$$

The equation for the heat flux can be checked by direct experiment over

- 349 -

the range of M numbers from 2 to 4 and $\frac{T_o}{T_e}$, from 0.4 to 1.2, and coincides with

existing data for heat exchange in an incompressible fluid (see Figs. 134 and 135).
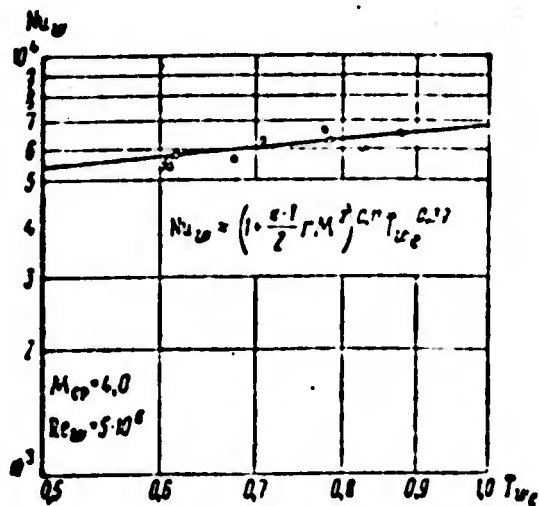
Fig. 134. Effect of temperature factor $\bar{T}_{w_e} = T_w/T_e$
on heat exchange
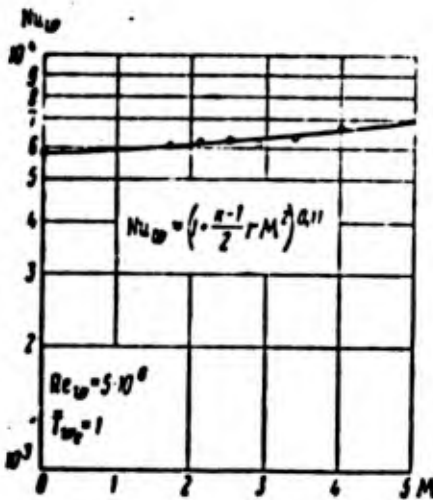
Fig. 135. Effect of M number on heat exchange

Taking it into consideration that when using the hydrodynamic analogy

the transformed equation accords satisfactorily with experimental friction

coefficients up to $M \approx 9$, the heat exchange equation can be recommended for use

as well at $M > 4$ and $\frac{T_w}{T_e} \geqslant 0,1$.

In order to apply the theoretical methods of the boundary layer in the

case $u_\infty \neq$ const, we must know the relationship between the heat flux and the local

characteristics of the local boundary layer.

The energy equation for the flat plate takes the form

$$Q_w = g \rho_\infty u_\infty c_p (T_e - T_w) \vartheta; \quad \vartheta = \int \frac{\rho u}{\rho_\infty u_\infty} \left[\frac{(T_w)_\infty - T_\omega}{T_e - T_w} \right] dy,$$

$$Q_w = \frac{1}{x} \int_0^x q_w \, dx.$$

Utilizing experimental data, we get

$$\frac{q_w}{g \rho_\infty c_p (T_e - T_w) u_\infty} = 0,013 \, Re_\theta^{-\frac{1}{4}} Pr^{-0.75} T_e^{-0.2} \left(1 + \frac{k-1}{2} r M^2 \right)^{-0.55} \quad (8.51)$$

Here $Re_\theta = \frac{u_\infty \theta}{\nu_\infty}$.

Sec. 37. Calculation of Heat Exchange in Neighborhood of

Critical Point of Plane and Axial Symmetric Body

During turbulent flow in the neighborhood of the critical point, the

boundary layer may be calculated by using the integral energy relationship and the

connection between heat flux and the local characteristics of the boundary layer,

derived for a case of the power velocity distribution law.

Let us consider the axial-symmetric case. Let us single out the contour abcd, in which the line bc coincides with the line of the current, and let us take it that a flow with parameters u_∞, $(T_0)_\infty$, ρ_∞ (Fig. 136) strikes the contour. In the section cd the flow parameters beyond the boundary layer are

$$\rho_1,\ u_1,\ (T_0)_1.$$

The energy balance condition gives us a heat flux receeding towards
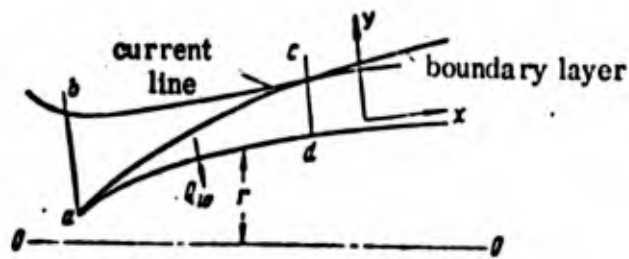
Fig. 136. Derivation of integral relationship for energy
for axially-symmetric flow

the wall is

$$Q_\bullet = m_{ab} c_p\,(T_0)_\infty - 2\pi c_p \int_0^\delta \rho u T_{00}\,(r+y)\,dy;$$

Here m_{ab} is the mass of gas flowing into the section ab $m_{ab} = m_{dc}$, since bc is the streamline

$$m_{ab} = 2\pi \int_0^\delta \rho u\,(r+y)\,dy.$$

Taking it that $r + y \approx r$, we get

$$Q_{\varpi} = 2\pi r c_{p} \rho_1 u_1 (T_e - T_{\varpi}) \int_0^\infty \frac{\rho u}{\rho_1 u_1} \left[\frac{(T_0)_\infty - T_{(0)}}{T_e - T_{\varpi}} \right] dy.$$

Let us designate

$$\theta = \int \frac{\rho u}{\rho_1 u_1} \left[\frac{(T_0)_\infty - T_{(0)}}{T_e - T_{\varpi}} \right] dy;$$

then

$$Q_{\varpi} = 2\pi r c_{p} \rho_1 u_1 (T_e - T_{\varpi}) \theta.$$

The heat flux density is related to the total flux by the condition

$$Q_{\varpi} = \int_0^x 2\pi r q_{\varpi} \, dx,$$

$$q_{\varpi} = 2\pi r \frac{dQ_{\varpi}}{dx}.$$

Finally we get

$$q_{\varpi} = \frac{1}{r} \frac{d}{dx} [r c_{p} \rho_1 u_1 (T_e - T_{\varpi}) \theta]. \qquad (8.52)$$

When there is flow round the leading, rounded section of an axially-symmetric body, $r \approx x$ in the neighborhood of the critical point. Furthermore, at small distances from the critical point, at which the flow velocity is small (up to $\lambda = u / a_{cr} \, (< 0.4)$), we can disregard the dependence of ρ_1 on x.

Then, at $T_{\text{w}} = $ const the energy equation, when it is taken into account that $u_1 = \beta x$, takes the form

$$\frac{q_{\varpi}}{c_{p} \rho_1 u_1 (T_e - T_{\varpi})} = \frac{d\theta}{dx} + 2 \frac{\theta}{x}. \qquad (8.53)$$

In order to establish the connection between the heat flux and the local characteristics of the boundary layer, let us apply the experimental data

- 353 -

for a flat plate

$$\frac{q_w}{g c_p \rho_1 u_1 (T_e - T_w)} = 0.013 \left(\frac{T_w}{T_e}\right)^{-0.3} \Pr^{-0.75} (1 + 0.2 r M_1^2)^{-0.55} \left(\frac{u_1 \theta}{v_1}\right)^{-\frac{1}{4}}.$$

Taking it into consideration that in the region under consideration

$M^2 \ll 1$, after substitution and integration, we get an equation for the heat flux

$$q_w = 3600 g c_p \rho_1^{1.3} x (T_e - T_w) \cdot 0.040 \left(\frac{\beta x^2}{v_1}\right)^{-\frac{1}{5}} \left(\frac{T_w}{T_e}\right)^{-0.16} \Pr^{-0.4} \quad \text{kcal/m}^2 \cdot \text{hr} \qquad (8.54)$$

It follows from this that at the most critical point at $\underline{x = 0}$, $\underline{q_{wr} = 0}$. But here there is still laminar heat exchange. The value $(q_w)_{lam} \neq 0$ at the critical point

/see (8.38) and (8.39)/
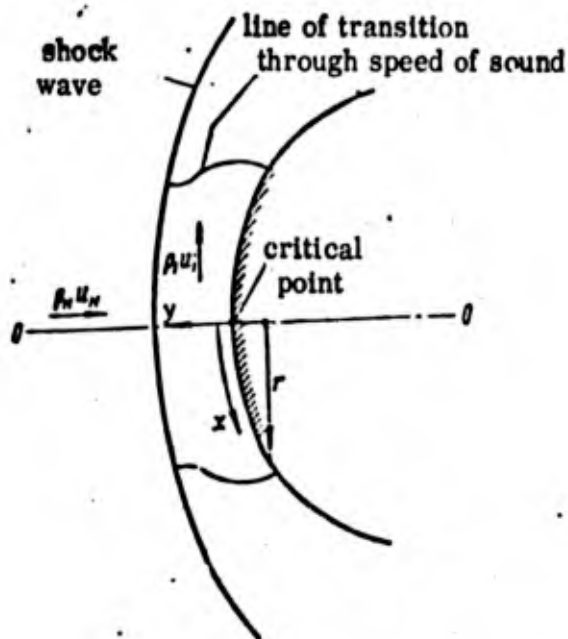
Fig. 137. Flow in neighborhood of leading critical point on axially-symmetric body

We can obtain an equation for the turbulent heat exchange in the neighborhood of the critical point on a flat body in a similar way

$$q_{\bullet}=3600\varsigma c_{p}\varrho_{1}3x\left(T_{e}-T_{\omega}\right)\cdot0.035\left(\frac{9x^{2}}{v_{1}}\right)^{-\frac{1}{5}}\left(\frac{T_{\tau}}{T_{e}}\right)^{-0.16}\mathrm{Pr}^{-0.6}. \tag{8.55}$$

In practice we have to calculate it with the formulae for laminar boundary flow up to values of $\underline{x}$ at which $(q_{\omega})_{\text{lam}} > (q_{\omega})_{\text{turb}}$, and from then on by the formulae for the turbulent boundary layer. This condition can be improved as we accumulate data on the transition point between laminar and turbulent boundary layers in the neighborhood of the critical point.

The value $\beta = \overline{(\partial u_1/\partial x)}$ in the case of supersonic flow around a body can be taken approximately at $\beta = a_{12}/r_0$, in which $\underline{r}_0$ is the radius of the end or the distance along the generator to $\varphi = 45°$ in the case of a spherical or cylindrical leading part (Figs. 137 and 138).
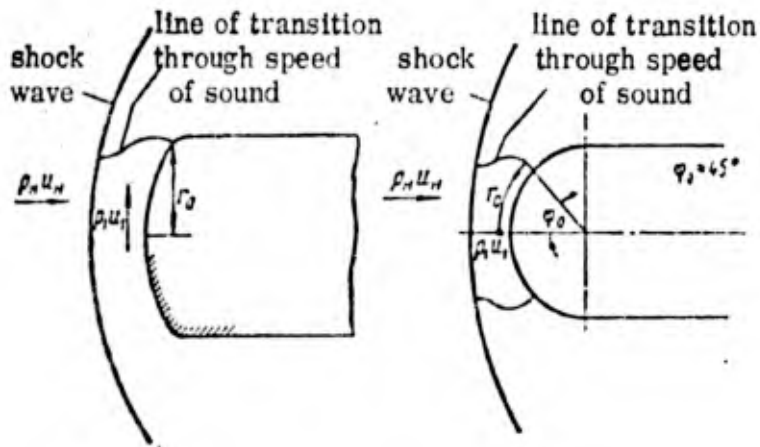
Fig. 138. Flow in neighborhood of leading critical point
of flat body

As is known from experimentation, when there is supersonic flow around

blunted bodies in the sections beyond the boundary layer, the velocity u attains

$a_{\text{кр}}$ $a_{\text{кр}}$.

Calculating heat exchange in a nozzle

With an accuracy of 15 - 30% the heat fluxes in the nozzle can be

calculated with the formula for a flat plate, if we start counting the distance

x in the chamber from the beginning of the nozzle. The values μ_1 and ρ_1 (in the formulae

have to be taken in each section of the nozzle for which we determine the heat flux.

The thickness of the boundary layer in this calculation is too small, while the

heat fluxes are too large. But on account of the fact that in the formula $q_w \sim (\theta)^{\frac{1}{5}}$

the error in the heat flux is insignificant. When calculating heat exchange on

the walls of a nozzle at $M \geqslant 3$, the errors may be more considerable. In this

case we make use of methods which make allowance for the developemnt of the boundary

layer in front of the sections in question, the so-called "prehistory". It follows

from the calculations and experiments that the heat flux in any section of a flat

nozzle is less than on a flat plate of equal length.

- 356 -

REFERENCES

1. Abramovich, G. N. Applied gas dynamics. Gostekhizdat, 1953.

2. Van Drayst. Problem of aerodynamic heating, "Problems of Rocketry", For. Lit. Press, 1957, No. 5.

3. Goldshteyn, S. Present state of hydrodynamics of viscous fluids. For Lit. Press, 1948.

4. Gukhman, A. A. and others. Fundamentals of teaching on heat exchange during gas flow at high velocities. Mashgiz, 1951.

5. Dorodnitsyn, A. A. Boundary layer in compressible gas, "Applied Mechanics and Mathematics", 1942, No. 1.

6. Kalikhman, L. Ye. Gasdynamic theory of transfer, "Applied Mathematics and Mechanics", 1946, No. 10.

7. Kochin, N. Ye. and others. Theoretical hydromechanics, Part II, Gostekhizdat, 1948.

8. Kutateladze, S. S. Fundamentals of theory of heat exchange, Mashgiz, 1957.

9. Loytsyanskiy, L. D. Aerodynamics of boundary layer. Gostekhizdat, 1941.

10. Loytsyanskiy, L. D. Mechanics of fluids, Gostekhizdat, 1957.

11. Prandtl, L. Hydroaerodynamics, For. Lit. Press, 1951.

12. Targ, S. N. Fundamental problems of theory of laminar flow, Gostekhizdat, 1951.

13. Khouart, L. Present state of aerydynamics of high velocities, For. Lit. Press, 1955.

14. Schlichting, G., Theory of boundary layer, For. Lit. Press, 1956.

15. Shirokov, M. F. Physical bases of hydrodynamics, Gostekhizdat, 1958.

16. Burgess, E. Guided ballistic missiles, For. Lit. Press, 1958.

CHAPTER IX

HEAT EXCHANGE DURING CHEMICAL REACTIONS IN

THE BOUNDARY LAYER

Sec. 38. Laminar Boundary Layer during Chemical Reactions in Gas

At the high gas temperatures which are attained in the combustion

chambers of liquid fuel and jet engines as well as in the boundary layer on the

surface of a body moving at high velocities, we have to take into account the

dissociation of molecules, the chemical reactions occurring in the boundary layer.

These reactions also take place in cases in which the *substance* fed to the boundary

layer for purposes of cooling may react with the gas of the outside stream. In

number of cases at high gas temperatures and high thermal flux we have to

give consideration to the destruction of the surface of the body - by melting or

evaporation. Here the particles of the destroyed surface may react chemically

with each other or with the gas in the outside stream. A case may also be

encountered in which the chemical reactions take place on the surface of the body.

The new branch of heat exchange during a chemical reactions is of

particularly great and topical importance in solving the problem of cooling

long-range rockets moving at high supersonic velocity. As is well known, at

such velocities there is considerable aerodynamic heating of the rocket parts

/14, 15/.

This process is particularly important when the rocket returns to the atmosphere, since in this case the increased supply of heat is considerably more intensive than the inverse thermal radiation. For example, if the velocity of a missile returning to the atmosphere is M = 15 - 22, at such high supersonic velocities of motion, a drag temperature of the order of 15000 - 25000°K is produced in the boundary layer near the wall of the missile /14, 15/. When such temperatures develop, there is dissociation of the air, which creates an extremely complicated gas-thermo-chemical problem, bordering on the realm of magnetogasdynamics. All this shows the necessity of ensuring special conditions for cooling the rocket and protecting its surface.

To solve the problem of protecting the rocket surface when moving at high supersonic velocities, we must carry out further research both in the use of the known types of coolant as well as search for new ones.

In particular, we are faced with the problem of further intensification of the cooling effect by using both phase transformations accompanying the absorption of heat (evaporation, sublimation, and so on), as well as additional use of the negative heat effects of the endothermal reactions which may occur in the cooling agent under corresponding conditions. Naturally, the practical application of the additional cooling effect of possible endothermal reactions

of dissociation of the coolant a may involve great difficulties.

First, the cooling agent itself and the decomposition products should

not be chemically aggressive with respect to the material of the heat exchanger

in which it is circulating, or with respect to the corresponding cooling surface

of the rocket. Secondly, the cooling agent and its *decomposition* (products should possess

the greatest specific g thermal capacity in order to ensure maximum heat removal

at the given temperature difference.

In principle, it is possible to step up the cooling effect by using

both phase transformations accompanying the absorption of heat, as well as the

additional absorption of heat through the completion of the endothermal reaction

with the heat transfer agent.

The study of heat transfer during chemical reactions is still in its

infancy, of course, and a great deal of experimental and theoretical research

will be required before it is successfully solved.

When there are chemical reactions in the boundary layer, we have to

take into account the additional emission or absorption of heat inside the

boundary layer. When considering the motion of a gas mixture as a whole, we have

to m keep it in mind that the physical parameters of the mixture $\rho, \mu, \lambda, D, Pr,$ etc. will

depend both on the temperature and the composition of it. In such cases we have to

consider the totality of the equations of motion, thermal conductivity and diffusion, since all these equations are inter related. In the general case we can add the conditions for the chemical reactions - the chemical kinetics equations - to the previous ones. On account of the complexity of the phenomena involved, we have to consider simplified systems. Let us now take a look at the laminar boundary layer, a although the derivations will be applied later to the turbulent boundary layer.

All the derivations applied to gas mixtures for which $Pr = \mu c_p / \lambda$ and $Pr_\mathcal{2} = \mu / \rho D$ are not very different from unity. The aim of this section of the book is to provide the preliminary information needed for the study of theoretical and experimental heat exchange during chemical reactions.

Boundary layer equations at low flow velocities during diffusion and chemical reactions

Let us introduce the concepts of gas - enthalpy

$$J_i = \int_0^T c_p \, dT + (J_{chem})_i \tag{9.1}$$

The enthalpy of the i-th gas component J_i is equal to the total energy consisting of the heat content of the gas $\left(\int_0^T c_{p_i} \, dT\right)_i$ and $(J_{chem})_i$ - the chemical energy of formation of the given substance from molecules of individual elements, equal to the energy which has to be expended in order to obtain this matter from the elements. For example, if heat is emitted during the combustion of hydrogen

- 360 -

and oxygen, the heat of formation is equal to the amount of heat released

during the reaction

$$H_2 + \frac{1}{2}O_2 = H_2O + Q$$

$$J_{\underset{chem}{H_2O}} = -Q = -57.8 \, \text{kcal/mole} = -3210 \, \text{kcal/kg}$$
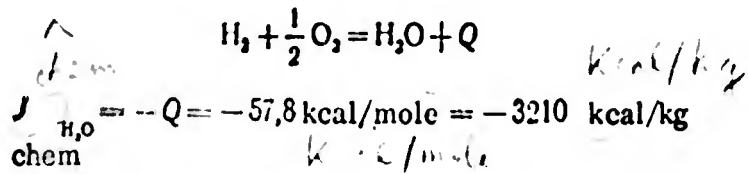
The chemical energy of H_2O comes out negative, since it is not

absorbed during the formation of the H_2O, but rather released. Here it is taken

that the heat of formation of H_2 and O_2 is equal to 0. The value J_{chem} thus

depends on the system of counting selected. Tables usually give data on the

heat of formation from elements taken into the state which is stable at 18°C

and   1 atm abs pressure. When making the calculations, it is of no importance

at all which system is selected, since we are dealing with differences in the heat

of formation of different components in the mixture.

If we consider a mixture of gases, the enthalpy - the total energy of

the mixture is obtained by summation

$$J = \sum_i C_i J_i \quad \text{kcal/kg} \tag{9.2}$$

Here C_i is the concentration by weight of the i-th component in

the   mixture.

When a gas mixture moves, the total energy of the released volume

may vary on account of the supply or removal of heat through conductivity,

er of energy directly by the influx or eflux of gas from the volume, and the transfer of energy during the movement of different molecules through diffusion.

The total energy flux at a low flow velocity through the area oriented in the direction of the y-axis x can be represented in the following form (disregarding diffusion thermal conductivity)

$$q_y = -\lambda \frac{\partial T}{\partial y} + \rho v J + \sum_i (Q_i) J_i. \qquad (9.3)$$

The first term represents the transfer of heat λ_2 thermal conductivity, the second term λ_2 convection, and the third through diffusing gases. Here Q_i is the amount of the i-th component diffusing through the area, J_i is the total energy of the i-th component. It is interesting to note that in this formula we do not need to take into account the emission or absorption of heat through the chemical reactions separately. During the chemical reactions, the total energy of the mixture J does not vary. This is indeed the advantage of introducing the concept of enthalpy J.
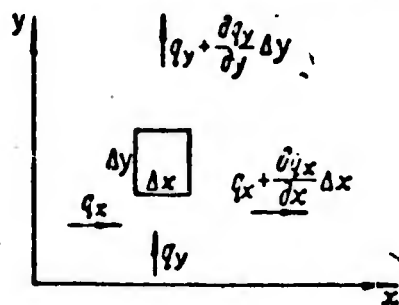
Fig. 139. Energy balance and elementary volume

$$\operatorname{div} \vec{q} = 0$$

and for a plane case (Fig. 139)

$$\frac{dq_x}{dx} + \frac{dq_y}{dy} = 0.$$

As usual in the theory of the boundary layer, in the expression

for Δq_x we can disregard the terms for thermal conductivity and diffusion in

$$q_x = \rho u J.$$

the direction of the x-axis.

This is implied by the evaluation of the orders of the individual

terms, and is a result of the slight thickness of the boundary layer.

The energy equation takes the form

$$\frac{\partial \rho u J}{\partial x} + \frac{\partial \rho r J}{\partial y} = \frac{\partial}{\partial y} \left(\lambda \frac{\partial T}{\partial y} \right) - \sum_i J_i \frac{\partial}{\partial y} (Q_i),$$

but

$$\frac{\partial \rho u J}{\partial x} + \frac{\partial \rho v J}{\partial y} = \rho u \frac{\partial J}{\partial x} + \rho v \frac{\partial J}{\partial y} + J \left(\frac{\partial \rho u}{\partial x} + \frac{\partial \rho v}{\partial y} \right).$$

From the continuity condition we get

$$\frac{\partial \rho u}{\partial x} + \frac{\partial \rho r}{\partial y} = 0.$$

- 363 -

Thus, we finally get

$$\rho u \frac{\partial J}{\partial x} + \rho v \frac{\partial J}{\partial y} = \frac{\partial}{\partial y}\left(\lambda \frac{\partial T}{\partial y}\right) - \sum_i J_i \frac{\partial}{\partial y}(Q_i). \qquad (9.4)$$

to this equation we must add the momentum equation and the diffusion equation

$$\rho u \frac{\partial u}{\partial x} + \rho v \frac{\partial u}{\partial y} = \frac{\partial}{\partial y}\left(\mu \frac{\partial u}{\partial y}\right) - \frac{\partial p}{\partial x}. \qquad (9.5)$$

$$\rho u \frac{\partial C_i}{\partial x} + \rho v \frac{\partial C_i}{\partial y} = -\frac{\partial}{\partial y}(Q_i) + (W_{chem})_i. \qquad (9.6)$$

The diffusion equation, which expressed the contuity condition for

the i-th component, disregarding thermal diffusion, takes into account the

consumption of the i-th component through chemical reactions $(W_{chem})_i$ in $kg/m^3 \cdot sec$.

The diffusion equation can be derived by compiling the balance of the i-th

component in the elementary volume.

The flow of the i-th component through the area normal to the y-axis
$M_y = \rho v C_i + Q^i_{diff}$
is equal to $\wedge$; through the area normal to the x-axis it is $M_x = \rho u C_i$ (disregarding

the diffusion flow along the x axis). The balance equation takes the form

$$\frac{\partial M_y}{\partial y} + \frac{\partial M_x}{\partial x} = (W_{chem})_i, \text{ and then } (9.6).$$

Let us consider a binary mixture by itself, i.e., a mixture consisting

of two components. In this case

$$C_1 + C_2 = 1; \quad Q_1 = -Q_2 = -\rho D_{12}(\partial C_1 / \partial y)$$

and D_{12} is the diffusion coefficient of the first component in the second: $D_{12} = D_{21}$

- 364 -

For a mixture consisting of several components, the diffusion flows Q_i are expressed in a more complex way in terms of the diffusion coefficients for each pair of components - the coefficients of binary diffusion. In a particular case, in which all the binary diffusion coefficients are equal, the expressions for Q_i retain their simple form

$$Q_i = -\rho D (\partial C_i / \partial y)$$

, in which $\underline{D}$ is the binary diffusion coefficient. Although all the operations from now on relate to a binary mixture, the final versions are still valid for a general case of a multicomponent mixture.

Let us transform the energy equation into another form. According to the definition of the enthalpy of a mixture $J = \sum J_i C_i$. Then

$$dJ = \sum J_i dC_i + \sum C_i dJ_i,$$

$$J_i = \int c_{p_i} dT + (J_{chem})_i; \quad dJ_i = c_{p_i} dT,$$

since $d(J_{изв})_i = 0$, because the heat of formation of each component is a fixed value. Hence,

$$dJ = \sum J_i dC_i + \sum C_i c_{p_i} dT.$$

but $\sum C_i c_{p_i} = \bar{c}_p -$ is the mean thermal capacity of the mixture, and

$$dJ = \bar{c}_p dT + \sum J_i dC_i.$$

The expression in the right-hand side of the thermal conductivity equation can now be transformed in the following way. The temperature derivative is equal to

$$\frac{\partial T}{\partial y} = \frac{\partial J}{\partial y} \frac{1}{\bar{c}_p} - \frac{\sum J_i \frac{\partial C_i}{\partial y}}{\bar{c}_p};$$

- 365 -

By substituting it into the right-hand side of the energy equation we get the following for a binary mixture

$$\frac{\partial}{\partial y}\left(\lambda\frac{\partial T}{\partial y}\right)+\sum\frac{\partial}{\partial y}J_i\left(\rho D\frac{\partial C_i}{\partial y}\right)=$$

$$=\frac{\partial}{\partial y}\left(\frac{\lambda}{c_p}\frac{\partial J}{\partial y}\right)+\frac{\partial}{\partial y}\left[\left(-\frac{\lambda}{c_p}\frac{\partial C_1}{\partial y}(J_1-J_2)+\rho D\frac{\partial C_1}{\partial y}(J_1-J_2)\right]=$$

$$=\frac{\partial}{\partial y}\left(\frac{\lambda}{c_p}\frac{dJ}{\partial y}\right)+\frac{\partial}{\partial y}\left[\rho D_{12}\left(1-\frac{\lambda}{c_p\rho D_{12}}\right)\frac{\partial C_1}{\partial y}(J_1-J_2)\right]. \quad (9.7)$$

$$\frac{\lambda}{c_p D}=Pr_2/Pr$$

$$Pr_s=\mu/\rho D_{12}$$

The formula $\wedge$ is equal to the ratio of the Prandtl diffusion number $\wedge$

$Pr=\mu c_p/\lambda$. to the Prandtl number. Having substituted this expression into

the energy equation, we get an equation in a new form

$$\rho u\frac{\partial J}{\partial x}+\rho v\frac{\partial J}{\partial y}=\frac{\partial}{\partial y}\left(\frac{\lambda}{c_p}\frac{\partial J}{\partial y}\right)+\frac{\partial}{\partial y}\left[\left(1-\frac{Pr_s}{Pr}\right)\rho D\frac{\partial C_1}{\partial y}(J_1-J_2)\right].$$

$$(9.8)$$

$$Pr_d=Pr$$

If we take it in this equation that $\widehat{}$, it acquires a form similar

to that of the energy equation for low velocities when there are no chemical

reactions, except that in this case the role of the heat content $c_p T$ is now

played by the total enthalpy $\underline{J}$. The physical meaning of this is that during flow

along a surface by a gas mixture, the heat exchange is determined both by the heat

energy of the flow as well as by the chemical energy which may become heat energy

$$Pr=Pr_d$$

on the walls. The condition $\widehat{}$ leads to the fact that the surplus chemical

energy in the outside flow over the chemical $\widehat{}$ energy of the gas at the temperature

at the wall is completely converted into heat energy. But if $Pr\neq Pr_d$ and the

processes of diffusion and thermal conductivity take place with different degrees

- 366 -

of intensity, it may happen that the conversion of chemical into heat energy is not complete. In the same way that when studying the boundary layer at high velocities in a case $Pr \neq 1$ we introduced the concept of the temperature recovery coefficient, when there are chemical reactions we can speak of the enthalpy recovery coefficient, which takes into account the degree of transfrmation of chemical energy into heat.

The heat flux transferred to the wall $\mathbf{z}$ is determined by the formula

$$q_w = \frac{\lambda}{c_p}\left(\frac{\partial J}{\partial y}\right)_w.$$

The derivatives

$$\left(\frac{\partial J}{\partial y}\right)_e \approx \frac{J_e - J_w}{\delta}.$$

in which J_∞ is the total enthalpy in the outer stream, J_w is the total enthalpy of the gas by the wall, δ is the thickness of the boundary layer. Then $q_x \sim \frac{\lambda}{c_p}\frac{J_e - J_w}{\delta}$.

In the same way that in studying flow at high velocities it was advisable to determine the heat-exchange coefficient $a = \dfrac{q_w}{(T_{(0)})_\infty - T_w}$, in the case of flow with chemical reactions it is convenient to determine this coefficient by the expression

$$\frac{a}{c_p} = \frac{q_x}{J_e - J_w}. \tag{9.9}$$

Here we are already taking into account the main effect of the chemical reactions on the heat flux by the fact that we are now dealing with enthalpy.

The value a may vary on account of variation in the physical characteristics

of the medium. As a first approximation, a can be taken from solutions for flow without chemical reaction, making allowance for the chemical reaction by substituting the values ρ, μ, λ, c_p into the final formulae and taking their chemical composition into account. For example, the heat flux on a plate can be calculated from (8.37)

$$q_w = 0,332 \frac{J_\infty - J_w}{c_{p_w}} \sqrt{\frac{u_\infty \rho_\infty}{\mu_w x}} \left(\frac{\mu_\infty \rho_\infty}{\mu_w \rho_w}\right)^{1/3}, \qquad (9.10)$$

in which $\overline{c_{p_w}}$ is the mean thermal capacity of the mixture at $T = T_w$.

J_∞ and J_w at the set temperatures T_∞ and T_w are determined from the chemical composition. If the temperatures are substituted for the enthalpy, we may make a large error. For example, in the combustion chambess of liquid fuel engines using a mixture of kerosene and oxygen, the temperature reaches approximately 3500° /16/. On account of strong dissociation of the combustion products, some of the chemical energy is not converted into heat. At a temperature of 1000° on the cooled wall the chemical energy may change to heat, i.e., there is recombination of the molecules. The temperature difference $T_{c\infty} - T_{c\omega} = 2500°$, the difference $\frac{J_\infty - J_w}{c_{p_w}} \approx 3500°$. So if we use the difference $(T_\infty - T_w)$ to determine the heat flux, we are liable to make a very large error.

Distribution of velocity, enthalpy and temperature across

the boundary layer

When there are chemical reactions, the $role$ of the temperature is

played by enthalpy. The equation for the distribution of enthalpy and velocity

across the layer in the case $Pr = Pr_d = 1$ during flow along a plate are similar

to each other. It is easy to see that by substituting condition $I = I_v^* + \dfrac{u}{u_o}(I_o - I_v)$

the energy equation becomes identical to the motion equation (at $dp/dx = 0$).

This condition

$$\frac{J - J_v}{J_o - J_v} = \frac{u}{u_o} \qquad (9.11)$$

is the similarity condition for the enthalpy and velocity profiles in the boundary

layer. The temperature distribution here may take an arbitrary form, depending

on the nature of the chemical processes in the boundary layer.

The similar condition for the velocity and enthalpy profiles implies

a relationship between the heat transfer and friction in the normal form

$$Nu = \frac{1}{2} c_f Re.$$

Here it should be kept in mind that in the formula for the number $Nu = \alpha x \big/ \lambda$

the value α is referred to the enthalpy drop $c_o = q_w / J_o - J_v$.

In the general case, if $Pr \neq Pr_d \neq 1$, the condition linking the friction

and heat transfer during chemical reactions can be written in the form

$$Nu = \frac{1}{2} c_f Re\, f(Pr, Pr_d).$$

- 369 -

Just as for an exact value of α, the form of the function $f(\overline{Pr, Pr}_d)$ can be

determined by solving the boundary layer differential equation. But to do this we

have to set ourselves the specific dependences of the chemical reactions.

Extensive experimental research is now going on to find these relationships.

Sec. 39. Equations for Laminar Boundary Layer during Chemical Reactions at High Flow Velocities

When the velocity of the flow is high, we have to make allowance for the

emission of heat in the boundary layer through friction and the work of pressure.

The amount of dissipated energy is determined by the formula $\Phi = \mu (\partial u/\partial y)^2$. The work

of pressure is equal to $\underline{u dp/dx}$.

The equation for the enthalpy distribution in the boundary layer

for a binary mixture, taking these terms into account, takes the form

$$\rho u \frac{\partial J}{\partial x} + \rho v \frac{\partial J}{\partial y} = \frac{\partial}{\partial y}\left(\frac{\lambda}{c_p} \frac{\partial J}{\partial y}\right) + \mu \left(\frac{\partial u}{\partial y}\right)^2 +$$
$$+ u \frac{dp}{dx} + \frac{\partial}{\partial y}\left[\left(1 - \frac{Pr_s}{Pr}\right)\rho D \frac{\partial C_1}{\partial y}(J_1 - J_2)\right]. \qquad (9.12)$$

The motion equation is

$$\rho u \frac{\partial u}{\partial x} + \rho v \frac{\partial u}{\partial y} = \frac{\partial}{\partial y}\left(\mu \frac{\partial u}{\partial y}\right) - \frac{dp}{dx}.$$

By multiplying the second equation by $\underline{u}$ and adding it to the energy

equation in exactly the same way as we did earlier when considering the boundary

layer in a compressible gas, we get after transformation

- 370 -

$$\rho u \frac{\partial J_{00}}{\partial x} + \rho v \frac{\partial J_{00}}{\partial y} = \frac{\partial}{\partial y}\left(\frac{\lambda}{c_p}\frac{\partial J_{00}}{\partial y}\right) +$$

$$+ \frac{\partial}{\partial y}\left[\mu\left(1 - \frac{1}{Pr}\right)\frac{\partial(u^2/2)}{\partial y}\right] + \frac{\partial}{\partial y}\left[\rho D_{12}\left(1 - \frac{Pr_d}{Pr}\right)\frac{\partial C_1}{\partial y}\left(J_1 - J_2\right)\right]. \quad (9.13)$$

(9.13)

$$J_{00} = J + \frac{u^2}{2}$$

Here $\wedge$ is the drag enthalpy or the total enthalpy of the gas mixture.

The equation derived is the most complete equation for the boundary layer energy in a compressible gas when there are chemical reactions. If the number $Pr = Pr_d = 1$, then the last two terms in the equation fall out, and the energy equation takes a form similar to that of the equation for low velocities, with the only difference that the part of the temperature is now played by the total drag enthalpy $J_{00} = \int c_p\, dT + J_{chem} + \frac{u^2}{2}$.

In actual fact, the numbers Pr and Pr_d differ from unity, but for most gases this difference is of the order of 30%. Here it is advisable to calculate on the basis off the assumption that $Pr = Pr_d = 1$ and then add a correction taking into account the difference in the Prandtl numbers from unity ($P_r < 1$ and $P_r < 1$). Physically speaking, this means making allowance for the fact that the surplus chemical energy and kinetic energy of the external stream are x transformed into heat on the wall to an incomplete extent.

The heat flux in the general case can be determined by the formula

$$q_w = \frac{\mu}{c_p}(J_{00} - J_w). \quad (9.14)$$

It might be thought when determined in this way that α would differ

from its value for a case in which there are no chemical reactions, principally

because of the variation in the physical properties of the medium.

In order to take the effect of the difference between the Pr and Pr_d

numbers from unity into account, we introduce the concept of the effective total

enthalpy $J_e < J_\infty$. Then $q_w = \alpha / \overline{c_p}(J_e - J_w)$. J_e is assessed experimentally.

Distribution of velocity and enthalpy across the boundary layer

Let us consider a case of flow along a ^{flat} plate in which $\frac{dp}{dx} = 0$.

The energy equation at $Pr = Pr_d = 1$ becomes identical with the momentum equation

on condition

$$\frac{J_\infty - J_w}{(J_\infty)_e - J_w} = \frac{u}{u_e} . \qquad (9.15)$$

It is easy to show that all the derivations regarding the temperature

distribution at $Pr = 1$ in a case of high flow velocity without chemical reaction

can now be extended to cover a general case in which the part of the temperature

is played by enthalpy, while the drag temperature is played by total enthalpy.

The condition relating the friction and heat transfer can be written

in the form

$$Nu = \frac{1}{2} c_f \, Re \, f(Pr, Pr_d).$$

$$Nu = \frac{ax}{\lambda} \quad \text{and} \quad \frac{a}{c_p} = \frac{q_w}{(J_e - J_w)}.$$

The values α as a first approximation can be taken from the solutions

derived without chemical reactions but with variation in the physical characteristics

of the medium /Eqs. (8.37) - (8.39)/.

Sec. 40. Different Cases of Flow in Boundary Layer with

Chemical Reactions and Methods of Calculation

Calculation of the boundary layer when there are chemical reactions

requires the setting of specific conditions for these reactions. In the general

case these conditions can be set in the form of reaction rates and temperature.

The number of these relationships should correspond to the number of possible

reactions in the mixture.

Let us go back to the system of equations for the boundary layer in

the case of a binary mixture

$$\rho u \frac{\partial u}{\partial x} + \rho v \frac{\partial u}{\partial y} = \frac{\partial}{\partial y}\left(\mu \frac{\partial u}{\partial y}\right) - \frac{dp}{dx};$$

$$\rho u \frac{\partial J_{00}}{\partial x} + \rho v \frac{\partial J_{00}}{\partial y} = \frac{\partial}{\partial y}\left(\frac{\lambda}{c_p} \frac{\partial J_{00}}{\partial y}\right) +$$

$$+ \frac{\partial}{\partial y}\left\{\mu\left[\left(1 - \frac{1}{Pr}\right)\frac{\partial (u^2/2)}{\partial y}\right] + \frac{\partial}{\partial y}\rho D\left(1 - \frac{Pr_s}{Pr_t}\right)\frac{\partial C_1}{\partial y}(J_1 - J_2)\right\};$$

$$\rho u \frac{\partial C_i}{\partial x} + \rho v \frac{\partial C_i}{\partial y} = \frac{\partial}{\partial y}\left(\rho D \frac{\partial C_i}{\partial y}\right) + W_i'.$$

Here the diffusion equation for each component contains the term $\underline{W}_i$

which corresponds to the rate of consumption of the given component in kg/sec $\cdot$ m^3.

The values $\rho, \mu, \lambda, D, Pr, Pr_d$ are functions of temperature and composition of the mixture at

each point on the boundary layer.

The solution of this problem in the general form, when the reactions occur inside the boundary layer, involves very great difficulties. But in a number of cases we can simplify . -- *it* . by making certain assumptions *resulting* *from* the physical pattern of the flow.

Case of chemically balanced flow in boundary layer

If the chemical reaction rates are excessive compared with the rate of transfer by diffusion and convection, it can be considered that at every point on the flow there is a composition corresponding to chemical equilibrium. This means that at each point the composition of the mixture is a *given* . function of temperature and pressure.

As an example ± let us look at the case of a chemical reaction of the first order $O_2 \rightleftarrows O + O$. The rate of consumption of the oxygen molecules O_2 is determined by the condition $W_{O_2} = V_1 - V_2$. Here V_1 is the rate of decomposition of O_2 into atoms, while V_2 is the rate of the reverse formation of O_2 molecules from atoms.

It follows from chemical kinetics that the reaction rates are

$$V_1 = k_1 \frac{C_1 \rho M_2}{M_1}; \quad V_2 = k_2 C_2^2 \frac{\rho M_1}{M_2} \quad \text{kg/m}^3 \quad \text{sec}$$

- 374 -

Here k_1, k_2 are the proportionality coefficients, depending on temperature. According to the Arrenius law $k = k_0 e^{-\frac{E}{kT}}$, where E is the activation energy. In the case of chemical equilibrium $V_1 = V_2$. If it is taken into account now that in our example $C_1 + C_2 = 1$, it is clear that at the set temperature and pressure the composition is determined.

In actual fact, the equilibrium is disturbed on account of diffusion and convection and $V_1 = V_2$ equals zero. But if the temperature and pressure in the stream are fairly high, the diffusion and convection terms are small compared with V_1, and V_2; $V_1 - V_2 = \varepsilon$ in which $\frac{\varepsilon}{V_1} \ll 1$ and $\frac{\varepsilon}{V_2} \ll 1$.

In order to satisfy the equation, we need only increase the velocity V_1 slightly above V_2, which is done by a very slight deviation in the concentrations C_1 and C_2 from their equilibrium values. This deviation is approximately $\frac{\varepsilon}{V}$. Thus, at fairly high reaction rates the diffusion equations are replaced by chemical equilibrium conditions. In each case the relationships $C_i = f_i(p, T)$ can be calculated. By knowing the composition we can then determine ρ, μ, λ and D as functions of temperature and pressure, after which the problem is reduced to the solution of only two equations: momentum and energy.

In the flow of air along a flat plate at very high velocities of the outer stream with dissociation, this problem has been solved by Mur (moore?) /7/

- 375 -

on the basis of certain simplifications. The calculation for equilibrium dissociation can be reduced to addition of the condition dependence of the physical properties of the gas on J - the enthalpy of the mixture - instead of the usual relationships for non-dissociated gas.

It is assumed that relative portion of atoms of each element across the boundary layer remains constant. The chemical equilibrium equations are used to calculate the variations in the molecular composition of the mixture consisting of O_2, N_2, O, N, and NO molecules. As a result we can plot the graphs (Figs. 140, 141 and 142). From then on the calculation is in no way different from the calculation of the boundary layer without chemical reaction except for the variable physical properties of the medium.

The results of the calculations show the variation in the heat exchange coefficient $\dfrac{\alpha}{c_{p_w}}$ from 10 to 15%; this is due to the fact that the main effect of dissociation is taken into account by replacing the temperature drop in the formula for heat flux by the enthalpy drop

$$q_w = \frac{\alpha}{c_{p_w}}[(J_0)_w - J_w].$$

It should be pointed out that although α/c_{p_w} varies only slightly, the heat flux may be considerably different from the value obtained without taking dissociation into account.

- 376 -
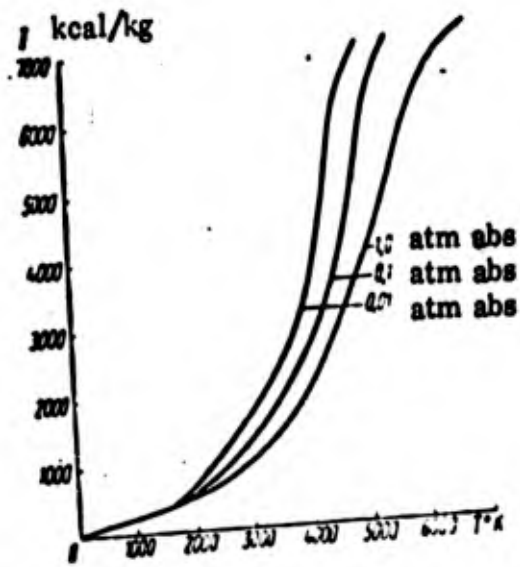
Fig. 140. Enthalpy of air as function of temperature
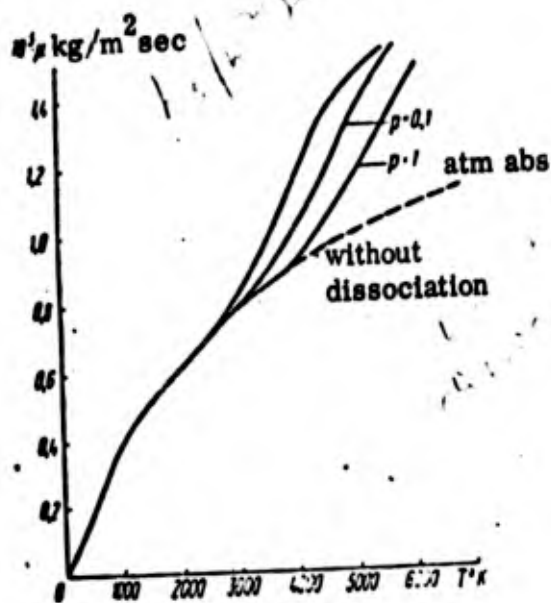
Fig. 141. Viscosity of air as function of temperature
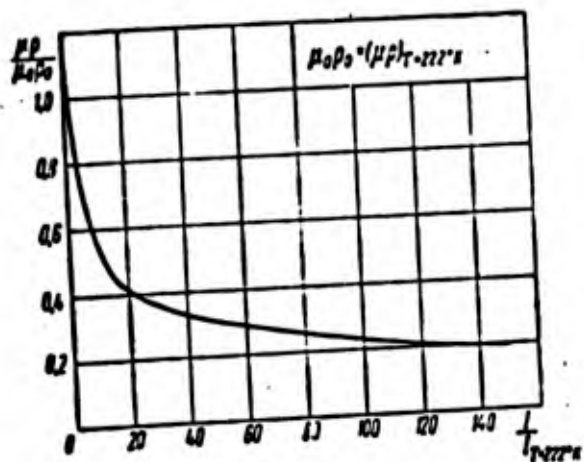
Fig. 142. Variation in $\mu\rho/\mu_0\rho_0$ as function of enthalpy

Example. A plate is moving through the air at a temperature $T_\infty = 300°$ and M = 10; the drag temperature $T_{00} = 6300°$. Let us assume that the static pressure is p = 0.1 atm abs. Let us determine the heat flux for the wall temperature $T_{W_1} = 2000°$ and $T_{W_2} = 4000°$ from two equations.

If we disregard dissociation, then $q = a(T_w - T_\varepsilon)$.,

$$q_{w_1} = 4300a, \quad q_{x_2} = 2300a.$$

If we take dissociation into account (disregarding the variation in $\propto$) we get $J_{(0)} \approx 0.24 \cdot 6300 = 1510$ and $q_{w_1} = \frac{a}{c_p}[(J_{(c)})_\infty - J_z]$. The values J_{W_1} and J_{W_2} are determined from the graph (Fig. 140) for p = 0.1 atm abs. So we get

$$J_{w_1} = 500 \ \text{kcal/kg}, \quad J_{x_2} \approx 2\times 0 \ \text{kcal/kg}$$

Then,

$$q_{x_1} = \frac{a}{0.24}(1510 - 500) \approx 4200a$$

and

$$q_{x_2} = \frac{a}{c_{p_w}}(1510 - 2000) < 0.$$

Thus, in the first case in which the temperature of the surface is below the dissociation point, we obtain an approximately true result. But if the temperature of the surface is ~ above this ~ point, the calculation when dissociation is disregarded gives the qualitatively opposite result - heating up of the plate whereas in actual fact the plate gives off its heat.

In the general case the effect of dissociation on the heat flux is
not very great, provided the temperature on both boundaries of the boundary layer
is below the dissociation point. But if this condition is not observed, the
effect of dissociation on the heat flux may be xx considerable.

Boundary layer with non-equilibrium dissociation.

If the chemical reaction rates are comparable with the transfer rates,
the chemical composition at each point in the stream depends on temperature and
pressure, and in addition is determined by diffusion. In this case we must solve
the diffusion equation, making allowance for the true kinetics of the chemical
reaction.
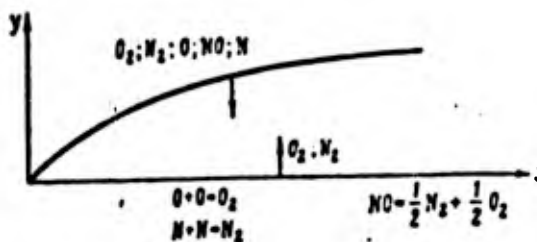
Fig.143. The case of chemical nonequilibrium in the
boundary layer

The problem is simplified when the flow is totally chemically unbalanced,
i.e., when the velocity of the stream is high so that the chemical reaction does
not have time to affect the composition of the mixture to any great extent.

When air flows round a flat plate, chemically unbalanced flow can be reduced to the case already considered by us for flow without dissociation. Indeed, the gas in the outside stream, which is at a low temperature, is not dissociated, while the chemical reactions do not have time to take place in the boundary layer. The opposite effect may occur when there is flow around a blunt-nosed body with a receding shockwave. When the temperature is raised, a chemical composition corresponding to equilibrium at this temperature is established beyond the shockwave.

If it is assumed that the composition of the gas does not vary in the boundary layer, the problem is reduced to the study of flow without chemical reactions, but with new physical properties differing from those of the air. Finally, we can imagine a case in which the chemical reactions only occur on the surface of the body through the catalyzing effect of the surface. Here we must make allowance for the diffusion of the reaction products from the wall to the boundary layer (Fig. 143).

General comments

The examples we have considered show that in the investigation of heat exchange at high velocities or at high temperatures we must have some idea of the

- 380 -

nature of the chemical processes taking place. Experimental study plays an enormous part in this problem. In order to reproduce the conditions under which the reactions occur in reality, we must strive for velocities and temperatures close to the real ones in the experimental models.

For approximate calculation of heat exchange in liquid-fuel engines and on the surface of flying craft we adopt the condition of chemical balance. The value α is taken from calculation without chemical reactions, but with correction for the variation in the physical properties of the medium /16/.

If there is considerable difference between the molecular weights of the gases in the mixture, we have to add to the energy and diffusion equations terms for the diffusion of thermal conductivity and thermal diffusion occurring through the tendency of lighter molecules to shift to the higher temperatures region, and the tendency of heavier molecules to shift to the lower temperature region. In certain cases these terms may attain the order of 10% of the principal terms in the boundary layer equations.

REFERENCES

1. Go, I. Effect of dissociation in hypersonic viscious flow, "Mechanics", For. Lit. Press, 1958, No. 1.

2. Kireyev, V. A. Physical chemistry, Goskhimizdat, 1956.

3. Lighthill, N. D. Dynamics of dissociated gas, "Problems of Rocketry", For. Lit. Press. 1956, No. 5.

4. Landau, L. B. and others. Mechanics of solid media, Gostekhizdat, 1954.

5. Levin, V. G. Physico-chemical hydrodynamics, Academy of Sciences Press, 1952.

6. Loytsyanskiy, L. G. Mechanics of liquids and gases. Gostekhizdat, 1950.

7. Mur, L. Solution of laminar boundary equations taking dissociation into account, "Mechanics", For. Lit. Press. 1953, No. 5.

8. Frank-Kamenetskiy, D. A. Heat transfer and diffusion in chemical kinetics, Academy of Sciences Press, 1947.

9. Schlichting, G. Theory of boundary layer, For. Lit. Press, 1956.

10. Lees, L. Laminar Heat Transfer Over Blunt-Nosed Bodies, Jet. Propulsion, No. 4, 1956.

11. Fay, J., Riddel, F. Theory of Stagnation Point Heat Transfer in Dissociated Air, JAS, 1958.

12. Rose, P., Stark, W., Stagnation Point Heat Transfer Measurements in Dissociated Air, JAS, No. 2, 1958.

13. Shirokov, M. F. and others. Heat transfer and friction in streams of reacting gas mixtures, "Scientific Higher School Reports", 1958, No. 1.

14. Vistas in Aeronautics, Pergamon Press, 1958.

15. Van Drayst, Problem of Aerodynamic heating "Problems of Rocketry", For Lit. Press. 1957, No. 5.

16. Burgess, E. Guided ballistic missiles, For. Lit. Press, 1958.

HYDRODYNAMIC METHODS OF FIRMLY PROTECTING SURFACES. SWEAT COOLING

In the preceeding sectins we have considered methods of calculating

the boundary layer for the heat flux from the gas to the wall. The surface

temperature occurring during aerodynamic heating may exceed the tolerated

temperature from the   point of view of strength, leading to destruction

of the surface. In such cases we must arrange for the surface to be cooled.

Sec. 41. Possible Methods of Cooling and Thermal Protection

a) The commonest method is convection cooling, during which the hot

stream is on one side of the surface while the cold liquid or gas is on the

other side, (Fig. 144);

When calculating the cooling of combustion chambers in liquid-propellent

engines, this form of cooling is termed external cooling (with respect to the

combustion chamber). When calculating the cooling of surfaces when there is flow

round the body on the outside, this form of cooling is termed internal cooling.

At very high heat fluxes it may happen that the temperature difference on the

$$(T_{e_1} - T_{e_2}) = \frac{q_w}{\lambda}\lambda$$

wall $_\wedge$ at the given thickness of the wall is very large, and despite   sufficient

cooling of the side T_{w_2}, the temperature T_{w_1} is still greater than the tolerance;

b) Barrier cooling is commonly used for combustion chamber walls and

jet engine nozzles. A stream of cold gas is fed through holes or a slot in the wall in the direction of the stream and protects the surface (Fig. 145).

Hot stream

cooling fluid
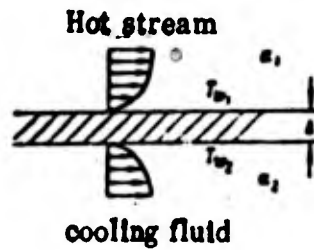
Fig. 144. Convective Cooling

Hot stream   mixing region

cold gas   cooled surface

Hot stream

coolant

Hot stream

coolant
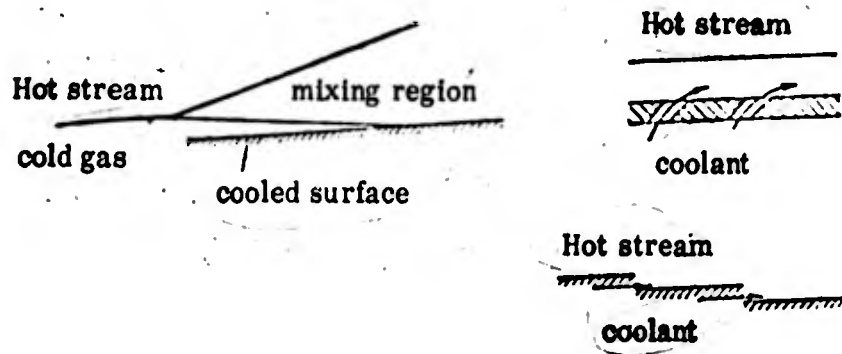
Fig. 145. Different systems of barrier cooling

The stream slowly mixes with the hot gas, as a result of which the surface temperature is increased. In practical cases there are several slots arranged in a line (Fig. 145);
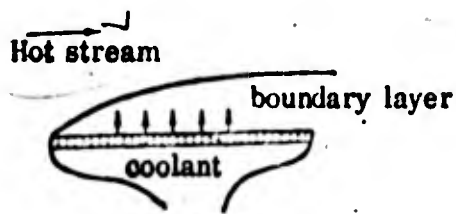
Fig. 146. Sweat cooling
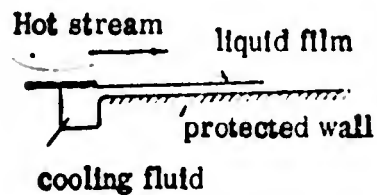
Fig. 147. Film cooling

c) Sweat cooling. The cold gas or liquid with the same properties
as in the outside stream or with different properties is fed through a porous,
permeable or perforated surface into the boundary layer (Fig. 146).

To keep the wall temperature constant, we have to feed the coolant
in accordance with a special regime. Sweat cooling is sometimes called gas
cooling, and if a liquid is used then it is termed condensate cooling;

- 384 -

d) Film cooling. The liquid here is fed through an orifice or slot and forms a protective film on the surface (Fig. 147). The film is carried along the surface by the stream and evaporates. Normally the film does not have time to completely evaporates, and is destroyed earlier through loss of stability and splattering. It is used for cooling combustion chambers and nozzles in liquid propellent engines, where one of the mixture components (usually a combustible one) serves as the coolant;

e) the use of protective coating with a high failure point and with a high-melting point and evaporation temperature;

f) the use of the internal thermal capacity during the short-term effect of thermal load. The inside parts of the construction may not have time to get really hot (Fig. 148). The surface of the body must be made of a material with a fairly low thermal conductivity and high thermal capacity γc;

g) at low heat fluxes occurring at high velocities, a large part is played by the removal of heat through radiation, which is the main type of cooling during flights at very high altitudes.

The calculation of convective cooling, provided the heat exchange coefficient α_1 and α_2 are known on either side, is not very difficult. In sweat,
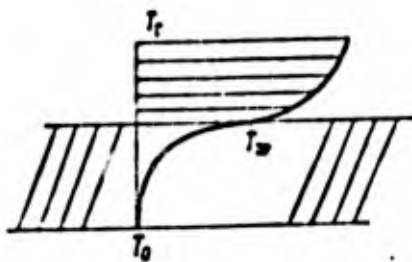
Fig. 148. Temperature distribution at any
moment of time in non-steady-state heating

barrier and film cooling the heat exchange coefficient is a function of the intensity

of the coolent feed. The calculation includes determination of the heat-exchange

coefficients during interaction between the coolent and the outside stream.

Sec. 42. Sweat Cooling

Laminar Flow in boundary layer

Let us consider the laminar boundary layer on a flat plate (Fig. 149)

at low flow velocities. There is flow around the plate at a velocity u_∞,

the coolent is fed through the porous surface at a vertical velocity v_w, which

in the general case is variable along the length $v_w = v_w(x)$
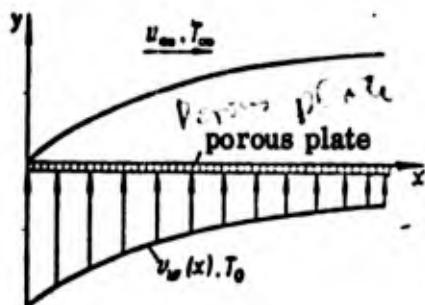
Fig. 149. Sweat cooling

The momentum equation for the laminar boundary layer is the same as during flow over an impermeable surface

$$\rho u \frac{\partial u}{\partial x} + \rho v \frac{\partial u}{\partial y} = \mu \frac{\partial^2 u}{\partial y^2}.$$

But when gas is fed through the wall, certain changes have to be made to the boundary conditions:

at $y=0$, $u=0$ and $v = v_w(x)$

The vertical velocity component by the wall differs from zero:

at $y=\delta$ $u=u_\infty$.

Deformation of the velocity profile in sweat cooling

The equations for motion and the above-described boundary condition imply

$$\rho_w v_w \left(\frac{\partial u}{\partial y} \right)_w = \mu \left(\frac{\partial^2 u}{\partial y^2} \right)_w .$$

Because $(\partial u / \partial y)_w = \tau_w / \mu$ greater than zero, since friction acts in the direction of the stream u_∞, when gas is fed ($\rho_w v_w > 0$) the second velocity derivative by the wall is $\partial^2 u / \partial y^2 > 0$.

This means that by the wall the velocity profile should bulge upwards (Fig. 150)

$$\left(\frac{\partial u}{\partial y} \right)_w = \mathrm{tg}\, a_1 .$$

- 387 -
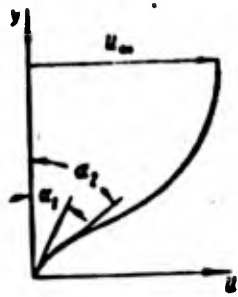
Fig. 150. Shape of velocity
profile in sweat cooling
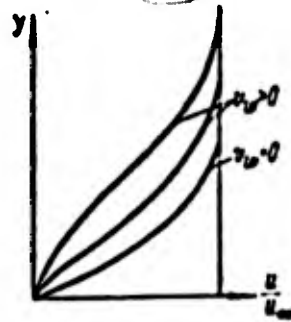
Fig. 151. Effect of gas feed
through surface on shape of
velocity profile

Since $\partial^2 u/\partial y^2 > 0$, $\overset{\frown}{}$ tan α should increase and the angle α between

the tangent to the profile and the y axis should be reduced; $\alpha_2 > \alpha_1$. But on

the boundary of the boundary layer $\partial u/\partial y = 0$, and the velocity in the boundary

layer : changes smoothly to the velocity of the outside stream. Hence inside the

boundary layer there must be an point of inflection at which $\partial^2 u/\partial y^2 = 0$, and above

which $\partial^2 u/\partial y^2 < 0$, i.e., there must be a decrease in the angle α. If $V_w = 0$,

the point of inflection is at the wall $\left[(\partial^2 u/\partial y^2)_w = 0 \right]$.

As the gas feed is increased, the profiles deform, and the point of

inflection moves away from the wall (Fig. 151.). The deformation increases as

the gas-feed rate is stepped up. At the same time as the deformation of the profile,

there is thickening of the boundary layer. In order to separate these two

phenomena, let us consider the dimensionless relationship

$$ \bar{u} = \frac{u}{u_\infty} = f\left(\frac{y}{\delta}\right) = f(\eta). $$

- 388 -

Let us substitute into the motion equation at $y = 0$

$$\rho_w v_w \left(\frac{\partial \bar{u}}{\partial \eta}\right)_w \frac{1}{\delta} = \mu_w \left(\frac{\partial^2 \bar{u}}{\partial \eta^2}\right)_w \frac{1}{\delta^2},$$

$$\frac{\left(\frac{\partial^2 \bar{u}}{\partial \eta^2}\right)_w}{\left(\frac{\partial \bar{u}}{\partial \eta}\right)_w} = \frac{\rho_w v_w \delta}{\mu_w} = f_w. \tag{10.1}$$

Thus, the deformation of the velocity profile within relative coordinates is

determined by the value $f_w = \rho_w v_w \delta / \mu_w,$ known as the parameter characterizing the profile

shape (shape-parameter), Fig. 152. The effect of the gas feed on the shape of the

profile is similar to the effect of a positive pressure gradient.
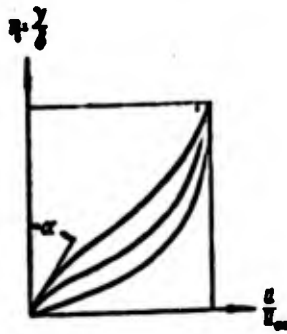
Fig. 152. Shape of velocity profile and dimensionless coordinates

The physical significance of the deformation of the velocity profile

can be explained in the following way. The gas fed through the wall does not have

a horizontal velocity component, as a result of which it slows down the motion

of the gas in the boundary layer. The drag exerts the greatest effect in

the part of the layer where the kinetic energy of the particles is less, i.e., by

the wall. When the pressure gradient is prolonged $dp/dx > 0$, when there is no gas

feed through the wall, the pressure is stepped up through a reduction in the velocity of the outside stream. The pressure across the boundary layer is constant. Particles near the wall with less kinetic energy are slowed down to a greater extent at the same longitudinal pressure drop.

Increase in boundary layer thickness. When the gas is fed through the surface, the velocity profile becomes less complete (Fig. 153). The total mass of decelerated gas is thereby increased - the boundary layer thickens.
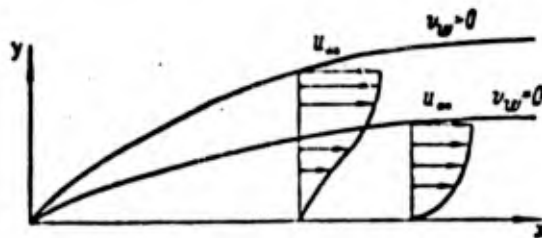
Fig. 153. Increase in thickness of boundary layer

Reduction in friction on the wall

$$\tau_w = \mu(\partial u/\partial y)_y \qquad \tau_w = \rho u_\infty/\delta(\partial \bar{u}/\partial \tau_1)$$

The friction on the wall $\wedge$ or in relative values $\wedge$. As can

$$\partial u/\partial \eta = tg \alpha$$

be seen from Fig. 152, $\wedge$ equals tan α is reduced when the coolant is fed in.

The thickness of the layer δ is increased. Hence, during sweat cooling there is a reduction in friction through the simultaneous action of deformation of the velocity profile and increase in the boundary layer thickness.

Shape parameter f $\wedge$ and coolant feed

The degree of deformation of the profile is described by the shape parameter, $f_w = v_w \delta/v_w$. Let us consider the physical meaning of this parameter

$$f_\mathrm{w} = \frac{v_w \delta}{\nu} = \frac{v_w^2 u_\infty}{u_\infty \nu} = \frac{v_w}{u_\infty} \cdot \frac{\delta}{x} \cdot \frac{u_\infty x}{\nu} . \qquad (10.2)$$

In flow along a plate

$$\frac{\delta}{x} \sim \frac{1}{\sqrt{Re}} , \quad \frac{v}{x^2} \sim \frac{1}{\frac{u_\infty x}{\nu}} .$$

Substituting this result into the equation for f_w, we get

$$f_\mathrm{w} \sim \frac{v_w x}{u_\infty \delta} .$$

The shape parameter is proportional to the ratio of the gas consumption through the plate to the consumption flowing through the boundary layer (Fig. 154).
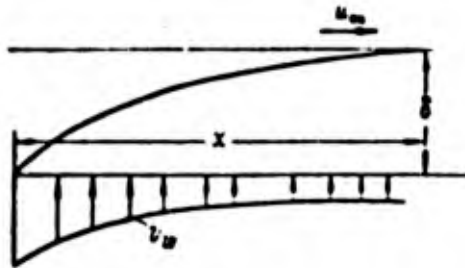
Fig. 154.   Determining physical significance of shape parameter of velocity profile

In the general case, f_w can be variable along the wall. But of special interest is a case in which $f_\mathrm{w} = $ const. If $f_\mathrm{w} = $ const, the deformation of the velocity profile occurs in all sections along the plate to an identical extent. Let us consider at which gas feed $v_\mathrm{w}(x)$ there will be a constant shape parameter

$$f_\mathrm{w} = \frac{v_w \delta}{\nu} = \frac{v_w}{u_\infty} \cdot \frac{\delta u_\infty}{\nu} .$$

but $\delta \sim x \sqrt{Re}$ and therefore

$$f_w \sim \frac{v_w}{u_\infty} \sqrt{Re}.$$

If $f_w = $ const, then $v_w \sim \frac{1}{\sqrt{x}}$. Thus, on a flat plate the shape of parameter f_w is constant when the gas is fed according to $v_w \sim 1/\sqrt{x}$.

Let us determine the variation in the inflection along the surface during laminar flow along a flat plate when $f_w = $ const. We will get

$$\tau_w = \mu \frac{u_\infty}{\delta} \left(\frac{\partial \bar{u}}{\partial \eta} \right)_w.$$

at $f_w = $ const $\left(\frac{\partial \bar{u}}{\partial \eta} \right)_w = $ const

and

$$\tau_w \sim \frac{1}{\delta} \sim \frac{1}{\sqrt{Re}} \sim \frac{1}{\sqrt{x}}.$$

Thus, if $v_w \sim \frac{1}{\sqrt{x}}$, then in every section the amount of coolant supplied is proportional to the friction.

All results that we obtain purely qualitatively can be derived strictly on the .... basis of solution of the differential equation of motion for the boundary layer.

Effect of feeding gas through the surface on temperature distribution and heat exchange

All the conclusions drawn above with regard to the effect of the gas feed

on velocity distribution and surface friction hold as well for heat exchange. There

is deformation of the temperature profile when the coolant is fed in (Fig. 155).

The thickness of the thermal boundary layer is increased. Since the boundary layer

equations do not vary, the relationship between friction and heat-exchange during

flow along a flat plate is retained in the form

$$c_H = \frac{c}{\rho_\infty u_\infty c_p} = \frac{1}{2} c_f \, Pr^{-\frac{2}{3}}.$$

The heat flux to the wall is

$$q_w = \lambda \left(\frac{\partial T}{\partial y}\right)_w = \frac{\lambda}{\delta_T} \left(\frac{\partial T}{\partial \eta}\right)_w.$$

in which

$$\eta = \frac{y}{\delta_T}.$$

When the coolant is fed in, the heat flux is reduced through deformation

of the temperature profile and thickening of the thermal boundary layer. The

deformation of the temperature profile is a function of the shape parameter $f_w \sim v_w \delta / \nu$.

If f_w = const, $v_w \sim 1/\sqrt{x}$, then the heat flux $q_w \sim 1/\sqrt{x}$.
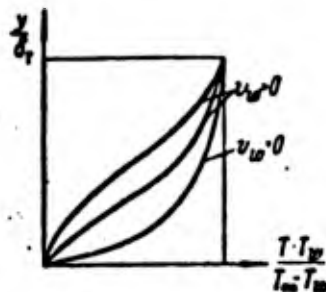
Fig. 155. Temperature and dimensionless
coordinate profile in sweat cooling

- 393 -

Thus, if the coolant is fed in according to $v_w \sim \frac{1}{\sqrt{x}}$, at a

constant wall temperature the heat flux is proportional to the consumption of

coolant. This condition is indeed desirable, since the heat reaching the wall

should be absorbed by the cooling gas.

Sec. 43. Method for Calculating Boundary Layer on Porous Surface

The laminar boundary layer equations in the partial derivatives can be

reduced in a number of cases to ordinary differential equations and solved numerically.

Examples of these solutions can be found in the references.

In the general case the solution can be found by using integral methods.

Integral relationships for laminar layer on plane porous surface

Let us compile a momentum equation for the outline singled out from the

plane plate (Fig. 156). We find

$$\int_0^a \rho u^2 \, dy + \Delta M u_\infty - \int_0^a \rho_\infty u_\infty^2 \, dy = -W.$$

Here ΔM is the amount of fluid flowing over the line $\underline{bc}$;

$$\Delta M = \int_0^a \rho_\infty u_\infty \, dy + \int_0^x \rho_w v_w \, dx - \int_0^a \rho u \, dy.$$
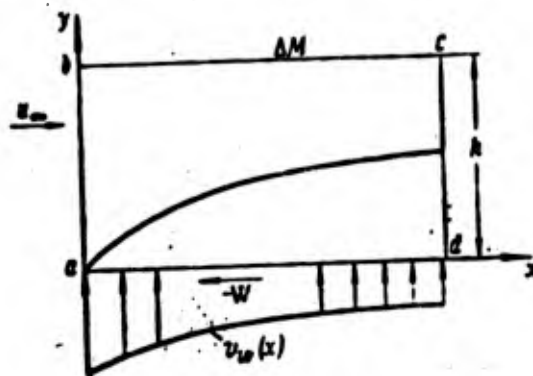
Fig. 156. Derivation of momentum equation
on porous surface

- 394 -

After substitution of $\Delta M \; \overbrace{\;}$ into the initial equation we get

$$W = \rho_\infty u_\infty^2 \int_0^\delta \frac{\rho u}{\rho_\infty u_\infty} \left(1 - \frac{u}{u_\infty}\right) dy - \rho_\infty u_\infty^2 \int_0^x \frac{\rho_z v_w}{\rho_\infty u_\infty} dx.$$

Here $\underline{W}$ is the total resistance acting on the plate of single width

$$W = \int_0^x \tau_w \, dx, \quad \tau_w = \frac{dW}{dx}.$$

$$\frac{\tau_w}{\rho_\infty u_\infty^2} = \frac{d\delta^{**}}{dx} - \frac{\rho_z v_w}{\rho_\infty u_\infty}. \tag{10.3}$$

The equation derived differs from the corresponding equation for an impermeable wall in the second term on the right-hand side.

The integral relationship for energy takes the form (at T_w = const)

$$\frac{q_w}{c \rho_\infty u_\infty (T_\infty - T_w) c_p} = \frac{d\vartheta}{dx} - \frac{\rho_z v_w}{\rho_\infty u_\infty}; \quad \vartheta = \int_0^\delta \frac{\rho u}{\varepsilon_\infty u_\infty} \left(\frac{T_\infty - T}{T_\infty - T_w}\right) dy. \tag{10.4}$$

These equations can be solved by replacing the velocity and temperature profiles by polynomials, only if the shape parameter f_w = const and the velocity and temperature profiles are deformed to the same degree while retaining their similarit, in different sections. But in this case, which corresponds to the cool nt feed a, $\rho_w v_w \sim 1/\sqrt{x}$, an analytical solution may also be obtained.

In the general case we have to resort to numerical calculation of the integral of relationship by breaking up the plate into small areas $\Delta \underline{x}$ and assuming f_w to be constant in each area.

Results of calculations, theoretical formulae and graphs

Flat plate in an incompressible liquid at $\rho_w v_w \sim \frac{1}{\sqrt{x}}$.

Figs. 157 and 158 show the curves for the variation in dimensionless

friction and heat exchange coefficients as a function of f_{-w} , when related by

the following equation

$$Nu = \frac{1}{2} c_f Re \, Pr^{\frac{1}{3}}.$$

Here it is taken that

$$f_w = 2 \frac{\rho_w v_w}{\rho_\infty u_\infty} \sqrt{Re}. \tag{10.5}$$

The corresponding values of $\tau_w^\wedge$ and q_w are determined from the equations

$$\tau_w = \frac{\theta'}{\sqrt{Re}} \rho_\infty u_\infty^2. \tag{10.6}$$

$$q_w = \lambda (T_\infty - T_w) \sqrt{\frac{u_\infty}{vx}} H' Pr^{\frac{1}{3}}. \tag{10.7}$$

It is interesting to note that at the final f_{-w} the friction on the wall

disappears.

The friction distribution across the boundary layer (Fig. 159) is

also determined from this solution. The maximum friction occurs inside the

boundary layer. The maximum points correspond to the points of inflection in

the velocity profile. The line passing through the inflection points is the

current line in the boundary layer (Fig. 160).
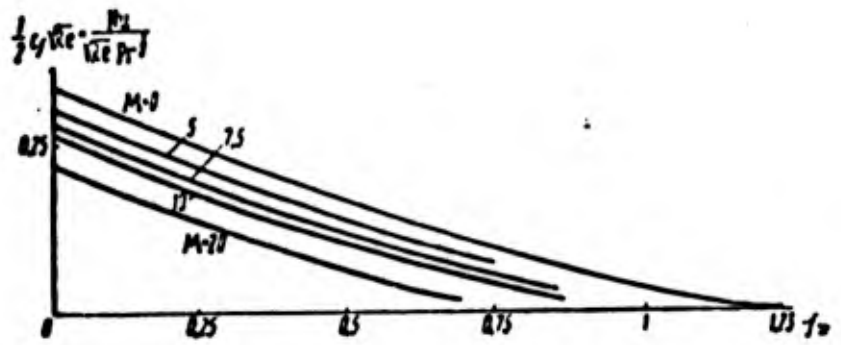
Fig. 157. Variation in friction and heat exchange coefficients as function of intensity of coolant feed in laminar flow
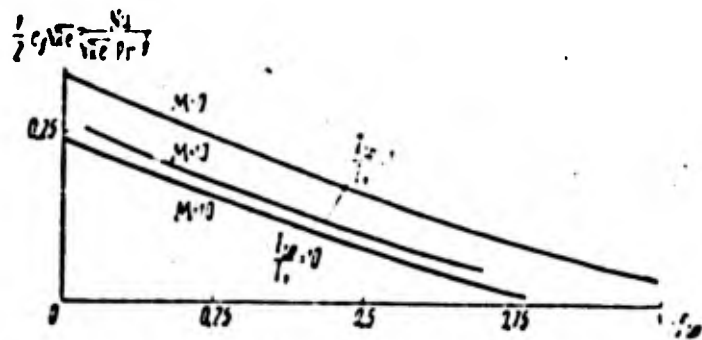
Fig. 158. Variation in friction and heat exchange coefficients as function of coolant feed intensity in laminar flow
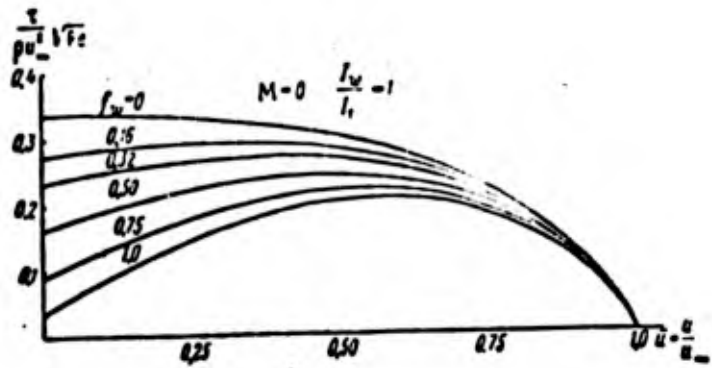
Fig. 159. Distribution of friction and half-boundary layer in sweat cooling

The total gas consumption through the porous plate over the length x from the leading edge is equal to the consumption through a section of the boundary layer taken at the same distance between the wall and the current line passing through the points of inflection on the profiles. This line, as it were, divides the gas fed through the surface from the outside stream. But it should be kept in mind that although there is no convective flow over this line, the molecular exchange between both parts (self-diffusion) is always present.

Flow of a compressible gas along a flat plate. When calculating the flow of a compressible gas, we have to use graphs (Fig. 157 AND 158) which show the variation in Θ' due to f_w at different M numbers and ratios of the gas enthalpy by the wall and in the stream.

From these data we can calculate the friction and heat flux, using the following equations

$$\tau_o = \rho_o u_o^2 \frac{\Theta'}{\sqrt{\frac{u_o \rho_o x}{\mu_o}}},$$ (10.8)

$$q_o = \lambda_o \frac{J_{\infty} - J_w}{c_{p_o}} \sqrt{\frac{u_o \rho_o}{\mu_o x}} \, \Theta' \, \mathrm{Pr}_o^{\frac{1}{3}}.$$ (10.9)

$$J_{\infty} = c_{p_o} T_{\infty} = c_{p_o} T_o \left(1 + \frac{k-1}{2} M_o^2\right)$$

Here λ is the drag enthalpy and J_w is the enthalpy of the gas at the wall temperature.
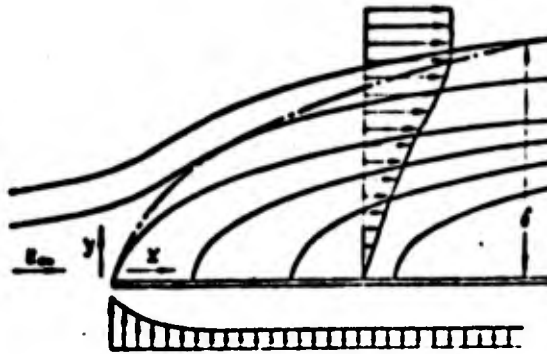
Fig. 160.   Streamlines in boundary layer in sweat cooling

In a case in which dissociation is possible in the boundary layer, the transition from the ⌒ temperatures to enthalpies enables us to take its effect into account.

Flow along the lateral surface of a cone in a supersonic stream. In order to make this calculation we can use the relationships established for a plate, keeping the following rule in mind. At the same distance from the leading edge, the heat flux and friction on a cone are greater than on a plate by a factor of $\sqrt{3}$, if the mass blast velocity is greater than the mass velocity on the plate by a factor of $\sqrt{3}$.

Thus, for the calculation we can use the same graphs as for the plate, taking the following equations into account

$$\tau_w = \frac{\theta'}{\sqrt{Re}}\,\sqrt{3}\,\rho_\infty u_\infty^2,$$ (10.10)

$$q_w = \lambda_\infty\,\frac{J_{0\infty}-J_w}{c_{p_\infty}}\,\sqrt{\frac{u_\infty\rho_\infty}{\mu_\infty x}}\,H'\,Pr_\infty^{\frac{1}{3}}\,\sqrt{3},$$ (10.11)

- 399 -

$$f_v = 2 \frac{\rho_0 r_0}{\rho_\infty \mu_\infty} \frac{\sqrt{Re_0}}{\sqrt{3}}. \qquad (10.12)$$

Here the subscript ∞ indicates the conditions on the boundary

layer boundary (on the surface of the cone during circumflow by an ideal gas).

<u>Flow in the neighborhood of the leading critical point on a flat and</u>

<u>axial-symmetric body.</u> In the neighborhood of a critical point the velocity

distribution corresponds to $u_1 = \beta x$. In order to determine the heat flux we can

use the following formulae: for a flat body

$$q_s = \frac{\lambda_w}{c_{p_w}} (J_1 - J_s) \sqrt{\frac{\beta}{\nu_w}} \theta'_{s,1} \frac{Pr^{\frac{1}{3}}}{(0.71)^{\frac{1}{3}}}, \quad (f_v)_{c,1} = \frac{\rho_z r_w}{\rho_w \sqrt{\beta \nu_w}}; \qquad (10.13)$$

for an axial symmetric body

$$\left. \begin{array}{l} q_w = \frac{\lambda_w}{c_{p_w}} (J_1 - J_w) \sqrt{\frac{\beta}{\nu_w}} \sqrt{3} \theta'_{0c} \frac{Pr^{\frac{1}{3}}}{(0.71)^{\frac{1}{3}}}, \\[3mm] (U_w)_{\infty} = \frac{3}{2} \frac{\rho_0 r_w}{\sqrt{3} \rho_w \sqrt{\beta \nu_w}}. \end{array} \right\} \qquad (10.14)$$

The graphs showing the variation in $\theta'_{s,1}$ and θ'_{μ} as a function of f are

contained in Figs. 161 and 162.
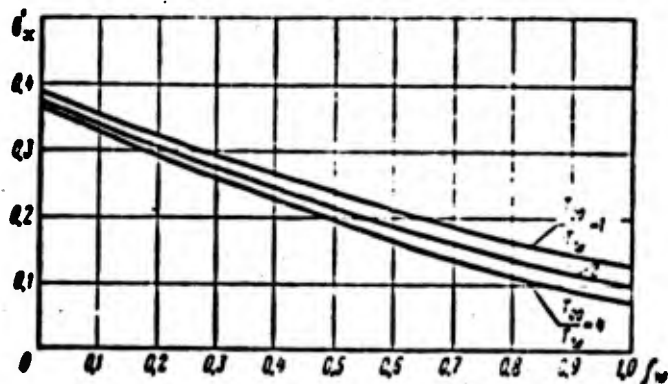
Fig. 161. Variation in θ'_w in sweat cooling in neighborhood
of leading critical point on axially-symmetric body

- 400 -

The graphs have been calculated for Pr = 0.71. In order to extend the solutions to cover other Pr numbers, the multiplier $Pr^{\frac{1}{3}}/0.71^{\frac{1}{3}}$ has been added to the expression for heat flux. The subscript $\underline{v}$ means the conditions at the wall temperature at the leading critical point.

when there is supersonic flow around a blunted body may $\beta = (\partial u \, \partial x)_{x=0}$

be taken as $\quad \beta = a_{s_f} \, r_0 \quad$.

Here α_{cr} is the speed of sound and $\underline{r}_0$ the distance between the critical point and the transition line through the speed of sound (the half-width of the blunted part when the end is flat, or the distance along the surface between the critical point and the section in which the central angle is $\varphi \approx 45°$).
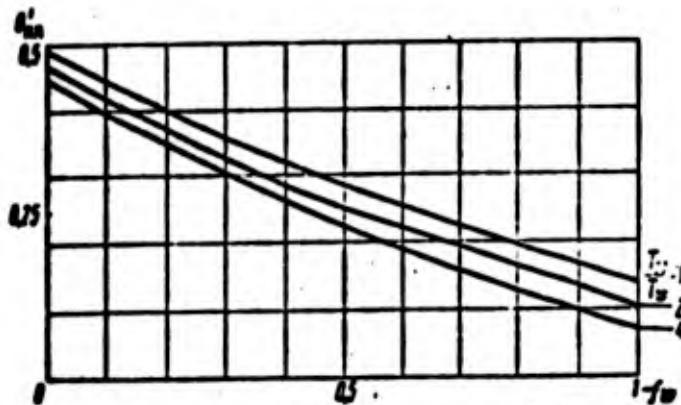
Fig. 162. Variation in θ'_{ax} and θ'_{pl} in sweat cooling in neighborhood of critical points on plane body

Heat balance during heat exchange on porous surface

Let us consider an area of the porous surface (Fig. 163) of length Δx and width 1. Cold gas $g G_{cool}$ with an enthalpy J_0 is fed through the plate from the underside. The enthalpy of the air at the plate outlet is J_{w} .
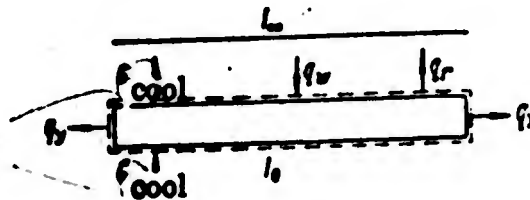
Fig. 163. Derivation of heat balance equation
for porous surface

Let us compile the balance of heat fluxes reaching the outline and emerging from it. We get

$$l\Delta x\, q_w + G_{cool}\, J_0 = G_{cool}\, J_w + l\Delta x\, q_r \dotplus \Sigma q_r.$$

Here q_r is the heat given off through radiation per unit area;

Σq_{γ_2} is the total heat loss through leakage.

$$q_w = \frac{a}{c_{p_a}}(J_a - J_w),\quad G_{cool} = g\rho_w v_w\,\Delta x\, l.$$

Dividing the initial equation by Δxl, we get

$$\frac{a}{c_{p_a}}(J_a - J_w) + g\rho_w v_w J_0 = g\rho_w v_w J_w + q_r + \frac{\Sigma q_\gamma}{\Delta x l}.$$

Disregarding radiation and leakage, we get

$$a = g\rho_w v_w c_{p_\infty} \frac{J_w - J_0}{J_\infty - J_w};$$

we have derived an equation relating the gas consumption to the heat-transfer

coefficient at set wall and stream temperatures.

It follows from the equation that the condition $J_\infty =$ const, $J_w =$ const

may only be satisfied if α is proportional to ρ_w, v_w . As we found earlier,

this condition holds in laminar flow along a flat plate when the coolant is

fed in accordance with $\rho_w v_w \sim 1'\sqrt{x}\,(f_w = \text{const})$.

The heat-transfer coefficient α may be expressed from solution of

the boundary layer equations

$$a = \lambda \sqrt{\frac{u_\infty}{v_\infty x}} \theta' Pr^{\frac{1}{3}}.$$

Substituting this relationships into the heat-flux balance condition,

we get

$$\lambda \sqrt{\frac{u_\infty}{v_\infty x}} \theta' Pr^{\frac{1}{3}} = g\rho_w v_w c_{p_\infty} \frac{J_w - J_0}{J_\infty - J_w};$$

$$\lambda = \frac{g\mu c_p}{Pr}.$$

After transformation we get

$$\frac{\rho_w v_w}{\rho_\infty u_\infty} \sqrt{\frac{u_\infty x}{v_\infty}} = \frac{(J_\infty - J_w)\theta'}{(J_w - J_0)Pr^{\frac{2}{3}}}.$$

But in the case of a plate we get

$$\frac{\rho_w v_w}{\rho_\infty u_\infty} \sqrt{\frac{u_\infty x}{v_\infty}} = \frac{1}{2} f_w.$$

Consequently,

$$\frac{1}{2} f_w = \frac{(J_\infty - J_w)}{(J_w - J_0)} \cdot \frac{w'}{Pr^{\frac{2}{3}}} \, .$$

We have derived this condition from the heat balance. Furthermore, we know the relationship between Θ' and f_w from solution of the boundary layer equations (Figs. 157 and 158).

Excluding Θ' from the equality, we get a graph showing the dependence of f_w on the parameter $\dfrac{J_\infty - J_w}{(J_w - J_0) Pr^{\frac{2}{3}}}$ (Fig. 164).
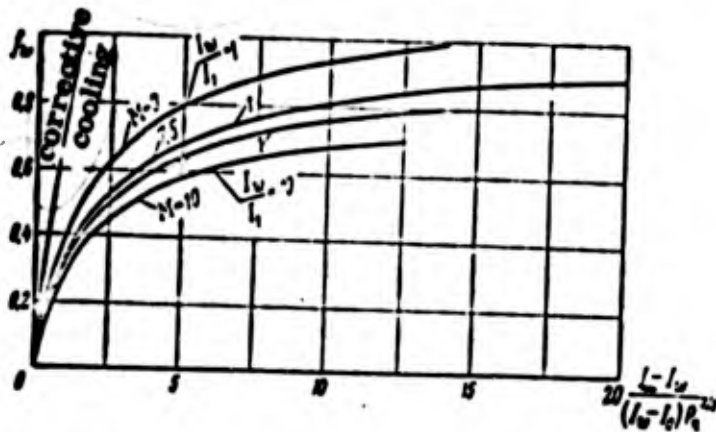

Fig. 164. Graph for calculating coolant consumption

This parameter $\dfrac{(J_\infty - J_w)}{(J_w - J_0) Pr^{\frac{2}{3}}}$ is usually given in advance, we can determine f_w directly from the graph and then work out the consumption of coolant per unit of area $\rho_w V_w$.

Let us consider the most advantageous case in convective cooling, when the wall is very thin and the heat exchange coefficient on the cold side is very high, since the coolent reaches the wall with an enthalpy J_0 and leaves it with an enthalpy $J_2 = J_w$. The balance condition can then be written in the form

$$q_w = \frac{a}{c_{p_w}}(J_w - J_0) = \rho_w v_w (J_w - J_0).$$

In actual fact, on account of the thermal resistance of the wall and the boundary layer on the cold side, the final enthalpy J_2 is less than J_w. The value α does not depend on the coolent consumption for practical purposes

$$\lambda \sqrt{\frac{a_w}{v_w x}}\, \theta_0' Pr^{\frac{1}{3}} = g\rho_w v_w c_{p_w} \frac{J_w - J_0}{J_w - J_w},\quad \theta_0' = \text{const.}$$

After transformation we obtain

$$f_w = 2\frac{J_w - J_w}{J_w - J_0}\,\frac{\theta_0'}{Pr^{\frac{2}{3}}}.$$

In the graph shown in Fig. 164 this equation corresponds to a straight line drawn from the origin of the coordinates at an angle of α, with $\tan \alpha = 2\theta_0'$.

For an incompressible fluid $2\theta_0' = 0.664$. The ratio f_w during convective and sweat cooling is equal to the ratio of the theoretical consumptions required for cooling. As can be seen, sweat cooling becomes particularly advantageous

- 405 -

at high temperature gradients.

<u>Theoretical graphs for flow in neighborhood of critical point</u>

Figs. 165 and 166 show graphs for the dependence of f_w on the

parameter

$$\frac{J_w - J_v}{(J_v - J_0) Pr^{\frac{2}{3}} (0.71)^{\frac{1}{3}}}:$$

for a plane case

$$\rho_w v_w = \rho_v f_w \sqrt{\nu_2 \beta}. \tag{10.15}$$

and for an axial-symmetric case

$$\rho_w v_w = \frac{2}{3} \sqrt{3} \rho_v f_v \sqrt{\nu_v \beta}. \tag{10.16}$$

<u>Disadvantages of sweat cooling</u>

Sweat cooling brings about a saving in coolant, but its use involves

great difficulties. One of them is the need to use a special porous material

with a lower degree of strength than a solid material. In order to be able to

feed the coolant through the porous surface, a certain pressure margin

has to be created.

In sweat cooling, the resistance to friction is decreased, but when

there is an outside flow round the body, the wave resistance is increased through

an increase in the thickness of the boundary layer, and this is particularly marked

- 406 -

on thin bodies at high M flight numbers. When the nozzle of a jet engine is
sweat cooled, there is a certain loss in thrust.

Fig. 167 shows the variation in the thickness of the impulse loss
and displacement on a flat plate as a function of f_{w} .

The value δ^{**} is determined from the impulse equation

$$\rho_\omega u_\omega^2 \delta^{**} = W' + M \cdot u_\omega$$
$$\text{cool}$$

at

$$f_\omega = 2 \frac{\rho_z c_z}{\rho_\omega u_\omega} \sqrt{Re} = \text{const.}$$

We get

$$\frac{\delta^{**}}{x} \sqrt{Re} = \frac{1}{2} c_f \sqrt{Re} + f_x.$$

Let us now consider what the outcome is when δ^{**} and δ^{*} in the
jet nozzle are increased. Let us suppose that for a nozzle calculated for an
ideal fluid we are given a constant total gas consumption. The thrust of this
nozzle of $R_{id} = mu_\alpha$ (Fig. 168). On account of the boundary layer, the true
nozzle has the thrust $R_t = \overline{m (u_a)_t} - \delta^{**} (\rho u_a^2)_t.$

The effective section at the outlet is decreased on account of the
thickness of the displacement, and we get $(u_a)_t < u_a$, through which the thrust
is reduced. But this loss in thrust can easily be recovered by widening

- 407 -
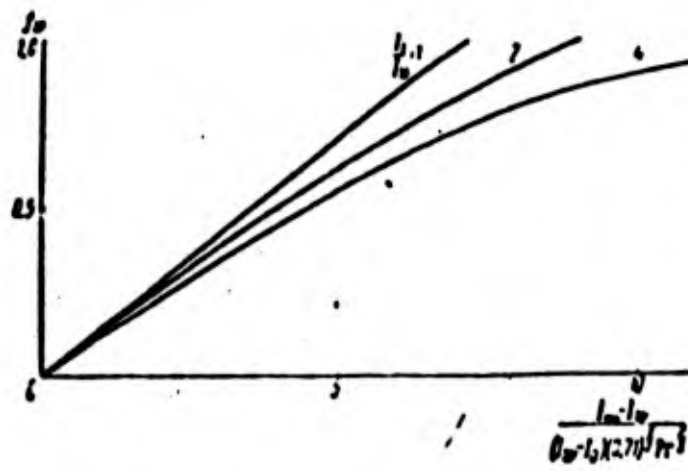
Fig. 165. Graph for calculating coolant consumption (plane body)
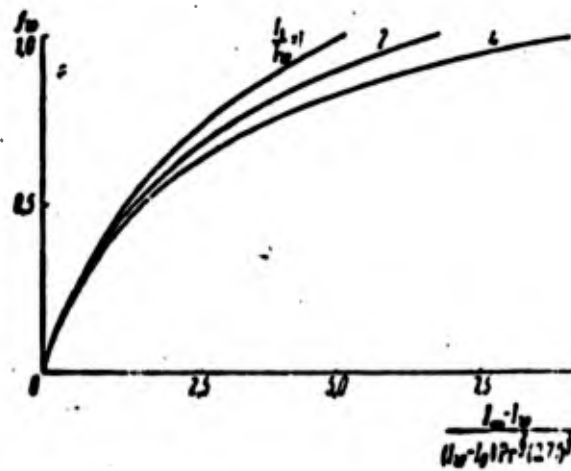
Fig. 166. Graph for calculating coolant consumption (axially-symmetric body)
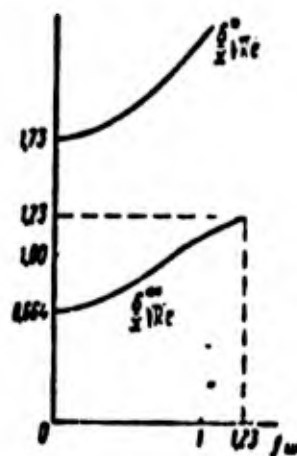
Fig. 167. Variation in thickness of displacement and impulse losses as function of coolant feed intensity

- 408 -

Fig. 168. Supersonic nozzle

the nozzle by a factor of δ^{*}.

Let us compare two cases, in one of which the cooling of the nozzle is convective and the coolant is fed to the combustion chamber, while in the other case cooling is effected by $k\iota$, combustible fed through a porous wall.

The bulk of the gas leaving the nozzle is the same $(\underline{m})$.

Let us consider that both nozzles have been corrected, each one by its emission thickness δ^{*}, and that they have a flow velocity at the outlet $\underline{u}_{\alpha}$.

Then

$$(R_{\zeta})_1 = mu_a - (\delta^{**})_1 \rho_a u_a^2,$$
$$(R_{\zeta})_2 = mu_a - (\delta^{**})_2 \rho_a u_a^2,$$
$$\Delta R_{\zeta} = R_{\zeta_2} - R_{\zeta_1} = -\rho_a u_a^2 [(\delta^{**})_2 - (\delta^{**})_1].$$

Thus, although the <u>friction</u> in the nozzle has been reduced, the thrust has dropped.

- 409 -

If the coolant contributes the extra mass, $\underline{M}_{cool}$, then

$$(R_x)_1 = mu_a - (\delta^{**})_1 \rho_a u_a^2.$$

$$(R_x)_2 = mu_a + M_{cool} u_a - (\delta^{**})_2 \rho_a u_a^2.$$

$$\Delta R_x = R_{x_1} - R_{x_2} = M_{cool} u_a - \delta_2^{**} \rho_a u_a^2 + \delta_1^{**} \rho_a u_a^2 = W_1' - W_2'.$$

In this case the thrust is increased by a value equal to the reduction in the resistance to friction in sweat cooling.

Sec. 45. Sweat Cooling by Gas with Physical Properties Differing From those of Oncoming Stream

In order to reduce the consumption of coolant, we have to select materials capable of absorbing large amounts of heat in such a way that at the set temperature difference between the wall $\underline{T}_w$ and the coolant $\underline{T}_0$, the enthalpy $\underline{J}_w - \underline{J}_0$ absorbed by the coolent is maximum. An evaporating coating is sometimes used in this purpose, the calculation of which can be reduced to that of the porous coolant. Furthermore, the weight consumption of coolant can be reduced by selecting a coolant with physical properties for which the reduction in the heat-transfer coefficient α is greater.

In such cases the boundary layer equations remain unchanged, but we now have to solve the complete system with regard for the diffusion equation. When compiling boundary conditions for these equations, we have to take the heat balance and material on the surface into account. The mass velocity of

- 410 -

of coolant feed and the gas concentration at the wall are related.

Material balance condition. Concentration of impurity at surface.

Let us consider for the sake of simplicity a binary mixture with two components. In the outside stream (Fig. 169) the gas concentration is $C_{g\infty} = 1$, $C_{cool\infty} = 0$, the rate of flow is u_∞. A coolant with concentration $C_{cool\,0} = 1$ is fed through the surface. Concentration of gases at the walls is designated C_{w_g}, $C_{w_{cool}}$, and $C_g + C_{cool} = 1$, the value C being measured in kg/kg.
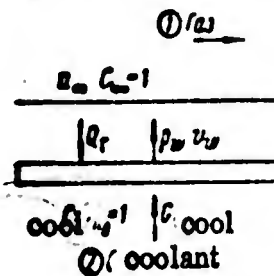
Fig. 169. Diagram of prous cooling by a gas with properties different from those of the flowing stream

The condition for the conservation of mass for the entire mixture is

$$Q_{cool} = g\rho_w v_w.$$

The continuity condition for the first component - the gas takes the form

$$\rho_w v_w C_{w_r} + (Q_{diff})_r = 0. \qquad (10.17)$$

The removal of gas by the stream $\rho_w v_w$ in steady-state conditions is

- 411 -

compensated by inverse diffusion stream Q_r. No gas passes through the wall. The

continuity condition for the second component - the coolant - is written in the form

$$\rho_w v_w C_{w_{cool}} + (Q_{dif})_{cool} = C_{cool}$$

or

$$\rho_w v_w (1 - C_{w_{cool}}) = Q_{dif_{cool}} \qquad (10.18)$$

The coolant fed through the wall is removed from it by diffusion and

convection. Adding the continuity equation for the two components, we get

$$Q_{dif_r} = - Q_{dif_{cool}}$$

In a binary mixture, the diffusion flow of the components is the

same in absolute terms

$$Q_{dif_r} = - \rho D_{r_{cool}} \left(\frac{\partial C_r}{\partial y} \right); \quad Q_{dif_{cool}} = - \rho D_{cool} \left(\frac{\partial C_{r_{cool}}}{\partial y} \right), \; D_{r_{cool}} = D_{cool_r} = D .$$

Thus, the conditions on the wall can bve written in the following form

$$C_{w_r} \rho_w v_w = \rho_w D \left(\frac{\partial C_r}{\partial y} \right)_w \qquad (10.19)$$

or

$$\rho_w v_w (1 - C_{w_{cool}}) = - \rho_w D \left(\frac{\partial C_{r_{cool}}}{\partial y} \right)_w . \qquad (10.20)$$

The concentration of the admixture at the wall is a function of the

mass velocity of the coolant feed

$$C_{w_{cool}} = \frac{\rho_w D \left(\frac{\partial C_{r_{cool}}}{\partial y} \right)_w}{\rho_w v_w} + 1. \qquad (10.21)$$

If $\rho_w V_w$ is very large, $C_w \to 1$. If the diffusion of theg gas from

the wall is large, $C_x \to 0$.

Heat balance on porous surface with physical properties of coolent

differing from those of outside stream

Let us compile the heat balance in the outline (Fig. 170). From now
on all values relating to the gas will be marked with the subscript 1, and those
relating to the coolent with the subscript 2. The heat flux reaching the outline
from the boundary layer through thermal conductivity and diffusion is

$$q_w = \lambda \left(\frac{\partial T}{\partial y}\right)_w +$$
$$+ \sum J_i \rho_w D \left(\frac{\partial C_i}{\partial y}\right)_w .$$

The amount of heat passing through the lower face together with the

coolant is $\quad g \bar{\rho_w v_w J_0}$, and the amounts of heat emerging through the upper face is

$g \overline{\rho_w v_w J_w}$. We get

$$q_w + g \rho_w v_w J_0 = g \rho_w v_w J_w.$$

Hence for a binary mixture

$$\lambda \left(\frac{\partial T}{\partial y}\right)_w + J_{1_w} \rho_w D \frac{\partial C_1}{\partial y} + J_{2_w} \rho_w D \frac{\partial C_2}{\partial y} + g \rho_w v_w J_0 = g \rho_w v_w J_w.$$
$$J_w = C_{1_w} J_{1_w} + C_{2_w} J_{2_w}$$

The enthalpy of the mixture is $\quad$, and J_{1_w} and J_{2_w} are the enthalpy of
each of the components at the wall temperature. Taking the relationship for J_w
into account, we get $\quad \lambda \left(\frac{\partial T}{\partial y}\right)_w + J_{1_w} \rho_w D \left(\frac{\partial C_1}{\partial y}\right)_w + J_{2_w} \rho_w D \left(\frac{\partial C_2}{\partial y}\right)_w =$
$$= g \rho_w v_w (-J_0 + C_{1_w} J_{1_w} + C_{2_w} J_{2_w}).$$

- 413 -

Taking the material balance condition into account, we get

$$\lambda \left(\frac{\partial T}{\partial y} \right)_{w} = g \cdots \cdots \; (J_{2_w} - J_0).$$ (10.22)

On the right-hand side we have the heat which has gone into warming up

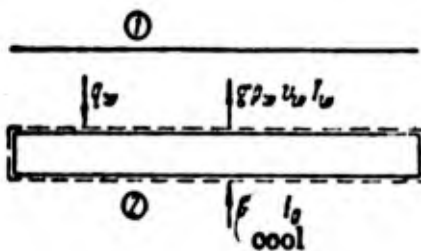the coolant from the initial temperature to the wall temperature.

Fig. 170. Derivation of heat balance equations

Thus, of the entire heat transferred from the stream to the wall

$$q_w = \lambda \left(\frac{\partial T}{\partial y} \right)_w + \sum J_{i} \rho_c D \left(\frac{\partial C_i}{\partial y} \right)_w .$$

only a certain part equal to $\overline{\lambda . (\partial T / \partial y)}$, goes into the wall to heat up the coolant.

The remainder $\overline{\Sigma J_{i} \rho_c D \partial C_i / \partial y}$ compensates the variation in enthalpy of the

stream equal to $(J_w - J_{2_w})$; J_{w} is the enthalpy of the mixture at the temperature T_{w}

may differ from the enthalpy of the coolant at the wall outlet J_{1_w}, although

the temperatures are the same on account of the different thermal capacities

and chemical energy of the component.

- 414 -

It follows from the material balance condition that when solving the boundary layer equations, we cannot set the gas concentration by the wall and the mass velocity of the feed on an arbitrary basis, since they are linked by the condition

$$\left(\frac{\partial C_2}{\partial y}\right)_z = \rho_z v_z (C_{2w} - 1).$$

In practical examples, we are required to determine the amount of heat transferred to the wall $q_{cr} = \Delta q_c$. This part of the total heat transferred from the stream to the wall is equal to

$$q_{cr} = \lambda \left(\frac{\partial T}{\partial y}\right)_w = g_{2z} v_{2z} (J_{2z} - J_0). \qquad (10.23)$$

In order to reduce the consumption of coolant, we must select material with a high enthalpy difference $(J_{2w} - J_0)$. If we use a gas as the coolant, then it should possess a high thermal capacity c_p. Among such gases are the light gases $H_2 (c_p = 3.5)$; He $(c_p = 1.25)$ /14/.

Materials with a high latent heat of vaporization can also be used. Among such materials are water $(r = 530 \text{ kcal/kg})$ /14/. Solid lubricants used for heat insulation may be made of materials capable of evaporating and absorbing large amounts of heat in the process. The maximum heat of evaporation is shown by carbon $(r \approx 12,000 \text{ kcal/kg})$ /14/. When selecting the material we should

also take into account the way in which the heat flux reaching the wall $q_{\wedge wall}$

$= \lambda \partial T / \partial y$ varies.

The weight consumption of coolant can be reduced by reducing $q_{\wedge wall}$.

Preliminary calculations and experimental data show that the use of gases with lower

density as coolants brings about a great reduction in the heat flux.

Eckert and Schneider /18/ have calculated the effect of feeding hydrogen

through a porous plate on the friction coefficient in air at low velocities. The

boundary layer equations take the usual form and the aforementioned material-

balance condition is taken into account in the boundary conditions. It has

been found from this calculation that at the same consumption by weight of

coolant, the friction is reduced considerably. The friction corresponds

approximately to the friction which would occur if a stream with a hydrogen

concentration equal to that of the wall flowed round the plate.

The resulting graph is shown in Fig. 171. Curve 1 shows the hydrogen

cooling, while curve 2 shows cooling effected by air.
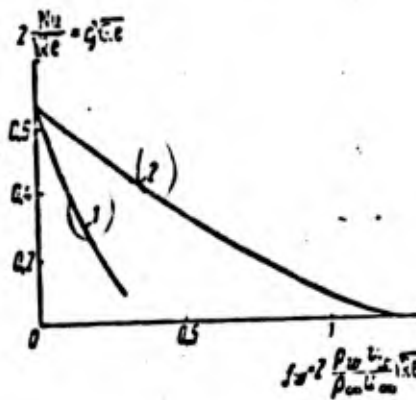
Fig. 171. Comparison of effectiveness in cooling by air (2), and
hydrogen (1)

In his publication /6/ Caernyy considers a boundary layer with an
interface. It is taken that on *the two* sides of the interface there is material
differ-ing in physical properties. In the particular case of friction along
a flat porous plate, as has been pointed out, the *streamline* emerging from the
leading edge of the plate separates the consumption of liquid fed through the
plate from the consumption of liquid arriving at the boundary layer from outside.
If we disregard diffusion, this line is impermeable. By solving the equations
for the external and internal parts of the boundary layer separately, and taking
the mutual effect of both parts into account through conditions on the interface,
the investigator has obtained an expression for the friction as a function of the
ratio of densities of the liquid fed in and the liquid in the outside stream.

Publication /4/ solves the problem of laminar flow around a
plate, taking the diffusion of water vapor into the boundary layer into
account and making certain assumptions for the sake of simplicity at the same time.

Sec. 46. Turbulent Boundary Layer on Porous Surface

A laminar boundary layer can only be established at low Reynolds numbers.
During flow along a porous surface, when the gas is fed to the boundary layer,
the stability of laminar motion is reduced and there is an earlier transition from

from (the) laminar to turbulent regimes.

During turbulent flow there is an increase in heat exchange and resistance, so that at low gas feed rates, sweat cooling may even produce negative results. When the consumption of coolant is further increased, the heat flux, even in the case of turbulent flow, becomes less than the flux on an impermeable surface in laminar flow.

Qualitative aspects of [the] effect of gas feed through surface on turbulent boundary layer

In general, the effect of feeding a mixture to the turbulent boundary layer is similar to the corresponding effect on a laminar layer. The velocity profiles are deformed and become curtailed (Fig. 172), and the thickness of the layer increases. At low feed rates, however, the profiles do not show points of inflection; when the coolant feed rate is further increased, however, there is in effect a point of inflection, and the velocity profile assumes a form similar to that of the profile in free turbulent flow. The deformation of the profile is similar to that of the velocity profile when the pressure gradient is positive.

Qualitatively speaking, we can distinguish three basic types of flow in a turbulent boundary layer with a vertical gas feed. At comparatively low feed intensities, its effect only shows up in the laminar sublayer. If the velocity

- 418 -

profile on an impermeable wall is close to linear in the sublayer (Fig. 173), then

at a low gas feed the velocity profile in the sublayer is deformed, and a

point of ⌒ inflection is obtained. When calculating this case we

assume that the flow in the outside part - the turbulent nucleus - has not changed,

and that all the relationships obtained for an impermeable surface can therefore

be used for the outside part. This theory, which is known as the "film" theory

accords satisfactorily with experiments, even at considerable gas feed rates.
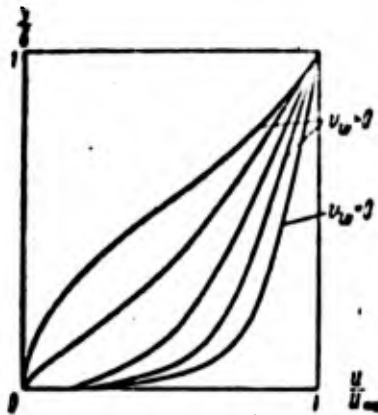
Fig. 172. Velocity profiles in turbulent flow
along porous surface
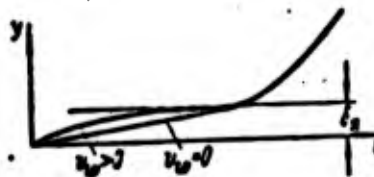
Fig. 173. Deformation of velocity profile in
laminar sublayer

When the feed is *further* ~~increased~~, the effect of the coolant begins to

show up in the turbulent part of the layer as well. This extremely important

case is the most difficult one to calculate theoretically. Here experimental

investigation acquires great importance. But *attempts have been* made to use a

method similar to the one for obtaining a logarithmic law for an impermeable

wall in order to solve this problem. The friction is represented in the form of

the Prandtl equation $\tau = \rho l^2 (du/dy)^2$ (1 is the mixing *length*). Here the gas feed is

taken into account by considering friction across the boundary layer to be variable.

The third flow regime on a porous surface corresponds to a consumption

of coolant for which the effect of the wall on the boundary layer is weakened,

and the boundary layer is rearranged in similar fashion to the boundary layer on

the edge of the turbulent stream. Here there is no longer any effect by the

Reynolds number. When the coolant feed rate is further increased, the boundary

layer separates from the wall completely. The friction and heat exchange

coefficients between the outside stream and the wall vanish completely at this

point.

When calculating this case, we can use the methods employed for free

turbulent flow. The consumption of coolant at which there is detachment of the

boundary layer corresponds approximately to the consumption carried away by the

- 420 -

boundary layer on the edge of the free turbulent stream.

Dimensionless characteristic of coolant feed intensity

In laminar flow the effect of the supply of mixture is described

completely by the shape parameter $f_{\alpha} = 2\dfrac{\rho_{\pi}v_{\pi}}{\rho_{\infty}u_{\infty}}\sqrt{Re} \sim \dfrac{\rho v_{\pi}\rho x}{\mu u_{\infty}\delta}$. The parameter

f_{π} is proportional to the ratio of the total consumption fed through the porous

surface and the consumption flowing into the boundary layer at the given section.

We can take it that a similar ratio describes the effect of the mixture feed

on the turbulent boundary layer as well.

In the boundary layer

$$\frac{\delta}{x} \sim \frac{\tau_{w}}{\mu u_{\infty}^{2}} \sim c_{H},$$

from which

$$\frac{\rho_{w}v_{w}x}{\rho_{\infty}u_{\infty}\delta} \sim \frac{\rho_{\pi}v_{w}}{\rho_{\infty}u_{\infty}}\frac{1}{c_{H}} = f_{\pi}.$$

This parameter can be used, no matter what the blasting intensity.

The experimental data can be processed in the form of the relationship

$$c_{H} = F\left(\frac{\rho_{v}v_{w}}{\rho_{\infty}u_{\infty}}\frac{1}{c_{H}}\right).$$

At low degrees of coolant feed intensity we can assume $\delta/x \sim c_{H_{0}},$ $f_{w} = (\rho_{w}v_{w}/\rho_{\infty}u_{\infty})(1/c_{H_{0}})$.

Here $c_{H_{0}}$ is the dimensionless heat exchange coefficient on an impermeable wall.

At $Re < 10^{7}$ $\dfrac{\delta}{x} \sim \dfrac{1}{Re^{0.2}}$ и $f_{w} \sim \dfrac{\rho_{\pi}v_{w}}{\rho_{\infty}u_{\infty}}Re^{0.2}.$

When the intensity is increased, the relationship between the thickness

of the boundary layer and the Reynolds number is weakened, and $\delta/x \sim$ const. In

this case $f_w = \rho_w v_w \, \rho_\infty u_\infty$.

Thus, in the general case

$$f_v \sim \frac{\rho_w v_w}{\rho_\infty u_\infty} \frac{1}{c_H},\tag{10.24}$$

Since c_H is not known beforehand, it is more convenient to represent

$f_v \sim \frac{\rho_w v_w}{\rho_\infty u_\infty} \mathrm{Re}^a$, in which n (0.2 - 0) decreases as the cool^a nt feed increases and the

Reynolds number $\mathrm{Re} = \frac{u_\infty x \rho_\infty}{\mu_\infty}$ increases.

Fundamentals of film theory of sweat cooling

Let us consider the equation for motion in a laminar sublayer in an

incompressible liquid (Fig. 174)

$$\rho u \frac{\partial u}{\partial x} + \rho v \frac{\partial u}{\partial y} = \frac{\partial \tau}{\partial y}.$$

In view of the fact that the thickness of the laminar sublayer is

very small $\delta_l / x \ll 1$, we can take it that inside it $\partial u / \partial x = 0$. It follows

from the continuity equation $\partial u / \partial x + \partial v / \partial y = 0$ that $\partial v / \partial y = 0$, and that therefore $v = v_w$.

The equation can now be written in the form

$$\rho v \frac{\partial u}{\partial y} = \frac{\partial \tau}{\partial y}$$

or

$$\frac{\rho v_w}{\mu} \mu \frac{\partial u}{\partial y} = \frac{\partial \tau}{\partial y}$$

- 422 -

and

$$\frac{v_w}{v}\tau=\frac{\partial\tau}{\partial y},$$

from which

$$\tau=Ce^{\frac{v_w}{v}y}.$$

At $\quad\overset{y=0\ \tau=\tau_w}{\wedge}\quad$ and $\quad C=\tau_w$. As a result we get

$$\tau=\tau_w e^{\frac{v_w}{v}y}.$$

Let us take it as the second condition that on the sublayer boundary

at $\quad y=\delta_4,\ \tau=\tau_4$.

$$\tau_4=\tau_w e^{\frac{v_w}{v}\delta_4},\quad \tau_w=\tau_4 e^{-\frac{v_w}{v}\delta_4}.$$

Thus, if the friction across the laminar sublayer is constant on an

impermeable wall, in sweat cooling the friction is less on the wall than on the

boundary of the laminar sublayer. In the film theory it is assumed that τ on

the border of the sublayer remains the same as when no coolant is fed through.
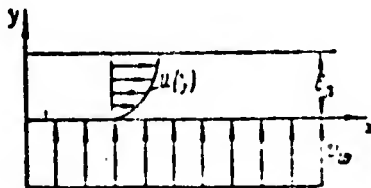
Fig. 174. Concept of film theory of sweat cooling

We are now left with determining the thickness of the laminar sublayer; experimental data for the velocity distribution in turbulent boundary layers tell us (Fig. 131) that the region of transition from laminar flow with linear velocity distribution in the laminar layer to turbulent flow with logarithmic distribution in the turbulent nucleus corresponds roughly to $u_\tau y/\nu = 10$,

In which $u_\tau = \sqrt{\dfrac{\tau_w}{\rho}}$; for $\tau_w = \tau_s$ $u_\tau = \sqrt{\dfrac{\tau_s}{\rho}}$.

The product $u_\tau y/\nu$, constructed along the lines of the Reynolds number, describes the stability of the flow in the laminar sublayer. Let us suppose that the transition from laminar to turbulent flow in sweat cooling occurs at the same value $u_\tau y/\nu = 10$.

The thickness of the laminar sublayer δ_l is then determined by the equation

$$\delta_l = \frac{10\nu}{\sqrt{\dfrac{\tau_s}{\rho}}}.$$

Thus,

$$\tau_w = \tau_s e^{-10\frac{v_w}{\sqrt{\frac{\tau_s}{\rho}}}} = \tau_s e^{-10\frac{v_w}{u_\infty}\sqrt{\frac{1}{2}c_{f_s}}},$$

in which $c_{f_s} = 2\dfrac{\tau_s}{\rho_\infty u_\infty^2}$ is determined from friction data for an impermeable wall

$$c_{f_s} = 0.057 \, Re_x^{-0.2} \text{ and } Re_x = \frac{u_\infty x}{\nu}.$$

- 424 -

Finally, in sweat cooling

and then

$$c_f = 0.057\, \mathrm{Re}_x^{-0.2} e^{-\frac{v_w}{u_\infty}\sqrt{\frac{10}{0.029 \mathrm{Re}_x^{-0.2}}}}$$

$$c_H = \frac{1}{2} c_f \mathrm{Pr}^{0.4}$$

$$q_* = 3600 g \rho u_\infty c_p (T_\infty - T_w) \cdot 0.029\, \mathrm{Re}_x^{-0.2} e^{-\frac{v_w}{u_\infty}\frac{10}{\sqrt{0.029 \mathrm{Re}_x^{-0.2}}}} \; \mathrm{kcal/m^2 hr.} \qquad (10.25)$$

Experimental relationships

Flow along a flat plate. Fig. 185 shows the velocity distribution in

the boundary layer. As the blasting intensity is increased, the thickness of

the layer increases, the velocity profiles become more and more asymptotic,

striving toward the form of the profiles at the *detachment* point of the boundary

layer when the pressure gradient is positive, *or* to the form of the profile

in free turbulent flow.
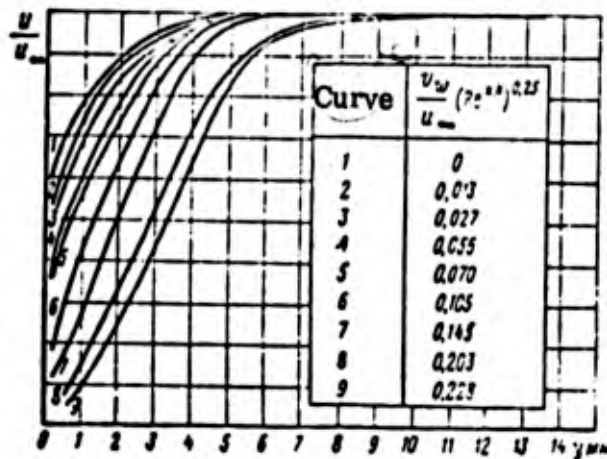
Fig. 175. Variation in shape of velocity profiles in increase in coolant feed intensity

Fig. 176 shows temperature profiles from which we can see similar

deformation when the coolant feed is increased. Fig. 177 shows experimental

curves for the ratio $c_H/(c_H)_{V=0}$ when air flows round a plate, and air and

helium are fed through a porous surface. Curves 1 and 3 have been obtained

at M-3, and a wall-stream temperature ratio $T_W/T_1 \approx 3.3$; $Re_x \approx 4 \cdot 10^6$ /9/.
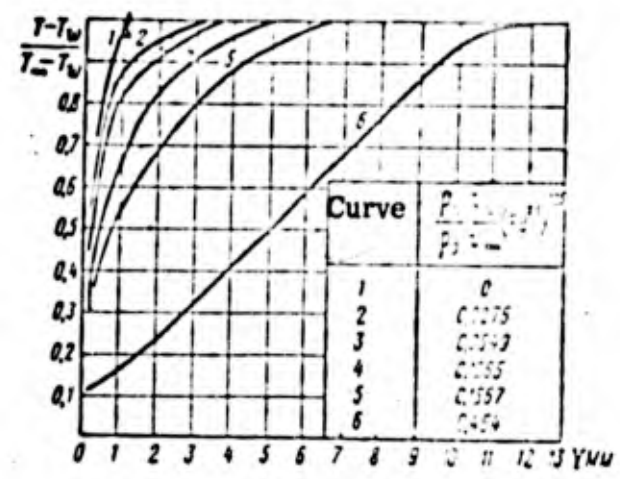
Fig. 176. Variation in temperature across boundary at different coolant feed intensities.
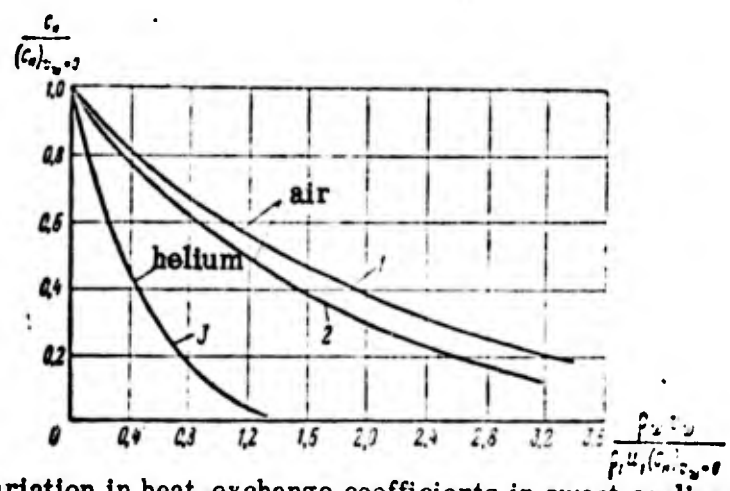
Fig. 177. Variation in heat-exchange coefficients in sweat cooling on plates with turbulent boundary layer

Curve 2 corresponds to experiments with low velocities at $\frac{T_z}{T_l} \approx 1$ and $M \approx 0$ over the

Reynolds number range $9 \cdot 10^4 \leqslant Re_x < 3.3 \cdot 10^6$ /2/. The ratio $\frac{h_z r_z}{\lambda_z \lambda_z} \frac{1}{(c_H)_{t_w=0}}$ is plotted

along the x-axis. These graphs can be recommended for use in calculations. Fig. 178

shows Hacker's experimental data /13/ for the friction coefficient (the curve

has been drawn through the experimental points with a spread of $\pm 10\%$).
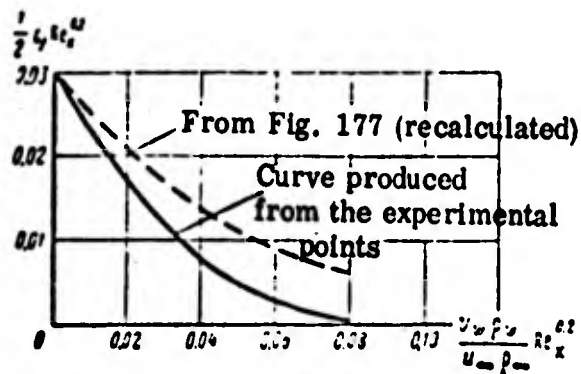
Fig. 178.   Variation in friction coefficients as function of coolant feed
intensity in turbulent flow

It also plots data for curve 2 from Fig. 178.

Experimentation has shown that when we attain the number

$$\frac{v_w \rho_w}{u_\infty \rho_\infty} Re_x^{\frac{1}{5}} = 0.03$$

the boundary layer is detached, and forced away from the wall, which accords with

the conclusions drawn from the above qualitative arguments. It should be pointed

out, however, that measurements under the extreme regime $\tau_w \approx 0$ are extremely inaccurate.

This publication refers to the fact that at high gas feed intensities

through the surface the velocity profiles are S-shaped and similar to those

in free turbulent streams.

REFERENCES

1. Avduyevskiy, V. S. and others. Laminar boundary layer in compressible gas on porous surface with heat and mass exchange. Herald of AS USSR, OTN, Mechanics and Machine Building, 1960.

2. Dorrans, R. and others. Effect of feeding mixture on surface friction and heat transfer in compressible turbulent layer, "Mechanics, For. Lit. Press, 1955, No. 3.

3. Krokko, L. Approximate theory of porous condenser or film cooling by reactive action, "Rocketry", For. Lit. Press, 1953, No. 5.

4. Samozvantsev, M. P. Evaporation of liquid with longitudinal flow around plate. "Heat Engineering", 1956, No. 5.

5. Shlikhting, G. Theory of boundary layer, For. Lit. Press, 1956.

6. Chernyy, G. G. Laminar motion of gas or liquid in boundary layer with interface, Herald of AS USSR, OTN, No. 6, 1958.

7. Eckert, E. and others. Method of calculating laminar heat transfer during flow round a cylinder of arbitrary section of air, "Mechanics", For. Lit. Press, 1956. No. 2.

8. Eckert, E., Schneider, P., Effect of Diffusion in an Isothermal Boundary Layer, JAS, 1956, No. 4.

9. Leadon, K., Scott, J., Mass Transfer Cooling at Mach N JAS, 1958, No. 1.

10. Eckert, E., Schneider, P., Mass Transfer Cooling of a laminar Boundary Layer by Injection of Sight-Weight Fouign Gas, JAS, 1958, No. 1.

11. Korkegi, R., Transition Studies and Skin Friction Measurements on an Insulate Flate Plate at a Mach Number of 5, 8 JAS, 1956, No. 2.

12. Leadon, K., Scott, J., Transpiration Cooling Experiments in a turbulent Boundary Layer at M-3, JAS, 1950, No. 8.

13. Hacker, K., Empirical Prediction of Turbulent Boundary Layer justability dlong a Flate Plate with the Constant Mass Addition at the Wall, Jet Propulsion, 1956, No. 9.

14. Kutateladze, S. S., and other. Textbook on heat transfer, Gosenergoizdat, 1959.

BARRIER AND COMBINED COOLING OF COMBUSTION CHAMBER

WALLS AND NOZZLES IN JET ENGINES

Barrier and combined cooling are the basic methods used to cool combustion

chambers and nozzles in jet engines. Systems of barrier and combines cooling

are shown in Fig. 179.
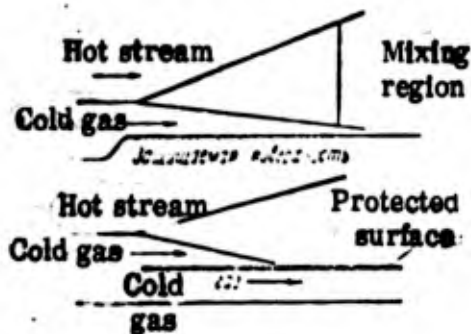
Fig. 179. Barrier and combined cooling

Barrier cooling is simple from the point of view of design. A high

pressure drop is not required to feed the cold gas through a slot, and air *fed*

from *a/* duct at the combustion chamber inlet is usually used for cooling purposes.

In the common designs there is a series of consecutive slots for feeding in the

cold air.

If there is a chance of high variation in pressure or pulsations in

the pressure along the cooled perimeter of the combustion chamber or nozzle,

it may transpire that in certain areas the cold jet, which possesses a small head

with respect to the mean pressure in the chamber, cannot overcome the counter-

pressure, *and this* may result in local overheating. If this is *a danger*, we have

to have a large pressure margin in the cavity with the cold gas, while an additional

resistance must be prevented in the outlet slot.

Sec. 47. Flow during Barrier and Combined Cooling

Let *us* use the term barrier cooling to mean the type of

cooling in which the wall on the outside is insulated or almost insulated, so

that we can disregard the removal of heat through the wall.

Let us first consider an ideal case in which there is no friction on

the wall. Here the wall may be regarded as the plane of symmetry of a free

turbulent jet in a high-speed stream (Fig. 180).

In *a* free stream we can single out *an* initial area in which

there is a constant velocity nucleus, a transient area and a *principal* area (Fig. 80).

For the sake of simplicity let us adopt a conditional system in which

the jet consists of an initial and a *principal* area.

Fig. 181 shows the velocity and temperature distribution in various

cross-sections of the free jet. In the initial area the temperature and velocity

on the stream axis remain constant and equal to their values in the outlet section.
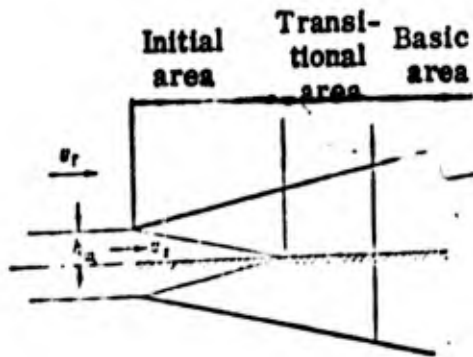
- 432 -

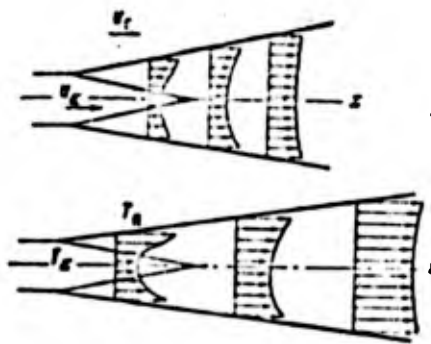Fig. 180.   Calculating boundary cooling

Fig. 181.   Velocity profiles and temperature
profiles in turbulent free jet discharged
into coflowing stream, velocity of which
is greater than discharge velocity.

In the   ˹principal˺ area there is a gradual variation in velocity and temperature of the

gas on the stream axis. As the distance from the outlet section increases, the

velocity and temperature tend to their values in the outside stream. This pattern

corresponds to a case in which there is no friction or heat exchange on a plate

situated in ˹the˺ /plane of symmetry in the stream.

Let us now consider the picture when there is a thermally± insulated

plate in the stream axis, and when there is friction (Fig. 182). On account of

- 433 -

this friction a boundary layer of thickness δ is formed on the surface.

In the boundary layer there is a drop in velocity to zero at the wall. Since the wall is insulated, the temperature across the boundary layer remains constant and equal to what it was on the layer boundary. The variation in temperature on the stream axis (wall temperature) is shown in Fig. 183. The continuous line corresponds to a case in which there is no boundary layer on the wall (no friction), while the broken line shows the case considered of a thermally insulated surface.

The calculations involves the problem of finding the temperature distribution along the wall and determining x_{ef} - the distance over which the temperature of the wall does not exceed the tolerance.

In combined cooling, the wall is protected by a cold stream on one side and is further cooled by the flow on the other. The velocity distribution across the boundary layer remains the same as in barrier cooling. The temperature distribution in this case is shown in Fig. 184.

Sec. 48., Calculation of Wall Temperature in Barrier Cooling

Initial area of stream

In order to calculate the initial area, we have to determine the flare angles of the displacement region of the stream α_1 and α_2 (Fig. 185).
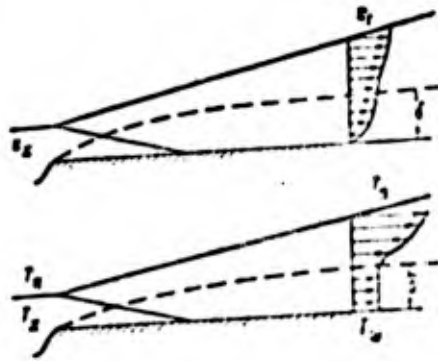
Fig. 182 . Effect of wall boundary layer on velocity and temperature distribution in barrier cooling
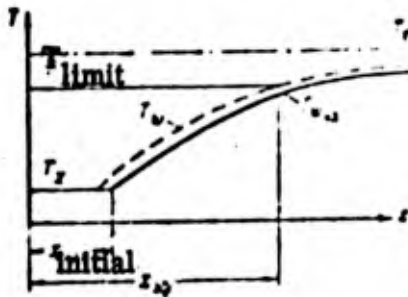

Fig. 183 . Variation in temperature of wall T_w in barrier cooling ($T_{w_{id}}$ without taking effect of wall boundary layer into account)
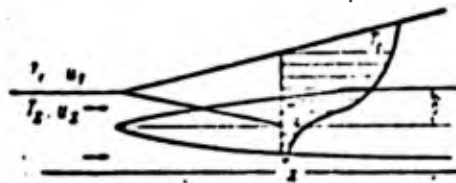

Fig. 184. Combined cooling

The angles α_1 and α_2 are functions of the velocity ratio $\underline{m} = \dfrac{u_{\kappa}}{u_g}$.

Fig. 186 shows the variation in the tangents of the flare angles of the displacement region $\tan \alpha_1$ and $\tan \alpha_2$ as functions of $\underline{m}$. The broken lines correspond to theoretical values, while the solid lines represent experimental values. The theoretical calculations show $\tan \alpha_1 = \tan \alpha_2 = 0$ at $\underline{m} = 1$. This is due to the fact that the turbulent viscosity $\mu_\tau = \epsilon l^2 (\partial u / \partial y)$ μ is proportional to the velocity gradient even at $u_g \rightarrow u_\tau, \partial u / \partial y = 0$.
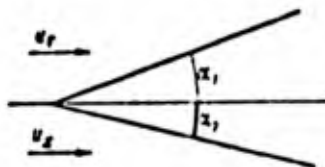

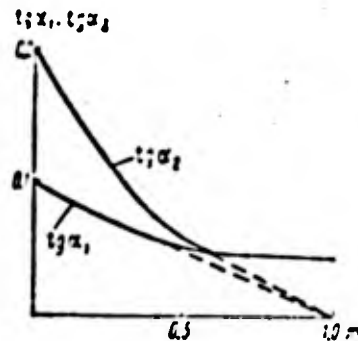Fig. 185. Flare angles of mixing region in initial area

Fig. 186. Variation in flare angles for mixing regions as function of $m = u_g / u_\tau$.

In actual fact, apart from turbulent viscosity, there is laminar viscosity, laminar diffusion and thermal conductivity, the effect of which begins to show up when the turbulent, thermal conductivity and diffusion are reduced.

The mixing streams also have an initial turbulence due to the presence

of the boundary layer along the wall dividing the stream, and to various

pertubations upstream. this, these factors (that) determine the width of the mixing

region at $u_\wedge = u_x$. But the least flare angle of the mixing region, and therefore

the greatest length of the initial area, where $T_w = T_{and}$, occurs at $u_x = u_q$.

In the general case we must distinguish between dynamic and thermal mixing

zones. Experiments show that at $m < 0.4$ the dynamic mixing zone is somewhat

narrower than the thermal one; at $0.4 < m < 1$ the outer boundaries of the

thermal and dynamic zones coincide. Let us take it throughout that the dynamic

and thermal mixing zones coincide.

In order to determine the length of the initial area, we must know

theposition of the "pole" of the mixing zone - the position of the point at

which the boundaries of the mixing zone intersect. If the wall dividing the

two streams is infinitely thin, the pole is located at the end of the wall, at

the point where the stream converges. If the wall thickness is increased, the pole
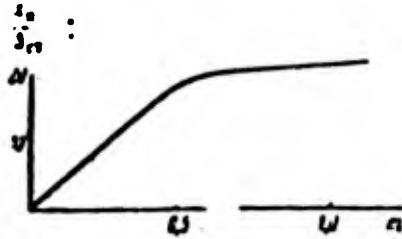
is displaced upstream (Fig. 187).

Fig. 187. Variation in position of pole
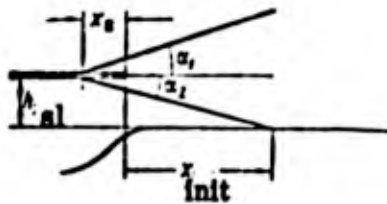in mixing region as function of wall
thickness

Fig. 188. Concept of pole of mixing region

The length of the initial area reckoned from the point of convergence

of the stream may now be calculated from the equation (Fig. 188)

$$x_{init} = \frac{h}{tg\,a_2}\cdot\frac{1}{st} - x_a.$$

(11.1)

in which $x_{-\alpha}$ is determined from the graph in Fig. 187, while tan α_2 is calculated

from the one in Fig. 186.

Calculation of principal area

A great deal of experimental research on free turbulent streams has

made it possible to find a universal law governing (the velocity distribution in the

principal area of the het

- 438 -

$$\frac{u_t - u}{u_t - u_{oc}} = \left[1 - \left(\frac{y}{b}\right)^{\frac{3}{2}}\right]^2. \tag{11.2}$$

Here y is the distance from the stream axis, and $\underline{b}$ is half the stream width.

The temperature distribution is taken to be similar to the velocity distribution

$$\frac{T_t - T}{T_t - T_{oc}} = \frac{u_t - u}{u_t - u_{oc}}. \tag{11.3}$$

The velocity and temperature distributions on the stream axis are then also similar to each other

$$\frac{T_{oc} - T_s}{T_t - T_s} = \frac{u_{oc} - u_t}{u_t - u_s}.$$

In order to determine U_{oc} and T_{oc} on the stream axis let us compile an equation for the momentum of the free stream, using the condition $p = $ const. Let us assume that on the stream axis there is a wall without friction or heat exchange (Fig. 189)

Then

$$h_s \rho_s u_s^2 + (b - h_s) u_t^2 \rho_t = \int_0^b \rho u^2 \, dy.$$

Having divided both parts of the equality by $b u_t^2 \rho_t$, we get, after transformation,

$$1 - \overline{h}_{s1}\left(1 - \frac{m^2}{n^2}\right) = \int_0^1 \left(\frac{u}{u_t}\right)^2 \frac{T_t}{T} \, d\overline{y}.$$

- 439 -

then

$$m=\frac{u_s}{u_r}, \quad n=\frac{T_s}{T_a}, \quad \bar{h}_{sl}=\frac{h_{sl}}{b}, \quad \bar{y}=\frac{y}{b}.$$

The integral on the right-hand side can be transformed on the basis of the condition

$$\frac{u_r-u}{u_r-u_{oc}}=\frac{T_r-T}{T_r-T_{oc}}=\left[1-\bar{y}^{\frac{3}{2}}\right]^2$$

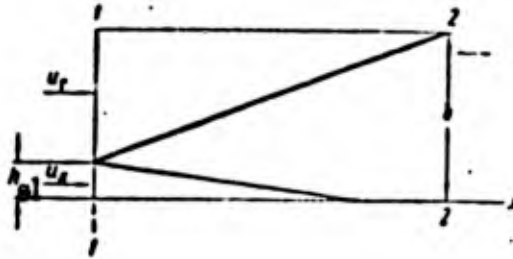so that it is a function of the value $\bar{u}_{oc}=u_{oc}/u_r$.

Fig. 189. Derivation of momentum equation

In the general case the calculations are complicated, but for practical purposes we can approximately determine the distribution of the axial values at $\underline{n}\approx 1$, $\underline{T_x}/\underline{T_y}\approx 1$.

This gives wall temperatures which are too high. In this case

$$\bar{h}_{sl}(1-m^2)=0.9(1-\bar{u}_{oc})-$$
$$-0.3155(1-\bar{u}_{oc})^2. \qquad (11.4)$$

This equality shows the relationship between $1-\bar{u}_{oc}$ and h_{sl}/b (Fig. 190).
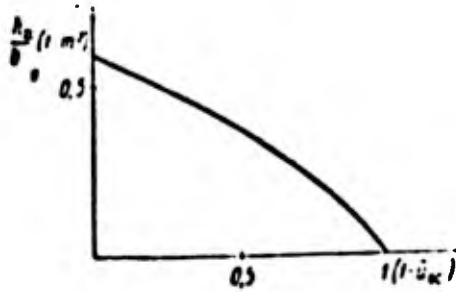
- 440 -

Fig. 190. Calculation of barrier cooling

Half the stream width is approximately equal to $b = \tan \alpha_1 (x \div x_a{}')$. Here

x is the distance between the converging point of the stream and the section under

consideration, x' is the distance between the converging point and the pole of the

basic area (where the boundary of the mixing region of the basic area intersects

the stream axis). Taking it for purposes of approximation that the boundaries

of the stream pass through the edge of the slot (Fig. 191), we get the equation

$$b = x \, \mathrm{tg}\, \alpha_1 + h_{sl}.$$

Taking the substitution into account (Fig. 190), we find the dependence

of $(1 - \bar{u}_{\alpha})$ on x, after which we derive u and T from the equations

$$\frac{u_{oc} - u_s}{u_t - u_s} = \frac{T_{oc} - T_s}{T_t - T_s} = 1 - \frac{1 - \bar{u}_{oc}}{m}. \tag{11.5}$$
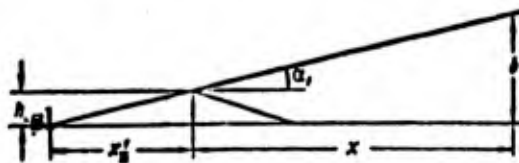

Fig. 191. Determining b

- 441 -

Calculation of wall boundary layer

Calculation of the initial and basic areas gives us the temperature and velocity distribution along the axis T_{Ax} (x) and u_{Ax} (x), the dependence of the stream width on the distance b (x) and the velocity and temperature distribution in the cross-sections of the stream

$$\frac{T-T_{oc}}{T_t-T_{oc}}=\frac{u-u_{oc}}{u_t-u_{oc}}=\left[1-\left(\frac{y}{b}\right)^{\frac{3}{2}}\right]^2.$$

This distribution is derived without regard for the effect of the boundary layer formed on the plate. In the first approximation it can be taken that the effect of friction on the wall is restricted to the region of the wall boundary layer.

In order to calculate the thickness of the boundary layer we can use the equation

$$\delta = 0{,}37\,(\nu/U)^{0.2}x^{0.8}. \tag{11.6}$$

In this equation U is variable on the boundary of the boundary layer, and the calculation has to be carried out by successive approximations. For practical purposes, however, we can take it that $U = \frac{u_t + \overline{u}_t}{2}$ when calculating the thickness of the layer, and that ν is determined as the temperature $T = \frac{\dot{T}_t + \widetilde{T}_t}{2}$.

Knowing the thickness of the boundary layer we can find the velocity and temperature on its boundary u_δ and T_δ from the equations for the distribution of u and T in different sections of the stream.

In combined cooling through a wall there is heat exchange. Barrier

cooling is a particular case at $q_w = 0$.

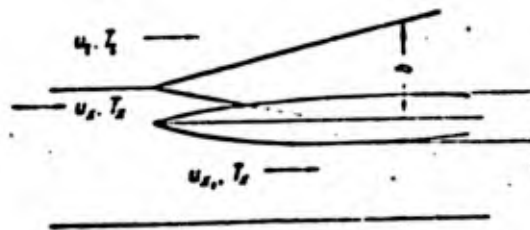The calculation of combined cooling is made in the following sequence

(Fig. 192)

Fig. 192. Combined cooling

1. At the set $m = u_x/u_s$ we find $\tan \alpha_1$ and $\tan \alpha_2$ (Fig. 188).

2. We determined the length of the initial sector $x_{init} = \dfrac{h \cdot sl}{tg\,\alpha_2} - x_s$

(x_π is determined from Fig. 182).

3. We calculate half the stream width $b = tg\,\alpha_1 x + h_{sl}$

4. From the graph in Fig. 190 we find $(1 - \overline{u}_{Ax})$.

5. We find u_{Ax} and T_{Ax} from the equation

$$\frac{u_{oc} - u_s}{u_t - u_s} = \frac{T_{oc} - T_s}{T_t - T_s} = 1 - \frac{1 - u_{oc}}{m}.$$

6. We find the thickness of the wall boundary layer

$$\delta = 0.37 \left(\frac{\nu_{cp}}{\frac{u_s + u_t}{2}} \right)^{0.2} x^{0.8}.$$

- 443 -

7. We find u_δ and T_δ

$$\frac{T_\delta - T_{0c}}{T_t - T_{0c}} = \frac{u_\delta - u_{0c}}{u_t - u_{0c}} = \left[1 - \left(\frac{\delta}{b}\right)^{\frac{3}{2}}\right]^2.$$

8. We find the heat-exchange coefficients

$$a_1 = 0.0225 \cdot 3600 g \gamma_\delta u_t c_p \left(\frac{u_t \delta}{\nu_\delta}\right)^{-\frac{1}{4}} \mathrm{Pr}^{-\frac{2}{3}}.$$

9. We find the heat-exchange coefficient with the outside

$$a_2 = 0.0296 g \gamma_{z_1} u_{z_1} c_p \left(\frac{u_{z_1} x}{\nu_{z_1}}\right)^{-0.2} \mathrm{Pr}^{-\frac{2}{3}}.$$

10. The wall temperature is determined from the equation

$$\frac{T_w - T_z}{T_\delta - T_z} = \frac{1}{1 + \frac{a_2}{a_1}};$$

at $\alpha_2 = 0$, $T_w = T_\delta$.

Sec. 50. Results of Calculations and Experimental Data

The velocity and temperature profiles obtained experimentally accord

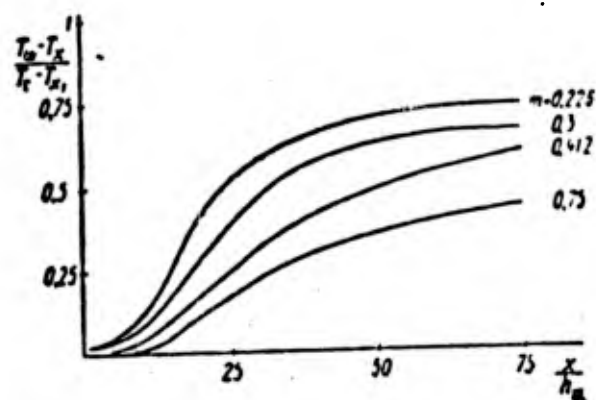satisfactorily with the data obtained by calculation by the system set forth above.

Fig. 193. Variation in wall temperature along insulated
surface as function of relative distance from slot
x/h_{sl} at different m

Fig. 193 shows the experimental temperature distribution along a thermally insulated surface in barrier cooling. It follows from the graph that when $m = u_x/u_s$ is increased, the effectiveness of the cooling is improved, and the distance x_{ef} over which the wall temperature remains lower than a value based on consideration of strength, is increased. Here the length of the initial area is also increased (Fig. 194).

Economic advantage of cooling. The consumption of coolant through a slot of height h and width equal to unity is determined from the equation

$$G_{cool} = h_s \rho_s u_s g \cdot 1.$$

Here the consumption per unit area of the protected surface is equal to

$$G = \frac{g \rho_s u_s h_s \cdot 1}{x \cdot 1} = \gamma_s \frac{u_s}{x} = \gamma_s u_s \frac{m}{x} \, kg/sec \cdot m^2 \qquad (11.7)$$

in which

$$\bar{x} = \frac{x}{h_{sl}}.$$

Having set ourselves some values of $\frac{T_v - T_s}{T_v - T_s}$, we find the corresponding values of m from the graph in Fig. 193 for different x, and then we find m/x.

Fig. 195 shows the dependence of G on m calculated at $u_s = 100$ m/sec. It follows from the graph that the economic advantage of barrier cooling decreases as $m = u_x/u_s$ increases. When the velocity u_x is increased, the consumption of

cool'nt increases more rapidly than the operational range.
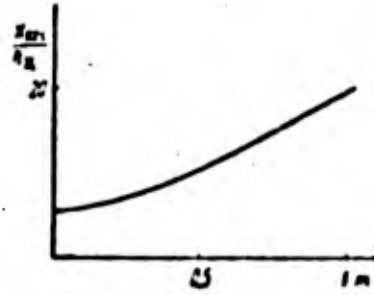

Fig. 194. Variation in length of initial area --
as function of m

Fig. 195. Variation in specific coolant consumption
in barrier cooling

References.

1. Abramovich, G. N. Theory of turbulent streams, Fizmatgiz, 1960.

Film cooling is used to cool and thus protect against erosion the walls of the combustion chambers and nozzles in liquid propellent rocket engines /1/. The need for film cooling arises in view of the fact that at high heat flows occurring in liquid-propellent rocket engine chambers, external cooling of the chamber is an extremely difficult problem on account of the considerable temperature difference between the inside and outside surfaces of the wall. Furthermore, if the fuel is used as the coolant, its thermal capacity may not be sufficient to absorb the transferred heat. At high heat flows there is also a danger of certain areas of the wall overheating with local boiling of the coolant.
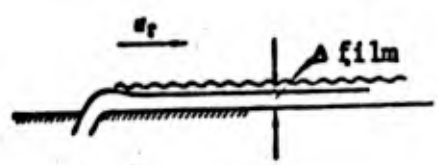

Fig. 196. Film cooling

For film cooling use is usually made of a liquid fuel which is fed to the surface through a special slot or series of holes (Fig. 196). The liquid film forms a film on the surface, which is carried away by the external flow through friction.

As ~~it~~ ~~moves,~~ *the liquid in the film* evaporates, absorbing the latent heat of evaporation. The

liquid vapor, reaching the boundary layer, acts on it in the same way as a gas fed

through a porous surface, and increases the thickness of the layer and reduces the

heat removal.

The film usually ruptures before it is fully absorbed, since there is

splashing on account of loss in stability. In the region *down-stream* ~~of~~

the beginning of the film rupture a gas curtain is created *with a*

temperature lower than that of the external flow. The gas film also protects the

surface over a certain distance.

51. Different Systems of Introducing the Liquid

There are different systems for introducing the coolant to the layer by

the wall (Fig. 197). The use of a porous surface is difficult on account of the risk

of the pores becoming clogged if the fuel contains an impurity. The point at which

the coolant is fed - the cooling belt - is located near the part of the structure

which is stressed to the greatest extent from the point of view of heat - the

critical cross section of the nozzle (Fig. 198.).

As the coolant use is made of one of the components of the combustible

mixture (usually the fuel) or else a specially neutral liquid, for example, water.

The difference is that the combustible reacts with the oxidizer of the external flow
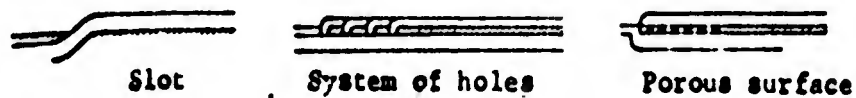
Slot   System of holes   Porous surface

Fig. 197   Different method of feeding a coolant

whereas a neutral coolant does not react and produces better cooling. But the use of a neutral coolant leads to a reduction in thrust per unit of weight of the total consumption of the fuel components and consumption of coolant.

Belt of cooling holes
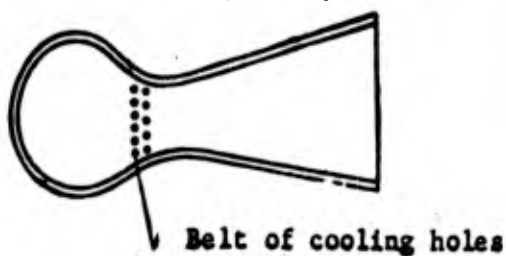
Fig. 198. Cooling critical section of nozzle

Parameters Requiring Determination in Calculating Film Cooling

A designer using film cooling is faced with the following problems:

1. The method of feeding the liquid to the wall layer, the geometrical dimensions of the slot or holes, their positioning, and the feed pressure.

2. Calculation of the amount of coolant required for the given length of surface to be cooled.

3. Temperature distribution along the surface.

4. Effect of the coolant on the engine thrust.

In order to solve these problems we have to study the flow of a liquid film when acted on by friction and evaporati[ng] at the same time.

Research shows that the method of feeding the liquid through a slot or by means of radial holes makes it possible to create a continuous film. The cleanliness of the surface plays an important part. Big scratches or strips of scale can deflect the film and create unprotected areas.

Fig. 119 shows the results of experimental determination of the critical
Cavitate?
feed rate for a coolant, at which the film is ruptured (Fig. 200) as a function of the slot width and gas velocity in the stream. The lower the velocity in the slot, the more reliable is the use of the stream. At high feed rates the film may be ruptured.

52. Stability of Film

No matter at what rate the coolant is fed to the surface, the films form waves through the action of the gas stream. When the feed rate is increased and the film thickens accordingly, waves are formed with a high period, and drops are torn from the surface of them (Fig. 201). The formation of the waves is connected with a loss in stability of the flow in the film (Fig. 202). At points where there is a concavity, the static pressure of the flow is less than $p_1 > p_2$. Consequently,

Fig. 199.

Coolant feed rate in m/sec

Air velocity in m/sec
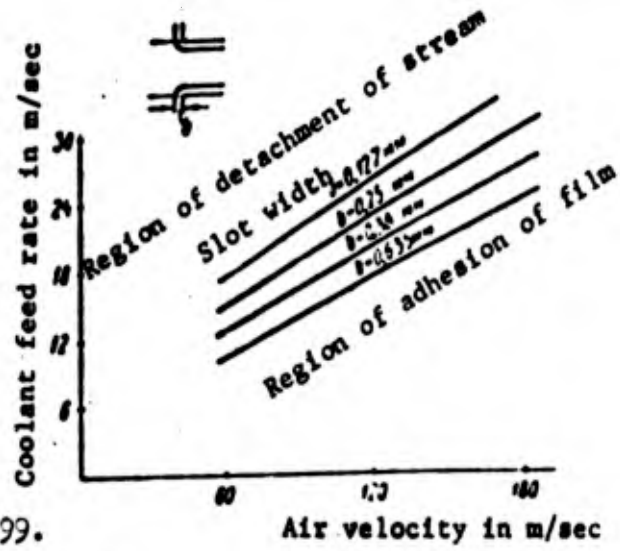
Regions of adhesion and detachment of film as function
of flow rate, coolant feed and width of slot

v/cool Formation of film

and air

v/cool Velocity greater than critical
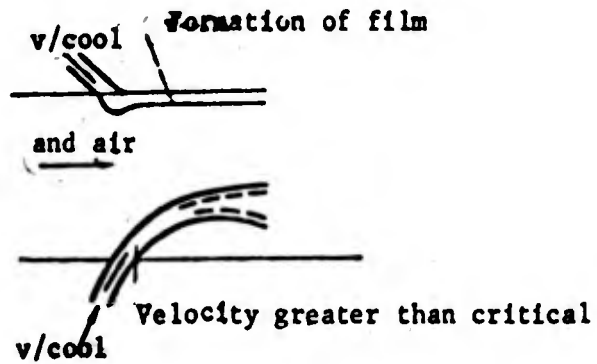
Flow under different conditions of coolant feed

Fig. 200.
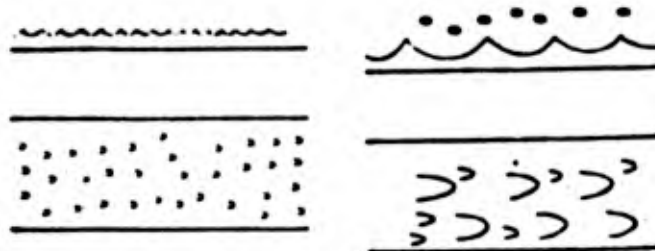
State of film surface during stable and
unstable flow

Fig. 201.

451

the pressure distribution in the outside flow is such that any undulation must

increase. This increase is counteracted by viscosity and surface tension.

The stability of the film should depend on the relationship between the

velocity of the liquid in the film and the rate of flow of the gas (Fig. 203). The

more viscous the liquid, the greater this difference *becomes*. On the other hand, an

increase in viscosity leads to the pertubations abating.

Experimental Investigation of Film Stability

In order to investigate the stability of the film, we carried out tests

with cold and hot external flow in transparent pipes. The liquid was let out

through a slot and visual observations were made. It was found that at small rates

of consumption, there are very small oscillations, and that the rupture of the film

at high rates of flow is due to the occurrence of long-wave oscillations.

In order to determine the length of the film, we measured the temperature

of the surface of a wall heat-insulated on the *opposite* side (Fig. 204). The length

of the film was determined from the sudden rise in temperature at the end of the

film.

It was found that when the consumption of the coolant increased, the length

of the film first increased in proportion to the increase in the consumption, but

then, beginning at a value $G_{cool} = G_{crit}$, began to slow down (Fig. 205).

452
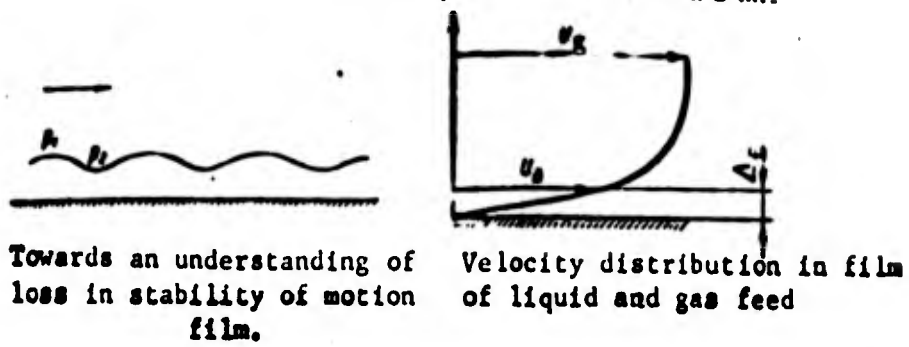
Fig. 202   Towards an understanding of   Velocity distribution in film
            loss in stability of motion   of liquid and gas feed
            film.

When compared with visual observations, it was found that the breaks in

the curve (Fig. 205) correspond to the occurrent of large oscillations and splashing

of the film. When the coolant consumption is high, the mass exchange between the

film and the flow is increased and the economic factor of the collant is reduced.
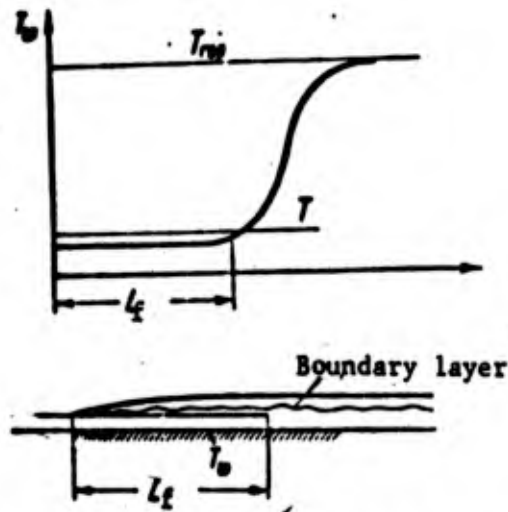
Fig. 204.   Temperature distribution along surface
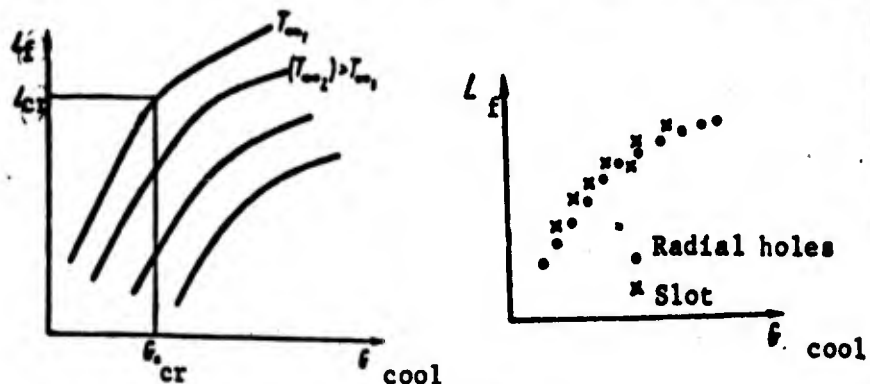
Fig. 205   Critical length of film as function of consumption of coolant

Effect of Individual Factors on Film Length

a) The Method of feed, provided the film adheres has little effect on the length or the critical length of the film (Fig. 206);

b) viscosity increases the film's stability;

c) rate of external flow, variation in pipe diameter has little effect on $\frac{L}{c} \cap \frac{G}{c} \cap$.

Parameters Determining Stability of Film

In the same way that the transition from laminar to turbulent flow in the boundary layer is determined by the number $\mathrm{Re} = u\rho x/\mu$, the stability of the flow in the film can be related to the number

$$\mathrm{Re}_\Delta = \frac{u_f \rho_f \Delta}{\mu_f} \tag{12.1}$$

Here u_f is the rate of motion of the liquid in the film, ρ_f and μ_f are the density and viscosity coefficient of the liquid, and Δ is the thickness of the film.

Fig. 207 Linear distribution of velocity in film.

Fig. 208. Variation in critical Reynold's number

Assuming that the velocity distribution in the film is close to linear

454

(Fig. 207), we get $G_{cool} = \frac{1}{2} g \varepsilon_f u \Delta b$, where $\underline{b}$ is the width of the film. This gives us

$$Re_\Delta = \frac{2G_{cool}}{g\mu_{cool}} \qquad (12.2)$$

If a cylindrical surface is being cooled,k then $\underline{b} = \pi \underline{D}$ and

$$Re_\Delta = \frac{2G_{cool}}{g_{cool}\pi D} \qquad (12.3)$$

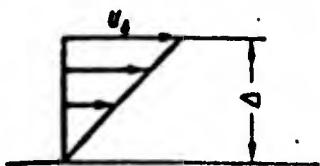The Re_Δ number describes the stability of the film. When it exceeds a

certain value $(Re_\Delta)_{cr}$, the film is ruptured.

Experimentation shows, however, that Re_Δ cannot describe the stability

completely. It transpires that in turn $(Re_\Delta)_{cr}$ is a function of the ratio of the

viscosities of the coolant and mixture of the vapor and gases of the external flow

at the surface of the film (Fig. 208). It follows from the graph that $(Re_\Delta)_{cr}$

increases as μ_{cool} decreases.

Determining $(Re_\Delta)_{cr}$

In order to determine $(Re_\Delta)_{cr}$ the hypothesis has been put forward that

the thickness of a stable film should not exceed that of the laminar sub-layer in

the boundary layer of the external stream (Fig. 209). If the thickness of the film

exceeds that of the laminar sub-layer $\Delta_f > \delta_{f\lambda}$ according to this hypothesis the stream

in the film then becomes unstable.

Study of experimental data on the velocity of distribution in a turbulent

boundary layer has shown that in the laminar flow region near the wall $u_* \delta / \nu < 10$

(Fig. 210). Here $u_\tau = \sqrt{\tau_w/\rho}$ Thus, the thickness of the laminar sub-layer is

$$\delta_s \approx \frac{(6 + 10)\,\nu}{u_\tau}\,.$$
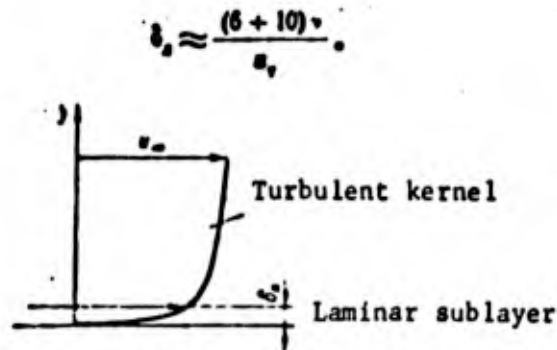
Fig. 209.   Velocity profile in turbulent boundary layer

This graph plots the experimental points obtained by Abramson when studying

the stability of films. The vertical axis shows $u\Delta/u_\tau$, while the horizontal axis

plots the corresponding value $\log u_\tau \Delta/\nu$ cool here u_s and Δ are calculated from the

critical value G_{crit} , at which the film loses stability.
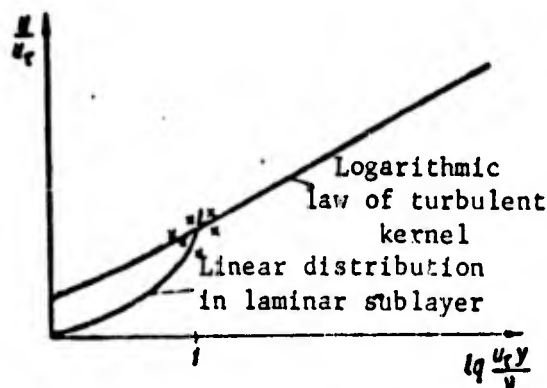
Fig.210. Velocity distribution in
semi-logarithmic coordinates

53.   EVAPORATION OF LIQUID FILM IN TURBULENT BOUNDARY LAYER

Calculation of the evaporation rate and, accordingly, the length over

which the film evaporates entirely can be made on the basis of the following

assumptions:

1. The consumption of coolant is less than critical; the film adheres

to the surface is stable.

2. There is no removal of heat through the wall and all heat reaching

the film goes into evaporating it.

If the coolant is liable to react with the external gas flow, the additional

heat emissions have to be taken into account.

54. Heat Balance Conditions and Mass

When the film evaporates, the heat reaching the surface is spent on warming

up the liquid to evaporation point and on latent heat of evaporation. The length

of the film at a known value of the heat transfer coefficient is

$$ l_f = \frac{G_{cool} \Delta J}{\frac{a}{c_{p_g}}(J_\infty - J_w)b} ; \tag{12.4}$$

$$(12.4)$$

here ΔJ is the heat absorbed by the liquid during heating and evaporating, in cal/kg;

a is the heat-transfer coefficient;

b is the width of the film ($b = \pi D$ for a pipe);

J_∞ is the gas enthalpy in external flow, and

J_w is the gas enthalpy at the film surface.

J_w is determined by the temperature and composition of the gas of the

surface
$$ J_w = \int \bar{c}_{p_g}\, dT + \Sigma C_i J_i.$$

The temperature of the film, and therefore the temperature of the gas on the surface, depends in turn on the concentration of vapor in the evaporating liquid

$$T_f = f[(C_{cool})_1].$$

To determine the concentration $(C_{cool})_w$, we can use approximate relationships which we obtained for a case in which gas is fed through a porous surface

$$(C_e)_{cool} \frac{1}{1 + \frac{J_e - J_0}{J_e - J_e}}.$$ (12.5)

The concentration of the coolant at the wall is already less than unity on account of removal through diffusion of the vapor into the boundary layer. At $C_w = 1$, the temperature of the film would be equal to the boiling point of the liquid at the given pressure in the external flow, which could lead to rapid destruction of the film through boiling of the internal particles of the film. At $C_w < 1$ evaporation occurs at a lower temperature than the boiling point, and the liquid only evaporates at the surface.

Condition $T_f = f[(C_{cool})_w]$ may be obtained from the critical dependence of the saturated vapor pressure on the temperature $T_f = f(p_{cool})$. In the given case p is equal to the partial pressure of the liquid vapor above the surface

$$p_{cool} = \rho \ RT_f$$

The heat transfer coefficient α may be taken from experimental data on porous cooling.

References

1. Knut Ye., Mekhanizm Plenochnogo Okhlazhdeniya, "Voprosy Raketnoy Tekhniki", IL, 1955, No. 6.

2. Kinney C., Abramson A., Internal Liquid Film Cooling Experiments with Air Stream Temperatures to 2000°F, NACA Report 1087, 1952.

3. Tsukrov M. Grekhem A., Plenochnoye Okhlazhdeniye Raketnykh Dvigateley, "Voprosy Raketnoy Tekhniki", IL, 1958, No. 1.

CHAPTER XIII

CONCEPT OF HEAT EXCHANGE IN RAREFIED GASES

Over the last few years flying craft have been able to attain ever higher layers of the atmosphere during flights. This applies particularly to supersonic craft. Ballistic missiles of the type V-2 used to reach 150 km. Artificial earth satellites move at altitudes of 150 - 1000 km at velocities of $\sim$8 km/sec.

When designing flying craft we must be in a position to determine the aerodynamic resistance and thermal flux. At such high velocities, the drag temperature reaches 10 - 20,000°. The heat flux, however, is reduced through a reduction in density. In order to make the calculation, we must know exactly the temperature and density at great heights. If we are to place instruments aboard a rocket moving at a great height, we must first calibrate them in highly rarefied wind tunnels. Investigation has shown that the flow of rarefied gases is different from flow at normal pressures.

Table 19

Sec. 55. Physical Parameters of Air at High Altitudes /4/

Altitude	T °K	P mm Hg	Number of particles per 1 cm³		
			N_2	O_2	O
0	297	760	$2 \cdot 10^{19}$	$5 \cdot 10^{18}$	0
20	232	241.8	$1.5 \cdot 10^{18}$	$3.7 \cdot 10^{17}$	—
40	240	2.65	$6.7 \cdot 10^{16}$	$1.7 \cdot 10^{16}$	—
60	420	0.23	$4.3 \cdot 10^{15}$	$1 \cdot 10^{15}$	—
80	160	$3 \cdot 10^{-2}$	$1.5 \cdot 10^{15}$	$3.8 \cdot 10^{14}$	—
100	240	$1 \cdot 10^{-3}$	$2.8 \cdot 10^{13}$	$7.6 \cdot 10^{12}$	—
150	410	$8.7 \cdot 10^{-6}$	$1.5 \cdot 10^{11}$	—	$1 \cdot 10^{11}$
300	1040	$3.3 \cdot 10^{-8}$	$4.7 \cdot 10^{7}$	—	$7 \cdot 10^{8}$

Sec. 56. Gas as a Totality of Separate Molecules. Free Path Length of Molecules.

When studying the flow of a gas at high rarefactions, we have to take into account the fact that the gas is a totality of individual molecules. When considering the molecular structure of gases it is assumed that the molecules are in continuously disorderly motion, that they collide with one another and strike against the surface of the body immersed in them. It is also assumed that the laws of the impact of elastic spheres are applicable to the molecular collisions. The interaction of molecules is disregarded in between collisions.

On the basis of these motions, we can introduce the concept of the free path length (free path of a molecule) as the distance traversed by the molecules from one collision to another. Since the molecules move at different velocities and have different free path lengths, we usually consider the mean free path of the

molecule l. The mean path and the number of molecular collisions involved depend

on the size of the molecules themselves, if they are regarded as spheres of finite

dimensions.

The kinetic theory of gases   shows that

$$l = \frac{1}{4\sqrt{2}\,\pi r^2 n}.$$ (13.1)

Here r is the so-called gas kinetic radius of the molecule, which is

a function of distance over which molecules may approach one another during

collisions; n is the number of molecules per unit volume; $4\sqrt{2}\,\pi r^2 = \sigma$ is the cross-

section of the particle.

The nature of flow around a body depends on the relationship l and the

size of the body L. If the ratio $l/L \ll 1$, the medium may be regarded as a solid

one (continuum). In this case all the laws of gas dynamics are applicable.

If l is comparable with the size of the body, we must take the

discretion of the medium into account. This region is the region of

rarefied gases. The value l increases as pressure decreases. It is only

possible to move from the gas dynamic region to the rarefied gas region through

reduction of pressure in the medium, or else by reducing the size of the body

under consideration.

As can be seen from Table 20, if the dimensions of the flow region

in question are $L \sim 1$ m, then the ratio $l/L < 0.001$ up to a flying altitude of

approximately 60 km. At greater heights we must take the rarity of the medium

into account.

Table 20.

Mean free path length of molecules at different heights

Altitude km	Pressure mm Hg .	Number of particles per 1 cm³	l in cm
0	760	$2.5 \cdot 10^{19}$	$8.6 \cdot 10^{-7}$
10.8	176.2	$7.3 \cdot 10^{18}$	$2.3 \cdot 10^{-5}$
32	6.45	$2.9 \cdot 10^{17}$	$7.7 \cdot 10^{-4}$
62	$1.55 \cdot 10^{-1}$	$4.5 \cdot 10^{15}$	$4.9 \cdot 10^{-2}$
84	$9.0 \cdot 10^{-3}$	$4.4 \cdot 10^{14}$	0.5
94	$2.1 \cdot 10^{-3}$	$3.6 \cdot 10^{13}$	2.8
100	$1 \cdot 10^{-3}$	$3 \cdot 10^{19}$	6
150	$8.7 \cdot 10^{-6}$	$2.5 \cdot 10^{11}$	2 000
300	$3 \cdot 10^{-6}$	$1.4 \cdot 10^{10}$	15 000
400	$1.16 \cdot 10^{-6}$	$3.9 \cdot 10^{9}$	55 000

Sec. 57. Relationship Between Viscosity Coefficient μ and Mean Free Path Length l

Let us consider the interaction between two layers of liquid at a distance

l from each other (Fig. 211). If there is a velocity gradient $\frac{\partial u}{\partial y} \neq 0$, in the direction

of the y-axis, at the distance l the flow velocities u differ from each other by

the value $\Delta u = u_2 - u_1 = l \frac{\partial u}{\partial y}$. On account of the chaotic motion of the molecules at a mean

velocity v, the particles may shift the distance l, keeping at the same time their

462

momentum in the direction of the x-axis, which they possessed in the previous layer.

The following momentum is transferred across the line 0 - 0

$$\rho \bar{v} \Delta u = \rho \bar{v} l \frac{\partial u}{\partial y}.$$

This momentum corresponds to friction between the top and bottom of the stream

$$\tau_0 \sim \rho \bar{v} l \frac{\partial u}{\partial y} \sim \mu \frac{\partial u}{\partial y}.$$

Thus, $\mu \sim \rho \bar{v} l$. The theory gives us the value $\mu = 0.499 \overline{\rho \bar{v} l}$. The mean velocity

Fig. 211. Concept of free path length
of molecule

of the molecules $\bar{v} \sim \sqrt{T} \sim a$, in which a is the speed of sound. Hence we can take it

that $\rho a l \sim \mu$ and

$$l \sim \frac{\mu}{\rho \bar{v}} \sim \frac{\mu}{\rho a}.$$

Sec. 58. Parameters Determining Boundaries of Gas Flow Regions

The degree of rarefaction of a gas is described by the ratio of the

mean free path length and the size of the region under investigation

$$\frac{l}{L} \sim \frac{\mu}{\rho a L} = \frac{U}{a} \frac{\mu}{\rho U L} = \frac{M}{Re_L}.$$

463

Here U is the flow velocity. As the M number increases and the Re number decreases, the degree of rarefaction of the medium is increased.

When considering a boundary layer the linear value determining the size of the region in question is the thickness of the boundary layer δ . The degree of rarefaction of the stream is described by the ratio $\frac{l}{\delta} = \frac{l}{L} \cdot \frac{L}{\delta}$.

Here L is the size of the body (for example, the distance from the leading edge during flow round the plate, the diameter of the sphere, and so on). We get

$$\frac{l}{\delta} = \frac{l}{L} \cdot \frac{L}{\delta} \sim \frac{M}{Re} \cdot \frac{L}{\delta}.$$

$\dfrac{\delta}{L}$ is the ratio of the boundary layer thickness to the size of the body - during laminar flow this is of the order of

$$\frac{\delta}{L} \sim \frac{1}{\sqrt{Re}}.$$

Thus in a case in which we can speak of the existence of a boundary layer (fairly high Re numbers), the ratio

$$\frac{l}{\delta} \sim \frac{M}{\sqrt{Re}}.$$

At very low Re numbers, when no boundary layer can be singled out, the size of the flow region around the body is of the order of the body size

$$\delta \sim L \quad \text{и} \quad \frac{l}{\delta} \sim \frac{M}{Re}.$$

Investigation has shown that at $l/\delta < 0.01$ we can disregard the discretion of the medium and regard the gas as a continuum.

464

$M/\sqrt{Re}<0.01$

Thus, the values $\wedge$ correspond to the continuum - gas dynamic region.

$M/\sqrt{Re}>0.01$

The values $\wedge$ correspond to rarefied gas flow. At very high degrees of rarefaction, when the free path length of the molecules is considerably greater than the dimensions of the body, when calculating flow around the body we can disregard the number of collisions between the molecules, compared with the number of collisions with the surface. This region is called the free-molecular flow region. It is characterized by $1/\delta>10$, or $\underline{M}/Re>10$. The region of free molecular flow is studied by methods involving the kinetic theory of gases.

Between the gas dynamic region and the free molecular flow region there is a transitional region which is very difficult to study. Two effects are observed in it.

The first is that the gas velocity by the wall is not equal to zero, and the gas glides along the surface at a finite velocity.
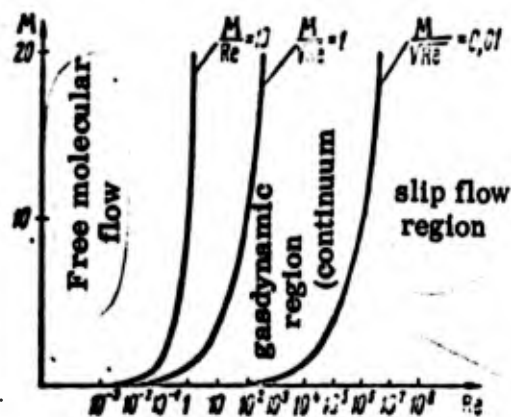

Fig. 212. Flow regions

465

This flow is therefore called slip flow. The second effect of the slip flow is the temperature discontuity at the wall during heat exchange between the gas and the surface. The gas temperature at the surface is not equal to the surface temperature. The boundaries of the slip region are determined by the relationship.

$$0,01 < \frac{M}{\sqrt{Re}} < 1. \tag{13.2}$$

Fig. 212 shows a graphic representation of the boundary of the gas flow regions:

$\frac{M}{\sqrt{Re}} < 0,01 -$ gas dynamic or continuum,

$0,01 < \frac{M}{\sqrt{Re}} < 1 -$ flow with slip,

$\frac{M}{Re} > 10 -$ free-molecular flow region.

These values have been put forward by Tzyam. They relate to aerodynamic phenomena in a gas and are approximate. It may be found during experimental investigation of individual aspects of heat exchange that the boundaries of the regions have shifted.

Sec. 59. Free Molecular Flow

Heat transfer and resistance during free molecular flow can be calculated from the kinetic theory of gases. Here it is assumed that the molecules colliding at a high velocity with the surface transfer the bulk of their energy to it and are

then reflected with considerably less energy, closer to the energy corresponding

to the wall temperature. The gas molecules striking the wall adapt themselves

to the conditions on the surface. This phenomenon is described by the adaptation

or accommodation coefficient

$$\sigma = \frac{E_{отр} - E_{вл}}{E_{ст} - E_{вл}},\tag{13.3}$$

in which $\underline{E}_{rf}$ is the energy of the reflected molecules, $\underline{E}_{wll}$ is the energy at

the wall temperature, and $\underline{E}_{in}$ is the energy of the incident molecules.

$\sigma < 1$ depends on the physical properties of the gas and the medium.

Calculation of the heat exchange consists in determining the difference

between the total energy supplied to the molecules impinging upon it, and the

energy carried away by the reflected molecules. In the general case we have

to take into account that the incident molecules have different energies, since

the velocities of thermal motion of the molecules are distributed in accordance

with Maxwell's law.

But at a high flight velocity of 6 - 8 km/sec, the thermal velocities

of the molecules can be disregarded ($v_{therm} \approx 500$ m/sec).

$$\frac{E}{E_{therm}} \sim \frac{(v_{fl})^2}{(v_{therm})^2} \sim 200;$$

here v_{fl} is the velocity of the flight.

In this case the energy of the molecules impinging upon the body is equal to

467

$$E_{\text{мол}} = N \frac{m(v_{\text{мол}})^2}{2} F_{\text{мид}}. \qquad (13.4)$$

Here $\underline{N}$ is the number of molecules hitting the surface per unit time,

$F_{\text{мид}}$ is the area of $\overset{\text{the middle of the}}{(\text{body},}$ and $\underline{m}$ is the mass of the molecule.

If the surface temperature is not too high ($\sim 1000°$), the approximate

value of the total heat flux is

$$Q = \frac{Nm(v_{\text{мол}})^2}{2 \cdot 427} F_{\text{мид}} \text{ kcal/sec}$$

$$Nv = n v_{\text{мол}} F_{\text{мид}};$$

here $\underline{n}$ is the number of particles per unit volume at the given altitude.

For a case of flow along a flat plate the following formula has

been theoretically derived

$$\alpha_{cp} = 0.170 \frac{\lambda}{x} \frac{Re}{M}. \qquad (13.5)$$

in which α_m is the $\overset{\text{mean}}{(\text{heat exchange coefficient}}$ over the length x.

Sec. 60. Slip Flow

This flow area is the least studied. As the gas becomes rarer, the

molecular flow equations for a continuum require further refinement. Apart from

the normal expressions for the heat flux, and friction, on the right-hand side

of the Navier-Stokes equations or the boundary layer equations we add terms of

a higher order. These generalized equations are termed Barnett equations.

As evaluations have shown, the additional terms in the expressions for

friction and heat flux relate to the ^principal terms as M^2/Re; they should therefore

only be taken into account at fairly high values of M^2/Re.

The additional terms in the Barnett differential equations are of a higher

order, on account of which we are required to add or vary the boundary conditions.

At the present time no solution of the Barnett equations have been obtained.

For calculations in the slip region we use an approximate method which

consists in applying the continuum equations and calculating the slip in the boundary

conditions. The slip may be expressed analytically by the following relationships.

For the velocity

$$u_{y=0} - u_e = l\left(\frac{\partial u}{\partial y}\right)_{y=l}.$$

Here $u_{y=0}$ is the gas velocity by the wall, u is the rate of motion

of the wall, l is the mean free path length of the molecules. We get similarly

for the temperature discontinuity

$$T_{y=0} - T_e = 1,996\,\frac{2-\sigma}{\sigma}\,\frac{k}{k+1}\,\frac{l\lambda}{\mu c_p}\left(\frac{\partial T}{\partial y}\right)_{y=l}. \tag{13.6}$$

Here σ is the accommodation coefficient, k is the adiabatic exponent,

λ is the thermal conductivity, $T_{y=0}$ is the gas temperature by the wall, T_{wall}

is the wall temperature.

For a flat plate under these conditions the solution hask been

theoretically derived as

469

$$a_{\epsilon\rho} = \frac{\lambda}{s}\, 0.52M \left\{ \exp \frac{Re\, Pr}{1.35M^2}\, \mathrm{erfc} \, \left] \sqrt{\frac{Re\, Pr}{1.35M^2}} - 1 + \frac{2}{\sqrt{\pi}} \,\right] \sqrt{\frac{Re\, Pr}{1.3 M^2}} \right\}. \qquad (13.7)$$

Here

$$\mathrm{erfc}(x) = \frac{2}{\sqrt{\pi}} \int_x^\infty e^{-t^2}\, dx \quad \text{и} \quad \exp(x) = e^x.$$

The corresponding value of α_m is also obtained for a case of flow

around a sphere. These values do not tally very well with experimental ones.

Sec. 61. Experimental Data

Experimental investigation of heat exchange was carried out in special

highly rarefied wind tunnels. The high degree of rarefaction was obtained by

using a system of oil diffusion b ter and vacuum pumps. Great difficulties

were experienced in boosting the steam in the nozzle. At very low Reynolds

numbers, which occurred in the experiments /Re = 10 - 1000/, the boundary layer

becomes so thick that it practically fills the entire nozzle section. In order

to improve the velocity and temperature fields in the cross-section of the nozzle

we sucked out the boundary layer through a perforated wall.

Fig. 213 shows the variation in the temperature recovery coefficient measured

$$r = \frac{T_\epsilon - T_\infty}{(T_{(0)})_\infty - T_\infty}.$$

470

with small spheres 2 - 12 mm in diameter as a function of the ratio $\sqrt{Re}/M$.

As can be seen from the graph, the temperature recovery coefficient is constant

at $M \sqrt{Re} < 0.2$.
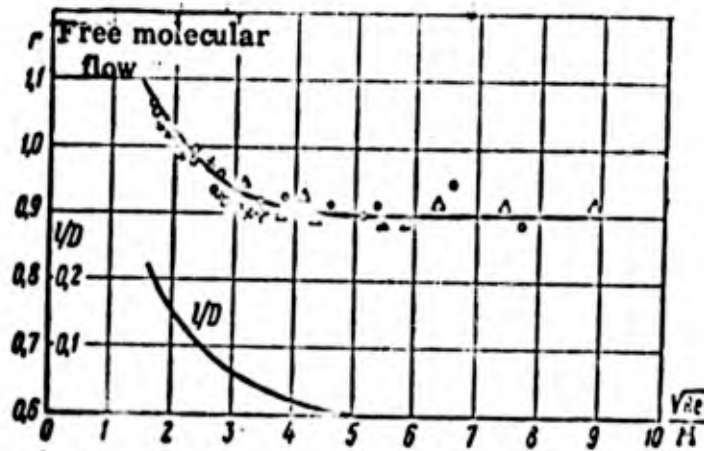
Fig. 213. Temperature recovery coefficient on sphere

As $M\sqrt{R_e}$ increases, the recovery coefficient increases and even exceeds

unity. In this case the equilibrium temperature is greater than the drag

temperature of the stream.

The same graph shows a curve for the ratio of the mean free path length l

and the sphere diameter D. As can be seen the deviation of the recovery coefficient

occurs at $l/D > 0.05$.

The graph in Fig. 214 plots the recovery coefficient for a flat plate.

The continuous line corresponds to the theoretical value $r = 7/6$ for a free -

molecular stream.

471

Fig. 214. Temperature recovery coefficient
on plate
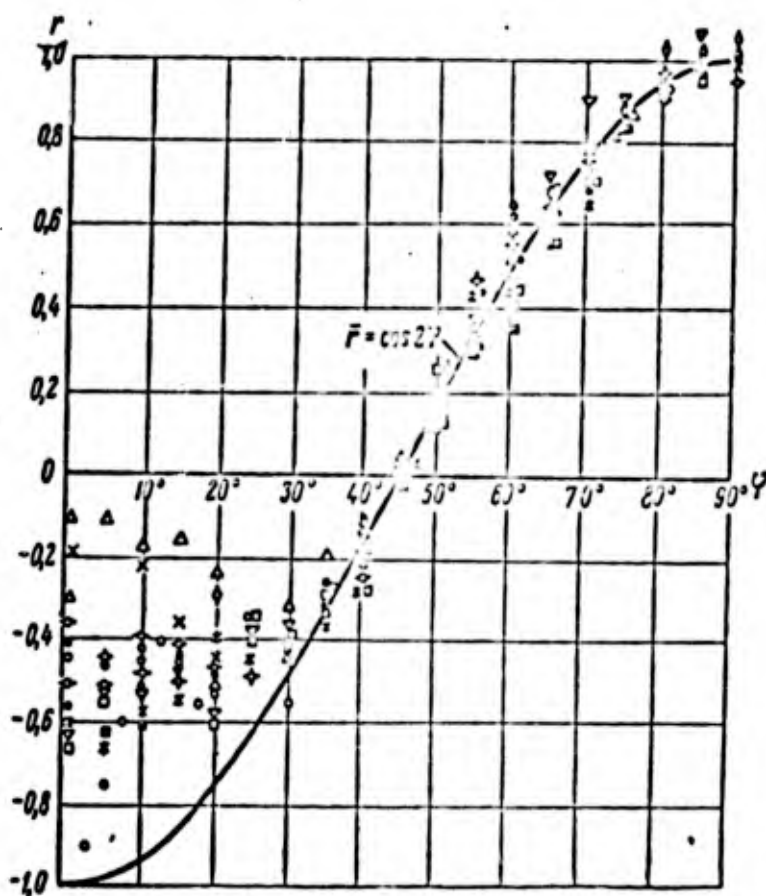
Fig. 215. Relative recovery coefficient as function of
attack angle φ

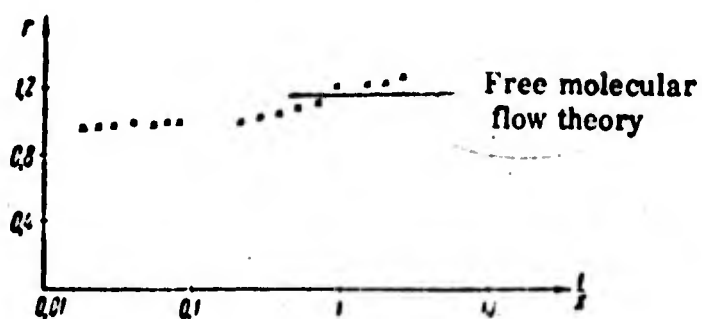Fig. 215 shows the experimental variation in the temperature recovery coefficient as a function of the angle of attack of a cylinder. The vertical axis plots the value

$$\bar{r} = \frac{r - r_{45°}}{r_{90°} - r_{45°}},$$

here $r_{45°}$ and $r_{90°}$ are the temperature recovery coefficients at attack angles on the cylinder $\varphi = 45°$ and $\varphi = 90°$. As can be seen from the graph, the coefficient falls as the angle φ decreases.

Fig. 216. $Nu = f(Re)$ as function for spheres

Heat-exchange coefficient. Fig. 216 is a graph showing the variation in the $Nu = a_{cp} D/\lambda$ as a function of the Re number for spheres. As can be seen, at low $Re = u D \rho / \mu$ the experimental points deviate from the line corresponding to the continuum. This deviation occurs earlier at high M numbers. Curves for different M numbers do not coincide.

473

Curves with different M numbers can be compatible if we plot the parameter $M/\sqrt{Re}$ or the reciprocal $\sqrt{Re}/M$ along the x-axis, rather th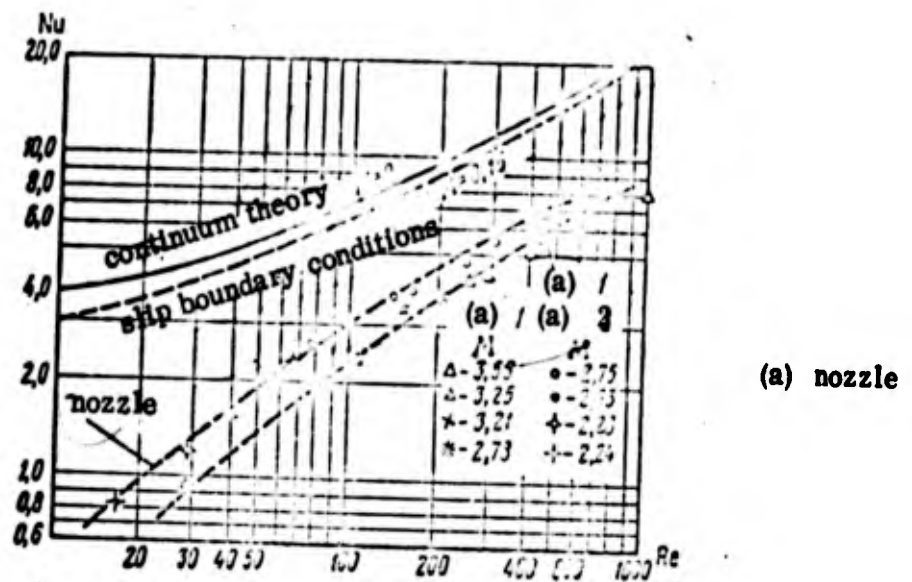an the Re number (Fig. 217). This confirms the right selection of the similarity parameter for rarefied gas in the form of $M/\sqrt{Re}$.
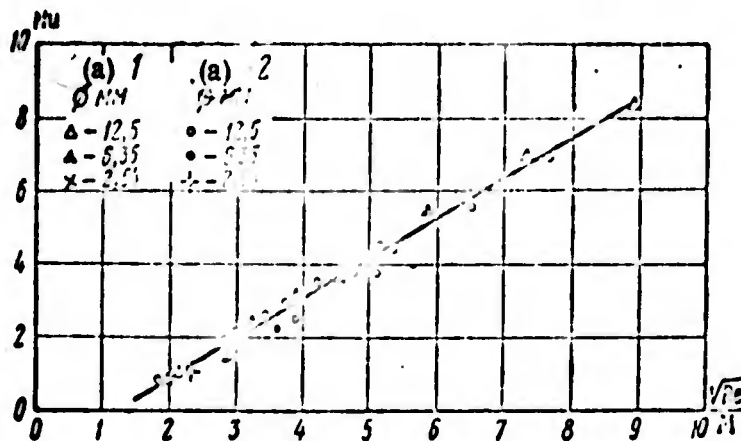
Fig. 217. Nu as function of $\dfrac{\sqrt{Re}}{M}$ for spheres

(a) Nozzle

<u>Flow region boundaries.</u> It follows from the graphs that the heat exchange and temperature recovery coefficients deviate from their corresponding

$$M/\sqrt{Re} > (0.05 \div 0.1)$$

values for a continuum at ⌄ . Thus, in this case the continuum region diverges somewhat, compared with the evaluations made by Tzyam.

It follows from experiments on determining the recovery coefficients that at $1/\underline{L} \sim 10$ there is a free-molecular flow.

474

REFERENCES

1.   Dreyk, R. Heat transfer from spheres to rarefied gas in supersonic flow "Problems of Rocketry" For. Lit. Press, 1953, No. 2.

2.   Dreyk, R. and others. Heat transfer in stream of rarefied gas at high velocity, "Problems of Rocketry" For. Lit. Press, 1954, No. 1.

3.   Zigel', K. Boundaries of aerodynamic regions "Mechanics", For. Lit. Press, 1952, No. 3.

4.   Mitra, S. K. The upper atmosphere, For. Lit. Press, 1956.

5.   Popov, S. G. Measurement of air currents, Gostekhizdat, 1948.

6.   Stelder, J. and others. Heat-transfer coefficient in stream of rarefied gas at high velocity, "Problems of Rocketry", For. Lit. Press, 1954, No. 1.

7.   Stalder, J. Heat transfer from stream of rarefied gas at high velocity of body, "Mechanics", For. Lit, Press, 1955, No. 2.

8.   Stalder, J. Comparison of theoretical and experimental data on rarefied gas flow, "Mechanics", For. Lit. Press, 1954, No. 3.

9.   Tzyan, S. Aerodynamics of rarefied gases, Collection of articles "Gas Dynamics", For. Lit. Press, 1950.

10.   Shaan, D. Aerodynamics at very high altitudes. "Mechanics", For. Lit. Press, 1957, No. 2.

11.   Shirokov, M. F. Physical fundamentals of gas dynamics, Gostekhizdat, 1958.

12.   Shirokov, M. F. Discontinuities in velocity and temperature by bodies of walls immersed in rarefied gases at velocities close to and greater than sound, Zhetf, Issue 6, 1958.

CHAPTER XIV

SOME ASPECTS OF THE CALCULATION OF THE HEAT-UP OF WINGED FLYING CRAFT; METHODS OF THERMAL PROTECTION

The foregoing sections in this book contain basic information from the theory of heat exchange and the boundary layer. Methods of solving very simple problems were used as illustrations. In actual calculations we have to take into account the joint effect on a number of factors, for example, the surface of a flying craft heats up in the atmosphere on account of friction against the air. The heated surface radiates some of the heat, through which the temperature of it is reduced. The remainder of the heat flux may move inside the part.

Calculation of the heating up of a flying craft includes determining the surface temperatures of the design elements, from which the heat is not transferred inside, the surface temperatures when heat is removed, and the temperatures of certain internal parts of the craft and the fuel. In a number of cases we have to calculate the thermal insulation of certain parts sufficient to ensure the temperature tolerance for the given part.

In the general case, the problems facing the designer depnd to a considerable extent on the purpose of the craft, its flight altitude and velocities, and involve a specific type of design. In this section we will deal, as an illustration, with

fundamentals of the calculation when applied to a craft flying through the

atmosphere at supersonic velocities, at altitudes of up to 30 - 40 km and at

$M \leqslant 5$. A flying craft of this kind must be equipped with a ram jet or a liquid

fuel jet engine. Under these circumstances the air is regarded as a solid medium

and its dissociation behind the shockwave in front of the leading edges and in

the boundary layer can be disregarded /1,6/.

It is natural that here we are only concerned with some of the aspects

of the problem and do not take the design details into account. The data

set forth below is merely an illustration of the application of equations and

methods of the theory of heat exchange. Detailed consideration for specific

design systems is left to special textbooks.

Sec. 62. Steady-State equilibrium Temperaure of Insulated Surfaces.

At the commencement of the flight, the temperature of the body is

gradually increased through acceleration and the gradual heat-up of the part.

During the actual flight the heat exchange conditions may also vary with the

altitude and velocity. But if these changes are fairly smooth, the variation in

time of the heat flux from the gas to the surface at each given moment may be

disregarded. Here we can speak of a steady-state surface temperature at different

points on the trajectory.

477

γ-angle of sweep

Section through AA
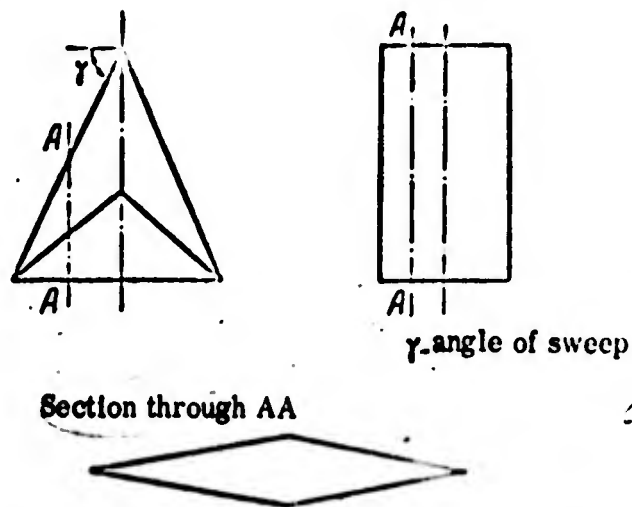
Fig. 218. Possible shapes of wings from above and
in cross-section

a) The temperature of the wing or fusilage surface at a distance from

the leading edge.

The wing of a supersonic aircraft, when viewed from above, can be

rectangular, triangular or some other shape (Fig. 218). In cross-section, the

wing may have a   rhomboid, triangular or   other   profile, comprised

of straight lines or lines which are fairly straight. The fusilage is usually

                    in shape,
a body very close /to a cylinder, except for the nose which is close to a conical.

In certain cases there may be an air collector - a supersonic diffus'r - in the

nose (Fig. 219). In all these cases, when calculating the boundary layer we

can disregard the longitudinal pressure gradient. Thus, when calculating the

thermal flux from the gas to the lateral surface we can use the solutions obtained

                    in an
for a flat plate or cone   approximation. The leading edge should be considered

separately.   478
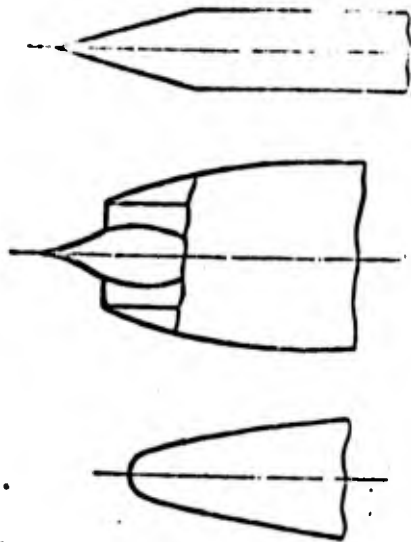
Fig. 219. Nose area of supersonic aircraft

It should be pointed out that this division is a conditional one. A heat-exchange calculation taking the development of the boundary layer along the surface of the wing or fusilage into account is more accurate. The blunting has an effect on heat exchange on the lateral surface both through more intensive build-up of the boundary layer   as well as variation in the flow parameters beyond the   boundary layer. At. $M > 10$ the heat flux on the lateral surface may be reduced through blunting by a factor of 20 or 30% or more.

Let us compile the heat balance for the following element of the surface

$$q_{con} = q_{p}.$$

Here q_{p} is the removal of heat from the wall through radiation, and q_{con} is the convective heat flux, which in the case of a plate can be determined from the equation

$$q_{con} = a(T_e - T_w).$$

(14.1)

479

The value α may be determined from Eqs. (8.37), (8.38), (8.39), (8.50), (8.54) and (8.55) in Chapter VIII.

Here $T_e = (1 + 0.2 r M_1^2)$. For a turbulent regime $r = 0.89$ and for laminar $r = 0.845$. The subscript 1 corresponds to parameters on the external boundary of the boundary layer. Hence if the wing is set at an angle of attach, we have to calculate first the velocity, density and M_1 number for ideal circumflow, taking the drag of the gas in the densification discontinuities at positive angles of attack and the expansion of the gas at negative angles into account.

Further,

$$q_\rho = 4.9 \varepsilon \left[\left(\frac{T_w}{100} \right)^4 - \left(\frac{T_{II}}{100} \right)^4 \right] \; \text{kcal/m}^2 \cdot \text{hr} \qquad (14.2)$$

Here ε is the coefficient of blackness of the surface, which is a function of the material of the wall, the state of its surface and the temperature.

Thus, to determine the temperature of the wall we must equate (14.1) and (14.2)

$$\alpha (T_e - T_w) = 4.9 \varepsilon \left[\left(\frac{T_w}{100} \right)^4 - \left(\frac{T_{II}}{100} \right)^4 \right]. \qquad (14.3)$$

The value α is a function of the ratio T_w / T_e. The equation should be solved either graphically, or by successive approximations.

If the blunted leading edge is set at an angle to the stream, as is the
case in a swept back wing, the heat flux is a function of the angle of sweep
(Fig. 220).
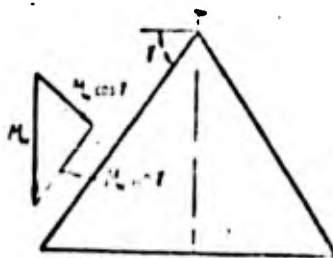
Fig. 220.   Decomposition of velocity into normal
and tangential components during flow around
swept-back wing

Here we should consider separately a case in which the stream velocity
component perpendicular to the leading edge is greater than the speed of sound
(supersonic leading edge) and less than the speed of sound ("subsonic leading edge").

In the first case a receded shockwave situated along the edge occurs
in front of it. In the second case there is no shockwave and the parameters of
flow at the surface can be calculated from the adiabatic drag condition. The
first case is determined by the condition (Fig. 220) $M_\infty \cos \gamma > 1$; the second case
by the condition

$$M_\infty \cos \gamma \leqslant 1. \tag{14.4}$$

In a turbulent regime the heat flux is found from the expression

$$q_{s0} = 0,023 \cdot 3 \cdots \rho_1 u_1 c_p \left(\frac{u_1^2}{\gamma_{a0}^2} \right)^{-\frac{1}{3}} (T_r - T_w).$$

(14,5)

in which

$$u_1 = u_\infty \sin \gamma;$$

$$\beta = \frac{a_{cr \cdot 1}}{\frac{b}{2}} \quad (at) \quad M_\infty \cos \gamma > 1;$$

$$\beta = \frac{2 u_\infty}{b} M_\infty \cos \gamma \quad at \quad M_\infty \cos \gamma < 1;$$

$$a_{cr \cdot 1} = a_\infty \sqrt{\frac{2}{k+1} \left(1 + \frac{k-1}{2} M_\infty^2 \cos^2 \gamma \right)};$$

ρ_1 is the density on the boundary layer; ν_w is the coefficient of

kinematic viscosity at a pressure on the critical line and wall temperature, and a_w

is the speed of sound in the oncoming stream; b is the thickness of the edge.

Sec. 63. Surface Temperature of Insulated Elements in Steady-State Flights

When there is a rapid gain in velocity or altitude, we have to take into

account the non-stationary nature of the heating-up both through the variation

in time in the heat exchange coefficient α as well as the heat through of the

part with time.

In the general case solution of this problem necessitates the use of

laborious methods of the thermal conductivity theory. But when calculating the

heat-up of thin walled shells, the calculations can be considerably simplified.

If the shell is fairly thin and a good conductor, it can be taken that the

temperatures of the inside and outside are equal, i.e., that the temperature drop

inside the shell is negligible. This is the case when the thermal resistance of

the body δ/λ is much less than the resistance of the boundary layer $1/\alpha$

$$\frac{1}{\lambda} \ll \frac{1}{a} \quad \text{at} \quad \frac{\delta a}{\lambda} = \text{Bi} < 1.$$

For example, for a steel shell

$$\delta = 1 \; \text{м.м}; \quad \lambda = 39; \quad a \approx 100, \quad \text{Bi} = 0,025.$$

When an aluminum shell is used Bi is still smaller.

On the basis of this condition we can compile the heat balance for the

element of the surface for an arbitrary moment in time

or

$$c\gamma\delta \frac{dT_z}{d\tau} = a(T_e - T_w) - 4,9 \left[\left(\frac{T_w}{100}\right)^4 - \left(\frac{T_{II}}{100}\right)^4\right]$$

$$\frac{dT_z}{d\tau} = \frac{1}{c\gamma\delta} \left\{ a(T_e - T_w) - 4,9 \left[\left(\frac{T_w}{100}\right)^4 - \left(\frac{T_{II}}{100}\right)^4\right] \right\}.$$

Here c is the thermal capacity of the wall material, γ is the specific

gravity of the wall material when disregarding the removal of heat from the shell

into the body.

In order to determine the variation of the surface temperature with

time, we divide up the entire segment of the flight into small intervals $\Delta\tau_i$.

Then, knowing $T_{w_{i-1}}$ and α_{i-1} from the preceding interval, the temperature

increment throughout the following interval can be determined from the equation

$$\Delta T_{w_i} = \frac{\Delta\tau_i}{c\gamma\delta} \left\{ a_{i-1}(T_{e_i} - T_{w_{i-1}}) - 4,9 \left[\left(\frac{T_{w_{i-1}}}{100}\right)^4 - \left(\frac{T_{II}}{100}\right)^4\right] \right\}.$$

α is determined for each moment in time by the usual formulae.

Ca culations show that in a number of cases the wall temperature in a non-stationary flight is much lower than the equilibrium temperature. Utilizing this fact, rocket designers are using duralumin even for boosting up to $M \approx 4 - 5$ ($T_{-\infty}$ up to 1200°C) /6/.

Sec. 64. Heat Insulation of Parts of Craft

In order to prevent overheating, the inside parts of the craft are insulated from the hot outside surfaces of the fusilage. In the part of the body containing the engine, protection has to be provided from the heat flux coming from the engine. Here we distinguish two cases. If it is possible to arrange for internal cooling, the thermal insulation must be selected in such a way that the amount of heat reaching the cell from the surface is equal to the amount of heat removed by the coolant.

The insulation chosen must be made of a material with a low specific gravity and high thermal resistance. The characteristic heat capacity of the insulator does not play any part here, since we are considering a stationary heat exchange regime. This case also includes large heat containers, for example, the fuel tanks. Here the thermal capacity of the insulators is slight compared with that of the fuel. In the examples given we could use as insulators material with a small thermal conductivity λ and relatively high coefficient of thermal diffusivity $\alpha = \lambda/\gamma c$. Among such materials we find, for example, air ($\lambda = 0.02$,

484

$\gamma = 1.29$ kg/m^3, $\lambda = 0.072$). Here the weight of the insulation is minimal.

For purposes of comparison we will point out, for example, that in as good an insulating material as cork plate ($\lambda = 0.036$, $\underline{a} = 0.00042$, $\gamma = 190$ kg/m^3) the characteristic thermal capacity is much higher, the thermal diffusivity is lower, but the weight of the material here is greater /6/.

The second case occurs whenever there is no internal cooling of the section and when the characteristic capacity is small. If the flight lasts for an unlimited time, the whole section will eventually acquire the temperature of the surface. But when the flying time is limited, we can select a heat insulating material, such that the temperature inside the section does not exceed the tolerance. For this the material must satisfy two requirements at the same time: it should have a low λ and a large $\gamma \subseteq$, or, what is the same thing, it should have as low a thermal conductivity as possible $\underline{a} = \lambda / \gamma \subseteq$. In this case air may prove unsuitable in view of its low thermal capacity /1, 6/. In practice we encounter several intermediate cases.

Sec. 65. Calculation of Single Layer of Heat Insulation when there is Slight Increase in the Heat Content of the Protected Part

This may be the case when the effective thermal capacity and permissible temperature increment of the body is small. Furthermore, let us consider that the flight time is relatively short. For the sake of simplicity we will take a flat body.

Let T_w be the temperature of the outer surface of the insulating material and T be the temperature of the surface of the body and the inside surface of the insulation.

Let us consider first how to determine the thickness of the insulation without making allowance for its thermal capacity $(c_{in}\cdot\gamma_{in}\approx 0)$. When there is insulation, little heat goes inwards, and the surface temperature is equal, with a fair degree of accuracy to the equilibrium temperature T_w determined from Eq. (14.3). The thermal resistance of the insulating material $R_{in} = \delta_{in}/\lambda_{in}$. Under these conditions the problem can be reduced to calculating the non-stationary heat of the body under a boundary condition of the third kind. An exact solution has been developed in the theory of thermal conductivity for the temperature distribution in a plate of infinite length and finite thickness /2/. The plate is heated on both sides (Fig. 221). We are given the temperature of the plate at the initial moment of time T_0, the temperature of the surrounding medium T_{ek}, and the heat transfer coefficient α. The variation of the temperature in all the sections of the plate with time is determined from the solution.

With certain assumptions, this solution can be used in our case. Let us suppose that the body in question is located in a medium at the temperature T_w. The heat-transfer coefficient between the surface of the body and the medium is $\alpha = \frac{1}{R_{in}}$.

..., in accordance with the true therm... insula..., ...ere is resistance

to heat exc... ...etween the outside medium at a temperature T_e . This

representation is possible since the temperature on the surface of the insulation

T_W virtually remains unchanged with time.

The conditional temperature of the outside medium in our case is T_W and

the condition heat-exchange coefficient is $\alpha_{ycл} = \dfrac{1}{R_{in}}$. Variation in the temperature

T_i in the boundary of the body is determined from the exact solutions /2, 3/

in the form

$$\theta = \frac{T_1 - T_0}{T_w - T_0} = f(\text{Bi, Fo}).$$

Here T_0 is the initial temperature of the body,

Biot number, $\quad - = \dfrac{\alpha_{ycл} d_\tau}{\lambda_{cr}} = \dfrac{\lambda}{\lambda} \dfrac{d_\tau}{h}$

Fourier Number $= \dfrac{a_\tau \tau}{d_\tau^2} = \dfrac{\lambda_\tau}{\gamma_\tau c_\tau d_\tau^2} : -$
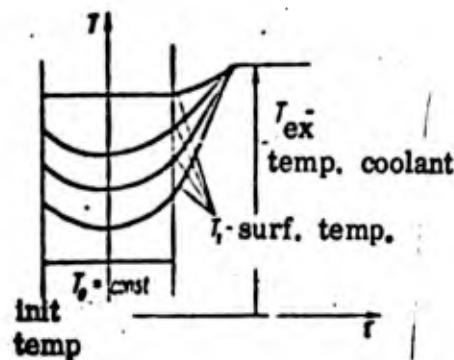

Fig. 221. Variation in temperature
of plate with time

The greatest possible increase in surface temperature $\left(T_1 - T_0\right)$ is the set

value. Since the flight time τ has also been set, the Biot number is uniquely

defined from graphs, and the required resistance of the insulation is therefore

$$R_{in} = \widehat{\delta}_{in}/\lambda_{in} \ .$$

As a result of the calculation it may appear that the required thickness of the insulating material cannot be ensured in the given part. An increase in this thickness can be created by reducing the permissible increase in temperature $(T_1 - T_0)$ or increasing Fo by reducing the product $(\gamma c d^2)$, or increasing the time τ .

In all cases it is advisable to use insulating material with a high characteristic thermal capacity. The shorter the flight time, τ , the more effective this will be. We will only describe here an approximate method, suitable for an extremely slight increase in surface temperature, i.e., at $\dfrac{T_{1_d}-T_0}{T_w-T_0} \ll 1$, where T_{1_d} is the permissible surface temperature of the body at the end of the heating up. In this case the surface temperature can be taken as equal to $T_{cp} = \dfrac{T_{1_d} + T_0}{2}$.

In order to determine the heat flux we use the solution of the problem of non-stationary heating of two infinite plates with an initial temperature T_m . One side of the first plate is kept at T_m , while the front side of the second one at the moment $\tau = 0$ acquires the temperature T_w , and is kept at it the whole time (Fig. 222).

Let us designate the parameters of one of the plates (insulation) λ_{3}, λ_{u3}, c_{u3};

and the parameters of the other plate (body) $\, \lambda_1, c_1, d_1 \,$ The problem is formulated

in the following way. Two plates of thickness δ_{T} (insulation) and d_{T} (body) are

in contact at a temperature $T_{cp} = \dfrac{T_{1} + T_{0}}{2}$ (Fig. 223). At an initial moment of time the

outside surface of the first plate (insulation) momentarily heats up to a temperature

T_{W}, which is then kept constant. The surface of the second plate (or to be more

exact, on the axis of the body) maintains a constant temperature T_{m} . We are

required to determine the temperature $T_{1}(\tau)$ on the contact surface, and the heat

flux passing through the contact surface $Q(\tau)$ in the time τ (see /2/, p. 238).
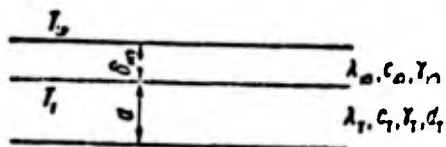

Fig. 222. For the determination
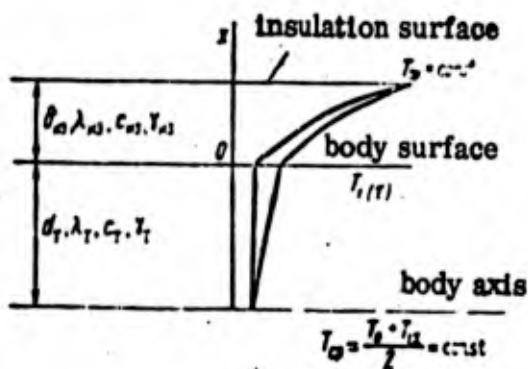of the thickness of the thermal
insulation

Fig. 223. Conditional calculation of insulation
at low variation in surface temperature

of body $\quad \dfrac{T_1 - T_0}{T_w - T_0} \ll 1.$

Having determined $q(\tau)$, we can replace the actual resistance of the insulation R_{in} by an effective value $(R_{in})_{ef}$, determined in such a way that the heat flux passing through this insulation in the time τ at a temperature difference $(T_w - T_{wall})$ under steady-state conditions is equal to the heat flux $q(\tau)$.
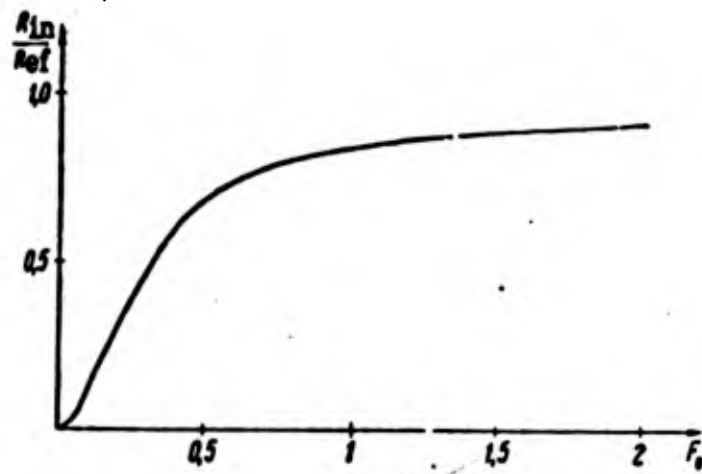
Fig. 224. Dependence $\dfrac{R_{in}}{(R_{in})_{ef}}$ from $Fo_{.} = \dfrac{a_{in}\tau}{\lambda_{in}^2}$.

The solution to the problem considered in the above-mentioned book by

Lykov gives us

$$\frac{Q(\tau)}{Q'} = f(Fo_{in}),$$ (14.6)

in which

$$Fo_{in} = \frac{\lambda_{in}}{c_{in}\gamma_{in}\delta_{in}^2},$$

$$Q' = \lambda_{in} c_{in} \delta_{in} (T_w - T_{wall}).$$ (14.7)

Let us introduce the effective heat resistance, which makes

allowance for the thermal capacity of the insulation on the basis of the condition

that the heat flux in the time τ under steady-state conditions is equal to Q_τ.

then

or

$$Q(\tau) = \frac{T_\bullet - T_{wall}}{(R_{in})_{ef}} =$$

$$\gamma_{in} c_{in} (T_\bullet - T_{wall}) \delta_{in} f(Fo_{in}) = \frac{T_\bullet - T_{wall}}{(R_{in})_{ef}} =$$

Then multiplying both sides of the equality by $R_{in} = \frac{\delta_{in}}{\lambda_{in}}$, and taking (14.7) into account, we get

$$\frac{f(Fo_{in})}{Fo_{in}} = \frac{R_{in}}{(R_{in})_{ef}}$$

or

$$\frac{(R_{in})_{ef}}{R_{in}} = f_1(Fo_{in}).$$

Fig. 224 shows the dependence of $\frac{R_{in}}{(R_{in})_{ef}}$ on $Fo_{in} = \frac{a_{in}\tau}{\delta_{in}^2}$.

At low Fo_{in}, the effective heat resistance of the insulation through internal thermal capacity is greater than under steady-state conditions. When Fo_{in} increases, i.e., all other things being equal, the effect of the thermal capacity of the insulation decreases as time increases.

The surface temperature of the protected part may be found by the method set forth at the beginning of this section if we were to replace the true value R_{in} by its effective value R_{ef}.

Sec. 66. Heat Up of Fuel in Tanks

When an aircraft is moving at a high speed, the fuel tanks must be firmly

insulated. The temperature of the fuel must not exceed its boiling point. In

a number of cases the maximum fuel temperature is determined from considerations

of ensuring the smooth supply of fuel to the engine, the spalling resistance of

the packing, prevention of cavitation in the feed lines, and so on.

The problem of heat insulation becomes particularly acute when designing

machinery for flights of the longest possible range. In this case the aircraft must

carry
tremendous reserves of fuel, the weight of which amounts to as much as 75% of

the total weight of the aircraft. By the end of the flight, which may last several

hours, the temperature of the fuel in the reserve tanks may become excessive. The

use of any heat insulating material means an increase in the dry weight of the

machinery and, accordingly, a reduction in the range of the flight.

The final fuel temperature is also a function of the make-up of the tanks

sequence
aboard the aircraft and the   in which they empty. The tanks which empty

first need not be insulated at all; those which empty last must be insulated to

the maximum extent. Fuel contained in one large tank   heats up more quickly

by the end of the flight than fuel contained in several tanks emptying one after

the other /1/.

Let us consider the calculation for the heating up of fuel in a cylindrical

tank. The lateral surface of the tank is the fusilage, around which there is a flow

492

of supersonic air. The tank remains full until the end of the flight, or is emptied under set conditions (Fig. 225).

The heat may reach the fuel through the wetted tank surface S_{wet} or through the non-wetted surface S_{hw} by convection and radiation heat exchange to the free surface of the fuel F.

Fig. 225. Fuel tank

Let us designate the volume of the fuel at an arbitrary moment of time as V, and its specific gravity and thermal capacity as γ_T and c_T. The heat balance equation can then be written in the following form

$$V \gamma_T c_T \frac{dT}{d\tau} = q_1 S_{cu} + q_2 F.$$

(14.8)

in which T is the temperature of the fuel, taken as identical throughout the volume, τ is the time, q_1 is the heat flux density through the wetted tank surface, and q_2 is the heat flux density to the free fuel surface.

In order to determine the variation in the temperature of the fuel T with time, we have to express q_1, q_2, V, S_{wet} and F in the form of time functions, after which we can numerically calculate the variation in T with respect to τ, by splitting up the entire flight time into finite intervals.

a) determining the heat flux density q_1 through the wetted surface.

The continuity conditions for the heat flux take the form

$$q_1 = a(T_e - T_w) - 4,9\varepsilon\left[\left(\frac{T_w}{100}\right)^4 - \left(\frac{T_H}{100}\right)^4\right] =$$

$$= \frac{\delta_{cr}}{\lambda_{cr}}(T_w - T_{w_1}) = a_r(T_{w_1} - T).$$

Here α is the heat-transfer coefficient from the outside stream to the wall, α_r is the heat-transfer coefficient from the inside surface of the wall to the fuel, ε is the degree of blackness of the outside surface, and $\delta_{cr}/\lambda_{cr} = R_{in}$ is the thermal resistance of the insulation.

Taking out the temperature of the inside wall T_r, we get

$$a(T_e - T_w) - 4,9\varepsilon\left[\left(\frac{T_w}{100}\right)^4 - \left(\frac{T_H}{100}\right)^4\right] = \frac{T_w - T}{\frac{1}{a_r} + \frac{\delta_{cr}}{\lambda_{cr}}} = q_1.$$

The solution of the first equality gives us the dependence of T_{wr} on T and then the variation in q_1 as a function of the variation in T.

b) determining the heat flux density through the free fuel surface F.

There may be heat exchange between the inside non-wetted surface of the tank S_{hw} and the free surface of the fuel through natural convection of gas and vapor above the surface of the fuel and also through radiation.

494

Let us use α_K to designate the coefficient of heat exchange through natural convection, referred to a unit area of the fuel surface. The degree of blackness of the inside surface of the tank и is designated ε_i, while that of the fuel is taken to that of unity. We can then introduce an effective degree of blackness, referred to unit area of free fuel surface ($\varepsilon_{эf}$), for the radiant heat exchange between the tank walls and the fuel surface.

The continuity condition for the heat flux can now be written in the following form

$$\alpha S_{нс}(T_e - T_в) - 4{,}9\varepsilon_i S_{нс}\left[\left(\frac{T_в}{100}\right)^4 - \left(\frac{T_{II}}{100}\right)^4\right] = \frac{{}''(T_в - T_{в_1})\lambda_{ст}}{\delta_{ст}} S_{нс} =$$

$$= \alpha_к(T_{в_1} - T)F + 4{,}9\varepsilon_{эf}F\left[\left(\frac{T_{в_1}}{100}\right)^4 - \left(\frac{T_{II}}{100}\right)^4\right] = q_2 F. \qquad (14.9)$$

This expression at a set value of F is used to determine q_2 as a function of the fuel temperature T .

Having calculating $\dot q_1(S, T)$ and $q_2(S, T)$, we can solve numerically the basic heat balance equation. The variation и in the volume of fuel V, the surfaces S _нw and F as a function of time can easily be determined at the set dependence of fuel consumption with time and the geometric dimensions of the tank.

Below we give examples of the use of theoretical relationships to determine the heat regime of the surface.

Example 1. We are required to determine the temperature of the aircraft

fuselage at a distance of 1 m from the leading edge.

$$H = 20 \ \text{км}, \quad M_H = 4, \quad T_H = 216,5°, \quad p_H = 41,77 \ \text{мм рт. ст.}, \quad \varepsilon = 0,82.$$

We are to consider the laminar and turbulent flow in the boundary layer.

Solution. The temperature is determined from the balance

$$q_{con} = q_{rad}$$

$$q_{con} = 0,82 \cdot 4,9 \left(\frac{T}{100}\right)^4.$$

In laminar flow

$$q_{con} = 0,332 \lambda_1 (T_e - T_x) \sqrt{\frac{u \rho_1}{\mu_1 x}}.$$

In turbulent flow

$$q_{con} = 0,029 \frac{\lambda_1}{x} (T_e - T_x) \left(\frac{u \rho_1}{\mu_1 x}\right)^{0,8} (1 + 0,2 r M_1^2)^{-0,55} \left(\frac{T_x}{T_e}\right)^{-0,2}.$$

$$M_1 = M_H, \ \rho_1 = \rho_H, \ \lambda_1$$

and μ_1 and λ_1 are the coefficients of viscosity and thermal conductivity

at T_H, $x = 1$ m, $T_2 = T_H (1 + 0.2 \ r \ M_H^2)$; for laminar flow $r = 0.845$ and for

turbulent flow $r = 0.89$.

Example 2. Determine the total amount of heat which has to be removed

from the bottom surface of the wing at an angle of attack 10°50' in order to keep

the surface temperature at 500°K. The flow conditions are laminar, the flight

altitude is $H = 37$ km, $M_H = 4$, $T_H = 255°$K, $\rho_H = 0.69 \times 10^{-3}$ kg cm/m. The

degree of blackness $\varepsilon = 0.8$.

<u>Solution</u>. The heat flux density is

$$q(x) = q_{con} - q_{rad} \sqrt{\frac{u_1 \rho_1}{\mu_1 x}} \lambda_1 (T_e - T_w) \theta'_w - \varepsilon c_0 \left(\frac{T_w}{100}\right)^4.$$

$$\sum q_x = 10 \int_0^{15} q(x)\,dx = 150 \left[\sqrt{\frac{u_1 \rho_1}{15 \mu_1}} 2\lambda_1 (T_e - T_w) \theta'_w - 4.9\varepsilon \left(\frac{T_w}{100}\right)^4\right].$$

Here $\lambda_1, u_1, \rho_1, \mu_1$ are the gas parameters beyond the density discontinuity.

The tables contained in /5/ give us the slope angle of the discontinuity

$\varphi_{dis} = 23°$, the M number beyond the discontinuity $M_1 = 3.23$, ρ_1 is the gas

density beyond the discontinuity, $\dfrac{\rho_H}{\rho_1} = 0.5.$.

$$T_{00} = T_H \left(1 + \frac{k-1}{2} M_H^2\right). \qquad k = 1.4.$$

$$\frac{T_1}{T_H} = \frac{(1 + 0.2 M_H^2)}{(1 + 0.2 M_1^2)}.$$

$$T_e = T_1(1 + 0.2 r M_1^2).$$

in which $\underline{r}$ is the recovery coefficient $\left(\underline{r} = 0.845\right)$

$$u_1 = M_1 a_1, \quad a_1 = 20.1 \sqrt{T_1}.$$

Knowing T_1, the tables give us the thermal conductivity λ_1 and the

viscosity coefficient μ_1 for air in a *Technical engineering* system.

The value θ'_w is determined from the curve or from the approximate equation

$$\theta'_w = 0.332.$$

Let us solve the same problem for turbulent flow in the boundary layer.

The convective heat flux is $q_w = \alpha(T_e - T_w)$.

Here

$$\alpha = 0.029 \frac{\lambda_w}{x} \left(\frac{u_1 \rho_w x}{\mu_w}\right)^{0.8} \left(\frac{T_w}{T_e}\right)^{0.2} (1 + 0.2 r M_1^2)^{0.11}.$$

$$\rho_w = \rho_1 \frac{T_w}{T_1}. \quad r = 0.89.$$

λ_{hr} and μ_{hr} are taken at a wall temperature T_w. $a_{xp} = a/0.9$.

$$\sum \varphi(x) = 25\left[\frac{0.029}{0.8}\frac{\lambda_w}{15}\left(\frac{a_{kp}\cdot 15}{\mu_w}\right)^{0.9}\left(\frac{T_w}{T_e}\right)^{0.2}(1+0.2rM_i^2)^{0.1}-\right.$$
$$\left.-0.8\cdot 4.9\left(\frac{T_w}{100}\right)^4\right].$$

Example 3.   Calculate the amount of cold air which has to be fed through a porous surface in order to cool it down to 500°K with air at $T_0 = 250$°K.

The surface is an axial symmetric end $r_0 = 3$ cm. The flow is laminar, radiation can be disregarded.

Flight conditions: H = 42, $u_H = 5.2$ km/sec, $\rho_H = 0.323\cdot 10^{-3}$ kg·sec^2/m, $T_H = 293$°K.

The graph for the relationship (see Fig. 166)

$$f_w = f\left(\frac{J_e - J_w}{(J_w - J_0)Pr^{\frac{2}{3}}(0.71)^{\frac{1}{3}}}\right)$$

gives us f_w, after which we determine

$$G_{cel} = g\rho_w v_w \pi r_0^2 = g\pi r_0^2\frac{2}{3}\sqrt{3}f_w\sqrt{\frac{\mu_w}{\rho_w}\beta}.$$

Here P_w is the density of the air at the forward critical point at wall temperature, μ_w is the viscosity coefficient at the wall temperature $\beta = \left(\frac{\partial a}{\partial r}\right)_{r=0} = \frac{a_{kp}}{r_0}$.

$$a_{kp} = 18.3\sqrt{T_{00}},\quad T_{00} = T_H\left(1+\frac{k-1}{2}M_H^2\right).$$

$$M_H = \frac{u_H}{a_H} = \frac{u_H}{20.1\sqrt{T_H}}\ .$$

$$\rho_w = 0.125\rho_0\cdot\frac{288}{T_w}.$$

ρ_0' is the total pressure beyond the straight discontinuity,

$$\frac{p_0'}{p_H} = \frac{1}{2}\left[\frac{(k+1)^{\frac{k+1}{k-1}}M_H^{\frac{2k}{k-1}}}{(4kM_H^2 - 2k + 2)^{\frac{1}{k-1}}}\right]$$

$$\frac{p_0'}{p_H} = \frac{166.7M_H^7}{(7M_H^2 - 1)^{2.5}}.$$

(Rayleigh's Equation)

498

The parameter $\dfrac{J_e - J_w}{(J_w - J_0) \, Pr^{\frac{2}{3}}(0.71)^{\frac{1}{3}}}$ is determined in the following way

$$J_e = c_p T_{(0)} \qquad (c_p = 0.24)$$

$$J_w = c_p T_c. \qquad J_0 = c_p T_{0}. \qquad (Pr = 0.71):$$

2) determine the amount of heat during convective cooling under the

same conditions

$$q_w = 0.39 \sqrt{3)_w} (T_{w0} - T_w) \left| \sqrt{\dfrac{\rho_{fw}}{\mu_w}} \right.$$

$$G_{0.1} = \dfrac{q_w \pi r_0^2}{c_p (T_w - T_0)}.$$

References

1. Van Drayst, Problem of aerodynamic heating, "Problems of rocketry" Foreign Lit.Press, 1957, No. 5.

2. Lykov, A. V. Theory of thermal conductivity, Gostekhizdat, 1952.

3. Mikheyev, M. A., Fundamentals of heat transfer, Gosenergoizdat, 1956.

4. Eckert, E., Engineering methods for calculating laminar and turbulent heat exchange and friction during flow round surfaces, "Problems of Rocketry", Foreign Lit. Press, 1957, No. 4.

5. Ferri, A., Aerodynamics of supersonic flow, Gostekhizdat, 1952, p. 458.

6. Burgess, E., Guided jet missiles, Foreign Lit. Press, 1956.

In designing liquid-propellant rocket engines one of the main problems is to

ensure reliable protection for the walls of the combustion chamber and nozzle from the

effect of the red-hot combustion products. At high gas pressures and temperatures, very

great heat flux occurs in the combustion chamber on account of convective and radiant

heat exchange. The specific heat flux on the chamber walls attains $5 \cdot 10^6$ kcal/m^2 · hour,

and $20 \cdot 10^6$ kcal/m^2 · hour in the critical cross section of the nozzle. The high

temperatures of the gases in the chamber increases the share of heat flux through

radiant heat exchange, the proportion constituting 20 to 30% of the total heat flux

in modern engines /1, 7/. Fig. 226 shows the rough distribution of specific heat
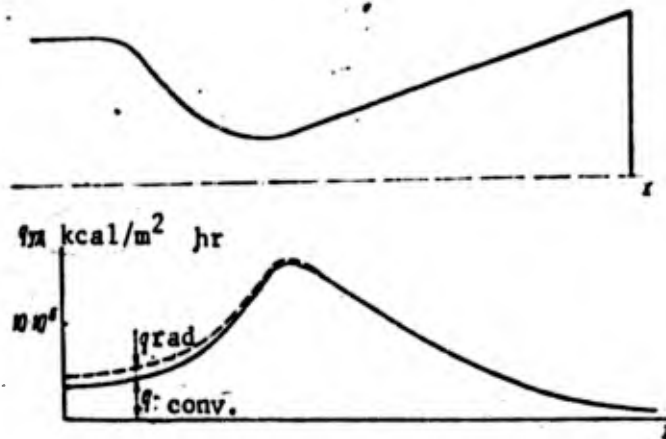
flux along the length of the chamber and nozzle.

Fig. 226.

Approximate Distribution of specific heat flux
along combustion chamber and nozzle in liquid-
propellant rocket engine.

It is an extremely difficult task to cool the chamber walls and nozzle under

these circumstances. For example, when there is outside liquid cooling, it is

necessary to provide for an extremely large consumption of fluid through the cooling

jacket. If fuel is used as the coolant, its thermal capacity may prove insufficient

to absorb the heat removed. Furthermore, at high specific heat *fluxes* there is a

considerable temperature *gradient* through the cooled wall, on account of which

it is difficult to ensure a fairly low temperature on the inside of the wall.

All these difficulties are made greater in present-day hopped-up engines

with increased pressure in the combustion chamber, and when using special high-calority

fuel. In these cases we have to use various combined systems of cooling. When

arranging for the cooling of a rocket engine, we have to ensure minimum energy loss

on overcoming the resistance of the jacket, or heat losses when the chamber is cooled

on the outside by a liquid which is not a combustion component.

Part of our problem is *a* (comparative *analysis* of the possible methods of

thermally protecting the chamber walls and nozzle from the viewpoint of the principle

involved in them in different cases. Examination of specific designs *can be found*

in special *studies,* (which also describe the relevant methods of calculation.

67. Distribution of *the* Heat *flux* Along *the* Combustion Chamber

In order to obtain a picture of the distribution of the specific heat *flux*

along the combustion chamber we can utilize the approximate formula for the

coefficient heat-exchange

$$z_q = 74.3 c_p (g\mu)^{0.14} \frac{G^{0.82}}{d^{1.82}} \left(\frac{T_{00}}{T_w}\right)^{0.35}$$

(15.1)

Here G is the gas consumption, d is the diameter of the chamber or nozzle, T_{00} is the ~~drag~~ temperature, T_w is the temperature of the wall. The values c_p and μ are determined at the wall temperature T_w.

The convective heat flow is determined from the expression

$$q_c = z_q(T_{00} - T_w),$$

(15.2)

in which c_p is the mean thermal capacity in the boundary layer.

As follows from the expression for q_c, the specific heat flux is more or less inversely proportional to $d^{1.82}$. The maximum heat flux occurs in the critical cross section of the nozzle.

In order to calculate the heat flux due to radiation we can use the empiric expressions /7/

$$q_{CO_2} = 3.5\sqrt[3]{p_{CO_2}l}\left[\left(\frac{T_{00}}{100}\right)^{3.5} - \left(\frac{T_w}{100}\right)^{3.5}\right] \quad kcal/m^2 \cdot hr$$

(15.3)

$$q_{H_2O} = 3.5 p_{H_2O}^{0.8} l^{0.6}\left[\left(\frac{T_r}{100}\right)^3 - \left(\frac{T_w}{100}\right)^3\right] \quad kcal/m^2 \cdot hr$$

(15.4)

Here p_{CO_2} and p_{H_2O} are the partial gas pressures and l is the reduced path length of the ray.

The gases remaining in the combustion chamber radiate to a considerably

lesser extent, on account of which we may assume

$$q_s = q_{CO_2} + q_{H_2O}.$$

The gas temperature T_g in the combustion chamber is equal to the *drag*

temperature T_{00}; as the gases move along the nozzle, the temperature T_g drops. Thus,

the heat fl*ux due to* radiation show/a maximum in the combustion chamber and *is*

reduced in the nozzle as the gas speeds up.   The variation in heat fl*ux* along the

chamber is shown in Fig. 226.

Consideration for heat exchange *due to* radiation of gases does not affect

the qualitative picture of the heat fl*ux* distribution.

68.   Methods of Thermal Protection of Chamber and Nozzle Surfaces

in Rocket Engines

Use of thermal capacity

The thermal capacity method is used in rocket engines which *operate* for a

short time, or when using fuels with low calorific value. The engine or its parts

are made of fairly thick metal. The heat coming from the hot combustion products

is taken *in* by the surrounding walls and heats them *up to* a [temperature] surface

permissable from the viewpoint of strength. This is taken as close
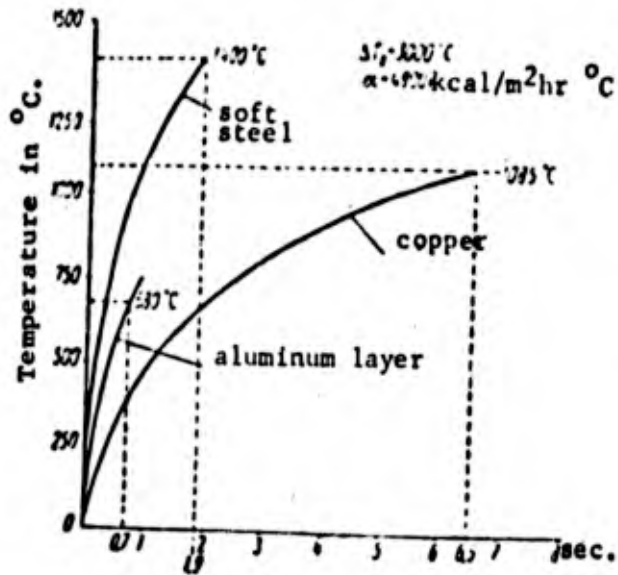
to melting point.

Fig. 227. Variation in thick wall temperature with time for different materials

Fig. 227 shows the increase in the wall temperature for three materials: copper, steel and duralumn. The curves are calculated for a case in which

$\frac{a}{c}$ = 4800 kcal/m^2 · hour · deg and for an initial temperature drop between

the gas and the wall $h \frac{\delta l_0}{c_p}$ = 3000°. When calculating the temperature we used the

theoretical solution (see p. 148 in /6/) for the problem of the heating of the

surface of a rod restricted on one side by an insulated lateral surface with a

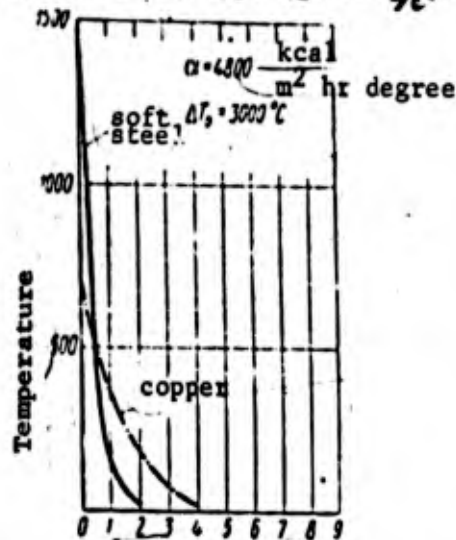boundary condition of the third type (given $\frac{a}{c}$ and T_{g0}).

Fig. 228. Temperature distribution with time in plate made of copper and steel.

Distance from hot surface in cm.

505

As can be seen from these curves, copper takes the longest time to heat up to the melting point. This is due to greater thermal conductivity through which heat removal inside the wall is increased. Fig. 228 shows the distribution temperature every two seconds after starting up in a plate made of steel and copper.

Use of the thermal capacity method is strictly limited in view of the need for heavy metal parts.

Use of High-Melting Materials

The use of materials with low thermal conductivity results in still steeper temperature curves than for steel. But if the melting point of the material is fairly high, or even equal to or greater, than the combustion point, a thin wall of high-melting material protects the part from heating up. On account of the poor mechanical properties of high-melting materials, the inside of the chamber is made of a high-melting material, which is then surrounded by a metal casing that can take the mechanical stresses. Another criterion for the suitability of a high-melting material is its response to the chemical action of the combustion products and ability to withstand a sudden increase in temperature.

Fig. 229 shows data for a number of materials with a high melting point. It also Compare) (their melting and softening points with the combustion points

506

of mixtures of oxygen and paraffin, nitric acid and paraffin, and hydrogen peroxide

and hydra~~zi~~ne hydrate /1/, /4/.

As can be seen from the graph, a number of materials *the* *exhibit* a fairly high

melting point. Experiments have shown the possibility of using graphite, tungsten

carbide and silicon. Most high-melting carbides and nitrides *would be able* withstand the

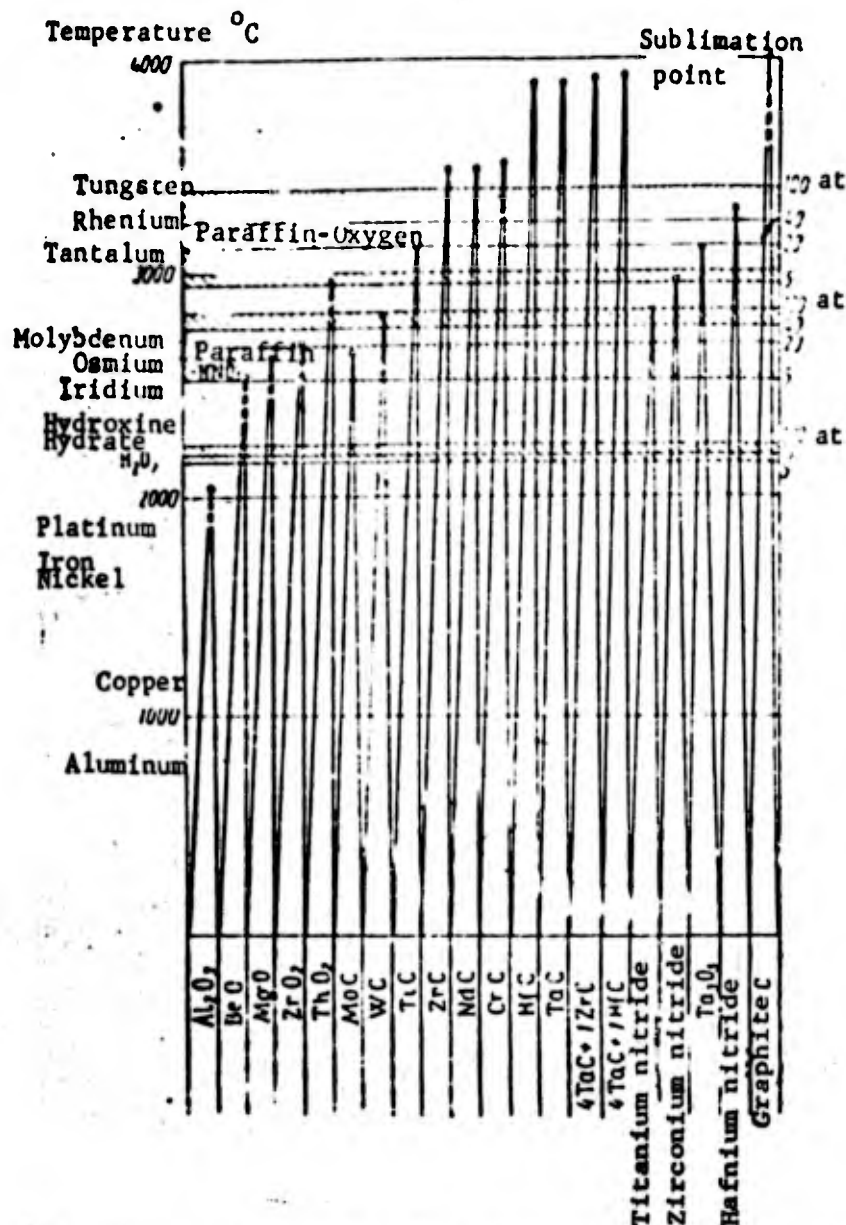highest temperatures developed by rocket engines.

Fig. 229. Softening and melting points of high-melting materials

<u>External Cooling</u>

External cooling is the commonest cooling method. The coolant circulates

through channels with a small cross section *attached to* the outside of the walls washed by

hot gas on the inside.

If the heat fl^{ux} from the gas to the wall . *has been determined*, in the calculation we

have to determine the rated consumption of coolant ensuring removal of the heat

received, and the rated coefficients *heat-exchange* on the *side* of

the coolant, at which the temperature of the *inside* surface of the wall does not

exceed the tolerances.

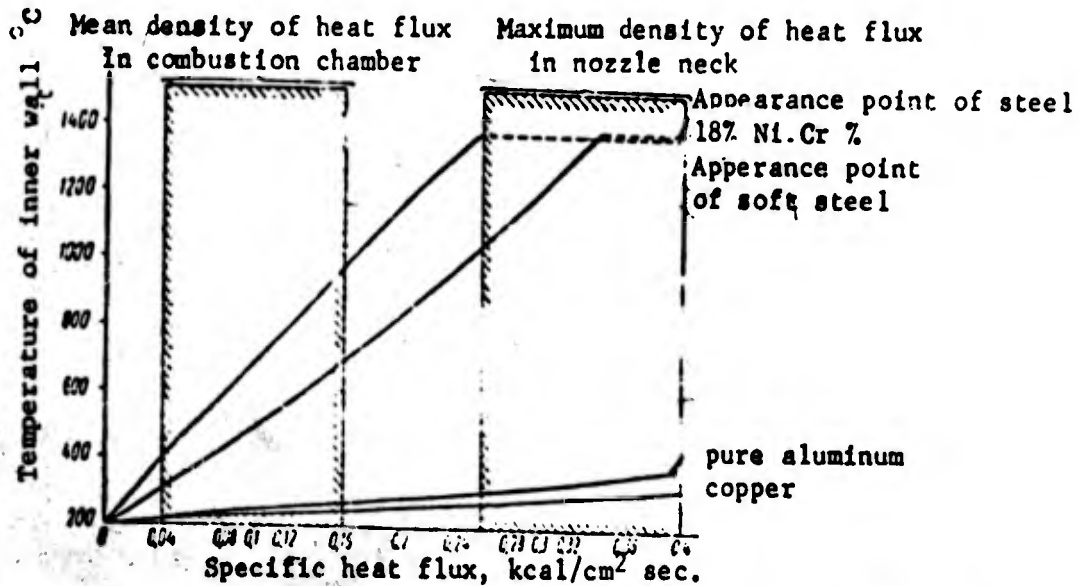Fig. 230.   Temperature of inside surface of walls 2.5 mm thick
using different materials as a function of the specific
heat flux.

Let us consider the factors on which the temperature of the inside surface

of the wall depends. At a given heat flow <u>q</u> and wall temperature on the side of the

coolant $T_{\underline{x}}$, the temperature of the surface on the hot gas side $T_{\underline{W}}$ is determined

from the expression

$$T_{\kappa} = q \frac{\delta}{\lambda} + T_{r}.$$

Here δ is the thickness of the wall and λ is the thermal conductivity.

If T_{x} is more or less constant, T_{w} increases with an increase in δ or a decrease in λ. The value δ cannot be lower than a certain limit, hence in order to reduce T_{w} we have to select materials with a high λ. In this case, however, we have to take into account that the surface temperature tolerances for different materials may be different.

Fig. 230 shows the temperature of the inside surface of the wall as a function of the specific heat fl^{ux} for four materials: soft steel, alloyed steel (18% Cr, 8% Li), copper and aluminum. In all cases the wall thickness is 2.5 mm. The temperature of the outside surface of the wall is 200°C.

As can be seen from the graph, aluminum, and particularly copper, show lower surface temperatures. When steel is used, the temperatures of the wall are higher. So although the melting point of steel is higher than that of aluminum and copper, the use of steel is restricted by a lower heat flux

509

Determining Heat Transfer Coefficients and Temperature

of Wall on Side of Liquid

It was assumed in the foregoing examples that the temperature of the wall

on the side of the liquid was fairly small and remained constant. This is the case

at fairly high values of the heat-transfer coefficient $\alpha_{\varkappa}$. In the general case, the

temperature of both surfaces should be determined from the heat balance condition

$$q = \frac{a_r}{c_p}(J_{\infty} - J_{\varkappa}) + 4.9 \left[\left(\frac{T_{\infty}}{100} \right)^4 - \left(\frac{T_{\varkappa}}{100} \right)^4 \right] = \frac{\lambda}{\delta}(T_{\varkappa} - T_{\varkappa}) =$$
$$= a_{\varkappa}(T_{\varkappa} - T_1) \tag{15.5}$$

The total heat resistance between the hot gas and the coolant is the sum

of the resistance of the boundary layer on the hot gas side, the resistance of the wall

and the resistance of the boundary layer on the coolant side:

$$R = \frac{1}{a_r'} + \frac{\delta}{\lambda} + \frac{1}{a_\varkappa}.$$

Here α_g' is the coefficient heat-exchange including heat transfer by

radiation.

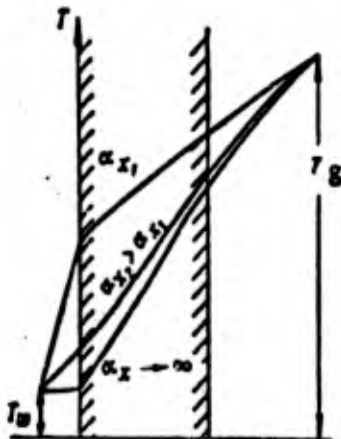
Fig. 231. Temperature distribution at different heat-transfer
coefficients from wall to coolant.

Variation in $a_{/l}$ has an effect on $\underline{R}$ only if $1/a_{/l}$ is of the order or greater than the remaining terms in the sum. As $a_{/l}$ increases, the last term decreases and the temperature of the wall on the outside tends to the temperature of the liquid. Fig. 231 gives a qualitative idea of the temperature distribution in the boundary cross section of the wall when $a_{/l}$ varies.

$a_{/l}$ may be determined by the empiric formula

$$a_s = z \frac{82.5}{d_e^{0.2}} \left(\frac{G_{cool}}{F_1}\right)^{0.8} \text{ kcal/ m}^2 \text{ hr degree}$$

Here

$$z = \lambda_x^{0.6} \frac{c_1^{0.4}}{(g\mu_1)^{0.4}} .$$

(15.6)

$F_{/l}$ is the area cross-section of the cooling channel, $d_{/e}$ is the equivalent diameter of the cross section of the channel, $d_e = \frac{4F_s}{\pi}$ and π is the perimeter of the cross section.

Since the heat fl^{ux} var^{u_s} along the length, the wall temperature is also a variable. During the calculation, the entire length is broken up into sectors and the value of T_w is determined for each one.

Checking the presence of enough coolant.

The greatest amount of heat which can be taken up by the coolant is determined by heating it to the boiling point at a set pressure in the cooling jacket. The heat balance condition can be written down in the following form:

$$\sum_i q_i f_i = \varepsilon c_{bol}(T_{out} - T_{in}).$$

(15.7)

Here q_i is the specific heat flow at the i-th sector, f_i is the area of the i-th sector of the chamber, c is the thermal capacity of the liquid at mean temperature, and T_{out} and T_{in} are the temperature of the liquid at the outlet and inlet of the cooling jacket, respectively.

When there is a large heat flux, it may be found that the consumption of a component is insufficient for purposes of cooling. In this case both components are used, or else internal or combined cooling systems are introduced.
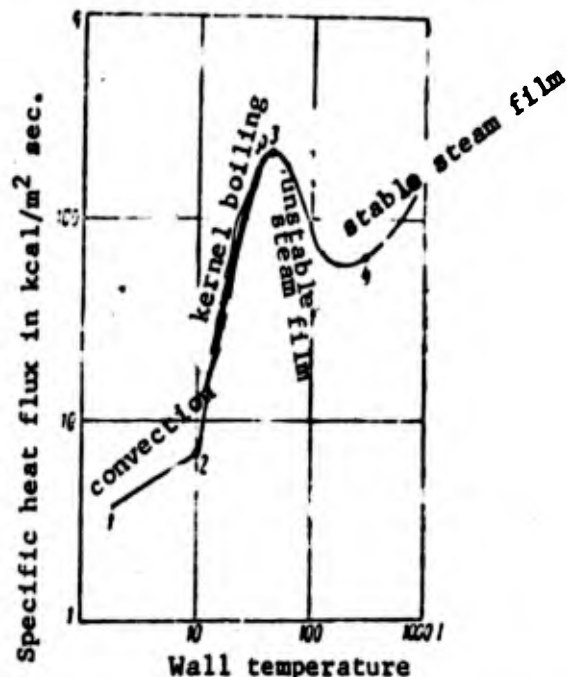

Fig. 232 Variation in heat flux during variation in wall temperature.

Surface Boiling of Liquids

If the temperature of the surface in contact with the coolant exceeds the boiling point, the formation of vapor begins in the boundary layer, although the bulk

512

of the liquid is at a temperature considerably below the boiling point.

Fig. 232 shows the variation in the wall temperature for three different sets of conditions. Between points 1 and 2 we find convective heat exchange conditions, i.e., the temperature of the wall is lower than the boiling point. At point 2 the boiling point is reached and small bubbles of vapor form by the wall and condense when the *stream* , the temperature of which is below the boiling point, moves inwards. The heat-exchange coefficient is increased through this process and the cooling conditions are therefore improved. The heat-exchange coefficient may be increased by a factor of 5 - 7. But if the temperature of the wall is further increased, there may occur film boiling, (which α *during j* falls sharply. In this case the surface may become dangerously hot and may fail.

When designing modern engines with external cooling, use is made of rated conditions with bubble boiling.

Internal Cooling of Combustion Chamber and Nozzle in

Rocket Engines

As has been shown above, the use of external cooling becomes difficult when the specific *heat flux* is stepped up. Furthermore, in a number of cases we have to protect the surface from chemical and mechanical action by the stream of red-hot gases. Here it is advisable to use internal cooling. In internal cooling,

513

a liquid or gas (see Chapter X) is forced through a number of slots or openings onto the surface.

It should be pointed out that the use of porous cooling is determined to a considerable extent by the availability of a spalling-resistant and suitably strong porous material. In order to keep the temperature of the combustion chamber and nozzle wall constant, the consumption of coolant has to be varied in proportion to the variation in the heat flux. But in view of the fact that the heat flux in the diverging area is sharply reduced, it is sufficient to feed the coolant through the chamber or nozzle wall just before the critical cross section.

Captions to figures.

Fig. 226. Approximate distribution of specific heat flux along chamber combustion and nozzle in liquid-propellant rocket engine

Fig. 227. Variation in thick wall temperature with time for different materials

Fig. 228. Temperature distribution with time in plate made of copper and steel

Fig. 229.   Softening and melting points of high-melting materials

Fig. 230. Temperature of inside surface of walls 2.5 mm thick using different materials as a function of the specific heat flux.

Fig. 231. Temperature distribution at different heat-transfer coefficients from wall to coolant

Fig. 232. Variation in heat flux during variation in wall temperature

References

1. Boden I and others. Some problems of heat exchange and cooling rocket engines. "Problems of rocketry," For. Lit. Press, 1952, No. 3.

2. Beyli S.(Payley?) Study of heat exchange to rocket engine fuel, ibid. 1955, No. 4.

3. Grinfild S. Calculation of heat-transfer coefficients in rocket engines, ibid., 1952, No. 1.

4. Ziblend I. Survey of modern methods of protecting and cooling rocket engine walls, ibid., 1955, No. 3.

5. Ziblend I. Problems of heat transfer in rocket engines, ibid., 1956, No. 4.

6. Lykov A. V. Theory of thermal conductivity, Gostekhizdat, 1952.

7. Sinyarev, G. B. and others. Liquid fuel rocket engines, Oborongiz, 1955.

CHAPTER XVI

HEAT CONDITIONS IN CRAFT FLYING IN UPPER LAYERS OF ATMOSPHERE
(ARTIFICIAL EARTH SATELLITES)

As the velocity of the flight is stepped up, the heat flux from the air

to the surface of such craft increases approximately in proportion to ρV^3. Flights

at velocities greater than 3 km/sec in the lower layers of the atmosphere are

virtually impossible. When the flight velocity is increased, however, the

centrifugal force offsetting gravity is increased and the   part played by the

aerodynamic buoyancy is reduced. On account of this the flight altitude may

be increased, and it becomes possible to fly in rarefied layers of the atmosphere.

At a flight velocity of ~ 7.9 km/sec, centrifugal force exactly balances gravity,

and the altitude of the flight is unrestricted. Here the air plays a negative

part, creates resistance and heats up the shell of the craft. At heights greater

than 200 km this resistance disappears for practical purposes. This altitude

region is indeed the region in which artificial earth satellites orbit the earth.

The aim of the present section is to give a brief description of the heat

conditions for artificial earth satellites.

When considering the heat regime for satellites, we   are faced with the

problem of determining the temperature of the internal and external parts and the

possibility of controlling them. Temperature control (of the instruments, apparatus and compartments assigned to living organisms) is essential if we are to prevent them overheating or becoming too cold. The problem is further complicated by the fact that during the flight there is no natural convection in the gas filling the satellite, which forces us to install artificial ventilation. The instruments and the living organisms give out heat, the satellite heats up on account of solar and terrestrial radiation, and at low altitudes through interaction with the surrounding medium. To avoid this over-heating, all the heat has to be taken away from the satellite.

This can be done most effectively by radiation from the surface. Here we have to satisfy two conditions. First, the amount of energy reaching the radiation surface from the outside and inside must be equal or less than the amount of energy radiated from the surface. Second, the temperature of the shell must be lower than that of the parts cooled inside.

These requirements are satisfied by proper selection of the dimensions of the radiation surfaces and emissivity characteristic is a function of wavelength. The sun's rays must be reflected from the surface, i.e., the blackness in the visible part of the spectrum A_s must be low, and at the same time the surface must radiate to a maximum extent, i.e., the blackness in the

infra-red region ξ corresponding to the region of characteristic radiation must be as close as possible to unity.

The output of the fan must be fairly low, since the energy reserves aboard the satellite are limited, and in addition, all the heat given out by the ventilator must also be removed by the cooling system. While the satellite is in motion, there may be moments when all the instruments are switched off or when their output is very small. This gives rise to the danger of overcooling, particularly when the satellite passes through the earth's shadow. If the control system is correctly designed, the temperature of the instruments should increase when the fan is switched off, and decreased when it is switched on. If the fan output is varied, it is always possible to keep the temperature within set limits.

An exact calculation of the temperature control system is complicated by the fact that the heat flux varies during the flight, the heating up and cooling down of the instruments is non-stationary, and the thermal capacity of the instruments or that part of it participating in the thermal exchange has to be included in the calculation.

Sec. 69. External Heat Sources

Radiant energy

The radiant energy is a sum of the longwave energy of radiation from the earth, radiation from the sun and solar energy reflected from the earth. The components of radiant energy coming from the earth are shown in Table 21. Each of the radiant energy sources mentioned is a variable in the general case, and a function of the position of the satellite with respect to the earth, the season, the state of the earth's surface, the atmosphere, and so on.

Since the satellite is moving at a great velocity and at fairly extensive distance from the earth's surface, though its trajectory passes over an extensive part of the globe, it can be considered that the radiant energy received by the satellite's surface is equal to a mean. Hence the amount of radiant energy can be calculated on the basis of the mean yearly heat balance of the earth.

The amount of radiant energy coming from the sun per unit   area perpendicular to the sun's rays at a mean distance between the sun and earth (beyond the earth's atmosphere) is determined by the solar constant S_0, which is equal to 1140 kcal/$m^2 \cdot$ hour /3/.

Columns 2 and 3 in Table 21 /3/ show the energy, shortwave and thermal radiation from the earth per unit surface.

Table 21

Type of radiant energy	In % S_0	E_0 kcal/m^2
Shortwave radiation		
1. Reflected from clouds into terrestrial space	27	—
2. Reflected into terrestrial space through disperion by atmosphere	7	—
3. Reflected into terrestrial space from earth's surface	3	—
Total reflected	37	—
Thermal radiation		
1. Radiation of atmosphere into terrestrial space	55	157.2
2. Characteristic thermal radiation of earth's surface	8	22.8
Total radiated	63	180

It follows from this table that the proportion of reflected solar

energy - the earth's albedo - is $\alpha = 0.37$.

The heat flux emitted per unit surface of the earth E_0 is determined

from the heat balance

$$S_0 \pi R^2 (1-\alpha) = E_0 4 \pi R^2; \quad E_0 = \frac{S_0(1-\alpha)}{4} = 180 \text{ kcal/m}^2 \cdot \text{hr} \qquad (16.1)$$

Radiation from the atmosphere plays a fundamental part. In order to calculate it ,

we introduce the concept of the effective radius R, determined in such a way that

the radiation from the surface of a sphere R is equal to radiation from the earth's

surface and from the atmosphere. It was taken in the calculations that the height

of the atmosphere was the upper limit of the troposphere, i.e., 12 km. In
accordance with this the effective radius of the earth was taken as $R = 6370$ km +
12 km, where $R_0 = 6370$ km is the earth's radius.

Heating due to earth's radiation

Let us consider a flat plate, the plane of which comprises the angle β
with a line joining the plate to the center of the earth (Fig. 233). If the
angle β is such that the plane of the plate does not intersect the earth's surface
$(\beta > \beta_2)$, the amount of heat reaching the plate through the earth's own
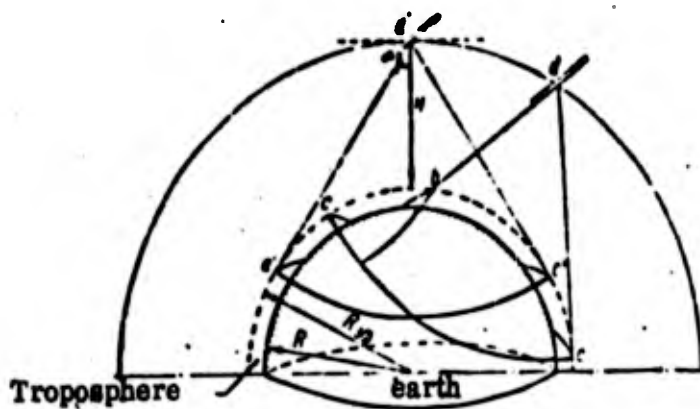radiation is not a function of the assumption with regard to radiation.

Fig. 223. Calculation of earth's own radiation
incident on inclined plane

The quality of the energy radiated by the earth and that passing through
a sphere of radius $(R_0 + H_0)$ shows that

521

$$4E_\bullet \pi R^2 = Q_3 4 \pi (R+H)^2; \quad Q_3 = E_\bullet \left(\frac{R}{R+H}\right)^2. \qquad (16.2)$$

where R is the effective radius of the earth, H is the flight altitude ($H = H_0 - 12$ km).

For a plate set at an angle $\beta > \beta_\gamma$.

$$Q_3 = E_\bullet \left(\frac{R}{R+H}\right)^2 \sin \beta. \qquad (16.3)$$

If the plane of the plate intersects the earth's surface $(\beta < \beta_p)$, the heat balance condition gives us the relationship

$$Q_{13} - Q_{23} = E_\bullet \left(\frac{R}{R+H}\right)^2 \sin \beta.$$

The specific heat flux falling on the plate on both sides, Q_{13} and Q_{23}, is here considerably dependent on the radiation law.

Let us assume that the amount of heat given off by an element of the earth's surface dF is determined by Lambert's law

$$dQ = \frac{E_\bullet}{\pi} d\Omega \cos \theta \, dF,$$

in which $d\Omega$ is the solid angle at which the plate is visible.

θ is the angle between the normal to dF and the direction towards the plate.

The total amount of heat reaching the plate on one side is obtained by integrating with respect to the earth's surface visible on that side. At $\beta = 0$ the plate is vertical, and the expression for the heat flux is written in the final form

$$(Q_3)_{i=0} = \frac{E_0}{\pi}\left\{ \arcsin\frac{R}{R+H} - \frac{R\sqrt{H^2+2HR}}{(R+H)^2}\right\}. \qquad (16.4)$$

Fig. 234 shows the dependence of the heat flux reaching the plate

on one side on the flight altitude and slope angle. On the right of the y-axis

we plot the amount of heat reaching the side of the plate from which the lesser

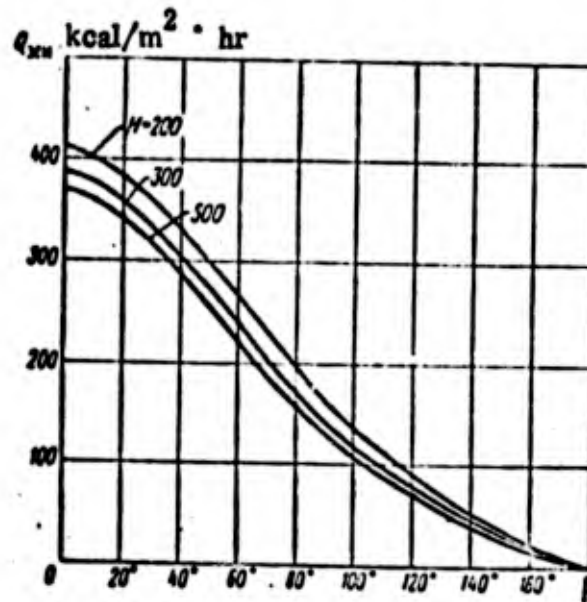part of the earth's surface is visible.

Fig. 234. Amount of heat received by plate through
earth's own radiation as function of angle
of slope of plate

The amount of heat reaching a spherically-shaped body can be determined from

the equation

$$(Q_3)_{u} = 2E_0\left(1 - \frac{\sqrt{H^2+2RH}}{R+H}\right)F_u. \qquad (16.5)$$

When calculating the heating up of a body of arbitrary convex shape, rotating

in space in a disordered way, we can use the expression derived for the spherical body.

523

The   effective area amid ships F   is equal to 1/4 of the entire surface
                                    - mid
of the body.

Heating up through reflection of solar energy from earth's surface

The heating up due to reflected solar rays depends on the shape and

orientation of the flying object, as well as on the mutual positioning of sun,

earth and object in question (Fig. 235). The amount of energy passing through

an area of sphere, radius $\underline{R}$ + $\underline{H}$, at an angle ψ , is, moreover, greatly dependent

on the distribution of the reflected energy in different directions. The reflection

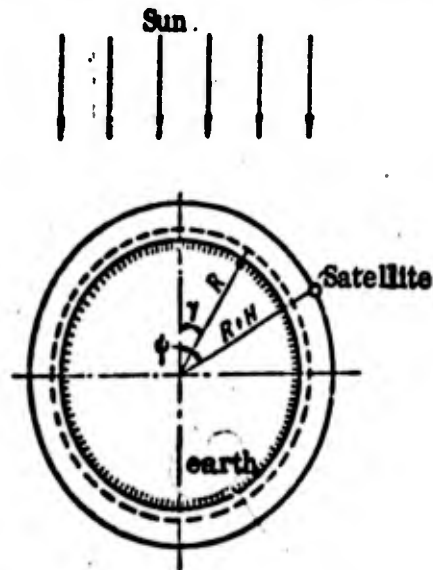may be specular and obey Lambert's law, or may be uniform in all directions.

Fig. 235. Mutual arrangement of sun, earth and satellite

The amount of solar energy reflected from a unit surface of the earth

is determined by the expression

$$Q_{om} = a S_0 \cos \gamma.$$

in which $\alpha = 0.37$; $S_0 = 1140$ kcal/m$^2 \cdot$ hour, γ is the angle between the normal

to the area and the direction of the solar rays. If the reflection obeys Lambert's

law, the amount of heat reflected from the earth's surface F is expressed by

$$Q_{om} = \frac{0.37 S_0}{\pi} \int_F \cos \gamma \cos \vartheta \, d\Omega \, dF \quad (\vartheta = \dot\psi - \gamma).$$

For a case in which all the earth's surface visible from the plate is
illuminated by the sun we derive the formula in the finite form

$$Q_{om} = 0.45 S_0 \cos \psi \times$$
$$\times \left\{ \left(\frac{R}{R+H}\right)^2 - \frac{H^2}{4(R+H)} - \right.$$
$$\left. - \frac{H^2 + 2RH}{\sqrt{8(R+H)^3 R}} \ln \frac{H+2R}{H} \right\} \tag{16.6}$$

The results of the calculation are shown in Fig. 236.   The values
calculated for a case of uniform reflection do not differ by more than 1 or 2%.

In this case

$$Q_{om} = \frac{0.45 S_0 \cos \psi \cdot 2}{3} \times$$
$$\times \left\{ \left(\frac{R}{R+H}\right)^2 + \frac{2(R+H)}{R} - \right.$$
$$\left. - \frac{\sqrt{H^2 + 2RH}}{R}\left[2 + \left(\frac{R}{R+H}\right)^2\right] \right\}. \tag{16.7}$$

If the reflection is specular (Fig. 237), the amount of heat reaching

an area is determined by the equation

$$Q_{om. sep} = a S_0 \frac{1}{4}\left(\frac{R}{R+H}\right)^2 \frac{\sin 2\gamma}{\sin \psi}. \tag{16.8}$$

in which $\gamma = f(\psi)$ is determined by the graph shown in Fig. 238. The amount of

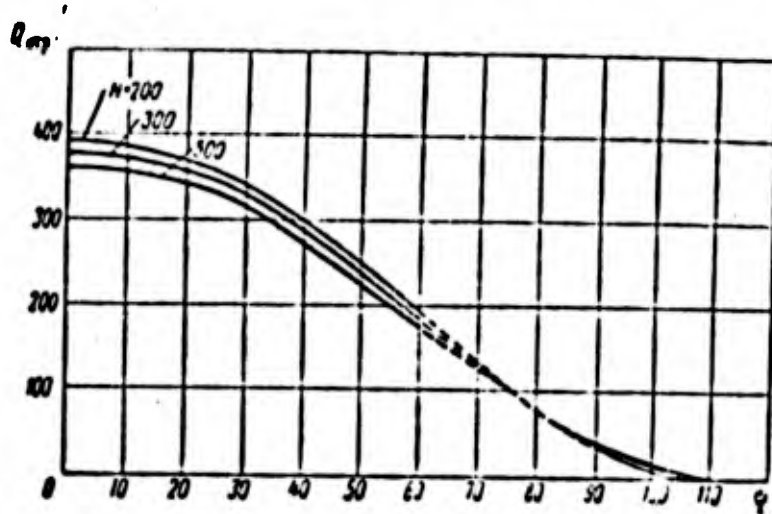heat energy reaching a unit surface of the plate at an angle β to the horizon

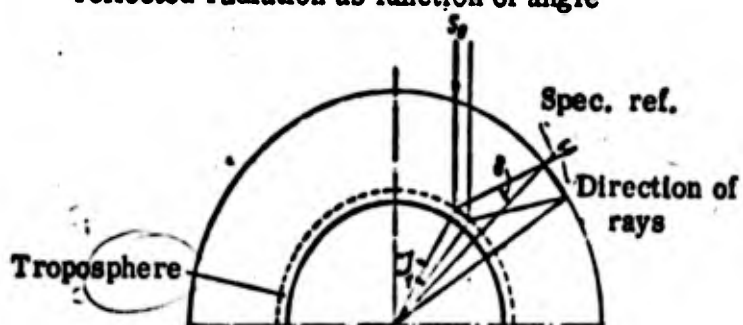Fig. 236. Amount of heat received by plate through sun's reflected radiation as function of angle

Fig. 237

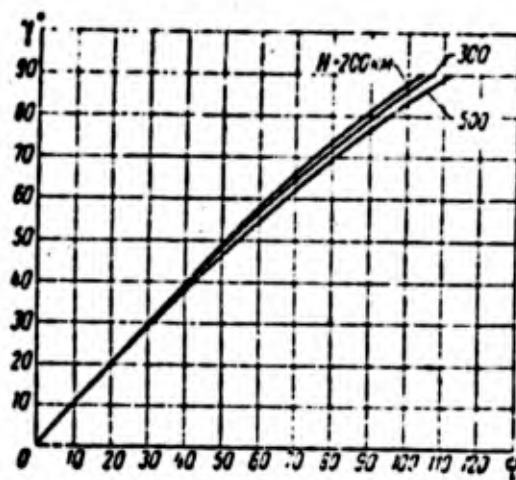Fig. 237. Calculation of earth's reflected radiation incident on inclined plate

Fig. 238

Fig. 238. Relationship between angles γ and ψ.

can be determined from the following expression

$$Q_{\substack{\text{spec. ref}}} = \frac{aS_0}{4}\left(\frac{R}{R+H}\right)^2 \frac{\sin 2\gamma}{\sin \psi} \frac{\cos(\beta + \delta)}{\cos \delta} .$$
(16.9)

in which

$$\delta = \arcsin\left[\frac{R}{R+H}\sin\gamma\right].$$

It is assumed that the specular reflection occurs at angles γ close

to $\pi/2$.

Fig. 236 shows the reflection according to Lambert's law for small γ

and according to the law of specular reflection for $\gamma \to \pi/2$.

In the general case of a body of arbitrary shape, the heat flux

per unit area amidships is calculated by the following formula

$$Q_{\substack{\text{spec. ref}}} = \frac{aS_0}{4}\left(\frac{R}{R+H}\right)^2 \frac{\sin 2\gamma}{\sin \psi} \frac{1}{\cos \delta} .$$

Heat up due to collision with air molecules and atoms

When atoms and molecules collide with the surface of the satellite, some

of the energy of the forward and backward degrees of freedom is transferred to the

wall. Hence for a unit area of surface at an inclined angle to the direction of

motion we get /2, 3, 4/

$$Q_{\text{mol}} = E_{it} + E_{iR} - E_w.$$
(16.10)

in which E_{it} is the forward motion kinetic energy of the incident molecules,

E_{iR} is the rotational energy of the molecules impinging on the plate.

527

When deriving this expression we assume that the accommodation coefficients for the forward (a_t) and rotational (a_R) degrees of freedom are close in size, and range from 0.68 to 0.95 and $a_t \approx a_R \approx 1$, for different construction materials, while the accommodation coefficient for a vibration degree of freedom $a_r = 0$ (see Chapter XIII).

Using the kinetic theory of gases, we can easily derive the following expressions /2/

$$E_{11} = n\left[\frac{mU^2}{2} + \frac{mv^2}{2}\phi(\beta)\right]. \qquad (16.11)$$

in which n is the number of particles striking the area per unit time,

$$n = \frac{Nv}{2\sqrt{\pi}}\left[e^{-\beta^2} + \beta\sqrt{\pi}\left(1 + \frac{2}{\sqrt{\pi}}\int_0^\beta e^{-S^2}dS\right)\right]. \qquad (16.12)$$

$$\beta = \frac{U}{v}\sin\theta;$$

N is the number of particles per unit volume;

v is the most likely velocity of thermal motion of the molecules

$$v = \sqrt{2kT};$$

k is the Boltzmann constant;

U is the velocity of the satellite;

θ is the angle between the plane of the area and the direction of the velocity;

$\underline{m}$ is the mass of the molecule;

$\psi\left(\beta\right)$ is a function which at $\beta > 2$ rapidly tends to a ⌐ constant, equal to 2.5.

The rotational motion energy of the instant molecules is

$$E_{iR} = n\frac{j}{2}\frac{mv^2}{2} = n\frac{j}{2}kT. \qquad (16.13)$$

in which $\underline{j}$ is the number of degrees of rotational freedom.

The energy of the reflected molecules is

$$E_w = \frac{\varkappa+1}{2(\varkappa-1)}nkT_w. \qquad (16.14)$$
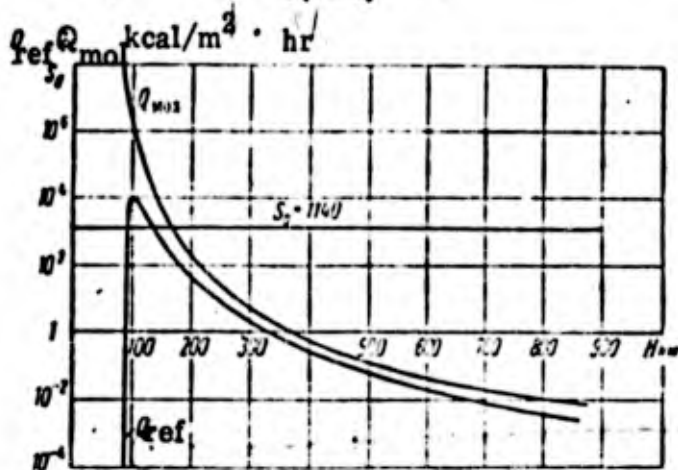

Fig. 239. Amount of heat received by plate through recombination of atoms and collisions with molecules as function of altitude

The ratio of the second and first terms in (16.11) is $\frac{\psi(\beta)}{\beta}$. For a flight at 200 km at ~ 8 km/sec (T_{atm} = 1000°K), this value may be of the order of 0.025. The accuracy with which the temperature of the atmosphere and molecular

concentration at high altitudes are determined is extremely small and for certain

models of the atmosphere the discrepancies attain several orders /8/. Hence in

the expression for forward motion of the incident molecules we can disregard the

second term $\frac{mv^2}{2} \div (\beta)$

If we ignore both the rotational motion energy of the incident molecules

and the energy of the respected molecules at the same time, we obtain a total error

not exceeding 5%. For high altitudes at which the air temperature increases

this error is greater, but the value Q_{mol} itself rapidly tends to zero, and can

be ignored at heights greater than 300 km (Fig. 239).

For altitudes of 100 km or more, we can use the following simple equation

with a fair degree of practical accuracy to determine the energy due to collisions

with molecules

$$Q_{mol.c} = n \frac{mU^2}{2}.$$

The accuracy which is determined by the accuracy with which we know the particle

concentration and temperature in the atmosphere.

Eq. (16.12) for determining n at large β takes the form $n = NU \sin \theta$.

X   Heating up due to recombination of oxygen atoms

It is assumed that at altitudes greater than (100 - 160) km the oxygen

is totally dissociated /2, 6/. During the flight of a satellite, there may be

530

ternary collisions and recombination of the atoms on its surface. The ratio of

a number of collisions between atoms and surface required for recombination and

the total number of collisions is termed the effective recombination. Experimental

research to study the recombination of atomic oxygen /4,5/ shows that for the

materials investigated   .

Thus, per unit surface $q_{rec} = n\sigma E$,

in which E is the recombination energy per one oxygen atom, equal to 2.541 ev,

n is the number of atoms colliding with the surface /10/.

Variation in the recombination energy as a function of altitude is

shown in Fig. 239.

Sec. 70.   Temperature Control

Since the satellite carries different scientific apparatus and instruments

aboard, we are faced with the problem of maintaining the temperature within set

limits. The amount of heat reaching the shell from outside is variable and

ranges within wide limits. The internal heat emission when the instruments are

working may also be variable. Under these conditions a special system of temperature

control is required to provide stabilization of the temperature of the instruments.

This system may be based on the absorption (or emission) of heat inside

the satellite, or on the removal of heat away from it. In the first case we can use

chemical reactions during which heat is given off or absorbed, or else the

temperature effect when the aggregate state of the material changes (melting,

evaporation, crystallization).

The most rational system is one in which the heat from the instruments

is transferred by a heat transfer agent to the radiation surface, which is at a

lower temperature than the instruments. The transfer of heat to the radiator is

controlled by the thermal resistance of the intermediate medium. The heat transfer

agent can be a gas set in motion by a fan, which then absorbs the heat from the

instruments and transfers it to the radiation surface. Any conducting material

with properly selected radiation coefficients A_s and ε can be used for the

radiator surface.

In order to reduce the amount of heat received through direct or

reflected solar radiation, A_s must be as small as possible. Furthermore, at

small A_s it is easier to carry out visual observations of the satellite from

the earth. On the other hand, the surface of the radiator should have a maximum

degree of blackness for the infra-red region of the sector   so as to increase

the energy flow radiated per unit area/

Figs. 240 and 241 show the variation in the emissivity of a surface as

a function of wavelength and the material used to make it. It also plots curves

for ideal and permissible coatings. Fig. 241 shows that polished metal surfaces are not suitable as radiator material.
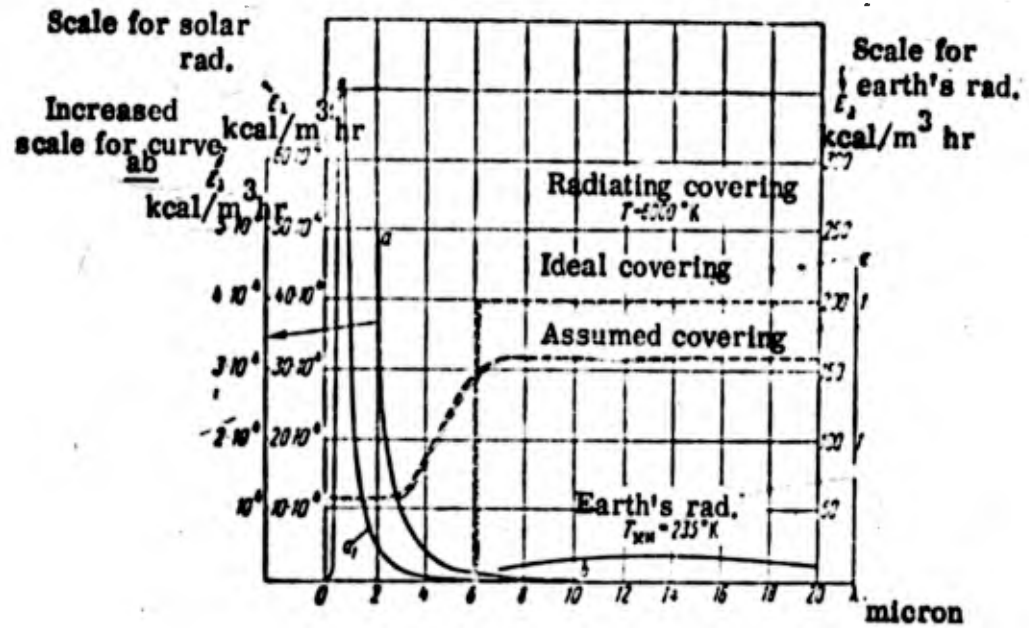

Fig. 240. Energy spectra of sun earth and degree of blackness of radiating covering as function of λ . Curve ab shows area a, b of curve for solar radiation on an enlarged scale
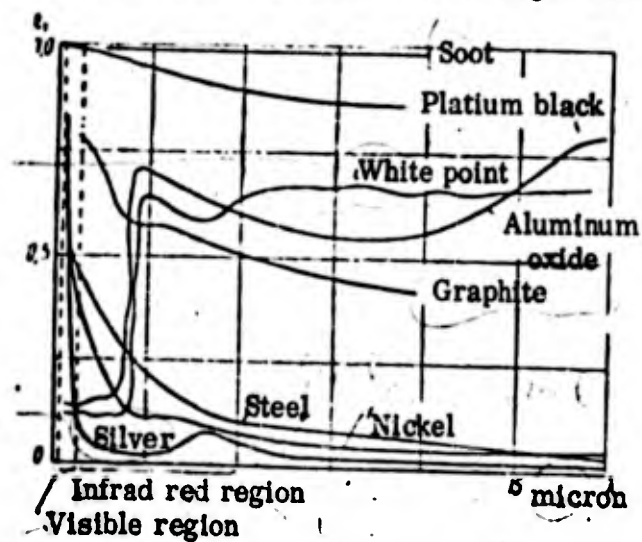

Fig. 241. Degree of blackness as function of wavelength for polished metals

Surfaces which do not conduct electricity, for example, white paint,

metal oxide films, make more suitable materials.

Let us consider the heat balance of the shell of the satellite rotating

in arbitrary fashion, though not too slowly, and let us make the average temperature

for the whole surface the temperature of its shell. A rotating satellite with an

infinitely conducting shell would also have the same temperature. In view of the

fact that the satellite receives external heat fluxes on only part of its

surface /for example heat through collision with molecules is received by the

middle section F_M , while radiation is emitted by the entire surface $(F)/$, it is

convenient to refer the heat flux to the mean surface in the middle (F_M). The

mean middle means the mean arithmetic area of the middle in all possible directions.

The heat supplied to the shell is used in heating it up and is radiated

into space. The heat-balance equation for ⌒ a thermally conductive

satellite shell, if it is assumed that the surface consists of $\underline{n}$ surfaces and

that each surface has its own coefficients A_S and ε , takes the form

$$\cdot \sum_{i=1}^{n} F_m \cdot \sum Q_i \Delta \tau + \sum_{i=1}^{n} Q_{ei} \Delta \tau = \sum_{i=1}^{n} m_e c_e dT_e +$$

$$+ \sum_{i=1}^{n} \varepsilon_i c_0 F_i \left(\frac{T_e}{100}\right)^4 \Delta \tau, \qquad (16.15)$$

in which $m_e c_e$ is the heat capacity of the shell;

Q_{int} is the heat reaching the shell from inside;

534

τ is the time;

$$c_0 = 4.06 \text{ kcal/m}^2 \cdot \text{hour} \cdot \text{deg}^4;$$

T_W is the temperature of the shell;

$\sum Q_c$ is the external heat flux

$$\sum Q_c = Q_{\rho e z} + Q_{\text{мол}} + \sum Q_{\text{эн}} + \Delta Q_{\text{зем. отр}} + AS_0 \qquad \text{(see Fig. 242).}$$

It can be seen from (16.15) that variations in the temperature of the shell, and therefore the temperature of the instruments, are decreased as the thermal capacity of the shell is increased. At a very high thermal capacity, the shell acquires a mean temperature, which is determined by the area of the radiator.
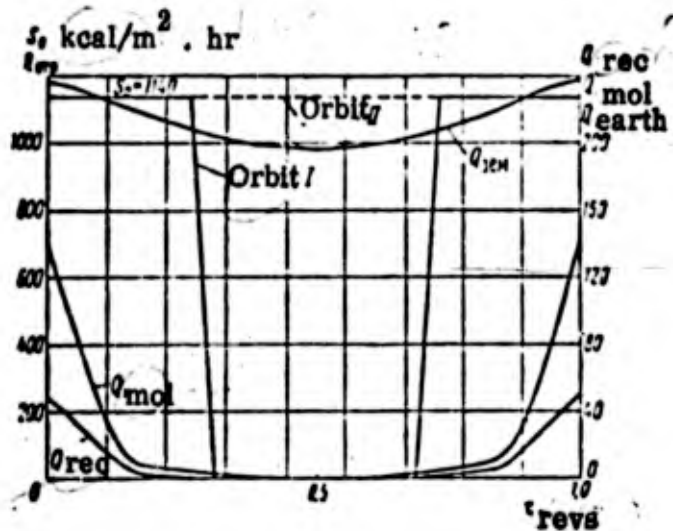

Fig. 242. Example of distribution of external heat flux incident on satellite during motion in circular orbit
$(H = 500 \text{ км})$.

For set external heat fluxes, internal heat emission and blackness there is a minimum area of radiator at which the heat removal can be assured for

set radiator temperature T_w. If the area of the radiator is finite, this

condition enables us to work out the minimum amount of heat given off inside the

satellite which can be removed through the shell at a set temperature T_w. The

amount of heat supplied to the surface of the radiator from inside is determined

from the heat balance of the inside assemblies. The heat emitted by the instruments

is partly spent on heating them up and partly removed to the wall.

To determine F_M in (16.15), let us use the rule, according to which

for any convex disorderly rotating body the ratio of the area of the entire

outer surface to the mean middle (to the mean shade) is a constant value and

equal to 4. In the particular case of a sphere, this is obviously $F/F_M = 4$.

Without loss of generality in the arguments, we can consider a satellite in

the form of a sphere with a good conducting shell. The conclusions drawn

remain valid for rotating satellites of any other shape as well.

If we consider the heat balance separately for different parts of the

surface with different coefficients A_S and ε, or at different intensities

of heat removal from inside, this rule is applicable to each separate area. In

this case when calculating the area F we only need take the visible outside

surface into account. The inside surface, although visible through an imaginary

section, is not considered. The surfaces in question must be plane or convex

and must not eclipse one another.

Sec. 71. Ventilation System

Let us now take a look at some of the features of controlling temperature by means of forced ventilation of gas in the cell. The gas flow set in motion by a fan passes through the radiator into tubes for cooling the instruments and returns to the air intake of the fan. The calculation includes determining the rated power of the fan and the geometrical parameters of the system.

Initial relationships are

$$N_0 = \frac{W_{sec} \Delta p}{\eta}, \tag{16.16}$$

$$Q_{wall} = c_p \gamma W_{sec} (T_2 - T_1) = F_p \alpha_p (\Delta T_{ef})_1 = F_{inst} \alpha_{inst} (\Delta T_{ef})_2. \tag{16.17}$$

Here N_f is the output of the fan at a volumetric consumption per second of W_{sec} and gradient Δp;

Q_{wall} is the amount of heat supplied to the radiation surface from inside;

$(T_2 - T_1)$ is the temperature difference between the radiator inlet and outlet;

γ is the specific gravity of the gas;

F_p and F_{inst} are the areas of the radiator and instrument surfaces participating in the heat exchange;

α_p and α_{inst} are the heat exchange coefficients.

The pressure head Δp is spent on overcoming hydraulic resistance in the system. Hydraulic resistance of the radiator is determined by friction against the

wall and local resistances. A large part is played inside the satellite by vortex losses during flow around the instruments. Using the condition of hydrodynamic analogy,

$$\tau_w = \frac{\lambda_p W_{sec}}{c_p g S_r}$$

we get

$$\Delta p = \frac{\lambda W_{sec}}{g S_r^2}\left[\frac{F}{F_r}\frac{T_1-T_2}{\Delta T_{ef}} + \zeta \frac{S_r^2}{S_i^2}\right] = \frac{\tau W}{g S_r^2}. \qquad (16.18)$$

here τ_{w} is the friction;

S_r is the flow area of the radiator;

$\dfrac{F}{F_o}$ is the ratio of the total radiator surface to the surface participating in the heat exchange;

S_i is the flow area of the cell;

ζ is the resistance coefficient of the cell.
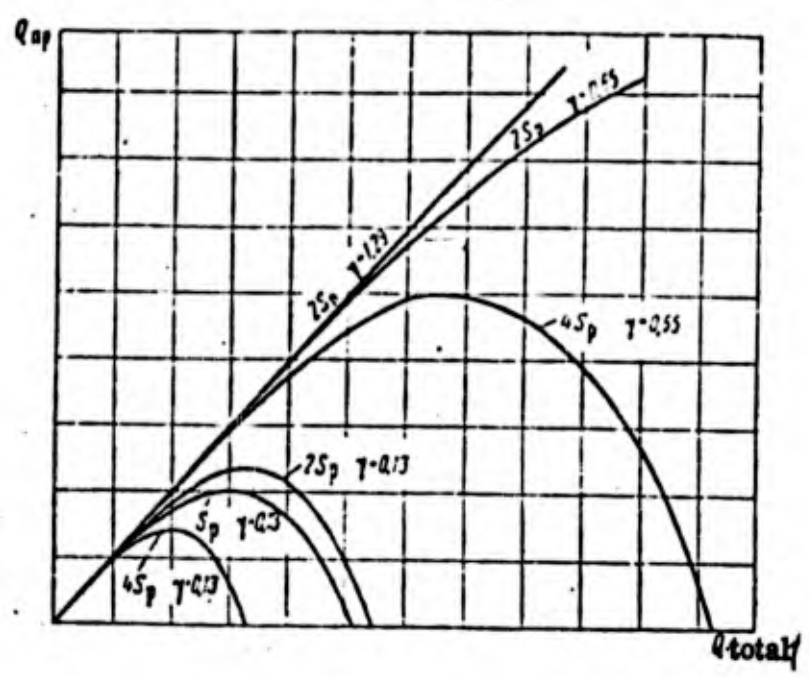
Fig. 243. Relationship between heat given out by instruments and total heat emission at different pressures of surrounding air (S_p through section of radiator)

After transformation, we get

$$N_s = \frac{Q_{cr}^3 M}{c_p^3 (T_2 - T_1)^3 \gamma^2 S_p^2},$$ (16.19)

in which M is a function depending mainly on the geometrical dimensions.

The temperature T_1 at the outlet from the radiator should not be lower than the smallest temperature permissible for the instruments. T_2 is always

slightly less than the maximum instrument temperature. It follows that when the permissible temperature range is narrowed the power required by the fan is greatly stepped up.

The relative proportion of energy spent on driving the fan increases in proportion to the square of the total output, including the fan output. In a steady-state regime

$$Q_{\text{wall}} = Q_{\text{inst}} + N_\ell \text{ н } \frac{N_\text{Д}}{Q_a} \sim Q_a^2.$$

At set parameters of the cooling system there is a maximum instrument output and a corresponding maximum fan output, at which cooling may still not have been effected (Fig. 243). When the output of the fan is further stepped up, the output of the instruments has to be reduced in order to keep the temperature constant. Otherwise, the fan will chiefly be working for itself.

If the instrument output is small, the amount of energy used to drive the fan becomes negligible, and the latter can be selected from purely functional considerations. In this case, instead of the smooth control we can apply step-by-step control, i.e., the fan is switched off when the maximum permissible temperature of the instruments is reached, and switches on when the air is cooled down to the minimum permissible temperature.

Here an important part is played by the thermal resistance of the

540

assembly and the gas $\underline{R}$ when the fan is turned off (Fig. 244).   It should be fairly

large in order for the temperature of the instruments when the fan is switched off

to be increased, since otherwise the instruments may become too cold and it will

no longer be possible to control it.
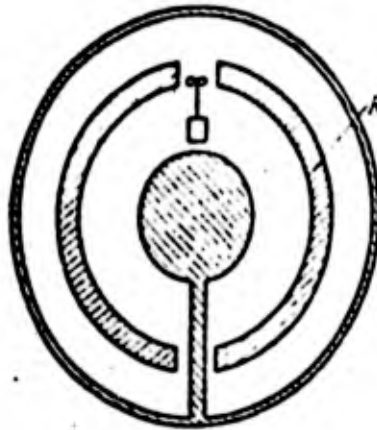
Fig. 244. Theoretical system of
satellite

Sec. 72. Radiation Surface

In the general case the radiation surface may include areas with

different values of $A_{\underline{S}}$ and ς . It is only possible to arrange for cooling if there

is an element in the satellite with a fairly low temperature. The part of the

shell of the satellite can serve as this element, since it is a radiator surface.

The heat received by the satellite shell is equal to

$$\Sigma Q_e = F_u [A_0 (S_0 + Q_{orp}) + \epsilon_0 Q_{3eu} + Q_{uoa} + Q_{peu}], \qquad (16.20)$$
$$Q_{uss} = \epsilon_0 F \left(\frac{T_w}{100}\right)^4 . \qquad\qquad (16.21)$$

in which F is the area of the outside surface of the shell,

T_w is the mean temperature of the outside surface of the shell,

A_s and ε_0 are the reduced coefficients of absorption in the visible and infra-red areas of the radiation spectrum.

Let us take it that the satellite shell consists of several parts, each one with its own radiation coefficient A_0 and ε in the visible and infra-red parts of the spectrum. For example, for a shell consisting of two parts, A_0 and ε are determined from the equations

$$A_0 = \frac{A_{s_1} + (n-1)A_{s_2}}{n},$$ (16.22)

$$\varepsilon_0 = \frac{\varepsilon_1 + (n-1)\varepsilon_2}{n},$$ (16.23)

in which A_{s_1}, ε_1 and A_{s_2}, ε_2 are the coefficients of radiation in the visible and

infra-red parts of the spectrum for the first and

second parts,

n is the ratio of the area of the total shell surface

to the area of the first part.

Let us take F_M to be $F_M = F/4$. It is clear from the equations that $0 < A_0 < 1$ and $0 < \varepsilon_0 < 1$.

For certain arbitrary values of A_0 and ε_0 we determine the temperature of the instruments for motion in an orbit, the plane of which is perpendicular to the direction of the sun's rays (Fig. 245), and we plot graphs showing

542

the variation in temperature as a function of motion of the satellite in its orbit (Fig. 246).

The calculation is repeated for the second extreme position of the orbit and we determine the range of A_0 and ξ, over which the temperature of the instruments keeps within the set values.
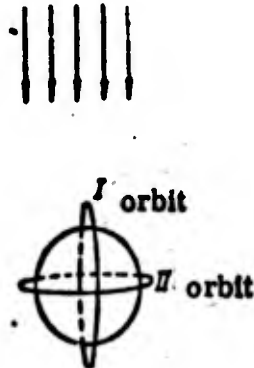

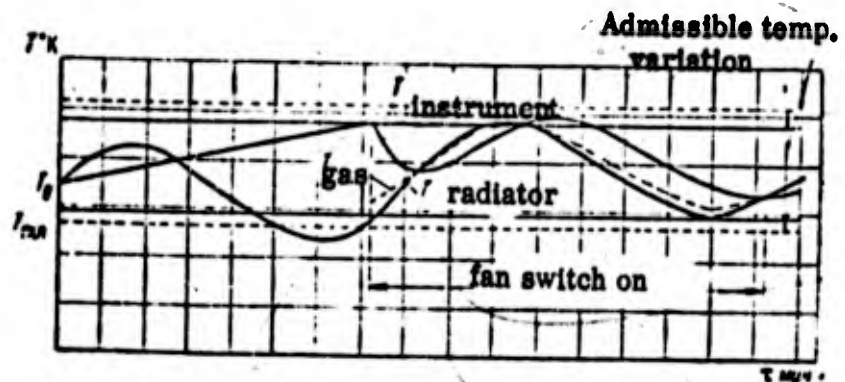Fig. 245. Position of two extreme orbits

Fig. 246. Heat conditions for satellite during motion through orbit

References

1. Adams, & Applicability of theory of continuum to artificial satellites and problem of hypersonic flights at high altitudes, "Problems of Rocketry", Foreign Lit. Press, 1958, No. 4.

2. Danilin, B. S., and others. "Progress in Physical Sciences", Vol. XIII, Issue 1, b, 1957.

3. Kondrat'yev, K. Ya. Radiant heat exchange in the atmosphere, Gidrometeoizdat, 1956.

4. Lavrovskaya, G. K. and other. Hydrogen atom and oxygen atom reactions on solid surfaces. "Journal of Physical Chemistry", Vol. 25, Issue 9, 1951.

5. Lavrovskaya, G. K. and other. Recombination of atoms on solid surfaces, Ibid, Vol. 26. Issue 8, 1952.

6. Mitra, S. K. The upper atmosphere, Foreign Lit. Press, 1955.

7. Ribo, G. Optic pyrometry, For. Lit. Press, 1957.

8. Stalder, J. and other. Transfer of heat to bodies moving at high velocities in upper layers of atmosphere. "Problems of Rocketry" For. Lit. Press, 1952, No. 5.

9, Tsyan, S. Aerodynamics of rarefied gases. Coll. "Gas Dynamics", For. Lit. Press, 1950.

544

10. Hansen, Some characteristics of upper layers of atmosphere involved in high velocity flight. "Problems of Rocketry", For. Lit. Press, 1958, No. 5.

11. Karpenko, A. O. and others. Temperature conditions for artificial earth satellites. Herald of AS USSR, Geophysics Series. 1957, No. 4, pp. 527-533.

12. Shmidt, U. and others. Temperature of satellite surface. "Problems of Rocketry", 1958, No. 3.

13. Cornog, R. Temperature equilibria in Space Vehicles. The Journal of the Astronautics Sciences, 1958, Vol. 4, Nos. 3-4.

14. Sandorf, P., Prigge, I. Termal control in a space vehicle, Journal of the Astronautics, 1956, Vol. VIII, No. 1.

15. Scientific problems of artificial earth satellites. Coll. Translations For. Lit. Press, Moscow, 1959.

The practical application of nuclear energy in engineering, particularly in transportation units, as is well known, is determined at the present time by a number of engineering problems. One of the most important branches of science determining progress in nuclear power engineering is heat transfer.

The great variety of _heating units_ utilizing energy from nuclear reactors /15, 16, 19/ prevents us giving a complete survey of the typical heat-exchange problems in power engineering. But if it is taken into account that most of the processes in the transfer of heat, _and in_ heat-exchange apparatus and devices are described fairly adequately in appendices to books on ordinary heat engineering, the task for this section is somewhat simplified.

Here we will discuss certain specific features of heat transfer when utilizing the heat from nuclear reactions in power reactors.

The problems will be considered in the followint order:

1. Heat released in nuclear reactions, forms of manifestation and energy carriers (micropicture).

2. Heat release in different parts of nuclear reactors, heat _flux_ (macropicture), processes of _heat_ transfer to the working substance in the power plant, and processes accompanying the harnessing of nuclear reaction heat (heat emission in parts of a power unit plant in the field of radiation, activation of

heat transfer agent, and so on).

73. Energy Release in a Nuclear Reactor

Nature of Nuclear Heat Release

Energy may be released in large quantities during two types of nuclear reaction. These are nuclear reactions involving the fission of the nuclei of heavy elements such as uranium, thorium, plutonium, and the reactions involving the combining of nuclei of light elements, for example, tritium (thermonuclear reactions). Although the latter are accompanied by a large energy release, they are far from practical application at the present time, though for the time being we will deal only with the energy release during fission reactions.

From the example of the fission of the isotope uranium U^{235} (Fig. 247) it can be seen that the energy appears in the form of (1) kinetic energy of the fragments fission, (2) kinetic energy from neutron fission, (3) β- and γ- radiation energy (instantaneous, accompanying the event of fission),(4) radioactive decay energy (α, β and γ) of the fission fragments; (5) energy from the protons and neutinos obtained during fission and further transformation of the fission fragments.

Present day experimental data /12/ describing the mean distribution of energy over these particles and radiations during the fission of U^{235} are given in Table 22.

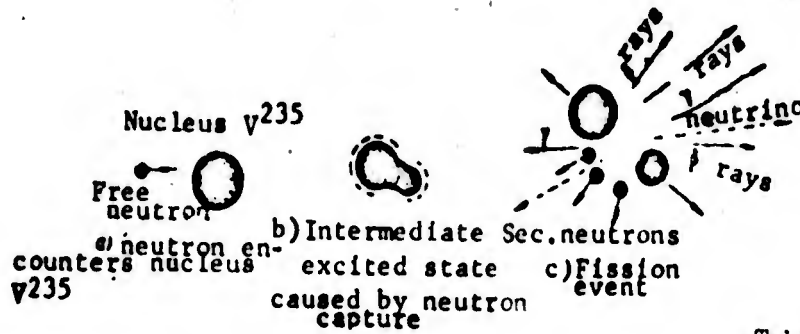Fig. 247. Diagram showing serial development of fission of U^{235}

Nucleus V^{235}

Free neutron

a) neutron encounters nucleus V^{235}

b) Intermediate excited state caused by neutron capture

Sec. neutrons

c) Fission event

γ rays

neutrino

γ rays

Table 22

Mean Particle Energy Distribution During Fission of U^{235}

Kinetic energy of fission fragments	162 Mev
γ- quanta of fission (instantaneous)	5 Mev
Kinetic energy neutrons	5 Mev
Energy of β- and γ- radiation of fission products	11 Mev
Energy of other types of radiation	10 Mev
Total	193 Mev

It is conventionally taken in engineering calculations that 200 million electron volts are produced per one fission event. This amounts to $19 \cdot 10^{6}$ kcal per 1 g of fissile matter, i.e., the calorific value of uranium "fuel" is more than a million times that of a chemical fuel.

In solving problems of heat transfer it is important to know where, in which parts of the reactor, and at what distance from the point of nuclear decay the energy is released.

548

As can be seen from Table 22, the fission fragments carry a large amount of energy. They hurtle away from the fission point in different directions at tremendous velocities (of the order of 10^6 m/sec). The energy level of the fragments would correspond to about 10^{12}°V, if all particles of matter moved at the velocities of the fragments.

The path length of the fragments depend on the medium, its density, stopping power and so on. In solid bodies, however, the fragment path does not exceed tenths of a millimeter. Such small distances are to a considerable extent explained by the fact that the fragments are strongly ionized and easily interact with particles of the medium. Along the stopping path the fragments undergo a series of collisions with particles of the medium, giving rise to different types of oscillation, altering the potential energy of the medium and causing displacement of the atoms in the crystal lattice. The energy then spreads from the fragment trajectory through the medium by the normal paths - thermal conductivity and radiation.

Taking into account the small fragment path lengths, it can be taken that their energy is released locally. It can be considered by the same token that the radiation of fission fragments occurs at the same fission point. The other fission energy carriers release β- particle energy locally, for practical purposes, since

549

their path lengths in solid bodies amount to 0.1 - 1.0 mm.

Local Heat Release

According to whether the reactor is homogeneous or heterogeneous, the heat release in the material of the active zone in the reactor is determined in different ways. In a homogeneous reactor, in which the fissile matter is uniformly distributed through the moderator, or sometimes mixed with the heat transfer agent, the task is comparatively simple.

The amount of heat released per hour per unit of volume depends on the number of neutrons passing through a unit of area (neutron flux $\underline{n}V\,n/cm^2 \cdot$ sec), on the concentration of fissile matter . on its tendency to capture neutrons with subsequent fission of the nucleus (σ_f in cm^2 or in barns* is the effective fission cross section).

Taking it into account that during one fission 200 mev energy is released, to obtain a thermal capacity of one kolowatt we need $\underline{c} = 3 \cdot 10^{13}$ uranium nuclei fissions per second, and to release 1 kcal in the course of an hour we need $\underline{c}_q = 3.49 \cdot 10^{10}$ fissions per second.

<u>Example.</u> In a homogeneous reactor using pure U^{235} with a graphite moderator, the uranium concentration is taken as such that per 1 m there are $5.76 \cdot 10^{25}$ uranium atoms (approximately 1% weight); and the total (macroscopic) fission cross-

---

* 1 barn = $10^{-24}\,cm^2$

section is
$$\Sigma_f = N_{\sigma_f} \quad cm^2$$

Assuming

$$\sigma_f = 549 \cdot 10^{-24} \quad cm^2$$

we get

$$\Sigma_f = 5.76 \cdot 549 \cdot 10^{-24} = 3.16 \cdot 10^4 \quad cm^2$$

For our example let us take a neutron flux in the center of the active

zone in the reactor equal to $\underline{nv} = 10^{13}$ neutron/cm^2 · sec. The total number of

fissions a second will then be

$$F = nv \Sigma_f = 10^{13} \cdot 3.16 \cdot 10^4 = 3.16 \cdot 10^{17} \text{ fissions per second in } m^3$$

The volumetric heat release is

$$q_v = \frac{F}{c_q} = \frac{3.16 \cdot 10^{17}}{3.49 \cdot 10^{10}} = 9 \cdot 10^6 \quad kcal/m^3 \cdot hr$$

Distribution of Heat Release in Reactor

The distributions of the neutron fluxes $\underline{nv}$ and therefore the heat releases

q are non-uniform through the active zone. During the chain nuclear reaction of U^{235}

fission, the neutrons are constantly being generated; some of them are absorbed by

the uranium atoms (for the most part the neutrons cause new fission events) or

other materials in the reactor; the diffusion processes cause a "leakage" of some

of the neutrons from the reactor. These processes can be calculated and solution

of the neutron balance equation makes it possible to derive a regularity for their

distribution through the active zone in the reactor, /4/.

For the simple case of a cylindrical reactor of finite length L

without a reflector, the distribution of the neutron flux through the volume of the

reactor is determined by the following equation

$$nv = (nv)_0 \cos\frac{\pi x}{L} \, J_0\left(\frac{2.405 r}{R}\right) \text{ s/cm}^2 \cdot \text{sec.} \qquad (17.1)$$

in which $(nv)_0$ is the neutron flux in the center of the active zone,

x   is the distance along the reactor axis, L is the length of the

reactor, r is the radial coordinate, R is the radius of the reactor, and J_0 is the

zero-order Bessel function.

In an actual reactor the neutron flux distribution is rather different

(Figs. 248 and 249). In order to make a rough estimation of the neutron distribution

in the active zone of the reactor with a reflector, L and R in Eq. (17.1) are

replaced by the imaginary values L' and R'; the latter are determined by extra-

polation of the curves $nv = f_1(x)$ and $nv = f_2(r)$ in the reactor with the reflector.

Equation (17.1) takes the form

$$nv = (nv)_0 \cos\frac{\pi x}{L'} \, J_0\left(\frac{2.405 r}{R'}\right) \text{ s/cm}^2 \cdot \text{sec.}$$

$$(17.2)$$

Accordingly, the distribution of the volume heat release in the two central

552

sections of the active zone is expressed by the following equations:

In the cross section $\quad q_o^{(")} = q_o . J_o \left(-\frac{2.405 r}{R'} \right) \qquad kcal/m^2. hr$

In the longitudinal section $\quad q_o^{(')} = q_o . \cos \frac{\pi x}{L'} \qquad kcal/m^2. hr$

In the heterogeneous reactor this method can be used to calculate the energy release in the heat-producing elements alone. All the physical constants for the calculation can be taken from scientific literature /1, 4, 8, 12, 20/.
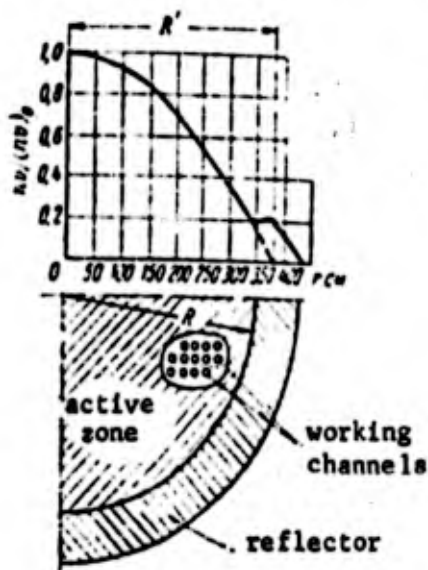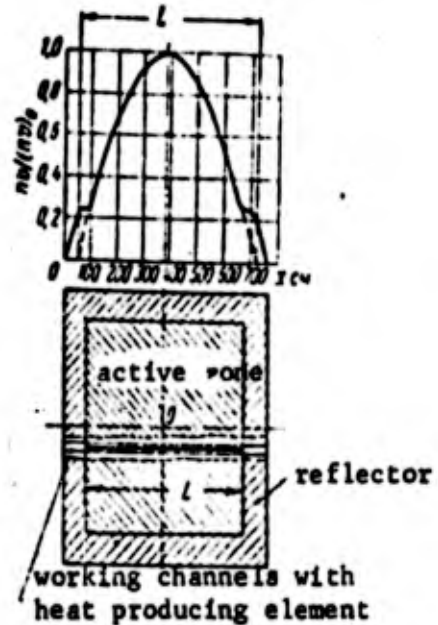

Fig. 248. Distribution of thermal neutron flux along radius of uranium graphite power reactor with reflector

Distribution of thermal neutron flux along length of uranium graphite power reactor with reflector
Fig. 249.

Heat release in the moderator and heat transfer agent, similar to heat release in the reflector, parts and reactor protection, is calculated in a different way, since it is determined by the absorption of energy solely by neutrons and γ-rays.

The neutron and γ-radiation have incomparably greater penetrating power than the fission fragments and β-particles. During fission, as well as during radioactive decay of the fission fragments, there occur neutrons and γ-quanta with different degrees of energy. The sphere of heat release from these radiations depends on their energy.

Fig. 250 shows another example of the distribution of the neutron stream in a reactor. The transfer of neutron and γ-quantum energy from the point of fission through the active zone does not distort to any great extent the conventional law of proportionality of the heat release to the neutron flux. But the removal of this small quantity of energy from the active zone by the neutrons and γ-radiation is a deciding factor in calculating the heat release outside the active zone or outside the heat producing elements in the heterogeneous reactor.

The absorption of neutrons and γ-quanta determines the heat release in the regulating rods and units of the reactor within the active zone.

Heat release through the neutron and γ-quantum energy is considerably more complicated by nature than in a nuclear reaction. The heat release depends not only on the properties of the material and particle energy, but also on the size and configuration of particular units of the reactor. It works out that the absorbing power of materials varies with the particle energy (Fig. 251). It is clear from

the

example given that if at small energies (0.5 mev) lead is superior to iron as a

protective material, when "hard " γ-rays pass through it, their absorptive powers
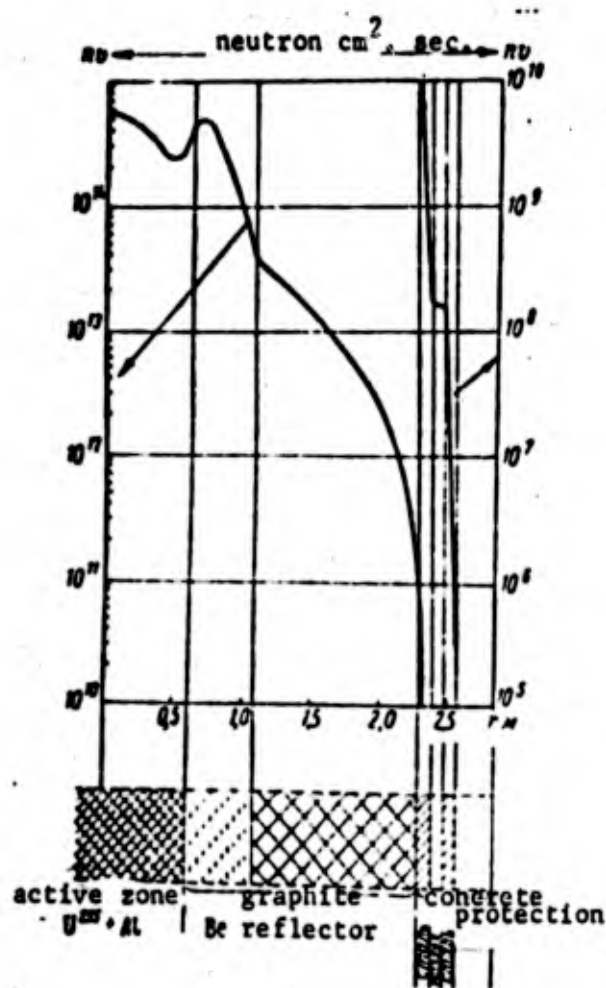
are hardly different.

Fig. 250. Distribution of neutron flux in cross section
of stationary research reactor.

Thus, in order to calculate the heat release from neutron and γ-radiation,

we have to solve a complex integral equation (with integration with respect to the

volume of the part, the type and shape of absorption, the particle energies, the

elements constituting the material of the part, and so on).

In practice the integral equation is solved by numerical methods, and is

most frequently replaced by summation *over the* areas within which the parameters

are averaged /12, 20/.

Volumetric heat release in the material when neutrons are absorbed and

quanta are emitted with energy $\underline{E}$ with a small free path length (in a heavy material,

for example, lead), can be calculated from *the following equation* [20].

$$q'_v(E) = n(E) \frac{EJ_0}{2} \mu_{en}(E) e^{-\alpha \mu b} \left\{ e^{\alpha \mu b} \left[-Ei(\mu b) \right] + \right.$$

$$\left. + Ei\left[-\mu b(1-\alpha) \right] \pm \ln \frac{1+\alpha}{1-\alpha} \right\} 1,37 \cdot 10^{-4} \; kcal/m^3 \; hr$$

Fig. 252 shows the results of the calculation of the function

$$F(\alpha, \mu b) = e^{-\alpha \mu b} \left\{ e^{\alpha \mu b} \left[-Ei(\mu b) \right] + Ei\left[-\mu b(1-\alpha) \right] \pm \ln \frac{1+\alpha}{1-\alpha} \right\}$$

for different values of α and $\mu \underline{b}$.

Taking this function into account, we get

$$q'_v(E) = 1,37 \cdot 10^{-4} \cdot n(E) \frac{EJ_0}{2} \mu_{en}(E) F(\alpha, \mu b) \; kcal/m^2 \cdot hr$$

Here $\underline{n(E)}$ is the share of neutrons bringing about γ-quanta with energy $\underline{E}$

during absorption;

$\frac{J_0}{\wedge}$ is the neutron flux every second through cm^2;

$\mu_{en}(E)$ is the coefficient of energy absorption of the γ-quanta in the

given material in cm^{-1},

$$\alpha = \frac{\sqrt{3 \Sigma_a \Sigma_t}}{\mu} \, ;$$

Σ_a is the neutron absorption coefficient in cm^{-1},

ε_{t} is the neutron transfer coefficient in cm^{-1},

$\mu (\varepsilon)$ is the linear absorption coefficient in cm^{-1},

b is the distance to the point at which the absorption of the γ-quantum

takes place in cm.

The physical constants required for the calculation can be borrowed from

/4, 6, 12, 20/ and other sources.

74. Transfer of Heat to Heat Removal Surfaces

This process of heat transfer within the heat-producing element is very

important because it determines the basic characteristics of suitability for work -

heat resistance (maximum temperatures in body and on surface of element), thermal

stresses (temperature distribution - maximum gradients and temperature differences

in the element), and transfer of heat to the coolant (temperature on heat-removal

surface).

As was found above, a characteristic feature of the energy release in

nuclear reactors is the heat-release volumetricity. The process of heat transfer

is somewhat complicated thereby. In order to take internal heat release into account*,

when deriving the general thermal-conductivity equation we have to compile a heat

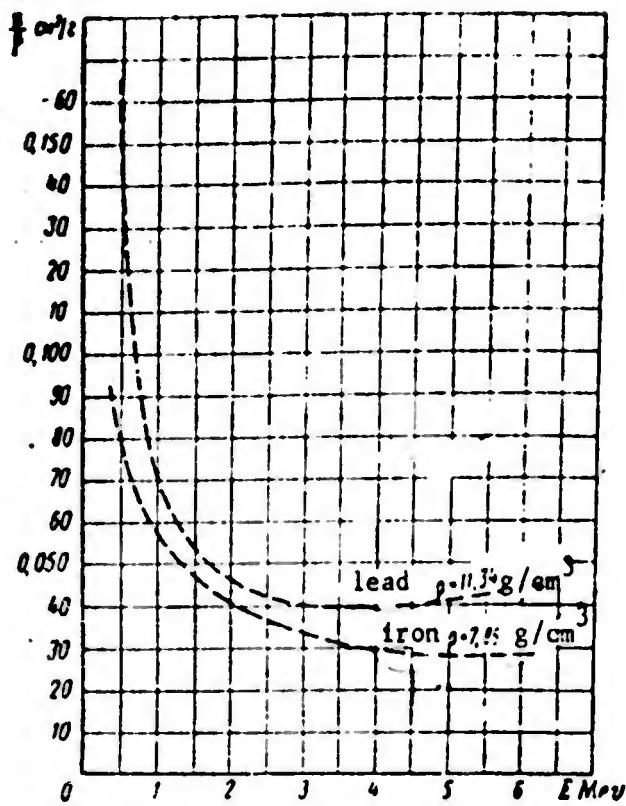balance for the element of the body volume dV.

557

Fig. 251. Mass absorption coefficients of
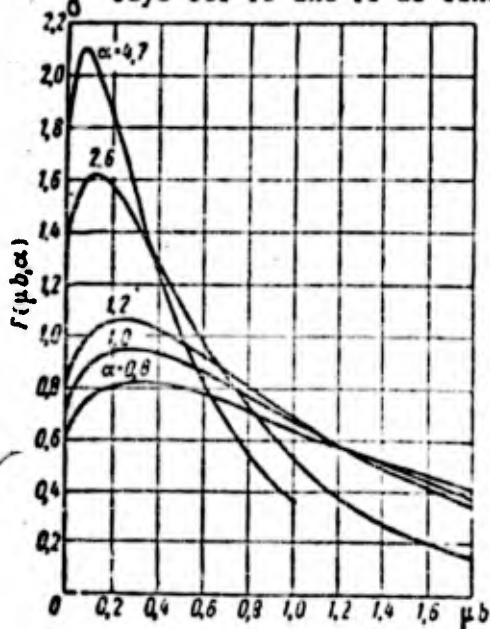γ-rays for Pb and Fe as function of hard radiation

Fig. 252. Absorption of
γ-radiation accompanying
the capture in an infinite
medium limited by by a plane

The integral parts of the heat balance are, accordingly,

a) dQ_1 is the heat released over the time $d\tau$ in the volume dV

The specific volumetric heat load* - the productivity of the internal heat sources /9/ - will be designated as q_v kcal/$m^3 \cdot$ hour, then

$$dQ_1 = q_v dV\, d\tau;$$

b) the amount of heat spent on heating up the volume element dQ_2 depends on the thermal capacity c, on the density of the body γ and on the rate of change in the temperature $dt/d\tau$, i.e.,

$$dQ_2 = c\gamma \frac{dt}{\tau:} dV\, d\tau;$$

c) some of the heat dQ_3 leaves the body through thermal conductivity and in the general case is determined by the equation

or

$$dQ_3 = -\lambda \left(\frac{\partial^2 t}{\partial x^2} + \frac{\partial^2 t}{\partial y^2} + \frac{\partial^2 t}{\partial z^2} \right) dV\, d\tau$$

$$dQ_3 = -\lambda \nabla^2 t\, dV\, dt.$$

Developing the heat balance equation

$$dQ_1 = dQ_2 + dQ_3,$$

we get

$$q_v dV\, d\tau = c\gamma \frac{dt}{d\tau} dV\, d\tau - \lambda \nabla^2 t\, dV\, d\tau$$

or

$$\frac{dt}{d\tau} = \frac{q_v}{c\gamma} + \frac{\lambda \nabla^2 t}{c\gamma}.$$

The general equation for thermal conductivity at $dt/d\tau = 0$ gives us an

equation for the stationary process ~~during~~ volumetric heat release

$$\nabla^2 t + \frac{1}{\lambda} q_v = 0. \tag{17.3}$$

Actual heat-producing elements, as will be shown below, have complex shapes -

ribbed rods, corrugated sheets, blocks with internal channels, and so on.

The solution of the thermal conductivity equation for such bodies is

extremely cumbersome. As an example, let us consider the solution of Eq. (17.3)

for heat producing elements with a very simple shape: a plane plate, cylindrical rod,

cylindrical pipe, with the condition that q_v and λ are invariable through the

volume of the body.

Flat Plate

If the plate is unrestricted in the directions $\underline{y}$ and $\underline{z}$, the thermal

conductivity equation takes the form

$$\frac{d^2 t}{dx^2} + \frac{q_v}{\lambda} = 0. \tag{17.4}$$

---

* A similar heat release pattern occurs in many other technical problems, for example,

when electric current is passed through a conductor, when high frequency current

is used to heat bodies, when a chemical reaction occurs in a body, and so on.

Let us solve Eq. (17.4) by assuming $\frac{dt}{dx} = u$; then by integrating first the equation

$$du = -\frac{q_v}{\lambda}\,dx.$$

we get

$$\frac{dt}{dx} = -\frac{q_v}{\lambda}x + C_1;$$

(17.5)

secondary integration gives us

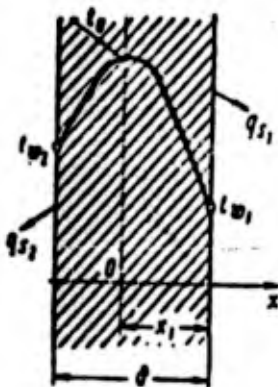$$t = -\frac{q_v}{\lambda}\cdot\frac{x^2}{2} + C_1 x + C_2.$$

(17.6)

Fig. 253. Temperature distribution in plate during volume heat release $q_{s1} + q_{s2}$ (showing derivation of equation).

For cases in which no other heat action is imposed upon the heat flux caused by volume heat release (for example, flow across a plate from an outside

---

In actual conditions, there is local non-uniformity of volume heat release in the reactor elements on account of neutron "corrosion", for example, in the body of an absorbing rod, and to a lesser extent, in the body of a heat producing element in a heterogeneous reactor. This fact must be taken into account in exact calculations of heat flux in reactors.

heat source), there is always a maximum temperature inside the plate (Fig. 253).

This fact may be utilized to find the integration constant C_1; this point in the

plate $dt/dx = 0$. Placing the origin of the coordinates ($x = 0$) in the ‾‾‾‾ section

where the temperature reaches a maximum, we get $C_1 = 0$ from Eq. (17.5). Under

these conditions Eq. (17.6) takes the form

$$t = -\frac{q_v}{\lambda} \cdot \frac{x^2}{2} + C_2.$$

(17.7)

The latter integration constant can easily be found from boundary

conditions. In the general case the heat removal may be different on each side

of the plate. The temperature of the plate surface is then $t_{\hat{w}_1} \neq t_{\hat{w}_2}$.

The integration constant can be determined from the conditions that at

$x = x_1$, $t = t_{w_1}$. Then

$$C_2 = t_{w_1} + \frac{q_v}{\lambda} \frac{x_1^2}{2}.$$

Substituting the value of C_2 obtained into Eq. (17.7) we get

$$t = t_{w_1} + \frac{q_v}{2\lambda}(x_1^2 - x^2).$$

(17.8)

If the distance x_1 is unknown, it can be found by using the condition

for finding C_2, i.e., $x = \delta - x_1$, $t = t_{w_2}$.

Solving the new equation

$$t = t_{w_1} + \frac{q_v}{2\lambda}[(\delta - x_1)^2 - x^2]$$

tpgether with Eq. (17.8), we get

$$x_1 = \frac{1}{2}\left[(t_{e_2} - t_{e_1})\frac{2\lambda}{q_0 \delta} + 1\right].$$

(17.9)

The equation determining the temperature field in a flat wall with bilateral heat removal finally takes the form*

$$t = t_{w_1} + \frac{q_0}{2\lambda}\left\{\frac{\delta^2}{4}\left[(t_{s_1} - t_{x_1})\frac{2\lambda}{q_0 \delta^2} + 1\right]^2 - x^2\right\}.$$

(17.10)

From (17.10) we can easily obtain expressions for the temperature in a plate with symmetrical heat removal $(t_{w_1} - t_{e} = 0)$

$$t = t_w + \frac{q_0}{2\lambda}\left[\left(\frac{\delta}{2}\right)^2 - x^2\right].$$

(17.11)

The maximum temperature difference in the plate with symmetrical heat removal is obtained from the condition $\underline{t} = \underline{t_0}$ at $\underline{x} = 0$

$$t_0 - t_w = \frac{q_0 \delta^2}{8\lambda}.$$

(17.12)

Cylindrical Bodies of Infinite Length

The general equation (17.3) in cylindrical coordinates, using the expression for $\nabla^2\underline{t}$ from Eq. (2.17) for the stationary process $dt/d\tau = 0$ and $dt/dz = 0$, takes the following form

$$\frac{d^2t}{d\rho^2} + \frac{1}{\rho}\frac{dt}{d\rho} + \frac{q_0}{\lambda} = 0.$$

To solve this equation we can use the same method as for Eq. (17.4), e.g., we assume

$$\frac{dt}{d\rho} = u.$$

Then,

$$\frac{du}{d\rho} + \frac{u}{\rho} + \frac{q_0}{\lambda} = 0.$$

(17.13)

Multiplying all the terms in the last equation by $\rho \, d\rho$, we get

$$\rho \, du + u \, d\rho + \frac{q_v}{\lambda} \rho \, d\rho = 0$$

and, accordingly,

$$d(\rho u) + \frac{q_v}{\lambda} \rho \, d\rho = 0. \tag{17.14}$$

Integrating Eq. (17.14), we get

$$\rho \frac{dt}{d\rho} = -\frac{q_v}{\lambda} \cdot \frac{\rho^2}{2} + C_1. \tag{17.15}$$

Separating the variables and integrating again, we get

$$t = -\frac{q_v}{\lambda} \frac{\rho^2}{4} + C_1 \ln \rho + C_2. \tag{17.16}$$

The integration constant C_1 and C_2 is determined from boundary conditions in each specific case.
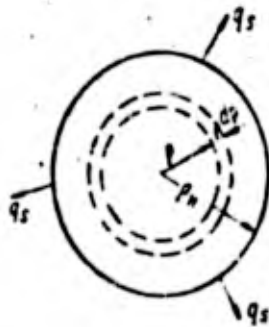

Fig. 254.
Calculation of temperature field in cross section
of cylindrical rod during volume heat release.

For a cylindrical rod (Fig. 254) at $\rho = 0$ $\frac{dt}{d\rho} = 0$ and $C_1 = 0$.

If the temperature on the rod surface $(\rho = \rho_H)$ is $t = t_H$, C_2 is found

from equation

$$C_2 = t_H + \frac{q_v}{\lambda} \frac{\rho_H^2}{4}$$

and, accordingly,

$$t = t_u + \frac{q_v \rho_u^2}{4\lambda}\left[1 - \left(\frac{\rho}{\rho_u}\right)^2\right].$$

$$(17.17)$$

The maximum temperature difference when $t = t_0$ and $\rho = 0$ is

$$t_0 - t_u = \frac{q_v}{\lambda}\cdot\frac{\rho_u^2}{4}.$$

$$(17.18)$$

Example. In a cylindrical rod $\underline{d} = 10$ mm in a heat producing element made of graphite with uranium 235, the amount of heat released is $q_\Lambda = 10$ kcal/m^3. hr let us assume $\underline{t} = 2300°$C, $\lambda = 12.5$ kcal/m·hour/deg (Fig. 255).

The temperature differential between the outside surface and the rod axis is

$$\Delta t = t_0 - t_u = \frac{q_v \rho_u^2}{4\lambda} = \frac{10^8\cdot 25\cdot 10^{-6}}{4\cdot 12.5} = 50°\,\text{C}.$$

For a cylindrical pipe with bilateral heat removal, the problem can be solved in the same way as for a flat plate. We will give the solution for the simplest case - cooling on the inside surface only (Fig. 256). Then at Λ, the integration constant, according to Eq. (17.15), is equal to

$$C_1 = -\frac{q_v \rho_u^2}{2\lambda}.$$

Eq. (17.16) then takes the form

$$t = -\frac{q_v \rho^2}{4\lambda} + \frac{q_v \rho_u^2}{2\lambda}\ln\rho + C_2.$$

$$(17.19)$$

The integration constant C_2 can be determined from the condition at $\rho = \rho_u, t = t_u$. then

$$C_2 = t_u + \frac{q_v}{\lambda}\frac{\rho_u^2}{4} - \frac{q_v}{\lambda}\frac{\rho_u^2}{2}\ln\rho_u.$$
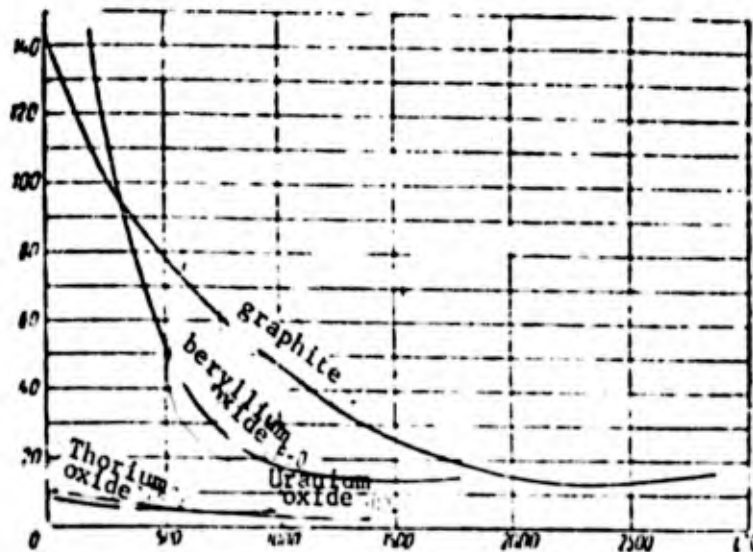
Fig. 255. Thermal conductivity coefficient of certain
non-metallic materials as function of temperature.
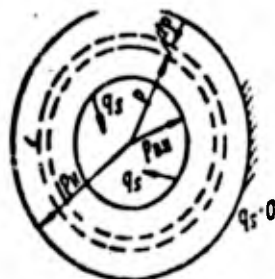
Fig. 256. Calculation of temperature field in pipe
wall during volume heat release.

The final form of the equation determining the temperature distribution
in the pipe wall is

$$t_a - t = \frac{q_v \rho_u^2}{4\lambda}\left[2\ln\frac{\rho_u}{\rho} + \left(\frac{\rho}{\rho_u}\right)^2 - 1\right].$$

(17.20)

The temperature difference on the pipe wall is determined from the equation

$$t_a - t_{вн} = \frac{q_v \rho_u^2}{4\lambda}\left[2\ln\frac{\rho_u}{\rho_{вн}} + \left(\frac{\rho_{вн}}{\rho_u}\right)^2 - 1\right].$$

(17.21)

566

We can derive an equation for the temperature distribution in a cylindrically shaped wall when the heat removal from the outer surface is $\wedge$ in a similar way. We get.

$$t_{en} - t = \frac{q_v \rho_{en}^2}{4\lambda}\left[\left(\frac{\rho}{\rho_{en}}\right)^2 - 2\ln\frac{\rho}{\rho_{en}} - 1\right]$$

or

$$t_{en} - t = \frac{q_v(\rho^2 - \rho_{en}^2)}{4\lambda}\left(1 - \frac{2\rho_{en}^2}{\rho^2 - \rho_{en}^2}\ln\frac{\rho}{\rho_{en}}\right).$$

(17.22)

... .

Generalization of different cases of volume heat release and *similarity conditions*

Analysis of
(the expressions given above for temperature distribution in bodies during volume heat release enables us to ascertain the proportionality in every individual case between the temperature drop and the complex $\wedge$ in which $\underline{R}$ is *the characteristic* linear dimension in the general case. The proportionality coefficient between the given complex and a temperature drop (Δt_{max}) on the length $\underline{R}$ may be expressed by the non-dimensional value $\tilde\Phi$. For example, for a cylindrical rod ($\underline{R} = \rho_H$)

$$:| = \Phi \cdot \frac{q_v}{4\lambda\phi} = {}^{2\pi w}/_\Gamma$$

for a flat plate ($\underline{R} = \frac{\delta}{2}$)

$$\Delta t_{max} = \frac{q_v R^2}{8\lambda}, \quad \Phi = \frac{1}{2};$$

for a cylindrical pipe with internal heat removal ($\underline{R} \neq \rho_H$)

$$\Delta t_{max} = \frac{q_v \rho_H^2}{4\lambda}\Phi.$$

in which

$$\Phi^{-1} = 2\ln\frac{r_n}{r_{nn}} + \left(\frac{r_{nn}}{r_n}\right)^2 - 1.$$

Thus, Φ expresses the difference between the temperature drop in the body and the temperature drop in the cylindrical rod ($\bar{\Phi} = 1$), so it can be tentatively called the shape factor or geometric factor.

In the general case the dimensionless value Λ can serve as a criterion of similarity for heat phenomena in volume heat release. Literature describes the use of this type of criterion /7/ known as the Pomerantsev criterion

$$Po = \frac{q_0 R^2}{\lambda \Delta t};$$

thus $Po = 4 \bar{\Phi}^{-1}$ /.

The identical nature of the Po criteria (or $\bar{\Phi}$), other conditions of similarity being satisfied, implies the similarity of the temperature fields in bodies of different sizes.

Temperature Field with Variable λ or q/λ

The above-given solutions can be expanded to cover a case in which the thermal conductivity coefficient of the material varies greatly with temperature. A linear approximation of temperature dependence in the form Λ is usually adequate. The temperature distribution is then expressed in the following way /9/.

For a cylindrical rod

$$t = -\frac{1}{b} + \sqrt{\left(\frac{1}{b} + t_0\right)^2 - \frac{q_0 r^2}{2b\lambda_0}},$$

(17.23)

for a cylindrical pipe with internal heat removal

$$t = -\frac{1}{b} + \sqrt{\left(\frac{1}{b} + t_\text{s}\right)^2 - \frac{q_v \rho_\text{s}^2}{2b\lambda_0}\left[2\ln\frac{\rho_\text{s}}{\rho} - \left(\frac{\rho_\text{s}}{\rho}\right)^2 - 1\right]}.$$ (17.24)

for a cylindrical pipe with external heat removal

$$t = -\frac{1}{b} + \sqrt{\left(\frac{1}{b} + t_\text{ss}\right)^2 - \frac{q_v \rho_\text{ss}^2}{2b\lambda_0}\left[\left(\frac{\rho}{\rho_\text{ss}}\right)^2 - 2\ln\frac{\rho}{\rho_\text{ss}} - 1\right]}.$$ (17.25)

This method can be used to take into account the variation q_v through the material of the reactor elements; the necessity may arise when calculating the heat release in a heat-producing element with a large concentration of fissile matter, when the external layers "screen" the internal ones from the neutrons, or in a regulating rod.

When the field of heat releases is set as a function of (body temperature), the solution, given linear approximation, will not be in any way different from the one at ; it is rather more complicated, however, to solve the problem when the heat release field is given as a function of (body geometry).

More general problems are solved in Lykov's monograph /7/.

Of particular interest are the problems of the distribution of temperature in multilayer walls, for example, a heat-producing element in a shell or with a protective covering; these problems can be solved by means of the above-mentioned methods.

Temperature Field and Thermal Stresses

As had already been pointed out, the temperature distribution determines the thermal stresses in the material of the heat-producing element or *some* other element in the reactor. Indeed, if we use equations from the elasticity theory /15/, we can see that the stresses are *determined both by the* temperature [distribution] *gradients* as well as the absolute values of the temperature

$$\sigma = \frac{\alpha E (\overline{T} - T)}{1 - \mu} \ \kappa \ell / c \mu^2,$$

(17.26)

in which **A** is the coefficient of linear temperature expansion,

E is the modulus of elasticity,

μ is the Poisson factor,

T is the temperature at the point in the body where there is stress σ, and

$\overline{T}$ is the mean temperature of the body, which in the general case is a function of the temperature distribution;

$$\overline{T} = \frac{\int_V T \, dV}{\int_V dV}.$$

For example, for a cylindrical rod the mean temperature is determined as follows

$$\overline{T} = \frac{\int_0^{\rho_\kappa} t(\rho) \rho \, d\rho}{\int_0^{\rho_\kappa} \rho \, d\rho} = t_\kappa + \frac{q_v \rho_\kappa^2}{8\lambda}$$

or

$$\overline{T} = t_\kappa + \frac{\Delta t_{max}}{2}.$$

570

The value $\overline{T} - \underline{T}$ is in turn proportional to $\dfrac{q_{\lambda}\lambda}{\lambda}$. Thus, it can be taken

that the thermal stresses are proportional to the complex of physical-mechanical

properties and the heat load

$$\sigma \sim \frac{\alpha E}{\lambda(1-\rho)} q_o.$$

In view of the fact that most high-temperature reactor materials do not

possess good constructional properties (ceramic materials, brittle metals), the

evaluation of their resistance to thermal stresses (spalling resistance) is of prime

importance.

When speaking of the spalling resistance of reactor materials, it is

essential to take into account the fact that when irradiated for some time by

neutrons and γ-quanta, the physical-mechanical properties of a material may be

altered. This (applies to the coefficient of thermal conductivity λ and the rupture

stress σ_{rup} in particular. The strength of the material may either increase or

decrease. Irradiation usually decreases thermal conductivity. We know of an

experiment /12/, in which the thermal conductivity of a quartz crystal decreased by

a factor of 300 after irradiation. It is also known, however, that at high

temperatures radiation damage to reactor materials is decreased to a considerable

extent, i.e., there is a sort of annealing of the materials. For example, λ of $\ln$

ceramics with a beryllium-oxide base decreases by a factor of 6 or more after prolonged

irradiation; after annealing at 1000 - 1100°C the radiation changes in λ reduce

considerably, and do not come to more than 15 - 30% of λ in an unirradiated material

/17/.

Thus, it is very important to keep in mind irradiation changes in thermal

conductivity when designing and constructing nuclear power reactors for use at low

and medium temperatures.

75. Heat Removal from Nuclear Reactors

Temperature Distribution in Heat-Producing Element Channel

As was demonstrated above, the temperature for the heat-release distribution

along the reactor takes the form

$$q_v = q_{v_0} \cos \frac{\pi x}{L'}.$$

Between the beginning of the active zone ($x = \frac{L}{2}$) and the cross section x

the heat released is $q_x x$, in which $q_x = \frac{q_v}{F_c}$ is the specific heat release per unit length

of the working channel, while F_c is the cross section of the heat-producing

elements in one channel ($q_v \sim q_x$).

The heat-up of the heat-transfer agent can be found from the condition

that all the heat released along the length x is taken up by the heat-transfer agent

$$Q_x = 3600 \, \dot{Q}_{sec} c (t_1 - t_{11}).$$

At the same time the amount of heat released in the reactor along the length x is

$$\int_{-\frac{\ell}{2}}^{x} q_x \, dx = q_{t_0} \int_{-\frac{\ell}{2}}^{x} \cos \frac{\pi x}{L'} \, dx.$$

The heat-up of the transfer agent is therefore

$$t_f - t_{f_1} = \frac{q_{t_0}}{3600 a_{sec.}} \int_{-\frac{\ell}{2}}^{x} \cos \frac{\pi x}{L'} \, dx.$$

By integrating we get the function

$$\Delta t_f = t_f - t_{f_1} = \frac{q_{t_0} L'}{3600 \pi a_{sec.}} \left(\sin \frac{\pi x}{L'} + \sin \frac{\pi L}{2L'} \right).$$

Attention should be given to the fact that the heat-up of the coolant depends solely on the working conditions. The values a and t_w do not have an effect on the heat-up, but are the result of the established reactor conditions.

The temperature wall can be determined from the heat-transfer to the gas. For instance, in the center of the reactor

$$q_{t_0} = a_0 (t_{w_0} - t_{f_0}) = a_0 \vartheta_0.$$

in which $\vartheta_0 = t_{w_0} - t_{f_0}$ is the temperature drop between the wall and the coolant in the middle of the reactor.

If we take it that a changes only slightly along the reactor and that the mean value a^*_{mean} can be used in the calculations, the *current* value of the

temperature drop θ along the reactor is determined by the following expression

$$\theta = \theta_0 \cos \frac{\pi x}{L'}.$$

The temperature of the wall of the heat-producing element t_w at each

point is determined in the following way

$$t_w = t_{f_1} + \Delta t_f + \theta.$$

Substituting expressions for Δt_f and θ into the equation we get

$$t_w = t_{f_1} + A_1 \sin \frac{\pi x}{L'} + A_2 + B \cos \frac{\pi x}{L'},\qquad (17.29)$$

in which A_1, A_2 and B are constants determined by the working conditions of

the reactor

$$A_1 = \frac{q_{s_1} L'}{3600 \pi G_s c_s}, \quad A_2 = A_1 \sin \frac{\pi L}{2L'}, \quad B = \frac{q_{s_1}}{a_{mean}} = \frac{q_v F_c}{F_s a_{mean}},$$

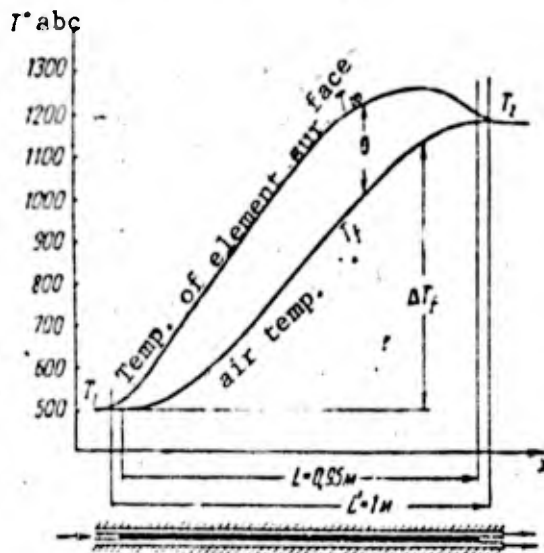in which F_s is the cooled surface of the heat-producing element per unit length.

Fig. 257. Temperature distribution along working channel of reactor

The relationship between q_v, F_k and F_s can be expressed in every individual case in terms of the geometric parameters of the active zone. For the specific example of an uranium graphite reactor, the temperature distribution in the center channel, calculated by Eqs. (17.29) and (18.29), is shown in Fig. 257.

The position of the cross section in which t_w obtains a maximum can be determined analytically as well by making the first derivatives (dt_w/dx) equal to zero.

Temperature Field in Reactor and Flattening

When considering the temperature distributions in the cross section of a reactor we must take into account the fact that heat release depends on radius

$$q_v = q_{v_0} J_0\left(2.405 \frac{r}{\rho'}\right) \text{ (for central cross section)}$$

$$q_v = q_{v_0} \cos \frac{\pi x}{L'} J_0\left(2.405 \frac{r}{R'}\right) \text{ (for any other points in reactor)}$$

A heat-release field of this kind, provided special measures are not adopted, means that the heat-up of the transfer agent in the peripheral channels is considerably less than in the center. This is very unfortunate from a thermodynamic point of view: the mean temperature of the heat-transfer agent at the

---

* This is admissible in the case of gas cooling; during cooling by a liquid or two-phase transfer agent, we have to calculate the heat transfer in stages by dividing up the reactor into several zones.

reactor outlet is lower than t_{f_2} in the central channel, and the efficiency is reduced during subsequent utilization of that heat.

In order to rectify this shortcoming we can apply various methods:

a) reducing the relative cooling surface in the peripheral channels;

b) artificial re distribution of the coolant consumption in different channels, and

c) profiling the concentration of fissile matter, and therefore the heat release through the active zone from the condition $t(r) \sim$ const.

This latter method is advisable as well for flattening the temperature along the reactor; in this case greater power can be obtained from a unit of volume of the reactor /22/.

Heat Transfer AGENTS

Both gases (air, hydrogen, carbon dioxide, helium, etc) and liquids (water, organic transfer agents, liquid salts and metals) are used as heat-transfer agents. They may be used in different power systems, i.e., with closed or open loops, with an invariable aggregate state, and with the heat-transfer agent changing from the liquid phase to the gas phase and back again, and so on.

Let us consider the basic requirements of a heat-transfer agent and the heat-removal system when applied to nuclear power reactors.

1. The set of requirements ensuring minimum action on the nuclear reaction.

a) the heat-transfer agent should not strongly absorb neutrons or have a negative effect on their moderation and scattering;

b) the volume through which the heat transfer agent flows in the active zone should be minim*al* as far as possible. This is essential in cases in which the transfer agent is not itself a moderator or heat-producing substance. In such cases the optimum volume of the transfer agent is determined by the physical calculations of the reactor.

2. Pumping the heat-transfer agent through should take away *as* little energy from the power plant as possible.

3. Optimum operating *characteristics*

a) chemical stability of the matter at high temperatures and when irradiated;

b) corrosion resistance *of* heat transfer agent and reactor elements in contact with heat transfer agent;

c) minimum liability to be activated by irradiation;

d) maximum freedom from activizing impurities.

All these requirements must be satisfied and at the same time the heat-transfer coefficient must be increased to the maximum extent, for from the point of view of increasing the economic nature it is not an advantage to increase power

by increasing the temperature difference between the heat-producing element and the transfer agent.

Research on the selection of heat-transfer agents satisfying this variety of requirements is being conducted on a fairly large scale /4/. The following heat-transfer agents may be of practical interest. In closed loop engines the heat-transfer agent is air, the characteristics of which are well known. Helium, nitrogen or carbon dioxide can be used for closed-loop reactors. Data for thermal conductivity, temperature conductivity and viscosity of these gases are shown in Figs. 258 - 269 /23/.

Heat Removal System

Systems for removing heat in nuclear power reactors can be classified on the basis of the following:

1. The type of heat removal from heat-producing elements - irradiant heat exchange

   - convection heat removal.

2. Type and phase state of heat transfer agent:

   - non-boiling liquid

   - boiling liquid,

   - inert or aggressive gas.
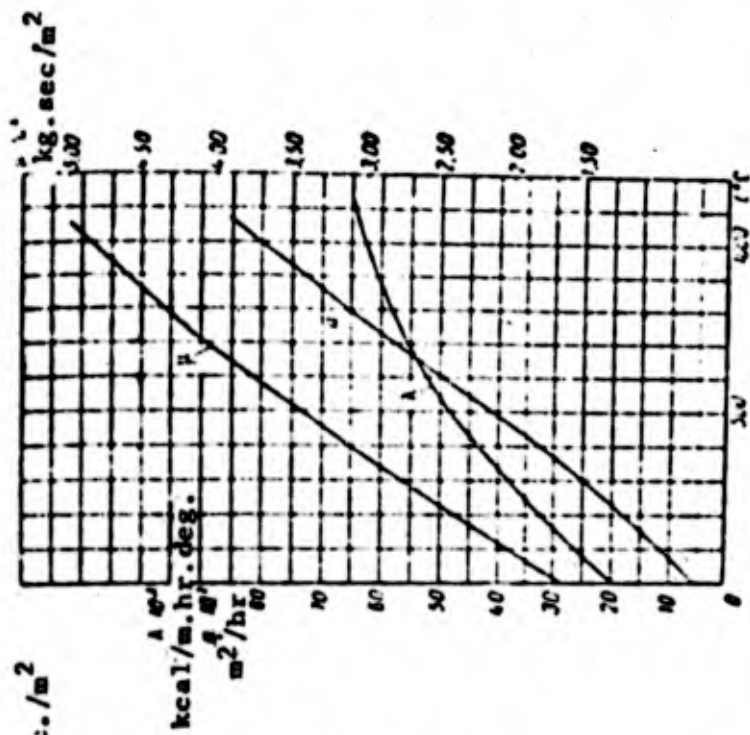
3. Design of heat-removal loop:

Fig. 258.
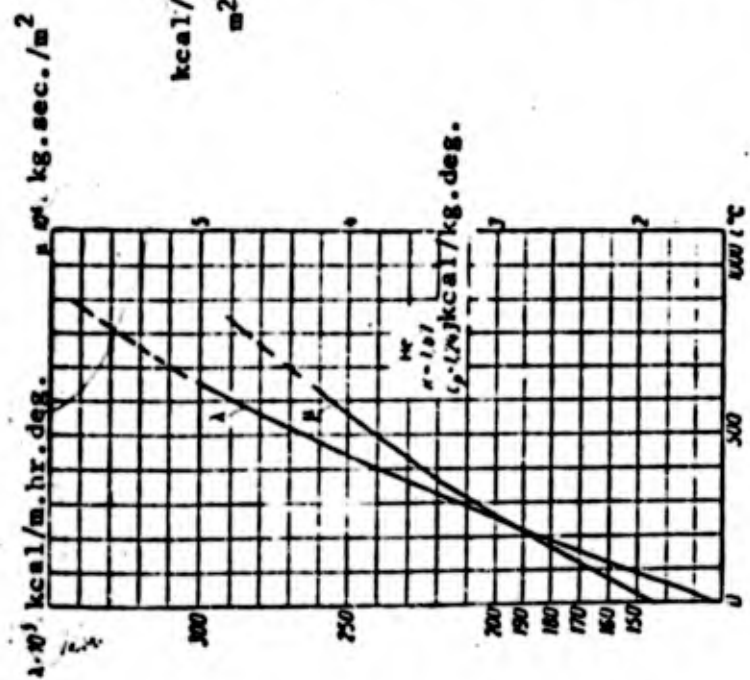Thermal conductivity and dynamic viscosity
of helium as function of temperature

Fig. 259.
Thermal conductivity and dynamic
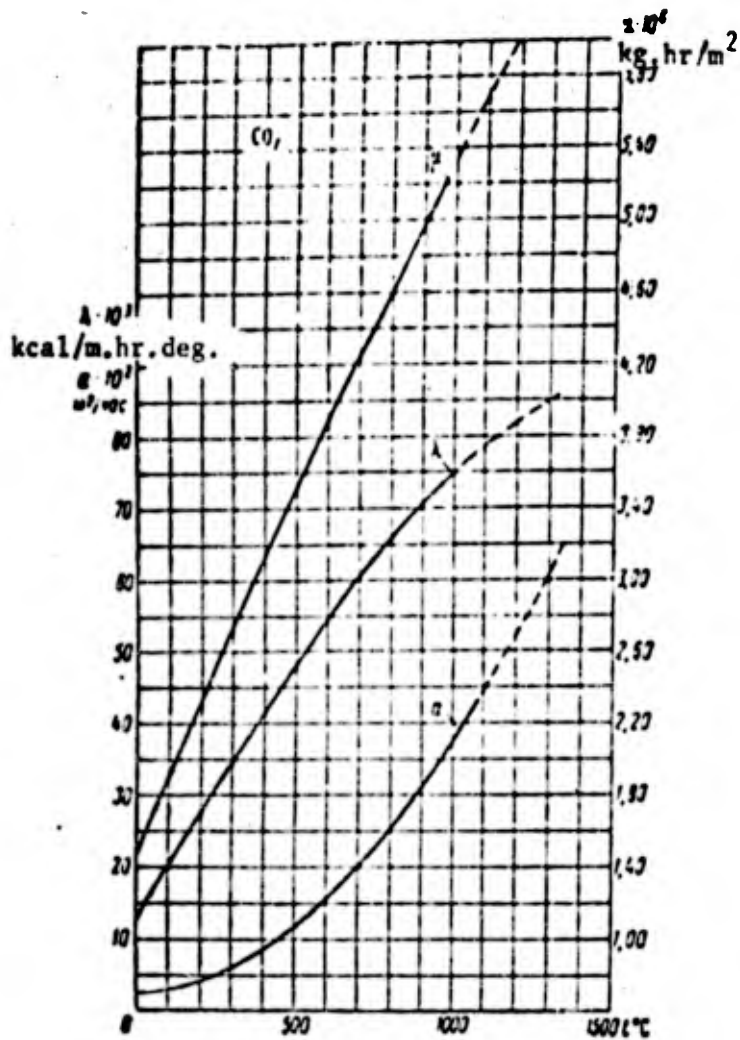viscosity of nitrogen as function of
temperature

579

Fig. 260. Thermal conductivity, thermal diffusivity
and dynamic viscosity of carbon dioxide
as function of temperature.

- open loop,

- closed loop,

- two-loop plants in which (heat engine operates with the working solid of the second loop without going through the reactor.

- with heat regeneration (heat-transfer agent is heated-up before reactor using heat not completely used up in heat machine) and so on.

Given the great variety of possibilities in heat removal, the process does not prevent any difficulty in principle, since similar systems have been widely used in heat engineering for some time. Admittedly, inorganic possibilities of obtaining high temperatures are typical of nuclear power engineering, consequently there are specific features in heat exchange at high temperatures - an increase in the share of radiant heat-exchange, an increase in the thermal conductivity of gases, and so on, which have not been very much studied so far.

Intensification of Heat Exchange as Method of Increasing Reactor's

Specific Power

The specific power which can be removed from a unit volume of the active zone in the reactor is limited by the heat removal and the admissible temperature drop in the heat-producing elements. Several ways of increasing the coefficient of heat transfer α to the transfer agent are known. The most practical and promising ones

581

are the following:

a) improvement *in* the design of the heat-producing elements;

b) use of liquid-metal transfer agents;

c) use of porous heat-producing elements.

Improvement in Design of Heat Producing Elements

At the present time when nuclear power engineering *is* still in its infancy, the variety of types and shapes of heat-producing elements prevents us from making a detailed analysis of them from the standpoint of heat transfer.

Matters are further complicated by the fact that in addition to the heat transfer, the life of heat-producing elements is determined by their spalling resistance. Furthermore, the consumption of expensive fissile matter on the construction of a reactor also depends on the shape and size of the heat-producing elements. It is known, for instance, that the best geometric shape, from the point of view of physics, in a gas-cooled heterogeneous reactor is a cylindrical rod.

Figs. 261 and 262 show examples of heat-producing element systems with different methods of intensifying heat transfer. When providing for more complicated element shapes, the following obligatory requirements must be kept in mind.
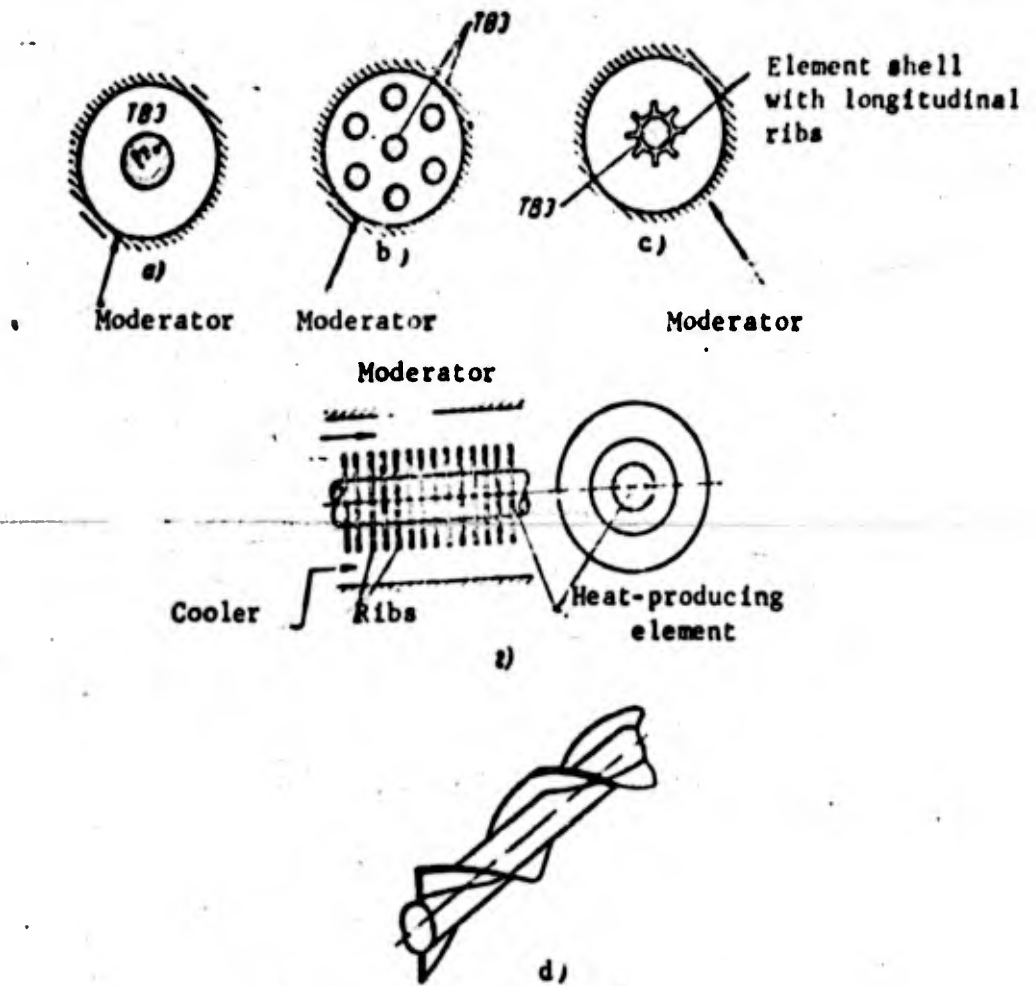
582

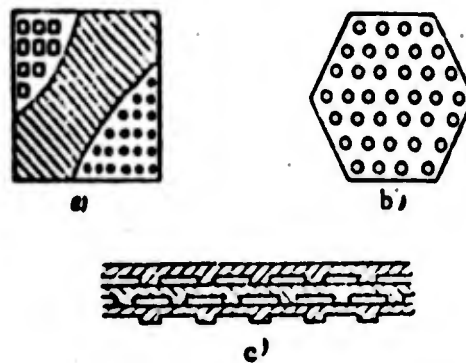Fig. 261. Example of systems for forming heat-releasing elements in heterogeneous reactor.

Fig. 262. Example of systems for forming heat releasing elements in homogeneous reactor.

The special shells - ribbing - must not cause:

a) the admission of any considerable quantity of undesirable (neutron absorbing) materials into the active zone;

b) an increase in the channel resistance beyond sensible limits.

Liquid Metal Heat Transfer Agent

The use of liquid-metal heat transfer agents for cooling reactors involves a number of unquestioned advantages*. Fused metals exhibit considerable thermal capacity and very high thermal conductivity, which is the reason for the smaller amount of heat transfer agent *which needs* to be pumped through the reactor. The hydrodynamic system here differs only slightly from the water systems, and losses pressure in the loop are not unduly increased.

Liquid metals have high melting points (see Table 23) /9/, hence high pressure can be maintained in the circulation system and there is no danger of a vapor film (crisis) occurring.

For a thermal neutron reactor liquid metal heat transfer agents are not particularly good on account of the relatively high neutron capture power. But for intermediate and fast neutron reactors, which, admittedly, necessitates an increase in the mass of the fissile matter, transfer agents such as liquid Na, K, Li, Po, Bi and mixtures of them are presently acceptable.

584

Some information liquid-metal transfer agents are given in Section 19, in Ch. 3.

Table 23.

	t °C	γ kg/m3	λ kcal/m hr.deg	c kcal/kg.deg	m^2·hr	m^2·sec ×10⁻	Pr
Lithium Li t_m-186°C t_b-1317°C	500	491	39	1.0	0.051	73.4	0.033
Sodium Na t_m-97.3°C t_b-878°C	500	823	49	0.304	0.195	28.9	0.0053
56.5% Bi+53.5P t_m-123.5°C t_b-1670°C	500	10130	12	0.035	0.031	13.6	0.0141
25% Na+75% K t_m- -11°C t_b- 784°C	500	751	18.5	0.231	0.107	26.7	0.009

As distinct from non-metallic liquid heat-transfer agents, metals are much more stable in the neutron and γ-radiation fields, but they are activated when flowing through the active zone a number of times; hence the loop has to be protected from radiation. At normal temperatures, metal transfer agents are usually in the solid state; this is a good thing from the viewpoint of repairing loop units without having to pour off all the metal, though it means that the reactor has to be pre-heated before being started up. The high electric conductivity of liquid metals enables us to use airtight electromagnetic pumps, gauges, and so on.

The negative properties of liquid-metal heat-transfer agents are their

high corrosion-erosion liability at high temperatures, the danger of a fire when

hermetically-sealed closed loop is broken, and high oxidibility, which causes oxides

to settle on the walls of heat exchanges, if oxygen gets into the system, and sharply

reduces the heat transfer coefficients.

The initial study of heat exchange with liquid metals /11/ shows that

dimensionless

dependences obtained for other fluids can be used to calculate them.

It was found later /10/ that the *dimensionless* dependence for heat exchange with

heavy fused metals was

$$Nu = (3 + 4.5)^{\bullet} + 0.014 Pe^{0.8}.$$

(17.30)

This equation tallies well with some of the ones formerly quoted by other

authors /8, 17/.

In Ref. /10/ the *dimensionless* equation for a range in variation $200 < Pe < 1400$

has been adjusted to $Nu = 5.9 + 0.015 \, Pe^{0.8}$.

If we compare water cooling and liquid lithium cooling at temperatures

from 300 to 500 C and $Re \approx 50,000$, there is reason to believe that the coefficients

of heat transfer from the channel wall to the liquid metal will be 5 to 10 times

greater than to water.

It is important to calculate the flow of liquid through the reactor

correctly. We can solve this problem by finding the optimum, taking into account the

hydraulic resistance of the system, power consumption of pumping and the gain in heat power in the reactor.

Cooling of Porous Body

If the heat-producing elements of a reactor are made in the form of a porous body with capillary *tubes*, this enables us to intensify the heat exchange to a considerable extent. Designers are now planning reactors of this type /3/.

Indeed, in small cross section channels flow is laminary, and, furthermore, the distance between the source and the heat consumer is reduced to a minumum, keeping the thermal resistance minimum. The striking results which can be obtained by reducing the channels in the heat exchanges can be seen from the following sample: when the size of the tube is reduced from 19 mm to 2.4 mm, the volume of the heat exchanger is reduced by a factor of 10, and the weight by a factor of 8. The heat transfer to the gas flowing along the small cross section channels can be calculated by *applying* /the theory of heat exchange in capillaries /2/.

Never and greater demands are being made on heat-transfer devices which

The free term depends on the state of the surface, i.e., whether it is oxidized, clean, unwetted, and so on.

play a very important part in the complicated systems of power plants. Last but

not least, progress in further intensifying convective heat exchange with different

media will be of exceptional value to nuclear power engineering.

References

1. Adamchuk Yu. V. Atlas of effective neutron sections of elements, edited by Academy of sciences of USSR, 1955.

2. Present state of hydroaerodynamics of viscous field, edited by S. Gol'shtein, vol. II, For. Lit. Press, 1948.

3. Gulmen K. Scientific and technical fundamentals of nuclear power engineering, Vol. II, Ch. X, For. Lit. Press, 1953.

4. Glesston S, and others. Theory of nuclear reactors, For. Lit. Press, 1954.

5. Dollezhal' N. A. and others. Uranium graphite reactor with high-pressure steam superheating, Atomic Energy, Vol. 5, Issue 3, 1957.

6. Kutateladze S. S. and others. Liquid Metal heat-transfer agents, Atomizdat, 1958.

7. Lykov A. V. Theory of thermal conductivity, Gostekhizdat, 1952.

8. Merrey R. Introduction to nuclear engineering, For. Lit. Press, 1955.

9. Mikheyev M. A. Fundamentals of heat transfer, third edit. Gosenergoizdat, 1956.

10. Novikov I. I. and others. Heat transfer and thermal-physical properties of fused alkaline metals, Atomic energy, 1956, No. 4.

11. Styrikovich M. A. and others. Certain regulations in heat transfer of boiling mercury under forced flow conditions, ZhTF, vol. 10, Issue 16, 1940.

12. Stefenson R. Introduction to nuclear engineering, Gostekhizdat, 1955.

13. Stsekli T. Reactor plants with open cycle for aircraft engines, Atomic engineering abroad, 1956, No. 8.

14. Timoshenko S. P. Theory of elasticity, ONTI, 1937.

15. Ford Dzh. Power reactor designs, Gosenergoizdat, 1956.

16. Chirkin V. S. Systems for removing heat from nuclear reactors, Atomic energy, 1956, No. 5.

17. As is.

18. As is.

19. Power reactors, Materials of International conference on peaceful uses of atomic energy, vol. 3, Gosenergoizdat, 1958.

20. Nuclear reactors, Materials of US Atomic Energy Com...

21. Ibid, v.1, 2, 1957.

22. As is.

23. Thermal physical properties of matter. Reference book

Gosénergoizdat, 1956.

24. As is.